Abstract Volume

30th Himalaya-Karakoram-Tibet Workshop Dehradun, India

6-8 October 2015

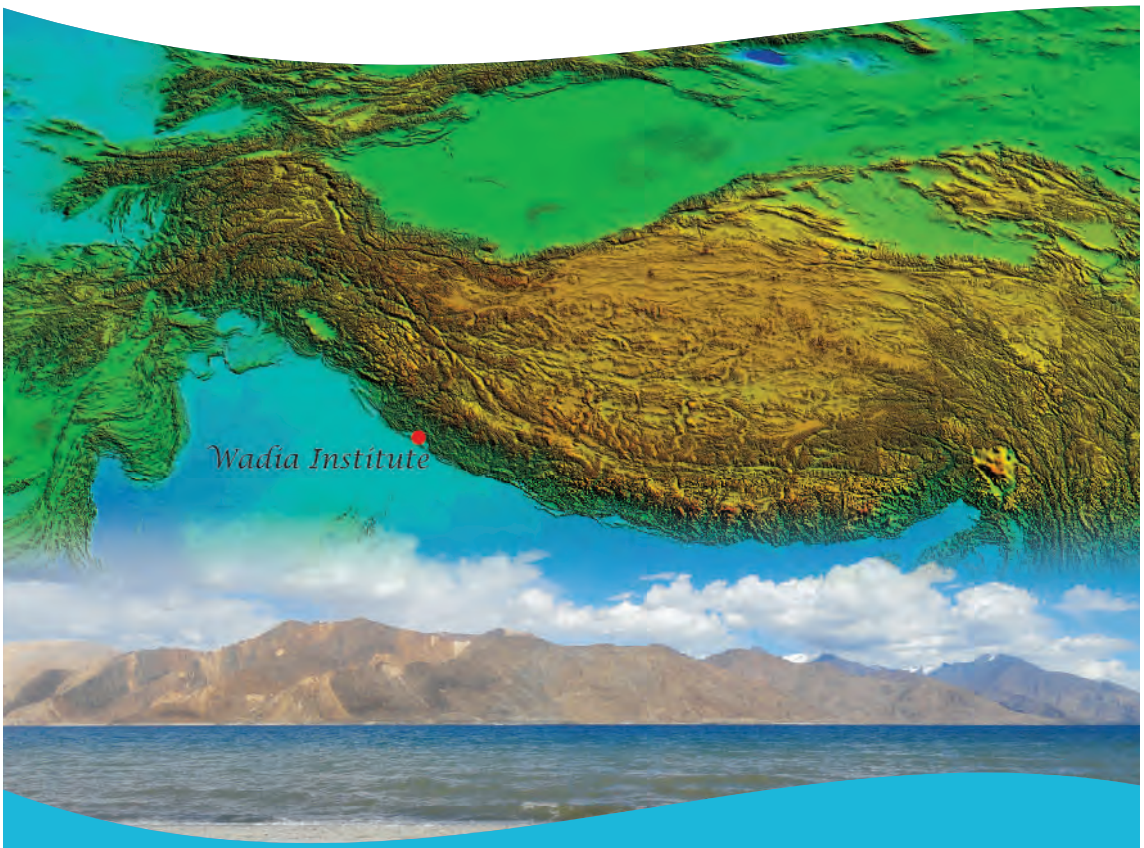

Wadia Institute of Himalayan Geology
Dehradun (India)

30th Himalaya-Karakoram-Tibet Workshop

WIHG, Dehradun, India

6-8 October 2015

Chairman

Anil K. Gupta

Core-Organizing Team

Rajesh Sharma (Convener)
Pradeep Srivastava
R.J. Perumal
Devajit Hazarika
S.K. Parcha
Barun K. Mukherjee

Editors

Meera Tiwari
Kishor Kumar
G. Philip
D.R. Rao
N. Suresh

Editorial Manager

Rambir Kaushik

Abstract Volume

30th Himalaya-Karakoram-Tibet Workshop
WIHG, Dehradun, India

6-8 October 2015

WADIA INSTITUTE OF HIMALAYAN GEOLOGY
(An Autonomous Institute of Department of Science & Technology, Government of India)
33, General Mahadeo Singh Road, Dehradun - 248 001
EPABX : 0135-2525100, Fax : 0135-2625212
Web : http://www.wihg.res.in

Contents

Kinematics and shear heat pattern of ductile simple shear zones with 'slip boundary condition': application in Himalayan tectonics

Kieran F. Mulchrone[1], Soumyajit Mukherjee*[2]
[1]*School of Mathematical Sciences, Dept. of Applied Mathematics,University College, Cork, IRELAND*
[2]*Dept. of Earth Sciences, Indian Institute of Technology-Bombay, Powai, Mumbai 400 076, INDIA*
[*]*soumyajitm@gmail.com*

Extrusion by Poiseuille flow and simple shear has been deciphered from large hot orogens, and partial slip boundary condition has been encountered in analogue models. Velocity and shear heat profiles are deduced for simple shear together with extrusive Poiseuille flow and slip boundary condition for Newtonian viscous rheology. A higher velocity at the upper boundary of the shear zone promotes higher slip velocity at the lower boundary. The other parameters that affect the slip are viscosity and thickness of the shear zone, and the resultant pressure gradient that drives extrusion. In the partial slip case, depending on flow parameters (resultant pressure gradient, density and viscosity) and thickness of the shear zone, the velocity profiles can curve and indicate opposite shear senses. The corresponding shear heat profiles can indicate temperature maximum inside shear zones near either boundaries of the shear zone, or equidistant from them. The developed model is applicable for extrusion of the Greater Himalayan Crystallines (GHC). Guo & Wilson (2012) deciphered influx of fluids into the GHC across its lower and southern boundary: the Main Central Thrust (MCT) from the Lesser Himalaya at south. This suggests that slip boundary condition might have prevailed at the MCT during the extrusion of the GHC by Poiseuille flow and/or simple shear.

An investigation into Uttarakhand disaster: a natural phenomenon or a result of multitude factors?

R.M. Devi[1], A.P. Dimri[2], Joystu Dutta[3]*
[1]*Indian Institute of Forest Management (IIFM), Bhopal, INDIA*
[2]*School of Environmental Sciences, Jawaharlal Nehru University, New Delhi, INDIA*
[3]*Sarguja University, Department of Environmental Sciences, Ambikapur, Chhattisgarh, INDIA*
[*]*joystu.dutta@gmail.com*

A natural disaster with torrential downpour and subsequent flash flood led to worst disaster on 16-17 June, 2013 devastating the Kedarnath region in Uttarakhand. This region is geo-morphologically vulnerable and tectonically active, and therefore, fragile and prone to disasters. Anthropogenic activities causing changes in land use, land cover, drainage, unplanned construction, unregulated tourism, etc. contributed towards enhancing the impact of this disaster. Continuous precipitation few days before the 16 June, 2013 followed by the sudden increase in precipitation during 16-17 June, 2013 lead to massive flooding of rivers. Loss of life, destruction of infrastructure, property and unestimated devastation to the ecology of the region made it one of the worst disasters that India had faced post the December, 2004 Tsunami. The event was associated with high intensity precipitation causing a flash flood which led to associated debris flow, sediment deposition, blockade, melting of glacier and several landslides. Preliminary data showed that a total of 745 landslides occurred along the river valleys of Mandakini, Mandani, Kali and Madhyamaheshwar. The debris created by these landslides was carried along with the flood water and added to the destruction. Most of the studies regarding the disaster are based on geo-morphological and hydrological aspects. The current study, however, attempts to seek an answer to the most pertinent and obvious question that intrigued the scientific world on a broader aspect: 'Was the Uttarakhand disaster solely a natural phenomenon or a result of multitude factors?'

To seek answers, we relied on meteorological models and baseline surveys. WRF model is used to simulate the Kedarnath disaster of 16-17 June 2013. Model simulated precipitation on comparison with corresponding observation and station data showed similar intensity and spatial distribution of precipitation. This extreme precipitation event was caused due to merging of two weather systems (Western Disturbance and Indian Summer Monsoon trough) over a region of variable orography. The interaction of the two systems occurred directly over Uttarakhand forming strong instability conditions. Further, the moisture incursion over this region of enhanced instability caused the formation of a temporary cloud cluster which persisted over Uttarakhand on 17 June 2013. This cloud cluster caused widespread torrential rain for a longer time period. Our baseline surveys indicated to the fact of unscientific river management, unplanned development along river beds and valleys, increasing population and unrestricted human establishments as some of the pivotal causes that lead to such humongous loss of life and property as an effect of the disaster.

July 25, 2015, Islambad Earthquake (IE), Pakistan-probable causative fault is Hazara Fault Zone (HFZ) or Hazara Lower Seismic Zone (HLSZ)?

MonaLisa[1], M. Qasim Jan[2]

[1]*Department of Earth Sciences, Quaid-i-Azam University (QAU), Islamabad 45320, PAKISTAN*

[2]*National Centre of Excellence in Geology (NCEG), University of Peshawar, Peshawar, Pakistan*

Islamabad, the capital of Pakistan, was badly shaken by an earthquake of magnitude 5.1 m_b at a depth of 26 km (according to United States Geological Survey (USGS)) and 10 km by Pakistan Meteorological Department (PMD). USGS marked the epicentral location of Islamabad Earthquake (IE) about 15 km NNE of Islamabad (Fig. 1) having the origin time of 01:59:55 (local time scale), with no apparent major damage in the epicentral area, i.e., in a circle of about 20 km radius, except in Abbottabad (a city located about 119 km NNW of Islamabad) where two woman and a child lost their lives due to roof collaps. An intensity of 5 on Modified Merculli Intensity (MMI) Scale has been assigned at the epicentral location. IE was felt in some parts of Kashmir and in North-West Frontier areas, i.e., Muzaffarabad, Bagh, Mirpur, Abbottabad, Murree, Peshawar, Swat, Malakand, and Mansehra. After the occurrence of a devastating October 08, 2005 Muzaffarabad Earthquake (7.6 Mw and 90 km NE of Islamabad), which took the death toll of more than 73,000, the IE badly scared the city of two million people. Rawalpindi (twin city of capital Islamabad) had previously experienced an earthquake of magnitude 5.2 M_L (USGS) on February 14, 1977. The preliminary seismotectonic studies of the IE interpret the activation of steeply dipping and NE striking right-

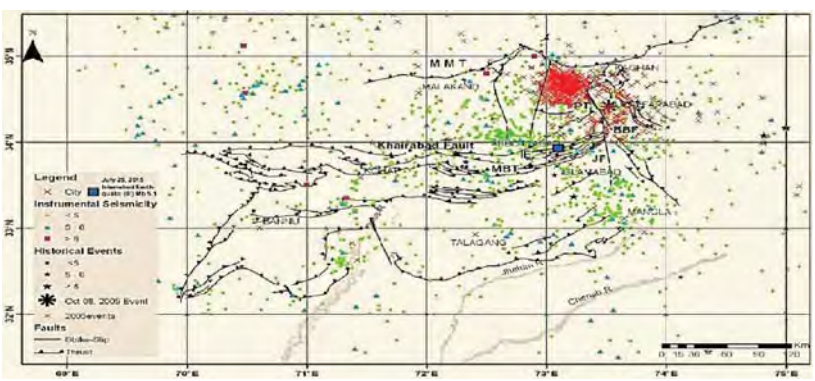

Fig. 1. Seismotectonic setting of the July 25, 2015 Islamabad Earthquake (IE), Pakistan (modified after MonaLisa 2009).

lateral strike slip fault with reverse component. The focal mechanism solution (FMS) of the IE and previously analyzed FMS by the authors and other workers from the epicentral area, tectonically known as Hazara Thrust System (HTS), indicates that either the Hazara Fault Zone (that corresponds to the Main Boundary Fault) or the Hazara Lower Seismic Zone was the cause of the IE. However, both local and international detailed seismological data of the IE will be required to determine the cause accurately. The correlation of location of the IE with the Bouguer gravity maps shows gravity lows, which are primarily related to the Tertiary sediments and crustal thickening under HTS.

Preliminary Seismic Hazard Evaluation of Makran Accretionary Zone (MAZ), Pakistan

MonaLisa[1], Frank Roth[2]

[1]*Department of Earth Sciences, Quaid-i-Azam University (QAU), Islamabad 45320, PAKISTAN*
[2]*Physics of the Earth, GFZ, German Research Centre for Geosciences, Potsdam, GERMANY*

The Makran Accretionary Zone (MAZ), located of the coast of Pakistan (geographic range as about 24-30°N, 61.5-68°E), having a long recurrence interval for large (>M_w 8) earthquakes and insufficient historical seismic data, is vulnerable but ill-prepared for future potential seismic hazards. Tectonically poorly understood MAZ has been studied on preliminary basis for the future probable major earthquakes. Including the 1945 M_w 8.1 earthquakes (which caused a tsunami) and April 16, 2013 M_w 7.8 earthquake (which hit southeastern Iran near the Pakistan border), the majority of the earthquakes show moderate seismicity (Fig. 1) with intermediate depth (50-100 km) based upon the catalogue recently prepared by Zare et al. 2014 for the area. Based upon the focal mechanism solutions carried out by previous workers and the authors, the eastern part of the MAZ seems to be seismically more active than the western part in Pakistan. A preliminary evaluation of potential seismic hazard with the available seismic as well as tectonic data and using the models of Heidarzadeh and Kijko 2010, the MAZ indicate the accumulation of strain along different tectonic features especially the eastern part (Fig. 1). Various surface and subsurface low-scale scattered

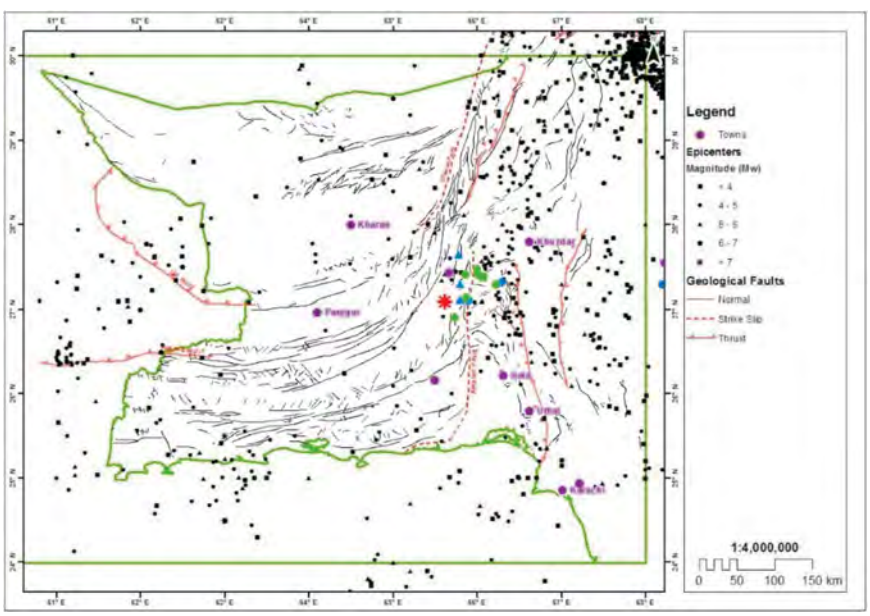

Fig. 1. Seismicity and Seismotectonics of Makran Accretionary Zone (MAZ), Pakistan.

structural features also indicate low magnitude future for the probable earthquake occurrences. However, neglecting these structural features can mean to be unprepared to a major earthquake in future. From this preliminary study of MAZ, we interpret that the complex interaction of the Indian/Arabian and Asian Plates may cause a serious threat for this part of country especially as the cities of Hyderabad and Karachi (Pakistan's largest and third largest cities) are located there. The integration of GPS and more geophysical data may improve this preliminary seismic hazard picture of the area.

The Nidar Ophiolite and its surrounding units in the Indus Suture Zone (NW Himalaya, India): new field data and interpretations

Nicolas Buchs, Jean-Luc Epard
Institut des sciences de la Terre, University of Lausanne, CH-1015 Lausanne, SWITZERLAND

The Nidar Ophiolite is located between the North Himalayan nappes and the Indus Suture Zone in the NW Himalaya in eastern Ladakh (India). Based mainly on geochemical argument, this ophiolite is classically interpreted as a relic of an intra-oceanic arc (Mahéo et al., 2000; Mahéo et al., 2004), which developed at around 140 Ma, prior to the collision between the Indian and Eurasian plates (Ahmad et al. 2008). From top to bottom, this ophiolite is composed of various sedimentary rocks (radiolarites, polygenic conglomerates and carbonates), volcanic rocks (pillow lavas, basaltic to andesitic in composition), gabbros (Fe-rich and layered gabbros, pegmatites and minor troctolites), serpentinites, dunites, pyroxenites and peridotites (mainly harzburgites).

The Nidar Ophiolite underwent an anchizonal metamorphism with preservation of primary structures (layering) and volcanic textures (pillow lavas). This study is mainly focused on new field observations across the ophiolite and the surrounding units. A new detailed geologic map of the ophiolite between the Nidar village and Kyun Tso area is presented. The upper part of the ophiolitic complex is an alternation of volcanic and sedimentary rocks (500-1000 m thick) and the lower part consists of large outcrops of gabbros (3000 m thick). These mafic rocks are separated from the serpentinized ultramafic rocks by a 200 m thick ophiolitic breccia and continental Indus Molasse slices. The Nidar Ophiolite is made up of the classical rock type succession (ultramafites, gabbros, pillow basalts, radiolarites), but the internal structure is far more complex than previously suggested. New field data (geologic and structural maps, lithologic sections, etc.) coupled with new geochemical analysis will help to constrain the geodynamic context and deformation history of this ophiolitic unit.

Ahmad, T., Tanaka, T., Sachan, H.K., Asahara, Y., Islam, R., Khanna, P.P. 2008. Tectonophysics, 451(1-4), 206-224.

Mahéo, G., Bertrand, H., Guillot, S., Mascle, G., Pêcher, A., Picard, C., De Sigoyer, J. 2000. Comptes Rendus de l'Académie des Sciences-Series IIA-Earth and Planetary Science, 330(4), 289-295.

Mahéo, G., Bertrand, H., Guillot, S., Villa, I., M., Keller, F., Capiez, P. 2004. Chemical Geology, 203(3-4), 273-303.

Early Palaeozoic garnets in the Jutogh Group, Himachal Himalaya, India: Its regional implication

O.N. Bhargava[1], M. Thöni[2], C. Miller[3]

[1]*INSA Honrary Scientist, 103, Sector 7. Panchkula 134109, INDIA*
onbhargava@gmail.com

[2]*Centre for Earth Sciences, Department of Lithospheric Research, University of Vienna, Althanstraße 14 / Room no. 2A487, A-1090 Vienna, AUSTRIA*
martin.thoeni@univie.ac.at

[3]*Institut für Mineralogie und Petrographie, Universität Innsbruck, Innrain 52, A-6020 Innsbruck, AUSTRIA*
christine.miller@uibk.ac.at

This paper documents early Palaeozoic garnets in the Naura Formation of the Jutogh Group. The Jutogh Group rocks form two belts: the Simla Klippe and the Chaur Mountain. The Chaur Thrust Belt above the Jaunsar and Kulu Thrust sheets extends towards the Satluj Valley and is overthrust by the Vaikrita Thrust Sheet, which is regarded as an upper digitation of the Jutogh, originated from a deeper level. The grade of metamorphism of the Jutogh varies from greenschist facies in the lower part to amphibolite facies (locally amphibolite-granulite transition) in the upper part. Several granitic bodies are present within the Jutogh Thrust Sheet, such as the Chaur Granite Complex, Khainchwa and Khadrala.

Coarsening of mineral grain size, particularly of garnet and staurolite, is observed in the Naura Formation, in the vicinity of the Chaur Granitic Complex, indicating that these minerals either pre-existed and grew coarser due to Chaur granitic activity, or were formed along with the Chaur Granite. Large size garnets up to 10 cm in diameter are confined to the mica-schist bands within the gneiss. Syn- to post-kinematic garnet growth with respect to the main foliation indicates its correlation with the regional tectono-metamorphic history.

Two garnet crystals (JU1, JU2) collected from Deola (30^0 48' 30.9"N: 77^0 25' 16.20"E), each c. 3 cm in size, were dated by the Sm-Nd TIMS method. For this purpose, c. 5 mm thick slabs were sawed out along the central part of the crystals. EMPA shows that both crystals are almandine rich (66-84) and zoned, with decreasing spessartine and increasing almandine and pryope from core to rim. The garnets are riddled with inclusions of quartz, plagioclase, ilmenite, apatite, biotite, chlorite, micro-zircon, and, importantly, Grt JU2 also contains inclusions of staurolite.

Slabs were cut into different domains, and from the crushed chips, including both core and rim parts, sieve and/or magnetic fractions were prepared (using the 0.07-0.30 mm gain size). Magnetic and/or handpicked splits, both leached and unleached, were used for analysis. Garnet crystal JU1 yielded a Sm-Nd isochron regression age of 485±19 Ma (for n= 8; MSWD = 6.6; ε_{Nd} = -6.1), while its rim part alone gave an age of 473±14 Ma. Crystal JU2 gave an age of 480±11 Ma (for n = 5; MSWD = 4.0; ε_{Nd} = -5.9); its rim part alone yielded an age of 477.9±6.2 Ma. When combining all analyses in one regression calculation, the resulting age is 479.7±8.5 Ma (n = 13; MSWD = 6.3; ε_{Nd} = -6.0) (Fig. 1). This "mean age" is interpreted as the time window of garnet crystallization. The results imply, that the garnets crystallized within one single coherent metamorphic event in the Early Ordovician (480±10 Ma), and there is no obvious indication that the more inclusion-rich core parts of the garnets are significantly older than their idiomorphic rims. The clearly negative initial (480 Ma) Nd isotopic composition (at ε_{Nd} = -6) is in line with a LILE-enriched, crustal source from which the garnets crystallized.

Several radiometric dates are available for the Chaur Granitic Complex. The foliated variety has given Rb-Sr ages of 1100±50 Ma and 930±115 Ma, the non-foliated variety an age of 526±46 Ma. Magmatic zircons defined a SHRIMP U-Pb age of 823±5 Ma for a quartz monzonite rock. However,

as the precise locations of the samples yielding different ages are not known, it is difficult to assess whether they stem from the same outcrop or from different varieties of granite. Rb-Sr ages of Khadrala Granite within the Jutogh Thrust Sheet are 460±18 Ma and 240±15 Ma. These published data would imply an earlier, pre-Cambrian metamorphism, some 823 Ma old or even older, possibly synchronous with the Jeori-Wangtu Gneissic Complex.

In literature, without substantiating with actual mapping, the name Jutogh has been arbitrarily tagged to any group of rocks having similar grade of metamorphism; e.g. Munsiari has been equated with the Jutogh, while it is an equivalent of the Kulu Thrust Sheet. No where, the granites in Jutogh or in its upper digitation Vaikrita have yielded older ages. Throughout its extension the Vaikrita Thrust Sheet contains Early Palaeozoic or younger granites, which however, due to their high altitude, remote location have not been systematically studied or dated. There is ample evidence that the Vaikrita and equivalent thrust sheets were not only initiated in the early Palaeozoic, but their granites, too, were exhumed as revealed by detrital zircons (525 Ma) in the Cambrian Tal Group (Lesser Himalaya) and the Kunzam La Formation (Tethyan Himalaya) at this time. These granites must have been located in close proximity to the Tethyan basin as revealed by granite pebbles in the Ordovician Conglomerate that rests, with angular unconformity, on folded Cambrian rocks. Feldspar pebbles in the Cambrian Tal Group of the Lesser Himalaya are smaller as compared to those of the Ordovician conglomerate, possibly due to greater distance of the basin from the granite source.

A Late Cambrian-Early Ordovician magmatic and deformational event seems wide-spread in the Himalaya, as evidenced by the numerous Early Palaeozoic intrusive rocks along the entire orogen; this event had repercussion all over the Indian subcontinent. In the Himalaya, the geodynamic nature of this event remained rather undefined up to now. We interpret our new age data in the context of this Early Palaeozoic event, which however, based on microfabrics, inclusion pattern and chemical zoning of the Jutogh garnets, give clear evidence for a regional tectonometamorphic process, that may have accompanied, and partly even promoted, the Ordovician igneous activities.

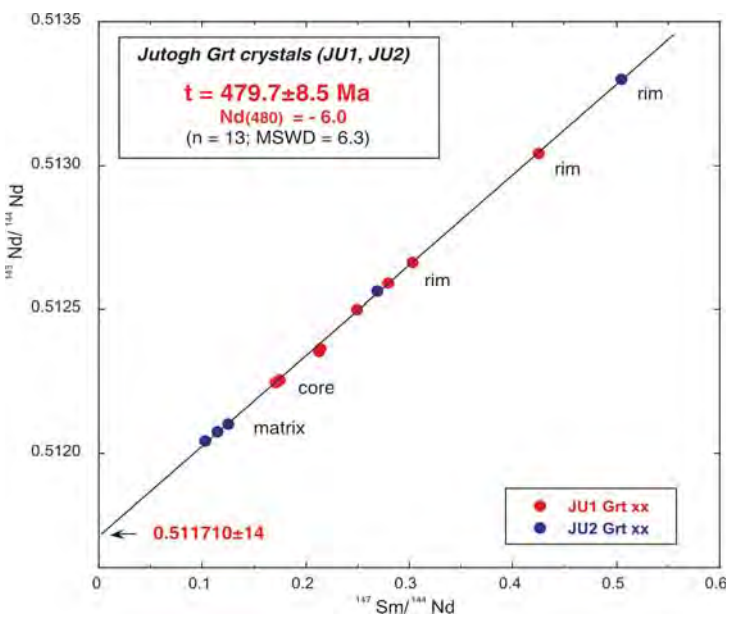

Fig. 1. Sm-Nd isochron plot for 13 fractions of two cm-sized single garnet crystals from the Naura Formation, Jutogh Group. The mean regression age of 479.7±8.5 Ma is interpreted as the time of garnet crystallization during an Early Ordovician tectonometamorphic event.

Variability in boreal spring precipitation over the last millennium in cold arid western Himalaya, India

Ram R Yadav[1], Akhilesh K. Yadava[1], Jayendra Singh[2]
[1]*Birbal Sahni Institute of Palaeobotany, Lucknow, India*
[2]*Wadia Institute of Himalayan Geology, Dehradun, India*

Precipitation in monsoon shadow zone of the western Himalayan region under the influence of mid-latitude westerlies is the dominant socioeconomic driver. However, our understanding on precipitation variability in perspective of decadal-century scale is not well understood due to spatially and temporally limited weather and high-resolution proxy climate records. Here we present the first boreal spring precipitation reconstruction for the western Himalaya extending back to the last millennium (1030-2011 CE) based on the annually resolved large tree-ring data set of Himalayan cedar (*Cedrus deodara*) and neoza pine (*Pinus gerardiana*) from ecologically homogeneous moisture stressed settings in Kinnaur, the western Himalaya. The reconstructed precipitation data revealed persistent long-term boreal droughts from 12th-early 16th century and pluvial from late 16th to recent decades. The late 15th and early 16th centuries CE displayed one of the driest episodes in 1490-1514 CE (206.20±6.81 mm), overwhelming any other 25-year mean in the reconstruction period, with precipitation ~15% lower than the long-term mean. The early part of the 19th century was the wettest in context of the past millennium with 1820-1844 mean precipitation (274±5.54 mm) being ~13% above the long-term mean.

The reconstructed boreal spring precipitation from the western Himalaya revealed consistency with the hydrological variations recorded from different locations in Central Asia under prevalent influence of westerlies indicating synoptic-scale changes in atmospheric circulation during the major part of the Medieval and Little Ice Age periods. As boreal spring precipitation is very important socioeconomic driver, protracted droughts in Central Asia during 12th to early 16th centuries caused severe contraction of the economy of the region. The boreal spring precipitation was observed to be above the long-term mean since the late 16th century. The protracted droughts and pluvial phases recorded in our reconstruction are in good agreement with historical proxy records available from different regions of the Central Asia. Many of the protracted severe hydrological conditions have been found to be associated with social upheavals and wars in the region.

Metamorphic CO_2-producing processes in the Himalaya: the contribution of calc-silicate rocks

Chiara Groppo[1,2]*, F. Rolfo[1,2], P. Mosca[2], G. Rapa[1]
[1]*Department of Earth Sciences, Via Valperga Caluso 35, Torino 10125, ITALY*
**chiara.groppo@unito.it*
[2]*CNR-IGG, Via Valperga Caluso 35, Torino 10125, ITALY*

Recent studies suggest that metamorphic degassing from active collisional orogens supplies a significant amount of CO_2 to the atmosphere, thus playing a fundamental role in the Earth's carbon cycle (e.g., Becker *et al.* 2008; Gaillardet & Galy, 2008; Perrier *et al.* 2009; Evans 2011; Girault *et al.* 2014). Quantifying the past-to-present metamorphic CO_2 flux from orogenic zones is therefore fundamental for our understanding of the deep carbon cycle (e.g., Mörner & Etiope 2002) and of the possible influence exerted by mountain building processes on the past, present and future climate.

Co_2 is produced during regional metamorphism in collisional contexts, where decarbonation reactions occur at relatively high temperatures within carbonate-bearing metasediments (e.g., calc-silicate rocks, impure marbles). The relative contribution this CO_2 has in the global carbon budget has long been debated (Rolfo *et al.* 2015). Previous studies aimed at constraining the metamorphic CO_2 flux related to regional metamorphism (e.g., Kerrick & Caldeira 1993; Ague 2000) mainly used

simple model reactions between end-members in the $CaO-Al_2O_3-SiO_2-H_2O-CO_2$ (CAS-HC) or in the $CaO-MgO-Al_2O_3-SiO_2-H_2O-CO_2$ (CMAS-HC) systems. However, natural calc-silicate rocks are much more complex than the CAS-HC and CMAS-HC model systems, because of the common occurrence of Ca-Mg-Fe solid solutions (e.g. garnet, clinopyroxene), as well as of K- (e.g., biotite, muscovite, K-feldspar) and Ca-Na (e.g., plagioclase, scapolite) silicates.

This study aims to define the CO_2-producing metamorphic reactions that occurred during the Himalayan metamorphic evolution. Detailed petrography (Rolfo et al., in press) and thermodynamic modelling of calc-silicate rocks (Groppo *et al.* 2013; submitted) in the CFMAS-HC ($CaO-FeO-MgO-Al_2O_3-SiO_2-H_2O-CO_2$) and NKCFMAS-HC ($Na_2O-K_2O-CaO-FeO-MgO-Al_2O_3-SiO_2-H_2O-CO_2$) systems are used to: (i) describe the types and abundance of the CO_2-source rocks (i.e. calc-silicate rocks); (ii) outline the CO_2 producing reactions, and (iii) surmise the amount of CO_2 released through these reactions.

The results obtained confirm that Himalayan calc-silicate rocks may act as CO_2-source during prograde heating, releasing internal-derived CO_2-rich fluids. Different fluid-producing reactions have been identified, involving the growth of: (a) garnet (in CFMAS-HC lithologies), and (b) clinopyroxene, zoisite and K-feldspar (in NKCFMAS-HC lithologies). CO_2 makes up 34-44% and 25-55% molar proportion of fluids in each respective reaction type (Groppo *et al.* 2013; submitted). Depending on whether the metamorphic system behaved as an open or closed system, the CO_2 produced could be released to the atmosphere and thus participate in the global carbon cycle.

Ague, J.J. 2000. Geology, 28, 1123-1126.
Becker, J.A., Bickle, M.J., Galy, A., Holland, T.J.B. 2008. Earth and Planetary Science Letters, 265, 616-629.
Evans, K.A. 2011. Geology, 39, 95-96.
Gaillardet, J., Galy, A. 2008. Science, 320, 1727-1728.
Girault, F., Perrier, F., Crockett, R., Bhattarai, M., Koirala, B.P., France-Lanord, C., Agrinier, P., Ader, M., Fluteau, F., Gréau, C., Moreira, M. 2014. Journal of Geophysical Research, Solid Earth, 119, doi:10.1002/2013JB010301
Groppo, C., Rolfo, F., Castelli, D., Connolly, J.A.D. 2013. Contribution to Mineralogy and Petrology, 166, 1655-1675.
Groppo, C., Rolfo, F., Mosca, P., Castelli, D. submitted. Contribution to Mineralogy and Petrology, submitted.
Kerrick, D.M., Caldeira, K. 1993. Chemical Geology, 108, 201-230.
Mörner, N.A,, Etiope, G. 2002. Global Planetary Change, 33, 185-203.
Perrier, F., Richon, P., Byrdina, S., France-Lanord, C., Rajaure, S., Koirala, B.P., Shrestha, P.L., Gautam, U.P., Tiwari, D.R., Revil, A., Bollinger, L., Contraires, S., Bureau, S., Sapkota, S.N. 2009. Earth and Planetary Science Letters, 278, 198-207.
Rolfo, F., Groppo, C., Mosca, P., Ferrando, S., Costa, E., Kaphle, K.P. 2015. In: Lollino, G. et al. (eds), Engineering Geology for Society and Territory. Springer International Publishing Switzerland, 1, 21-25.
Rolfo, F., Groppo, C., Mosca, P. Italian Journal of Geosciences (In press).

Cretaceous-Tertiary Boundary C, O and Hg Isotope Chemostratigraphy from Northern and Southern Hemispheres, India-Asia collision and Evolution of the Himalaya

V.C. Tewari[1*], A.N. Sial[2]
[1]Scientist (Retd.), Wadia Institute of Himalayan Geology, 33 GMS Road, Dehradun 248001, INDIA
**vinodt1954@yahoo.co.in*
[2]NEG-LABISE, Dept. Geology, UFPE, Recife, BRAZIL

The Cretaceous-Tertiary Boundary (KTB) sections studied from the Northern and Southern Hemispheres for the carbon, oxygen and mercury isotopes include (a) Europe (Stevns Klint, Gubbio,

Padriciano), (b) India (Um Sohryngkew Meghalaya, Jhilmili, Central India), and (c) South America (Bajada del Jagüel, Cabra Corral, Poty Quarry) in Brazil and Argentina. Complete KTB sections display strong negative $\delta^{13}C$ excursions at the KTB, while in near-complete sections, gradual fall of $\delta^{13}C$ values predates the KTB. Volcanogenic CO_2 enrichment of the atmosphere during the KTB transition led to large negative $\delta^{13}C$ excursions. O-isotope signals recorded a warming event predating the KTB, likely related to Deccan phase 2, followed by strong cooling at the KTB, probably related to high amounts of SO_2 released to atmosphere by the Deccan phase 2 and accumulated in the KTB transition. Warming events in the early Danian are, perhaps, related to early eruptions of Deccan phase 3. Almost all sections exhibit three Hg spikes. The one which predates the KTB and the spike that coincides with the KTB layer are likely related to Deccan phase 2. A third spike, probably related to the Deccan phase 3, is present in the early Danian in almost all sections. $\delta^{202}Hg$ values for the KTB layer at Stevns Klint, Gubbio, Um Sohryngkew, Meghalaya and Jagüel Formation (1 to 2‰) lie within the range for volcanogenic Hg. The Indo-Myanmar Orogenic Belt (IMOB) is interpreted as representing the eastern suture of the Indian Plate., which was formed due to the collision of the the Indian Plate with the Myanmar Plate. The Manipur Ophiolite Zone contains diverse fauna, predominantly foraminifera *Globotruncana* sp., *Nummulites* sp., *Bolivina* sp., algae and gastropods indicative of marine environment. The random carbonate limestone samples from different sections have been analysed for the carbon and oxygen isotope analysis for comparison of regional isotopic variation in the eastern Tethys ocean, NE India. $\delta^{13}C$ varies from +0.49 to +2.22‰ (V-PDB) and $\delta^{18}O$ range from -7.14 to -11.19‰ (V-PDB). Northward anti-clockwise movement of India, its collision with Asia, rise of the Himalaya and closure of the Tethys ocean has been discussed.

Paleoglaciations in the Himalaya and future implications

Vinod C. Tewari

Scientist (Retd.), Wadia Institute of Himalayan Geology, 33 GMS Road, Dehradun 248001, INDIA
vinodt1954@yahoo.co.in

The past sea level changes in the geological history of the earth confirm that the climate change, tectonic movements, sedimentation and volcanism are interrelated. The major cooling and warming events of the Himalaya and their relationship with the sea level rise and fall has been studied in detail. Blainian (Marinoan) Neoproterozoic glaciation is a major paleoclimatic change on earth due to the ice albedo. Neoproterozoic or low latitude glaciation record in all the continents indicates equatorial glaciation at sea level (Hoffman 2008; Tewari 2007, 2012, 2013). Pre-Ediacaran Blainian glaciation (Blaini Diamictites) and the pink cap dolostone represents the period of Snow ball earth in the Lesser Himalaya (Tewari 2012, 2013 and the references therein). Post-Ediacarn glaciations such as Ordovician to Silurian times and Carboniferous to Permian (Lower Gondwana) is well recorded in the Tethyan and the Ranjit window in Sikkim, NE Himalaya. During Cambrian and Ordovician through Permian, the sea levels have fluctuated. These variations result in rapid sea level rise after the Permian/Triassic and continued upto Cretaceous-Paleogene. Recent studies have shown that Pre-Mesozoic to Mesozoic and Tertiary earth has suffered extreme warm and cold periods (Histon et al. 2013). The global sea level is rising according to the report of the IPCC (Intergovernmental Panel on Climate Change). Due to the global temperature rise, the sea level may rise even more in future if the present trend of global warming is continued. This is due to the increase in green house gases in the atmosphere. The melting of glaciers is caused by the global warming and the expansion of sea water due to the melting of the Antarctica and Greenland is related to temperature increase.

The beginning of Paleogene is marked by a rapid warming event (Paleocene-Eocene Thermal Maximum or PETM). Global temperature rose to 5°C and this warming continued after the PETM

reaching a maximum in the Eocene about 50 million years ago. This is also recorded in the Paleocene-Eocene carbonates of South Shillong Plateau in Meghalaya, east India (Tewari et al., 2010a,b, and references therein). This green house event was followed by ice-house event around 15 million years ago and ice sheets developed in northern hemisphere. India was moving northwards during this period and the uplift of the Himalaya changed the climate of the region and new vegetation started developing. The paleoceanic and paleocontinental reconstructions suggest that about 300 million years ago India occupied high latitudes and was closer to the south pole (Antarctica). India started moving northward in anti-clockwise direction around 75 million years ago and was a big island. The collision of India with Eurasia formed the Himalaya and the fossil occurrences from the Higher Himalaya indicate about 3000 m uplift from last 12 million years. The evidence of Last Glacial Maxima and Little Ice Age are also well known from the Himalayan lake sediments and cave deposits (speleothems). To conclude, in order to predict the future climate it is interpreted that past-global climate changes have to be properly understood. The recent global climate variations like global warming and melting of the Himalayan glaciers are relevant to the future of the Third Pole (Himalaya-Karakorum-Tibet region) in particular. Past climate studies can help us in understanding the mechanism of future climate change in the Himalaya. The recent GLOF (Glacial Lake Outburst Flood) in Chorabari lake and the subsequent devastating natural disaster occurred in the Kedarnath shrine and downstream areas in the Garhwal Himalaya is an eye opener to understand the mountain meteorology and implications of climate change on Himalayan environment.

Petrology of lawsonite-blueschist facies metasediments from the Western Himalaya (Ladakh, NW India)

Franco Rolfo[1]*, C. Groppo[1], H.K. Sachan[2], S.K. Rai[2]

[1]Department of Earth Sciences, Via Valperga Caluso 35, Torino 10125, ITALY

**franco.rolfo@unito.it*

[2]Wadia Institute of Himalayan Geology, 33 GMS Road, Dehradun 248001, INDIA

High pressure metamorphic rocks are scanty in the Himalayan collisional orogen. Beside rare eclogite (Lombardo & Rolfo, 2000), few blueschist occur along the Yarlung-Tsangpo Suture (ITS), i.e. the suture marking the India-Asia collision. The petrographic features of blueschist-facies lithologies have been described in the western portion of the ITS in Swat, NW Pakistan and in Ladakh, NW India (e.g., Guillot et al., 2008 and references therein). Barring a recent paper on blueschist from the far eastern Himalaya (Ao & Bhowmik, 2014), modern petrologic studies on the relatively more abundant blueschist from the western Himalaya are still lacking.

The best occurrence of blueschist in the western Himalaya is that of the Shergol ophiolitic mélange, which outcrops over a distance of 250 km along the ITS and consists of several thrust slices sandwiched between the Nindam-Naktul-Dras nappe to the north, and the Lamayuru nappe to the south. Blueschist lithologies are heterogeneous and dominated by volcanoclastic sequences rich in mafic material with subordinate interbedding of metasediments. Prior to this study, P-T estimates based on conventional thermobarometry suggested T = 350-420°C and P = 9-11 kbar (Honegger *et al.* 1989).

West of the village of Tringo, blueschist facies metasediments are particularly abundant and suitable for petrologic modeling. They show the typical lawsonite-blueschist (LBS) facies assemblage quartz+phengite+lawsonite+Na-amphibole+garnet. Lawsonite and strongly zoned garnet porphyroblasts overgrow the main foliation defined by high-celadonite phengite (Si $\geq$ 3.83 a.p.f.u.). Petrologic results obtained from pseudosection calculations in the MnNKCFMASH model system constrain peak P-T conditions to 430-470°C, 18-19 kbar, i.e. at significantly higher P than previously estimated. The following exhumation still occurred in the LBS-facies field, allowing the preservation of lawsonite.

Petrologic modeling also suggests a very moderate effect of Fe^{3+} in the system, as well as significant addition of H_2O near peak conditions to allow lawsonite formation. According to the reconstructed P-T evolution, the Shergol blueschists are the result of cold subduction along a very low to low thermal gradient ('early' prograde: ca. 5°C/km; 'late' prograde: ca. 7-8°C/km). Such a low geothermal gradient was followed also during exhumation, in order to preserve lawsonite in the studied lithologies. This P-T evolution is consistent with a mature subduction zone system in an intra-oceanic subduction setting, as also suggested by Ao & Bhowmik (2014) for blueschist from the far eastern Himalaya.

Ao, A., Bhowmik, K. 2014. Journal of Metamorphic Geology, 32, 829-860.
Guillot, S., Mahéo, G., de Sigoyer, J., Hattori, K.H., Pêcher, A. 2008. Tectonophysics, 451, 225-241.
Honegger, K., Le Fort, P., Mascle, G., Zimmerman, J.L. 1989. Journal of Metamorphic Geology, 7, 57-72.
Lombardo, B., Rolfo, F. 2000. Journal of Geodynamics, 30, 37-60.

Uplift and Growth of the northwest Pamir

Rasmus Thiede[1*], Edward Sobel[1], Paolo Ballato[1], Konstanze Stübner[2], Mustafo Gadoev[3], Ilhomjon Oimahmadov[3], Todd Ehlers[2], Manfred Strecker[1]
[1]Potsdam University, Erd- und Umweltwissenschaften, Potsdam-Golm, GERMANY
[*]thiede@geo.uni-potsdam.de
[2]University of Tübingen, Institut für Geowissenschaften, Tübingen, GERMANY
[3]Acad of Science of Republic of Tajikistan, Inst. Geology, Seismology, Dushanbe, TAJIKISTAN

The Pamir is the most prominent active mountainous region within Central Asia, forming the northwestern tail of the Tibetan plateau. Although many of the large-scale tectonic features are now thought to be understood, the details of uplift and orogenic growth in most places are still poorly constrained, but crucial for evaluating first order geodynamic models.

To assess the impact of tectonic uplift on the geomorphic evolution of the plateau, we performed several standard morphometric analyses. In detail, we analyzed local topographic relief, the overall character of the drainage network, fluvial knick points and river concavities. We have also begun measuring Apatite (AHe) and Zircon U-Th-Sm/He (ZHe) as well as apatite fission track ages to obtain the timing of upper crustal cooling related to rock uplift.

Here we focus on the western and northwestern unglaciated margin of the Pamir, Darvaz and Peter-I Range, where we observe key geomorphic characteristics of the fluvial network. Drainage pattern and DEM analysis indicate that the Panj River forms a major base level controlling river network draining the entire central and western margin of the Pamir. Fluvial network constraints indicate that it has been established in the geologic past, has facilitated deep valley incision when crossing Darvaz Range but not been uplifted significantly. Within the Darvaz Range, bounded by the Darvaz fault zone in the northwest and Badakhshan fault zone in the southeast, we discovered extensive low-relief landscapes with gentle, concave longitudinal upstream river profiles. These are interrupted by major knick points and steep downstream segments, draining towards the deeply incised trunk and base level controlling Panj River. Prior to uplift, this landscape was eroded to a low relief landscape, has partly been covered by upper Neogene sediments. Preliminary ZHe and AHe ages indicate that uplift of the Darvaz Range was underway by 15 Ma and may have accelerated since then. We suggest that (1) the western flank of the Pamir has had surface uplifted on the order of 1 to 2 km starting sometime during the middle Miocene; (2) the internal portion of the western Pamir has facilitated deep valley incision during late Cenozoic and base level of the major Panj drainage has maintain at its low elevation.

Tectonic deformation zones across the Himalaya of northwest India

Rasmus C. Thiede[1*], Johannes Faruhn[1], Saptarshi Dey[1], Marcus Nennewitz[1], Bodo Bookhagen[1], Vikrant Jain[2], Manfred Strecker[1]

[1]Potsdam University, Department for Earth- and Environmental Science, Potsdam, GERMANY

[*]thiede@geo.uni-potsdam.de

[2]IIT-Gandhinagar, Ahmedabad, INDIA

The Himalaya is the most prominent active mountain range, forming the southern margin of the world's largest orogenic plateau. Although the large-scale features of this active orogenic wedge are now thought to be understood, the details of seismotectonic behavior in most places are still poorly constrained, but crucial, for instance, for any geo-hazard evaluation. The precise rates of crustal shortening, their changes through time, and the spatial distribution of active deformation across the orogenic domains are often unknown. For instance, it is unclear whether the range thickens homogenously as a result of contemporaneous thrusting on many faults or whether it is localized on major range-bounding thrust fault zones, where deformation is localized. For the past decades, several Himalayan research groups favoured that active deformation and crustal shortening dominantly accommodated along the toe of the wedge (e.g., Yeats and Lillie, 1991; Raiverman et al., 1994, Powers et al., 1998; Lave and Avouac, 2000). In this context, it has been proposed that the Main Frontal Thrust (MFT) forms the direct surface expression of the Main Himalayan Thrust (MHT), which is commonly considered to be the main basal detachment and decoupling horizon between the under-thrusting Indian craton and Himalayan wedge.

Recent advances in Nepal, using Geodetic, InSAR, Seismicity, and geomorphic landscape analysis, combined with low temperature chronology have identified three first-order active deformation zones within orogenic wedge (Grandin et al., 2012; Jackson and Bilham, 1994; Pandey et al., 1995; Wobus et al., 2003; Herman et al., 2010; Harvey et al., 2015); in addition to (a) the known deformation accommodated within the here narrow Sub-Himalaya belt, (b) uplift is proposed in the hanging wall of the Main Boundary Thrust (MBT) (e.g., Lave and Avouac, 2001) or related faults bounding southern margin of Lesser Himalaya, as well as the growth of the Lesser Himalayan duplex bounding the southern margin of High Himalaya (Cattin & Avouac, 2001; DeCelles et al., 2001, Robinson et al., 2003; Lang et al., 2010), by detaching Indian cover units and integrating these in orogenic wedge in the vicinity of major time transient flat-ramp-flat structure along the MHT (e.g., Bollinger et al., 2004; Robert et al., 2012).

Due to the northward bend of the Himalayan arc in the northwestern India, the convergence between the underthrusting India and Himalayan wedge is oriented obliquely. This geometric setting provides a unique opportunity to study deformation patterns within the wedge and detect important differences to the arc-perpendicular convergence.

Our key tectonic observations are as follows:

Segments of the MFT grow arc-parallel in contrast to the strongly undulating trend of the MBT resulting in a strongly curved topographic front characterized by re-entrants and pronounced salients, such as the Kangra and Dehra Dun Re-entrant as well as the Nahan Salient. Consequently the width of the Sub-Himalaya changes strongly along strike and does not follow the curved trend of the MBT. This deformation pattern demonstrates that MBT and MFT developed independently from each other and that deformation within Sub-Himalaya is decoupled from growth of Himalayan wedge.

In contrast to the deformation pattern observed in central Nepal, the western Himalaya shows that the majority of Holocene shorting is accommodated along the out-of-sequence Jwalamukhi-Thrust (JMT) within the center of Kangra-Re-Entrant. The Jwalamukhi Thrust is located in the

center of the Sub-Himalaya and probably only minor parts of the total shortening is accommodated along the MFT during the Holocene (Saptarshi et al., submitted).

We observed top-to-west thrust ramps that are uplifting early Tertiary Subathu and Dhramsala formation along the eastern margin of the Kangra-Re-Entrent and within the footwall of the here north-south trending segment of the MBT. This is supported by recent observations of GPS measurements and topographic relief analysis (Bannerjee and Bürgmann, 2002; Malik et al., 2007; Kundo et al., 2014). This pattern of deformation strongly suggest that the Sub-Himalaya is more strongly connected and effected by the under-thrusting of India rather than triggered by deformation of the Himalayan wedge, behaving here as regit indentor.

Along the southern margin of High Himalaya a time transient flat-ramp-flat structure along the MHT trigger underplating and extent of the internal growth of LH-duplex. The lateral extent of this duplex is recognized by high exhumation rates derived from spatial distribution of young low temperature chronology data and geomorphic landscape analysis (e.g., Thiede et al., 2009; Morell et al., 2015). This has been well documented eastern extent of Kulu-Jari-Rampur Window, where a continous zone of rapid exhumation run into Gharwal and Kumaun Himalaya, exposed along southern flanks of High Himalaya.

In contrast new and previously published low temperature transects (Deeken et al., 2011) across the Dhauladar Range, further to the west, indicate continuous uplift and fault displacement with rates in the range of 1-2 mm/yr along the MBT-fault zone hanging wall bounding the Kangra-Re-Entrant in the north since the late Miocene. Interestingly, in this segment a flat-ramp-flat geometry within the MHT has not been recognized (Deeken et al., 2011). This is in contrast to the Kinnauer, Gharwal and Kumaun areas further east. We suggest that the Beas River valley forms the boundary between these segments.

In summary all above observations provide a key for understanding the location of the main decoupling horizon and where strain is accommodated between the under thrusting Indian units and the Himalayan wedge. Therefore, we would suggest that the MBT is directly linked with the MHT forming the basal detachment horizon rather than the MFT, as it is usually proposed.

Back structures (back-faults and back-folds) from collisional orogen: field findings from Lesser Himalaya, Sikkim, India

Narayan Bose*, Soumyajit Mukherjee
Department of Earth Sciences, IIT Bombay, Powai, Mumbai 400076, Maharashtra, India
**narayan.bghs@gmail.com*

Back structures (back folds and back shears) with hinterland-ward vergence have been reported from several collisional orogens. Recognition of back structures is important in tectonics, resource, and earthquake studies. Back structures have so far been reported in mesoscale from Greater Himalayan Crystallines (Mukherjee, 2013) and Lesser Himalaya (Bose and Mukherjee, 2015) from Bhagirathi river section, western Himalaya, India. Our fieldwork in the Paleoproterozoic phyllites, quartzites of Daling Group (Lesser Himalaya, Sikkim, India) revealed brittle back shears of both top-to-N/NE (up) back-reverse and top-to-N/NE (down) back-normal faults at three zones (BSZA, BSZB, BSZC). No secondary brittle shear zones, neither R1 nor R2, were found associated with these zones. The BSZA is extremely well developed ~3 km N to Damthang, where the Daling Group quartzites contain brittle back shear Y-planes with up to 5 cm thick fault gouge. Here the back shear Y-planes clearly cut the fore-shear Y-planes indicating the back shear post-dated the top-to-S/SW fore-shears. Geochronologic dating of fault gouge can constrain the absolute timing of back deformation. The fault gouge within the Y-planes of back shear sometimes contains faint P-planes of same back shear sense. The Y-planes are at places sub-horizontal and

dip moderately elsewhere. The BSZB near Singtam shows back shears in the form of brittle P-planes bound by Y-planes, and a single meter-scale overturned-isoclinal synformal back fold with ~ENE dipping limbs and axial plane. At places, ductile shear indicators S-planes bound by C-planes were found parallel to P- and Y-planes, respectively. Thus back thrusting that initiated in the ductile regime probably continued in the same sense in the brittle regime. The BSZC is well exposed from W of the village Kyongsa (near Geyzing) up to a nearby 'Farm Science Centre'. Top-to-NE (up) back shears were observed in this location in terms of Y- and P-planes in schistose rocks, quartz sigmoids and few back folded quartz veins. Whether BSZA, BSZB and BSZC constitute a single back-thrust zone remains indeterminate. Other than BSZA, BSZB and BSZC, back shears are present in the Lesser Himalaya in Sikkim but are less ubiqutous. Only at two locations between Ravangla and Tarek, back shears were observed in cm-scale sheared quartz veins. This work along with the previous reports of back shear (Mukherjee, 2013; Bose and Mukherjee, 2015) indicates plausibly such structures are more common in the Himalaya. Presence of back structures probably connotes a critical taper mechanism of deformation.

Mukherjee, S 2013. International Journal of Earth Sciences, 102, 1851-1870.
Bose, N., Mukherjee, S. 2015. Tectonic Studies Group.

Depositional scenario and climate variability during the late Quaternary in the Tangtse Valley, Ladakh, Trans-Himalaya, India

Randheer Singh*, Binita Phartiyal
Birbal Sahni Institute of Palaeobotany, Lucknow 226007, INDIA
**randheer.singh@gmail.com*

The Tangtse River Valley (Ladakh) in the Trans-Himalayan range is a cold and arid desert due to strong influence of westerlies. In this area, the strike-slip Karakoram Fault (KKF) bifurcates into two strands viz., the SW Tangtse Strand and the NE Pangong Strand (Rutter, 2007). To the east of the valley Pangong Tso, the longest lake in Ladakh, shows high and distinct palaeo-strandlines giving clues about the wider extent of the lake area in the past. During this high lake level, the valley has served as a spillway for the Pangong Tso, therefore flooding and damming the entire Tangtse Valley, resulting in the formation of a lake. Presence of various features like strath terraces (26 m), offset of streams (200-400 m), wide valley filled with debris flow, fault scarps, debris cones, river toe cutting, abandoned channels, gorges and straight river course with the swirls, expresses the neotectonic activity in the area. Varied sedimentary architecture with fluvial episodes intervened by the lacustrine pulses, flood events, colluvial and glacial activity are preserved. Documentation based on 14 Carbon (AMS) and OSL chronologies of the sediment sections (lacustrine and fluvial) throughout the valley was done (Phartiyal *et al.*, 2015).

A fluvial depositional environment existed in the valley around 48 ka and 30-21 ka, a period marked with comparatively arid conditions with cold and dry climate interspersed by flooding. The valley has been incised to depths of 40-50 m in the upper part. Much of the incision took place between 22 and 9.6 ka to ~130 m in the lower part. Aggradation (sediment fill) occurred from 9.6-5.1 ka followed by another incision phase of ~5 m with varying incision rates in different stretches of the Tangtse Valley. The incision rate ranges from 0.3 to 1.2 mm yr^{-1} in the upper part and reaches as high as 10.8 mm yr^{-1} in the lower valley.

Strong evidence reveals the presence of a lake with ~50 km extent, between ~9.6 and 5.1 ka occupying the present day Tangtse Valley as the sixth basin of Pangong Tso towards the west. This event of wet and warm conditions coincides with periods of high lake levels in Tibet, China and as well as intensified monsoon periods over the Indian subcontinent. Lacustrine deposits comprising buff coloured clay, silt and alternating sand facies association were recorded on both valley walls in a continuous

strandline varying between ~40-50 m levels from the present day river. Typical lacustrine facies and flood facies are exposed below the Shachukul village. In the Shachukul-Taruk site four sections were studied for their climatic history using environmental magnetism and loss on ignition as proxies.

Increased catchment weathering and enhanced concentration of detritus input led to an increased Magnetic Susceptibility (MS), susceptibility of Anhysteretic Remanent Magnetization (ARM) and Saturated Isothermal Remanent Mangetization (SIRM) those reflect a colder phase. During warm periods, on the other hand, due to deposition of fine sediments values of MS, susceptibility of ARM and SIRM reduced in this high altitude cold desert region. The variations in the studied parameters divide the lacustrine span into 4 zones (Z1-Z4). The ~20 to ~16 ka (Z1), ~7.2 to ~6.7 ka (Z3) and ~6.7 to ~5.1 ka (Z4) shows a shift towards cold climate conditions. The set up of Z1 is synchronous to LGM period with peak around 18 ka. Zone 4 is much colder than that of Z3 and having short, but intense cold phases. A stable lake condition with a warm climate record is seen in ~16 to ~7.2 ka (Z2) corresponding to well known enhancement of Indian monsoon (15.2 ka) and climate amelioration. LOI data shows a trough whereas MS, susceptibility of ARM and SIRM values an enhancement around 8 ka may be the signature of the prominent cold excursion 8.2 ka event in warm Holocene.

A 9.7 m thick (flood facies) displays the characteristics of a natural levee unit. This is a younger horizon depicting a later flood event (~3 ka). This section consists of intermittent clay and sand having cross bedded sand, slity sand layers. In this section at ~3 m level, an 80 cm horizon of sand with well-preserved accumulation of sub fossils was observed. The recovered wood and bone fragments reveal an age of 3140±35 ^{14}C yr BP and 3400±40 ^{14}C yr BP respectively. The preservation of soft tissue in this assemblage points to a quick burial which was likely a result of a short term flood event. In section, majority of the pronounced peaks in MS positively correlate with the susceptibility of ARM indicating predominance of Single Domain (SD) magnetite. The authigenic SD magnetite indicate less oxygenated water condition for a short while due to the turbid water of flood event in flood facies section. High magnetic susceptibility indicates high ferromagnetic content.

Phartiyal, B., Singh, R., Kothyari, G.C. 2015. Palaeogeography, Palaeoclimatology, Palaeoecology, 422, 11-24.
Rutter, E.H., Faulkner, D.R., Brodie, K.H., Phillips, R.J., Serale, M.P. 2007. Journal of Structural Geology, 29, 1315-1326.

Modelling the Crust beneath the Kashmir valley in North-western Himalaya

Ramees R. Mir[1,2,*], Imtiyaz A. Parvez[1,2], Vinod K. Gaur[1], Ashish[1], R. Chandra[3], Shakil A. Romshoo[3]

[1]*Academy of Scientific and Innovative Research (AcSIR), CSIR-Fourth Paradigm Institute Campus, Bangalore, INDIA*

**ramizmir752@gmail.com*

[2]*CSIR-4PI (erstwhile CSIR-CMMACS), Bangalore 560037, INDIA*

[3]*Department of Earth Sciences, University of Kashmir, Srinagar 190006, INDIA*

We investigate the crustal structure beneath five broadband seismic stations in the NW-SE trending oval shaped Kashmir valley sandwiched between the Zanskar and the Pir Panjal ranges of the northwestern Himalaya. Three of these sites were located along the southwestern edge of the valley and the other two adjoined the southeastern. Receiver Functions (RFs) at these sites were calculated using the iterative time domain deconvolution method and jointly inverted with surface wave dispersion data to estimate the shear wave velocity structure beneath each station. To further test the results of inversion, we applied forward modelling by dividing the crust beneath each station into 4-6 homogeneous, isotropic layers. Moho depths were separately calculated at different piercing points from the inversion of only a few stacked receiver functions of high quality around each piercing point.

These uncertainties were further reduced to ±2 km by trial forward modeling as Moho depths were varied over a range of ±6 km in steps of 2 km and the synthetic receiver functions matched with the inverted ones. The final values were also found to be close to those independently estimated using the H-K stacks. The Moho depths on the eastern edge of the valley and at piercing points in its southwestern half are close to 55 km, but increase to about 58 km on the eastern edge, suggesting that here, as in the central and Nepal Himalaya, the Indian plate dips northeastwards beneath the Himalaya. We also calculated the Vp/V_s ratio beneath these 5 stations which were found to lie between 1.70 and 1.76, yielding a Poisson's ratio of ~0.25 which is characteristic of a felsic composition.

Late Cenozoic Records of the River System of Northwestrn Himalaya

Rohtash Kumar
Scientist (Retd.), Wadia Institute of Himalayan Geology, 33 GMS Road, Dehradun 248001, INDIA
rohtashgpt@gmail.com

Late Cenozoic fluvial stratigraphic records of the Himalayan foreland basin (HFB) represented by Siwalik and post-Siwalik deposits, were studied to understand the river response to allogenic forcing at variable time scale. The Siwaliks in the Indian domain initiated around 13 Ma and terminated around 0.2 Ma due to tectonic deformation along the Himalayan Frontal Trust (HFT). Fluvial architecture and associated facies suggest deposition far away from the mountain front which gradually migrates toward basin around 5 Ma with no bounding frontal thrust (similar to present Ganga basin). The Siwaliks initiated with fine-grained facies, but during the Middle Siwalik time (around 10 Ma) the fluvial architecture reveals that large river systems were evolved. The continued tectonic deformation due to northward migration of the Indian plate, the Himalayan mountain front gradually shifted southward, and large gravelly alluvial fans were deposited in the proximity of the basin margin around 5 Ma (Upper Siwalik). These deposits neither indicate major incision nor formation of paleo-valleys, therefore indicating either balance in sediment flux and basin subsidence or their signatures are not visible due to identical lithologies. Noteworthy influx of boulder to pebble size clasts indicate major surface uplift at around 5 Ma all along the Himalaya mountain front (i.e., MBT) rather than a response to a more erosive climate since the onset of north Hemispheric Glaciation. This uplift is more widespread and is responsible for the generation of much of the modern drainage system. This fluvial architecture reveals variation in temporal and spatial deposition style at million year scale. However, direct climatic signatures are not evident, although stable isotope geochemistry suggests variability at million year scale.

Facies character in the Siwalik rocks in the Lish River section, Darjeeling District, West Bengal, India: depositional environment and palaeogeography

Suchana Taral
Geological Studies Unit, Indian Statistical Institute, 203 B. T. Road, Kollkata 700108, INDIA
suchanataral100@gmail.com

About 1.5 km thick succession of Siwalik rocks exposed in the Lish River section in the foothills of Darjeeling Himalaya has been studied in detail to examine the sedimentological attributes of the deposits. Seven facies recognised in the succession are: (F1) massive to stratified conglomerate; (F2) Cross-stratified medium to coarse-grained sandstone; (F3) Low-angle cross-stratified very fine- to medium-grained sandstone; (F4) Hummocky and swaley stratified sandstone (F5) Wave or combined flow ripple laminated fine sandstone-siltstone; (F6) Laminated dark grey mudstone with

rippled sandstone-siltstone layer; (F7) Fractured grey to brown mottled mudstone. Based on their preferred occurrences, geometry and palaeocurrent pattern, these facies can be grouped into four facies association representing: (FA1) Conglomeratic sandstone of braided rivers, displaying a dominantly southward transport; (FA2) Erosively-based multi-storey coarse-grained sandstone complex showing a dominantly southward flow representing large distributary channels; and (FA3) generally flat-based, low-angle laminated to wave rippled, very fine- to medium-grained sandstone showing a highly variable and complex palaeocurrent pattern representing delta mouth bar and terminal distributary channel complex; (FA4) Grey mudstone with interlayered thin sandstone beds, locally with gleyed palaeosols, root traces and coaly beds inferred to represent interdistributary bay fill deposits. The deposits show occurrence of stacked, 12-20 m thick coarsening-upward units, typical of prograding deltaic succession.

In the western Himalaya, Siwalik succession has been typically inferred to represent a fluvial deposit resembling the Kosi-like large megafans of proximal Ganga plain. Siwalik rocks of the Tista Valley, eastern Himalaya have some important differences with those of the western Himalaya: (i) the red mudstone and calcareous palaeosols typical of western Himalaya are completely absent in the eastern Himalaya. In contrast, grey mudstone, gleyed palaeosols and coaly beds are common in eastern Himalaya. (ii) Abundant vertebrate fossils reported from the western Himalayan Siwalik succession are absent in the eastern Himalaya and in contrast marine trace fossils like *Rosselia*, *Rhizocorallium Ophiomorpha* and *Chondrites* are common. A rich palynotaxa indicating brackish water influence has been reported together with occurrences of foraminifers. (iii) In western Himalaya, most of the sandstone units form fining upward succession and a unimodal palaeocurrent pattern typical of fluvial sandstones, whereas many sandstone bodies in the Tista valley form coarsening upward succession with abundant wave-generated structures and polymodal palaeocurrent pattern, typical of shallow marine environment. Whereas a large number of transverse alluvial system has been documented from the western and central Himalaya, a marginal marine basin or a large lake has not been documented posing a problem for basin-wide palaeogeographic reconstruction. Documentation of shallow marine and deltaic depositional environment in the Siwalik succession therefore much better explains the regional palaeogeographic setting of the Siwalik foreland basin.

High resolution climatic changes through Pleistocene-Holocene transition in Northwest Indian Himalaya by using speleothems

Bahadur Singh Kotlia[1], Anoop Kumar Singh[1], Jaishri Sanwal[2], Syed Masood Ahmad[3], Lalit Mohan Joshi[1]

[1]Centre of Advanced Study in Geology, Kumaun University, Nainital 263002, INDIA
[2]Geodynamics Unit, Jawaharlal Nehru Centre for Advanced Scientific Research, Bangalore 560064, INDIA
[3]CSIR-National Geophysical Research Institute, Uppal Road, Hyderabad 500 007, INDIA

A high resolution $\delta^{18}O$ and $\delta^{13}C$ record from a U-Th dated stalagmite from Kalakot Cave (33°13'19" N : 74°25'33" E; Alt. 826 m) located in Rajouri Distt, Jammu and Kashmir Himalaya reflects variation in the amount of monsoon precipitation for the periods of Pleistocene-Holocene transition. This foremost record of the stalagmite based high resolution climatic changes from NW Himalaya between ca. 16.3-9.5 ka BP is presented using a suite of proxies, e.g., mineralogy, U/Th dating, growth rate, $\delta^{18}O$ and $\delta^{13}C$ variations. The ages, obtained by U/Th dating and linear interpolation show consistency despite large errors due to lesser amount of Uranium in the samples. The results reflect the effect of Indian Summer Monsoon (ISM) and Westerlies. The $\delta^{18}O$ and $\delta^{13}C$ values range from -5.41 to -8.82‰ and -7.09 to -10.84‰, respectively. The Hendy test results suggest that the

stalagmite was formed in isotopic equilibrium. The growth rate is ca. 23-47 μm/year with fluctuations. During a few multi-century events (e.g., ca. 14.5-14.2, 12.8-12.5, 11.0-10.8, 9.8-9.6 ka BP), the growth was comparatively slower which can be well correlated with the enriched $\delta^{18}O$ and $\delta^{13}C$ values. In general, five stages of the climate pattern are suggested with three global events, e.g., Older Dryas (OD), Allerød period and Younger Drays (YD) at ca. 14.3-13.9, 13.9-12.7 and 12.7-12.2 ka BP. The precipitation strength was weaker during the OD and YD, but was stronger during the Allerød interstadial. We suggest that the Late Pleistocene-Holocene records from the locations influenced by the ISM and Westerlies reveal variations from those sites dominated only by the ISM. Since the time interval of multi-century scale events has been found different in various parts of globe, we believe that the variation in their commencement, duration and termination can be attributed to the latitude location, response time and temporal resolution.

The Performance of RegCM with Different Convective Parameterization Schemes in North Pakistan Himalaya Region

Bushra Khalid*[1, 2], Pir Shaukat Ali[3, 4]

[1]*ICCES, Institute of Atmospheric Physics, Chinese Academy of Sciences, Beijing 100029, CHINA*

[2]*Department of Environmental Sciences, International Islamic University, Islamabad 46000, PAKISTAN*

**kh_bushra@yahoo.com*

[3] *Global Change Impact Studies Center, Islamabad 46000, PAKISTAN*

[4]*Institute of Atmospheric Physics, Chinese Academy of Sciences, Beijing 100029, CHINA*

Regional Climate Models (RegCM) are one of the most important tools that are used in the development of present/future climate projections and impact studies. The realistic simulation of RCMs and its suitable use in impact studies greatly depends on the validation, configuration, and integration of different models and processes (i.e. hydrology, oceanology, energy, and ecology) (Giorgi and Francisco, 2000; Sylla et al., 2010). In the last few decades a lot of effort has been made for improved simulation of regional climates but it still involves certain issues. These issues include the selection of an appropriate Convective Precipitation Scheme (CPS) and the bias correction for different regions which greatly depends on the performance of these schemes (Pal et al., 2007). Hence, this study is conducted to explore the performance of different schemes under coupled and uncoupled RCMs with Ocean Model for East/South Asia region. Different schemes under RCM are integrated and validated for East/South Asia region after dividing it in three sub regions as Huang-Huai-Hai (3H), Tibetan Plateau (TP), and North Pakistan (NP). The output of RegCMs is used as input to the University of British Columbia (UBC) hydrological model in offline mode for the future climatic changes and to explore the performance of two-way coupling of RegCMs with Ocean Model for the period of 2041-2050 and 2071-2080. To explore the coupled setup of RegCM and MITGCM, RegCM is run independently (uncoupled mode) and concurrently (coupled mode) with MITGCM. Results show that RegCM is able to properly reproduce the circulation of East/South Asian monsoon. The performance of the model is highly affected by the CPSs and greatly influenced by region and seasonality. Over Western Ghats, Bay of Bengal, and southeast of China, Grell scheme exhibited the least Root Mean Square Error (RMSE) values as compared to the observed data. Over Huang-Huai-Hai (3H), Tibetan Plateau (TP), and most part of China, Tiedtke scheme simulated summer precipitation with higher correlation (0.6-0.85). However, none of the CPSs is able to capture the seasonal variation over North Pakistan (NP). The RegCM's data biases were corrected before using as input to calibrated UBC model. Projections of future climatic change show increased air temperature and precipitation by 1.8°C and 14% for 2041-2050 and 4.3°C and 23% in 2071-2080 respectively. The results of RegCM show the increased temperature during spring and winter as compared to summer season. The regions of higher latitude show more increase in precipitation and temperature than lower

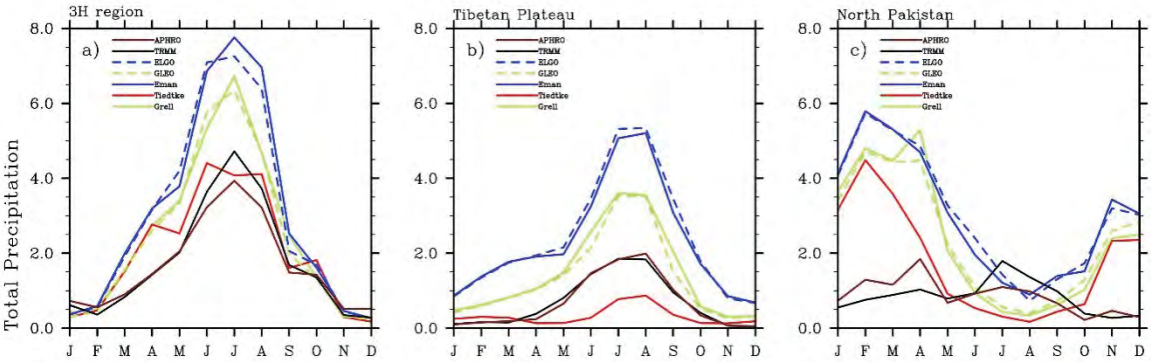

Fig. 1. 1998-2002 average monthly precipitation (mm day-1) using Tiedtke, Grell, Emanuel, GLEO and ELGO convective schemes and in APHRODITE, TRMM data over 3H (a), TP (b) and NP (c) sub-regions.

Table: *Seasonal root mean square error (RMSE) for precipitation and temperature over 3H region, North Pakistan and Tibetan Plateau (Italic bold with less RMSE value for each season).*

		Precipitation				Temperature			
	CPSs	MAM	JJA	SON	DJF	MAM	JJA	SON	DJF
3H region	Tiedtke	1.07	1.09	0.51	0.34	0.78	2.08	1.26	2.73
	Grell	1.25	1.94	0.59	0.30	1.66	1.94	1.49	2.58
	Emanuel	1.68	3.50	0.75	0.38	1.19	0.88	1.02	2.49
	GLEO	1.18	2.19	0.49	0.36	1.55	1.24	1.53	3.12
	ELGO	1.79	3.62	0.72	0.37	1.18	0.82	1.01	2.49
North Pakistan	Tiedtke	1.85	1.17	0.85	3.35	6.34	4.97	5.97	6.29
	Grell	3.44	1.09	1.03	3.72	7.57	8.22	7.72	6.40
	Emanuel	3.74	0.99	1.72	4.41	7.20	7.03	7.35	6.32
	GLEO	3.19	1.02	1.20	3.72	7.68	8.34	8.06	6.87
	ELGO	3.85	0.92	1.68	4.36	7.31	7.19	7.55	6.35
Tibetan Plateau	Tiedtke	0.53	1.28	0.46	0.37	2.20	3.06	1.87	4.03
	Grell	0.87	1.91	0.61	0.54	4.06	2.79	2.19	4.23
	Emanuel	1.52	3.37	1.69	1.00	4.19	2.22	2.33	4.79
	GLEO	0.83	1.83	0.50	0.50	4.26	2.92	2.71	4.86
	ELGO	1.59	3.64	1.81	0.97	4.34	2.28	2.56	4.79

latitudes. Future runoff is projected to increase by 36% in 2041-2050 and 56% for 2071-2080 in summer season. Moreover, the rate of increased temperature is high during 2041-2050 while relatively low in 2071-2080. The results of both coupled (RegCM and MITGCM with BATs and CLM) and uncoupled approaches were also compared and preliminary results were obtained for the Mediterranean region. It is found that generally the coupled results are poorer and show more biasness when compared with observed data. Further work is required in future for the substantial refinement of coupling approach for the realistic simulations of RegCMs for different regions.

Giorgi, F., Francisco, R. 2000. Geophysical Research Letters, 27, 1295-1298.
Pal, J.S., Giorgi, F., Bi, X., Elguindi, N., Solmon, F., Rauscher, S.A., Steiner, A.L. 2007. Bulletin of the American Meteorological Society, 88, 1395-1409.
Sylla, M.B., Coppola, E., Mariotti, L., Giorgi, F., Ruti, P.M., Dell'Aquila, A., Bi, X. 2010. Climate Dynamics, 35, 231-247.

Climatic and tectonic scenario during Holocene in Ladakh, western Tibetan Plateau

Binita Phartiyal*, Anupam Sharma, Debarati Nag
Birbal Sahni Institute of Palaeobotany, Lucknow 226007, INDIA
**binitaphartiyal@gmail.com*

The spatial and temporal setting of the Spituk palaeolake, along the Indus River, in Trans-Himalayan fringe of Western Tibetan Plateau, was analyzed for palaeoclimate reconstruction and tectonics during the Holocene, using geomorphic, sedimentological, mineralogical, mineral magnetic and geochemical proxies as the lake records count for one of the best archive to record high resolution climatic data from the terrestrial regime. This region is a cold arid high altitude dessert and is dominated by the western disturbances. The Indian Summer Monsoon (ISM) effect in the area is only seen in periods of strengthened monsoons, which penetrates into the Himalayan barrier due to the northward shift of the ITCZ (Bookhagen et al., 2005). The AMS and OSL chronologies bracket the lake record from 10800-1000 yr BP. Seismic activity is recorded at 10800-10400; 9400; ~6600-6400; and 5900 and 5600 yr BP by the presence of multiple layers of seismites. The extent of this lake was ~65-70 km covering an area of 235 sq km with good exposures at Spituk (~3213 m), Gupuk (~3225 m) and Jingshan sites (~3240 m) along with several smaller scattered on both banks of the River Indus. This lake was formed after the Younger Dryas by blocking of river by precipitation induced debris flow and seismicity. Two lacustrine phases (~9000-7200 and 5900-3000 yr BP) show stable lake conditions occupying the whole valley and have a synchronous relationship between the highest variation in monsoon intensity; high $\delta^{18}O$ values in the Guliya core, rise in temperature and high solar insolation with the older phase indicative of warmer and humid conditions resulting from the ISM for the sustenance of this lake while the younger lake phase can be seen as contribution of the westerlies. Arid, cold stages are seen prior to and between these two lake phases intercalated with shorter pulses of detrial input also at ~11200, 9800, 8300-7900, 6000 1000 yr BP during the entire span.

Bookhagen, B., Thiede, R.C., Strecker, M.R. 2005. Geology, 33, 149-152.

Late Quaternary tectonics and fluvial aggradation in monsoon dominated Saryu River valley: Central Kumaun Himalaya

Girish Ch. Kothyari[1*], Khayingshing Luirei[2]
[1]Institute of Seismological Research, Raisan, Gandhinagar 382009, INDIA
[2]Wadia Institute of Himalayan Geology, 33 GMS Road, Dehradun 248001, INDIA

The present study has been carried out with special emphasis on the aggradational landforms to explain the spatial and temporal variability in phases of aggradation/incision in response to climate changes and tectonic activity during the Late Quaternary in the Saryu River valley in Central Kumaun Himalaya. The valley has preserved, (a) Cut-and-fill terraces (FT) with thick alluvial cover, (b) Debris flow terraces (DFT), and (c) bedrock strath terraces with thick fluvial cover (FST). Morphostratigraphy of the terraces reveals that the oldest landforms preserved south of the Main Central Thrust (MCT) are

fluvial deposits reworked by debris flow developed between 32-49 ka in the middle to late part of Marine Isotopic Stage (MIS-3). Major phase of valley fill aggradation is dated to be between 11 ka and 26 ka. This event corresponds to the intensified Indian Summer Monsoon (ISM). Following this, a period of accelerated incision/erosion owing to an increase in uplift rate and more intense rainfall occurred as evident from strath terraces. The last phase of fluvial aggradation was regionally extensive and corresponds to the strengthening of the early Holocene ISM. A gradual decline in the monsoon strength between 10 to 5 ka resulted in reduced fluvial discharge and lower sediment transport capacity of the Saryu River, leading to incision of the fill sediments and the underlying bedrock, leading to the development of strath terraces. The study suggests that fluvial dynamics in the Saryu valley were modulated by monsoon variability during the time of sediment deposition and background tectonics, provides post-deposition modification of the landforms. Six major phases of bedrock incision have been estimated during 50 ka (3 mm/yr in MCT zone), 32 ka (0.43 mm/yr in BT zone), 16 ka (0.75 mm/yr in AT zone), 12 ka (1.3 mm/yr in BJT zone), 8 ka (5.38 mm/yr) and around 5 ka (2.1 mm/yr in NAT zone). We postulate that between 9-5 ka the terrain witnessed relatively enhanced surface uplift (2-5 mm/yr).

1D Velocity structure of the Garhwal-Kumaun Himalaya

Sanjay S. Negi[1], Ajay Paul[1], P. Mahesh[2]

[1]Wadia Institute of Himalayan Geology, 33 GMS Road, Dehradun 248001, INDIA

[2]Institute of Seismological Research, Gandhinagar 382009, INDIA

The Himalaya, subjected to be one of the most seismically active terrain, elucidates many large to great earthquakes viz., the 1803 (Kumaon), the 1833 (Kathmandu), the 1897 (Shillong), the 1905 (Kangra), the 1934 (Bihar/Nepal), the 1950 (Assam), and the recent 2015 (Nepal) earthquake. The occurrence of these earthquakes, which are potentially significant in terms of seismic hazard could possibly be affected by the regional tectonics (Robinson et al., 2006). However, this necessitates a high-precision earthquake location which is a paramount pre-requisite for precise seismotectonic interpretation and seismic hazard assessment.

In order to precisely monitor the seismic activity and to improve local earthquake locations we estimate the 1D velocity structure of Garhwal-Kumaun Himalaya by utilizing 368 well located earthquakes, recorded by 14 broad band stations in permanent mode. The events have $rms_{av} \leq 0.8$ secs and azimuthal gap $\leq 200^{o}$, with minimum five or more P- and S-phase readings. For the travel time inversion, 2075 P wave arrival and 2074 S wave arrivals have been used. We use VELEST routine program (Kissling et al., 1994) to simultaneously invert for earthquake locations and to obtain optimum 1D-velocity structure.

Mahesh et al. (2013) limited their velocity structure study to 20 km depth. In the present work, an attempt has been made to further extend the understanding of the deeper crustal structure. The initial observation indicates that nearly 87% of the hypocenter locations are confined to the depths of 20 km, while the remaining 13% lies between 20 and 50 km. The stable and representative Vp/Vs ratio of 1.73 was obtained by using the Wadati plot.

The preliminary velocity model has been obtained using the travel time plot, where we estimated three linear trends with crossover distances at 159 and 198 km. The slopes or the slowness of the regression were used to obtain the velocities for Pg, P*, and Pn. This method provides the three layer model with the thickness of upper and the lower crust as 20 and 26 km. The travel-time-distance method provides a subtle understanding of the Moho depth approximated at ~46 km.

We inverted several initial models, parameterizing the upper crust with 3 km layer thickness and the lower crust by 4 to 6 km. The initial velocity models considered for inversion are from the

Depth (km)	Vp(km/s)	Vs(km/s)
0	5.83	3.21
3	5.84	3.38
5	5.85	3.41
20	6.25	3.57
27	6.45	3.74

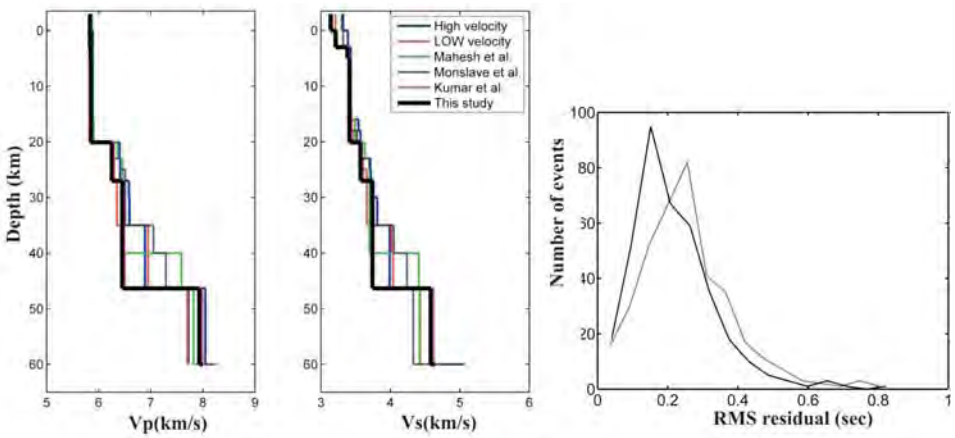

Fig. 1. The final velocity model for a) P wave (dark black line), and b) S wave (dark black line); where the colored lines are the various other models considered for inversion, **c)** The improved rms residual (solid dark line) and the initial rms (dashed lines) for the considered earthquakes in the study region.

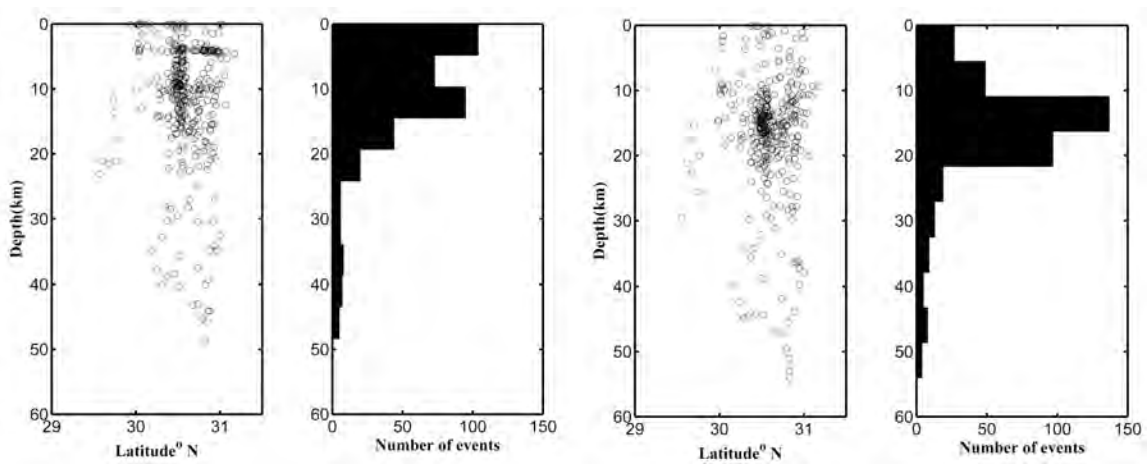

Fig. 2. The earthquake distribution plots a) For initial hypocentral locations (depth vs latitude (left) and depth vs number of earthquakes (right)); b) For final hypocentral locations (depth vs latitude (left) and depth vs number of earthquakes (right)).

Kumaun and Garhwal Himalaya (Mahesh et al., 2013), Kangra-Chamba region (Kumar et al., 2009), Nepal Himalaya (Monsalve et al., 2006) and travel-time-distance curve method from this study. The velocity-depth inversion result shows the minimum of 0.236 rms corresponding to the velocity estimates from travel-time-distance method.

We estimate a 4 layer optimum 1D velocity model for the region (Table 1) where, the moho depth we consider is calculated from the travel time-curve method. The stable velocity model is

evaluated upto the depth of 35 km (Fig. 1 a,b). Fig. 1(c) shows the decrease in the rms residual peak against the number of earthquake for new velocity model.

Our result show improved hypocentral location of earthquakes and significant shift in them provided by their dense clustering between 10 and 20 km (Fig. 2). This perhaps delimits the seismicity around Main Himalayan Thrust and supports the flat ramp system beneath the MCT. The results obtained could be further coupled to estimate the 3D tomography and resolve the complex seismotectonics in the deeper part of this region.

Robinson, D.P., Das, S., Watts, A.B. 2006. Science, 312 (5777), 1203-1205.

Kissling, E., Ellsworth, W.L., Eberhart-Phillips, D., Kradolfer, U. 1994. Journal of Geophysical Research, 99(B10), 19,635-19,646,

Mahesh, P., Rai, S.S., Sivaram, K., Paul, A., Gupta, S., Sarma, R., Gaur, V.K. 2013. Bulletin of the Seismological Society of America, 103 (1), 328-339.

Kumar, N., Sharma, J., Arora, B.R., Mukhopadhyay, S. 2009. Bulletin of the Seismological Society of America, 99 (1), 95-109.

Monsalve, G., Sheehan, A., Schulte Pelkum, V., Rajaure, S., Pandey, M.R., Wu, F. 2006. Journal of Geophysical Research: Solid Earth (1978-2012), 111(B10).

Identifying out-of-sequence thrusts in the Chitwan Intermontane Valley, Central Nepal, using longitudinal river profiles and SL index analysis

Ananya Divyadarshini, Vimal Singh

Department of Geology, University of Delhi, Delhi 110007, INDIA

Continued convergence of the Indo-Eurasian plates since early Cenozoic has led to large scale thrusting and movement of tectonic blocks (causing numerous great earthquakes), giving rise to the Himalaya (LeFort, 1975). The present day convergence rate between the Indo-Eurasian plates ranges from 40 to 50 mm/yr resulting in accumulation of large amount of stress across the Himalayan Belt (Bilham et al., 1997). Around 10 to 20 mm/yr of shortening is taken up by movement of thrust sheets in the frontal part of the Himalaya (Wesnousky et al., 1999; Lave and Avouac, 2000; Kumar et al., 2001). However, historical record of great earthquakes reveals absence of large magnitude surface rupture events in the last few centuries. There is presence of several seismic gaps along which nearly two-third of the Himalaya belt stays unruptured by recent earthquakes, thereby increasing the expectancy of large magnitude earthquakes in the near future (Bilham, 2004). This requires a good knowledge of active structures capable of taking up slip across the Himalaya. The Main Frontal Thrust (MFT; also called as the Himalayan Frontal Thrust or HFT) is shown to be the most active thrust, taking up maximum convergence across the Himalayan belt (e.g. Wesnousky et al., 1999; Lave and Avouac, 2000). But active faults (out-of-sequence thrusts deforming Quaternary landforms) have also been reported to the north of the MFT (e.g., Malik and Nakata, 2003; Singh et al., 2008).

In this study, we investigate Chitwan intermontane valley located in a *seismic gap* in the central part of the Nepal Sub-Himalaya. This area has observed a period of quiescence since the last 200 to 500 years (Khattri, 1987). Absence of great earthquakes in the past few centuries and relatively higher convergence rates along the central Himalaya (Bilham et al., 1997; Mugnier et al., 2004) makes this area vulnerable. Epicenters of the recent 2015 earthquakes occurred to the north of the Chitwan intermontane valley, but there is no evidence of surface rupture during these earthquakes. It is therefore essential to identify potential structures along which rupturing could occur in case of a great earthquake. In order to do so we have employed longitudinal profile analysis and SL index analysis of the rivers flowing within the dun. Since it is well known that most of the convergence

occurs along MFT we have excluded it from our analysis. The results of the analysis are then correlated and integrated with the landforms of the area. The Chitwan intermontane valley is bounded to its north by the Inner Churia Range (Inner Siwaliks) which is thrusted over the Quaternary sediments along the Central Churia Thrust (CCT). The Inner Churia Range is separated from the Lesser Himalaya by the Main Boundary thrust (MBT). Another structure viz., Barakot fault (BKF) is present to the north of the CCT (Kimura, 1995). The Frontal Churia Range (Outer Siwaliks) marks the southern boundary of the Chitwan intermontane valley, and it is thrusted over the Indo-Gangetic Plains along the MFT.

Longitudinal profile and SL index analysis of 18 rivers flowing within the Chitwan intermontane valley shows knick points and high SL index values (anomalous zones) in certain reaches. The anomalous zones are correlated laterally to trace the extent of structures present within the intermontane valley. Seven active faults are identified within the Chitwan intermontane valley, which includes the CCT 1, Jharahi Thrust (JHT), Belani Thrust (BT), Danda Thrust (DT) and West Chitwan Thrust (WCT), in the western part of the valley, and the CCT 2 and Shaktikhor Thrust (ST), in the eastern part of the valley. Landforms showing displacement along these structures further support our findings. Although the CCT 1, CCT 2 and JHT are identified in the field, outcrops of the BT, DT, WCT, and ST could not be observed due to poor outcrops. However, the topographic expressions of these thrusts suggest existence of these faults. The active structures identified within the Chitwan intermontane valley represent out-of-sequence thrusts displacing Quaternary landforms and are thus potential rupture zones in the area apart from the MFT.

Bilham, R., Larson, K., Freymueller, J., Project Idylhim members, 1997. Nature, 386, 61 -63.
Bilham, R. 2004. Annals of Geophysics, 47, 839-858.
Khattri, K.N. 1987. Tectonophysics, 138 (1), 72-92.
Kimura, K. 1995. The Science Report of the Tohoku University, 7th Series, 45 (2), 103-120.
Kumar, S., Wesnousky, S. G., Rockwell, T.K., Ragona, D., Thakur, V.K., Seitz G.G. 2001. Science, 294, 2328-2331.
Lave, J., Avouac, J. P. 2000. Journal of Geophysical Research, 2000, 105 (B3), 5735-5770.
LeFort, P. 1975. American Journal of Science A275, 1-44.
Malik, J.N., Nakata, T. 2003. Annals of Geophysics, 46,917-936.
Mugnier, J.-L., Huyghe, P., Leturmy, P., Jouanne, F. 2004. In: Mc Clay, K.R. (Ed.), 'Thrust Tectonics and Hydrocarbon Systems: AAPG Memoir 82, 91-114.
Singh, V., Tandon, S.K., Singh V., Mukul, M., Thamo-Bozso, E. 2008. Current Science, 94, (5), 623-628.
Wesnousky., S.G., Kumar, S., Mohindra, R., Thakur, V.C. 1999. Tectonics, 18, (6), 967-976.

Late Pleistocene-Holocene record of aggradation and incision of Indus River, Ladakh, NW Himalaya: Role of paleoclimate and tectonics

Anil Kumar, Pradeep Srivastava
Wadia Institute of Himalayan Geology, 33 GMS Road, Dehradun 248001, INDIA

This study examines the geomorphic evolution of Indus River in the region from Nyoma to Dah Hanu, in Ladakh, NW Himalaya during the past 83 ka. Based on the (i) river valley profile, (ii) Stream Length (SL) gradient index, and (iii) terrace configuration, this stretch of the river could be divided into four segments. Segment-I, from Nyoma to Mahe was a braided channel, with average gradient of 0.75 m/km, a maximum width of 3.9 km and older floodplains showing tight meanders. Segment-II, from Mahe to Upshi, the river flows into a deep and narrow gorge with gradient of 7.2 m/km and a fill terrace. Segment-III, from Upshi to Spituk had a channel gradient of 1.8 m/km with a wide valley (Leh). The valley in this segment is flanked by fans and channel fill deposits. Segment-IV, from Spituk to Dah Hanu, the channel gradient was 4 m/km with a fill terrace and 2 levels strath

terraces. SL-index, varied from segments I to IV, where Segment-I shows the lowest values the Segment-IV the highest, and was inferred to be independent of lithology.

Sedimentology of valley fills suggested that aggradation and formation of fill terraces was controlled by channel bound processes. Optically Stimulated Luminescence (OSL) ages suggest that valley filling and progradation of lateral outwash fans along the Indus occurred during in three pulses at ~52 ka, ~28 ka and ~16 ka respectively which from palaeoclimatic records were wetter conditions.

Strath terraces in the Segment-IV suggests bedrock incision rates between 1.2-3 mm/a and that the strath surfaces suggest two palaeo Indus profiles. Upper profile at 147±26 m above river level (arl) was optically dated to 64±4 ka and this gave an average erosion rate of 2.3±0.6 mm/a. Lower profile at 65±15 m arl had an optical age of 46±4 ka, gave average erosion rate of 1.4±0.4 mm/a. Both the profiles diverge downstream implying a base level fall in the downstream region. Comparison of our record with the Nanga Parbat Harmosh Massif (NPHM), indicate an increase in the bedrock incision rate from Nimu to NPHM suggests that besides uplift along the local faults, rapid incision in the NPHM region added to bedrock incision and formed strath terraces of Segment-IV.

Are late Eocene-Oligocene calcretes of the western Himalaya linked to climatic aridity in India?

B.P. Singh
Centre of Advanced Study in Geology, Banaras Hindu University, Varanasi 221005, INDIA
drbpsingh1960@gmail.com; bps_geol@bhu.ac.in

Pedogenic calcretes develop in soil vadose zone under arid to semiarid climatic conditions (Tandon, 1999; Singh and Tandon, 2002; Alonso-Zarza, 2003). This paper correlates the occurrence of pedogenic calcretes in the western Himalaya with the climatic aridity prevailed during Late Eocene-Oligocene in India. Calcrete occurs in the Lower Murree and Dagshai formations within red/brown mudstones host. They show variegated colour with dominance of the white patches. They also show profile development as well as variation in their development stage. In many profiles, nodular calcrete of soft and hard varieties occur in a hierarchical manner. In a complete profile, powdery calcrete is followed by soft and hard nodule calcretes, and laminar calcrete. Ten such calcrete profiles are recorded in a 35 m thick succession in the Kalakot area of Jammu and Kashmir, India. These calcretes possess both alpha and beta fabric elements. The alpha fabric elements are floating grains, corona structures and micronodules, while the beta fabric elements are pellets, rhizoliths, alveolar septal fabric, filamentous calcite, fungal boring and *Microcodium*-like structures. The stable carbon and oxygen isotope varies between -8.5 to -11.2‰ and -8.5 to -12.6‰, respectively.

Calcrete profiles of stage 3 and 4, containing rhizoliths, pellets, filamentous calcite, fungal borings and *Microcodium*-like structures, have developed by pedogenic processes in soil vadose zone. Large negative stable carbon (-8·5 to -11·2‰) and oxygen isotope values (-8·5 to -12·6‰) suggest that the studied calcretes formed under the influence of meteoric water and soil organic matter in dry subtropical climatic conditions. The stable carbon isotope values, determined from the studied calcrete samples, suggest level of atmospheric carbon dioxide ~465 ppmV at low productivity. These imply that the calcretes of the western Himalaya formed at higher level of atmospheric carbon dioxide than the present day value in arid to semiarid climatic conditions between 20 to 30ºN latitudes.

Alonso-Zarza, A.M. 2003. Earth Science Review, 60, 261-298.
Singh, B.P., Tandon, S.K. 2002. Journal of the Geological Society of India, 60, 75-89.

Tandon, S.K., Kumar, S. 1999. In: Singhvi, A.K. & Derbyshire, E. (eds.), Paleoenvironmental Reconstruction in Arid Lands. Oxford & IBH Publ. Co., New Delhi, pp. 109-152.

Behaviour of Little Ice Age (LIA) in Northern vs. Southern sites in Asia

B.S. Kotlia
Centre of Advanced Study in Geology, Kumaun University, Nainital 263002, INDIA

The Late Holocene climate of the Himalaya shows inverse correlation with sites solely influenced by the Indian Summer Monsoon (ISM), largely because of the additional role of the Westerlies in the Indian Himalaya. Within the Indian Himalaya itself, even today, there are different precipitation regimes from Central Himalaya to the northwest Himalaya, the wet periods in the former show reverse pattern in the later, as confirmed by the Standardized Precipitation Index (SPI) which provides an improved selection to develop short to long-term records for the Himalayan region which has, so far, very limited high resolution records for the Holocene period.

Variations in petrography, stable isotopes, reflectance, and luminescence along the central growth axis of a 14.5 cm stalagmite from Panigarh cave indicate cooler and slightly wetter conditions in the Himalayan foothills of northern India during the Little Ice Age (LIA), which lasted from AD 1489-1889 based on deposition of calcite, and AD 1450-1820 based on rapid changes in $\delta^{18}O$ values. Conditions were warmer and drier during the preceding Medieval Climate Anomaly (MCA) and also in the post-LIA periods, as evidenced by deposition of aragonite. In contrast to the Himalaya, the core area of the Indian Summer Monsoon (ISM) was dry during the LIA and wetter during the MCA and post-LIA period. Cave records and other proxies in Asia record a dry LIA in the south and at the same time wet conditions further north.

Variations in solar irradiance are believed to have determined the strength of the ISM by varying the frequency of El Niño and La Niña events over time, which produce weak and strong ISM, respectively. Low (high) levels of irradiance produce more El Niños (La Niñas). A high frequency of El Niño events during the LIA brought drought conditions to the core ISM area but triggered more monsoon 'breaks' that brought higher precipitation to the Himalaya. At the same time, lower solar irradiance cooled the North Atlantic and Eurasian land mass reducing the south-to-north temperature and pressure gradients that drive the ISM, increased snow cover and persistence in Eurasia, which weakens the ISM, and pushed more depressions along the path of the southern winter jet which brought more winter precipitation to the Himalaya. Another possible explanation for increased LIA precipitation at Panigarh Cave is that there was an increase in fall/winter/spring precipitation due to the Southern Winter Subtropical Jet funneling depressions along the southern margin of the Tibetan Plateau.

Climate variability during Late Quaternary in Khalsi-Saspol paleolake, along River Indus, Ladakh, Trans-Himalaya: A multi-proxy approach

Debarati Nag*, Binita Phartiyal
Birbal Sahni Institute of Palaeobotany, Lucknow 226007, INDIA
**debarati_nag@yahoo.co.in*

The Indus river valley is tectonically unstable, exhibiting a complex topography, landscape relief and varied Quaternary sedimentation. The region lies in the Indus Suture Zone (ISZ) of Trans Himalaya in the northern limit of Indian Summer Monsoon (ISM) and trajectory of westerly winds. The major geomorphic landforms include alluvial fans, debris cones, fluvio-lacustrine deposits, scree and talus cone

are present throughout the study area. This strategically located region hosts a plethora of sedimentary archives and provides a rare opportunity to decipher the temporal changes in climatic-tectonic interactions and consequent landform evolution of the area. During the Quaternary a ubiquitous mass movements and catastrophic land sliding transported material from steep slopes to valley bottoms is seen which was responsible for forming lakes (preserved as thick piles of fine sediments), while the outburst floods redistributed sediment down valley. Three phases of lake formation are recorded, at ~35-26 ka (Lamayuru palaeolake); 17-13 ka (Rizong) and 14-5 ka (Khalsi and Saspol); and 10 to ~1.5 ka (Spituk-Leh) (Phartiyal et al., 2013; Nag and Phartiyal, 2014). Special account of the palaeolake sequences and the seismites (soft sediment deformation structures) are undertaken as the mark of the river damming and tectonic pulses. The lake formation can be attributed jointly to the tectonic activity as well as the deglaciation after the Last Glacial maximum (LGM) and Holocene warming and previous records show that Indian Summer Monsoon (ISM) intensity was more during the lake phases. These lake sediments are the resultant of geologic and climatological interactions and being more continuous in nature can provide a more complete record of past climate variability.

The present study focuses on sediment characterization (sand, silt, clay percentages), total organic content (moisture content, carbonate content, loss on ignition), mineral magnetic analysis (magnetic susceptibility, Anhysteric Remnanent Magnetisation) in association with ^{14}C (AMS) and optically stimulated luminescence chronology of sequences at Khalsi and Saspol villages (parts of a major lake system - Khalsi-Saspol palaeolake) to reconstruct the late Quaternary tectono-climatic history. Choking of the narrow Indus river channel by huge amount of debris generated during the deglaciation after LGM gave rise to the Rizong palaeolake at ~17 ka and subsequently the rising water level led to the formation of the Khalsi-Saspol landslide dammed valley lake. The total area of the lake is around 370 sq. km extending from Nimo to Khalsi at elevation more than 3200 m asl. Both the sections are composed of variations of clay, silt and sand and associated with several meters of fluvial sediments, with a mixed facies signifying interchanging sedimentary environment. At Saspol the clay-silt lacustrine deposit is punctuated by sandy influxes. The percentage of clay (68%) and silt (25%) and minor sand (7%) for the Saspol section is noted. Most of the fining up sequences are concentrated in the lowermost 12.9 m of the section. For the Khalsi section clay (13%), silt (73%) and sand (14%) is recorded. The entire sequence till 13.5 m shows alternations of fine grained sand and mud while 13.5 to 15 m records undisturbed clay bed and thereafter silt content again increases. Based on sediment content, organic matter and magnetic parameters supported by ^{14}C (AMS) chronology Saspol section is broadly divided into three climatic zones: SZ1 (3 subzones), SZ2 (3 subzones) and SZ3 (5 subzones) and Khalsi section is classified into five climatic zones: KZ1 (7 subzones), KZ2 (5 subzones), KZ3, KZ4 and KZ5. SZ1 is correlated to KZ1 and KZ2. SZ2 is correlated to KZ3 and SZ3 is correlated to KZ4. The formation of the lake was initiated at ~14.6 ka. Fluctuating energy condition depicted by grainsize analysis of zone 1 (SZ1) with variable magnetic susceptibility values and low TOC percentage, assigned zone 1 from 14.6 to 10.8 ka (SZ1 and KZ1 and 2). The most stable and highest lake level is recorded at 10.8 to 8.3 ka, which is Zone 2 (SZ2). This zone records undisturbed clay bed, low magnetic susceptibility and high TOC. Return of high energy condition, high susceptibility and decreasing TOC are documented from 8.3 to 6 ka and thereafter breaching of the lake led to the return of fluvial regime. Seismites reported from 8.7 m level at ~10 ka of the Khalsi section leaves the footprint of tectonic activity at that time which conform with the report of seismic activity at 10 and 6 ka by Phartiyal et al. (2013) from Spituk palaeolake section of Leh valley. This study is an attempt to learn the causative factors for the formation of the lake in terms of climate and tectonic perturbances and aims at study and reconstruction of palaeolakes and the palaeoclimate from the lower reaches of the Indus River in the Indian territory.

Nag, D., Phartiyal, B. 2014. Quaternary International 371, 87-101.
Phartiyal, B., Sharma, A., Kothyari, G.C. 2013. Chinese Science Bulletin 58, 142-155.

Formation of Wrinkle Ridge along the Piedmont Belt in the Eastern Himalayas

Chandreyee Goswami Chakrabarti[1*], Prasun Jana[2], Pallavi Mahato[1]
[1]*Department of Geology, University of Calcutta, Kolkata 700089, INDIA*
**chandreyee.goswami75@gmail.com*
[2]*P-961, Block A, Lake Town, Kolkata 700089, INDIA*

Ongoing tectonic activity in the Himalayan terrain is often well revealed by prominent tectonically controlled geomorphic features within the Piedmont belt. In the Himalaya, geomorphic expressions like displaced and warped Late Pleistocene and Holocene surfaces along active faults in the frontal zone, the signatures of palaeo-lake formation due to movement along active faults, gullied surfaces marked by ravines and the development of canyons/deep narrow gorges, entrenched channels and tilted terrace surfaces are indicative of active tectonic and fault displacement, and its influence over the evolution of the landscape.

The Piedmont area east of the Tista River is located within the foreland basin in front of the active Fold Thrust Belt (FTB) in the Eastern Himalayas where Quaternary sediments occur as distinct terraces formed over the fan deposits which are dissected by southerly flowing rivers. In the piedmont belt located between the Murti and the Neora rivers, two prominent E-W trending and south facing scarps from north to south are Matiali and Chalsa scarps. They are identified and interpreted as ramp anticlines over north dipping blind thrusts representing the MBT and HFT respectively (Gansser, 1964, Nakata, 1972, 1989; Guha et al., 2007; Goswami Chakrabarti et al., 2013). There are a set of conjugate normal faults along the Neora and the Murti rivers, which has uplifted the interfluve area and has guided the present drainage pattern of that area (Goswami et al., 2012).

In an adjacent area, the piedmont fan surface within the Jaldhaka and Gathia interfluves is highly deformed and are bounded by the imposing ca. 60 m high northerly facing Thaljhora scarp in the north and the subdued south facing Chalsa scarp in the south (Fig. 1). In this contribution, we report another northerly sloping small scarp of 5 m height between the Thaljhora and the Chalsa scarp (Fig. 2). The river profiles obtained from the Cartosat I DEM of this area show nick points while crossing either the Thaljhora scarp or the small northerly sloping scarp. We interpret these two northerly sloping and E-W trending scarps as back thrusts forming a wrinkle ridge pair. As this scarp is very small, the southerly flowing smaller rivers originated from the Thaljhora scarp start incising the fan surface forming deep gorge sections while crossing this scarp. The Jaldhaka River shows a sharp easterly bend parallel to the trend of the fault underlying the newly identified scarp. The major

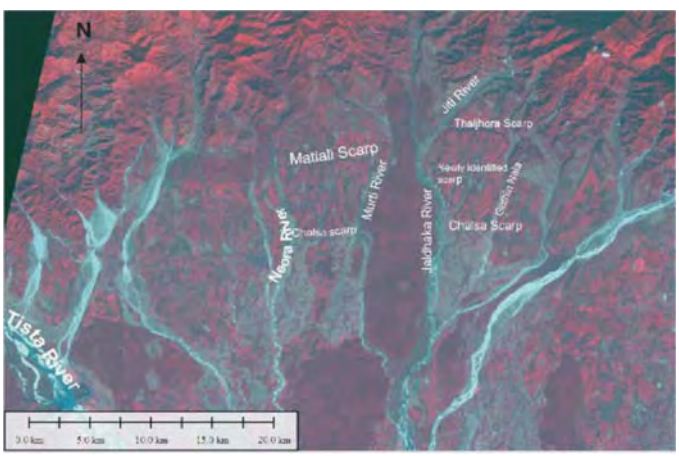

Fig. 1. The area showing different rivers and scarps in the eastern Himalayan piedmont belt.

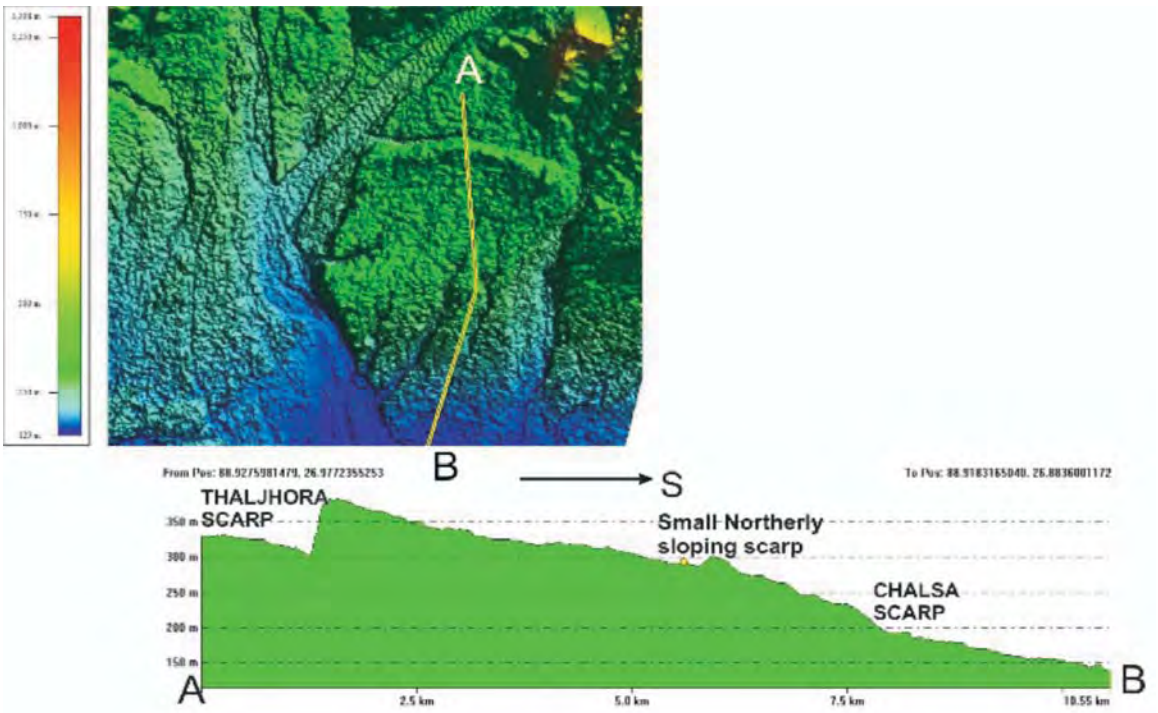

Fig. 2. Longitudional profile on the fan surface showing the Thaljhora scarp, small northerly sloping scarp and the Chalsa scarp from north to south.

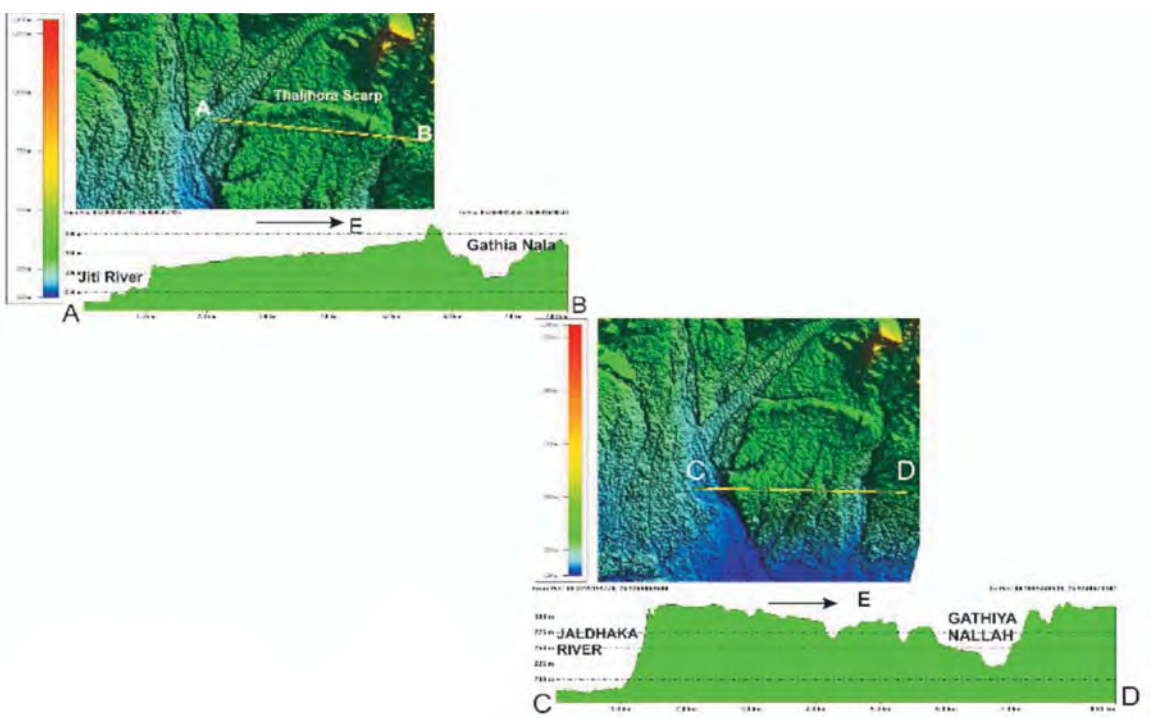

Fig. 3. The transverse profile along the fan surface showing easterly tilting in northern portion and westerly tilting in southern portion.

drainage system of this area is controlled by the two NNW-SSE and N-S faults along the Jaldhaka River and the Gathia Nala respectively. The Jiti River in the NW corner of the area also flows along a NE-SW trending fault and meets Jaldhaka River after negotiating the Thaljhora scarp. The interfluve area between the Jaldhaka River and the Gathia nala is uplifted compared to the adjacent area by two faults along these two rivers but the amount of upliftment is not same along two faults. In northern portion of the fan surface, the fault along Gathia nala has uplifted the eastern side of the Thaljhora scarp more than the western part .This has resulted in bogging of the Thaljhora River at the back of the scarp and it is now flowing towards west to meet Jiti River. In contrast, the western side of the newly identified scarp has been uplifted more than the eastern portion by the fault along the Jaldhaka River indicating a rotational component between these two faults (Fig. 3).

Though the study area is adjacent to the Neora-Murti interfluve area and the Matiali scarp and the Thaljhora scarps are almost in the same latitude, this area is much younger than the Neora Murti interfluve area and in terms of antiquity, the Thaljhora scarp is younger than the Matiali scarp. In the previous area, the fault underlying the Chalsa scarp is the youngest whereas in the present study area the fault along the Chalsa scarp is the oldest. Time sequential analysis of drainages from toposheets, IRS P6 LISS-III, Resourcesat 2 LISS IV images, and Cartosat I data shows that the Jaldhaka River course has shifted towards east in last twelve years while the Gathia Nala has shifted towards west. The confluence of the Jiti River and Jaldhaka River has shifted towards south in recent years indicating the southern backthrust as well as the transverse faults are still active.

Gansser, A. 1964. Geology of the Himalayas. Interscience, Wiley, New York, 289p.
Goswami (Chakrabarti), C., Mukhopadhyay, D., Poddar B.C. 2013. Quaternary International, 298, 80-92.
Goswami, C., Mukhopadhyay, D., Poddar, B.C. 2012. Frontier of Earth Science in China 6 (1), 29-38.
Guha, D., Bardhan, S., Basi, S.R., De, A.K., Sarkar, A. 2007. Journal of Asian Earth Sciences 30, 464-473.
Nakata T. 1989. Geological Society of America, Special Paper No. 232, 243-264.
Nakata,T. 1972. Tohoku University Science Reports, 7th Ser. (Geography) 22, 39-177.

Shear-wave Velocity Structure of the Crust in Northeast India

Dipok K. Bora[1*], Devajit Hazarika[2], Kajaljyoti Borah[3]
[1]Department of Physics, Diphu Government College, Diphu, Karbi Anglong 782462, INDIA
**dipok23@gmail.com*
[2]Wadia Institute of Himalayan Geology, 33 GMS Road, Dehradun 248001, INDIA
[3]Department of Earth Sciences, Indian Institute of Science Education and Research, Kolkota 741246, INDIA

We investigated the seismic shear-wave velocity structure of the crust beneath nine broadband seismological stations of the Shillong-Mikir plateau and its adjoining region of northeast India by using teleseismic *P*-wave receiver function analysis. The inverted shear wave velocity models show ~34-38 km thick crust beneath the Shillong plateau which increases to ~37-38 km beneath the Brahmaputra valley and ~46-48 km beneath the Himalayan foredeep region. The gradual increase of crustal thickness from the Shillong plateau to Himalayan foredeep region is consistent with the underthrusting of Indian Plate beyond the surface collision boundary. A strong azimuthal variation is observed beneath SHL station. The modeling of receiver functions of teleseismic earthquakes arriving the SHL station from NE backazimuth (BAZ) shows a high velocity layer of thickness 6 km within depth range 2-8 km along with a low velocity zone within ~8-13 km. In contrast, inversion of receiver functions from SE BAZ shows high velocity zone in the upper crust within depth range ~10-18 km and low velocity zone within ~18-36 km. The critical examination of ray piercing points projected over the geoelectric section clearly indicates that the waves arriving from SE BAZ pierce the extremely high resistive zone that also shows high shear-wave velocity. This high resistive and high velocity zone may indicate effect of crystalline rocks of the Shillong Plateau.

Proposed Geo-Park (Stromatolite Fossil Park) development at Mamley area, South Sikkim with emphasis on promotion of Geotourism in Sikkim Himalaya

Indira Sharma[1*], Prakriti Pradhan[1], V.C. Tewari[2#]

[1]Mines, Minerals & Geology Department, Government of Sikkim, Gangtok, INDIA

[*]sharmaindira89@gmail.com

[2] Ex-Scientist, Wadia Institute of Himalayan Geology, 33 GMS Road, Dehradun 248001, INDIA

[#]vinodt1954@yahoo.co.in

The Geotourism holds a great potential for preservation of significant geological structures and mountain ecology in the Sikkim Himalaya, NE India. Sikkim Himalaya is well known for the highest Himalayan peak in India (Kanchendzonga), scenic landscape along Teesta River valley, glaciers and high altitude lakes, biodiversity hot spots, unique Tibetan customs, mythology and history. Geologically significant sites in the South Sikkim Lesser Himalaya needs to be preserved immediately and developed as Fossil Parks since these are located very close to the ongoing and proposed new hydro power projects, road and tunnel constructions and other developmental civil constructions (Tewari, 2014). The Meso-Neoproterozoic stromatolites are very well preserved in the Buxa Dolomite Formation in the Rangeet river valley near Tatapani, along the road from Tatapani to Reshi and Namchi town to Mamley village (present study). Highly diversified assemblage of characteristic taxa *Colonella columnaris, Conophyton garganicus, Kussiella kussiensis, Baicalia* sp., *Jurusania* sp., *Minjaria* sp., *Gymnosolen* sp., *Kalpanaella* new form (Tewari, 2011)*, Stratifera* sp., *Colleniella* sp., *Tangussia* sp., and *Nucliella* sp., etc. are well developed in the south Sikkim Himalaya (Tewari, 2011 and the references therin). The chert bands associated with the stromatolites have yielded the organic walled microfossils *Siphonophycus* sp., *Eomycetopsis* sp., *Obruchevella* sp., *Myxococcoides* sp. and *Oscillatoriopsis* sp., (Schopf et al., 2008; Tewari, 2011). The Laser Raman Spectroscopic and Confocal Laser Scanning Microscopy has shown that these bacteria are biogenic and can also be useful in search for the extraterrestrial life on Mars and other planets (Tewari, 2011). Recent astrobiological studies have shown that stromatolites or microbially induced sedimentary structures and bacterial microorganisms may be found on Martian surface. Therefore, the stromatolite fossil park may be urgently developed at Mamley to preserve these rare evidence of early life, its evolution and diversification in India from the South Sikkim Lesser Himalaya. The other equally important evidence of Permian glaciation is also well preserved at Tatapani where large Gondwana Ranjeet Boulder Beds (glacial diamictites) indicate strong past evidence of glacial cool climate (Tewari, 2011). The present paper dealt with the development of the stromatolite fossil park at Mamley in South Sikkim to raise the scientific awarenes in the local community and the preservation of the geo-site for future geotourism in the Sikkim State.

Tewari, Vinod C., 2014. Journal of the Nepal Geological Society, Volume 48, Special Issue, pp.41.

Tewari, Vinod C., 2011. In: Tewari, Vinod & Seckbach, Joseph (Eds.), Stromatolites : Interaction of Microbes with Sediments. Cellular Origin, Life in Extreme Habitatas and Astrobiology, Volume, 18, pp.497-522, Springer - Verlag, Heidelberg, Germany.

Mathematical analysis on seismic profiles provides a new approach of delineating subsurface geometry an application in the Himalayan Foreland Thrust belt

Joyjit Dey
Indian Institute of Technology, Khargpur 721302 (WB), INDIA

In active collisional zones like the Himalaya it is very common to find out structures related to large amount of orogenic contraction. For brittle-ductile rock deformation there are two main types of fault-related folds that can accommodate large collisional shortening in foreland thrust belts, i.e. fault-bend folds and fault-propagation folds. However, in the north-west frontal thrust belt of Himalaya the seismic interpretation of sub-surface geometry is ambiguous due to the difference in proposed model of various authors. Though fault-bend and fault-propagation models have found to be convincing, but no simplified and direct method is yet to known to differentiate and testify various published models of fault-related folds. Here a predicted angular function for quantitative geometric relationships between fault shape and fold shape has been found to be a straight forward tool to test the fault-related folds directly from the seismic profile. Use of distance-displacement (dD) method on the seismic profile to cross-check and predict the relative propagation rate of the fault and folds also serves a good mechanism to decipher subsurface geometry of structures. Two seismic profiles Kangra-2 and Kangra-4 of Kangra re-entrant, Himachal Pradesh, are used in this study to test the fault-related folding associated with Balh anticline, Paror anticline, and calculated the amount of shortening along the JwalamukhiThrust, Jhor fault that lie between Himalayan Frontal Thrust (HFT) and Main Boundary Thrust (MBT) in the Himalayan foreland. The results are obtained by transformation of seismic time profile to depth profile using the time-depth conversion diagram, and it has been used to identify whether the interpreted structures are reasonable or not. Lastly, this method has been applied to delineate subsurface feature above MFT of Dehradun reentrant.

This study signifies a great insight in the interpretation of subsurface seismic pattern and provides an important and simplified tool for the geologists to interpret and predict the existence of fault related folding in the subsurface structure.

Early Campanian calcareous nannofossils from Chikkim Formation, Spiti Valley, Tethys Himalaya, India

Jyotsana Rai[1], Deb Brat Pathak[2], Bindhyachal Pandey[2]
[1]*Birbal Sahni Institute of Palaeobotany, Lucknow 226007, INDIA*
[2]*Department of Geology, Banaras Hindu University, Varanasi 221005, INDIA*

We first report here precisely datable, moderately preserved and reasonably diversified calcareous nannofossil assemblage comprising twenty eight species from the Upper (Shale) Member of the Chikkim Formation from its type area near Chichim village of the Spiti Valley. The Chikkim Formation exposed in the Spiti valley, belongs to the Tethyan Himalayan belt of the Indian Territory. This formation is underlain by the Giumal Formation (Berriasian - Early Aptian interval) and is further subdivided into Lower (Limestone) and Upper (Shale) members. Though this formation (~150 m thick) was earlier dated to range in age from Albian to Early Maastrichtian. The sectioned study of planktonic foraminifers from Chikkim Formation has provided broad Late Albian to Santonian age for Lower Member and a probable Late Campanain to ?Maastrichtian age for Upper Member (Bertle & Suttner, 2005). The present study precisely constrains the ammonite devoid Upper Member by calcareous nannofossil data. This precise age bracketing is based on calcareouas

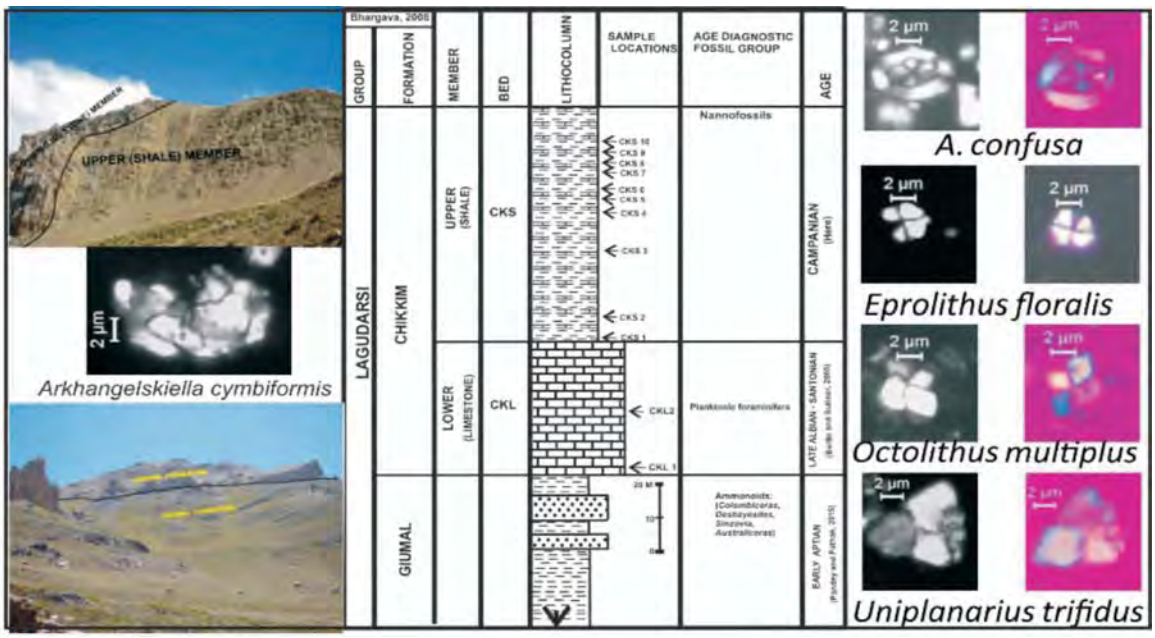

nannofossils recovered from eight productive out of eleven samples collected from major profile of the Chikkim Formation from its type area. The nannotaxa include *Arkhangelskiella confusa, A. cymbiformis, Braarudosphaera bigelowii, Calculites obscurus, Cyclagelosphaera margerelii, C. reinhardtii, Cribrosphaerella ehrenbergii, Discorhabdus* cf. *D. ignotus, Eprolithus floralis, Eiffellithus gorkae, E. turriseiffelii, Micula decussata, M. staurophora, M. cubiformis, M. praemurus, Manivitella pemmatoidea, Octolithus multiplus, Prediscosphaera grandis, P. ponticula, Prediscosphaera* sp., *Monomarginatus quaternarius, Reticapsa crenulata, Rhagodiscus indistinctus, Tranolithus orionatus, Tegumentum stradneri, Uniplanarius trifidus, Watznaueria barnesiae, W. fossacincta.* The most abundant species in the present assemblage is *W. barnesiae* which is usually an abundant species in Cretaceous environments, being capable to adapt to fluctuating and/or extreme conditions (Mutterlose, 1991).

The FAD of *A. cymbiformis* and the LAD of *E. floralis* is taken here to indicate the base of Campanian. Therefore, the age assigned for Upper Member of Chikkim Formation is UC 13b^{BP} (Burnett, 1998) of Early Campanian. The occurrence of *Uniplanarius trifidus* and *A. cymbiformis* suggests the presence of early Late Campanian *Quadrum sissinghii* Zone (CC21, Sissingh, 1977). The record of *U. trifidus* and *O. multiplus* from basal most part of the Upper (Shale) Member indicates the presence of CC21/ CC22 zones of Campanian age.

Burnett, J.A. 1998. In: Bown, P.R. (ed.), Calcareous nannofossils biostratigraphy. British Micropaleontology Society Series, Chapman & Hall, London, p. 132-199.
Bertle, R.J., Suttner, T.J. 2005. Cretaceous Research, 26, 882-894.
Mutterlose, J. 1991. Palaeontographica (B) 221: 27-152.
Sissingh, W. 1977. Geol. Mijnbouw, Den Haag, 56: 37-65.

Holocene out-of-sequence thrusting in the Kangra re-entrant, NW Sub-Himalaya, India

Saptarshi Dey[1*], Rasmus C. Thiede[1], Taylor F. Schildgen[2], Hella Wittmann[2], Bodo Bookhagen[1], Manfred R. Strecker[1]

[1]Institut für Erd & Umweltwissenschaften, Universität Potsdam, Karl Liebknecht Str. 25, Haus 27, Potsdam 14476, GERMANY

**geosaptarshi@gmail.com, Saptarshi@geo.uni-potsdam.de*

[2]GeoForschungsZentrum Potsdam, Telegrafenberg, Potsdam 14473, GERMANY

The Himalayan orogenic wedge comprises several morphotectonic sectors separated by thrust fault systems that have accommodated the convergence between India and Eurasia. The Sub-Himalaya thrust belt, the youngest and lowest sector of the wedge, exposes foreland-basin sediments that are deformed by several thrust systems. Geodetic data reveals 14±1 mm/yr of present-day shortening in this region. The southernmost thrust fault that separates the contiguous foreland from the orogen, the Main Frontal Thrust (MFT), is thought to accommodate most of the crustal shortening in this region. However, the Kangra re-entrant in the NW Sub-Himalaya records out-of-sequence deformation within the orogenic wedge, where Quaternary reactivation of the Jwalamukhi Thrust (JwT) and other thrust faults have caused transient filling of the intermontane Kangra Basin.

To assess the degree of out-of-sequence thrusting in the Sub-Himalaya we combine morphometric analyses with cosmogenic nuclide (^{10}Be) exposure dating of fluvial terraces. The best-preserved aggradation phase was followed by episodic re-incision, which formed four terrace levels with mean ages of 8.4±0.8 ka, 6.6±0.7 ka, 4.9±0.4 ka, and 3.2±0.3 ka. Steepened stream segments that are independent of lithology and back-tilted terraces record neotectonic activity in the Kangra re-entrant. Holocene differential uplift across the JwT can be deduced from the offset of the 8.4 ka terrace, which helps to determine a shortening rate 6.6 to 7.4 mm/yr for the Holocene. This result suggests that out-of-sequence thrusting along the JwT accommodates most of the Holocene shortening within the Kangra re-entrant, leaving only a minor component of shortening for the MFT farther south.

The geochemistry and petrography of Permo-Carboniferous sandstones from the Spiti region, Tethys Himalaya, Himachal Pradesh, India: An excellent preservation of paleoclimatic record

Shaik A Rashid*, Javid A Ganai

Department of Geology, Aligarh Muslim University, Aligarh 202002, INDIA

**rashidamu@hotmail.com*

Major and trace element chemistry along with detrital modes of the Permocarboniferous Kanawar Group (consisting of Lipak, Po and Ganmachidam formations) sandstones from the Spiti Valley, NW Tethys Himalaya were determined to infer their provenance, paleoweathering conditions and their depositional setting. Based on the composition and the whole rock geochemistry, the sandstones are classified as quartzarenites, sublitharenites and subarkose types. They are characterized by moderate to high SiO_2 contents, moderate K_2O/Na_2O ratios and relatively low mafic contents. The sandstones exhibit uniform REE patterns which are similar to the upper continental crust and post-Archean shales with LREE enrichment, flat HREE and negative Eu anomalies. The petrographical data indicate quartz-rich sedimentary source, medium to high grade metamorphic and plutonic (granitic) parent rocks for the Spiti sandstones. The nature of the feldspar observed, from most altered to euhedral pristine minerals corresponding to Carboniferous to lower Permian sandstones, strongly indicate a

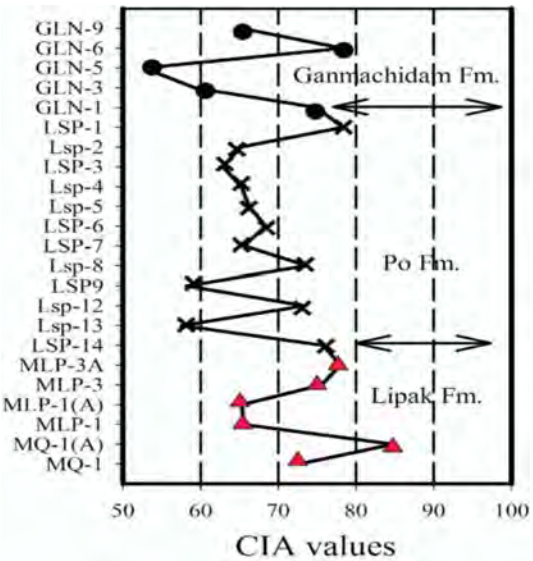

change in climate from most favorable conditions for rapid feldspar alteration (i.e warm and humid) to conditions where negligible alteration is possible (i.e. arid and glacial). Major and trace element geochemistry suggest a typical passive continental margin with minimal intra-basinal sediment recycling. The chemical index of alteration (CIA) values of the Spiti sandstones indicate low and moderate to intense degree of chemical weathering of the source. When the CIA viewed as a paleoclimate indicator, it is found that the CIA values of these sandstones accorded with inferences based on sedimentologic and paleontological evidence, discriminating well between warm-humid (indicated by high CIA values) and arid-glacial (representing low CIA) conditions in the Spiti basin. The results thus document a complete record of glacial and interglacial phases in the Permocarboniferous Spiti sandstones and the interpretations are consistent with other such studies on the Phanerozoic glaciation events on Gondwana supercontinent.

Paleoseismology of Nepal Himalaya and 2015 Gorkha Earthquake

Soma Nath Sapkota[1], L. Bollinger[2], P. Tapponnier[3]
[1]Department of Mines and Geology, NEPAL
[2]Deapartment Analyse Surveillance Environment DASE, FRANCE
[3]Earth Observatory of Singapore, EOS

Department of Mines and Geology in collaboration with Department Analyse Surveillance Environment (DASE) France monitors the seismicity of Nepal since 1978. Monitoring seismicity in this part of the Himalaya lead us to better understand the seismotectonics and earthquake nucleation process. A belt of seismicity, at a depth of 10-20 km, follows approximately the front of the higher Himalaya along the 3000-3500 m topographical contours. This midcrustal seismic cluster is interpreted to fall within a zone of interseismic stress accumulation characterized by high uplift rate inferred from geodetic measurements. A network of 29 continuous GPS stations within the territory of Nepal Himalaya complement the seismic network since 2002, monitoring the convergence rate between northward moving Indian plate and the Tibetan plateau. Result from this network shows that the Main Himalyan Thrust fault (MHT) is currently locked between the higher Himalaya and the Main Frontal Thrust, 100 km southward, and accumulates a slip deficit in this part of the Himalaya at a rate of approximately 1.8 cm/yr.

Himalayan region has been shocked by 6 great earthquakes in the past century including recent April 25, 2015 Mw 7.8 Gorkha Earthquake: 2005 Muzzafarabad Pakistan (Mw 7.6), 1905 Kangra (Mw 7.8), 1934 Bihar Nepal (Mw 8.4), 1987 Shillong (Mw 8.3) and 1950 Assam (Mw 8.6) earthquakes. The region between 1905 Kangra Earthquake and 1934 Bihar Nepal Earthquake between 78°E and 84°E has not produced any major earthquake since more than four centuries and stands for being a large seismic gap in the Himalayan region. The high seismogenic potential of this locked fault zone exposes the North-Western Himalaya and the densely populated region of nearby Ganges basin in India to a high level of seismic risk. Better understanding the future seismic behavior within this seismic gap is one of the major challenges to be taken up by the scientific community in the region. This paper will focus on the present understanding of the seismicity of the Himalaya and impending seismic hazard of the region.

The location and earthquake rupture history of the active faults being critical to assessing the seismic hazard in the Himalayan region, this paper will describe the surface ruptures discovered and studied in Nepal. It will try to answer some fundamental questions such as; how complete is the historic record for M>8 earthquake in the region? What structures generate these very large earthquakes?, and do they rupture to the surface or they stopped before reaching the surface as 2015 Gorkha Earthquake? To address these questions this presentation will confront the historical records with the results of geomorphic and paleoseismic studies conducted along the MFT in Nepal. The MFT has been chosen as a main target because deformed river terraces show that late Pleistocene and Holocene deformation across the Nepal Himalaya is expressed on the frontal fold above the MFT. The surface trace of the MFT therefore provides an opportunity to document whether large earthquake in the MFT rupture the surface, and if so, to determine there size and recurrence as demonstrated by the first report by Sapkota et al., 2013 of the surface ruptures on the same MFT segment of two of the largest historical earthquakes that occurred in central eastern Nepal (AD 1934: M8.4 and AD 1255: M>8).

A review on out-of-sequence deformation in the Himalaya

Soumyajit Mukherjee
IIT Bombay, Powai, Mumbai 400 076, INDIA
soumyajitm@gmail.com

Out-of-sequence deformation in the Himalaya has been mainly by thrusting. Out-of-sequence thrusts (OOSTs), usually N/NE dipping foreshear planes, occur inside the Sub-Himalaya (SH), Lesser Himalaya (LH) and Greater Himalayan Crystallines (GHC). Where absolute dates are available, the youngest slip within the SH is near the Janauri anticline (India) at ~1400-1460 AD, within the LH is the Munsiari Thrust (India) at ~1-2 Ma, and in GHC is the Main Central Thrust Zone in Marsyandi valley (Nepal) during Holocene (~0.3 ka). Except the Riasi Thrust (Kashmir, India), the Paonta Thrust (Himachal Pradesh, India) in the Siwalik, the Tons Thrust (Garhwal region, India) within the MCZ zone, crustal shortening related to OOST in the Himalaya has been insignificant. The major litho/stratigraphic contacts within the SH and the GHC at places acted as an OOST. OOST in the SH were detected mainly based on geomorphological observations. On the other hand, more quantitative geochronologic studies detect ~22 Ma up to Holocene OOST in the GHC based on age jump, especially within the MCT Zone. Crustal channel flow (specifically for the GHC) and/or critical taper model with or without erosion explain the Himalayan OOSTs.

Study of out-of-sequence deformation in collisional terrains is important in the context of seismicity, petroleum geoscience and tectonics. Thrusting is the most common manifestation of out of sequence deformation in the Himalaya from Pakistan in the west up to Arunachal Pradesh (India) in east. Other than faulting, less common mode of out-of-sequence deformation in the Himalaya has

been fracturing related to earthquakes. Examples from India are from Nurpur, Nadha, Kala Amb and Rampur Ganda (Himachal Pradesh), Lal Dhang and Ramnagar (Uttarakhand), and Punjab.

The vast stretch of Siwalik, Lesser Himalaya (LH) and Greater Himalayan Crystallines (GHC) consist of several out-of-sequence thrusts (OOSTs) that usually strike NW and dip NE. OOSTs (in the Himalaya) have been recognized by (i) they cut across recent sediments, (ii) geomorphic indicators e.g., landslides, (iii) trials in cross-section balancing exercises, (iv) disparity in geochronologic age across a tectonic plane. The first three techniques have been more applied on Siwalik, whereas the fourth method has been worked more profusely in the GHC.

Some of the OOSTs in Salt Range (Pakistan) and Barsar Thrust and Majhaur Thrust in the Indian Siwalik are backthrusts. Rates of crustal shortening related to OOSTs usually are trivial compared to Himalayan tectonics. Notwithstanding, the Riasi Thrust is an OOST that seems to be accommodated significant crustal shortening. OOSTs can either be surface breaking (South Kalijhora Thrust in Darjeeling, India) or blind ('SjBt' in Himachal Predesh, India), can have gentle, moderate or steep dip, and may have an in-sequene deformation history with or without associated drag folds. Out-of-sequence faulting can display oblique slip (Muzaffarabad Fault: Siwalik, Pakistan; possibly Garampani-Kathgodam Fault: Siwalik, India), normal faulting (e.g. Singhauli Fault in Siwalik: Himachal Pradesh, India; Salt Range: Pakistan), strike slip (Ganga- and Yamuna-Tear Fault in Siwalik, near Dehradun, India), and significant dip slip component (Tamar Khola Thrust, GHC, Nepal). Single OOSTs, such as the Kala Amb Fault, Pinjaur Garden Fault, Hajipur Fault (Himachal Pradesh), Munsiary Thrust (Uttarakhand, India), and Main Dun Thrust in LH and the Physiographic Transition from the MCT Zone (Nepal), on higher resolution reveals more than one strands of coeval/different activation timings. The Siwalik Himalaya along the Himalayan trend varies in critical taper condition. Intensity of deformation along individual OOST can vary along its length, such as the Medlicott-Wadia Thrust and the Main Dun Thrust. Temporal variation of slip rate of OOST is also deciphered for the Medlicott-Wadia Thrust, and varied slip along the Kathgodam-Garampani Fault.

At places in between the Upper- and the Lower-Siwalik (e.g., Paonta Thrust, Pinjaur Thrust and Nahan/Nalagarh Thrust in Himachal Pradesh, Chaura-Marin Thrust in Nepal, South Kalijhora Thrust in Darjeeling, India), between the Upper- and the Middle-Siwalik (e.g. Soan Thrust in Himachal Pradesh, Ramghat Thrust in Arunachal Pradesh, India), between Lower Siwalik and alluvium (e.g. Nalagarh Thrust: L Himachal Pradesh, India), the upper- and the lower-LH (Bari-Gad Kali-Gandaki Fault), and between the upper GHC and lower GHC (Zimithang Thrust in Arunachal Pradesh, India) defines the OOST. Lithological contacts in different units of the Himalaya thus favourably acted as the OOST at few places, which is common in many other regional shear zones (Gerbi et al., 2015's review). However, such thrusting amongst major lithologic division does not exist everywhere in the Siwalik. For example, the structural cross-section along Dun valley does not have any thrust between Upper- and Middle-, and between the Middle- and the Lower-Siwalik (see fig. 4 of Thakur and Pandey, 2004). Secondly, the Chamuhi Fault (Himachal Pradesh, India) developed wholly inside the Upper Siwalik unit. Additionally, due to litho-facies variation along the Himalayan trend, not all the major-lithologic/stratigraphic contacts can be traced continuously. Finally, the contact between the GHC_U and the GHC_L in Nepal is the pre-India-Eurasia collisional Higher Himalayan Detachment (HHD), which is quite different from OOST.

OOST within the GHC has been reported from 13 or more spot locations in various Himalayan sections. Except few sections, The MCT Zone reactivated/acted like OOST as discrete thrusts, as deciphered most notably from the Marsyandi valley in Nepal. OOSTs of unconstrained mechanisms exist as the contact between domes/windows ans klippens with GHC and LH.

The deepest exhumation of the hanging wall block of the OOST in GHC has been around Kakhtang. OOST in GHC links in a complicated way with the deformation of the GHC and also the

LH, and spans ~22 Ma up to the Holocene. OOST in the GHC has been deciphered noting (significant) age jump of rocks across the Himalayan trend. However, the jump has also been explained by duplexing mechanism. Secondly, whether any age jump really exists has also been questioned. Whether duplexing was followed by OOST has remained uncertain. While Robert et al. (2011) and Grandin et al. (2012) almost negated OOST in the GHC, Kohn et al. (2001) from an alternate petrologic study supported the OOST activity within the GHC.

One would expect higher shear strain near the OOST in Siwalik, SH and GHC. Such a quantitative study is yet to be undertaken. However, even if higher strain is obtained near a tectonic plane/zone, it cannot act as an independent proof for OOST. This is because pre-Himalayan/pre-Collisional ductile shearing (as in Montomoli et al., 2013) might be the other possibility.

Erosion and crustal shortening during channel flow can produce age jump in the GHC, hence can explain OOST in GHC (Beaumont et al., 2007). On the other hand, Mukherjee et al. (2012) analogue modeled GHC's channel flow, same as restricted channel flow of Wang et al.'s (2013) and Hollister and Grujic's (2006) mechanism, where OOST generated without any erosion of the extruded material. Whether OOST can form for a weak channel flow in some Himalayan section is yet to be explored though models. OOST can also be explained easily by critical taper mechanism with or without enhanced erosion. Recent finding of OOST of $STDS_U$ indicates more complicated tectonics of the GHC.

Mitigation and bioengineering measures for prevention of Surbhi Resort Landslide, Mussoorie Hills, Uttarakhand Lesser Himalaya, India

Victoria Z. Bryanne[1]*, Vinod C. Tewari[2#]

[1]*Mahadev Residency - III, Anand Vihar, Jakhan, Rajpur Road, Dehradun 248001, INDIA*

**victoriabryanne@gmail.com*

[2]*Scientist (Retd.), Wadia Institute of Himalayan Geology, 33 GMS Road, Dehradun 248001, INDIA*

[#]*vinodt1954@yahoo.co.in*

Recent cloud bursts and Glacial Lake Outburst Flood (GLOF) in the Uttarakhand Himalaya have triggered catastrophic landslides. Heavy monsoon precipitation lashed Uttarakhand has again caused devastation and a series of new landslides in the region. Surbhi Resort Landslide is located near the hill station of Mussoorie in Garhwal Himalaya, India, in Upper Krol Limestone. After intense rain in August 1998, the Krol sedimentary deposits suddenly gave way as a deep-seated landslide, blocking the main Mussoorie-Kempty artery for 15 days. In 2005, the velocity of the slide was determined to be 4-14 mm/yr by previous workers, thus still active even if with a modest intensity. However, since huge amounts of Quaternary debris are still lying on the slope, another high intensity rainfall or cloud burst could trigger another large-scale failure. Recently, Venkateswarlu and Tewari (2014) and Bryanne and Tewari (2014) have done various geotechnical and geological studies of the rock and soil samples from the Surbhi landslide zone and have suggested the possible causes of the landslide in the area. Based on these detailed investigations, following mitigation and bioengineering measures are suggested. To lower the ground water table, a series of horizontal drains should be installed at the base of the crown portion of the slide. This would generate an additional discharge which has to be channeled down Rangaon-ka-Khala, the natural channel, down the slope to Aglar River flowing in the valley below. To prevent further surface erosion, Rangaon-ka-Khala must be bioengineered with shrubs and grasses such as *Eriophorum comosum, Saccharum spontanum, Pogonatherum spp.* and *Woodfordia fruticosa* while the surrounding slope must be reforested with *Quercus leucotrichophora, Alnus napelensis, Pinus spp.*and *Cedrus spp.* Check dams must be constructed on the entire 3.5 km stretch of Rangaon-ka-khala to lower the velocity of the water. This

could be done either as gabions or in the form of live fascines of *Salix tetrasperma* or *Dalbergia sissoo*.The catchment area above the Mussoorie-Kempty road can be expected to collect 60,000 m^3 in 24 hours in a 25 years reoccurrence cloud burst. Thus proper drains (40 cm in dia.) on the inside of the road must be installed. The flow velocity at these extreme events would be 4.8 m/s, which is slightly above the recommended value. If this water is allowed to flow down Rangaon-ka-Khala it will most certainly lead to a major debris slide with a vertical velocity of almost 100 m/s with huge erosive power. For this reason, this discharge should be channeled down in plastic or cement lined pipes, preferably to the west of Siyagaon village which is reported as stable rather than in the landslide zone itself. It is concluded, that these mitigation measures and bioengineering plantation would certainly help stabilize the Surbhi landslide area and to prevent another similar disaster in future which destroyed the water mills and fields of the surrounding villages. These measures may also be applicable for the other active landslide zones in the NW (Jammu & Kashmir) and NE (Darjiling-Sikkim) Himalaya.

Bryanne, Victoria Z., Tewari, V.C. 2014. Jour. Ind. Geol. Cong., Vol. 6(2), pp. 57-77.
Venkateswarlu, B., Tewari, V.C. 2014. In: Innovative Practices in Rock Mechanics, Bangluru, pp. 329-336.

Morphotectonic evolution of the Siwalik Hills between the Yamuna and the Markanda Exits, NW Himalaya

Mahak Sharma[1], Vimal Singh[2*]
[1]Department of Geology, Kurukshetra University, Kurukshetra 136119, INDIA
[2]Department of Geology, University of Delhi, Delhi 110007, INDIA
** vimalgeo@gmail.com*

The geomorphic evolution of the Himalaya and its bordering areas is significantly influenced by tectonic activities associated with the collision of Indian and Eurasian plates. The southern limit of the Himalaya is generally marked by a major thrust developed during the Himalayan orogeny viz., the Himalayan Frontal Thrust (HFT) or the Main Frontal Thrust (MFT). It is considered to be the most active fault that has folded and uplifted the Siwaliks to form the outermost structural hills. The Himalaya has expanded both spatially and vertically ever since it came into existence. The Himalaya expands spatially by southward migration of its mountain front by breaking new thrusts. The mountain front of the Himalaya has migrated from the Main Central Thrust (MCT) to the Main Boundary Thrust (MBT) to the MFT in past 23 Ma. The migrating mountain fronts have huge impact on the drainage network that in turn impacts sedimentation and geomorphology of the Indo-Gangetic Plains. Thus, understanding of the development of landforms due to migrating mountain front is important. We investigate the area between the Markanda and the Yamuna exits in the NW Himalaya and reconstruct the morphotectonic evolution of the outermost Siwalik Hills (also known as Dhanaura range in this area) between the two exits.

Using geomorphic indices such as mountain front sinuosity ratio, hypsometric analysis, stream-length index value, and basin asymmetry, and other analysis such as drainage divide profile, basin shape and structural data investigations a morphotectonic evolution model of the area has been postulated. According to the model a blind thrust has resulted in the uplift of the surface from which antecedent drainages such as Matar ki Khol, Somb nadi, Pathrala nadi etc. originated. These were the first expression of the Siwalik hills in the area. It was followed by development of Pataliyon anticline giving rise to some new south flowing drainages. Three segments of the MFT have been identified. The eastward segment (i.e., Segment 3) developed first resulting in formation of Kalesar Syncline. The other two segments (1 and 2) of the MFT are probably contemporaneous. The anticline developed over these segments joined to give rise to Dhanaura anticline. The Dhanaura anticline

formed a barrier to the antecedent drainages resulting in drainage reorganization (streams joined to increase their discharge and cut through the barrier). Apart from the Dhanaura anticline, there exists an unidentified structure along which change in the magnitude of dip in the bedrock is observed. These have resulted in some local structures to which drainages have responded. Structures and drainages in the study area interacted to give rise to present day morphology.

Regional correlation of the Carbonate rocks from Ophiolitic Mélange Zone in Manipur, North East Himalaya India with Indus-Tsangpo Suture Zone of Ladakh Himalaya

Vinod C. Tewari
Scientist (Retd.), Wadia Institute of Himalayan Geology, 33 GMS Road, Dehradun 248001, INDIA
vinodt1954@yahoo.co.in

The Indo-Myanmar Orogenic Belt (IMOB) is interpreted as representing the eastern suture of Indian plate and it was formed due to the collision of the Indian plate with the Myanmar plate. The ophiolite sequence in this region is highly tectonised, dismembered and shows three phases of deformational events broadly comparable to the Himalayan orogeny and sea floor spreading of the Indian Ocean. These ophiolites are represented by dismembered mafic and ultramafic rocks with closely associated oceanic pelagic sediments and occur as folded thrust slices occupying the highest tectonic levels and are brought to lie over distal shelf sediments. The ophiolite complex is haphazardly juxtaposed along faults or they consist of lensoid slices interbedded with Disang Group of rocks. The Lower Disang sediments were intermixed with pelagic cherts and limestone. The flyschoid Disang Formation gradually merges into the post-orogenic mollassic Barail Group of rocks towards the west. The mélange zone is characterized by the occurrence of exotic blocks of varying size, fossiliferous limestone, marl, sandstone, mafic rocks and conglomerate embedded in matrix of flyschoid rocks. On the basis of faunal assemblages (radiolarian, planktonic foraminefera) in the olistolithic blocks of pelagic limestone and cherts, the Naga-Manipur ophiolites has been assigned to range in age from Upper Cretaceous to Eocene.The olistoliths are generally formed due to slope instability and deformed in a trench setting and these tectonic blocks have emplaced in the ophiolitic mélange by subduction process.

Olistoliths (exotic blocks of limestones) have been recorded from different tectonic zones of western Ladakh Himalaya, Indus-Tsangpo Suture Zone. Microbially laminated structures (microbial oncolites) are known from Dras area in Zanskar shelf associated with olistoliths and foraminifera of Cretaceous age. The limestone blocks are also found associated with olistoliths and oncolites in Lamayuru Formation (Triassic-Paleogene age). The olistolithic limestone and the foraminiferal assemblage suggest shallow marine depositional environment for both the Manipur Ophiolitic Zone and the Indus-Tsangpo Suture Zone. The Carbonates of the olistoliths within MOB show variable oxygen and carbon isotope data ranging $\delta^{18}O‰$ (PDB) from -6.29 to -11.40‰ (PDB) whereas $\delta^{13}C‰$ (PDB) show ranging from 0.89 to 2.74‰ (PDB). The $\delta^{13}C‰$ (PDB) and $\delta^{18}O‰$ (PDB) ratios of carbonates from the Manipur ophiolitic mélange zone show close similarity with the marine limestone. Their overall isotopic signatures indicate the humid and warm paleoclimatic conditions in shallow marine environment.

In the Indus-Tsangpo Suture Zone of NW Himalaya, the olistoliths from the Lamayuru Complex has yielded reworked pelagic foraminiferal limestone, brachiopods, ammonites, algae, bryozoans etc and suggest shelf to pelagic wide range of sedimentary environment. The olistoliths from Manipur Ophiolitic Mélange Zone has also suggested shallow shelf (carbonate ramp) to basin margin carbonate facies. These olistoliths might have been emplaced in the MOC due to Indo-

Myanmar tectonic process, climatic and oceanographic changes. There are two olistoliths of different ages in the ophiolitic zones of the Naga-Manipur ophiolites of Northeast India. First, the pre mid Eocene olistolith is pre-subduction related and the second olistrostromal trench contains dismembered ophiolites and olistoliths of younger mid Eocene age. The stable isotope data from the carbonates of the olistoliths indicate shallow shelf sedimentation. It is also strongly supported by the close association of Late Cretaceous-Eocene limestone and chert yielding radiolarian, small and larger foraminifera and algae. The occurrence of two ophiolite complexes accreted during Cretaceous and mid Eocene are restricted to the western part of the MOC, however the juxtaposed suture of mid Cretaceous and Late-Oligocene are found in eastern part. The pre and post Indian-Eurasian plate collision sedimentation, closing of the Neotethys ocean and the regional correlation of the western and eastern Neotethys has been discussed.

Geomorphological and climatic changes in the Chang La pass region of Ladakh Range during the Quaternary

Priyanka Joshi*, Binita Phartiyal
Birbal Sahni Institute of Palaeobotany, Lucknow 226007, INDIA
** priyanka. joshi@gmail.com*

Chang La (La=Pass; third highest pass of the world 5200 m) catchment of the Ladakh Range comes in the southwestern part of the Tibetan plateau - a cold, arid and high-altitude dessert. This Trans-Himalayan region is mountainous with river Indus and its tributaries (Shyok, Tangtse and Nubra) are seen occupying the valleys along sutures/faults *viz.* the Indus Suture Zone (ISZ), the Shyok Suture Zone (SSZ) and the Karakorum Fault (KF). The region lies in the rain shadow of NW Himalaya having an arid to hyper arid climate and dry steppe vegetation. Being a cold arid desert and only receives precipitation during winter months (December-March) due to westerly disturbances that originate in the Mediterrainean, Caspian and Black seas. This mountain range is ~570 km long with parts in Tibet, India and Pakistan, separating the Indus and the Shyok valleys in the downstream side, the Tangtse and Indus valley in the middle stretches and cut by River Indus at near Nyoma and Loma (upstream) where the river is seen flowing north of this range. The rock type exposed belongs to the Ladakh Range (Ladakh batholith) and Shyok Suture Zone.

The Chang La area is a typical glaciated area with the snow cover during winter months and only at the summit and passes during the summer time. Erratics, huge boulders, moraines, enormous amount of rock debris and wide valleys with flat areas are seen. Three streams join to make the main Changla stream. There are some pro-glacial lakes present in this region which are spotted in the area, although there is no such glacier in the area as of today. Two lakes are seen (towards the eastern side) of the pass at an altitude of 4983 m and 4853 m respectively. Five patches of dry lake sediments are seen placed over a moraine between 4737-4707 m levels. These patches have ~190 cm of buff coloured clay, silt and sand layers. Centimeter scale organic layers, drop-stones and scattered pebbles (bottom) are seen. The base is gritty and the moraine deposit is seen after 190 cm. The highest lake at Tsoltak shows decreasing lake levels with water at only some patches of the wide flat area. The thickness of the sediments is 150 cm with two permafrost layers, one at 65-80 cm from the top and the second 105 cm from the top to the base. The top layer shows mottling and melting during the summer months while the second layer is hard, black and indicates a permanent frost zone. Another lake at 4835 m at the outlet of the first lake is joined by another stream which hosts a pro-glacial lake at 5225 m. Here the permafrost is seen at 85 cm from the top. This too shows signs of decreasing water levels. Diatoms frustules in the camebian tests have been recently reported from this lake (Farooqui et al., 2015). These lakes drain off in form of Chang La stream which becomes narrower and flows in a gorge before joining the Tangtse River, a tributary of the Shyok River.

The other part of the water divide of this pass drains into the River Indus with lake Zhingral (4764 m) which is also seen over an ancient moraine deposits. It is a rocky lake with very little sediment, fed by small streams and rivulets coming from the western side of the Chang La pass. Being a high-altitude and a cold dessert, enormous amount of unconsolidated sediment (generated due to frost action/physical weathering) lies loose on the high-angled slopes and the valley floor damming the drainage and forming lakes. The glaciers are absent from the region but the moraines and these lakes can tell us about the glacial history of these areas through time. Our ongoing studies from these lakes will throw light on the changing geomorphology of the region as well as the climatic variations that have occurred in this area through time.

Farooqui, A., Aggarwal, N., Jha, N., Phartiyal, B. 2015. International Journal of Current Microbiology and Applied Sciences, v(7), 472-485.

Trilobite fauna of Cambrian Series 2 (Stage 4) - Series 3 (Stage 5) boundary from the Parahio Valley (Spiti), Northwest Himalaya, India

Birendra, P. Singh[1], Nancy Virmani[1], O.N. Bhargava[2], Naval Kishore[1], Aman Gill[1]
[1]Center of Advanced Study in Geology, Panjab University, Chandigarh160014, INDIA
[2] INSA Honorary Scientist, 103, Sector-7, Panchkula 134109, INDIA

Globally, the First Appearance Datum (FAD) of *Oryctocephalus indicus* is considered to be a good point to define a GSSP by the International Subcommission on Cambrian Stratigraphy (Sundberg et al., 1999; Geyer & Shergold, 2000; Sundberg et al., 2011) and can be used for defining the base of the as yet unnamed Series 3 (Stage 5) of the Cambrian system (Yuan et al., 1997; Sundberg et al., 1997; Zhao et al., 2001; Peng & Babcock, 2005; Babcock et al., 2005, Sundberg et al., 2011, Geyer & Peel, 2011; Peng et al., 2012 GTS). In the Himalaya, the *Oryctocephalus indicus* has been known from the Parahio valley section (Spiti) but its stratigraphical range (FAD and LAD) is not established (Hayden, 1904; Reed, 1910; Jell & Hughes, 1997; Peng et al., 2009; Singh et al., 2014). Peng et al., (2009) stated that *Oryctocephalus indicus* level, which constitutes the lowest trilobite level of Reed (1910) in the Parahio valley, is no older than the base of yet unnamed Cambrian Stage 5 (Series 3). Though, Peng et al., (2009) could not locate the *Oryctocephalus indicus* level in the Parahio Valley and Sumna khad sections, they "projected" this level to be at 200 m from the base of the Parahio Valley section (Peng et al., 2009).

In the present work we demarcate the base of the Cambrian Series 3 (Stage 5) or Cambrian Series 2 (Stage 4) - Series 3 (Stage 5) boundary in the Parahio valley section (Spiti) and also the stratigraphic range of the *Oryctocephalus indicus* Zone. The studied section lies north of the Parahio River along the steep slope exposed on left bank of the Parahio River near the Maopo encamping ground, Parahio Valley, Spiti. The section is an ideal candidate for demarcation of the Cambrian Series 2 (Stage 4) - Series 3 (Stage 5) or "Lower-Middle" Cambrian boundary as it bears FAD and LAD of the globally important taxon *Oryctocephalus indicus.* Along this section the Kunzum *La* (=Parahio) Formation is more than 700 m thick, though we measured only 280 m of the section from the lowest exposed rocks in this section. Within 280 m of this section, 18.2 m thick succession from the base yielded the faunal elements of the basal part of the Cambrian Series 3 (Stage 5), stratigraphic range (FAD and LAD) of *O. indicus* and the Cambrian Series 2 (Stage 4) - Series 3 (Stage 5) boundary. The basal most rock exposed along this section is a thick medium to coarse grain sandstone unit (7.38 m thick), overlain by the thin layer of argillaceous limestone unit (0.36 m; carbonate-shale mix). Upward the section is dominated by bluish-grey shale (4.64 m) succeeded by an alternating siltstone-sandstone unit (5.82 m). The Cambrian Series 2 (Stage 4) - Series 3 (Stage 5) boundary is placed at the FAD of the *Oryctocephalus indicus* which lies at 7.74 m from the base of the above referred section. *Eosoptychoparia* (*Danzhaina*) sp., and *Danzhaiaspis* sp., are recorded for the first time from the Cambrian of the Indian Himalaya and they emerged with *Pagetia significans* and *O.*

indicus from the base of the Cambrian Series 3 (Stage 5). The FADs of taxon *Pagetia* and *Kunmingaspis* predates the FAD of *O. indicus* along the Parahio valley section. More than five species of *Pagetia* are recognised along the section. *Pagetia* ranges from Cambrian Series 2 (Stage 4) to Cambrian Series 3 (Stage 5) and its occurrence in Parahio valley section is consistent with the global occurrences. The taxon *Kunmingaspis* and *Pagetia* are long ranging. We propose the Parahio Valley as a reference section for the GSSP of the base of the Cambrian Series 3.

Babcock, L.E., Peng, S., Geyer, G., Shergold, J.H. 2005. Geoscience Journal, 9, 101-106.
Geyer, G., Peel, J.S. 2011. Bulletin of Geosciences, 86(3); 465 - 534.
Geyer, G., Shergold, J. 2000. Episodes, 23, 188-195.
Hayden, H.H. 1904. Memoirs of the Geological Survey of India, 36, 1-121.
Jell, P.A., Hughes, N.C. 1997. Special Papers in Palaentology, 58, 1-113.
Peng, S., Babcock, L.E. 2005. Journal of Stratigraphy, 29: 92, 93, 96. (In Chinese with English title).
Peng, S., Babcock, L.E., Cooper, R.A. 2012. In: Gradstein, F., Ogg, J. & Smith, A. (eds), Geological Time Scale-2012. Cambridge University Press, 1-590.
Peng, S., Hughes, N.C., Heim, N.A., Sell, B.K., Zhu, X., Myrow, P.M., Parcha, S.K. 2009. Paleontological Society Special Publication, 6, 1-95.
Reed, F.R.C. 1910. Palaentologia Indica, 21, 1-38.
Singh, Birendra, P., Virmani, N., Bhargava, O.N., Kishore, N., Gill, A., 2014. Journal Paleontological Society of India, 59(1), 81-88.
Sundberg, F.A., Mccollum, L.B. 1997. Journal of Paleontology, 71,1065-1090.
Sundberg, F.A., Yuan, J.-L., Mccollum, L.B., Zhao, Y.-L.1999. Acta Palaeontologica Sinica, 38, 102-107.
Sundberg, F.A., Zhao, Y.L., Yuan, J.L., Lin, J.P. 2011. Bulletin of Geosciences, 86(3), 423-464
Yuan, J.-L., Zhao, Y.-L., Wang, Z.-Z., Zhou, Z., Chen, X.-Y., 1997. Acta Palaeontologica Sinica, 36(4), 494-524. [in Chinese with English abstract]
Zhao, Y.-L., Yuan, J.-L., Peng, J., Yang, Y.-N. 2011. In: Hollingsworth, J.S., Sundberg, F.A., Foster, J.R. (eds), Cambrian Stratigraphy and Paleontology of Northern Arizona and Southern Nevada. Museum of Northern Arizona Bulletin, 67.

Multi-proxy provenance record of Cenozoic exhumation along the flanks of the eastern Qaidam basin, northern Tibetan plateau

Brian K. Horton[1]*, Meredith A. Bush[2], Joel E. Saylor[3], Junsheng Nie[4]
[1]Dept. of Geological Sciences and Institute for Geophysics, Jackson School of Geosciences, University of Texas at Austin, Austin, TX 78712, USA
**horton@jsg.utexas.edu*
[2]Dept. of Geological Sciences, Jackson School of Geosciences, University of Texas, Austin, TX 78712, USA
[3]Dept. of Earth and Atmospheric Sciences, University of Houston, Houston TX 77204-5007, USA
[4]MOE Key Laboratory of Western China's Environmental Systems, College of Earth and Environmental Sciences, Lanzhou University, Lanzhou 73000, CHINA

Application of multiple provenance techniques to Cenozoic clastic fill of the eastern Qaidam basin helps define the exhumation histories of distinctive source regions in the flanking ranges of the northern Tibetan plateau. Along the northeastern basin margin, a detrital record of protracted subsidence, uplift-induced exhumation, and basin isolation is preserved in the ~6 km thick Cenozoic succession within the Dahonggou anticline. Temporal shifts among fluvial and subordinate lacustrine systems record long-term progradation of basin-margin deposystems and increasingly proximal sediment sources that reflect the activation and basinward advance of upper crustal deformation. Sediment provenance results from U-Pb geochronology, sandstone petrology, and heavy mineral analyses suggest initial late Paleocene-early Eocene derivation from igneous, metamorphic, and sedimentary sources, consistent with the Permian-Triassic magmatic-arc rocks that dominate the

southern (Kunlun Shan) and western (Altyn Shan) basin margins. Upsection provenance variations are attributed to middle Eocene-Oligocene derivation from early Paleozoic and Mesozoic igneous and metamorphic rocks to the north in the central to northern Qilian/Nan Shan. The progressive reduction of igneous sources and persistence of metamorphic sources is consistent with derivation from newly activated northern source areas in the southern Qilian/Nan Shan during early-middle Miocene shortening along the frontal Nan Shan-North Qaidam thrust belt. These results are supported by paleocurrent analyses revealing an early Eocene shift from roughly axial to transverse (from east-directed to southwest-directed) dispersal of sediment. Variations in lithofacies, composition, U-Pb ages, and paleoflow are consistent with late Paleocene-early Eocene exhumation along the southern basin margin during earliest Kunlun Shan uplift followed by middle Eocene and younger exhumation to the north in the Qilian/Nan Shan. The upsection disappearance and reappearance of diagnostic U-Pb age populations can be attributed to the successive input of sedimentary and magmatic sources during drainage reorganization and progressive unroofing of multiple thrust sheets that record basinward (southward) encroachment of Qilian/Nan Shan shortening into the Qaidam Basin.

Tectonic and topographic control over erosion in the Arunachal Himalaya

Vikas Adlakha[1*], Akhil Kumar[2], R.C. Patel[2], Nand Lal[2]

[1]Wadia Institute of Himalayan Geology, 33 GMS Road, Dehradun 248001, INDIA

** vikas.himg@wihg.res.in*

[2]Department of Geophysics, Kurukshetra University, Kurukshetra 136119, INDIA

Radiometric thermochronological dates provides estimate about the long-term exhumation rates, the patterns of which can be assessed with respect to structure, geomorphic and climatic records to unravel the evolution of the landscape on millennial time scale (Reiners and Brandon, 2006). Arunachal Himalaya, the area which has undergone intense deformation during its evolution (Kumar, 1997) and is strongly affected by monsoon climate since Miocene (Dettman et al., 2001; 2003; Bookhagen and Burbank, 2010) forms a suitable geological cite to understand landscape evolution in terms of Tectonics, Climate and Erosion. A total of forty six apatite fission track (AFT) cooling ages, thirty nine from western Arunachal Himalaya (Adlakha et al., 2013) and seven new AFT ages from Higher Himalayan Crystallines in the central Arunachal Himalaya reveal marked variations in millennial scale erosion rates. In western Arunachal Himalaya, the AFT ages in the Higher Himalayan Crystallines (HHC) range from 1.3±0.1 to 2.9±0.3 Ma, while in the central Arunachal Himalaya these ages range from 5.0±0.8 to 17.6±2.5 which reveal an interesting along strike variation in exhumation rates of HHC in the Eastern Himalaya. The AFT cooling ages in the Lesser Himalayan Sequence (LHS), western Arunachal range from 5.7±0.6 to 13.3±1.4 Ma and are similar in range with the HHC of central Arunachal Himalaya. Exhumation Rates in the HHC of the central Arunachal Himalaya range from 0.17 to 0.58 mm/a since ~12 Ma.

The data reveals: (i) a distinct correlation of topography and erosion, (ii) out-of-sequence faulting in the western Arunachal Himalaya and window zone formation in central Arunachal Himalaya at ~6 Ma ago, (iii) a poor correlation of precipitation and erosion. Despite the interplay between the tectonic rock uplift and surficial erosion by climatic precipitation for landscape denudation in active orogens, we suggest here a prime control of tectonics for the evolution of landscape in the Eastern Himalaya.

Adlakha, V., Lang, K.A., Patel, R.C., Lal, N., Huntington, K.W. 2013. Tectonophysics, 582, 76-83, doi:10.1016/ j.tecto.2012.09.022.

Bookhagen, B., Burbank, D.W. 2010. Journal of Geophysical Research, 115, F03019, doi:10.1029/2009JF001426.
Dettman, D.L., Kohn, M.J., Quade, J., Ryerson, F.J., Ojha, T.P., Hamidullah, S. 2001. Geology, 29, 31-34.
Dettman, D.L., Fang, X.M., Garzione, C.N., Li, J.J. 2003. Earth and Planetary Science Letters, 214, 267-277.
Kumar, G. 1997. Geological Society of India Publication, Bangalore, 217 p.
*Reiners, P.W., Brandon, M.T.2006. Annual Review of Earth Planetary Science, **34**, 419-466.*

Stable isotopic studies of the Early Pleistocene pedogenic nodules and gastropod shells from the Pinjor Formation of the Upper Siwalik Subgroup exposed in the vicinity of Panchkula (Haryana)

Simran Singh Kotla[1], Rajeev Patnaik[1], Ramesh Kumar Sehgal[2], Aditya Kharya[2]
[1]C.A.S in Geology Panjab University, Chandigarh 160014, INDIA
[2]Wadia Institute of Himalyan Geology, Dehradun 248001, INDIA

The Early Pleistocene is marked by severe climatic fluctuations all over the world. This was the time when several mammalian dispersal events took place including those of our own ancestors. In India, the well dated highly fossiliferous Pinjor Formation represents Early to Middle Pleistocene time interval. A 6 m swamp/pond deposit representing ~12,000 yrs, belonging to the Pinjor Formation exposed near the village Nadah, Panchkula (Haryana) was subjected to high resolution (35 samples of pedogenic nodules and gastropods at about 15-17 cm interval) stable isotopic study (carbon and oxygen isotope). The samples were powdered and analyzed using Continues Flow Isotope Ratio Mass Spectrometer (CF-IRMS) at the Wadia Institute of Himalayan Geology, Dehradun (India). According to Azzaroli and Napoleon (1982), the age of the studied section (swamp/pond) is about 1.8-2 Ma. The $\delta^{13}C$ value of pedogenic nodules is between -6.3 to 1.9‰ VPDB. The enrichment of ~15‰ in $\delta^{13}C$ values of pedogenic nodules (soil carbonate) with respect to the soil respired CO_2 due to fractionation from gaseous diffusion and equilibrium exchange between two phases (soil carbonate and soil respired CO_2).Whereas, the average $\delta^{13}C$ values of gastropod shell is -0.6‰ VPDB ±2.0‰ (with enrichment 14-15‰). The stable carbon isotopic values of pedogenic nodules as well as gastropod shell suggest the dominance of C4 vegetation in the Early Pleistocene. The $\delta^{18}O$ value of pedogenic nodules and gastropod shell is 24.4‰ VSMOW ±1.4‰ and 26.6‰ VSMOW ±3.7‰, respectively (with an enrichment of 14-15‰ due to fractionation) indicating presence of warm and humid climatic condition. The Carbon and oxygen isotopic ratios are expressed relative to the Vienna Pee Dee Belemnite (VPDB) and Vienna Standard Mean Ocean Water (VSMOW) respectively, using the standard notation (δ) of ‰ (permil). The precision of carbon and oxygen isotope ratio measurement in carbonate phase is ±0.1‰.

This is first ever data set from the Pinjor Formation being presented here to understand the Pleistocene climate and vegetations changes and their bearing on the mammalian dispersals and extinction.

Traces fossils of *Scoyenia* ichnofaceis from the Pinjor Formation (Pliocene), Nadah locality, Siwalik foothills

Ravi. S. Chaubey*, Birendra P. Singh
Department of Geology, Panjab University, Chandigarh 160014, INDIA
** ravischaubey@hotmail.com*

The fluvial Siwalik Group (>7000 m) in foothills of Himalaya comprises of freshwater molasse sediments and ranging in age from early Miocene (18 Ma) to middle Pleistocene (0.7 Ma)

(Patnaik, 2003). We recorded trace fossils of *Scoyenia* ichnofacies (Seilacher, 1967) from the Pinjor Formation (Siwalik Group) exposed near the Ghaggar River along the road leading to village Nadah. The studied section belonged to Pliocene age (1.8 Ma) (Tandon et al., 1984) and well known for their faunal and floral assemblages i.e rodents, gastropods, ostracods, pollens-spores and charophytes (Patnaik, 2003; Bhatia, 1996, 1999; Rao & Patnaik, 2001). The trace fossil assemblages recorded in the present studies include ichnogenus *Beaconites*, *Cylindrichum, Fuersichnus, Sagittichnus*, *Scoyenia, Steinichnus* and *Taenidium*. Integration of physical sedimentology and ichnology is used for paleoenvironmental interpretation. The dominance of horizontal traces of deposit feeders and abundant meniscate burrows indicates low-energy setting preferably of fluvial (flood plain and crevasse splays) and lacustrine systems. The low to moderate ichnodiversity and localized high abundance indicate the *Scoyenia* ichnofacies of continental deposit.

Bhatia, S.B., 1999. India. Aust. J. Bot. 47, 49-74.
Bhatia, S.B., 1996. Palaeogeographic and Palaeoecologic implications. Pub. C.A.S. 5, 99-106.
Patnaik, R., 2003. Palaeo, Palaeocli, Palaeo, 197, 133-150
Rao, M.R., Patnaik, R., 2001. Palaeobotony 50,267-286. Seilacher, A., 1967.
Tandon, S.K., Kumar, R., Koyama, M., Nitsuma, N., 1984. J. Geol. Soc. India 46, 429-437.

Nepal Earthquake 2015: it's tectonic implication

Santanu Baruah*, Manoj K. Phukan, Saurabh Baruah, Ranju Duarah
Geoscience Division, CSIR-NE Institute of S&T, Jorhat 785006, INDIA
**santanub27@gmail.com*

The seismotectonics of Nepal Himalaya has been examined using the broadband waveform data of the Mw 7.8 Nepal earthquake of 25th April, 2015 and its major aftershock which occurred of Mw 7.3 of 12th May, 2015. The fault plane solutions for these events were derived using the broadband data of NEWSN, CSIR-NEIST Jorhat. The northerly dipping E-W trending nodal plane is found to be the causative fault plane which coincides with the MBT. Attempt is also made to examine the spatial changes to the local stress field resulting from the 25th April, 2015, Mw 7.8 Nepal earthquake. Results indicate an apparent clustering of aftershocks slightly westward of the main thrust, which is consistent with the modeled zone of promoted normal failure. Using existing models, we found a high number of aftershocks to be consistent with triggering by the mainshock, suggesting that static stress is a dominant control in the months following a large earthquake in this area.

Late Quaternary Fluvial deposits and Landscape evolution along the Yamuna River: Implications to peripheral forebulge tectonics of Ganga plain

Rupa Ghosh[1]*, Pradeep Srivastava[1], U.K. Shukla[2], R.K. Sehgal[1], R. Islam[1], Pankaj Srivastava[3]
[1]Wadia Institute of Himalayan Geology, 33 GMS Road, Dehradun 248001, INDIA
**rupaghosh2006@gmail.com*
[2]Departament of Geology, Banaras Hindu University, Varanasi 221005, INDIA
[3]Department of Geology, University of Delhi, Delhi 110007, INDIA

Ganga basin is a foreland basin formed in response of collision of Indian and Eurasian plates. The sediments deposited in this basin are sourced from Himalaya and peninsular region. The Yamuna River, a Himalaya bound river, drains through the southern Ganga Plain where it is joined by several cratonic tributaries. Dissected ravines and deeply incised gullies along Yamuna, Betwa and Dhasan, a

characteristic feature of this region provide good opportunity to study the past depositional environment and its interaction with climate and tectonics of the forebulge. Therefore in this study efforts are made to (i) map the litho-sections and understand the sedimentary style and role of bulge tectonics, and (ii) calculate the rate of sediment erosion in response to the ravine forming processes. The studied sections show a regional pedogenic surface at the base which traversed by conjugate set of calcrete filled fractures. Besides field based observations the occurrence of paleosol is confirmed using geochemical proxies (CIA) and micromorphology. Sitting unconformably on this is a cratonic sourced large scale cross bedded gravel unit. This unit also yielded a fossil skull of elephant (*Elephas hysudricus*) and several vertebrate fossils, molar fragments. The luminescence age of this units ranges from 100-60 ka making paleosol >100 ka. The age of the uppermost youngest horizon of cliff sections is 11 ka. We believe that the paleosol horizon marks the tectonic activity along the peripheral bulge which is followed by wet and warm climatic conditions depositing gravels sourced from already uplifted peripheral bulge between 100-60 ka. Topographic characteristic of ravines was derived from Cartosat-1 based DEM using ArcGIS tools and in conjunction with the chronology the rate of erosion due to ravine process was calculated for time scale of 10^4 yrs.

Paleocene-early Eocene high elevation of the Linzizong Arc and Crustal Mass Balance implications for large-scale subduction of Continental crust during Himalayan collision

Miquela Ingalls[1], David B. Rowley[1]*, Brian Currie[2], Shanying Li[2], Gerard Olack[1], Ding Lin[3], Albert Colman[1]

[1]The University of Chicago, Department of the Geophysical Sciences, 5734 S. Ellis Ave, Chicago, IL 60637, USA

**drowley@uchicago.edu*

[2]Miami University, Department of Geology, 620 E. Spring St, Oxford, OH 45056, USA

[3]Institute for Tibetan Plateau Research, Chinese Academy of Sciences, Beijing, CHINA

We reconstruct the ~55 Ma paleo-elevation of the pre- to syn-collisional Linzizong arc by coupling carbonate-derived oxygen stable isotope measurements ($\delta^{18}O_c$) with paleotemperatures derived from the Δ_{47}-'clumped' isotope paleothermometer ($T(\Delta_{47})$). We estimate a pre- to early syn-collisional (~54±2 Ma) paleo-elevation of the Penbo/Linzhou region of >4100±550 m. This provides the first well-constrained elevation estimate of the pre-collisional Linzizong volcanic arc in the southern Tibetan Plateau. Our results indicate that high relief at low latitude prevailed on the Asian margin confirming previous inferences based on field geological observations. We perform numerical calculations of post-collisional crustal mass balance using the pre-collisional elevation and crustal thickness, and the recently reconsidered diachronous collisional age of India-Eurasia, together with up to date global plate kinematic constraints that all integration of the mass flux as a function of time. We find that ~50% of the collision-related crustal mass cannot be accounted for by the mass preserved in excess crustal thickness (in Himalaya, Tibet, and adjacent Asia), Southeast Asian tectonic escape, and exported eroded sediments. This implies large-scale subduction of continental crust, amounting to ~15% of the total oceanic subduction flux since 56 Ma during this continent-continent collision. Contamination of the mantle by direct input of continental crustal materials rather than crust-derived sediments may be more significant than previously thought and may be responsible for crustal geochemical anomalies in mantle-derived melts.

Fluid-rock interaction: the isotope perspective

Igor M. Villa
Institut für Geologie, Universität Bern, 3012 Bern, SWITZERLAND
Centro Universitario Datazioni e Archeometria, Università di Milano Bicocca, ITALY

Fluid-rock interactions can manifest themselves with a great variety of effects, from engineering geology and water resource management to petrology.

Among the geophysical and geochemical techniques suited to study the influence of water on minerals and rocks, the use of stable and radiogenic isotopes have an important role. Oxygen isotope ratios ($\delta^{18}O$) provide constraints on the paleoclimatic signature of surface waters, but also on the provenance of hydrothermal waters in alteration zones. In turn, faults that acted as conduits for fluid ingress can be better understood if the $\delta^{18}O$ of the authigenic gauge rocks is taken into account.

Radiogenic isotopes (Sr, Pb, and Ar) can also contribute to the fingerprinting context. Especially stepwise leaching of hydrothermally altered minerals is able to trace the extent of recrystallization and the source of the circulating fluids. Feldspar minerals are especially prone to interaction with aqueous fluids, and imaging (back-scattered electrons, cathodoluminescence, transmission electron microscopy, etc.) can suggest a sample choice that maximizes the information on the hygro-chronologic evolution of a rock.

Slope instability and geotechnical characteristics of the slope materials along the Mansa Devi Hill bypass road, Haridwar Township

Ruchika S. Tandon[1]*, B. Venketeshwarlu[1], Vikram Gupta[2], Rajesh Sharma[1,2]
[1]National Geotechnical Facility, 11-C, Circular Road, Dehradun 248001, INDIA
[1]ruchika_ddn@yahoo.co.in
[2]Wadia Institute of Himalayan Geology, 33 GMS Road, Dehradun 248001, INDIA

Mansa Devi Hill Bypass (MDHB) road was constructed during 1958 on the slope of the Mansa Devi Hill to negotiate the traffic in a famous holy place, Haridwar. The road runs at an elevation ranging between 300 and 396 m asl and is about 12 km long on the Mansa Devi Hill slope having a relief of about 277 m. The Mansa Devi Temple is located at the top of the hill, whereas a dense network of commercial and industrial area is located towards its base. A rail-route connecting the township also runs to the close proximity of the hill.

Every year, a number of small scale isolated landslides and rock fall reported during monsoon period along this road. A major landslide occurred in the area during 1998 termed as "Mansa Devi Landslide" that damaged a cumulative stretch of 1000 m of bypass road and also blocked the railway route. Therefore, it is extremely important to identify and demarcate zones that are vulnerable to landslide and to quantify the geotechnical properties of rocks and soil constituting the Mansa Devi Hill. This will help to plan for corrective measures so as to minimize the effect of the landslides present along the MDHB road.

The present study reveals the presence of seven vulnerable zones along MDHB road that have been identified based on adverse joint conditions, high rate of weathering, road subsidence and tensional cracks on the hill slope. The soil/rock samples were analyzed to characterize the geotechnical properties of slope materials. The laboratory test confirms the soil having low cohesion and high permeability and classify as 'clayey-silt' with high plasticity. The rock exposed in the area ie sandstone and mudstone classify as weak rocks having unconfined compressive strength is >22 MPa.

It has further been noted that most of the vulnerable zones are located dominantly where the MDHB road is aligned on the weaker mudstone. Since mudstone weathers very easily on coming in contact with water, as revealed by the slake durability index, it is utmost important to realign the road at certain places, and a proper drainage network is to be installed on the slope, so as to minimize the ingress of water into the slope. This will help to reduce the landslide hazard along the MDHB road.

Tectonic and metamorphic discontinuities in the Greater Himalayan Sequence in Central Himalaya: insights from natural examples and numerical modelling

R. Carosi[1], C. Montomoli[2], S. Iaccarino[2], A. Piccolo [3], M. Faccenda[3], D. Visonà[3]

[1]Dipartimento di Scienze della Terra, University of Torino, ITALY

[2]Dipartimento di Scienze della Terra, University of Pisa, ITALY

[3]Dipartimento di Geoscienze, University of Padova, ITALY

The Greater Himalayan Sequence (GHS) is the main metamorphic unit of the Himalayan belt, stretching for ~2400 km, bounded to the South by the Main Central Thrust (MCT) and to the North by the South Tibetan Detachment (STD) whose contemporanous activity controlled its exhumation between 23 and 17 Ma (Godin et al., 2006). Several shear zones and/or faults have been recognized within the GHS, usually regarded as out of sequence thrusts. Recent multitechiques investigations in the GHS in Central-Eastern Himalaya allowed the authors to identify two different levels of tectonic and metamorphic discontinuities, above the MCT, both characterized by a top-to-the SW sense of shear (Carosi et al., 2010; Montomoli et al., 2013, 2014; Iaccarino et al., 2015): a higher (Kalopani and Tyar shear zones) and a lower tectono-metamorphic discontinuity (Higher Himalayan Discontinuity: Montomoli et al., 2014). U-Th-Pb in-situ monazite ages provide ages of initiation at ~36 Ma of the upper tectonic and metamorphic discontinuity and at 26-24 Ma for the lower one, continuing up to ~17 Ma. Data on the P and T evolution testify that these shear zones affected the tectono-metamorphic evolution of the belt and different P and T conditions have been recorded in the hanging-wall and footwall of the discontinuities. The GHS is consequently divided into three tectonic sub-units and peak metamorphisms were reached in different times in each sub-unit. When the mid unit underwent prograde meamorphism the upper one underwent exhumation by activation of the upper discontinuity. When mid unit was exhumed by activation of the lower discontinuity the lower one underwent prograde metamorphism. All the GHS underwent exhumation during the activation of the MCT.

The actual proposed models of exhumation of the GHS, based exclusively on the MCT and STD activities and considering the GHS as a single tectonic unit, are not able to explain the occurrence of the Higher Himalayan discontinuity and other older in-sequence shear zones. Any model of the tectonic and metamorphic evolution of the GHS should account for the occurrence of the tectonic and metamorphic discontinuities within the GHS and its consequences on the metamorphic path. The channel flow model proposed by Beaumont et al. (2001) implies a coherent exhumation of the GHS due to the focused monsoonal erosion acting on the southern flank of the Himalayas. However, channel flow model is not consistent with the occurrence of the several tectono-metamorphic discontinuites within the GHS, indicating a sequential exhumation of different GHS sub-units (Montomoli et al., 2013, 2014; Iaccarino et al., 2015).

We have numerically simulated the interaction between surface and exhumation processes in post-subduction collisional orogens. Two kinds of collisional orogens are obtained: asymmetric and symmetric ones. Asymmetric collisional orogens feature the occurrence of a channel flow-like behaviour, high crustal temperatures and exhumation of partially molten rocks, while symmetric orogens features lower crustal temperatures and different patterns of exhumation. The asymmetric

models have been chosen to test the influence of surface processes. By taking a fixed value of focused erosion rate, the timing of the focused erosion and sedimentation rate are independently varied. The results give several insights: 1) focused erosion is not a necessary condition for the exhumation of the partially molten rocks; 2) timing of the focused erosion controls the dynamics of the channel flow and, consequently, the exhumation processes; 3) the sedimentation rate may induce first order modifications on the evolution of the orogeny; 4) sequential exhumation of high grade metamorphic sub-units is achieved when the focused erosion is activated at the final stage of the collision.

Beaumont, C., Jamieson, R.A., Nguyen, M, Lee, B. 2001. Nature, 414, 738-742.
Carosi, R., Montomoli, C., Rubatto, D., Visonà,, D. 2010. Tectonics 29, TC4029.
Godin, L., Grujic, D., Law, R.D., Searle, M.P. 2006. Geol. Soc. London. Sp. Publ., 268, 1-23.
Iaccarino, S., Montomoli, C., Carosi, R., Massone, H-J, Lamgone,, A., Visonà, D., 2015. Lithos, 231, 103-121.
Montomoli, C., Carosi, R., Iaccarino S. 2014. In: Mukherjee, S., Carosi R., Mukherjee B.K., Robinson D., van der Beek P. (eds), Tectonics of the Himalaya. Geol., Soc. London Special Publication, 412.
Montomoli, C., Iaccarino, S., Carosi, R., Langone, A., Visonà, D. 2013. Tectonophysics, 68, 1349-1370.

Monazite U-Pb age and fluid inclusion of cordierite migmatite in far-eastern Nepal

Takeshi Imayama[1]*, J. Yamamoto[2], T. Takeshita[3], K. Takahata[2], K. Yi[4]
[1]Dept. of Earth and Environmental Sciences, Chonbuk National University, Jeonju, 561-756, SOUTH KOREA
**t.imayama@gmail.com*
[2]The Hokkaido University Museum, Sapporo, 060-0810, JAPAN
[3]Dept. of Natural History Sciences, Hokkaido University, Sapporo, 060-0810, JAPAN
[4]Geochronology Team, Korea Basic Science Institute, Chungbuk, 363-883, SOUTH KOREA

Cordierite migmatites of the upper High Himalaya Crystalline Sequence in far-eastern Nepal was investigated. The petrography and microstructure show that the migmatites were formed by biotite dehydration melting (biotite + sillimanite + plagioclase + quartz → cordierite + garnet + K-feldspar + melt) during the early decompression stage of the upper HHCS. Secondary cordierite replacing garnet was formed during decompression or cooling. P-T pseudosection yields the peak P-T condition of P = ca. 5.5 kbar and T = ca. 800°C. Raman spectrometry analyses of fluid inclusions suggest that the H_2O-rich fluids were trapped in garnet during biotite dehydration melting, whereas CO_2-rich fluid were trapped or modified in quartz during decompression or cooling. Retrograde pressure condition calculated by CO_2 density and CO_2/H_2O ratio of fluid inclusions in quartz is 3-4 kbar at 650-800°C. Monazites include cordierite, biotite, K-feldspar, plagioclase, sillimanite, and quartz. Monazites U-Pb ages obtained by SHRIMP yields the age range from 27 to 14 Ma, with the cluster of ages at 25 Ma. The ca. 25 Ma is interpreted as the timing of biotite dehydration melting. These data suggest that the cordierite migmatites in far-eastern Nepal are accompanied by Early Oligocene low-pressure anatectic processes, and prolonged high temperature metamorphism of the upper HHCS might be continued during exhumation until 14 Ma.

Lithium isotopes as a tracer for silicate weathering in the Ganga basin

Waliur Rahaman[1, 2], Friedhelm von Blanckenburg[1], Jan A. Schuessler[1]
[1]*GFZ German Research Centre for Geosciences, Potsdam, GERMANY*
[2]*ESSO-National Centre for Antarctic & Ocean Research, Goa, INDIA*

Lithium (Li) stable isotopes have been successfully used as a proxy for silicate weathering. The advantage of this proxy is that Li is primarily derived from weathering of silicate rocks (Kısakűrek et al., 2005; Millot et al., 2010) and does not participate in biotic processes (Lemarchand et al., 2010). In previous studies, reconstruction of marine Li isotope records were assessed (Hathorne and James, 2006; Misra and Froelich, 2012). They show steady increase in δ^7Li since the late Cenozoic. This increase has been attributed to the uplift of the Himalaya. Thereby an increase in denudation and shifting of the weathering regime from transport limited (flat topography) to weathering limited (mountain) regime occurred (Misra and Froelich, 2012). In a subsequent study by Pogge von Strandmann and Henderson (2015) this interpretation was challenged. These authors suggested instead that the steady increase of δ^7Li reflects enhanced production of secondary minerals in the flood plain, rather than weathering in mountains.

To resolve these issues, we carried out a systematic study of Li isotopes in the modern day Himalayan river basins. As on today, only a single study is available (Kısakűrek et al., 2005) restricted to the mountain region of the Nepal Himalaya. We measured Li isotopes in the Ganga river system (main stream and major tributaries) draining from the Himalaya to the plain in all three compartments (water, suspended and bed sediments). The Ganga river system drains through diverse geomorphic and tectonic settings with variable climate, and therefore, Li isotope study in the Ganga basin provides a unique opportunity to better understand Li isotope fractionation and its controlling factors.

Inverse model calculation based on our data shows that dissolved Li is primarily derived from silicate rocks. However, contributions from evaporites and dissolution of saline/alkaline soil are also contributing in the plain. The dissolved riverine δ^7Li shows a large range from 12.9 to 22.6‰. The isotope values show a systematic increase from upstream in the Himalaya at Rishikesh to the final out flow in the plain at Manikchak (Fig. 1). This observation is consistent with the decrease of δ^7Li in its counter phase (particulate river loads). This indicates that Li isotope fractionation during weathering and river transport is responsible for the observed spatial evolution of δ^7Li along the Ganga river system.

Remarkably, dissolved δ^7Li values show a nonlinear relation with denudation rate and weathering intensity. This observation is consistent with the prediction derived in the model of Bouchez et al. (2012). The lower δ^7Li values are observed both in the areas of higher denudation (weathering-limited regime) and lower denudation (transport-limited regime) rates, whereas the highest values are observed in intermediate geomorphic regions with moderate weathering intensity and denudation rates. Our study demonstrates a link between the Li isotope proxy and the weathering regime in modern river basins. Hence, we can improve the understanding of the controlling factors of Li isotopes fractionation during weathering. This has important implications for the unequivocal interpretation of the late Cenozoic oceanic δ^7Li records.

Bouchez, J., von Blanckenburg, F., Schuessler, J.A. 2013. American Journal of Science, 313, 267-308.
Hathorne, E.C., James, R.H. 2006. Earth and Planetary Science Letters, 246, 393-406.
Kısakűrek, B., James, R.H., Harris, N.B. 2005. Earth and Planetary Science Letters, 237, 387-401.
Lemarchand, E., Chabaux, F., Vigier, N., Millot, R., Pierret, M.-C. 2010. Geochimica et Cosmochimica Acta, 74, 4612-4628.
Millot, R., Vigier, N., Gaillardet, J. 2010b. Geochimica et Cosmochimica Acta, 74, 3897-3912.
Misra, S., Froelich, P.N. 2012. Science, 335, 818-823.
Pogge von Strandmann, P.A.P., Henderson, G.M. 2015. Geology, 43, 67-70.

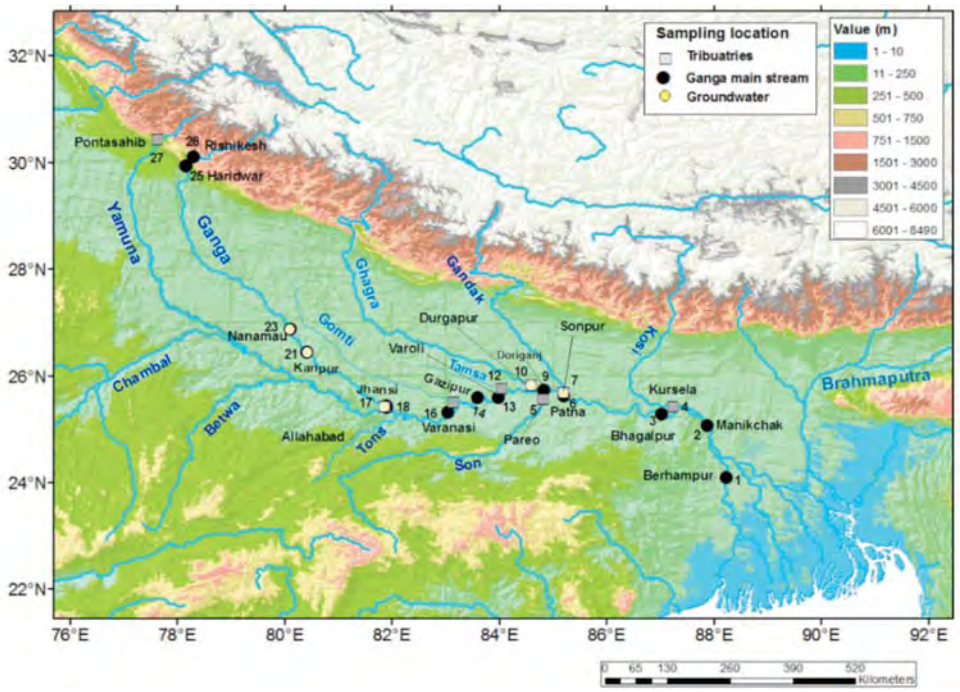

Fig.1. Sampling locations shown in the DEM map of the Ganga basin.

Channel width variations and controls in drainage networks of Dehradun

Sukumar Parida[1*], S.K. Tandon[2], Vimal Singh[1]

[1]Department of Geology, Chhatra Marg, University of Delhi, Delhi 110007, INDIA

**paridasukumar@gmail.com*

[2]Department of Earth Sciences, IIT Kanpur, Kanpur, INDIA

Channel width is an important parameter of river geometry, which reflects the response of a channel to the tectonic, topographic, lithologic, structural, and climatic controls in a particular reach of a river. The width pattern of a channel affects the efficiency of sediment transfer between the geomorphic compartments of a river system. For the rivers originating in the Lesser Himalaya, active tectonics plays a major role as it controls the space, energy and material supplied to a river system. In this zone, large sediment buffer zones like intermontane valleys exist that trap huge amounts of sediments and over geological timescale they also release these sediments. The width of the rivers flowing through such zones may provide important information regarding connectivity between different geomorphic compartments. Dehradun is one such intermontane valley that shows remarkable variability in the patterns of channel width. Also, the Dehra Dun basin acts as a sediment buffer zone and affects the sediment flux to the Ganga and the Yamuna river systems.

The rivers in Dehradun originate both from the northern boundary flanked by the Lesser Himalaya (the Mussoorie Range; Avg. elevation 2200 m) and the southern boundary flanked by the Siwalik Hills (the Mohand Range Avg. elevation 800 m). Due to higher elevation and the relatively larger basin area, the northern rivers are bigger (Tandon and Singh, 2014). For this study, we selected six major streams (the Asan River, Sitla Rao, Suarna Rao, the Song River, the Suswa River, and Jakhan Rao) originating from the Lesser Himalaya in the northern part.

The channel width in the mountainous region varies generally from 5 to 20 m. In the middle and lower reaches, the width variation is mostly between 100 to 400 m. The channel widths of the

Asan River system vary less in comparison to the Song River system. Channels widen as they cross the structural zones i.e., the Main Boundary Thrust (MBT), the Santaurgarh Thrust (ST) and the Bhauwala Thrust (BT) as a result of the change in the river gradient across the structures. Large sediment supply from the weak zones (i.e., fault related zones) to the rivers can also make them transport limited resulting in the deposition of the sediments. In addition, deposition may lead to channel bed armouring, which in turn causes the channel widening by bank erosion. The middle reaches receive sediment flux not only from the Lesser Himalayas, but also from the uplifted older surfaces in the valley. All the rivers show widening in their middle reaches except for the Asan River. The Jakhan Rao widens as it exits from the mountains which may be a result of change in gradient. In the lower reach, the river narrows down significantly, which could be a result of channel bank stability due to changes in lithology (i.e., increase in cohesive material). The decrease in channel width in the lower reach of the Jakhan Rao can also be attributed to agricultural land use practices and forest cover along both the banks. For the rivers flowing within the valley, the channel width increases gradually on the northern slope and maintains almost similar width as they flow in the axial part of the valley.

Most of the southern rivers (flowing from the Mohand Range) become indistinct before the confluence with their trunk rivers due to anthropogenic activities usually associated with farming. The results suggest that the mid-reaches of the Dehradun Rivers are relatively well connected with their upstream reaches. But the connectivity between the mid-reaches and the lower reaches is poor in most of the Dun Rivers. From this study it is found that the channel width variation in the upper and middle reaches is largely controlled by the structures. However, in the lower reach, the width variation pattern of the rivers is mostly influenced by anthropogenic factors such as man-made embankments and land use practices.

Tandon, S.K., Singh, V. 2014. Landscapes and Landforms of India, 135-142.

Deciphering the Meso-Cenozoic tectonic history of southern Eurasia using thermochronology on Central Asian faults

Stijn Glorie[1,*], Johan De Grave[2], Wenjiao Xiao[3], Alan Collins[1]

[1]Centre for Tectonics, Resources and Exploration (TRaX), Department of Earth Sciences, School of Physical Sciences, The University of Adelaide, Adelaide SA 5005, AUSTRALIA

**Stijn.glorie@adelaide.edu.au*

[2]Dept. Geology & Soil Science, MINPET Group, Ghent University, 281-S8 Krijgslaan, Ghent 9000, BELGIUM

[3]Xinjiang Research Center for Mineral Resources, Xinjiang Institute of Ecology and Geography, Chinese Academy of Sciences (CAS) and Division of Tethys Research Center, Institute of Geology and Geophysics, CAS, CHINA

The mountainous Central Asian landscape (to the north of the Himalayas and Tibet) predominantly formed as a response to recurrent tectonic deformation (e.g. Hendrix et al., 1992; De Grave et al., 2007; 2013; Glorie et al., 2011). The cause for these episodes of deformation is not yet fully understood. It has been suggested widely that the most recent pulse of intracontinental deformation that affected Central Asia, is related to distant forces that originate at the India-Eurasia collision zone (e.g. Molnar and Tapponnier, 1975; Knapp et al., 1996; De Grave et al., 2007). Subduction of the Tethys Ocean led to convergence and collision of Gondwana-derived India into Eurasia, which generated stresses that caused shortening and uplift in the Himalayas and Tibet (e.g. Harrison and Copeland, 1992; Wang et al., 2001). Continuous convergence between India and Eurasia and the growth of the Tibetan plateau induced convergence-driven (e.g. Abdrakhmatov et al.

1996) and/or flexure related (Aitken, 2011) stresses that propagated into the Eurasian interior where it deformed the weaker crust of Central Asia (e.g. Knapp et al., 1996; Wang et al., 2001). This deformation is preferentially accommodated by strength heterogeneities such as pre-existing fault zones within the crust of Tibet and Central Asia (e.g. England and Houseman, 1985), resulting in fault reactivation and associated rapid exhumation (Walker et al., 2007; Clark et al. 2010; Jolivet et al. 2010; Glorie et al., 2011; 2012; De Grave et al., 2013; Glorie and De Grave, 2015). The reactivation history of these fault systems, hence, not only archives the associated exhumation history of the Central Asian mountain ranges, but also maps out the strain distribution in this region, which provides unique insights into the dynamics of the Meso-Cenozoic collisions at the Eurasian margin such as the India-Eurasia collision (e.g. Peltzer and Saucier, 1996; England and Molnar, 1997; Glorie and De Grave, 2015).

This study documents that besides the occurrence of preserved Early Mesozoic geomorphic features (such as internally drained plateaus or old erosion surfaces), most of the current Central Asian relief is related to an important phase of Late Jurassic-Early Cretaceous exhumation. This Mesozoic exhumation pulse is thought to be related with the progressive consumption of the Palaeo-Tethys Ocean and associated collisions of Gondwana-derived terranes to Eurasia in the south and to the closure of the Mongol-Okhotsk Ocean to the northeast. Major fault systems within southern Central Asia (Tian Shan) record Cenozoic episodes of fault-induced rapid exhumation during the Early Palaeogene (~55-45 Ma) and Oligocene (~33-22 Ma) to Miocene (~10-8 Ma), related with the consumption of the Neo-Tethys and subsequent India-Eurasia collision (Glorie and De Grave, 2015). Our findings indicate a major episode of fault reactivation since ~33Ma, which correlates well with a ~35 Ma age for the India-Eurasia collision (Aitchison et al., 2007; Jiang et al., 2015). Although many of the hypothesised links between intracontinental exhumation and the prevailing plate-margin tectonic processes need to be tested further, they allow a first-order insight into stress propagation pathways from the Eurasian margin to the continental interior. Ongoing research focusses on fault systems in the verges of the Tian Shan (Uzbekistan and China) to further constrain the dynamic response of the collisions at the southern margin to Central Asia.

Abdrakhmatov, K.Ye., Aldazhanov, S.A. et al. 1996. Nature, 384, 450-453.
Aitchison, J.C., Ali, J.R., Davis, A.M. 2007. Jour. Geophys. Res., 112, B05423.
Aitken, A.R.A. 2011. Geology, 39, 459-462.
Clark, M.K., Farley, K.A., et al. 2010. Earth Plan. Sci. Lett., 296, 78-88.
De Grave, J., Buslov, M.M., Van den haute, P. 2007. Jour. Asian Earth Sciences, 29, 188-204.
De Grave, J., Glorie, S., et al. 2013. Gondwana Research, 23, 998-1020.
England, P., Houseman, G. 1985. Nature, 315, 297-301.
England, P., Molnar, P. 1997. Science, 278, 647-650.
Glorie, S., De Grave, J., et al. 2011. Tectonics, 30, TC6016.
Glorie, S., De Grave, J. et al. 2012a. Tectonophysics, 544-545, 75-92.
Glorie, S., De Grave, J., 2015. Geoscience Frontiers, in press.
Harrison, T.M., Copeland, P. et al. 1992. Science, 255, 1663-1670.
Hendrix, M.S., Graham, S.A. et al. 1992. GSA Bulletin, 104, 53-79.
Jiang, T., Aitchison, J.C., Wan, X. 2015. Gondwana Research, in press.
Jolivet, M., Dominguez, S., et al. 2010. Tectonics, 29, TC6019.
Knapp, J.H., 1996. Nature, 384, 406-409.
Molnar, P., Tapponnier, P., 1975. Science, 189, 419-426.
Peltzer, G., Saucier, F., 1996. J. Geophys. Res., 101, 27943- 27956.
Wang, Q., Zhang, P.-Z. et al. 2001. Science, 294, 574.

Paleoflood records in Himalaya

Pradeep Srivastava[1], Y.P. Sundriyal[2], Anil Kumar[1], Suman Rawat[1], Naresh Kumar[2], R.J. Wasson[3], Rajesh Agnihotri[4], Narendra Meena[1], Alan Zieglar[3]

[1]Wadia Institute of Himalayan Geology, 33 GMS Road, Dehradun 248001, INDIA

[2]HNB Garhwal University, Srinagar, INDIA

[3]Inst. of water Policy, National University of Singapore, SINGAPORE

Floods are one of the most effective agents of erosion and sediment transport in the mountainous regions such as the Himalaya. On geological time scales, the build-up of the fertile Ganga basin, that sustained several civilizations, is a consequence of recurring floods in the Himalaya. But due to population pressure, flood events in watersheds of the Himalaya can also put societies under great risk. The flood of June 2013 in the Alaknanda river valley, Garhwal Himalaya, witnessed the loss of more than 6000 human lives and economic damage of ~$250 million. Therefore the understanding of flood events on different time scales is required for better (i) flood forecast (ii) civil planning (iii) understanding of geomorphological evolution of mountains.

In the wetter southern front of the Himalaya, our understanding of paleofloods mostly comes from a 1900 yr record described from flood sediment in the Alaknanda basin. The record suggests that between about 80AD (or CE) to about 1667 CE the floods show no pattern and recur on average every 176 years. There is then a cluster from about 1714 to 1745 CE that can be attribute to a negative phase of the Arctic Oscillation, then three floods after this cluster with an average frequency of about 40 years and these occur with a higher frequency than during the first episode. Further, our investigation involving study of glacial outwash fans and AMS ^{14}C chronology from the headwaters of the river Mandakini (tributary of the Alaknanda river) suggests that a moraine dammed lake breached and a catastrophic flood took place in the middle of the 9-8th century AD that possibly destroyed an agro-based civilization and soon thereafter a major Hindu shrine of Kedarnath came into being. In the eastern Himalaya in the Darjeeling Himalaya extreme floods took place in the years 1899, 1950 and 1968, the years that coincide with similar kinds of events in Garhwal. In the NE Himalaya, in the head waters of the Brahmaputra River, there is evidence of glacially dammed lakes that breached and caused catastrophic floods at 10-8 ka and 2-1 ka (Montgomery et al., 2004). In the lower part of the valley there is sedimentary evidence in the form of thick piles of massive sands with luminescence ages of 21 ka (at Tuting), 8 and 6 ka (Yinkiyong and Geku). In the Ladakh Himalaya that lies in the rain shadow of the SW Indian Monsoon a paleoflood record was studied at the confluence of the rivers Indus and the Zanskar at Nimu. The deposits, composed of 25 flood couplets of fine sand-clayey silt, sit at ~29 m above the river level. This is twice as high as the last catastrophic flood recorded in the region in the year 2010. The chronology indicates that these floods are clustered in the Holocene monsoon optimum between 11-9 ka.

Therefore, the published and new data from the Indus and Alaknanda Rivers indicate that (i) climatically wetter phases witness a high frequency of extreme flood events, and (ii) during the Holocene monsoon optimum the monsoon front extended much into the north beyond Ladakh and induced high floods in the region.

Abnormal rainfall event of 2013 at Uttarakhand (India): Searching operative natural and anthropogenic forcing factors from long-term climate time series

Rajesh Agnihotri[1], Koushik Dutta[2], H.M. Joshi[3], Jayendra Singh[4], Pradeep Srivastava[4], Nishchal Verma[3], C. Sharma[1] M.V.S.N. Prasad[1] and Y.P. Sundriyal[5]

[1]Radio and Atmospheric Science Division, CSIR-National Physical Laboratory, New Delhi 110012, India
[2]Department of Earth and Planetary Sciences, Northwestern University, Evanston, IL60208, USA
[3]Department of Electrical Engineering, Indian Institute of Technology, Kanpur, India
[4]Wadia Institute of Himalayan Geology, Dehradun, India
[5]Department of Geology, HNB Garhwal University, Srinagar (Uttarakhand), India

Extreme rainfall events are expected to become more common as a result of changing climate. Hazards like flash-floods and landslides in mountainous regions caused by anomalous rainfall are expected to increase. The northern Indian state of Uttarakhand located at the southern front of the Himalaya has several major tourist attractions and the area has undergone significant changes of land use in the last few decades. The state witnessed three-day long disastrous spell of rainfall during June 15-172013, when excess of 600 mm rainfall occurred within just 36 hours. This anomalous rainfall triggered numerous landslides, causing heavy debris flows and flash-floods and river bed elevation in the Mandakini River and overall catchment of the Ganges. Landslide driven channel blocking and breaching also had cascading effect on the disaster. The catastrophic event caused heavy damage in the vicinity of Kedarnath temple, costing thousands of human and animal lives along with huge capital loss of infrastructure and resources (Ziegler et al., 2014).

The anomalous rainfall event of June 2013 in Uttarakhand came as a surprise as overall monsoonal rainfall in this region has been steadily declining since ~1960's (Basistha et al., 2009). This prompted us to investigate relationship of long-term rainfall variability of Uttarakhand with other relevant climate variables (*e.g.*, monthly air temperatures) and climate tele-connections (*e.g.*, Arctic Oscillation index).Owing to paucity of long monthly rainfall time series for the region, we have used gridded monthly rainfall and air temperature data from Global Precipitation Climatology Project Version 2 (GPCP V2) and NCEP 20th Century Reanalysis V2C (both datasets available from http://www.esrl.noaa.gov). These data were obtained over a 4×4ºgrid (28ºN to 32ºN; 78ºE to 82ºE) covering most parts of Uttarakhand, and analyzed using advanced time series and statistical methods. Modeled change in precipitation and temperature are compared using the Global climate model output, from the World Climate Research Program's (WCRP's) Coupled Model Inter comparison Project phase 3 (CMIP3) multi-model dataset (Meehl et al., 2007).Our study utilized hence, monthly series of rainfall and temperature data covering time span of last ~110 years (AD 1901-2009), in tandem with some other key climate variables and obtained key results. The major outcomes of the study pertaining to Uttarakhand region are:

Abrupt increase in pre-monsoon (April-May) air temperatures after 1997

Statistically significant upward trend in early monsoon precipitation (May-June) relative to the later monsoon months (July-September) after 1990s

More common early monsoon anomalous rainfall events during negative phases of Arctic Oscillation

A reduction in early monsoon (March-May) precipitation by about 5% has been predicted formid-21st century relative to the current values by ensemble average results of CMIP3 model using the high and medium emission scenarios of greenhouse gases.

In view of the above observations we attempted to address the question: 'Has vulnerability of the region in terms of anomalous heavy rainfall events increased in the concurrent global warming era?'

ZieglerAD, Wasson RJ, Bhardwaj A, Sundriyal YP, Sati SP, Juyal N, Nautiyal V, Srivastava P, Gillen J, Saklani U. 2014. Hydrological Processes, 28(24), 5985-5990, DOI: 10.1002/hyp.10349
Basistha A, Arya DS, Goel NK. 2009. Int. J. Climatol., 29, 555-572,DOI: 10.1002/joc.1706
Meehl GA, Covey C, Taylor KE, Delworth T, Stouffer RJ, Latif M, McAvaney B, Mitchell JFB. 2007. Bulletin of the American Meteorological Society, 88(9): 1383-1394, DOI: 10.1175/BAMS-88-9-1383

Discovery of Bathonian-Cenominan Palynomorphs from the Eastern Karakoram Block, and their Tectonic Implication

Rajeev Upadhyay[1], Ram-Awatar[2], Samir Sarkar[2], Saurabh Gautam[2]
[1]Department of Geology, Kumaun University, Nainital 263002, INDIA
[2]Birbal Sahni Institute of Palaeobotany, 53 University Road, Lucknow 226007, INDIA

We report a diverse and well preserved fossil palynomorphs for the first time from a marine sedimentary sequence of the eastern Karakoram block, northern India. The assemblage contains a number of dinoflagellates cysts - *Nannoceratopsis gracilis, Ctendodinium tenellum, Gonaulacysta Jurassica, Tanyosphaeridium jurassicum, Rigaudella filamentosa, Sentusidinium villersensis* in association with *Araucariacites australis*, *Classopollis classoides, Tricolpites longus* and *Biretisporites eneabbaensis* spore and pollen grains. Besides, in the assemblage *Cyclonephelium vannophorum, Pterodinium cingulatum* and *Pterodinium pterota* are also present which referable to Middle-Late Jurassic/Early Late Cretaceous age (~166-105 Ma) of the sediments. Based on the present discovery, it is suggested that before the final accretion of the Cimmerian microplates to the Asia, a narrow and elongated sedimentary basin, oriented in a NW-SE direction, at latitude of ~25-30°N was existed. At that time, Karakoram block was situated near the already welded Qiangtang block of Asia. Besides, it is also inferred that the northern and eastern Karakoram blocks were connected during the late Jurassic/Cretaceous time. The activity and dextral offset of Karakoram fault separates and displaced the sedimentary sequence of northern and eastern Karakoram blocks by ~150 km.

Late Quaternary climate fluctuations in Ladakh and its comparison With global climate record

Ravish Lal[1], N.C Pant[1], H.S Saini[2], S.A.I. Mujtaba[2]
[1]Department of Geology, University of Delhi, Delhi, INDIA
[2]Geological Survey of India, Faridabad, INDIA

Ladakh, in northwestern part of India, is an elevated plateau marked by continental island arc setting, is tectonically active and has a major active fault traversing through it. The region has average precipitation. around 100 mm/yr mainly as snow fall. Climate is dominantly influenced by Mid-latitude westerlies coming from the north and a minor influence of the Indian summer monsoon. Geographically Quaternary process may be independent of global influence so it is a test case for finding out global versus regional climate influence on account of a unique high altitude and low latitude setting. Significant climatic fluctuations during Late Quaternary have been recorded within climate archives from Glacial, fluvial and lacustrine deposits preserved in different parts from this region. Considering Late Quaternary period fluvial and lacustrine records are more consistent and they allow good interpretation.

A composite 60 m thick sequence observed on the right bank of Indus River near Leh, known as Spituk deposit constitutes a 80 ky to 40 ky complete record of a paleolake which extended for over ~200 sq km areally. OSL dating of quartz grains for strategically selected samples in this sequence

indicate presence of cold climate sequence corresponding to MIS 4. The base of this laminated sequence is marked by a fluvial unit at MIS 5a. Interrupted deposits of this paleolake are present upto 30 km upstream of Spituk. Though the origin of this lake was considered to be a moraine but our resent investigations indicated it to be a glaciofluvial deposit of >150 m thickness. There is a widespread ~100 ka glacial activity (~MIS 5) in the Ladakh region. This is evidenced by 98±3 ka age of the moraine near Darbuk and ~106 ka at Hanle. This appears to be the last most widespread glaciations in Ladakh.

A refined stadial-interstadial chronostratigraphy of the Ladakh region has been prepared which shows that the region was influenced by the global climate events but these were modified by the unique geographic factors of this terrain.

Remote Sensing based pre- and post-event analysis of Landslides in Bhagirathi Valley: The June 2013 extreme event

Shweta Singh[1*], Rakesh Bhambri[2], Pradeep Srivastava[2], R.J. Perumal[2], Manish Mehta[2]

[1]D.B.S. (P.G.) College, Dehradun 248001, INDIA

**shwetasinghgeo24@gmail.com*

[2]Wadia Institute of Himalayan Geology, 33 GMS Road, Dehradun 248001, INDIA

The June 2013 event in Uttarakhand Himalaya is regarded as the most destructive flood event occurred during the past millennium. The state experienced heavy down pour from 15 to 17 June 2013 in the northern regions of India. In the headwaters of Ganga system, in Kedarnath region, the excess rainfall and snow melt lead to the bursting of moraine-dammed Chorabari Lake causing flash flood in the downstream regions. Many villages were washed away and ~5000 people died. The major cause of loss was not only the heavy rainfall but failed evacuation measures that could not be effectively operated due to landslide driven road blocked and damages. Landslides in areas are general hazard but the situation in the fateful year worsen due to the extreme rainfall that led to the creation of many new and re-activation of several dormant landslides. In this work, we generated the pre- and post-event landslide inventory and attempted to understand the pattern with respect to the geology and rainfall distribution in the Bhagirathi valley. This might help in damage assessment and to create a possible landslide warning system. The mapping was based on visual interpretations of satellite images that included parameters *viz.* shape, size, tone and texture of landslides and pre- and post-events image changes. A set of five important topographic factors such as slope, aspect, elevation, area and re-occurrence of landslides were analyzed using GIS.

The landslide inventory shows that the event generated total number of 456 new landslides. The total number of pre-event landslides were 2315 that covered ~13.5 km^2 whereas post-event landslides (2771 count) cover ~15.7 km^2. This shows landslide area has increased overall by 2.2 km^2. The increase in landslide number has its direct relation with the geology of the area. It was observed that maximum new landslides were generated in the vicinity of the Main Central Thrust zone that also coincided with the maximum rainfall followed by the rim of the Tehri dam site in Lesser Himalaya with phyllitic rocks of Chandpur affinity.

Exhumation and emplacement of the Himalayan metamorphic nappe and its northward lateral cooling, originated from delamination and break-off of Indian slab

Harutaka Sakai[1]*, H. Iwano[2], T. Danhara[2], T. Kawakami[1], K. Nakamura[1]
[1]Division of Earth and Planetary Sciences, Kyoto University, Kyoto 606-8502, JAPAN
**hsakai@kueps.kyoto-u.ac.jp*
[2]Kyoto Fission-Track Co. Ltd., Kyoto 603-8832, JAPAN

One of the prominent structures of the Himalayan orogenic belt is huge metamorphic nappe, covering the whole Lesser Himalaya and extending ~2000 km in E-W directions with width of ~100 km. We undertook the Himalayan nappe project in eastern and central Nepal Himalaya, in order to reveal the kinematic and thermal history of the nappe that has a key to understand how the Himalaya was built. We carried out zircon and apatite Fission-Track (FT) dating, zircon U-Pb dating and muscovite ^{40}Ar-^{39}Ar dating for the metamorphic nappe and underlying metamorphosed Lesser Himalayan Sediments (LHS).

The metamorphic nappe exposed on the ground at 15-14 Ma, judging from the same cooling age (zircon, apatite, muscovite) of 14.4 Ma from the Yellow Band and granite intrudes into the Qomolangma detachment (Sakai et al. 2005). It advanced southward at 3-4 cm/yr, and the nappe front reached the present position behind the MBT by 11-10 Ma (Sakai et al., 2013b).

The nappe front and underlying LHS cooled down till 240°C of closure temperature of zircon FT by 10 Ma, and those of middle part of the nappe cooled down till 240°C by 6-5Ma (Sakai et al. 2013a). It indicates that the isotherm of 240°C within the nappe retreated toward the NNE at the rate of ~10 km/Ma (Sakai et al., 2013b). The northern part of the nappe to the south of Mt. Everest shows much younger zircon FT age of 4-3 Ma and apatite age of 1.2-0.8 Ma.

P-T condition of the basal part of the metamorphic nappe is consistent from the nappe front to the Higher Himalaya, ranging in width of 80 to 120 km: maximum temperature is about 750°C and maximum pressure is 11-12 kb (e.g. Yoneshiro & Kizaki, 1996; Guillot, S., 1999; Kohn, 2009). Zircon U-Pb ages of partially melted gneiss at the base indicates that prograde metamorphism occurred at 45-25 Ma, and decompression melting occurred at 22-15 Ma. It suggests that metamorphism occurred at the middle crust in horizontal attitude without pressure gradient, and rapid exhumation occurred at 22-15 Ma.

After simple calculation on the position of the metamorphic rocks in the Higher Himalaya under 12 kb, we concluded the rocks were located at 53 km to the north of the partially melted mid-crust of Tibet at present. It suggests that the Himalayan nappe was originated from partially-melted mid-crust of Tibet. Delamination and break-off of the mantle from the Indian continental crust must have caused rapid exhumation of the metamorphic belt and following by emplacement of nappe.

One-million-year-long climatic changes and northward migration of depositional center caused by probable syn-depositional faulting, Revealed by the Paleo-Kathmandu Lake drilling project

M. Setoguchi, R. Fujii, M. Mampuku, H. Sakai*
Division of Earth and Planetary Sciences, Kyoto University, Kyoto 606-8502, JAPAN
**hsakai@kueps.kyoto-u.ac.jp*

The Kathmandu Valley, located in the midland of the Nepal Lesser Himalaya, is filled with Pleistocene thick lacustrine and fluvial sediments, and considered as a good archive of the past

monsoon climate and environmental changes in Central Himalaya (Sakai, 2001a). We undertook core-drilling of lacustrine sediments in the central and southern marginal part of the basin, and have continued multi-proxy analyses of the core ranging in age from ca. 600 to 13 ka (e.g. Sakai et al., 2006, Mampuku et al., 2008, Hayashi et al., 2009). Recently, we conducted analyses of pollen, micro-fossil and organic chemistry on the additional core drilled at Champi (CP) in the southern part of the basin. As the result, we could have reconstructed vegetation and climate changes from ~1000 to 500 ka. In this paper, we present newly reconstructed pollen and micro-fossil (sponge spicules, phytoliths, plant fragments) diagram, and discuss on the one-million-year-long climatic record after joining new data. Furthermore, we discuss on the northward migration of depositional center, probably caused by faulting along the Chandragiri Fault running in the valley.

Newly analyzed core was collected at Champi at 1424 m asl, 4 km north of the valley margin, and called CP core. It is 114 m long and divided into four parts: basal 11 m is the Lukundol Formation showing fluvial and swamp facies, and the middle 47 m is the Kalimati Formation comprising of lacustrine clay. Upper two parts consist of transition zone of 22 m and uppermost Sunakothi Formation

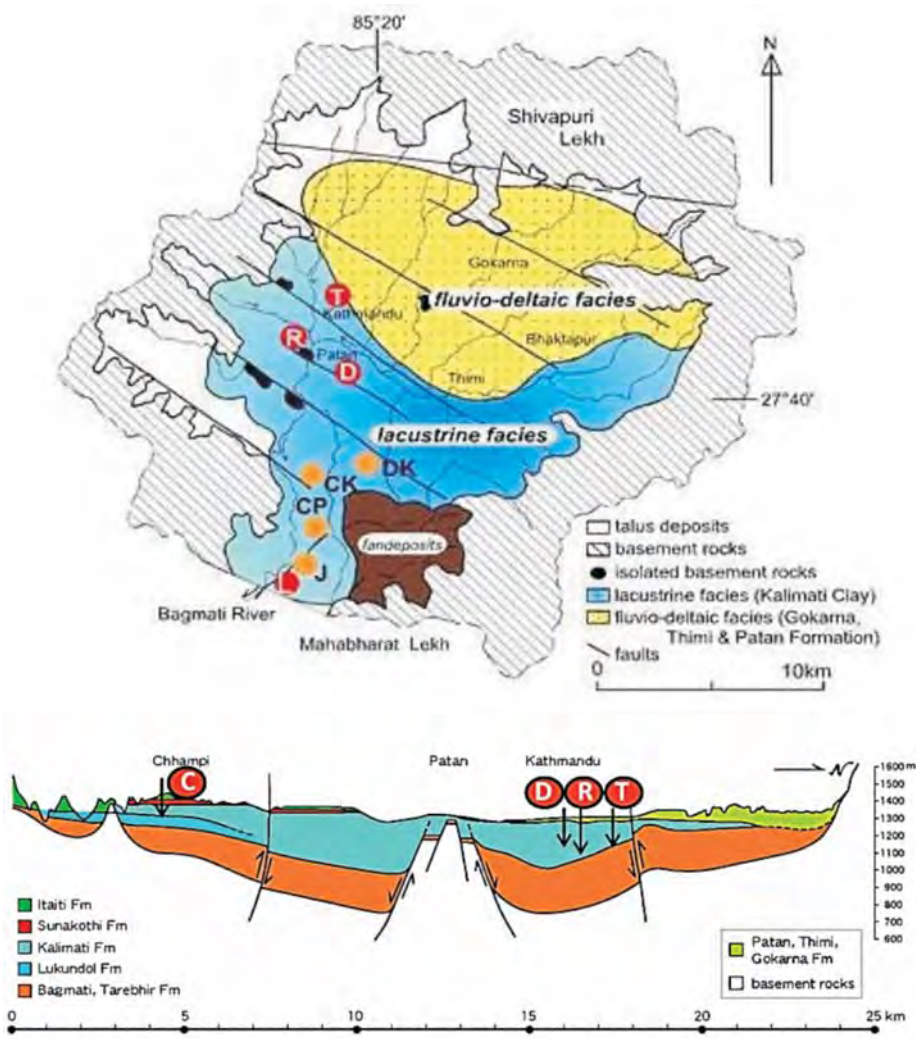

Fig. 1. Simplified sedimentary facies distribution map of the Kathmandu Basin sediments (Sakai, 2001b) and schematic geological cross-section of the Katmandu Basin. Drill sites (C, D, R, T) are also shown.

of the deltaic facies. The basal part of the Kalimati Formation is assigned to the age of Jaramillo event during 1070-990 Ma, and Brunhes-Matuyama boundary is estimated to be 78 m in depth.

On the basis of changes in relative abundance and assemblage of fossil pollen, nine pollen zones are constructed. Pollen zone 9, 7, 5, 3 and 1-b indicate cold and dry climate and zone 8, 6, 4, 2 and 1-a indicate warm and wet climate. Cold index (*Abies, Tsuga*) and dry index (*Artemisia ,* Chenopodiaceae, Gramineae) increase during period of cold climate after zone 7. The ratio of arboreal pollen starts cyclic change after zone 5. A comparison of the pollen zones with MIS (marine isotope stage) indicates that pollen zones from 8 to 2 correspond to MIS 27-15. The pollen diagram suggests that climate of the Kathmandu Valley became cool and dry at 900 and 700 ka (pollen zone 7 and 5), and cyclic climatic change started at 700 ka. These changes seem to correspond to abrupt increase and cyclic changes of global ice volume in the MPT (Elderfield et al., 2012).

Abrupt and rapid decrease of sponge spicule and diatom at around 50 m in depth suggests rapid lowering of lake-water-level. In addition, sedimentary facies changes from lacustrine clay to prodeltaic bioturbite and delta front sandstone, and both TOC and C/N ratio rapidly decrease at the same horizon. These changes are likely to have been caused by tectonics, because the pollen zone 2 (MIS 15) indicates warm and wet climate that implies increase of lake-water-level.

On the other hand, lake-water-level recorded at RB core started gradual increases at the same period (Sakai, 2001b, Hayashi et al., 2009). Difference of altitude of MIS 15 in CP core at 1374 m and RB core at 1126.5 m suggests relative uplift of southern basin and relative subsidence of northern basin after lowering of lake-water-level in the southern basin at ca. 540 ka. This difference seems to have been caused by an active fault, Chandragiri Fault (Asahi, 2003), running between southern and northern basin.

Asahi, K., 2003. Jour. Nepal Geol.Soc., 28,1-8.
Elderfield, H., Ferretti, P., Greaves, S., Crowhurst, S., MaCave, I.N., Hodell, D., Piotrowski, M. 2012. Science, 337,704.
Hayashi, T., Tanimura, Y., Kuwahara, Y., Ohno, M. Mampuku, M., Fijii,R., Sakai, H., 2009. Quaternary Research, 72, 377-387
Mampuku. M., Yamanaka, T., Uchida, M., Fujii, R., Maki, T., Sakai, H., 2008. Climate of the Past, 4, 1-9.
Sakai, H., 2001a. Jour. Nepal Geol. Soc., 25, Special Issue, 1-8.
Sakai, H., 2001b. Jour. Nepal Geol. Soc., 25, Special Issue, 9-32.
Sakai, H., Sakai, Hideo, Yahagi. W., Fujii, R., Hayasjhi, T., Upreti, B.N., 2006. Palaeogeography, Palaeoclimatology, Palaeoecology, 241, 16-27.

Modeling of movement of continental plates to predict lithospheric weather on the region of Pamir-Tibet belt

M.S. Dufour[1]*, M.B. Ignatyev[2#], T.S. Katermins[3], V.A. Nenashev[2]
[1]Institute of Earth Science, St-Petersburg State University
**dufourms@rambler.ru*
[2]St-Petersburg State University of Aerospace Instrumentation
[#]ignatmb@mail.ru
[3]Niznevartovsk State University, Russian Federation

The lithospheric weather is the state of the tectonic ensembles in space and time. Contemporary satellite radio-navigation permits to determine the coordinates of reference points with the high accuracy and to create the computer simulation system for predict lithospheric weather by means of modeling of movement of continental plates and fractures on basement of geological and geophysical dates. In our report we consider to use our simulation system for decision of tectonic task of Pamir-Tibet belt.

History of Earth Science Researches and Tectonic framework of Himalayan Mountain Region to Save the fragile Ecology and Effect of Global Climatic Changes for the Survival of Human Civilization

Anshu K. Sinha
Former Director BSIP, Lucknow;
Present address: B 602, Vigyan Vihar, Sector 56, Gurgaon 122011, INDIA
anshuksinha@gmail.com

The geology of the Himalaya is a record of the most dramatic and visible creations of modern plate tectonic forces. The Himalayas, which stretch over 2400 km between the Namche Barwa syntaxis in Tibet and the Nanga Parbat syntaxis in Pakistan, are the result of an ongoing orogeny - the result of a collision between two continental tectonic plates. This immense mountain range was formed by tectonic forces and sculpted by weathering and erosion. The Himalaya-Tibet region supplies freshwater for more than one-fifth of the world population, and accounts for a quarter of the global sedimentary budget.

Topographically, the belt has many superlatives: the highest rate of uplift (nearly 10 mm/year {Heim, A. & Gansser, A. (1939). "Central Himalaya; geological observations of the Swiss expedition 1936". Schweizer. Naturf. Ges., Denksch. 73 (1): 245}.Nanga Parbat), the highest relief (8848 m at Mt. Everest Chomolangma), among the highest erosion rates at 2-12 mm/yr, the source of some of the greatest rivers and the highest concentration of glaciers beside of the polar regions. This last feature earned the Himalaya its name, originating from the Sanskrit for 'the abode of the snow'.

In the Early Carboniferous, an early stage of rifting developed between the Indian continent and the Cimmerian Superterranes. During the Early Permian, this rift developed into the Neotethys ocean. From that time on, the Cimmerian Superterranes drifted away from Gondwana towards the north. Nowadays, Iran, Afghanistan and Tibet are partly made up of these terranes.

While most of the oceanic crust was "simply" subducted below the Tibetan block during the northward motion of India, at least three major mechanisms have been put forward, either separately or jointly, to explain what happened, since collision, to the 2500 km of "missing continental crust". The first mechanism also calls upon the subduction of the Indian continental crust below Tibet. Second is the extrusion or escape tectonics mechanism (Molnar & Tapponnier 1975) which sees the Indian plate as an indenter that squeezed the Indo-China block out of its way. The third proposed mechanism is that a large part (~1000 km (Dewey, Cande & Pitman 1989) or ~800 to ~1200 km) of the 2500 km of crustal shortening was accommodated by thrusting and folding of the sediments of the passive Indian margin together with the deformation of the Tibetan crust.

Colonel Sir George Everest, son of Tristram Everest, was born on 4th July 1790 in Greenwich, England. He had a brilliant academic career and was appointed in 1818 as Lambton's Chief Assistant in the Great Trigonometrical Survey of India. In 1830 he became the Suveyer General of India and Superintendent of the Great Trigonometrical Surveys. He completed one of the most stupendous works in the whole history of science by measuring the Great Meridional Arc of India and finding thereby the parameters of the earth which lead to the determination of mathematical surface, in the form of spheroid still used in India as Everest Spheroid. Everest retired from India in 1843 and died in 1866, at the age of 76. In 1856 Sir Andrew Waugh, Surveyor General of India, proposed that the peak be named after Everest. In 1865 the peak was named MOUNT EVEREST (8848 m).

The great Arc of Meridian, began in 1800, was the longest measurement of Earth's surface ever to have attempted. Its 1600 miles of inch-perfect survey nearly took 50 years -carried from southern tip of Indian subcontinent up into the frozen waste of the Himalayas. William

Geological Features of Himalayas

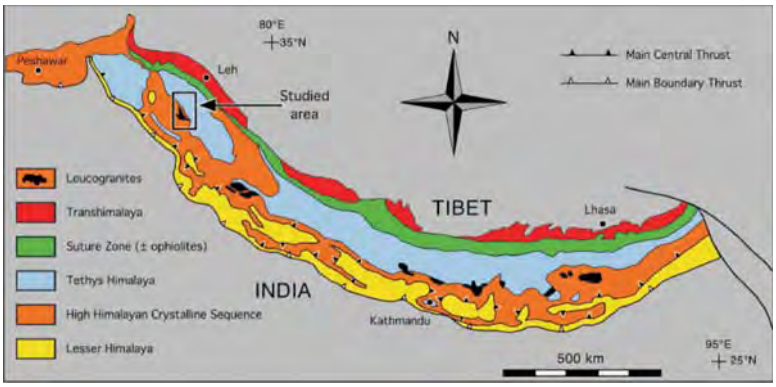

Geological profile through Himalayas

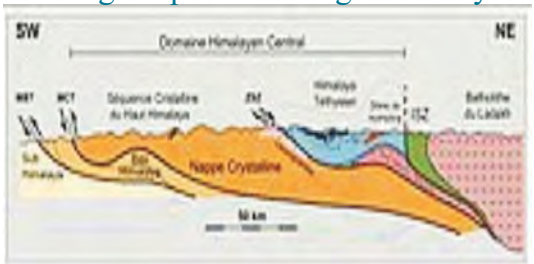

Lambton, an endearing genius, conceived the idea; George Everest, an impossible martinent, completed it. Both found the technical difficulties horrendous. The ARC also resulted in the first accurate measurements of the Himalayas, an achievement which was acknowledged by the naming of the world's mountain in honour of EVEREST. More important still, the ARC significantly advanced our knowledge of the exact shape of our planet.

Global warming responsible for recession of Himalayan glaciers at alarming rate is a serious matter of concern for the survival of human civilization in the Indo-Gangetic plain.

The stress and strain caused due to plate motion is responsible for frequent earthquakes in this region making enormous loss of human life.

Present day kinematics of Himalayan Frontal Thrust in Garhwal and Himachal Himalaya through GPS measurements: Role of Geoid, Topography and Gravitational Potential Energy

S. Rajesh
Wadia Institute of Himalayan Geology, 33 GMS Road, Dehradun 248001, INDIA
Satraj@wihg.res.in

The Himalayan Frontal Thrust (HFT) is the southernmost plate boundary thrust (Gansser, 1964) that morphologically separates the Sub-Himalayan Siwalik Hills from the alluvium of Ganga Plain. The ongoing India-Eurasia tectonic collision has produced HFT and other series of imbricate thrust systems; where, variable convergence rates, crustal shortening, mass accumulation, high topography and major thrust earthquakes are observed (Ambraseys and Bilham, 2000; Banerjee and Burgmann, 2002;). There were three major thrust earthquakes occurred in the Northwest and Central Himalaya during the last 100 years, including the latest M 7.9 April 25th 2015 Nepal earthquake. None

of these events reportedly produced any surface rupture along their frontal part (Wesnousky et al., 1999). However, palaeoseismological observations on uplifts of fault terrace deposits of late Quarternary and Holocene from the Himachal Himalaya and historical records from the Kumaon Himalaya suggest active deformation of HFT in the past at century to millennium scales (Kumar et al., 2001; Philip et al., 2012; Mugnier et al., 2013). Thus implying, the plausible recurrences of the Major or Great Magnitude earthquakes in the region. Although, the estimated geological deformation rates would give the long term visco-elastic response of the thrust; but are not necessarily comparable to the instrumentally measured rates of short term deformation (Hindle et al., 2002). But the latter would provide threshold deformation rates, which set the criticality for the occurrences of Major or Great earthquakes. This emphasizes the need to instrumentally monitor the present day movement of the HFT at Garhwal and Himachal Himalaya. What is the sense of movement of HFT with respect to stable India? Is it commensurate with the expected southward propagation of the frontal thrust system? If not so, what are the blocking factors that contain the locking process of frontal thrust system.

The investigation was carried out at two sub areas in Dehradun and Kangra re-entrants in Garhwal and Himachal Himalaya respectively (Fig. 1), where continues GPS measurements along with campaign data have been used. GPS data have been processed using GAMIT and obtained the combination solutions with GLOBK and generated the velocity vectors. Apart from geodetic data, I have also computed (Coblentz et al., 1994) the Gravitational Potential Energy (GPE) change using the Earth Gravity Model (EGM2008) and CRUST1.0 model. The SRTM 3 Arc Sec data have been used to compute the topographic effect on GPE. EGM2008 model have been used to compute the lithospheric density effects of a lithospheric column of thickness 125 km on GPE.

Results show that in the Kangra re-entrant the velocities are NNW-SSE with respect to the stable Eurasia. But for the case of Dehradun re-entrant the velocity vectors are mainly NNE-SSW. Thus there exists difference in their azimuthal horizontal velocities with respect to the stable Eurasia. However, with respect to stable India reference frame the observed velocities are significantly low throughout the frontal part right from the Himachal to the Dehradun region; and hence, in general, the HFT appears kinematically dormant or locked. For the case of Dehradun re-entrant a ninety degree offset in the directions of frontal displacements though their displacement magnitudes are negligible, but directions show along the arc movement of HFT. While in the Kangra network, frontal displacements are oriented towards SW and the sense of movement is perpendicular to the arc. Both compressional and extensional principal axes of strain in the study region are of the order of tens of micro-strain, which are three orders of magnitude more with respect to the stable peninsular region. In Dehradun re-entrant between the HFT and MBT (Main Boundary Thrust) the compressional regime is dominating, which appears complicated in both N-S and E-W directions at different magnitudes. In the Kangra network the extensional regime is present only at the north of MCT.

What possibly caused the negligible movement and consequent restrained southward propagation of HFT with respect to the stable Peninsular India is being discussed by considering the scenarios (1) the role of N-S oriented transverse ridge systems and lineaments as stress 'diffusers' (Rajesh et al., 2011) that abuts the HFT, (2) HFT is at present in the lean phase of its strain dissipation as a visco-elastic relaxing thrust and hence no more strain accumulation is taking place; unless, a great magnitude event should occur in the region and re-activate the whole frontal thrust, (3) and finally, the enhanced topography and mass accumulation at the Lesser and Higher Himalaya. Would that induce a gravitational potential energy driven southward frontal propagation of HFT? This GPE driven radial flow might have ceased or countered by the ongoing crustal under thrusting process along the convergent zone.

The first scenario, in fact represents a case of ridge-thrust collision. But the intriguing aspect is whether such transverse structures, like the Delhi-Haridwar Ridge (DHR), Mahendragrh-Dehradun

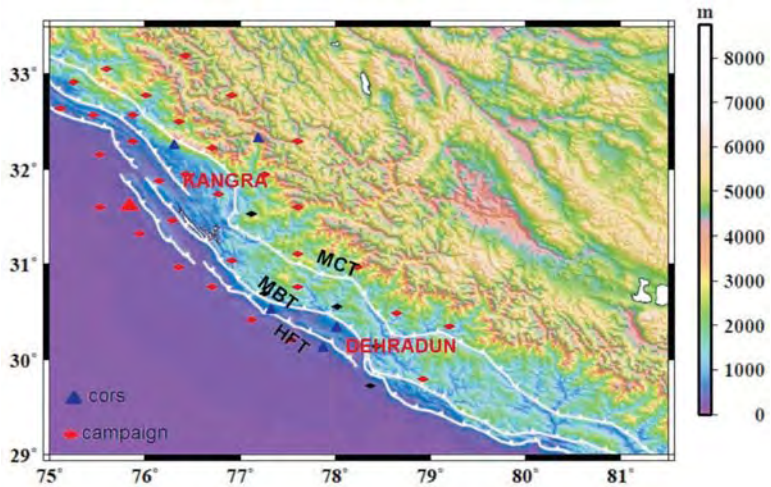

Fig. 1. The study area is located in the Kangra and Derhadun re-entrants in NW Himalaya. Blue triangles represent location of permanent GPS stations and red are the campaign observation points.

Lineaments (MDL) (Gahalaut and Kundu, 2012; Ravi Kumar et al., 2013), are really continuing and abutting beneath the HFT. I have analysed the existing Bouguer gravity data (GSI-NGRI 2006) available in the frontal, sub and higher Himalayan region. Gravity results indeed corroborate that the DHR, MDL and numerous other transverse structures like Haridwar Tear Fault, Moradabad Fault are abutting beneath the Himalayan frontal thrust system. The same has been corroborated by analyzing the soft sediment thickness variation by H/V technique (Nakamura, 1989).

The second scenario considered HFT as a visco-elastic relaxing thrust. If there are no southward bound blocking ridge systems against the relaxing HFT, then there would have been some degree of southward propagation of HFT due to stress transfer as a consequence of seismic energy release (of the order of 10^{15} J) from the seismogenic MCT zone. But rheologically the frontal Shiwalik material, such as boulders and conglomerate are too weak to hold the transferred stress from the seismogenic MCT zone. Thus rather than strain accumulation and occurrence of earthquakes; passive long term creep is happening at the HFT. This long term creep process at the HFT is currently ceased by the blocking of the abutting N-S transverse structures.

The role of GPE change on the frontal displacement of HFT is two pronged, owing to the crustal mass accumulation and subsequent topographic build up. Both these factors result relatively enhanced GPE (75-125 x 10^{11} N/m) in the Lesser and the Higher Himalayan region. High GPE values are observed in these areas where extensional regime is prevailing. The low GPE values are characterized by compressional regime, and are observed throughout close to the MCT zone. The enhanced GPE-driven radial mass flow from the Lesser and the Higher Himalayan regions exert substantial radial pressure to the frontal side and hence it should aid the southward displacement of HFT. This exerted radial pressure is mainly contributed by the topographic mass above the geoid datum. But crust and lithospheric masses below the geoid datum also deform along the convergent zone, which is opposite that of topographic aided southward bound radial flow. Thus there exists stress transfer between the mass flow happening below and above the geoid datum. The difference in the stresses due to the GPE driven flow and that of the ongoing convergence process along the convergent zone should determine the critical stress required to displace the HFT. This critical stress can be obtained through modelling and integration of results from accurate regional or local crustal velocity structures from seismic tomography, rheology, GPS measured surface displacements and velocity vectors etc.,

Ambraseys, N.N., Bilham, R. 2000. Current Science, 79, 45-50
Banerjee, P., Burgmann, R. 2002. Geophysical Research Letters, 29. 10.1029/2002GL015184,
Coblentz, D.D., Richardson, R.M., Sandiford, M. 1994. Tectonics, 13, 929-945
Gahalaut, V.K., Kundu, B. 2012. Gondwana Research, 21, 1080-1088.
Gansser, A. 1964. Geology of the Himalaya. Interscience, New York, NY, 298p.
Hindle, D., Kley, J., Klosko, E., Stein, S., Dixon, T., Norabuena, E. 2002. Geophysical Research Letters, 29,10.1029/2001GL013757.
Kumar, S., Wesnousky, S.G., Rockwell, T.K., Ragona, D., Thakur, V.C., Seitz, G.G. 2001. Science, 294, 2328-2331.
Mugnier, J.L., Gajurel, A., Huyghe, P., Jayangondaperumal R., Jouanne, F., Upreti, B. 2013. Earth-Science Reviews, 127, 30-47.
Nakamura, Y. 1989. Quarterly Report. Railway Technical Reseach Inststitute. 30 (1) 25-33.
Philip, G., Bhakuni, S.S., Suresh, N. 2012. Tectonophysics, 580, 160-177.
Rajesh, S., Majumdar, T.J., Krishna, K.S. 2011. 7th International Conference on Asian Marine Geology, held at National Institute of Oceanography (NIO), Goa -India, 11-14 October 2011 (ICAMG-7), 142p.
Ravi Kumar, M., Mishra, D.C., Singh, B., Venkat Raju, D. Ch., Singh, M. 2013. Journal of Geological Society of India. 81, 61-78.
Wesnousky, S.G., Kumar, S., Mohindra, R, Thakur, V.C. 1999. Tectonics, 18, 967-976

Geodynamics in the frontal Mishmi hills, with reference to morphotectonic studies integrated with geophysical data, in Arunachal Pradesh, India

R.K. Mrinalinee Devi[1*], Siddhartha K. Lahiri[2#], Jamini Boruah[2], R. Duarah[1]
[1]*Geoscience Division, CSIR-North-East Institute of S&T, Jorhat 785006, INDIA*
******mrinalineerk@rediffmail.com*
[2]*Department of Applied Geology, Dibrugarh University, Dibrugarh, INDIA*
[#]*siddharthalahiri2@gmail.com*

Study on tectonic activities, with the help of geomorphology, is an important tool in understanding geodynamics of the frontal Mishmi Hills. Mishmi Thrust brought the metamorphic Mishmi Crystalline rocks over the Brahmaputra Alluvium as well as over the Lesser Himalayan sedimentary rocks at places. In the Arunachal Himalaya the Lohit River drains from north to southward with a sinuous trend (sinuosity ~1.11). This transverse river passes through the eastern limb of the Eastern Syntaxial Bend and takes a right angle turning at Parsuramkund while debouching from its hilly sojourn to the plains, due to the presence of shutter ridge along its channel and follows an almost straight course westward, with sudden increase of braided characteristics, signifying excessive sedimentation, almost covering recent deformational activities in the valley. In these areas, morphometric studies try to discover the sub-surface structural patterns of the region. Drainage, lineaments and other related basin parameters provided important clues to better understanding about the valley-range relationship substantiated with different geophysical data of the subsurface.

In the present study, an area of about 5000 km^2 has been taken up covering the Eastern Syntaxial belt of the Himalayas across the Lohit River and it has been observed that in a span of 35 plus years (1975-2011) the surface relief of the Lohit River and Lohit Valley has witnessed significant changes. So, we hereby try to understand the fluvial processes and dynamics in the Lohit Valley, morphometric characterization and the nature of tectono-geomorphic controls in the eastern Himalayan Syntaxial part of the Brahmaputra basin, with inputs of active tectonics activity of the frontal Arunachal Himalaya.

Slip Model of the 2015 Mw 7.8 Gorkha, Nepal Earthquake derived from coseismic offsets from GPS Time series

Sanjay K Prajapati[1*], Param Gautam[2], V.K. Gahalaut[1]
[1]Center for Seismology, Ministry of Earth Sciences, New Delhi, INDIA
**sanjay.kp@nic.in*
[2]Wadia Institute of Himalayan Geology, 33 GMS Road, Dehradun 248001, INDIA

A good spatial coverage of continuous GPS stations in the region affected by the 2015 Mw 7.8 Nepal earthquake, as well as far field station in the neighboring north India, allow us to model the coseismic slip distribution of this event. We inverted coseismic offsets from 15 GPS site of Nepal and India to derive the slip distribution. Coseismic offsets ranging from 1890 mm near to epicenter to ~3 mm or less at sites far from the epicenter are estimated from the GPS time series analysis. The earthquake occurred through predominant thrust slip on a 160 km long and 50 km wide rupture on the Main Himalayan Thrust (MHT) that trend NW-SE. The inverted slip distribution fits to all the coseismic offsets well (95%). The slip distribution indicates that notable slips (>4 m) occurred on the sub-horizontal decollement at the depth of 10-15 km, north of Kathmandu. The derived seismic moment is 7.84 x 10^{20} Nm (Mw 7.9), which is consistent with that derived from seismological data. We also computed static stress using coseismic slip distribution which explains the aftershocks pattern of the region and imply that stress increased in the southern and northern regions, neighboring the rupture. The increased stress in the western region is worth noting from the seismic hazard point of view as the last earthquake in that region probably occurred in 1505. Increase in stress to the south of Kathmandu is also a matter of concern; however, it is known whether this is a stress weakening or stress strengthening region.

Thecamoeba and Diatom record from high altitude pristine lakes of Chang La Pass: potential indicators of climate induced ecology

Anjum Farooqui*, Sunil Shukla, Binita Phartiyal
Birbal Sahni Institute of Palaeobotany, 53, University Road, Lucknow 226001, INDIA
**afarooqui_2000@yahoo.com*

Surface sediments were collected from two lakes (Zhingral and Tsoltak) of cold and arid Chang La Pass catchment in Ladakh Range at an altitude of ~5000 m. Structurally, the area lies in the vicinity of the Karakorum Fault (KF) with surrounding peaks exceeding 6000 m altitude. As the region lies in the rain shadow of North West Himalaya it has dry steppe vegetation. These lakes drain off in form of Changla stream to join the Tangtse river, a tributary of the Shyok River towards the east and Indus River towards the west. Enormous amount of unconsolidated sediment (generated due to frost action/physical weathering) lies loose on the high-angled slopes and the valley floor damming the drainage and forming lakes. The glaciers are absent from the region but the moraines and these lakes provide signals of climatic variations and the changing geomorphology of these areas through time. It is therefore, important to assess the prevailing biotic forms in the lakes as proxies to interpret the past climatic events in the vertical stack of the lake sediments. The surface samples were analyzed for biotic forms such as Thecamoebians and Diatoms as these proxies are short lived and serve as potential indicators of even the slightest change in the climate induced ecology. About 12 species of Thecamoebians were recorded dominated by *Centropyxis aerophila, C. aerophila sphaginicola, C. sylvatica, C. arcelloides, C. aculeata*. Most of these are agglutinated forms and typical of those surviving in stressed conditions in varied ecological niche and also indicate good primary productivity which sustained these heterotrophs. Diatom community was represented by 14 species

belonging to 9 genera. The observed diatom species were quantitatively enough in numbers, however, the diatom population shows a poor species diversity as a whole which is suggestive for the presence of somewhat stable environmental conditions.

'Shaanxilithes ningqiangensis' from the Tal Group (Cambrian), Nigali Dhar Syncline. Lesser Himalaya, India and Its biostratigraphic significance

C.A. Sharma[1], Birendra P. Singh[1], O.N. Bhargava[2], Naval Kishore[1]
[1]*Center of Advanced Study in Geology, Panjab University, Chandigarh 160014, INDIA*
[2]*INSA Honorary Scientist, 103, Sector-7, Panchkula 134109, INDIA*

The enigmatic *Shaanxilithes ningqiangensis has been reported* from the earthy dolomite Member (Krol Group) and calcareous siltstone beds of the Earthy Siltstone Member (Tal Group), occupying a position above the Krol-Tal juncture and below the Chert Member (Shaliyan Formation, Tal Group), of the Nigali Dhar Syncline, Lesser Himalaya, India. We recovered 40 well preserved ribbon-shaped, meandering specimens of *S. ningqiangensis* showing closely spaced annulations that lacked branching (Fig. 1). The beginning and terminal points are indistinguishable. In certain cases, individual specimens are characterized by irregular, low-angle to high-angle sinuosity. It has been variously described as body fossil, ichnofossil and algae (Xing et al., 1984; Li et al., 1997; Hua et al., 2004; Webster et al.,, 2007; Shen et al., 2007; Zhuravlev et al., 2009; Cai and Hua, 2011; Zhuravlev et al., 2011; Rogov et al., 2012, Meyer et al., 2012; Tarhan et al., 2014). Detailed study of this enigmatic fossil is needed to resolve the long standing controversy regarding its phylogenetic and stratigraphic placements, which will be important contributions to the evolutionary history of metazoans. Originally, *S. ningqiangensis* was reported from the late Neoproterozoic (Ediacaran) of southern and central China (Sichuan, Shaanxi, Quinghai and Guizhou provinces and Ningxia Hui Autonomous region), Siberian platform and India (Xing et al., 1984; Hua et al., 2000; Hua et al., 2004; Shen et al., 2007; Weber et al., 2007, Zhuravlev et al., 2009; Cai & Hua, 2011; Zhuravlev et al., 2011; Meyer et al., 2012; Tarhan et al., 2014). *Shaanxilithes* is considered an Ediacaran organism that spans the Precambrian-Cambrian boundary, an interval marked by significant taphonomic and ecological transformations that include not only innovation but also probable extinction. All the past well constrained finds of *S. ningqiangensis* are restricted to Ediacaran age. However, according to a recent publication the stratigraphic status of *S. ningqiangensis-bearing* Earthy Siltstone Member is rendered uncertain, though the overlying Chert Member in the adjoining Korgai Syncline has yielded definite early Cambrian acritarchs (Tiwari, 1999). The moot question is whether the Earthy Siltstone Member represents an Ediacaran

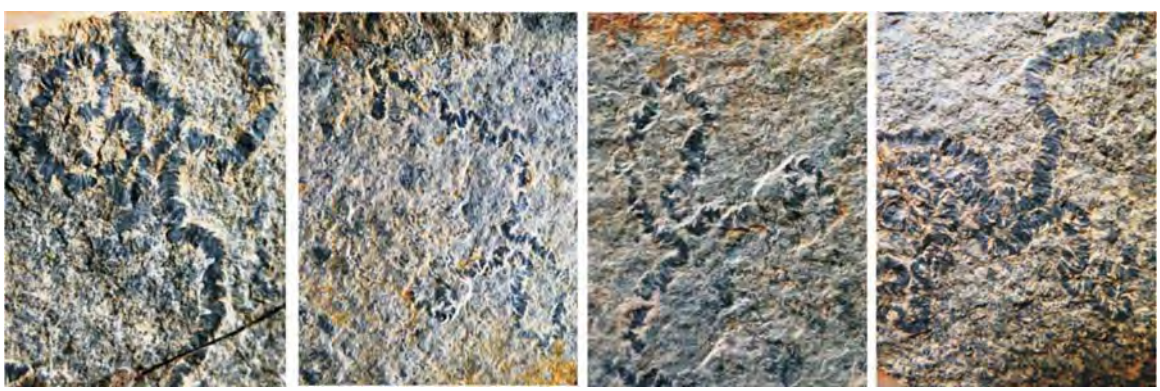

Fig.1. *S. ningqiangensis* recovered from the Earth Siltstone Member (Tal Group) of the Nigali Dhar syncline.

or an early Cambrian age? It would be interesting to find if *Shaanxilithes,* so far known from Ediacaran sequences, could it transgress to the early Cambrian or in simple words could it withstand the Pc/C Boundary event?

Cai, Y., Hua, H. 2011. Geological Magazine, 148, 329-333.
Hua, H., Chen, Z., Zhang, L. 2004. Journal of Stratigraphy, 28, 265-269. [In Chinese, English abstract].
Li, R., Yang, S., Li, W. 1997. Geological Publishing House, Beijing, 99 pp. [In Chinese].
Meyer, M., Schiffbauer, J.D., Xi, A., S., Cai, Y., Hua, H. 2012. Palaios, 27, 354-372.
Rogov, V., Msrsuin, V., Bykova, N., Goy, Y., Nagovi, Tsi, N., Kochnev, B., Karlova, G., Grazhdanki, D. 2012. Geology, 40, 395-398.
Shen, B., Xi, A., S., Dong, L., Zhou, C., Li, U.J. 2007. Journal of Paleontology, 81, 1396-1411.
Tarhan, L.G., Hughes, N.C., Myrow, P., Bhargava, O.N., Ahluwalia, A.D., Kudryavtsev, A.B. 2014. Palaeontology, 57, 283-298.
Tiwari, M., 1999. Precambrian Research, 97, 99-113.
Webster, B., Steiner, M., Zhu, M.-Y. 2007. Palaeogeography, Palaeoclimatology, Palaeoecology, 254, 328-349.
Xing, Y., Ding, Q., Luo, H., He, T., Wang, Y. 1984. Geological Magazine, 121, 155-170.
Zhuravlev, A. Yu, G. Vintaned, J.A., 2011. Geological Magazine, 148, 329-333.
Zhuravlev, A.Y., Vintaned, G., Ivantsov, J.A., Yu, A. 2009. Geological Magazine, 146, 775-780.

Using the 'crystal signature' of mylonites to demarcate the Main Central Thrust (Alaknanda region, Garhwal Himalaya)

Nicholas J. Hunter[1]*, R.F. Weinberg[1], C.J.L. Wilson[1], V. Luzin[2]
[1]*School of Earth, Atmosphere and Environment, Monash University, Clayton Campus, VIC 3800, AUSTRALIA*
**nicholas.hunter@monash.edu*
[2]*Bragg Institute, Australian Nuclear Science and Technology Organisation (ANSTO), Lucas Heights, NSW, 2234*

During plastic deformation, quartz typically develops a crystallographic preferred orientation (CPO), which reveals information about the stress, temperature, strain and key deformation mechanisms associated with shear zone mechanics (Lister and Hobbs, 1980; Schmid and Casey, 1986; Kruhl, 1996; Pennacchioni et al., 2010). Such information is critical for understanding major tectonic processes and the rheological weakening of the crust, and therefore comprehensive CPO analyses are of particular importance to a complete understanding of deformation processes during the Himalayan orogeny. An additional and particularly remarkable aspect of CPOs is their ability to reveal information even in rocks where there is no visible appearance of deformation. Because deformation fabrics are typically recognized based on the juxtapositions between two or more phases, evidence of strong shearing in monomineralic rocks, such as quartzites, can be difficult to observe in the field and under petrographic microscope. When analyzed using crystallographic diffraction techniques, however, they can reveal strong CPOs associated with plastic deformation (e.g., Heilbronner and Tullis, 2002).

It is for these reasons that CPO analysis is essential for determining the pattern of strain distribution in the Main Central Thrust (MCT), where a deep crustal slice comprising the High Himalayan Crystallines (HHC) has been emplaced atop Proterozoic rocks of the Lesser Himalayan Sequence (LHS). It is uncertain whether the MCT comprises a broad zone of ductile shear (Davidson et al., 1997), or a varying number of narrow thrust planes (Hodges et al., 1996; Bhattacharyya and Mitra, 2014). Analysis of CPO patterns along the region of deformation can help address these problems by unraveling the 'crystal signature' of the MCT, and can be used as semi-quantitative estimates of the strain distribution and style of deformation.

We have used neutron diffraction and electron back scatter diffraction techniques to study the crystal signature of quartz in mylonitic rocks along the MCT, exposed in the Alaknanda region of the Garhwal Himalaya (NW India; Fig. 1a). A number of workers have described two mylonitic shear

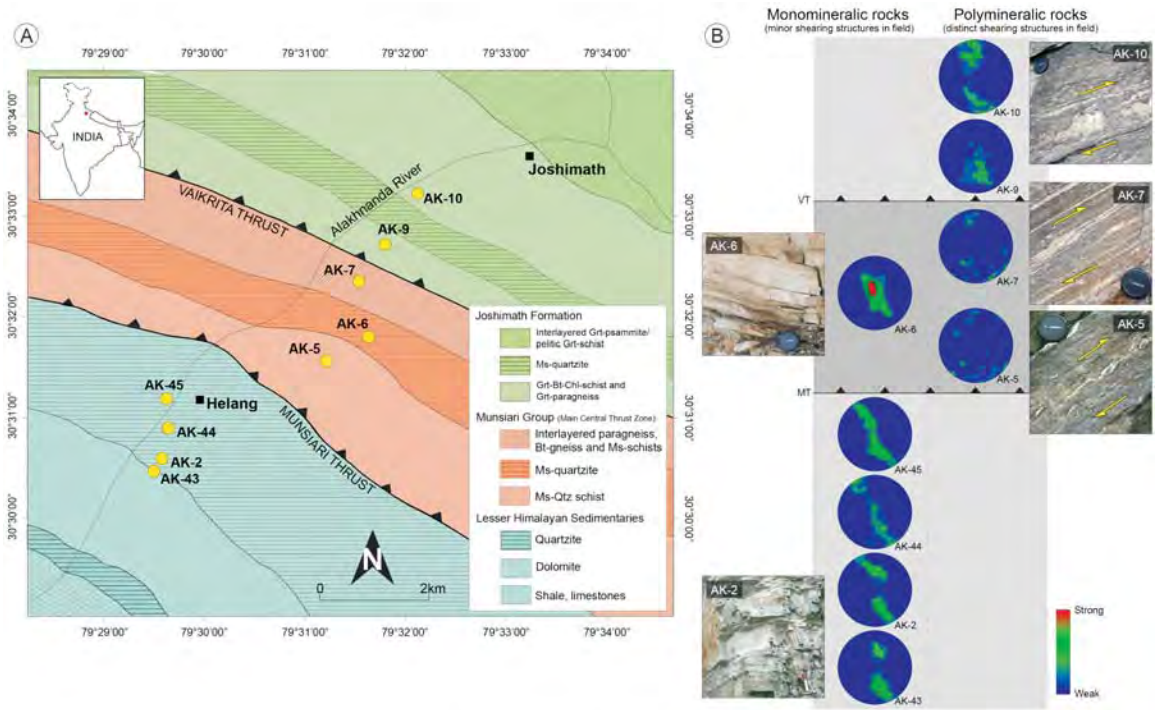

Fig. 1. (a) Geological map of the Alaknanda region in the Garhwal Himalaya, NW India (inset). Locations of samples used in this study are indicated. The proposed Munsiari and Vaikrita thrust planes are shown. (b) Contoured stereographs showing the distribution of the [0001] crystallographic axis of quartz in monomineralic and polymineralic rocks of the Alaknanda region. Axial data was collected from 500 grains in each sample. Photos of field areas from which samples were collected are provided for comparison with crystallographic data. Note the contrasts in visible shearing (yellow arrows) between monomineralic and polymineralic rocks. Based on CPO intensity and field observations, a high strain zone is approximated (dark grey).

zones in this area, the Munsiari and Vaikrita Thrusts, which are separated by a massive quartzite unit (Fig. 1a; Valdiya, 1980; Jain et al., 2014; Shreshtha et al., 2015). These two mylonites, part of the Munsiari Group, comprise interbanded gneiss and schist with distinct evidence of shearing in the field and under petrographic microscope (Srivastava and Srivastava, 2010; Jain et al., 2014). The quartzite separating the mylonites, conversely, shows only minor evidence of shearing.

We show, using CPO data that this quartzite is also strongly deformed, and together with the mylonites mark the highest strain zone in the region (Fig. 1b). The deformation can be better understood by comparing the crystal signature across the monomineralic quartzites and polymineralic mylonitic rocks. The CPO patterns in monomineralic rocks of the LHS, in the footwall of the MCT, are very strong and are associated with extensive crystal-plastic deformation (dislocation glide and climb). The strength of CPOs increases up-structure and peaks in the quartzite unit situated between the Munsiari and Vaikrita Thrusts (Fig. 1b). Deformation experiments have linked strong CPO patterns such as these to high shear strains ($\gamma > 6$) and temperatures of ~500ºC (Stipp et al., 2002; Heilbronner and Tullis, 2006; Pennacchioni et al., 2010). The increasing asymmetry of the CPO distribution up-structure also suggests a transition from dominant coaxial to non-coaxial strain (top-to-the-SSW thrusting). Where CPOs in monomineralic rocks is stronger along the shear zone, polymineralic rocks CPOs are comparatively weaker (Fig. 1b). This observation is concomitant with the transition from coarse-grained clast-matrix fabrics to homogenous fine-grained fabrics, and suggests a change from dislocation creep to grain size sensitive deformation mechanisms, such as grain boundary sliding or diffusion creep (Platt and Behr, 2011).

Overall, the crystal signature of the MCT contains information not immediately apparent from field or petrographic observations. Our data shows that the strength of monomineralic rock CPOs continues to increase between the proposed Munsiari and Vaikrita Thrusts; there is no decrease or plateau in the strain intensity as might be expected between two thrust planes. Therefore, we propose that the MCT is actually one continuous zone, at least 2 km wide and including not only the gneissic mylonites but also the quartzite in between. Our results demonstrate that describing shear zones based exclusively on the visible appearance of the rocks can be deceptive and that the true location and nature of the MCT is better understood when the crystal signature is considered.

Bhattacharyya, K., Mitra, G. 2014. Journal of Asian Earth Sciences 96, 132-147.
Davidson, C., Grujic, D.E., Hollister, L.S., Schmid, S.M. 1997. Journal of Metamorphic Geology 15, 593-612.
Heilbronner, R., Tullis, J. 2002. Geological Society, London, Special Publications 200, 191-218.
Heilbronner, R., Tullis, J. 2006. Journal of Geophysical Research: Solid Earth 111, B10202.
Hodges, K.V., Parrish, R.R., Searle, M.P. 1996. Tectonics 15, 1264-1291.
Jain, A., Shreshtha, M., Seth, P., Kanyal, L., Carosi, R., Montomoli, C., Iaccarino, S. 2014. Journal of the Virtual Explorer 47, 34.
Kruhl, J.H. 1996. Journal of Metamorphic Geology, 14, 581-589.
Lister, G.S., Hobbs, B.E. 1980. Journal of Structural Geology 2, 355-370.
Pennacchioni, G., Menegon, L., Leiss, B., Nestola, F., Bromiley, G. 2010. Journal of Geophysical Research B: Solid Earth 115.
Platt, J.P., Behr, W.M. 2011. Geology 39, 127-130.
Schmid, S.M., Casey, M. 1986. AGU, Washington, DC, pp. 263-286.
Shreshtha, M., Jain, A.K., Singh, S. 2015. Current Science 108, 1107-1118.
Srivastava, H.B., Srivastava, V. 2010. Journal of the Geological Society of India 75, 152-159.
Stipp, M., Stünitz, H., Heilbronner, R., Schmid, S.M. 2002. Journal of Structural Geology 24, 1861-1884.
Valdiya, K.S. 1980. Tectonophysics 66, 323-348.

An overview of the Earthquake triggered Landslides in the Indian Himalayas

Subhay K. Prasad*, Ravi S. Chaubey, Birendra P. Singh
Center for Advanced Studies in Geology, Panjab University, Chandigarh 160014, INDIA
**subhay.lovely@gmail.com*

Himalaya is one of the most active mountain belts representing continent-continent collision and leading to high rate of devastation in the form of landslides, avalanches and slope failures either under the influence of gravity, continuous uplift and earthquake generated triggers leading to slope failures. Such slope failures are primarily endangering the habitations, strategically important roadways and loss of life.

Recently the Nepal earthquake (25th April, 2015) of magnitude 7.5 (USGS) at a shallow depth (~15 km) and epicenter (34 km) east-southeast of Lamjung (Nepal), jolt for 50 seconds triggered an avalanche on Mount Everest, killing at least 19 peoples. A major aftershock (6.7 M) occurred on 26th April 2015 in the same region and this triggered landslide in the Langtang Valley and fresh avalanches on Mount Everest.

The most important and recent earthquake recorded in India was at Sikkim on 18th September, 2011 at Indo-Nepal border, 68 km northwest of Gangtok, Sikkim, India (Rajendran *et al.* 2011) which triggered several hundreds of landslides in the adjoining regions with a moment magnitude (Mw) of 6.9 at a shallow depth of 19.7 km (USGS). More than 354 landslides were reported post-earthquake by National Remote Sensing Center (NRSC) within the Indian Territory after this massive earthquake (Gupta et al., 2015) which also killed atleast 111 people.

In the Northwestern Himalaya the most significant earthquake recorded in the past were 8th Oct, 2005 Kashmir Earthquake magnitude 7.6 (USGS), 20th October, 1991 Uttarkashi Earthquake magnitude 6.8 (Thakur and Sushil K.. 1994); 19th January, 1975 Kinnaur Earthquake magnitude 6.8 (Khattri et al.,, 1978). 4th April, 1905 Kangra Earthquake magnitude 7.8 (Ambraseys and Bilham, 2000). Such major earthquakes in the region have caused massive landslides.

The northwest Himalaya is comparatively well studied in terms of Paleoseismic activities preserved in the lacustrine deposits. Manifestation of such paleo-lake profile in the Spiti-Sutlej river basin (Joshi et al., 2010) gives an evidence of landslide lake formations near Morang, Sumdo, Kioto, Phaldhar, Atargoo, Hurling (Bhargava and Bassi, 1998). The South Tibetan Detachment System (STDS) is tectonically active all along its strike length in Himalaya-Tibet and Northeastern region of Indian plate and it may be possible that a major earthquake more likely will occur in the northwestern Himalaya along the Kaurik-Chango Fault Complex (KCFC), which was recently proved to be active during the Quaternary (Draganits et al., 2014a,b; Neumayer et al., 2004). Further the Kinnaur region of northwest Himalaya is currently endure critical denudation at rapid rate characterized by mass movements such as landslide, slope failure, rockfall etc. at places Urni where the NH-22 is blocked and a landslide lake on the Sutlej River has formed recently. Similar activation of landslides also witnessed at Maling Nala in Kinnaur. These activities in this region can be attributed to the Neotectonic activity along the STDS.

Ambraseys, N., Bilham, R. 2000. Current Science, 79 (1), 45-50.
Bhargava, O.N., Bassi, U.K. 1998. Memoirs of the Geological Survey of India, 124.
Draganits, E., Grasemann, B., Janda, C., Hager, C., Preh, A. 2014a. Engineering Geology, 169, 14-29.
Draganits, E., Gier S., Hofmann, C., Janda, C., Bookhagen, B., Grasemann, B. 2014b. Journal of Asian Earth Sciences, 90, 157-172
Gupta, V., Mahajan, A.K., Thakur, V.C. 2015. Himalayan Geology, 36(1), 81-90.
Joshi, M., Kothyari, Girish C., Ahluvalia, Arun, Pant, Pitambar D. 2010. Journal of Geographic Information System. 2, 169-176.
Khattri, K.N., Rai, K., Jain, A.K., Siinvhal, H., Gaur, V.K., Mithal, R.S. 1978. Tectonophysics, 49(1-2), 1-21.
Neumayer, J., Wiesmayri, G., Janda, C., Grasemann, B., Draganits, E. 2004. Austrian Journal of Earth Sciences, (95/96), 28-36.
Rajendran, K., Rajendran, C.P., Thulasiraman, N., Andrews, R., Sherpa, N. 2011. Current Science, 101, 1475-1479.
Thakur, V.C., Sushil, K., 1994. Terra Nova (Wiley), 6 (1), 90-94.

Mantle upwelling at the Neo-Tethyan spreading center was originated From a deep (~410 km) and reduced source

Souvik Das[1,*], Barun K. Mukherjee[2]
[1]*Physical Research Laboratory, Navrangpura, Ahmedabad 380009, INDIA*
**souvikdasgeology@gmail.com*
[2]*Wadia Institute of Himalayan Geology, 33 GMS Road, Dehradun 248001, INDIA*

The mantle tectonites in ophiolites along Indus Suture Zone (ISZ) are supposed to preserve the signatures of mantle upwelling at the Neo-Tethyan spreading center. Petrological knowledge of the generation of mid ocean ridge basalt strongly suggests that melting in a spreading center is restricted to <90 km depth (O'Leary et al., 2010). They are present as magmatic rocks (basalt and mafic cumulates) within ophiolites. But geophysical studies have shown that the root of the mantle upwelling beneath a spreading centre extends up to much greater depths (>100-410 km; Su et al., 1992; Zhao et al., 1997). To fill this knowledge gap primary mineral inclusions, micro textures and fluid inclusions were studied in ultramafic rocks of a well preserved Tethyan ophiolite (Nidar valley, SE Ladakh, ISZ). With the aid of petrography, Laser Raman spectroscopy and Electron Probe Micro

Analyses (EPMA), recently we discovered systematic high pressure mineral phase transitions from two peridotites of Nidar ophiolite (coesite→quartz, high-pressure $C2/c$ clinoenstatite→orthoenstatite, and β-Mg_2SiO_4→Cr spinel exsolution needles in olivine; Das et al., 2015). The phase stability of these Ultra High Pressure (UHP) minerals requires derivation from mantle transition zone (~410 km). One UHP peridotite bears unusual Fe_2O_3 glass and disordered microdiamond along with methane inclusion within primary α-Fe_2O_3 grains which indicate a primary low fo_2 deep mantle environment. The other UHP peridotite shows primary C-H fluid inclusion and graphite crystals in olivine along with H_2O fluid inclusions, which also supports a reduced origin. There are report of high pressure reduced nitrides and oxides from another Tethyan ophiolite (Dobrzhinetskaya et al., 2009) which also advocates for a deep and reduced source for ultramafic parts. The UHP phase transitions and other solid and fluid inclusions altogether infer that the mantle upwelling in the Neo-Tethyan spreading center began its journey from a reduced (and hence enriched?) and deep source.

Das, S., Mukherjee, B.K., Basu, A.R., Sen, K. Jr. 2015. In: Mukherjee, S., Carosi, R., van der Beek, P.A., Mukherjee, B.K. & Robinson, D.M. (eds), Tectonics of the Himalaya, Geological Society of London, Special Publication, 412, doi: 10.1144/SP412.12.

Dobrzhinetskaya, L.F., Wirth, R., Yang, J., Hutcheon, I.D., Weber, P.K., Green, HW. II 2009. Proceedings of National Academy of Sciences USA, 106 (46), 19233-19238, doi: 10.1073/pnas.0905514106.

O'Leary, J.A., Gaetani, G.A. & Hauri, E.H. 2010. Earth and Planetary Science Letters, 297, 111-120, doi: 10.1016/j.epsl.2010.06.011.

Su,W. J.,Woodward, R.L. & Dziewonski, A.M. 1992. Nature, 360, 149 - 152, doi: 10.1038/360149a0.

Zhao, D., Xu, Y., Wiens, D.A., Dorman, L., Hildebrand, J., Webb, S. 1997. Science, 278, 254-257, doi: 10.1126/science.278.5336.254.

Oblique motion, slip partitioning and seismic hazard in the NW Himalayan arc

Vineet K. Gahalaut[1*], Bhaskar Kundu[2], Rajeev Kumar Yadav[3], Sonalika Chaudhury[3]

[1]National Centre for Seismology, Ministry of Earth Science, New Delhi, INDIA

**vkgahalaut@yahoo.com*

[2]Department of Earth & Atmospheric Science, National Institute of Technology, Rourkela, INDIA

[3]National Geophysical Research Institute, Hyderabad, INDIA

Himalayan frontal arc accommodates about 2 cm/yr of convergence of the India Eurasia convergence. This convergence is accommodated through stick and slip on the seismogenic detachment under the Outer and Lesser Himalaya. According to the oblique convergence model, the India-Eurasia convergence is arc normal in the Central Himalayan region but to the east and west of it, it becomes oblique to the structural trend and frontal thrusts of the Himalaya. This obliquity results in partitioning in which the shear component is absorbed by pure shear on the generally east west trending strike slip faults in the southern Tibet and predominantly arc normal motion in the Himalayan frontal arc. GPS measurements have been very useful in exposing such complexities in tectonics and geodynamics and also in constraining plate motion, convergence, slip partitioning and in assessing seismic hazard in the region. Such measurements in the Nepal region, confirms that the entire motion of ~19 mm/yr between the southern Tibet and India is accommodated through thrust motion, with no oblique motion and no shear motion in southern Tibet through slip partitioning. To the west, in the Kashmir Himalaya, our recent GPS measurements suggest that in the Kashmir Himalaya the oblique motion of 17±2 mm/yr between the southern Tibet and India plate is partitioned between dextral motion of 5±2 mm/yr on the Karakoram fault system and oblique motion of 13.6±1 mm/yr. The oblique motion in the frontal arc is also consistent with the P axes of the earthquake focal

mechanisms. Thus the partitioning of the India-Southern Tibet oblique motion is partial in the Kashmir Himalayan frontal arc. In this model, the Karakoram fault marks the northern limit of the NW Himalayan sliver. The Kaurik Chango rift, a north-south oriented seismically active cross-wedge trans-tensional fault appears to divide the sliver in two parts causing varying translatory motion on the Karakoram fault on either side of the Kaurik Chango rift. Another important aspect of these measurements is its implication for seismic hazard. These measurements suggest a locking width of 175 km, against the locking width of ~100 km in the neighbouring Garhwal Kumaun and Nepal Himalaya, and it is a matter of debate. Elsewhere in the Himalaya, the earthquakes of Himalayan seismic belt and the 3.5 km topographic contour coincide with the downdip edge of the locked zone. But here in the Kashmir Himalaya, they do not guide us to decide the width of locked zone in the Kashmir Himalaya, as the seismicity is almost NIL and the 3.5 km topgraphic contour surrounds the Kashmir valley.

New constrains of the vertical offset of the Beichuan fault in Longmen Shan mountain belt (Sichuan, China) from a high-resolution petrological study

Laura Airaghi*, Julia de Sigoyer, Pierre Lanari, Olivier Vidal
Institut des Sciences de la Terre (ISterre), BP 53 - 38041 Grenoble Cedex 9, FRANCE
**laura.airaghi@ujf-grenoble.fr*

The paradox of high topography but low convergence rates in the Longmen Shan mountain belt (Shen et al., 2005), at the eastern margin of the Tibetan plateau (Sichuan, China, Fig. 1) leaded to an underestimation of the seismic hazard prior to the Wenchuan earthquake Mw 7.9 (2008). During the earthquake the rupture affected the Beichuan fault with a complex pattern, some segments underwent pure dextral strike slip while other slid with a thrusting and dextral strike slip movement as shown by INSAR and post-seismic field works (de Michele et al., 2010a,b; Liu-Zeng et al., 2009). In the hanging wall of the thrusting segment the Pengguan massif (South China basement) is exhumed while in the hanging wall of strike slip segment sedimentary cover still crops out (Fig. 1). The Wenchuan earthquake could therefore represent a characteristic earthquake on the eastern border of Tibetan plateau.

Paleoseismological studies (Densmore et al., 2007; Ran et al., 2010) have constrained the quaternary activity of the Beichuan fault and thermochronological data acquired on the hanging wall of the fault attest for a rapid exhumation at 11 Ma of the basement (Godard et al. 2009) which however seems to have started earlier, at Oligocene time (Tan et al., 2014). The total offset of the Beichuan fault remains unknown. In order to answer this question petrological and chronological analysis were performed on samples of both basement and sediments in the hanging wall of the Beichuan fault.

Samples collected in the Neoproterozoic basement close to the Beichuan fault (Pengguan massif, Fig. 1) show shear zones underlined by a green schist metamorphic assemblage (chlorite+micas+epidote+quartz) (Fig. 2). Since granites are naturally less reactive than sediments to metamorphic transformations and since green schist facies conditions are difficult to estimate, a high-resolution petrological approach has been here used. X-Ray chemical maps were performed with an Electron Microprobe in order to retrieve the chemical heterogeneities within metamorphic minerals. Maps where then processed with the XMapTools program (Lanari et al., 2014) that allows to visually associating chemical heterogeneities of metamorphic minerals to microstructures (Fig. 3b).

Two structurally and chemically different generations of white micas were observed in the samples from the Pengguan massif. The first generation of micas developed at the expense of the K-Feldspar grains. The celadonite content of these micas of micrometric scale, varies between 0.05 and 0.18 while muscovite is comprised between 0.68 and 0.85 (Mica 1 in Fig. 3). Minimal pressure is estimated at 2-4 kbar according the empirical barometer of Massonne et al. 1987, while temperature

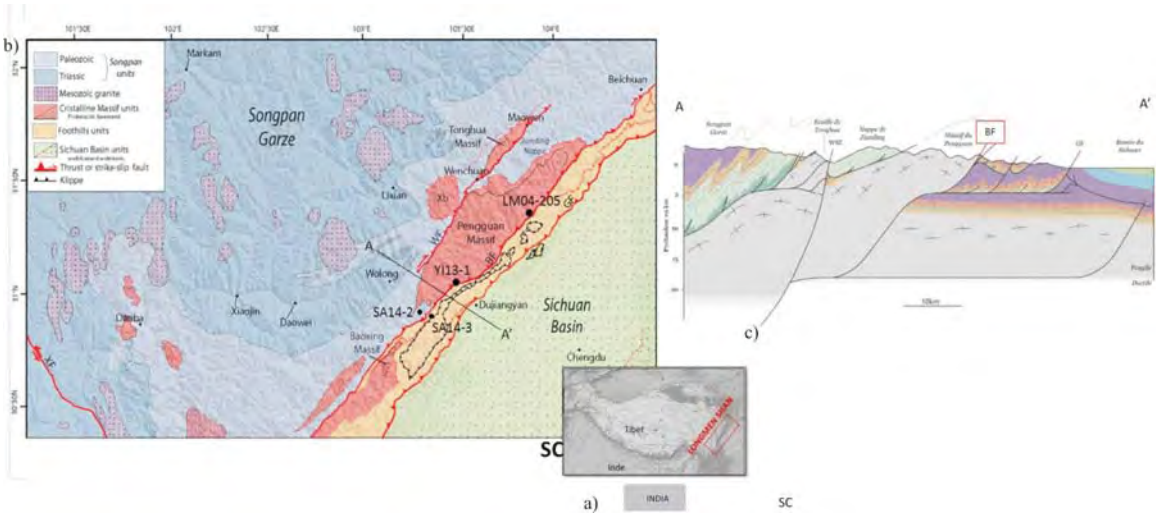

Fig. 1. (a) SRTM of the Tibetan plateau showing the location of the Longmen Shan. (b) Simple geological map of Longmen Shan mountain belt at the eastern margin of Tibetan plateau. Collected samples are shown in black (YI13-1, LM04-205, SA14-2 and SA14-3). Xb: Xuelongbao massif, WF: Wenchuan Fault, BF: Beichuan fault, SC: South China craton. (c) NW-SE geological cross section: the South China basement (the Neoproterozoic Yangtze terrane of Pengguan) is exhumed along the Beichuan fault on younger sediments.

Fig. 2. Samples were collected on the hanging wall of the Beichuan fault in the basement where green schist metamorphic shear zones (chlorite + mica + epidote) developed.

is calculated at 300±50°C from equilibrium thermobarometric modelling of Dubaq et al., 2010. This generation of white mica could be related to a fluid-rich alteration event.

The second generation of micas, of some tents of micrometers in length, has a higher celadonite content (0.30-0.48) and a lower muscovite content (0.45-0.60) (Fig. 3). Since this generation is observed in deformed samples only, along shear zones, together with chlorites, it is associated to a green schist metamorphic event accompanied by deformation. Pressure and temperature conditions of the green schist metamorphic event were estimated with chlorite-mica (+quartz + water) multiequilibrium thermobarometric modelling (Dubaq et al., 2010; Vidal et al., 2006) at 270±30°C, 6-8 kbar. Temperatures of 350 (±50) °C were also deduced from the graphitization of carbonaceous material characterized by Raman Spectroscopy in the sedimentary cover of the Pengguan massif (samples SA14 in Fig. 1). Such P-T conditions reveals of a cold gradient across the basement in the hanging wall of the Beichuan fault.

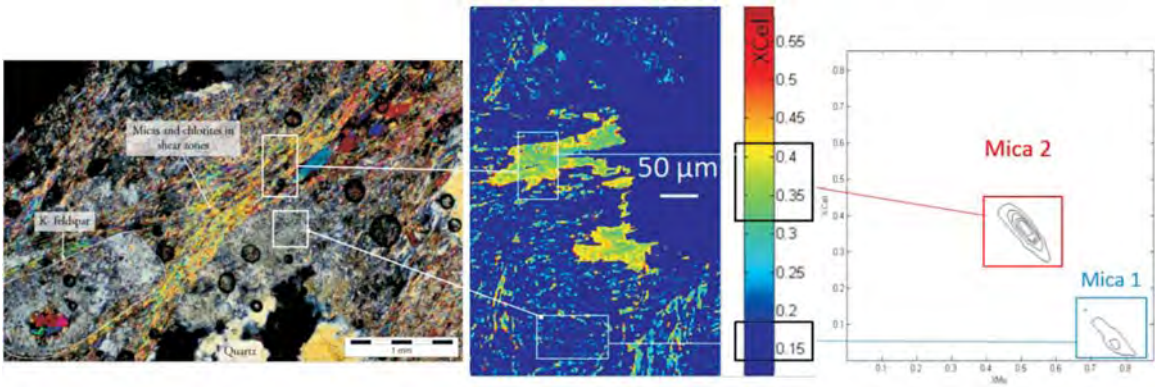

Fig. 3. (a) Uncrossed polar microscopic images of samples from the basement in the hanging wall of Beichuan fault. a) Uncrossed polar images of metamorphic green schist assemblage (epidote and chlorite develops from the breakdown of magmatic amphiboles) of the metagranite. The first generation of micas developed at the expense of k-feldspar grain is observed in the cross-polar image in the frame (sample LM04-205). (b) Chemical map of celadonite content (Xcel) of with micas obtained with XMapTools program. (c) Two generations of white micas observed in the chemical map (b) in a XMuscovite vs XCeladonite diagram.

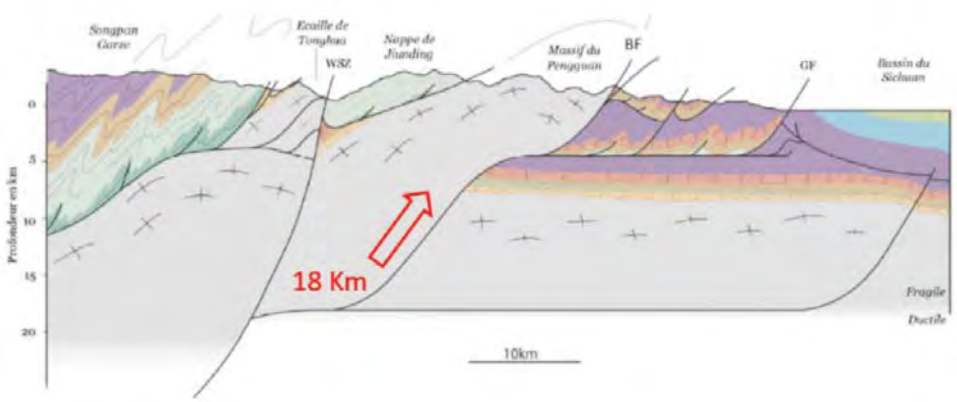

Fig. 4. Geological cross section across the Longmen Shan (see Fig. 1 for location). The P-T conditions of green schist shear zone in the hanging wall of Beichuan fault suggest that the Pengguan massif was exhumed from a depth of 18 Km.

The second step consisted of dating the alteration and metamorphic events which have affected the rocks of the basement on the hanging wall of the Beichuan fault. Micas of the first generation were too small to date by conventional methods. However hydrothermal allanites (REE-rich epidotes) probably formed from the break-down of monazites during the same fluid-rich alteration event could have been dated. Laser ablation-ICPMS Th-Pb dating on allanites provides ages of 680±28 Ma, slightly younger than the age of 742±4 Ma estimated by $^{40}Ar/^{39}Ar$ dating of magmatic amphiboles for the granite crystallization. This magmatic age is coherent with the 827 to 741 Ma activity of the South China basement (Billerot, 2011). The alteration event during which the first generation of mica crystallize seems then associated to a post-magmatic fluid circulation occurred at the granite emplacement depth of 5-10 km.

A first attempt to date by $^{40}Ar/^{39}Ar$ the second generation of micas has also been carried out but, due to the small size of micas grains compared to the spot width, further analyses are required. Although a precise dating of the green schist metamorphic event is needed, estimated P-T conditions

at which this event occurred (270±30°C, 6-8 kbar) suggest that the basement of the Pengguan massif was exhumed along the Beichuan fault from a depth of 16-21 km (Fig. 4). The total denudation in this area is estimated at about 1 mm/yr since the last 10 Ma (Godard et al., 2010), therefore a part of the basement exhumation (about 10 km) is clearly related to the vertical offset of the Beichuan fault. At 18 km a decollement level is observed by geophysical imaging (Robert et al. 2010; Fielding et al., 2013) and the epicenter of the May 2008 Wenchuan earthquake was located at about 15 km depth. Comparison of results from distant sampled sites (70 km) along the Beichuan fault reveals the spatial continuity of the 18±2 km of exhumation for the basement suggesting similar vertical offset along this thrusting segment of the Beichuan fault.

Billerot, A. 2011. Ph.D thesis, Université Henri Poincaré, Nancy-Université.
Godard, V., Pik, R., Lavé, J., Cattin, R., Tibari, B., de Sigoyer, J., Pubellier M., Zhu, J. 2009. Tectonics, 28, TC5009.
Densmore, A., Ellis, M., Li, Y., Zhou, R., Hancock, G., Richardson, N. 2007. Tectonics, 26, TC4005.
Dubaq, B., Vidal, O., De Andrade, V. 2010. Contrib. Mineral Petrol, 159, 159-174.
Fielding, E., Sladen, A., Li, Z., Avouac, JP., Bürgmann, R., Ryder I. 2013. Geophysical Journal International, 194, 1138-1166.
Lanari, P., Vidal, O., de Andrade, V., Dubacq, B., Lewin, E ;, Grosch, E. Schartz, S. 2014. Computers & Geosciences, 62, 227-240.
Liu-Zeng, J., Zhang, Z., Wen, L., Tapponier, P., Sun, J., Xing, X., Hu, G., Xu, Q., Zeng, L., Ding, L., Ji, C., Hudnut, K., van der Woerd, J. 2009. Earth and Planetary Science Letters, 286, 355-370.
Massonne, H., Schreyer, W. 1987. Contrib. Mineral Petrol, 96, 212-224.
de Michele, M., Raucoles, D., de Sigoyer, J., Pubellier, M., Chamot-Rooke, N. 2010a. Geophysical Journal International, 1-7.
de Michele, M., Raucoles, D., Lasserre, C., Pathier, E., Klinger, Y., Van Der woerd, J., de Sigoyer, J. Xu, X. 2010b. Earth planets Space, 62, 875-879.
Ran, Y., Chen, L., Chen, J., Wang, H., Chen, G., Yin, J., Shi, X., Li, C., Xu, X. 2010. Tectonophysics, 491, 141-153.
Robert, A., Zhu, J., Vergne, J., Cattin, R., Chan, L., Wittlinger, G., Herquel, G., de Sigoyer, J., Pubellier, M., Zhu, L. 2010. Tectonophysics, 491, 205- 2010.
Shen, Z-K., Lü, J., Wang, M., Bürgmann, R. 2005. Journal of Physical Research, 110, B11409.
Tan, XB., Lee, YH., Chen, WY., Cook, KL., XU, XW. 2014. Journal of Asia Earth Sciences, 81, 91-104.
Vidal, O., de Andrade, V., Lewin, E., Munoz, M., Parra, T., Pascarelli, S. 2006. Jour. Metam. Geol., 24, 669-683.

Geneses of pseudotachylytes from brittle-ductile transition zone in the Asia/Indian boundary: a new seismic duplexing model for the Eastern Great Counter Thrust

Zhiqin Xu[1], X Zhou[1], Deng-Zhu B[2], Guan-Wei Li[1], Han-Wen Dong[1]
[1]Institute of Geology, Chinese Academy of Geological Sciences, Beijing, 100037, P.R. CHINA
[2]Geological Survey of Tibet, Tibet, P.R. CHINA

The E-W trending duplexing structures with foliation steeply dipping to south occur along the Eastern Great Counter Thrust (EGCT), south Tibet. The EGCT is composed of three slices from south to north, including the Triassic flysch of the Tethys Himalayan, Yarlung-Zangbu ophiolites representing the Neo-Tethys oceanic fragment and Luobusa-Langxian conglomerates (the eastern segment of the Gangrinboche conglomerates) overlying the Gangdese granite, respectively, which are seperated by two 'S' shape backthrusts (Fig. 1).

The main backthrust develops in the Latest Oligocene-Early Miocene mylonitic Luobusha-Langxian conglomerate. The Luobusha scientific drilling (1800 m in depth) reveals that the mylonitic conglomerate as a deformed wedged shape inserts between the Luobusha ophiolite and Gangdese granite. The field and microstructure observations firstly show that large volumes of mm

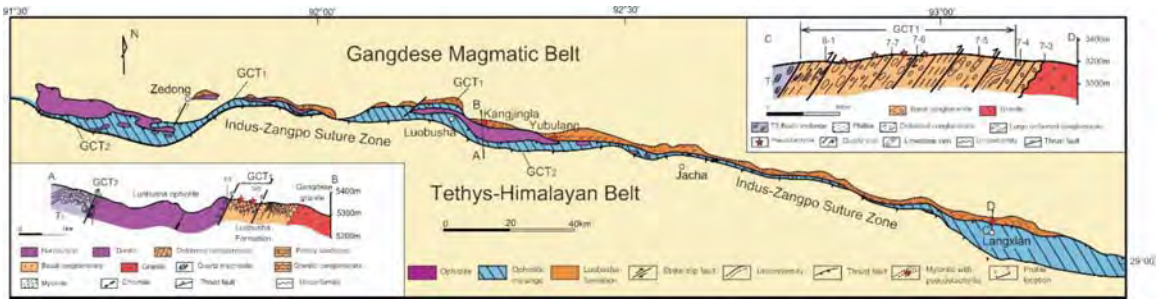

Fig. 1. Schematic tectonic map of the Eastern Great Counter Thrust (E.GCT) along the Yarlung-Tsangpo suture zone (YTSZ) (A) (modified by geological maps of Zedong and Milling areas); Cross-section of the Luobusha mylonitic thrust shear zone with pseudotachylite veins(A-B); Cross-section of the Langxian mylonitic thrust shear zone with pseudotachylite veins(C-D).

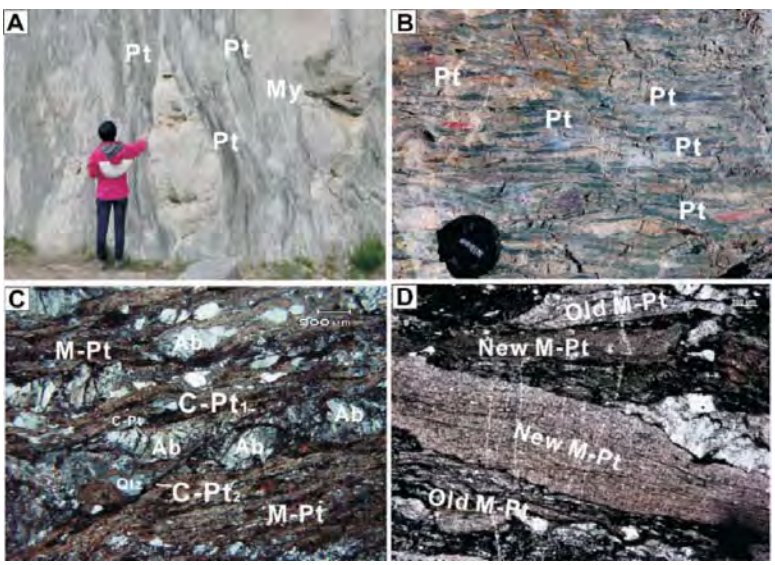

Fig. 2. Field photograph and microphotograph of the Luobusha-Langxian along the East Great Counter Trust (EGCT) showing the pseudotachylyte (Pt) in the mylonites (My) from the conglomerates. C-Pt: cataclasite-related pseudotachylyte.

to cm scale pseudotachylyte veins distribute in the mylonitic conglomerates (Fig. 2). Multiple repeated generations of pseudotachylyte veins and mylonitizations, as well as cataclasite, indicate that the mylonitic conglomerate wedge was transformed from crystal-plastically to brittle domain.

The pseudotachylytes consisting of different directions microlites, and flow structures within a fine-grained matrix display typical melt-origin features. The distribution of pseudotachylyte in the mylonites indicates that the earthquakes nucleated at the base of the brittle-dominated seismogenic zone and propagated through the brittle-ductile transition into the ductile-dominated regime of the crust about 12-16 km in depth.

The coexistence of multiple overprinting generations of voluminous Cataclasite-related pseudotachylyte veins (C-Pt) and Mylonite-related pseudotachylyte (M-Pt) veins indicates that there had been a series of large earthquakes, accompanying repeatedly seismic slips, representing the activity of EGCT during Early Miocene. It dragged the conglomerates into the crustal brittle-ductile transition at 12-16 km depth along the EGCT, which was subsequently exhumed the surface above >5 km.

Study of snout fluctuation and geomorphology of Dunagiri glacier linked with pollen deposition pattern in the Dunagiri valley, Uttarakhand, India

Vinit Kumar[1*], S.K. Yadav[2], A. Mishra[2], A. Trivedi[3]
[1]*Wadia Institute of Himalayan Geology, 33 GMS Road, Dehradun 248001, INDIA*
[*]*vinit@wihg.res.in*
[2]*Department of Geology, University of Lucknow, Lucknow 226007, INDIA*
[3]*Birbal Sahni Institute of Palaeobotany Lucknow 226007, INDIA*

Dunagiri glacier is a north facing 5.5 km long and 0.5 km in width (valley glacier) covers an area of 2.56 sq km lying in the fifth order Girthiganga basin of Dhauliganga valley. The glacier is bounded by latitudes 30°32' to 30°35'N and longitudes 79°53' to 79°54'E, in Chamoli district of Uttarakhand. The glacier is broad in the accumulation zone lying in NW direction with several transverse crevasses and separated by ablation zone lying in N direction having thick mantle cover of dump moraines, supra glacier lakes and three levels of lateral moraines and a terminal moraine at different elevations and positions.

The snout fluctuation of Dunagiri glacier was earlier examined during 1985 to 1992 (by GSI). This period characterized oscillatory nature of snout. The morainic levels at different position and altitudes (snout at 4373 m) show past extension of the glacier at down valley from the snout at elevation up to 3367 m. The field investigations coupled with satellite data and SOI toposheet has enabled to delineate the different levels of moraines and map the landforms associated with the glacier area. The field observations and visual interpretation of satellite data have revealed that there are three levels of lateral and a terminal moraine well identified in the field. On the basis of recent position of snout and the location of these deposits, the total retreat of glacier is calculated as about 123 m from 1992-2013. The total recession of glacier during the period of 21 years was about 123 m with an average rate of 5.8 m/yr. The above observations show that the glacier retreated with a steady state except for the marked fluctuations in the snout positions.

The pollen analysis of 8 surface samples collected in a transect from the Dunagir glacier snout to Ruwing village in Garhwal Himalaya (Latitude 30°35′34.3″ and Longitude 79°53′29.3″) was carried out to understand the pollen deposition pattern of the various plant taxa/groups in relation to their composition in the regional vegetation. In general, the pollen rain assemblage depicts dominance of arboreals (trees and shrubs) over non-arboreals (herbs). The encounter of conifer pollen such as *Pinus wallichiana*, *Abies*, *Cedrus*, *Picea,* etc. (temperate pollen) in the glacier region denotes their transportation by the upthermic winds. The record of broad-leaved thermophillous elements such as *Querecus*, *Betula*, *Corylus*, *Carpinus* and *Juglans* in low to moderate frequencies deciphers their restricted presence in the moist and shady depressions. Even then, they are under-represented compared to their factual occurrence in the region. This discrepancy regarding their display in the pollen rain could be attributed to their low pollen productivity since majority of them are entomophillous. Among the non-arboreals, the high values of grass pollen together with good presence of sedges, Chenopodiaceae/Amranthaceae, Caryophyllaceae, Brassicaceae, Asteraceae and *Artemisia* in the pollen rain correspond with their occurrence in the ground flora.

This comparative database derived on the pollen deposition pattern of various extant plant taxa/groups provides a modern analogue for precise assessment of pollen sequence from the morainic deposits from the region in terms of past vegetation and climate change.

Kinematics, fabrics and geochronology analysis in the Médog shear zone, Eastern Himalayan Syntaxis

Hanwen Dong*, Zhiqin Xu
Institute of Geology, Chinese Academy of Geological Sciences, Beijing 100037, CHINA
**donghanwen123@126.com*

The Himalaya orogen is a classic example of an orogenic system created by continent-continent collision (Dewey and Burke, 1973; Yin and Harrison, 2000). It is bordered by four large boundaries: the Yarlung-Tsangpo suture to the north, the Main Frontal Thrust (MFT) to the south, the left-slip Chaman fault to the west, and the right-slip Sagaing fault to the east (Yin, 2000). The EHS represents the east termination of the main Himalayan orogen. Understanding the tectonics of the EHS plays a key role in constructing the origin and evolution of the Himalaya orogen belt. Thus, the kinematics, microstructure, geochronology and fabric analyses of the deformation structures are critically important.

The EHS, structurally below the Trans-Himalayan plutonic belt, is a high-grade metamorphic terrane. This terrane primarily consists of orthogneiss and paragneiss with high amphibolite-granulite facies that are often interlayered with high-pressure granulites and mantle-derived mafic-ultramafic xenoliths (Liu and Zhong, 1997). These rocks experienced high grade metamorphism in the upper green schist to upper amphibolite or granulite facies (Liu and Zhong, 1997; Zhong and Ding, 1996). The EHS is confined by boundary faults, including the sinistral-shearing Dongjiu-Milin fault to the west and the dextral-slipping Médog Shear zone to the east (Burg et al., 1998; Xu et al,. 2008, 2012; Zhang et al., 1992; Zhang et al., 2004). The Médog shear zone has preserved considerable significant information on the structural and tectonic evolution of the EHS. In this study, we report kinematics, fabrics and geochronology data of the Médog shear zone in the EHS. Analyses of the crystallographic preferred orientation (CPO) of quartz (EBSD analysis) demonstrated that there are three major slip systems: (i) basal <a> slip, (ii) prism [c] slip, and (iii) prism <a> slip. These slip systems are consistent with microstructures of low-temperature shearing, medium-temperature shearing and high-temperature shearing, respectively. U-Pb zircon *in situ* dating with LA-MC-ICP-MS from granitic plutons consistently yielded an age of 64-63.3 Ma. However, the syn-kinematic granites exhibited ages of 29.4-28.6 Ma. We interpret that the former resulted from the India-Eurasian plate collision. The latter suggests that the dextral shearing along the Médog shear zone was initiated during the Early Oligocene. The $^{40}Ar/^{39}Ar$ analysis indicates that the Médog shear zone experienced three tectonothermal events from the Late Oligocene to the Pliocene, e.g., ~23.4 Ma, 16.9-12.6 Ma and ~5.3 Ma.

Burg, J.P, Nievergelt, P., Oberli, F., Seward, D., Davy, P., Maurin, J., Diao, Z., Meier, M. 1998. J. Asian Earth Sci., 16(2), 239-252.
Dewey, J.F., Burke, K.C.A. 1973. J. Geol., 683-692.
Liu, Y., Zhong, D.L. 1997. J. Metamorph. Geol., 15(4), 451-466.
Xu, Z.Q., Cai, Z.H., Zhang, Z.M., Li, H.Q., Chen, F.Y., Tang, Z.M. 2008. Acta Petrol. Sin., 24(7), 463-1476 (in Chinese with English abstract).
Xu, Z.Q., Ji, S.C., Cai, Z.H., Zeng, L.S, Geng, Q.R., Cao, H. 2012. Gondwana Res., 21(1), 19-36.
Yin, A. 2000. J. Geophys. Res., (1978-2012), 105 (B9), 21745-21759.
Yin, A., Harrison, T.M. 2000. Annual Review of Earth Planet. Sci., 28(1), 211-280.
Zhang, J.J., Ji J.Q., Zhong, D.L., Ding, L., He, S.D. 2004. Sci. China (Ser. D: Earth Sci.), 47 (2), 138-150.
Zhang, Z.G., Liu, Y.H., Wang T.W. 1992. Science Press, Beijing. p. 185 (in Chinese).
Zhong, D.L., Ding, L. 1996. Chinese Sci. Bull., 41 (1), 87-88.

Susceptibility mapping of Landslide Hazards in the Tribal Belt of Chamba-Bharmour region Western Himalaya, Himachal Pradesh, using Geo-spatial Techniques

Kamini Singh[1]*, Anjali Singh[2], Ajay Kumar Arya[1]

[1]Centre of Advance Study in Geology, University of Lucknow, Lucknow 226001, INDIA

******geo.kaminisingh@gmail.com*

[2] Department of Anthropology, University of Lucknow, Lucknow 226001, INDIA

The landslide hazards are one of the natural phenomena in the highly vulnerable and geodynamically active mountains, like Himalaya, where the ongoing collision of India-Eurasian plates has allowed the generation of a high mountain chains characterized by steep unstable slopes. Landslide hazards are the third largest natural agent of destruction in the Himalaya (Biyani, 2006) which causes enormous damage not only to structures like roads, tunnels, dams, bio-engineering structures, etc but also takes a toll of human life.

The present study aims at investigating the landslide susceptible zones in tribal belt of Chamba-Bharmour region situated between the Zanskar and Dhauladhar ranges under the Ravi catchment of Himachal Pradesh. The slope stability in the region is mainly governed by the local geology, geomorphology and tectonism. The causative factors responsible for inducing instability includes, undercutting or toe erosion by Ravi River, lithology, over steepened slopes, increase in weight and creation of slippery surfaces in rocks due to percolating rain waters, violent seismic shaking, cloud bursts and anthropogenic activities, etc. The highest incidences of landslides occur due to heavy precipitation in monsoon periods and thereby affecting the traffic movement on the important routes. One such important pilgrim route is Chamba-Bharmaur road, where landslides disrupt traffic movement every year and also power supply for long periods. The area falls under the seismic zone V of the Seismic Zonation Map of India. From seismicity point of view, the area falls in the western extremity of the Kangra reentrant, which is continuously converging, giving a shortening rate of 14±2 mm/yr, and there is also a 20 km long N35°W-S35°W trending segment of neo-tectonically active fault stretching along Ravi River (Joshi, 2004), and thereby making the Chamba town more vulnerable for landslide hazards.

A vulnerability and susceptibility map was prepared using Remote Sensing and GIS technique of the region. The regional susceptibility mapping of Landslide Hazard in the terrain results to delineate the area into different zones of three relative classes i.e. High-, Moderate- and Low-susceptible zones. The High Hazard zones are restricted to upstream part of Ravi River in the area as it is under high influence of anthropogenic activities and natural river undercutting. The investigations carried out suggests that most part of area is highly susceptible to Landslide Hazards which always pretense a threat to mankind, and sometimes also blocking the progress of developmental projects in the area. Therefore, the susceptibility categorization in the area will assist the planners and developer in selecting the favorable sites for the developmental schemes, even if hazardous terrains cannot be avoided altogether.

Comparative evaluation of ground water storage using GRACE-GPS data in highly urbanized region in Uttar Pradesh, India

Saksham Arora[1], Suresh Kannaujiya[2], Param K. Gautam[3], Anjali Singh[4], Ajanta Goswami[2], Prashant K. Champati[2]

[1]Indian School of Mines, Dhanbad, INDIA
[2]Indian Institute of Remote Sensing, Dehradun 248001, INDIA
[3]Wadia Institute of Himalayan Geology, 33 GMS Road, Dehradun 248001, INDIA
[4]Indian Institute of Technology Roorkee, Roorkee, INDIA

As the groundwater sustainability depends on recharge, discharge rate of the ground water and the consumers, it is often problematic to accurately quantify the ground water resources availability on the large scale. In the present effort we have tried to evaluate the Ground Water Storage (GWS) in the highly populated and industrial region of India. With this goal we selected two districts Meerut and Lucknow of Uttar Pradesh (UP) state in India. Meerut region is highly populated and industrial compare to Lucknow. To achieve the goal, ten years data of Gravity Recovery and Climate Experiment Satellites (GRACE), Soil Moisture Contents (SMC), Rain Fall (RF) from 2003 to 2012, bore-hole data of 42 wells from May 2005 to November 2010 and one year Global Positioning System (GPS) data of the year 2012 of International GNSS Service (IGS) station LCKI of Lucknow region have been included in the study. We performed processing of entire data set with the consideration of all necessary constraints. The obtained results have been analyzed in two phases (i) seasonal variation (pre-monsoon, monsoon and post-monsoon) of each year separately that reflect the seasonal/climatic variation and it does not affect GWS much, and (ii) Comparative analysis also has been done for each season with each year from 2003 to 2012 and found the overall depletion in GWS in entire UP. The Meerut region which is relatively highly urbanized shows more depletion rate -2.76±0.87 cm/yr compare to the depletion rate of -1.46±0.74 cm/yr at Lucknow. From the study we found that the over extraction of the groundwater due to the continuous urbanization is the major factor, which was more responsible for the depletion of ground water resource compared to the meteorological effect. If proper measurements are not taken soon to ensure sustainable ground water usage, that day is not far away when Uttar Pradesh will face a severe shortage of ground water.

Kinematic model for the development of Tista-Rangit Dome, Darjeeling-Sikkim Himalaya (DSH)

Subhajit Ghosh[1]*, Puspendu Saha[1], Santanu Bose[1], Nibir Mandal[2], S.K. Acharyya[2]

[1]Department of Geology, University of Calcutta, Kolkata 700019, INDIA
**cugeol.subhajit@gmail.com*
[2]Department of Geological Sciences, Jadavpur University, Kolkata 700032, INDIA

Along the entire length of the Himalayan mountain belt, the Lesser Himalayan fold-thrust belt is characterized by several of orogen-transverse domal tectonic windows (McQuarrie et al., 2008). Our kinematic analysis shows the mushroom shape map pattern of the Tista Dome (Fig. 1) resulted from orogen parallel F3 and orogen transverse F4 fold interference, which invoke a new conceptual model of superposed buckling in the mechanically stratified litho-tectonic systems for the development of tectonic windows in the context of Himalayan geology (Bose et al., 2014). But, the fold interference model along with the orogen transverse F4 folds remains a very controversial issue in the light of dominant brittle crustal deformations and antiformal thrust stack models (Bhattacharyya and Mitra, 2009). Our structural mapping indicate orogen parallel F3 folds with NE-SW to NW-SE axial planes are rotated to its present orientation by the later orogen-transverse F4

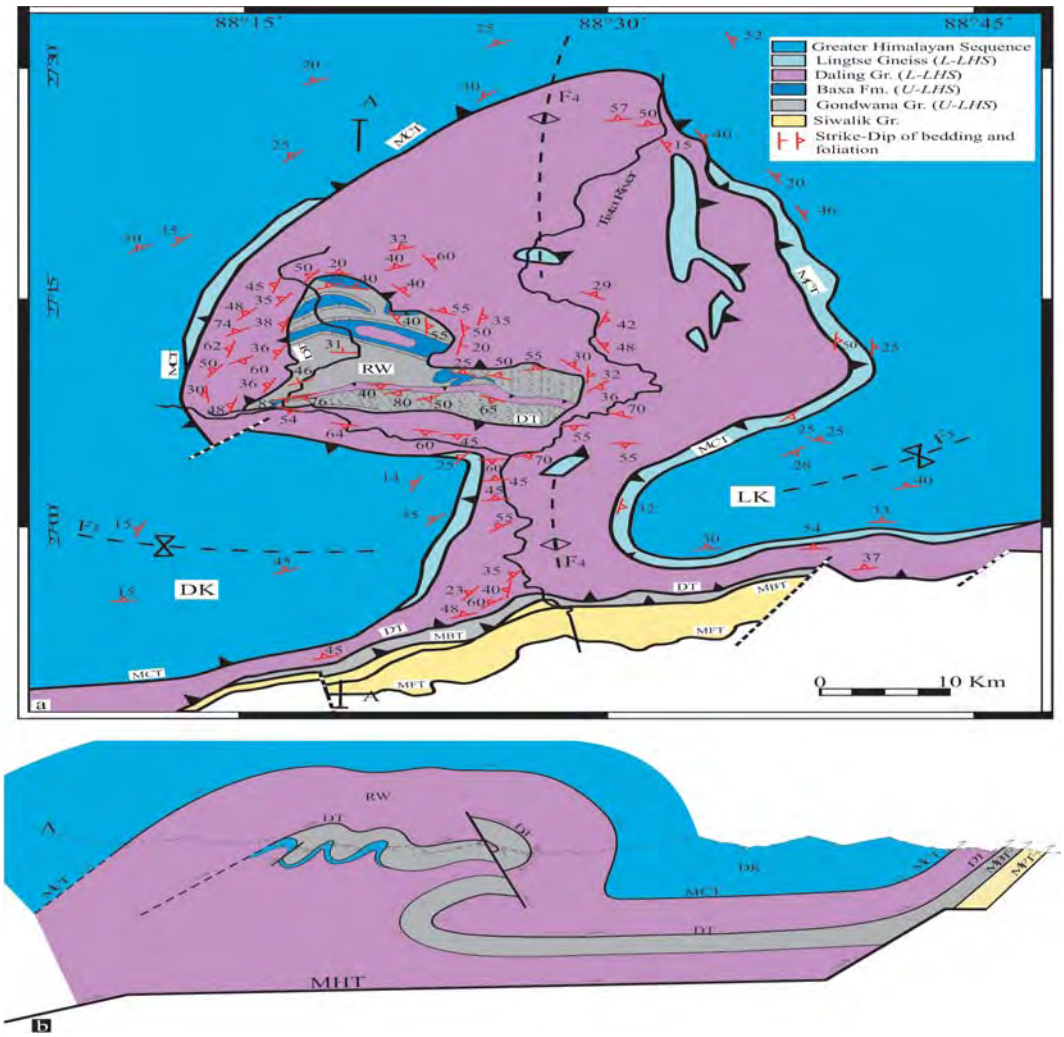

Fig. 1. (a) Geological map of the Tista Dome (TD), DSH. Regional axial traces of F3 and F4 are shown. A part of the Gondwana Gr. of rocks marked by dash lines indicates Rangit- Phongla slates. DK - Darjeeling klippe, LK - Lava klippe, RW - Rangit Window. Note that the strike variations around the Rangit window (RW) define a domal structure. (b) N-S structural profile (AA') across the TD (after Bose et al., 2014).

folds with N-S axial plane characterized by an association of Types 1 and 2 interference patterns. We substantiate this superposed buckling model with results obtained from analogue experiments. The model explains contrasting F3-F4 interferences in the Lesser Himalayan Sequence (LHS).

Secondly, the Daling Thrust (~Ramgarh Thrust ~Sumar Thrust) (DT) delineates a zone of intense shear localization around the Rangit Window (RW) in the Lesser Himalayan Sequence (LHS) of the Darjeeling-Sikkim Himalaya (DSH). Microstructural studies of deformed quartzite samples indicate a transition of bulging (BLG) to sub-grain rotational (SGR) recrystallization mechanism with increasing distance from the DT. Based on the quartz piezometer (Stipp et al., 2003; Holyoke and Kronenberg, 2010), our estimates reveal strong variations in the flow stress (59.12 MPa to 16.53 MPa) over a distance of ~1.2 km from the DT. Deformation mechanism maps constructed for different temperatures show the strain rates (10^{-12} S^{-1} to 10^{-14} S^{-1}) remain within the natural limits (Twiss and Moores, 2007). Finally, we present a mechanical model to provide a possible explanation for the cause of stress intensification along the DT.

Bhattacharyya, K., Mitra, G. 2009. Gondwana Res., 16, 697e715 doi:org/10.1016/j.gr.2009.07.006.
Bose, S., Mandal, N., Acharyya, S. K., Ghosh, S., Saha, P. 2014. Journal of Structural Geology, 66, 24-41.
Holyoke, C.W., Kronenberg, A.K. 2010. Tectonophysics, 494, 17-31. doi:10.1016/j.tecto.2010.08.001.
McQuarrie, N., Robinson, D., Long, S., Tobgay, T., Grujic, D., Gehrels, G., Ducea, M. 2008. Earth Planet. Sci. Lett. 272, 105e117 http://dx.doi.org/10.1016/j.epsl. 2008.04.030.
Stipp, M., and Tullis, J. 2003. Geophysical Research Letters, v. 30, 2088, doi: 10.1029/ 2003GL018444.

Variety and complexity of boudinage in the heart of Almora Crystalline zone

Arun K. Ojha*, Deepak C. Srivastava#
Dept. of Earth Sciences, IIT Roorkee, Roorkee 247667, INDIA
**ojhaarun323@gmail.com #dpkesfes@gmail.com*

Structural analysis along Khairna - Almora sections of Kumaun Lesser Himalaya reveals wide variety of structural features which requires logical explanations. Among these, boudins are both common and intriguing. Boudinage is the disruption of layers, bodies or foliation with in a rock mass in response to bulk extension along enveloping surface (Ramsay and Huber, 1987; Davis and Reynolds, 1996; Passchier and Druguet, 2002; Goscombe et al., 2004; Twiss and Moores, 2007 and others). These structures are commonly formed by layer parallel extension in rocks with considerable competence contrast across layering (Ramsay and Huber, 1987; Davis and Reynolds, 1996; Passchier and Druguet, 2002; Goscombe et al., 2004; Twiss and Moores, 2007). A variety of boudins are found such as; Pinch-and-swell, Barrel boudins and Fish mouth boudins. Several workers have already mentioned their findings of boudins in Almora area (Valdiya, 1980; Agrawal and Bali, 2008). All the boudins are developed in Quartzite bands that are enclosed in matrix mica schist.

This study reports a new variety of boudin; 'Self-organised boudin' (Fig. 1). This new kind is completely different from the classical varieties, because of the following characteristics; (i) combination of pinch-and-swell and Fish mouth structure, and (ii) pinching of one layer lies adjacent to the swelling of another neighbour layer.

Following two hypotheses are proposed for the origin of these boundins:

(1) Extension superimposed by shearing: The boudins in individual layer first generate due to layer parallel extension and then organise themselves due to shearing (Fig. 2). Whether the layer parallel extension and shearing processes were simultaneous or sequential is not clear at this stage.

(2) Interference: These 'Self-organised boudins' can develop in an extensional regime in multi-layered rock; with closely spaced competent layers (Fig. 3). Because of close spacing, the zone of contact strains of

Fig. 1. Field photograph of the 'Self organised boudin' found in layers of interbedded quartzite and schist.

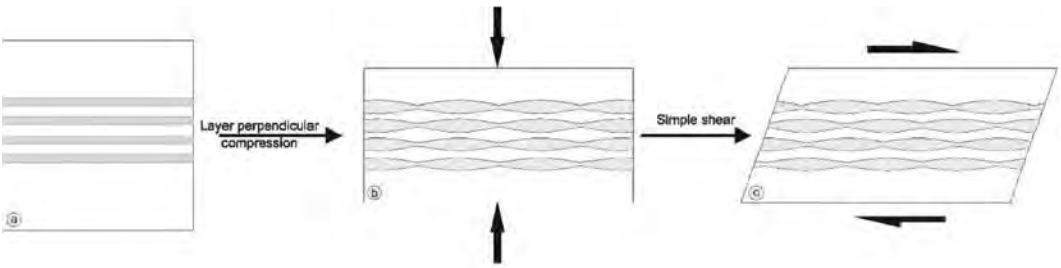

Fig. 2. Representation of combined effect of layer parallel extension and simple shear in boudin formation. (a) Initial parallel layers of high competent (grey) and low competent (white) rock. (b) Formation of boudins by layer parallel extension. (c) Readjustment of boudins because of shearing.

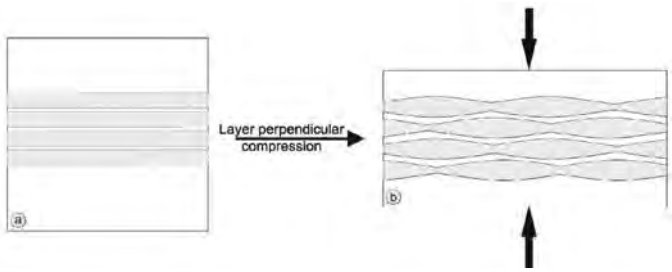

Fig. 3. Graphical representation of formation of 'Self-organised boudins' by interference. (a) Initial layering of high competent (grey) and low competent (white) rock. (b) Formation of boudins by interference because of layer parallel extension.

two adjacent competent layers interferes. This hypothesis has already been used to define similar structures in quartz veins within Levan schist of Scotland, in mesoscopic scale (Cosgrove, 1997).

Agrawal, K.K., Bali, R. 2008. Journal Earth Science India, Vol. I(III), 119-124.
Cosgrove, J.W. 1997. Tectonophysics 280, 1-14.
Davis, G.H., and Reynolds, S.J. 1996. Structural Geology of Rocks and Regions (2nd Edition): New York, John Wiley and Sons, Inc., 776 p.
Goscombe, B.D., Passchier, C.W., Hand, M. 2004. Journal of Structural Geology 26, 739-763.
Passchier, C.W., Druguet, E. 2002. Journal of Structural Geology 24, 1789-1803.
Ramsay, J. G., Huber, M. I. 1987. The Techniques of Modern Structural Geology. Volume 2: Folds and Fractures. Academic Press, London. 391 p.
Twiss, R.J., Moores, E.M. 2007. Structural Geology, second ed. Freeman, New York. 736p.
Valdiya, K.S. 1980. Geology of the Kumaon Lesser Himalaya, Wadia Institute of Himalayan Geology, Dehradun, India 291p.

Direct Estimation of Rupture Depths of Earthquake Fault From GPS and InSar

Zhen Fu[1], Caibo Hu[2], Haiming Zhang[3], Huihui Xu[3], Yongen Cai[3]
[1]*Institute of Geophysics, China earthquake Administration 100081, CHINA*
[2]*College of Earth Science, University of Chinese Academy of Sciences, Beijing 100049, CHINA*
[3]*School of Earth and Space Sciences, Peking University, Beijing 100871, CHINA*

Rupture depth of an earthquake fault is important parameters for characterizing the earthquake rupture and studying earthquake mechanics. It has been inferred from aftershock distribution, seismic reflection and refraction imaging. However, the results from different methods

are often significantly different. Dislocation theory in an elastic half space indicates that if a seismic ruptures directly runs up to the ground surface, there exist zero points of horizontal strain in the surface deformation, which correspond to the rupture depths, except for pure strike-slip faults. In this study, we use numerical simulations to investigate the possibility of inferring rupture depths from zero-strain points for cases of buried faults and heterogeneous media. The results show that the correspondence of zero-strain points to the rupture depths can be influenced by the heterogeneity of the underground media and the stress field. For buried faults, the correspondence relationship is approximately valid when the fault depth is <1 km. In addition, the range of earthquake fault dip angles can be estimated by horizontal displacements on the ground. We also study how to determine the rupture depths of faults from InSAR data after large earthquakes, and successfully apply the method to the 2008 Wenchuan earthquake. The method proposed here, which determines the parameters of fault geometry according to surface deformation, is simple and easy to perform. With independent of aftershocks, it can provide valuable constraints to kinematic inversions.

Biostratigraphy of the Cambrian succession of the Parahio Valley, Spiti region, Northwest Himalaya

Nancy Virmani[1*], Birendra, P. Singh[1], O.N. Bhargava[2], Naval Kishore[1], Aman Gill[1]
[1]Center of Advanced Study in Geology, Panjab University, Chandigarh 160014, INDIA
**nancy15.geo@gmail.com*
[2] INSA Honorary Scientist, 103, Sector-7, Panchkula 134109, INDIA

Additional collection of new faunal elements comprising trilobites and ichnofossils from four sections has led to refine the existing Cambrian biostratigraphy (Peng et al., 2009, Singh et al., 2014) of the Parahio Valley, Spiti region, Northwest Himalaya. The identified faunal assemblages (Table 1) are: the *Oryctocephalus indicus* Zone (earliest Middle Cambrian, Series 3 (Stage 5)), the *Bhargavia prakritika* level (earliest Middle Cambrian, Cambrian Series 3, Stage 5), *the Yuehsienszella cf. szechuanensis* level (latest Early Cambrian, Cambrian Series 2, Stage 4), and trace fossil assemblage zones viz., the *Diplichnites-Rusophycus-Hormosiroidea* assemblages Zone and the *Planolites- Phycodes* assemblage Zone (Early Cambrian). The *Yuehsienszella* cf. *szechuanensis* level constitutes the lowest trilobite level in the studied section (Table 1); occurring stratigraphically below the *Oryctocephalus indicus Zone* (Cambrian Series 3, Stage 5) indicates a latest Early Cambrian age (Cambrian Series 2, Stage 4). The *Oryctocephalus indicus* Zone (Cambrian Series 3, Stage 5) contains *Oryctocephalus indicus*, *Pagetia significans*, *Pagetia taijiangensis*, *Pagetia miaobanpoensis*, *Pagetia* sp., and *Kunmingaspis pervulgata, which is* age equivalent to the basal part of the earliest Middle Cambrian (Series 3, Stage 5).

The *Bhargavia prakritika* level occurs 12 m above the *O. indicus* Zone and is dominated by the abundant specimens of *Bhargavia prakritika* (Singh et al., *under review*). The *Planolites-Phycodes* assemblage Zone (Early Cambrian) occurs below the least known trilobite level i.e. *Yuehsienszella cf. szechuanensis* level (Cambrian Series 2, Stage 4); whereas the *Diplichnites-Rusophycus-Hormosiroidea* assemblage Zone is ranging in rocks of the Cambrian Series 2, Stage 4 (latest Early Cambrian) to the Middle Cambrian (Cambrian Series 3, Stage 5). The *Oryctocephalus indicus* Zone (Cambrian Series 3, Stage 5) contains *Oryctocephalus indicus*, *Pagetia significans*, *Pagetia taijiangensis*, *Pagetia miaobanpoensis*, *Pagetia* sp., and *Kunmingaspis pervulgata, which is* age equivalent to the basal part of the earliest Middle Cambrian (Series 3, Stage 5). The *Bhargavia prakritika* level occurs 12 m above the *O. indicus* Zone and is dominated by the abundant specimens of *Bhargavia prakritika* (Singh et al., *under review*). The *Planolites- Phycodes* assemblage Zone (Early Cambrian) occurs below the least known trilobite level i.e. *Yuehsienszella cf. szechuanensis* level (Cambrian Series 2, Stage 4); whereas the *Diplichnites- Rusophycus-Hormosiroidea*

Table 1. *The various faunal assemblages / zones / levels with their corresponding faunal elements, age and localities in the Parahio valley, Spiti region, Northwest Himalaya.*

Assemblages / Zone / level	Trilobite/ ichnofauna	Locality	Age
Bhargavia prakritika level	*Bhargavia prakritika*	Classic Parahio Valley section	Middle Cambrian (Cambrian Series 3, Stage 5).
Oryctocephalus indicus Zone	*Oryctocephalus indicus*, *Pagetia significans*, *Pagetia taijiangensis*, *Pagetia miaobanpoensis*, *Pagetia* sp., *Kunmingaspis pervulgata*	Classic Parahio Valley section	Middle Cambrian (Cambrian Series 3, Stage 5).
Yuehsienszella cf. szechuanensis level	*Yuehsienszella cf. szechuanensis*	Section B (above Khemangar khad locality, lower part of the Parahio Valley section)*	latest Early Cambrian (Cambrian Series 2, Stage 4)
Diplichnites-Rusophycus-Hormosiroidea Assemblage Zone	*Diplichnites, Psammichnites, Monomorphichnus, Diplocraterion, Treptichnus*,*D imorphicnus, Helminthopsis, Cruziana, Gordia, Hormosiroidea, Curvolithus,* myriapod trackways and arthropod scratch marks	Sections A & B (A at Khemangar khad and B above the Khemangar khad locality, lower part of the Parahio Valley section)* and Section C (at Kaltarbo locality, 1.8 km SW of the Maopo encamping ground)	Cambrian Series 2, Stage 4 (latest Early Cambrian) to Middle Cambrian (Cambrian Series 3, Stage 5)
Planolites-Phycodes Assemblage Zone	*Planolites*, *Phycodes*	Sections A & B (A at Khemangar khad and B above the Khemangar khad locality, lower part of the Parahio Valley section)* and Section C (at Kaltarbo locality, 1.8 km SW of the Maopo encamping ground)	latest Early Cambrian (Cambrian Series 2, Stage 4)

** For details of the location see Virmani et al., (2015)*

assemblage Zone is ranging in rocks of the Cambrian Series 2, Stage 4 (latest Early Cambrian) to the Middle Cambrian (Cambrian Series 3, Stage 5).

Peng, S., Hughes, N.C., Heim, N.A., Sell, B.K., Zhu, X., Myrow, P.M., Parcha, S.K. 2009. Paleontological Society Special Publication, 6, 1-95.
Singh, Birendra, P., Virmani, N., Bhargava, O.N., Kishore, N., Gill, A. 2014. Journal Paleontological Society of India, 59(1), 81-88.
Singh, Birendra P., Virmani, N., Bhargava, O.N., Kishore, N., Gill, A. (under review). Revision of trilobite Genus Bhargavia from the Spiti Himalaya, India.
Virmani, N., Singh, Birendra P., Gill, A. Journal Geological Society of India, 85, 557-566.

Continuous GPS time series analysis of MPGO Ghuttu, Central Himalaya, India

Param K. Gautam*, Naresh Kumar, Chandra P. Dabral
Wadia Institute of Himalayan Geology, 33 GMS Road, Dehradun 248001, INDIA
**param@wihg.res.in*

In the present work we investigated the deformation pattern of GPS station Ghuttu and also made an effort to find out the parameters that are responsible for the anomalous behavior in the GPS

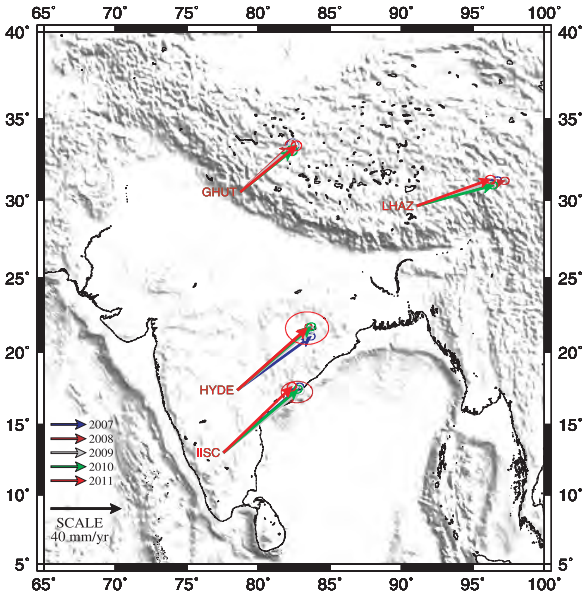

time series. With this objective we analyzed the continuous five years data (2007-2011) of GHUT station through GAMIT/GLOBK software in ITRF05 reference frame on 95% confidence level and generated daily time series plots of each year's separately. It is found 40±2 mm/yr horizontal motion and 41±3° rotation from east for GHUT while 48±4 mm/yr horizontal motion with rotation of 18±2.5° has been estimated for LHAZ site. The comparative analysis indicates convergence between GHUT and LHAZ with the rate of convergence ~15 mm/yr and ~23 mm/yr respectively. Here we have also examined anomalous changes in the time series of GHUT before, after and during the occurrence of local earthquakes for both cases when the earthquake lies within or out of strain radius and tried to detect any relation of such changes with the occurred earthquake. For this purpose we considered seven local earthquakes of magnitude range 4.5 to 5.7 that are selected on the basis of strain radius equation $\rho=100.43^{M}$ of Dobrovolsky et al. (1979). In the analysis, we inferred that the earthquake source parameters (M, Fd and Ed) and strain radius (ρ) play important role to change the behavior of time series that may consider as earthquake precursor parameters.

Ediacaran-early Cambrian ichnofossils from Mongolia, China and Newfoundland show geographically asynchronous appearance and evolution of metazoans

Tatsuo Oji[1], Takafumi Mochizuki[2], Sersmaa Gonchigdorj[3], Stephen Q. Dornbos[4], Keigo Yada[1]

[1]Nagoya University, Nagoya, 464-8601, JAPAN

[2]Iwate Prefecture Museum, JAPAN

[3]Mongolian University of Science & Technology, MONGOLIA

[4]University of Wisconsin-Milwaukee, Milwaukee, WI 53211, USA

We have been studying ichnofossils (trace fossils) from the late Ediacaran-early Cambrian marine siliciclastics and carbonates of western Mongolia, South China and Newfoundland, Canada, in order to clarify the pattern and the process of 'the Cambrian Explosion', namely the evolution and diversification of metazoans. Our main focus is on the geographic comparison of ichnofossils from different geographic areas from this age interval. Our study shows that the ichnofossil sizes, and also the activities of ichnofossil producers, which are expressed by the bedding plane bioturbation index,

have increased asynchronously among these areas. In the earliest Cambrian, the ichnofossil sizes were larger and the activities of benthic animals were greater in western Mongolia and South China than in Newfoundland. Paleogeographic reconstruction in early Cambrian shows that Mongolia and South China were located in low latitude near the equator, whereas Newfoundland was located in high latitude in southern hemisphere. Namely the size increase of benthic animals and an increase of benthic activities had started earlier in low latitude than in other areas in the early Cambrian.

Our recent survey of the late Ediacaran of western Mongolia also showed that large (up to 1 cm in diameter) and penetrative trace fossils are abundantly found in bedded limestones. Such a new discovery shows that evolution of metazoans had occurred earlier than previously considered, at least locally in the late Ediacaran.

Characteristics of metamorphic rock magnetic fabrics in the Nyalam area of the southern Tibet and its geological significance, China

Zou Guangfu[1*], Zou Xin[2,5], Mao Ying[3], Mao Qiong[4]

[1]*Chengdu Institute of Geology & Mineral Resources, Chinese Geological Survey, Chengdu 610082, CHINA*
**zguangfu@163.com*
[2]*Department of Psychology, Peking University, Beijing 100871, CHINA*
[3]*Chengdu Comprehensive Rock and Mineral Testing Center, Chengdu 610081, CHINA*
[4]*Institute of Exploration and Development, NorthChina Oilfield, Renqiu 062552, CHINA*
[5]*China Ocean Press, Beijing 100081, CHINA*

The Precambrian metamorphic belt in Nyalam region located in southern Himalayan Plateau is important study area for the formation and evolution of the Himalayan orogen and Tibetan Plateau uplift history. It has a complex tectonic deformation history that recorded the relevant information of crustal movement and deformation characteristics in southern Tibet Plateau. The study area is important for the geologists because of its structure and multiple deformation active that has been recognized to understand the formation and evolution of the Himalayas. However, it is to be noted that the existing studies mainly focused on the regional geology, petrology, geochronology aspects, fracture initiation activities and other aspects, but relatively speaking, the studies lack the understanding of fine structural deformation, and deformation of the Regional tectonic strain type and structure orientation of principal stress.

In this paper we report Precambrian rock magnetic fabrics in the Nyalam area of southern Tibet. We studied the deformation of times and deformation and metamorphism of Precambrian metamorphic in Nyalam region, and the Southern Tibet Detachment system (STDS) and the Main Central Thrust (MCT) of deformation characteristics. Also, we have studied regional tectonic stress strain type and orientation of the main structure, and other aspects in Nyalam region. The magnetic fabric, tectonic strain characteristics, structural principal stress directions and kinematic characteristics of the Precambrian metamorphic basement area have been discussed in great detail in this paper. The studies have significant meaning as they provide a new evidence of the Precambrian metamorphic basement in the formation of the Himalayan orogenic evolution and stress field conversion process.

The analytical results of magnetic fabrics show that the values of H are high (>10% in general), so the ductile deformations of the Precambrian rock is strong. The orientation of the maximum principal stress inferred from the minimum magnetic susceptibility is nearly S-N, NE-SW and NW-SE. The Flinn diagram of the magnetic fabrics shows that the strain pattern are oblate and constrictional type. Magnetic foliation of great majority of rock samples is well developed and the magnetic lineation is poor, and the magnetic susceptibility ellipsoid is flattened. The magnetic lineation of the minority rock samples is well developed and the magnetic foliation is poor and the

magnetic susceptibility ellipsoid is prolate. Acording to the geological field and the magnetic fabrics, there are 3 times tectonic stress field in SN directed extruding, NW-SE directed extruding,NW-SE directed extension. It shows that the Nyalam area has undergone process the orientation of SN, NW-SE nappe structure and NW-SE directed extension structure. The change of tectonic stress is reflected by the field characteristics of the Precambrian rock magnetic fabrics that is the direct responding result of the arc-continental, continent-continental collision between the India and Asian continents in the late part of the Late Cretaceous to Late Eocene and subsequently shifted to intra-continental convergent, the plateau uplifting and extension structure stage since the Late Eocene.

Late Quaternary displacement of the Karakoram Fault: evidence from Nubra and Shyok valleys, Ladakh Himalaya

Watinaro Imsong[1]*, Falguni Bhattacharya[2], Mishra, R.L[1], Sarat Phukan[3]

[1]Wadia Institute of Himalayan Geology, 33 GMS Road, Dehradun 248001, INDIA

**imsongnar@gmail.com*

[2]Institute of Seismological Research, Gandhinagar 382421, INDIA

[3]Department of Geological Sciences, Gauhati University, Guwahati 781014, INDIA

In Northwestern Himalaya, the right-lateral Karakoram fault (KF) has displaced the Jurassic-Cretaceous Karakoram batholith from the Gangdese batholith with a displacement of ~1000 km causing the eastward extrusion of Tibetan Plateau (Matte et al., 1996; Molnar and Tapponier, 1975; Peltzer and Tapponier, 1988). However, in a more recent study, Searle, et al., (1989, 1996; 2010) suggested that the displacement is less than ~120-150 km and the movement along the fault initiated since early to mid-Miocene. Based on the geomorphic evidences, variable rate of displacements have been obtained during the Quaternary period suggesting that the KF is still active.

In the present study we investigated Nubra and part of Shyok valleys to ascertain the nature and magnitude of activity along the KF. Towards this we used morphotectonic derivatives and Quaternary

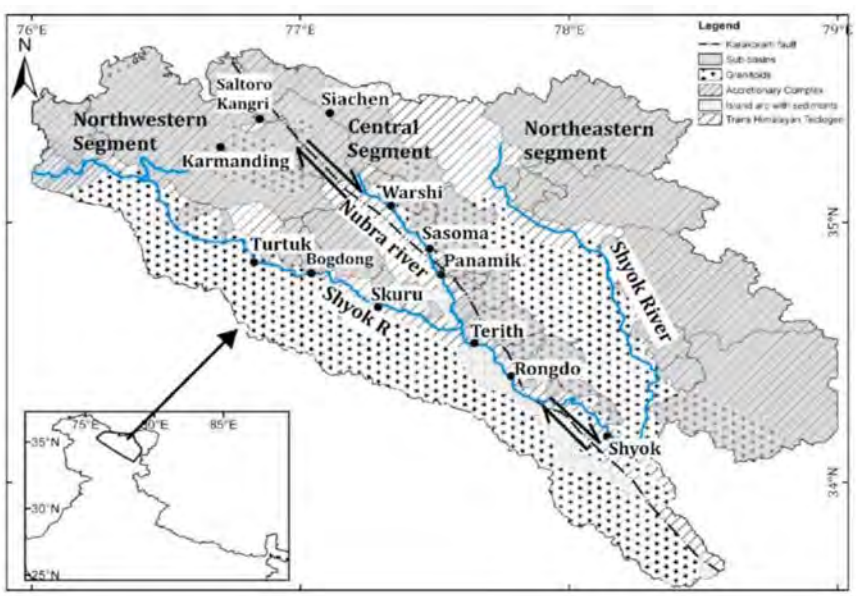

Fig. 1. Lithotectonic map of the Study area modified after Seismotectonic Atlas of India prepared by Geological Survey of India (2000) showing the trend of KF. Three segments viz. northeastern, central and northwestern are marked. The shaded area represents the sub-basins selected for morphometric analysis in the study area.

landforms to ascertain the magnitude of displacement (Fig. 1). In order to provide tentative time periods, we used the existing chronology on the displaced landforms.

The morphometric indices suggests that compared to the eastern segment the central segment between Nubra valley and part of Shyok river is undergoing relatively high deformation and accords well with the sense of movement along the KF. The geomorphic expression of right lateral displacement is well represented by the presence of shutter ridges (in bedrock streams), deflection of the alluvial streams, preferential tilt in the alluvial fans and displaced lateral moraines.

Tentative chronology for the initiation of displacement along the bedrock and alluvial suggests that the bedrock stream deflection was initiated close to ~180 ka and 60 ka respectively, whereas the alluvial stream deflection is dated between early Holocene (~10 ka) to late Holocene (~2 ka). The above age estimates are broadly in accordance with the data obtained by Brown et al. (2002) and resonate well with the field stratigraphy. The study suggests that KF is providing the accommodation space to the north directed compression, however, it does not contribute significantly in terms of attaining relief (Searle, 1996; Brown et al., 2002).

Brown, E.T., Bendick, R., Bourles, D.L., Gaur, V., Molnar, P., Raisbeck, G.M., Yiou, F. 2002. Jour. Geophys. Res., 107(B9), 2192.

Matte, P., Tapponnier, P., Arnaud, N., Bourjot, L., Avouac, J.P., Vidal, Ph., Qing, L., Yusheng, P., Yi, W. 1996. Earth and Planetary Sc. Lett., 142, 311-330.

Molnar, P., Tapponnier, P. 1975. Science, 189(4201), 419-426.

Peltzer, G., Tapponnier, P. 1988. Jour. Geophys. Res., 93(B12), 15085-15117.

Searle, M.P., Rex, A.J., Tirrul, R., Rex, D.C., Barnicoat, A., Windley, B.F. 1989. Metamorphic Geol. Soc. America, Special Paper, 232, 47-73.

Searle, M.P. 1996. Tectonics, 15(1), 171-186.

Searle, M.P., Parrish, R.R., Thow, A.V., Noble, S.R., Phillips, R.J., Waters, D.J. 2010. Jour. of the Geol. Soc. London, 167, 183-202.

Coseismic offset due to the April 25, 2015 Gorkha, Nepal Earthquake

Rajeev Kumar Yadav*, P.N. Singharoy, S. Gupta, P. Khan, J.K. Catherine, V.K. Gahalaut

CSIR-National Geophysical Research Institute, Hyderabad 500007, INDIA

**rs123_bhu@yahoo.co*

The April 25, 2015 Gorkha Earthquake (Mw 7.8) was one of the largest earthquakes of recent time in the active Himalayan thrust belt. We have observed significant coseismic offsets at sites in the adjoining Indo-Gangetic plains, the largest being about 7 mm towards north at Patna, Bihar. In this presentation we have compared various available slip models of this earthquake derived from seismic back projection, GPS data, InSAR data etc. We have estimated the coseismic displacement at various sites of Indian GPS networks Nepal for spherical layered earth due to the available five slip models (USGS, 2015; Avouac, 2015; Yagi, 2015; Wang, 2015; and Galetzka, 2015). We found that the slip model of USGS and Yagi have large inconsistency with observed coseismic displacement at the nearby GPS stations (KKN4, CHLM, SNDL, and NAST, in Nepal) and have good consistency at far field GPS stations. The average root mean square error of coseismic displacement is less for slip model derived by Galetzka et al., (2015) from the inversion of GPS and InSAR data, as compared to the other slip models. We have used a linear inversion scheme to derive the slip distribution on the finite fault in layered earth (CRUST2.0) using coseismic offsets at the GPS stations of Nepal and India. We have found reduced root mean square error as compared to the other available slip models of the earthquake. The estimated moment magnitude is consistent with that reported by other authors. The ruptured segment is about 130

km and majority of the slip occurred between the epicenter of the main shock (Mw 7.8) and its largest aftershock (Mw 7.3).

Avouac, J-P., Meng, L., Wei, S., Wang, T., Ampuero, J-P. 2015. Nature Geosciences, DOI: 10.1038/NGEO2518.
Galetzka, J. et al. 2015. Science express, 0.1126/science.aac6383.
USGS, 2015. Http://earthquake.usgs.gov/earthquakes/eventpage/us20002926#scientific_finitefault.
Wang, K., and Fialko, Y. 2015. Geophysical Research Letter, doi: 10.1002/2015GL065201(Accepted).
Yagi, Y., Okuwaki, R. 2015. Geophysical Research Letter; doi: 10.1002/2015GL064995 (Accepted).

Influence of anthropogenic groundwater unloading in Indo-Gangetic plains on the April 25, 2015 Mw 7.8 Gorkha, Nepal Earthquake

Bhaskar Kundu[1*], Naresh Krishna Vissa[1], V.K. Gahalaut[2,3]
[1]*Department of Earth and Atmospheric Sciences, NIT Rourkela, Rourkela, INDIA*
**rilbhaskar@gmail.com*
[2]*CSIR-National Geophysical Research Institute, Hyderabad, INDIA*
[3]***National Centre for Seismology, Ministry of Earth Sciences, New Delhi, INDIA***

Groundwater usage in the Indo-Gangetic plains exceeds replenishment of aquifers, leading to substantial reduction in the mass. Such anthropogenic crustal unloading may promote long-term fault slip or may modulate seismic activity in the adjoining Himalayan region to the north. Our simulation using GRACE data and hydrological models of such a process indicates that the April 25, 2015 Mw 7.8 Gorkha, Nepal earthquake was probably influenced, upto some extent, by the anthropogenic groundwater unloading process in the Indo-Gangetic plains. The groundwater withdrawal leading to crustal unloading in the Indo-Gangetic plains of the Bihar and eastern Uttar Pradesh states of India, causes a significant component of horizontal compression which adds to the secular interseimic compression at the seismogenic depth (5-20 km) on the Main Himalayan Thrust (MHT) beneath the Himalayan arc, and at hypocentral depth of the Gorkha, Nepal earthquake. This effect enhances the Coulomb stress on the locked zone of MHT.

Aftershock sequence of Gorkha Earthquake 2015

Lok Bijaya Adhikari
National Seismological Centre, Kathmandu, NEPAL

On 25th April 2015 at 11:56 AM local time a large earthquake of magnitude M 7.8 (ML 7.6) occurred with epicenter Barpak of Gorkha district, Nepal. Epicenter of this devastating earthquake lies about 75 km North West of Kathmandu, the capital city of Nepal. The earthquake lies at the rim of the High Himalayan range. affecting Kathmandu valley, which claimed about 9000 lifes and destroyed more than 6,00,000 houses. More than 400 aftershocks of magnitude greater than 4 ML have been recorded and still aftershocks are frequent in the region. The distribution of aftershock defines a main 140 km long ESE trending structure, parallel to the mountain range. In addition to the main region illuminated by the aftershocks, we observe a second seismicity belt located southward, under the Kathmandu basin and northern part of the Mahabharat range. Many aftershocks within this belt have been felt by the 3 million inhabitants of the Kathmandu valley.

The mystic Main Central Thrust revisited throughout the Greater Himalayan Crystalline duplex

A. Alexander G. Webb[1]*, Dian He[2,3], Kyle P. Larson[4], Aaron J. Martin[5], Tyler K. Ambrose[4,6], Hongjiao Yu[2,3]

[1]School of Earth and Environment, University of Leeds, Leeds, UK
** a.a.g.webb@leeds.ac.uk*
[2]Dept. of Geology and Geophysics, Louisiana State University, Baton Rouge, USA
[3]Shell International Exploration and Production Inc., Houston, USA
[4]Earth and Environmental Sciences, University of British Colombia Okanagan, Kelowna, CANADA
[5]División de Geociencias Aplicadas, IPICYT, San Luis Potosí, MEXICO
[6]Department of Earth Sciences, Oxford University, Oxford, UK

Two longstanding problems in Himalayan tectonics, i.e., (i) how the Himalayan crystalline core was developed and emplaced, and (ii) the description of the Main Central Thrust (MCT), may now be resolved by recent work on the bounding and internal faults of the Greater Himalayan Crystalline complex. Work on the first problem has generated most of our Himalayan tectonic models: wedge extrusion, channel flow, tectonic wedging, critical taper, etc. The second problem has proved a key difficulty in testing these models. This is because the 'nature, position, and the role' of the 'mystic' MCT (as famously phrased by Upreti, 1999) bounding the base of the crystalline complex in tectonic models has never been a settled issue. MCT definitions based on chemistry, lithologies, metamorphism, timing, combined aspects, etc., have commonly held for one region, yet failed along other portions of the orogen. We put forward a hypothesis based on exploration of the southern limits of the South Tibet Detachment (STD), i.e., the upper bound on the Greater Himalayan Crystalline complex, and 'tectonic discontinuities' within the Greater Himalayan Crystalline complex:

We argue that footwall accretion and/or duplexing has dominated each phase of Himalayan mountain-building (He et al., 2015). The Greater Himalayan Crystalline complex itself appears to be a duplex: a stack of thrust horses, with each horse recording a similar but temporally distinct pressure-temperature evolution. In this model, the STD is the roof thrust of the duplex and the 'tectonic discontinuities' are the thrust faults bounding the horses. We consider the MCT to be both the base of the crystalline core during its emplacement and the Himalayan sole thrust during that period. This helps explain some of the complexity in recognizing the MCT. If the Greater Himalayan Crystalline complex was assembled as a largely in-sequence thrust duplex, then the basal thrust of each thrust horse represents a segment of the MCT. The MCT would have been long-lived on fault flats. Along the fault ramp where the duplex horses were accreted, the development of each new horse would correspond to (a) the cessation of motion on a structurally high segment of the MCT, and (b) the initiation of motion on a structurally low segment of the MCT. In this view, the Greater Himalayan Crystalline complex now contains multiple strands of the MCT. Multiple occurrences of the same fault can be readily understood within the theoretical framework of a duplex (Larson et al., In Press).

Another element of MCT mystery involves the question of reactivation, potentially as recently as the Pliocene (Harrison et al., 1997). We understand some apparent MCT reactivation in the context of out-of-sequence faulting. Perhaps one out of every ten south-directed thrust faults observed in the Himalaya is an out-of-sequence fault (Webb, 2013). Such faults disrupt the upper plate of the Himalayan orogen and locally coincide with (and cut) pre-existing faults, including strands of the MCT. Monazite evidence for extensive MCT reactivation in the central Himalaya may alternatively reflect Lesser Himalayan duplex development (Robinson et al., 2003) and/or metasomatism (Martin et al., 2007).

Harrison, T.M., Ryerson, F.J., Le Fort, P., Yin, A., Lovera, O.M., Catlos, E.J. 1997. Earth and Planetary Sciences Letters, v. 146, p. E1-E7.

He, D., Webb, A.A.G., Larson, K.P., Martin, A.J., Schmitt, A.K. 2015. International Geology Review, v. 57, p. 1-27.

Larson, K.P., Ambrose, T.K., Webb, A.A.G., Cottle, J.M., Shrestha, S. (In press). Earth and Planetary Sciences Letters, doi:10.1016/j.epsl.2015.07.070.

Martin, A.J., Gehrels. G.E., DeCelles, P.G. 2007. Chemical Geology, v. 244, p. 1-24.

Robinson, D.M., DeCelles, P.G., Garzione, C.N., Pearson, O.N., Harrison, T.M., Catlos, E.J. 2003. Geology, v. 31, p. 359-362.

Upreti, B.N. 1999. Journal of Asian Earth Sciences, v. 17, p. 577-606.

Webb, A.A.G. 2013. Geosphere, v. 9, p. 572-587.

Source parameters and Static stress changes associated with the M_w7.8 2015 Nepal Himalayan earthquake

Prantik Mandal

CSIR-National Geophysical Research Institute, Hyderabad 500007, INDIA

**prantikmandal62@gmail.com*

We measure source parameters for the 25th April 2015 Nepal earthquake through inversion modeling of S-wave displacement spectra from RTZ components recorded at eighteen broadband stations. The average seismic moment and source radius are estimated to be 1.27 x 10^{20} N-m and 7454 m, respectively, while the mean corner frequency and moment magnitude are calculated to be 0.0986 Hz and (7.270.24), respectively. The average radiated energy, stress drop and crustal Q values are found to be 2.74 x 10^{16} Joules, 38.14 and 1774, respectively. The mean apparent stress is calculated to be 2.38 MPa, which agrees well with the estimates for the Tibet-Himalayan and Mexican subduction zone thrust earthquakes. The large radiated energy and high apparent stress associated with the 2015 Nepal event can provide an explanation for the widely felt intensity data at distances up to 1900 km.

The moment tensor inversion for multiple point sources is performed on the band-passed (0.008-0.10 Hz) displacement data of the 25 April (M_w 7.8) and 12 May (M_w 7.3) 2015 events, from seventeen broadband stations in India. Results reveal that the 25 April event (strike=318°, dip=26°, rake=93°) ruptured the shallow part (at 16 km depth) of the north dipping (~15°) Main Himalayan Thrust (MHT) while the 12 May event (strike=29°, dip=18°, rake=30°) rocked the north dipping (~18°) deeper part of the MHT (at 26 km depth). The P-axis orients toward NE, which is parallel to the direction of convergence of the Indian plate suggesting an N-S shortening in the brittle upper India crust while T-axis orients toward E-W, which is parallel to the strike of MHT in the Nepal Himalaya.

We modelled the Coulomb failure stress changes (CFS) produced by the slips on the fault planes of the 25 April event (USGS's W phase MT solution: strike=290°, dip=7°, rake=101°) and 12 May event (our estimated MT solution: strike=29°, dip=18°, rake=30°). A strong correlation with occurrences of aftershocks and regions of increased positive CFS is obtained below the Kathmandu basin, Nepal. We notice that predicted CFS show a positive Coulomb stress of 0.269 MPa and 0.195 MPa on the fault plane of the 25 April event and 12 May event, respectively. These small modelled stress changes can lead to trigger events if the crust is already near to failure, but, these small stresses can also advance the occurrence of future earthquakes. The main finding of our CFS modelling implies that the 25 April event increased the Coulomb stress by 0.195 MPa at 26 km depth below the site of the 12 May event, thus, this event can be termed as triggered. We propose that the seismic hazard in the Himalaya is not only caused by the slip on the shallow part of MHT, rather, the occurrence of large triggered event on the deeper part of MHT can also enhance the seismic hazard in the Nepal Himalaya.

Geomorphic evolution of valley-fill deposits of Srinagar (Garhwal) valley, NW Himalaya

Rahul Devrani*, Vimal Singh
Department of Geology, University of Delhi, New Delhi, INDIA
**rahuldevrani18@gmail.com*

In the last decade several studies have highlighted the importance of valley-fill deposits. These studies (e.g., Juyal et al., 2010; Ray and Srivastava, 2010) have mainly linked the occurrence of deposits of different time periods with the climatic shifts. However, these studies overlooked the role of tectonics and local processes such as sediment flux from tributaries, hillslopes, river damming etc. In order to understand the evolution of valley-fill deposits in an area, it is important to investigate both local as well as regional processes.

The Alaknanda valley in the Ganga River basin is located in one of the world's most dynamic mountain chains i.e., the Himalaya. Large amount of valley-fill deposits occur along the Alaknanda River in its different reaches. In this study we investigate the widest reach of the Alaknanda River for the evolution of valley-fill deposits in this part. Bounded by a regional structure i.e. NAT (North Almora Thrust) in the east and a narrow gorge near Kirtinagar in the west, the Srinagar valley stores 1.35×10^8 m^3 of sediments. On the basis of presence and absence of the valley-fill deposits, the valley is divided in to two parts - eastern part where thick valley-fill deposits occur and western part where the deposits are mostly absent. Geomorphic and field investigation suggest that seven levels of terraces and five levels of debris flow surfaces are present in the Srinagar valley. The terraces present in the eastern part are mostly composed of q_i (axial river deposits), q_t (local stream deposits) and q_h (hillslope deposits), whereas the terraces towards western part are mostly strath terraces. Further, an epigenetic gorge is identified by geophysical investigation (i.e., resistivity survey) on the northern bank of the Alaknanda River over which part of Choras town is located. Variation in the thickness of the valley-fill deposits in the valley is ascribed to the uneven bedrock topography in the valley which is in turn related to the presence of structure, erosion by the tributary and the trunk rivers.

The present study shows the geomorphic evolution in the Srinangar valley and occurrence of valley-fill deposits as an interplay of the regional and local geomorphic processes, which act on an initial (bedrock) topography. The geochronological data suggests that the epigenetic gorge in the Srinagar valley was abandoned before 80 ka and the sediments in this valley were filled by the axial river deposits (q_i) due to pulses of climatic events. Difference in valley-fill deposits in the Srinagar valley is ascribed to the structures present in the valley.

Juyal, N., Sundriyal Y., Rana N., Chaudhary, S. 2010. Journal of Quaternary Science.
Ray, Y., Srivastava, P. 2010. Quaternary Science Reviews.

Tectono-metamorphic evolution of the Tethyan Sedimentary Sequence (SE Tibet)

C. Montomoli[1*], S. Iaccarino[1], B. Antolin[2], E. Appel[2], R. Carosi[3], I. Dunkl[4], L. Ding [5], D. Visonà[6]

[1]Dipartimento di Scienze della Terra, Via S. Maria 53, 56126, Pisa, ITALY
**chiara.montomoli@unipi.it*
[2]Institute for GeosciencesTubingen, University of Tubingen, GERMANY
[3]Dipartimento di Scienze della Terra, Via Valperga Caluso 35, 10125, Torino, ITALY
[4]Geoscience CenterGottingen,University of Gottingen, GERMANY
[5]Institute of Tibetan Plateau ResearchBeijing, Chinese Academy of Sciences, CHINA
[6]Dipartimento di GeoscienzePadova, Via Gradenigo 6, 35131, Padova, ITALY

The Tethyan Sedimentary Sequence (TSS), one of the major tectonic units of the Himalayan belt cropping out in the inner portion of the Himalayan belt, has been investigated in SE Tibet to unravel its tectonic and metamorphic evolution. In SE Tibet the TSS is mainly represented by a Triassic flysch (Antolin et al., 2010) deformed under very-low to low-grade metamorphic conditions (Crouzet et al., 2007, Dunkl et al., 2011).

Along other sections of the belt most of the attention has been paid till now to the relations between the TSS and the STDS (Godin, 2003; Carosi et al., 2007; Kellet and Godin, 2009) focusing on the relations between the development of several generations of folds and the activity of the STDS. The study area offers an almost complete transect of the TSS from the southernmost portion, close to the STDS and the inner one approaching the suture zone allowing to depict a much more complete tectonic and metamorphic evolution of the TSS unit itself.

Meso and microstructural analysis highlighted that the Tethyan Sedimentary Sequence recorded at least three phases of ductile defomation, all of them associated to the development of folds and related axial plane foliations. A prominent D1 deformation is progressively overprinted by a D2 deformation approaching the Yarlung Tsangbo suture zone to the North.

Structural analysis allowed recognising two different first-order structural domains: (i) a southern domain in which D1 is the prominent deformation, and (ii) a northern domain in which the D2 overprint predominates upto transpose D1 deformation. F2 folds show a regional backward vergence (northward) with respect to the southward verging F1 folds. Finite strain data show an increase of D2-related strain moving from South to North. The further tectonic evolution is characterized by the development of brittle-ductile shear zones often localized on the inverted limbs of F2 folds. Kinematic indicators are mainly represented by S-C structures and point to a top-to-the-North sense of movement. A later D3 tectonic phase is associated to upright metric to decametric folds.

Detailed microstructural petrological investigations have been conducted on selected chloritoid-bearing schist. SEM based chemical maps and EMPA profiles have been conducted on chloritoid schist and reveal how a core to rim increase of Mg, compensated by the decrease of Fe and Mn, is systematically present in chloritoid (X_{Mg} from 0.12-0.17). Moreover, white mica shows a statistically change in composition as function of microstructural position: S1 white micas have a lower Si^{4+} (3.02-3.07 a.p.f.u.) content with respect to S2 white micas (3.09-3.15 Si^{4+} a.p.f.u.). A P-T pseudosection in the MnO-Na_2O-CaO-K_2O-FeO-MgO-Al_2O_3-SiO_2-H_2O-TiO_2 model chemical system has been constructed and support P-T condition of S1 equilibration close to 0.45-0.50 GPa and 400-425°C, while the P-T condition of S2 is around 0.75-0.80 GPa and 500-530°C

It is worth to note that the new P-T-d data on polydeformed chloritoid schists point out to an increase of both temperature and pressure from D1 to D2 deformation indicating prograde

metamorphism related to burial during D1-D2 phases and support that F2 folds developed in a compressive tectonic framework during crustal thickening in the time span of 35-25 Ma.

The integration of our new deformation and P-T data with available literature data will help to deconvolve the long lasted history of this tectonic unit, far away to be well understood.

Antolín, B., Appel, A., Montomoli, C., Dunkl, I., Ding, L., Gloaguen, R., El Bay, R. 2011. Geological Society of London Special Publications 349, 99-121 DOI 10.1144/SP349.6

Carosi, R., Montomoli, C., Visonà, D. 2007. Journal of Asian Earth Sciences, 29, 407-423

Crouzet, C., Dunkl, I., Paudel, L., Arkai, P., Rainer, T.M., Balogh, K., Appel, E. 2007. Journal of Asian Earth Sciences 30, 113-130.

Dunkl, I. Antolín, B., Wemmer, K., Rantitsch, G., Kienast, M., Montomoli, C., Ding, L., Carosi, R., Appel, E., El Bay, R., Xu, Q., von Eynatten, H. 2011. Geological Society of London Special Publications 353, 45-69, DOI: 10.1144/SP353

Godin, L. 2003. Journal of Asian Earth Science 22, 307-328

Kellet, D.A., Godin, L. 2009. Journal of the Geological Society London 166, 1-14, doi: 10.1144/0016-76492008

Deformation and very low grade metamorphism of Siwalik rocks south of Bomdila Thrust, Potin-Doimukh section, southwestern Arunachal Pradesh

Abhijit Patra[1]*, A. Banerjee[1], Sk. Md. Equeenuddin[2], D. Saha[1]

[1]Geological Studies Unit, Indian Statistical Institute, Kolkata 700108, INDIA

**abhi.patra2010@gmail.com*

[2]Earth and Atmospheric Sciences, National Institute of Technology, Rourkela 769008, INDIA

In the Potin-Doimukh section of southwestern Arunachal Pradesh, the northwesterly dipping Bomdila Thrust (≡MBT) separates the Bomdila Group of rocks including the Bomdila granite gneiss in the north from the Permo-Carboniferous Gondwana and the Neogene Siwalik rocks in the south, the latter constituting the bulk of sub-Himalaya to frontal Himalaya in this domain. Two strands of the MBT are recognized (MBT1 and MBT2), and deformed Ranigunj Formation equivalent rocks (cf. Bhareli Formation, Kumar, 1997) are sandwiched between these two fault strands. The linear belt of ~200 m (maximum) wide coal bearing Ranigunj Formation is characterized by hard, compact, medium grained pale yellow to buff coloured feldspathic sandstone interstratified with carbonaceous shale, and very thin sub-bituminous coal bands. South of MBT2, the folded and faulted Lower Siwalik rocks (cf. Dafla Fm.) occur in the hanging wall of the Tipi Thrust (Singh, 2007). The Lower Siwalik (Dafla Fm.) consists of medium to fine sandstone alternating with thin, gray to dark gray mudstone and carbonaceous shale; floating pebbles of sandstone and occasional mudstone and woody (lignitic) fragments occur in the thicker sandstone units. South of Tipi Thrust, Middle and Upper Siwalik rocks (cf. Subansiri and Kimin Fm.) occur with moderately to steeply dipping strata showing local overturning. The Middle Siwalik succession consists of trough cross stratified, very coarse (locally up to granule-pebble size clasts) to fine grained sandstone intercalated with fine sandy mudstone; whereas the Upper Siwalik consists of friable, medium to coarse, salt-and-pepper sandstone interstratified with matrix supported conglomerate horizons with common occurrence of carbonaceous shale fragments. The hanging wall of Tipi Thrust is a crush zone (Sibson, 1977), exhibiting cataclasites with mm scale deformation bands (Fossen et al., 2007) and phyllo-silicate bands with smears of carbonaceous and calcareous material along fractures. Brittle fracturing and small meter scale faults are common and close to the MBT1, the Gondwana sandstone and carbonaceous shale are strongly sheared giving rise to foliated cataclasites. On the hanging wall of MBT1, sheared granite gneisses and meta-psammites of the Bomdila Group show ductile to brittle-ductile deformation features including proto-mylonites and shear bands.

Table 1. *KI values, sample location for IC studies with respect to stratigraphy and structural level.*

Sample No	Kubler index# [KI] (Δ°2Θ Cu-Kα)	Location	Litho-stratigraphic position	Metapelitic zone (depth, km) [on the basis of basin maturity, Frey and Robinson, 1999]
Ita 28	0.88493622	In between MBT1 & MBT2	Ranigunj Formation	Diagenetic zone
Ita 25b	0.20473242	~136m away of MBT2 at the footwall	Lower Siwalik	Upper anchizone to Borderline Epizone
Ita 07c	0.22740588	~320m away of MBT2 at the footwall; core of an upright antiform		
Ita 05b	0.21984806	~3.3km away of MBT2 at the footwall; core of an upright antiform		
Ita 33	0.17450114	~4km north of Tipi Thrust at the hanging wall within crush zone; core of an upright antiform		
Ita 19	0.21984806	~1.8km south of Tipi Thrust at the footwall; normal limb of an overturned synform	Middle Siwalik	

 # Illlite crystallinity is inversely proportional to KI

Since the Siwalik and Gondwana rocks are conspicuously folded and faulted in the Doimukh-Potin section, a preliminary examination of the mineralogical reconstitution of these sedimentary strata by XRD analysis of selected samples was undertaken. Results of XRD analysis (clay size fraction) of one Gondwana sample and five Siwalik samples show the common occurrence of chlorite, smectite, illite-muscovite, kaolinite, quartz and plagioclase feldspar. While calcite is present in the Siwalik samples, the Gondwana samples are devoid of carbonates. The "*illite crystallinity*" technique is considered for the first basal reflection of di-octahedral illite-muscovite taking into account c. 10 Å peak, and the standardized *illite crystallinity* (IC) was measured. Except one sample of Gondwana shale, the Kübler Index (KI values) are <0.25 (Table 1), implying maximum burial depth of 12 km and the temperature just above 300°C (Frey & Robinson, 1999 & references therein), had the clay mineral reconstitution was due to burial alone. As the estimated maximum thickness of the Siwalik Group is 7-8 km (Vaidyanadhan and Ramakrishnan, 2010), and Siwalik samples are from the crush zone above the Tippi Thrust or core of folds or, the effect of cataclastic deformation and tectonic loading on clay mineral reconstitution was assessed from the preliminary data. Taking into account the sample location in relation to the major dislocations, namely Tipi Thrust, MBT2 and MBT1, the preliminary data suggest lower KI close to the fault lines or fold cores except one Gondwana sample occurring between MBT1 and MBT2 (Table 1). The Siwalik Group of rocks suffered anchizone to borderline epizone transformation of clay mineralogy. Proximity of locations of analyzed samples for *illite crystallinity* studies to fold cores or fault lines lead us to propose that enhanced cataclastic deformation in this zones facilitated mineralogical

transformation via localized shear heating, and/or channeling of hydrothermal fluids. However, we cannot altogether rule out contribution of detrital clay minerals, degraded micas or altered feldspar in modifying the KI values in the analyzed samples. The lone Gondwana sample with apparent low *illite crystallinity* (KI~0.88) goes against any major contribution of burial metamorphism or any significant influence of detrital minerals.

Fossen, H., Schultz, R.A., Shipton, Z. K., Mair, K. 2007. Journal of the Geological Society, London, 164, 1-15.
Frey, M., Robinson, D. 1999. Blackwell science.
Kumar, G., 1997. Geological Society of India, Bangalore.
Sibson, R. H. 1977. Journal of Geological Society London, 133, 191-213.
Singh, T. 2007. Journal Geological Society of India, 70, 339-352.
Vaidyanadhan, R., Ramakrishnan, M. 2010. Geological Society of India, Bangalore, 889-906.

Paleoclimatic reconstructions using Biochemical modeling in tree ring cellulose isotope data from Western Himalaya and Karakoram

Trina Bose[*,1], Saikat Sengupta[2], R. Ramesh[1], Supriyo Chakraborty[2]
[1]*Physical Research Laboratory, Ahmedabad, INDIA*
**trinabose@yahoo.com*
[2]*Indian Institute of Tropical Meteorology, Pune, INDIA*

In the present scenario of climate change, detail knowledge of the climate system especially its long term variabilities are required (Crowley, 2000; Marcott et al., 2013). Tree ring cellulose isotope datasets due to their stable temporal resolution are one of the primary sources of climatic variability information in recent past (Mann and Jones, 2003; Mann et al., 2008; Brienen et al., 2012). However the reconstructions produced from such data are variably dependable due to statistical process involved in producing these (Crowley, 2000).

There are myriad reasons of statistical regressions giving limited correlation with instrumental data. Firstly, these regressions are usually run using nearest meteorological station data which might be hundreds of kms away, lacking quality control and sparsely available in time. There is no uniformity of which temperature (say) is being reconstructed among the temperature reconstructions. Moreover, the correlation coefficients of the regression lines are low ($r \leq 0.6$) which undermine the quality of reconstruction. In some cases correlation are higher due to detail filtering and complex statistics applied but this does not remove the site specific characteristics of these analyses. This problem becomes specially severe in complex terrains like those in Himalayan ranges and rest of Central Asia.

Cellulose formation in all of the trees (including the ring bearing ones) is mostly the same basic physiochemical process as they all undergo C3 metabolic process. This process and resultant isotopic fractionation have been modeled from experimental information on live trees (Farquhar et al., 1982; Roden et al., 2000; Hughes, 2002). Evans (2007) used these relations as forward models to determine isotopic values of wood cellulose. Managave et al. (2010) tested similar forward models for a trial and error interpretation of the unknown inputs. Although some papers (e.g. Treydte et al., 2009) identified some processes in long term data, but no process based reconstructions were given till now.

Among many benefits of process based reconstruction models, the primary is that the parameter being reconstructed and their dependabilities will stay constant in time and space. This will make the resultant reconstructions more easily interpreted in terms of observed physical processes in present and their variabilities in the past. In presence of basic meteorological data i.e.

temperature and humidity estimates, the pCO_2 of the atmosphere has been reconstructed from carbon isotope data from tree ring cellulose (Bose et al., 2014). The processes involving oxygen and hydrogen isotope fractionations provide information about humidity, temperature and source water isotopic compositions. Some of these process based fractionation model outputs from Himalaya and Karakoram will be discussed.

Bose, Trina, Chakraborty, Supriyo, Borgaonkar, Hemant, Sengupta, Saikat, Ramesh, R. 2014. Current science, 107(6), 971.
Brienen, Roel J.W., Helle, Gerd, Pons, Thijs L. Guyot, Jean-Loup, Gloor, Manuel 2012. Proceedings of the National Academy of Sciences, 109(42), 16957-16962.
Crowley, Thomas J. 2000. Science, 289 (5477),270-277.
Evans, M.N. 2007. Geochemistry, Geophysics, Geosystems, 8(7).
Farquhar, Graham D., O'leary, M.H., Berry, J.A. 1982. Functional Plant Biology, 9(2),121-137.
Hughes, Malcolm K. 2002. Dendrochronologia, 20(1),95-116.
Managave, S.R., Sheshshayee, M.S., Borgaonkar, H.P., Ramesh, R. 2010. Geophysical Research Letters, 37(5).
Mann, Michael E., Jones, Philip D. 2003. Geophysical Research Letters, 30(15).
Mann, Michael E., Zhang, Zhihua, Hughes, Malcolm K., Bradley, Raymond S., Miller, Sonya K., Rutherford, Scott, Ni, Fenbiao 2008. Proceedings of the National Academy of Sciences, 105(36),13252-13257.
Marcott, Shaun A., Shakun, Jeremy D., Clark, Peter U., Mix, Alan C. 2013. Science, 339(6124),1198-1201.
Roden, John S., Lin, Guanghui, Ehleringer, James R. 2000. Geochimica et Cosmochimica Acta, 64(1),21-35.
Treydte, Kerstin S., Frank, David C., Saurer, Matthias, Helle, Gerhard, Schleser, Gerhard H., Esper, Jan 2009. Geochimica et Cosmochimica Acta, 73(16),4635-4647.

Kinematic evolution of local, transport-parallel L-tectonites from eastern Sikkim Himalayan fold-thrust belt: Insights into progressive deformation

Jyoti Prasad Das[*,1], Kathakali Bhattacharyya[1], Matty Mookerjee[2]
[1]*Indian Institute of Science Education and Research Kolkata, Mohanpur 741246, INDIA*
**jpd15rs028@iiserkol.ac.in*
[2]*Department of Geology, Sonoma State University, Rohnert Park, CA 94928, USA*

In the Sikkim Himalayan fold-thrust belt (FTB), the Pelling Thrust (PT) lies in the footwall of the Main Central Thrust (MCT; Bhattacharyya and Mitra, 2014). The PT fault rocks are locally characterized by an L-tectonite mylonite zone along a linear, N-S trending, discontinuous klippe, unlike anywhere else in the Himalayan orogen. This zone lies in close spatial association with L>S, and S>L mylonites, and is folded along a N-S trending synform (Fig. 1). In this study, we address the kinematic evolution of this rare deformational structure.

Shear-sense analysis on the asymmetric feldspar porphyroclasts of the orthogneissic fault rocks record a dominant transport parallel flow (N to S) with a subsidiary transport perpendicular flow (W to E) (Das et al., 2014). Based on recrystallized quartz grains (Stipp et. al., 2002) and quartz c-axes fabric opening angle (Kruhl, 1998), deformation temperatures of the mylonite zones are estimated at ~420-435±30°C and at ~370-520±50°C, respectively. To estimate vorticity at various stages of progressive deformation, we analyzed four different strain markers that record different incremental strain stages: a) porphyroclasts, b) subgrain, c) oblique grain shape fabric, and d) quartz c-axis fabric. The estimates of kinematic vorticity numbers (W_k) from S>L, L>S and L-tectonite zones using these markers range from $0.44<W_k<0.99$, where porphyroclasts show a range of W_m=0.53-0.74, subgrain records W_n=0.66-0.92, oblique grain shape fabric records W_n=0.62-0.80, and quartz c-axis records W_n=0.44-0.99. Such a range in kinematic vorticity number suggests a general deformation with L-fabric from the hinge zone of the fold recording the highest W_k. The variation in W_k recorded by different markers indicates a non-steady state deformation. W_m (from porphyroclasts) and W_n (from

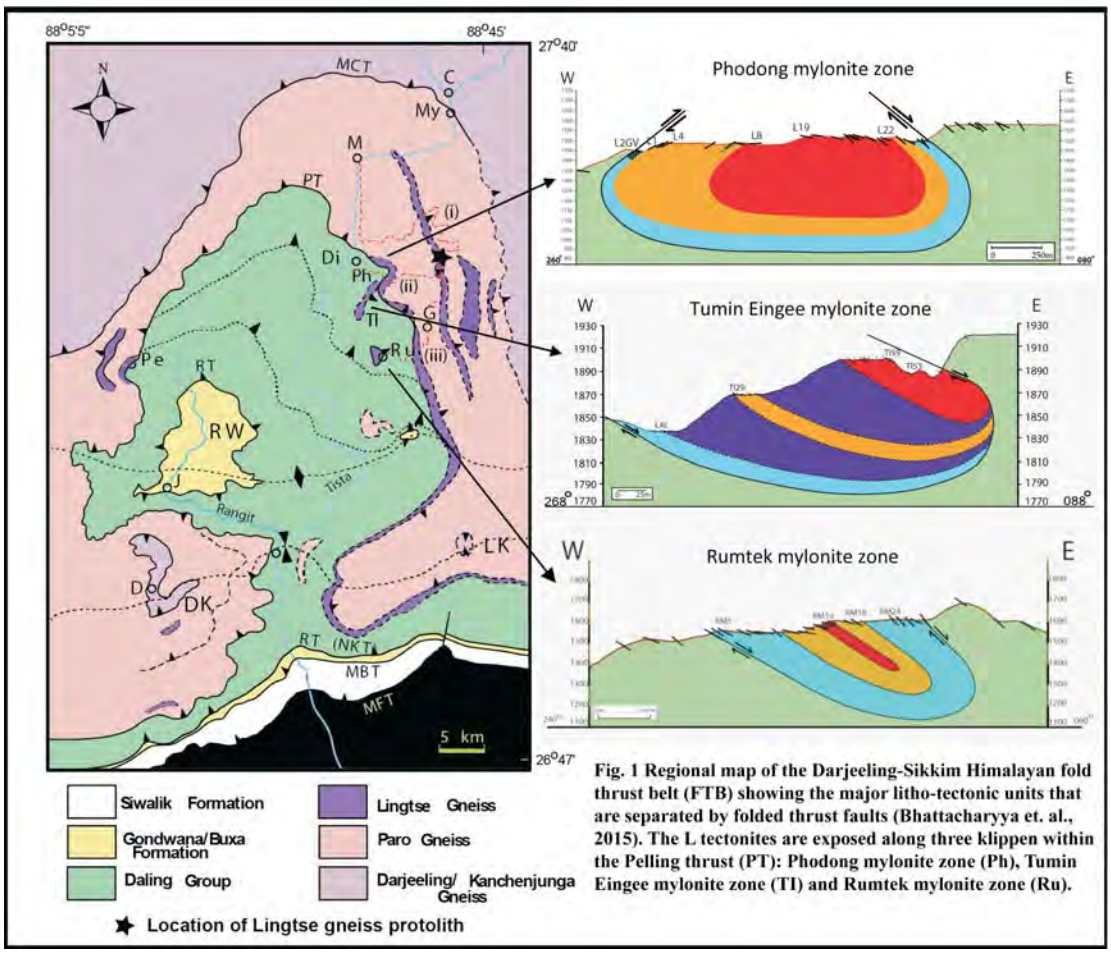

Fig. 1 Regional map of the Darjeeling-Sikkim Himalayan fold thrust belt (FTB) showing the major litho-tectonic units that are separated by folded thrust faults (Bhattacharyya et. al., 2015). The L tectonites are exposed along three klippen within the Pelling thrust (PT): Phodong mylonite zone (Ph), Tumin Eingee mylonite zone (TI) and Rumtek mylonite zone (Ru).

oblique fabric) show a smaller variation from N-S than W_n from subgrains. Based on this, we interpret subgrains as the best marker of vorticity variation in this zone. Based on W_k, we concluded that the relative contribution of simple shear decreased from Phodong mylonite zone (~30-75%) in the north to Rumtek mylonite zone (~37-47%) in the south. Quartz crystallographic fabric records a type-II crossed girdle in the strongest L-fabric. As the dominance of linear component decreases, the fabrics record type-I crossed girdle and flattening patterns. There is no particular trend observed along transport parallel (N-S) direction, and the fabric geometries suggest that they have undergone intense shearing and high temperature deformation. W_k values from the PT fault rocks, immediately north of the klippen, records a dominant simple shear deformation. Comparison of these results with published datasets from similar structural positions in the western Himalaya (Jessup et. al., 2006; Law et. al., 2013) suggests that these mylonites record a greater amount of pure shear (~48-63%). These vorticity data support the proposed lateral ramp model of Bhattacharyya et al. (2015) which explains the mechanism of the formation of the L-tectonite in this region.

Bhattacharyya, K., Mitra, G. 2014. Journal of Asian Earth Sciences 96, 132-147.
Bhattacharyya, K., Dwivedi, H.V., Das, J.P., Damania, S. 2015. Journal of Asian Earth Sciences 107, 212-231.
Das, J.P., Dwivedi, H.V., Bhattacharyya, K. 2014. Rock Deformation and Structures (RDS-III) Abstract, 27-28.
Jessup, M.J., Law, R.D., Searle, M.P., Hubbard, M.S. 2006. In: Law, R.D., Searle, M.P., Godin, L. (eds.), Channel Flow, Ductile Extrusion, and Exhumation in Continental Collision Zones. Geological Society, London, Special Publications, vol. 268, pp. 379-414
Kruhl, J.H. 1998. Journal of Metamorphic Petrology, 16, 142-146.

Law, R.D., Stahr, D.W., Francsis, M.K., Ashley, K.T., Grasemann, B., Ahmad, T. 2013. J. Struct. Geol., 21-53.
Stipp, M., Stünitz, H., Heilbronner, R., Schmid, S. 2002. Journal of Structural Geology, 24, 1861-1884.

MOR and OIB magmatism in the Ophiolite of Indo-Myanmar Orogenic Belt, NE India: Implication for magma mixing at the spreading zone in the southeastern Neo-Tethyan Ocean

S. Khogenkumar*, A. Krishnakanta Singh, R.K. Bikramaditya Singh
Wadia Institute of Himalayan Geology, GMS Road, Dehradun 248001, INDIA
**sksingh@wihg.res.in*

Coexistence of tholeiitic Mid-Ocean Ridge Basalt (MORB) type and alkaline Ocean Island Basalt (OIB) type mafic volcanics is reported from the Manipur Ophiolite Complex (MOC), Indo-Myanmar Orogenic Belt (IMOB), NE India. The IMOB is interpreted as representing the eastern suture of the Indian plate which was formed due to the collision of the Indian plate with the Myanmar plate (Gansser, 1980). Highly tectonised and dismembered mafic and ultramafic rocks closely associated with pelagic sediments are preserved in this belt as ophiolites, which also show three phases of deformational events broadly comparable to the Himalayan orogeny and sea floor spreading of the Indian Ocean. These ophiolitic suits of rocks occur as folded thrust slices riding over the distal shelf sediments of Eocene to Oligocene age (Acharyya et al., 1990). Such ancient oceanic crust preserved as ophiolites could be generated in diverse tectonic settings (Coleman, 1981). They can be produced in a mid-oceanic ridge (MOR), supra subduction zone (SSZ) or within plate environment (Aldanmaz et al., 2008).

It is generally accepted that geochemical characteristics of mafic volcanics from ophiolites can be used as a robust tool for investigating the petrogenetic and geodynamic evolution of the ancient oceanic lithosphere (Saccani et al., 2004). Immobile elements present in such rocks preserve the very distinctive identity of their magma source. For having such significance, over the years, great efforts have been made to study the geochemical and petrological affinity of mafic volcanics of the MOC. Nonetheless, a satisfactory interpretation on its magma source and tectonic implication has not been reached yet though Singh et al. (2008) reported preliminary geochemical data of limited pillow basalts. So, new geochemical and petrological dataset of mafic volcanics from the MOC are presented in this paper with an attempt to constrain the petrogenetic processes behind the generation of mafic volcanics of this ophiolite complex.

Mafic volcanics of the MOC exhibit a wide range of geochemical variations indicating derivation from two distinct mantle sources. The MORB type basalts have low TiO_2 concentrations (0.6-1.6 wt. %), which can further be subdivided into normal-MORB (N-MORB) with low Zr/Nb <20 and enriched-MORB (E-MORB) with high Zr/Nb >20. Conversely, the OIB-type mafic volcanics are characterized by high concentration of TiO_2 (1.3-3.5 wt. %), which shows compositional range from pure OIB to Plume-type MORB (P-MORB) testified by high Zr/Y ratio >6 and low Zr/Y ratio <6, respectively. Tholeiitic MORB-type exhibits almost flat REE patterns with slightly LREE depleted patterns ($(La/Sm)_N$ = 0.62-1.03) whereas alkaline OIB-type shows LREE enrichment pattern as compared to HREE ($(La/Sm)_N$=2.27-3.44; $(Sm/Yb)_N$=2.56-3.29). Petrogenetic modelling suggests that 20% partial melting of depleted mantle within spinel stability facies zone at a depth of <90 km is responsible for generation of MORB tholeiites and <5% partial melting of enriched mantle or plume material at garnet facies stability zone (>90 km) is responsible for production of alkaline OIB-type. Geochemical signatures of E-MORB and P-MORB further suggest possible scenario of mixing of depleted N-MORB melt and enriched OIB melt. It is therefore likely that mafic volcanics of the MOC were derived from chemically heterogeneous magma sources

erupted at the sea floor spreading zone in the south-eastern neotethys as MORB, and OIB in the form of intra plate seamounts at the backyard of the spreading ridge axis. Later, due to prolonged subduction of the Indian plate beneath the Myanmar plate and afterward collisional activity, they might have accreted along the Indo-Myanmar Orogenic belt as upthrust ocean crust.

Acharyya, S.K., Ray, K.K., Sengupta, S. 1990. Earth Planet. Sci. Lett., 99(2), 187-199.
Aldanmaz, E., Yaliniz, M.K., Guçtekin, A., Goncuoglu, M.C. 2008. Geol. Mag., 145, 37-54.
Coleman, R.G. 1981. Jour. Geophy. Res., 86, 2497-2508.
Gansser, A. 1980. Tectonophysics, 62, 37-52.
Saccani, E., Photiades, A. 2004. Lithos, 73, 229-253.
Singh, A.K., Singh, N.I., Devi, L.D., Singh R.K.B. 2008. Jour. Geol. Soc. India, 72, 168-174.

Holocene extreme hydrological events reconstructed using paleo-flood sequences in the middle Satluj Valley, western Himalaya, India

Shubhra Sharma[1,*], A.D. Shukla[3], B.S. Marh[2], S.K. Bartarya[1]
[1]Wadia Institute of Himalayan Geology, 33 GMS Road, Dehradun 248001, INDIA
**shubshubhra@gmail.com*
[2]Himachal Pradesh University, Shimla, INDIA
[3]Physical Research Laboratory, Ahmedabad, INDIA

In a dynamic terrain like Himalaya sedimentary records of paleo-floods are scanty. Some evidences pertaining to the past floods up to last 1000 years have been reported from the Alaknanda Valley (Srivastava et al., 2008; Wasson et al., 2008; 2013). In the present study, the palaeoflood sequences from the middle Satluj Valley around Sunni and Tattapani (31°14'43.6" N, 77°07'04.8" E; 31°14'41.8" N, 77°05'41.2" E; Fig. 1) are discussed, which are dated as the early Holocene. Optical chronology indicates that the floods were generated during early Holocene (~9 ka) and mid to late Holocene (~6-4 ka).

Each flood unit with distinct fining upward characteristic is differentiated by weak to moderately developed paleosols. Most of the deposits are associated with tributaries suggesting their deposition in a slack water environment. Based on sediment texture, grain size analyses and degree of weathering, ascertained using Chemical Index of Alteration (CIA). Around seven flood couplets preserved in a tributary stream have been discerned at Sunni. Compared to this, at Tattapani around five flood couplets separated by clayey sand and bedded calcretes are preserved.

The flood sediment provenance have been ascertained using the CIA and the Al_2O_3-CaO*+Na_2O-K_2O (A-CN-K) compositional space diagram. The average CIA values of the Higher Himalaya Crystalline (HHC) and the Tethyan Sedimentary Sequence (TSS) calculated based on the major elemental data of Richard et al. (2005) indicate a range of 58 and 59.5, respectively. These values compare well with the unweathered paleo-flood horizons at Sunni (54.8 to 59.4), thus suggesting a major contribution from the Higher Himalaya. Further, the A-CN-K diagram shows the clustering of paleo-flood sediment values around average HHC. Landslides are known to occur during early Holocene in the HHC zone (Bookhagen et al., 2005). Thus, Holocene floods are ascribed to landslide lake outburst floods (LLOFs) generated in the HHC, as also suggested in other studies (Wasson et al., 2008, 2013).

Climatically the early Holocene floods are ascribed to the strengthened Indian Summer Monsoon (ISM) whereas, the mid-to late Holocene floods correspond to the declining phase of the ISM. We hypothesise that the early Holocene floods in the Satluj Valley were caused due to the abnormal monsoon events associated with intensified ISM, whereas, mid to late Holocene floods

Fig 1. Geological map of the study area. Sites of major paleo-flood deposits are marked by red stars.

during the weakened ISM can be ascribed to the interaction between monsoon circulation and southward penetrating mid-latitude Westerlies. Such interactions are suggested to be more frequent during the weakened ISM in the western Himalaya (Vellore, 2015). Interestingly, during both intensified and weakened ISM, floods were generated in the Higher Himalaya as indicated by the geochemical proxies.

Bookhagen, B., Thiede, R.C., Strecker, M.R. 2005. Geology, 33(2), 149-152.

Richards, A., Argles, T., Harris, N., Parrish, R., Ahmad, T., Darbyshire, F., Draganits, E. 2005. Earth and Planetary Science Letters, 236(3), 773-796.

Srivastava, P., Tripathi, J.K., Islam, R., Jaiswal, M.K. 2008. Quaternary Research, 70, 68-80.

Vellore, R.K., Kaplan, M.L., Krishnan, R., Lewis, J.M., Sabade, S., Deshpande, N., Rao, M.R. 2015. Climate Dynamics, 1-30. DOI 10.1007/s00382-015-2784-x.

Wasson, R.J., Juyal, N., Jaiswal, M., McCulloch, M., Sarin, M.M., Jain, V., Srivastava, P., Singhvi, A.K., 2008. Journal of Environmental Management, 88, 53-61.

Wasson, R.J., Sundriyal, Y.P., Chaudhary, S., Jaiswal, M.K., Morthekai, P., Sati, S.P., Juyal, N. 2013. Quaternary Science Reviews, 77, 156-166.

Tectonics and sedimentation of Saltoro Molasse of Shyok Suture Zone (SSZ) of Nubra Valley, Ladakh Trans-Himalaya and Karakoram, India

Mujtuba Rashid*, Rakesh Chandra

Department of Earth Sciences, University of Kashmir, Hazratbal, Srinagar, INDIA

**amrzubin@yahoo.co.in*

The Shyok back-arc basin resulted due to the subduction, collision and accretion of the Indian Plate along the southern margin of the Eurasian Plate. Several igneous, sedimentary and

metamorphic rock types occur and are sandwiched between the Ladakh Batholith to the south and the Karakoram Batholith to the north. The marine sedimentary succession in the lower Shyok area is represented by the Saltoro Flysch. It is overlain by molasse sediments of the Saltoro Formation. Tectonics has exerted significant control on the production, dispersal, accumulation and lithification of these sediments due to continuous convergence of the Indian plate below the Asian plate. In Nubra Valley, these sediments occur as an apron like sedimentary sequence, moderately folded, resting in thrust contact with Shyok Volcanics and the Saltoro Flysch in the south and Shyok Ophiolitic Melange in the north. Detail sedimentological study suggests that deposition of the Saltoro Molasse is caused by braided river system. The bed forms are generally plane and few scouring at their bases. The compactional structure such as mud cracks formed mainly due to desiccation and shrinkage either by expulsion of water or sub-areal drying. The molasse displays an overall decrease in pebble size in conglomerate from the southern contact. The percentage of pebbles in groundmass also decreases away from the southern contact suggesting that the initial deposition was adjacent to the Ladakh magmatic arc. Petrographic study of sediments reveal the presence of clasts of Khardung Volcanics, Shyok Volcanics, Saltoro Flysch, Ladakh and Karakoram Batholiths in abundance suggesting that the sedimentation in Shyok back-arc was active even after the closure of the Indus Tsangpo Suture Zone. These sediments are traversed by several parallel young dykes, suggesting that Shyok back arc basin was magmatically active even after the closing of the SSZ.

Formation of late Quaternary piggy-back Kangra basin to the south and Chamba pull - apart basin to the north of the Dhauladhar range: Partitioning of convergence in NW Himalaya

V.C. Thakur, M. Joshi

Wadia Institute of Himalayan Geology, 33 GMS Road, Dehradun 248001, INDIA

Dhauladhar range (D-range), trending NW-SE, lies south of the Pir Panjal range between the Beas and Ravi rivers. It lies in the outer Lesser Himalaya with steep gradient and abrupt physiographic and tectonic break to the south against the Siwalik foreland basin of the Kangra reentrant. The southern margin of the D-range is demarcated at the base by the closely spaced Main Central Thrust (MCT) and the Main Boundary Thrust (MBT) which are responsible for the uplift and exhumation of the mountain range. The altitude at the water divide of the D-range decreases from 4800 m in the southeast to 2800 m in the northwest along the regional orogenic trend. The structural and stratigraphic framework is continuous and is the same along the D-range. Based on altitude and climate-tectonic features, the range is divided along the regional strike into two segments, the eastern segment with altitude between 4800 m and ~4000 m and the western segment with altitude between 3500 and 2800 m. An intermontane, post-Siwalik, Kangra basin is developed south of the D-range eastern segment front in the Kangra area. The valley-fill terraces occur along the Ravi river in the Chamba basin to the north and to the rear side of the D-range western segment. The main body of the D-range is made of lower Paleozoic granite massif, and the granite has been used as a marker lithology in tracing the provenance for the Kangra basin and the Ravi river terraces. The D-range was affected by glaciation-deglaciation during the last glacial cycle and the LGM, and the eroded flux is preserved in the Kangra basin to the south and the Chamba basin to the north of the D-range. The Kangra basin is filled with the post-Siwalik late Quaternary debris flow fans. The fans largely consist of granites derived from the Dhauladhar granite with subordinate provenance from the lower Tretiary and Lesser Himalayan formations. The proximal to middle part of the fans is dominated by debris flows with out-size large granite boulders. The fluvial deposits are associated in the middle to distal part of the fans. The fan sediments have yielded OSL ages ranging from 78-30 ka, 40-32 ka and 16-7.5 ka. There are glacial lakes and small glaciers on the crestal parts of the of the D-range western segment at altitude ranging from 4000-48000 m. The occurrence of

glacier erratics and moraine lobes on the southern flank of the D-range at altitude as low as 2600 m in some locations suggests that the extent of glaciation was similar to that described in Garhwal and Rohtang in Lahaul area. There are pedogenised loess horizons occur within the fan sediments, indicate cold-arid followed by warm-wet climatic episodes. The warm-wet climate as indicated by pedogenised soils prevailed during the interglacial periods. The Kangra fans are largely debris flows emanated from the D-range as a consequence of deglaciation and deposited in the intermontane basin. The Kangra basin was developed as a piggy-back basin over the hanging wall of the Jawalamukhi Thrust (JT). The strath terraces developed along the Baner river across the hanging wall of the JT give OSL ages of 76 ka, 30 ka, 20 ka and 12 ka as abandonement ages. The bed rock uplift ages of the straths are consistent with the depositional ages of the Kangra basin fans, indicate reactivation of the JT synchronous with the aggradation in the piggy back basin. The Chamba region lies on the northern side of the Dhauladhar range water-divide. The Ravi river largely flows to the northwest on the northern flank of the D-range. In the upstream as well as the down stream of the Chamba basin, the Ravi river flows in narrow confined valley, characterized with the lack of terraces. Whereas well preserved valley-fill terraces and debris flow fans occupy the ~3 km wide and ~20 km long river valley of the Chamba basin. Four levels of terraces are recognized in the basin. The terraces T4, T3, T2 are the valley- fill, whereas T1 is the strath terrace. The heights of these terraces from the river beds are 188 m, 89 m, 54 m, and 10 m respectively. The OSL dating of the terraces indicate two major aggradation phases at 72-46 ka and 37-6 ka, separated by an incision phase. The valley fill terraces in the Chamba area, representing a major aggradational climatic episode, were deposited in a graben of a pull-apart basin. The basin was developed as step - over to the right of the reactivated Chamba thrust with right-lateral strike - slip movement. The kinematics of Kangra and Chamba basins formation indicates normal convergence for the former and dextral shear for the latter, indicate late Quaternary partitioning. The partitioning may be due to oblique convergence in the northwest Himalaya. This is consistent with the GPS estimated horizontal velocity rates in the Kashmir Himalaya indicate both normal convergence and dextral shear.

Proterozoic seismites in a tide-wave interactive depositional system, Saknidhar Formation, Garhwal Lesser Himalaya, India

Biplab Bhattacharya[1,*], Moloy Sarkar[1], Sumit K. Ghosh[2,3,#]

[1]Department of Earth Sciences, Indian Institute of Technology, Roorkee 247667, INDIA

** bb.geol.dgc@gmail.com, bbgeofes@iitr.ac.in*

[2]Wadia Institute of Himalayan Geology, 33 GMS Road, Dehradun 248001, INDIA

[3]Present address: 7 Kalimandir Enclave, GMS Road, Dehradun 248001, INDIA

#skgwihg@gmail.com

The Lesser Himalayan succession is dominantly represented by Proterozoic marine siliciclastic-carbonate successions (Ghosh, 1991; Valdiya, 1995; Shukla and Pant, 1996; Jiang et al., 2003). The Saknidhar Formation, commonly considered as a transitional phase between the Proterozoic argillaceous Chandpur Formation and the arenaceous Nagthat Formation, is represented by thick- to thin-bedded sandstone with interbedded mudstone/shale (Kumar and Dhaundiyal, 1980). The rocks show evidences of several phases of deformation related to the Himalayan tectonics.

Sedimentologically, the overall succession shows alternate juxtaposition of channel-filling and tide-wave influenced facies architecture. The channel-filling depositional systems are recorded in the thick-bedded mature to immature sandstone facies associations with meter-scale cross-strata sets. Lateral accretion of cross- strata sets confined within major channel morphology is the characteristic of the sandstone facies. Intermittent thin argillite dominated facies associations represent over bank deposits within a shifting channel system. These are generally characterised by

thin-bedded sandstone-mudstone heterolithic facies associations with definite signatures of marine tide-wave led sedimentation. Tide-generated sedimentary features include, (i) mud draped sandstone foresets with variable foreset thickness, (ii) laterally-accreted cross strata set with reactivation surfaces, (iii) mutually opposite cross-strata set, separated by subhorizontal, planar-laminated sandstone-claystone heteroliths, and (iv) alternate sequence of sand-dominated and mud-dominated tidal rhythmites. Wave features are relatively less abundant and include accretionary hummocks and wave ripples within the medium- to fine-grained sandstone-mudstone heterolithic facies. Mutual interactions of two exclusive processes, the tidal currents and the wave oscillations, are evident from the characteristic modifications in the morphology of the primary structures. Overall facies architecture suggests deposition in a fluctuating tide-dominated subtidal channel-filling to open intertidal flat depositional system with minor wave interferences.

Few heterolithic beds within the tide-wave led succession bear soft-sediment deformation structures (SSDS). The SSDS include, (i) recumbently folded foreset laminae within cross-strata set, (ii) syn-sedimentary step faults, (iii) various water escape structures and flow structures, (iv) load and flame structures, (v) brecciated mud layer, etc. Soft sediment deformation structures form during or shortly after deposition, when sediments become liquefied and/or fluidized under the influence of a dynamic trigger of sufficient strength (Allen, 1982; Seth et al., 1990; Owen, 1995; Bhattacharya and Bandyopadhyay, 1998; Van loon, 2009). Such SSDS bearing beds are restricted at distinct stratigraphic horizons separated by beds having no signatures of soft-sediment deformations, and are characterized by: (i) episodic deformational events with no fixed time intervals between deformations, (ii) complete absence of evidences of gravity-induced mass-movement or sudden sediment loading in vertically associated facies types, and (iii) the deformation structures resemble in morphology with those described from other seismically-induced deformed horizons. Thus, the SSDS-bearing beds are identified as seismites formed by liquefaction and fluidization of water-saturated, unconsolidated sediments by earthquake shock-induced ground shaking (Seilacher, 1984; Seth et al., 1990; Owen, 1995; Moretti and Van Loon, 2014).

The seismites, reported for the first time from the Saknidhar Formation, signify episodes of syn-sedimentary paleoseismic events related to tectonic activity in the basin. Evidently, these earthquake events and there manifestations are much older than the age of Himalayan tectonics, and record phases of tectonic disturbances in the marginal Tethyan marine basin during the Late Meso-(?) - Early Neoproterozoic time. Since a rift-related tectonic setup has been envisaged for this basin (Valdiya, 1995; Ghosh et al., 2012), these seismites are interpreted to form by earthquake events triggered by fault activities under riftogenic tectonisms.

Allen, J.R.L. 1982. Vol. II. New York: Elsevier, 663.
Bhattacharya, H.N., Bandyopadhyay, S. 1998. Sedimentary Geology, 119, 239-252.
Ghosh, S.K. 1991. Sedimentary Geology, 71, 33-45.
Ghosh, S.K., Pandey, A.K., Pandey, P., Ray, J., Sinha, S. 2012. Sedimentary Geology, 261-262, 76-89.
Jiang, G., Sohl, L.E., Christie-Blick, N. 2003. Geology, 31, 917-920.
Kumar, G., Dhaundiyal, J.N. 1980. Journal of the paleontological Society of India, 23-24, 58-66.
Moretti, M., Van Loon, A.J. 2014. Journal of Palaeogeography, 3, 162-173.
Owen, G. 1995. Journal of Sedimentary Research, A65, 495-564.
Seilacher, A. 1984. Marine Geology, 55, 1-12.
Seth, A., Sarkar, S., Bose, P.K. 1990. Sedimentary Geology, 68, 279-291.
Shukla, U.K., Pant, C.C. 1996. Journal of the Geological Society of India, 47, 431-445.
Valdiya, K.S. 1995. Precambrian Research, 74, 35-55.
Van Loon, A.J. 2009. Geologos 15, 3-55.

The 25 April Gorka earthquake Pre-, co- and post-deformations From GPS measurement

Francois Jouanne
Universite de Savoie Mont Blanc, FRANCE
**fjoua@univ-savoie.fr*

The 25 April 2015 Gorka earthquake gives the first opportunity to study a major Himalayan earthquake documented by geodetic data. Geodetic determination of the deformation before the earthquake, i.e., during interseismic periods has been performed by GPS (Jouanne et al., 1999, 2004; Ader et al., 2012), leveling comparison (Jackson and Bilham 1994) and Insar (Grandin et al., 2012). The coseismic deformation associated by the 25 April Gorka earthquake and its main aftershock on 12 May 2015 have been quantified by GPS and Insar (Avouac et al., 2015; Galetzka et al., 2015) whereas the postseismic deformation has been mainly recorded by permanent GPS measurements.

The Gorkha earthquake probably occurred in the area of the Main Himalayan Thrust (MHT) in central Nepal that had already been affected by a similar earthquake in 1833 and released probably the slip deficit accumulated since 1833. This particular earthquake illustrates an important type among earthquakes in the Himalaya: giant earthquakes had brought movement on all the MHT whereas others earthquakes could only affect a segment of the MHT or, like, in the case of the Balakot earthquake, a ramp that connects the MHT and the surface (Mugnier et al., 2013).

We present interseismic deformation quantification documented by episodic and continuous GPS measurements during the 1995-2015 period that analyzed in the IGB08 reference frame with reprocessed orbits and introduction of discontinuities considered in the IGB08 reference frame determination. GPS time series allow to underline the lack of slow slip events along the Main Himalayan Thrust during the 20 last years covered by GPS data, we can then suppose that all the slip deficit accumulated between the major earthquakes are released during earthquakes and afterslip in years following the main shock.

We have considered two hypotheses to simulate the interseismic deformation: (i) the MHT is the only main active fault, or (ii) the MHT and also the Western Nepal Fault System (WNFS) (Murphy et al.; 2013), that allows a strain partitioning in western Nepal, are considered in the inversion as main active faults. Simulations reveal that the southern part of the Main Himalayan Thrust is fully locked during interseismic period, whereas a few mm/yr slip may exist along the WNFS. The locking appears to be induced by a brittle-ductile transition along the MHT in western Nepal, west of Dhaulagiri whereas in central and eastern Nepal the locking is probably induced by a brittle-ductile transition along the MHT but also by the flat-ramp transition of the MHT (Berger et al.,

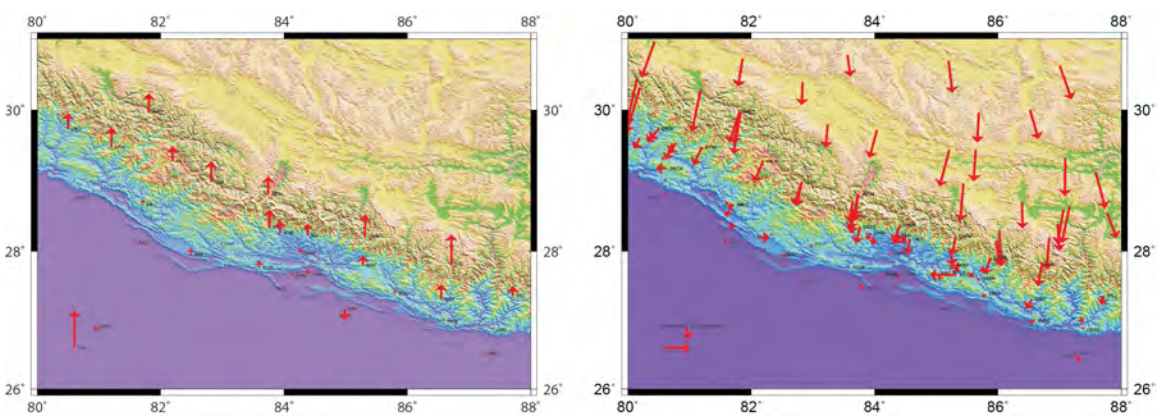

Fig. 1

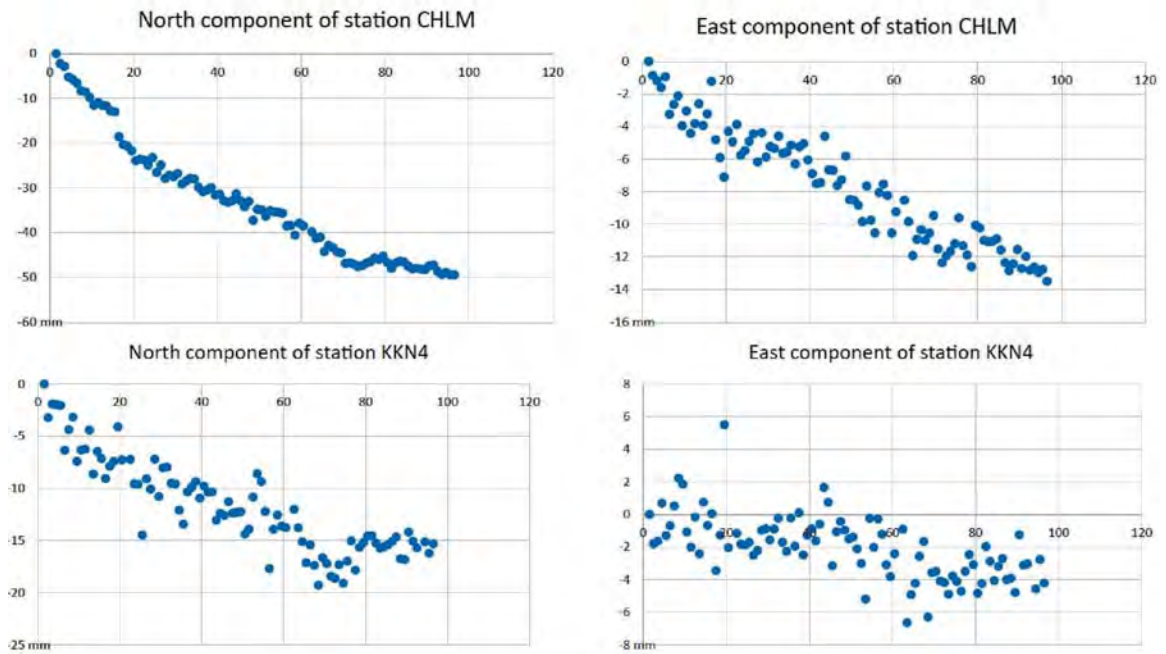

Fig. 2. Time series of the CHLM and KKN4 Caltech permanent station. The daily positions are plotted as displacement in mm versus the number of days after the Gorkha earthquake. The jump in the CHLM time series corresponds at the main aftershock, the Mw 7.2 12 May earthquake. CHLM station is located 55 km north of Katmandu whereas KKN4 is located 10 km north of Katmandu.

2004). This simulation also underlines that a giant earthquake of Mw ≥8.6 can affect western Nepal and India between the Gorkha longitude and Kangra in India and perhaps further if the 1905 Kangra earthquake has not released all the slip deficit previously accumulated. Such a case already occurred after the 1255 event, when there was still the potential for a slip of several meters for the Mw ~8.1 1505 event (Mugnier et al., 2013).

The coseismic rupture, as studied by Insar, high-rate GPS, static GPS and inversion of teleseimic waves, revealed a coseismic rupture initiation in the Gorka area was propagated eastward with a steady state velocity of 2.8-3.3 km/s (Galetzka et al., 2015; Avouac et al., 2015; Grandin et al., submitted). This slow rupture velocity may explain the moderate acceleration during the earthquake (0.2 g). The rupture affected the MHT between 15 km depth and the latitude of Katmandu.

To record postseismic displacements induced by the Gorka earthquake and its main aftershock (12 May 2012, Mw 7.2) we have deployed a network of 16 permanent GPS stations, all around the area affected by the earthquakes. This network has been designed to complement the GPS network installed by Caltech (Galetzka et al., 2015). These measurements will allow to test (i) the existence of afterslip south of the segment of the MHT affected by the main shock, releasing a part of the slip deficit along this southern part of the MHT, and (ii) the existence of afterslip also in the ruptured area or down dip along the MHT as it has occurred after the 2005 Balakot earthquake. We will also test if a part of postseismic deformation is controlled by viscous relaxation of stress increases north of Katmandu. If a significant afterslip occurs along the MHT between the Main Frontal Thrust and the southern end of the ruptured area, this phenomenon will decrease the seismic hazard to the south of Katmandu whereas if no afterslip occurs along the southern part of the MHT, a Mw 6.9 earthquake will probably occur to transfer along the southern edge of the MHT the 4 m coseismic slip of the 25 April 2015 earthquake.

Preliminary results obtained with the Caltech permanent station data available at Unavco, suggest that an important postseismic deformation is occuring north of Katmandu with a southward displacement reaching 5 cm 100 days after the main shock at the CHLM station 55 km north of Katmandu, and southward displacement reaching 1.4 cm during the same time span at the KKN4 station 10 km north of Katmandu. The time series of CHLM shows a jump of ~6 mm induced by the Mw 7.2 May 12, 2015 earthquake. It must be underlined that this time series reveal probably two contributions, a first one corresponds at the main shock with a first attenuation tendency, whereas after the 12 May the time series reveal the sum of the two contributions: a postseismic deformation linked to the Mw 7.8 earthquake and a second one linked to the second earthquake.

With these preliminary results, it seems that the postseismic deformation is mainly important in the high chain area and that the eventual creep south of Katmandu is not very important and probably not susceptible to transfer the coseismic slip along the southern part of the MHT, in other words these very preliminary results could suggest that the coseismic will be transfer along the MFT by one or several earthquakes. More data along a longer period will be presented at the time of the meeting.

Avouac, J.-P., Meng, L., Wei, S., Wang, W., Ampuero, J.-P. 2015. Nat. Geosci. 10.1038/ngeo2518.

Ader, T., et al. 2012. J. Geophys. Res., 117, B04403, doi:10.1029/2011JB009071.

Berger, A., Jouanne, F., Hassani, R., Mugnier, J.L. 2004. Geophys. J. Int., 156, 94-114.

Galetzka, J., Melgar, D., Genrich, J.F., Geng, J., Owen, S., Lindsey, E.O., Xu, X., Bock, Y., Avouac, J.P., Adhikari, L.B., Upreti, B.N., Pratt-Sitaula, B., Bhattarai, T.N., Sitaula, B.P., Moore, A., Hudnut, K.W., Szeliga, W., Normandeau, J., Fend, M., Flouzat, M., Bollinger, L., Shrestha, P., Koirala, B., Gautam, U., Bhatterai, M., Gupta, R., Kandel, T., Timsina, C., Sapkota, S.N., Rajaure, S., Maharjan, N. 2015. Science. 2015 Aug 6. pii: aac6383.

Jackson, M., Bilham, R. 1994. J. Geophys. Res., 99, 13, 897-13,912.

Jouanne, F., Mugnier, J., Pandey, M., Gamond, J., Le Fort, P., Serrurier, L., Vigny, C., Avouac, J.-P. 1999. Geophys. Res. Lett., 26 (13), 1933-1936.

Jouanne, F., Mugnier, J., Gamond, J., Le Fort, P., Pandey, M., Bollinger, L., Flouzat, M., Avouac, J. 2004. Geophys. J. Int., 157, 1-14.

Jouanne, F., Awan, A., Madji, A., Pêcher, A., Latif, M., Kausar, A., Mugnier, J.L., Khan, I., Khan, N.A. 2011. J. Geophys. Res., 116, B07401, doi:10.1029/2010JB007903.

Grandin, R. et al. 2012. Geology, 40, 1059-1062.

Mugnier, J.L., Huyghe, P., Gajurel, A.P., Upreti, B.N., Jouanne, F. 2011. Tectonophysics, doi:10.1016/j.tecto.2011.05.01.

Mugnier, J.L., Gajurel, A., Huyghe, P., Jouanne, F., Upreti, B.N. 2013. Earth-Science Reviews, 127, 30-47, doi : 10.1016/j.earscirev.2013.09.003.

Murphy, M.A., Taylor, M.H., Gosse, J., Silver, C.R.P., Whipp, D.M., Beaumont, C. 2013. Nature Geosciences, 7, 38-42; doi: 10.1038/NGEO2017.

Deciphering tectonic history using drainage network, An examples from the western Himalaya

Ramendra Sahoo*, Vikrant Jain#

Discipline of Earth Sciences, IIT Gandhinagar, Palaj 382355, INDIA

**Ramendra.sahoo@iitgn.ac.in #vjain@iitgn.ac.in*

Tectonic process has always fancied Earth Scientists, as it causes large scale reshaping of earth's surface. These processes are endogenous in nature. So sometimes, their responses get constrained to Earth's interior, while at other times, they get exposed on Earth's surface. Geomorphologists have been using these exposed responses for years, both qualitatively and quantitatively, for interpreting the tectonic history of an area. Some of the widely used characteristic responses are cross sectional attribute (i.e. Long profile of river, hypsometry and planar attribute (i.e. Channel pattern). But, most of these

surface exposures get easily destroyed or diluted by agents of erosion. Drainage network is one of the surficial features that conserve the response of the sub surface processes. So there have been extensive study on drainage network and it's characteristics over the last century, which started in a qualitative sense (Zernitz, 1932) and later evolved into a more robust quantitative science, with beautiful insights from Horton (1945), Strahler (1957), Shreve (1966), etc. Extraction of this drainage network needs a modelled earth surface, from which we can work out the gradient directions. DEM data is used for such analysis. The accuracy of these data is dependent upon their spatial resolution. We have estimated the sensitivity of the morphometric parameters of the drainage network to the spatial resolution of our source data. We have taken digital elevation data (DEM) of different resolution (30 m and 90 m) for the area of Nahan salient, provided by SRTM and extracted the required parameters using ArcMap 10.0. We carried out a student t-test on both the sample and found no statistically significant difference between the morphometric ratios derived from the 2 different source data.

The resultant drainage network of given magnitude were analyzed through the Random Topology model (RT model) (Shreve, 1966). RT Model is based on the fact that responses to natural forcings are random due to the heterogeneity in the forcings itself along with the random noises (Shreve, 1966). While most models for studying the processes - response interaction, are empirical in nature, we have established a theoretical base for the RT model using the law of Thermodynamics and theory of Information Entropy (Shannon, 1948). The theoretical analysis has been verified from the extracted drainage network data in the tectonically active area of Kangra recess.

Horton, R. 1945. Bulletin of the geological society of America, 56, pp.275-370.
Shannon, C.E. 1948. The Bell System Technical Journal 27, 379-423.
Shreve, R. 1966. Journal of Geology, 74, 17-37.
Strahler, Arthur N. 1957. Trans. AGU 38 (6), 913.
Zernitz, Emilie R. 1932. The Journal of Geology 40 (6), 498-521.

Multiple channel-flows in the Higher Himalaya: Evidences from Indian hot springs

Rajkumar Ghosh
Department of Earth Sciences, IITBombay, Powai, Mumbai 400076, INDIA
Rajkumarghgeol@gmail.com

Genesis of Out-Of-Sequence Thrusts (OOSTs) within the Higher Himalaya might be explained by 'multi-channels concept'. Mukherjee (2015) compiled OOST locations in the Higher Himalaya. The OOST and the present day hot springs near it might be interrelated. Evidence of thermal anomalies are also documented by increasing grade of rocks as one moves towards N/NE from the Main Central Thrust (MCT) (review by Ghosh, 2013, unpublished report). As the OOST is comprised of shear zones, 'shifting in channel flow' can also be attributed to the OOST activation along the Himalayan arc as the shifting in channel flow resulted from superposition of ductile shear zones. However, under this condition, the shear zones should be exposed at a spatial distance of >50 km (Lockett et al., 1982) along the Himalayan arc, consisting of multi-channel flows. However, the shear zones may broaden with depth and parallel shear zones can merge with each other at a certain distance <10 km (Bak et al., 1975; Watterson, 1979).

Therefore, shear zone shifting in Higher Himalaya can interpret Toijem, Kalopani, ModiKhola, Physiographic Transition (PT), Khumbu, High Himal Thrust and Nyalam Thrust, Chaura Thrust, Sarahan Thrust, Jhakri Thrust. From geophysical data, Unsworth et al. (2005) documented that volume of mid-crustal partial melt (2-4%) in NW Himalaya is less than that in NE Himalaya (5-12%). Therefore, difference of crustal melt volume can lead to support the possibility of having different channels below Himalaya.

Although the channel below NW-Himalayan mainly documents as a fossilized record of channel (consistent with the Chaura Thrust, activation age 4.9-1.5 Ma; Jhakri Thrust: Miller et al., 2000). The 'reactivated channel flow' (see, Harris 2007) at the central part of the Nepal represents an active OOST in the Marsyandi river valley. Here, the erosion and the exhumation rates are higher than other parts of the Himalaya. Whereas, beneath the erosional front, 'tunneling channel flow' is stabilized (see, thermo-mechanical model LHO-66 of Jamieson et al., 2002). Using magnetotelluric data from Southern Tibet, Unsworth et al., (2005) interpreted the partially molten layer, similar to the crustal melt. In this regard, Wobus et al., (2005) has suggested an activation age of 15-0.01 Ma for OOST in this area. In addition, the reactivation of these shear zones may be the result of buried distributaries of the main channel as well as 'mid-crustal channel' (Leech, 2008) source for OOSTs. Another, supporting evidence for 'palaeo-channel' (Leech, 2008) as a package of Greater Himalayan Sequence (GHS) are migmatites and leucogranites in the footwall of the South Tibetan Detachment (STD). Recently, Bao et al. (2015) revealed from geophysical evidence that two crustal channels are present beneath SE Tibet.

Evidence of such channels exists in the Higher Himalaya that can be correlated with the hot springs as well as with the presence of the OOSTs. From the cluster of OOSTs and hot springs data, confirms the channel below the north-western Higher Himalaya (only three OOSTs). Channel below NW Himalaya can also be confirmed in addition to the major distributaries of the channel (with major number at least ten of OOSTs and maximum number of hot springs) in the central part of the Himalaya and few in Eastern Himalaya. However, the eastern part of the Himalaya represents the last/narrower part of the channel as evidenced from the Kakhtang-Zimithang Thrust. Metcalfe (1993) proposed that late activity in the MCT and circulation of hydrothermal fluids generated from local hot springs may source for young white mica in the MCT zone. Hot springs are located nearby OOSTs, like: Unoo Bridge, Jeori and right bank of Satuj River near dam site of Nathpa, and also right bank of Satluj near Jhakri. Therefore, it is suggested that hot springs are linked up with different hot channels beneath in Higher Himalaya.

Bak, J., Sorensen, K., Grocott, J., Korstgard, J. A., Watterson, J. 1975. Nature, 254, 556-569.
Bao, X., Sun, X., Xu, M., Eaton, D. W., Song, X., Wang, L., Wang, P. 2015. Earth Planetary Sci. Letters, 415, 16-24.
Ghosh, R. 2013. Unpublished APS report, IIT Bombay. pp. 1-19.
Harris, N. 2007. Journal of the Geological Society, 164(3), 511-523.
Jamieson, R.A., Beaumont, C., Nguyen, M.H., Lee, B. 2002. Journal of Metamorphic Geology, 20(1), 9-24.
Leech, M.L. 2008. Earth and Planetary Science Letters, 276(3), 314-322.
Lockett, J.M. Kusznir, N.J. 1982. Geophysical Journal International, 69(2), 477-494.
Miller, C., Klötzli, U., Frank, W., Thöni, M., Grasemann, B. 2000. Precambrian Research, 103(3), 191-206.
Mukherjee, S. 2015. Geological Society of London, 412
Unsworth, M.J., Jones, A.G., Wei, W., Marquis, G., Gokarn, S.G., Spratt, J.E., Roberts, B. 2005. Nature, 438(7064), 78-81.
Watterson, J. 1979. U.S.G.S. Office of Earthquake Studies.
Wobus, C., Heimsath, A., Whipple, K., Hodges, K. 2005. Nature, 434(7036), 1008-1011.

Tso Morari coesite eclogite: garnet inclusion and geochemical patterns and implications for the newly proposed diapiric ascent model

Patrick J. O'brien*, Franziska D.H. Wilke
Dept. of Earth & Environmental Sciences, Universität Potsdam, GERMANY
**Obrien@geo.uni-potsdam.de*

The eclogites of the Tso Morari dome have been the subject of numerous research projects in the last few years especially following the excursion linked to the 2008 HKT workshop. One of these recent publications by Chatterjee and Jagoutz (2015, Contr. Min. Pet.), in contrast to all previous

studies, proposes exhumation of the Tso Morari eclogite by diapiric ascent through the overlying mantle wedge. This new model is based on a pressure-temperature path derived for the eclogite comprising a very low temperature (ca. 400°C, 2.6 GPa) for the peak pressure stage (just below the coesite field) followed by significant heating (to ca. 700°C at 1.8 GPa) during initial exhumation. The deduced path is rather surprising because the studied rock has essentially the same mineral chemistry, microstructures and garnet zoning profiles as in previous studies but the inclusion-host relationships, omphacite zoning, garnet zoning and multi-stage amphibole evolution has been interpreted quite differently to previous authors. The majority of previous studies also note a significant heating episode but this occurs at much lower pressures and postdates the major part of the exhumation history. How robust is this new interpretation?

The critical sample is a carbonate-bearing eclogite from a well-known location south of Sumdo village. This eclogite body is clearly recognisable in Fig 13 of Berthelsen (1953 Medd. Fra. Dansk Geol. Forening.), and has provided samples for more than a dozen major publications. Despite the clear description of eclogite in this early work and the recognition of their origin as metamorphosed equivalents of Late Palaeozoic Panjal Trap dolerites (following on from the reports of garnet-bearing metabasites in Tso Morari orthogneiss from Hayden, Mem. G. S. India, in 1904), it was to be 40 years until de Sigoyer et al. (1995, Eur. J. Min.) confirmed metamorphic high-pressure conditions for these rocks. Reporting on the discovery of coesite from eclogites in Pakistan, O'Brien et al. (2001, Geology) pointed out the high probability of this phase also in Tso Morari eclogite (reworking the mineral compositional data for sample TS34 of de Sigoyer et al. 1995) and a few years later (Sachan et al., 2004, Eur. J. Min.) coesite was confirmed here too.

Detailed study of the magnesite and dolomite-bearing eclogite combined with thermodynamic modelling linked to trace and major element zoning patterns and sequential changes in inclusions (e.g. Wilke et al., 2015, Lithos, 231, 77-91) allows a check of the conclusions reached by Chatterjee and Jagoutz (2015). Firstly, it will be shown that strong growth zoning of garnet makes it difficult to choose the appropriate composition for a particular P-T stage. In addition, different omphacite generations (in the matrix and as inclusions in garnet) with different jadeite content, must also be separated and the interpretation of phases as inclusions rather than as later reaction products along cracks leads to further problems in P-T determination. Further, interpretation of inclusion phases as pseudomorphs after lawsonite has important implications for the expected PT path. Finally, multi-equilibria pseudosection modelling to deduce PT fields must use realistic fractionation steps to correctly account for the effect of garnet zoning on effective bulk composition. Once all these problems are carefully avoided the PT path for diapiric exhumation through the mantle disappears and a deep, fast subduction and fast exhumation history including a marked heating at around 10 kbar emerges: a path directly comparable to that of the coesite-eclogite of the Kaghan Valley, Pakistan.

North-east transgression of the eastern Himalayan syntaxis: Insights from low temperature thermochronology

Dnyanada Salvi[1,*], George Mathew[1], Barry P. Kohn[2], Kanchan Pande[1]
[1]Department of Earth Sciences, IIT, Powai, Mumbai 400076, INDIA
**Dnyanadasalvi@iitb.ac.in*
[2]School of Earth Sciences, University of Melbourne, Victoria 3010, AUSTRALIA

The rapidly uplifting eastern syntaxial zone of the Himalayan orogen has been extensively studied in the recent years. Numerous studies highlight the contrast of a central fast eroding dome made up predominantly of Indian crust, surrounded by a much more slowly eroding Asian crust. While a majority of the studies attribute this setting to tectonic aneurysm, more recent works

recognise the role of accelerated fluvial erosion due to an antecedent river. Seward and Burg (2008) used the particularly young AFT and ZFT cooling ages from the Namche Barwa (NB) dome to propose the expansive growth of the syntaxis towards the northeast. The expansive growth the NB antiform can be better understood by analysing thermochronological data of the complete GHS ridge that forms the eastern syntaxial zone. The Siyom valley region represents the southwestern part of the syntaxial zone. Based on the available data from the NB and our thermochronological results we attempt to unravel the thermal evolutionary history of entire NE GHS region.

We used multiple low temperature thermochronometers to understand the upper crustal evolution of the western limb of the Siang antiform. Our data suggest two phases of cooling in the rocks of the Siyom valley based on their thermal evolution. Biotite $^{40}Ar/^{39}Ar$ ages range between 24-13 Ma indicating that rocks of the Siyom valley have undergone an initial slow phase of cooling since Early Miocene related to decompressional melting. Zircon (ZHe) and apatite (AHe) helium and apatite fission track (AFT) ages support a second substantially increased rate of cooling and exhumation since the Late Miocene. Data from the lower thermochronometers (AHe and AFT) manifest a significantly higher rate of exhumation at least since the Pliocene.

An assessment of the thermochronometric ages from the Namche Barwa region indicate a similar slowly cooling rockmass throughout the Early and Middle Miocene (23-11 Ma) followed by a rapidly cooling phase beginning thereafter, sustained to the present. The entire extent of the GHS ridge seems to have deformed in a similar fashion from the Mechuka region, north-eastwards up to NB.

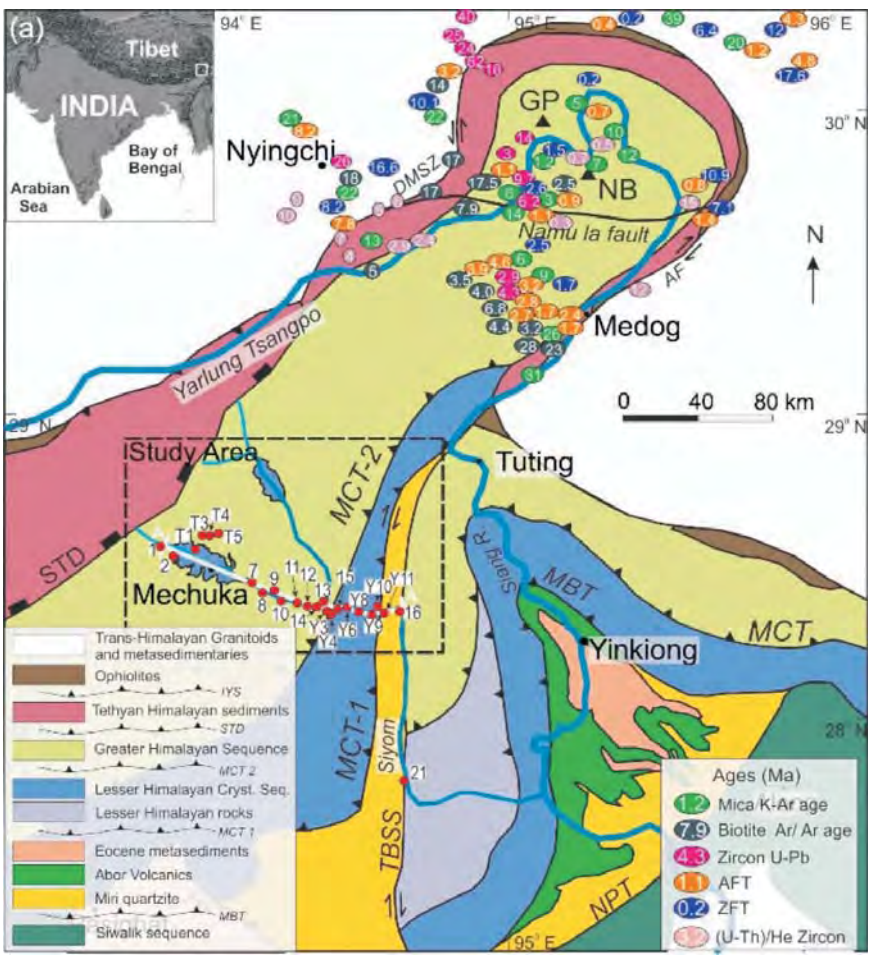

We compare the cooling rates from the Siyom valley transect across the GHS with similar studies towards the northeast of the study area along Doxiong La and Namche Barwa. Cooling rates for samples from the Siyom valley transect have an average lower cooling rate of 10°C/Myr for $^{40}Ar/^{39}Ar$, while the AFT (110°C) to surface temperature (20°C) cooling rate is 30°C/Ma. This indicates non-uniform cooling of the samples at the deeper (above 330°C isotherm) and shallow (above 110°C isotherm) crustal depths. A similar transect across the GHS from the Aniqiao fault up to Doxiong La gives a slightly higher cooling rate of ~600 C/Ma for the ArB ages (Yu et al., 2011). Parallel comparison along Namche Barwa for ArB closure temperature (~330°C) to AFT (110°C) and AFT to surface temperature imply an average cooling rate of ~130°C/Ma in the core of NB (Tu et al., 2015). This shows that the NB massif uplifted very rapidly from ~330°C isotherm to surface since ~5.5 Ma. Thus the cooling rate is seen to increase gradually from the southwest towards the north-east across the east Himalayan GHS.

The E-W shortening induced uplift and exhumation in the Siyom valley since the Late Miocene implies that the crustal antiform, which presently extends north-eastwards and contains the NB and GP peaks, initiated in the Mechuka region. With continued shortening along the E-W and N-S, the zone of rapid exhumation slowly shifted from Mechuka, towards the northeast and has concentrated over the NB-GP massif today. Protracted erosion and uplift of the underlying rockmass has given rise to an apparent northward movement and bending of the suture.

Seward, D., Burg, J.P. 2008. Tectonophysics 451, 282-289. doi:10.1016/j.tecto.2007.11.057
Tu, J., Ji, J., Sun, D., Gong, J., Zhong, D., Han, B. 2015 J. Asian Earth Sci. 105, 223-233.
Yu, X., Ji, Q., Gong, J., Sun, D., Qing, J., Wang, L., Zhong, D., Zhang, Z. 2011. Chi. Sci. Bull. 56, 11, 1123-1130. doi: 10.1007/s11434-011-4419-x

Formation of late Quaternary Ravi river terraces in Chamba region, NW Himalaya: Coupling of Climate and Tectonics

Mayank Joshi*, V.C. Thakur
Wadia Institute of Himalayan Geology, 33 GMS Road, Dehradun 248001, INDIA
**mayank.geo@gmail.com*

The tectonically active and climatically influenced mountain ranges of the Himalaya are drained primarily by the Indus, Ganga and Brahmaputra river systems that carry huge amount of sediments, generated through denudation of mountain ranges as landslides, fluvial erosion and deglaciation. The erosion and aggradation by these river systems sculpts the Himalayan landscape and forms terraces and alluvial fans in the mountain valleys and foreland areas, thus providing a testimony of erosion and aggradation as climatic perturbations (Ray and Srivastava, 2010; Dutta et al., 2012) and tectonic uplift (Lave and Avouc, 2000).

In this work, amongst 5 rivers of the Indus river system we studied the aggradation and incision history of the Ravi river in Chamba, NW Himalaya, in order to understand the coupling between tectonics and climate in terraces genesis. The four levels of distinct river terraces T4, T3, T2 and T1 are found along the Ravi river among which three levels of terraces T4, T3, T2 are the valley fill and the lowest one i.e., the T1 is the strath terrace (Fig. 1). The terrace litho-facies indicate that the river valley aggradation occurred as channel bar deposits and debris flow deposits. The terrace sediments attribution is the surrounding catchment area of Ravi river including the Dhauladhar range. The glacial advancement upto 2600 m also has been observed on the northern flank of Dhauladhar range which is similar in the neighboring Rohtang area (Owen et al., 2008; Owen, 2009). We infer that the sediments generated due to the glaciation processes at the higher reaches were

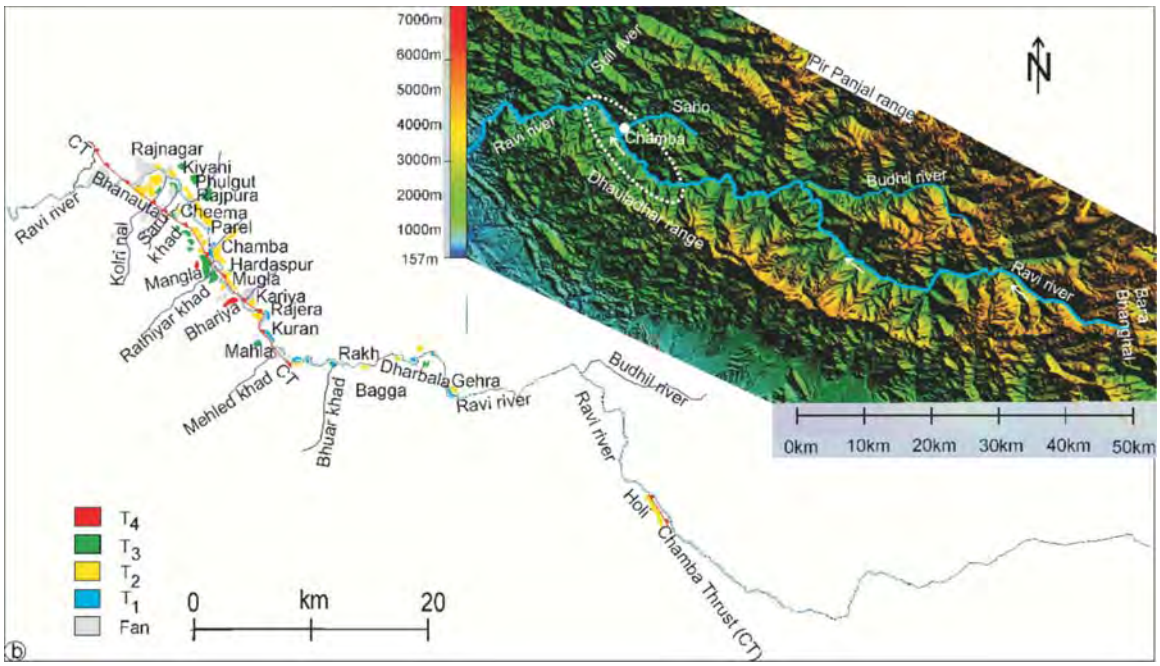

Fig. 1. SRTM map (inset) show the Dhauladhar range to the south and Pir Panjal range to north of the study area, Chamba region. The dotted ellipse denotes the Chamba basin outline. b) Terraces distribution map of the Ravi river shows four level of terraces. The terraces are largely confined in the NW-SE segment of the river in the Chamba basin.

carried down during deglaciation/higher monsoon periods. The OSL chronology of Ravi river terraces indicate two major aggradation phases between 72-46 ka and 37-6 ka along with intermittent incision phases. The terrace formation time span in Chamba area is nearly consistent with the Indian Summer Monsoon (IMS) oscillations and the Marine Isotopic stages. Therefore, our study indicates that the terraces were deposited along the 17 km long and 2.5 km wide Chamba basin and were developed during the reactivation phases of Chamba Thrust with right-lateral strike-slip movement.

Dutta, S., Suresh, N., Kumar, R. 2012. Palaeogeography, Palaeoclimatology, Palaeoecology, 356, 16-26.
Lavé, J, Avouac J.P. 2000. Journal of Geophysical Research: Solid Earth (1978-2012), 105(B3), 5735-5770.
Owen, L.A., Caffee, M.W., Finkel, R.C., Seong, Y.B. 2008. Journal of Quaternary Science, 23(6-7), 513-531.
Owen, L.A. 2009. Quaternary Science Reviews, 28(21), 2150-2164.
Ray, Y., Srivastava, P. 2010. Quaternary Science Reviews, 29(17), 2238-2260.

Numerical analysis of progressive Pawari landslide zone, district Kinnaur, Himachal Pradesh

Vipin Kumar, Vikram Gupta*
Wadia Institute of Himalayan Geology, 33 GMS Road, Dehradun 248001, INDIA
**vgupta@wihg.res.in*

Landslides, caused by natural as well as anthorpogenic factors, are one of the major hazards which result in the social as well as economical loss worldwide. It has been reported that about 15% of the Indian landmass is prone to landslides that cost millions of rupees and approximately 200 lives per year. Landslide hazard zonation is the first step towards understanding the landslide hazards in the area and is being practiced for a long time. It helps to demarcate areas that have higher potential for landslide activities. However, for quantitative assessment, slope stability analysis through finite

element method (FEM) is preferred. FEM not only helps to simulate the actual field conditions through mathematical equations but also predicts the potential unstable zone.

In the present study, Pawari landslide zone (31º33'20.3"N; 78º16'49.2"E) located in the Satluj valley, in the Kinnaur district of Himachal Pradesh has been numerically modelled and analysed for landslide hazard assessment. It lies in the rainfall shadow zone having an annual rainfall of about 120 mm. It is an old landslide zone and has observed to be enlarging during recent times. It is about 500-700 m long, 4.5-5 km wide affecting about 5 km strentch of the national highway (NH-22). The headquarter of the Kinnaur district, Reckong Peo, having about 2397 habitants is located uplsope of the landslide zone at an elevation of about 2450 m. The rock type constituting the area are mainly granitic schist and quartzite belonging to the Higher Himalaya. Geomorphologically, the drainage on the entire slope is more or less parallel.

Both natural and anthropogenic factors are responsible for the occuerence of this landslide. Natural factors mainly include thick and loose debris constituting pebbles and boulders of granitic gneiss in the clay-silt-sand mixture, resting on the steep slope of granitic gneiss which is highly jointed, whereas anthropogenic factors are mainly six road cuts on a single slope and heavy discharge of the entire Reckong Peo township into the slope.

High spatial resolution Cartosat-1 image has been used for the preparation of six cross sections of the landslide zone. These were validated with field survey. Rock and debris material properties were tested in the laboratory. Numerical modelling through Finite element analyses of these slopes has been attempted using phase2 software (ver. 6.0). It has been observed in the model that the slopes are developing considerable stresses and has been documented in the field at various locations in the form of bulging of the retaining walls and development of the ground fissure within the landslide zone. The results from this study will help to plan preventive measures so that its affects, in the future, can be minimised.

Nepal Earthquake evidence from GNSS data at the Everest Pyramid Lab

Giorgio Poretti[1], Federico Morsut[1], Franco Pettenati[2]

[1]Dipartimento di Matematica e Geoscienze - University of Trieste - OGS, ITALY
[2]OGS - Istituto di Oceanografia e Geofisica Sperimentale, ITALY

The Himalayan GNSS network - Started in 1982 with one station at the EvK2Cnr Pyramid Laboratory in Nepal, after 2004 a network of 4 GNSS stations was installed in the Karakorum with the purpose of creating a network that might follow the geodynamic evolution of the Himalayan orogeny. After 2009 the GNSS stations were linked in Internet and the data (in Rinex format) made available to the scientific community through the server of the Dipartimento di Matematica e Geoscienze of the University of Trieste. In this occasion the Pyramid point was shifted to a new location more stable from a geological and topographic point of view.

The data recorded at the New Pyramid permanent station (now GNSS) were processed on a daily basis with precise ephemeris providing the Precise Point Positions (PPP) that indicate the northwards movement of the EvK2Cnr Pyramid Laboratory. The coordinates of the Pyramid Lab were also verified analyzing the correlations with three permanent stations of the IGS world-wide GNSS network. These stations are located in Lhasa (Tibet) and two in Lucknow (India). The distance of these points from the EvK2Cnr Pyramid Lab is rather high but they can be calculated with reliable accuracy for the rather large amount of data available.

The movement of the Pyramid Laboratory during the April 25, 2015 Earthquake - In order to detect an eventual permanent shift of the point during the earthquake the distances of the Pyramid Lab from the three IGS stations have been computed before and after the earthquake.

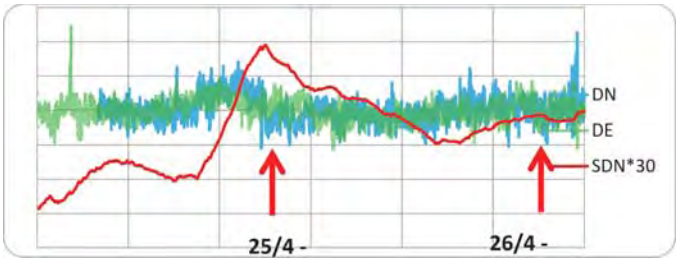

Fig.1. The movement of the Pyramid Laboratory GNSS station N and E components.

Differential analyses of the data during the earthquakes - Particular attention was devoted to the recordings obtained during the days before, during and after the earthquakes and their processing with the PPP techniques and with differential method provided an interesting behavior. A special technique allowed to compute the kinematic site coordinates of the Pyramid point every 30" and to determine the distances from the original point.

Positions during the last three years (2012-2014) - In order to determinate the position of the EVK2Cnr Piramid Laboratory GNSS Station, reference was made to the nearest IGS stations: Lhasa (LHAZ), Luknow (LCK3-LCK4) and Kitab (KIT3). The following tables show positions and their relative error (RMS) for single components: X, Y, Z for Cartesian coordinates and North, East, and High (Up) for Geographic coordinates. All these positions were calculated with the Double Difference technique, using 24 hours RINEX data (GPS and GLONASS where possible) and the Precise Ephemerides (from CODE datacenter).

During the earthquake (25/04/2015) - With the data of the 25th of April, it was possible to do two kinds of analyses: four hours (from 04:00 to 08:00 UTC) of RINEX data with a Double Difference technique and twenty-four hours (whole day) of RINEX data with a Precise Point Positioning (PPP) technique. Both the approaches produced data that were processed later as Kinematic data, so it was possible to distinguish and plot the movement of every component every 30 seconds, compared to an average value of position. In figure 1, are plotted the North, East and Up values as difference between the average position during that period and the kinematic value. As it is possible to see, there are two "inversions" compared to the normal trend: the first one is set at 5:55 UTC and the second one at 6:15 UTC, very close to the official recorded time for the earthquake (6:11 UTC).

The East component has a similar behavior, while the Up value changes very quickly in that same period of time. The change is more marked and the position changes quickly (2 cm in 30 seconds), for both the North and East components; Up instead does not present particular differences. It is possible to state that there was a horizontal movement, with a period of settlement and followed by a normal trend, but with a centimeter difference in position.

This movement is more noticeable in the following images, with two graphs plotted using the kinematic values, obtained from a PPP analyses.

Integral analyses of the coordinates variations during the earthquake - In order to provide a better insight, a new function was defined that adds up the single changes for each component, from the beginning of the observations. A very simple analyses allow to point out the movement of the earth crust through the earthquake and to point out the oscillations of the points of the Pyramid laboratory. An integral function adding up the data from the beginning of the observations interval provides the filtered sequence presented in Fig. 1. for the North component. It can be seen that the constant average movement of 5 mm/day assumes a sharp increase for 8 hours up to the moment of the 7.9 shock of the 25th of April at 5.55 UTM and then it decreases for about 16 hours. This behavior can be enhanced normalizing the input data.

Conclusion - One can conclude that the seismic movements can be recorded and detected by a GNSS

station that can point out not only the intensity of the tremors of the earthquake but also the amount of the shifts of the point at the permanent GNSS station location at every instant before and after the seismic event. The constant increase of the N and U components before the earthquake might suggest a sequential analysis for a possible warning in the case of a systematic processing of the data.

3-D seismic velocity structure of the lithosphere beneath the Nepal Himalayas and the recent Nepal earthquake

Javed Raoof[1,*], Sagarika Mukhopadhyay[1], Ivan Koulakov[2, 3]

[1]*Department of Earth Sciences, IIT Roorkee, Roorkee 247667, INDIA*

**rjavediitroorkee@gmail.com*

[2]*Trofimuk Institute of Petroleum Geology and Geophysics SB RAS, Prospekt Koptyuga, 3, 630090, Novosibirsk, RUSSIA*

[3]*Novosibirsk State University, Novosibirsk, Russia, Pirogova 2, 630090, Novosibirsk, RUSSIA*

The northward relative motion of the Indian plate with respect to the Eurasian plate resulted in the onset of the continent-continent collision processes. As a consequence of that complex Himalayan-Tibetan system was created ~50 Ma ago. Tectonically it is still an active zone. This region is one of the most interesting and complicated regions of the world in terms of geotectonics and seismicity. The tectonic pattern of this region is very complex because of the interactions between the Indian and Eurasian plates and the active north-south convergence along the great Himalayan arc that lead to significant shortening and thickening of the crust. The causal mechanisms of the mountain building in the Himalayas and Tibet have been extensively discussed by many authors (e.g., Dewey and Bird, 1970; Molnar and Tapponier, 1975; Seeber et al., 1981; Allegre et al., 1984). As the Indian plate moved northwards with respect to the Eurasian plate the sedimentary heaps together with its older crystalline roots were complexly folded, faulted and thrusted, hence brought about varied crustal structure all along the ~2500 km long Himalayan arc from west to east. The most popular and accepted tectonic model of the Himalayan collision was proposed by Seeber et al. (1981) stated that the Indian plate underthrusts the Eurasian plate along a gentle north dipping (4-10°N) detachment surface called Main Himalayan Thrust (MHT).

In this study we made an attempt to evolve 3-D seismic velocity structure of the lithosphere beneath the Nepal Himalayas based on tomographic inversion of regional earthquake data. We have analyzed the data obtained from International Seismological Bulletin, contributed by the regional networks in northern India (run by India Meteorological Department, IMD) and Nepal (run by the Department of Mines and Geology, Nepal, DMN) for the years of 2004-2014. In total, we have used the information obtained from 78 seismograph stations installed in the northern India and Nepal. In total, 15085 P- and 6285 S-arrival times from 1167 events in the study region were selected for this study. The study area lying between latitudes 25-31°N and longitudes 79-90°E is shown in figure 1, along with the distributions of stations, selected events and tectonic features. We have attempted to correlate the observed seismic velocity structure with the recent Nepal earthquake that occurred on 25 April, 2015 together with its aftershocks. We have also correlated and interpreted the inferences derived from afore-mentioned observations in conjunction with some of the previous studies in order to better understand and clarify the interactions among different structural segments and the tectonics and their consequences on the seismic activity in response to the geodynamic processes. The data for the hypocentres of the mainshock and their aftershocks are obtained from the Incorporated Research Institutions for Seismology (IRIS).

The analysis of the data has been performed utilizing the iterative tomographic algorithm LOTOS (Koulakov, 2009; Koulakov et al., 2010). The processing begins with the preliminary source

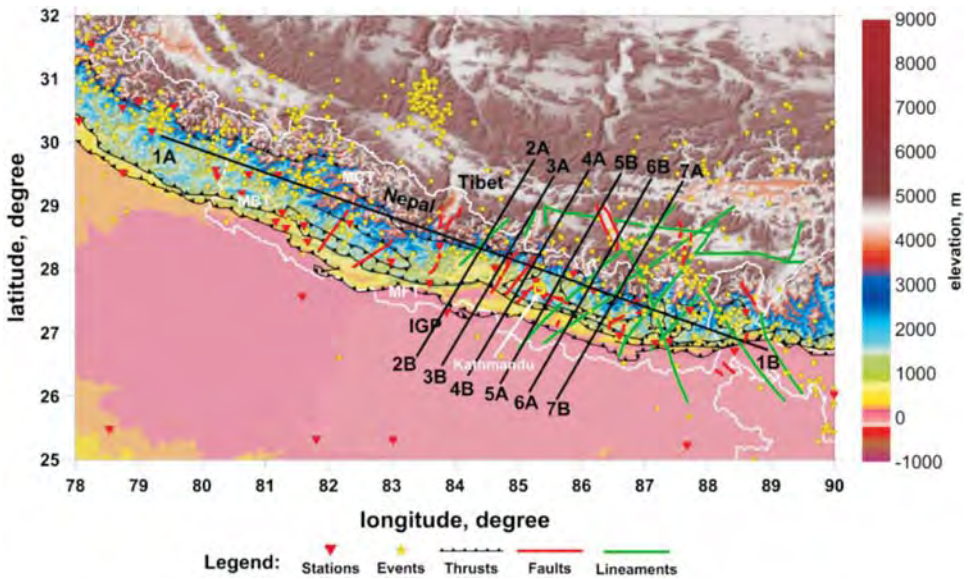

Fig.1. Map of the study region and data distributions. Black lines show locations of the profiles (shown by numbers and the two ends are represented as A and B) selected for visualization of the tomographic results in vertical sections. Background is topography.

locations with the utilization of reference table containing the travel times in the reference 1-D velocity model. The inversion was performed simultaneously for the 3-D P- and S-velocity distributions, source parameters and station corrections. The matrix was inverted utilizing the LSQR technique (Paige and Saunders, 1982; Nolet, 1987). The inversion results obtained utilizing 4 differently oriented (0°, 22°, 45° and 67°) grids were averaged into one model which then was used to update the 3-D model for the next iteration.

From the tomographic analysis we have obtained the heterogeneous lithosphere structure beneath Nepal Himalayas. We have obtained a low-velocity anomaly in the upper part of the model down to depths of ~40 to ~80 km. The results are well supported by a similar study recently conducted in the study region inferring about the variation of the crustal thickness all along/across the strike of the Nepal Himalayas (Koulakov et al., 2015). Earlier several researchers have developed regional tomographic models of the Himalayan-Tibetan region that depict images of the lithosphere in order to understand the geodynamics of the Himalayan-Tibetan orogen (e.g., Li et al., 2008; Koulakov, 2011). Several other researchers locally conducted their studies based on receiver function analysis, deep sounding profiles and local earthquake tomography (e.g. Hauck et al., 1998; Galve et al., 2002; Kind et al., 2002; Kumar et al., 2005; Mitra et al., 2005; Ramesh et al., 2005; Schulte-Pelkum et al., 2005; Rai et al., 2006; Mukhopadhyay and Sharma, 2010). Their findings provide reliable, but too local and sparse information for conceptualization of the geodynamics of the entire Himalayan-Tibetan system.

In line with the objectives, we have obtained reliable 3-D seismic velocity structure of the lithosphere beneath Nepal Himalayas. From the obtained tomographic image we infer that the seismic structure of the lithosphere is heterogeneous along and across the strike of the Nepal Himalayas. We have obtained negative P- and strongly negative S-velocity anomalies and high Vp/Vs ratio with patches of negative P- and positive S-velocity anomalies with low Vp/Vs ratio within top 80 km. The uppermost negative-velocity anomaly may represent the crustal part whereas the lowermost positive-velocity anomaly represents the uppermost mantle. Similar results obtained by Koulakov, et al. (2015) support our findings. The varying architecture of the seismic velocity anomalies, as seen in our tomographic image may be attributed to the variable mechanical properties of the two colliding plates

(Indian/Eurasian). We interpret that the obtained velocity anomalies pattern may represent the weaker and/or rigid segments of the Indian plate that may cause the weaker and/or rigid folding-thrusting in the Himalayan collision zone (Koulakov et al., 2015). The patches of the high S-velocity anomalies and low Vp/Vs ratio may represent thicker and more rigid segments of the Indian plate, possibly the relicts of the ancient crystalline roots that cause more compression in the Himalayan thrust zone. Contrastive, the low velocity anomalies and high Vp/Vs ratio in the upper part may represent presence of thicker layers of sediments and/or highly fractured fluid filled medium.

We observe from the seismicity plotted over the obtained horizontal slices and cross-sections of seismicity velocity anomalies that most of the events are concentrated at and/or near the junction/boundary of the high/low velocity anomalies and low/high Vp/Vs ratio. This corroborate well with the inferences derived by many workers (e.g., Zhao et al., 2000). The distribution of earthquakes suggests that the effective elastic thickness of the lithosphere is varying in the entire region, in other words there is varying mechanical strength of the lithosphere. These interfaces/boundaries separate the two anomalous zones. At places, these interfaces show the pre-existing faults and weak zones that correlate well with the existing tectonic features. These zones are the weak zones of the seismogenic crust. The weak zones of the seismogenic crust are subjected to the tectonic stresses and are capable of generating large crustal earthquakes (Zhao et al., 2000). A large portion of the Himalayan seismic tremors are shallow and happen at ~15 to ~20 km mostly on the MHT (Main Himalayan Thrust).

A catastrophic earthquake Mw=7.9 struck Central Nepal (Goda et al., 2015) on 25 April, 2015 (local time 11:56 a.m.), hypocenter located in the Gorkha region (27.77°N 85.37°E; 12 km

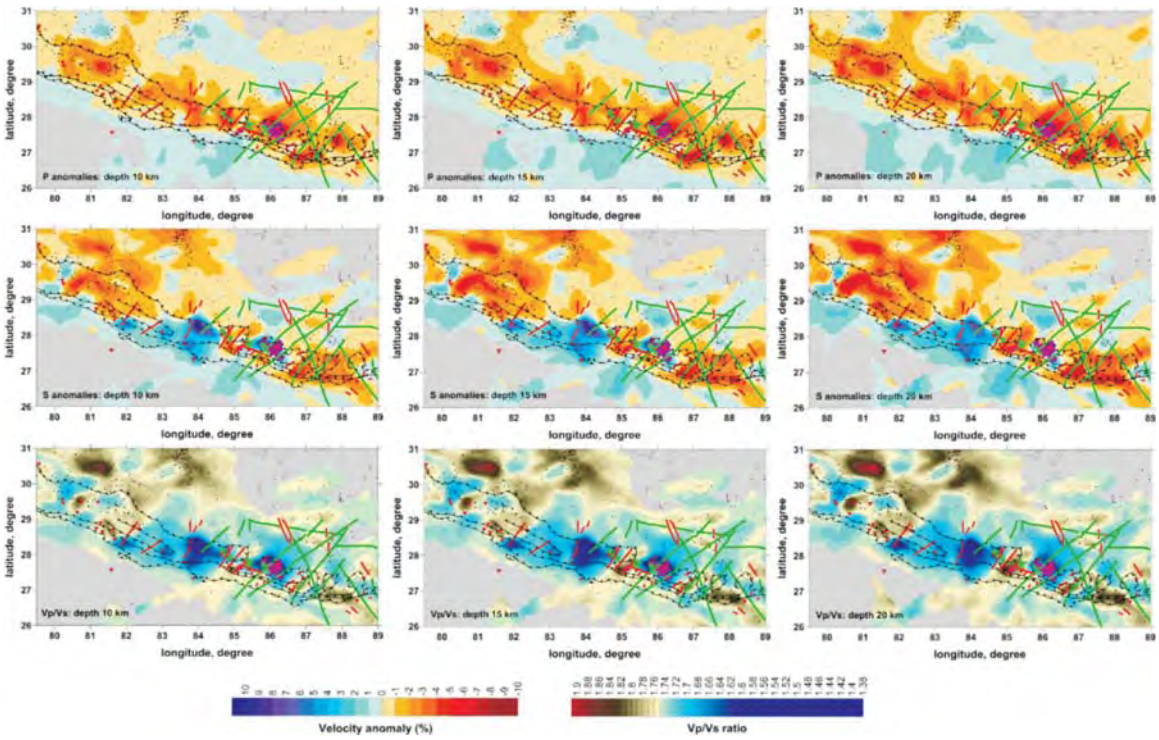

Fig.2. Horizontal slices obtained through real data inversion (at 10, 15 and 20 km depths). Events and seismograph stations are shown with black dots and red inverted triangles respectively. Green and purple stars are showing the April 25, 2015 (Mw=7.9) and May 12, 2015 (Mw=7.2) events respectively. Aftershocks are shown with green and purple dots.

depth) about 80 km north-west of Kathmandu) occurred at the underthrusting interface along the Himalayan arc between the Indian plate and the Eurasian plate (Avouac, 2003; Ader et al., 2012). The earthquake rupture propagated from west to east and from deep to shallow parts of the shallowly dipping fault plane (USGS, 2015). This was the largest event since 1934, Mw=8.1 Bihar-Nepal border earthquake (Ambraseys and Douglas, 2004; Bilham, 2004) in the region. We have plotted the mainshock together with some major aftershocks. Immediately after the mainshock, a moderate Mw=6.6 aftershock struck near the hypocenter. It can be noticed that majority of the aftershocks occurred in the Kodari region (north-east of Kathmandu). Soon after the mainshock a notable event Mw=7.2 occurred on 12 May, 2015 towards the east of Kathmandu (27.56°N 86.1°E; 12 km depth). The rupture propagated eastwards for about 140 km, unzipping the lower edge of the locked portion of the fault, and represents the zone of presumably high and heterogeneous pre-seismic stress at the seismic-aseismic transition (Avouac et al., 2015).

We have plotted these earthquakes and find that they occur at/near the junction of the two anomalous zones of high/low seismic velocities and low/high Vp/Vs ratio (Fig. 2). The patterns of the observed low-velocity anomalies and high Vp/Vs ratio may correspond to the alignments of faults and the high-velocity anomalies and low Vp/Vs ratio may represent the rigid blocks. These earthquakes occurred at MCT (Main Central Thrust) and coincide with the existing tectonic elements in the region.

Ader, T., Avouac, J. P., Liu-Zeng, J., Lyon-Caen, H., Bollinger, L., Galetzka, J. 2012. J. Geophys. Res., 117, B04403.
Allegre, C. O., Courtillot, V., Tapponnier, P., Hirn, A., Mattauer, M., Coulon, C., Xu, R. 1984. Nature, 30, 17-22.
Ambraseys, N. N., Douglas, J. 2004. Geophys. J. Int., 159, 165-206.
Atkinson, G.M., Wald, D.J. 2007. Seismol. Res. Lett., 78, 362-368.
Avouac, J.P. 2003. Adv. Geophys., 46, 1-80.
Bilham, R. 2004. Ann. Geophys., 47, 839-858.
Dewey, J.F., Bird, J.M. 1970. J. Geophys. Res., 75, 2625-2647.
Galvé, A., Sapin, M., Hirn, A., Diaz, J., Lépine, J. C., Laigle, M., Gallart, J., Jiang, M. 2002. Geophys. Res. Lett. 29, L15308.
Goda, K., Kiyota, T., Pokhrel, R.M., Chiaro, G., Katagiri, T., Sharma, K., Wilkinson, S. 2010. Frontiers in Built Environment, 1, 8.
Hauck, M.L., Nelson, K.D., Brown, L.D., Zhao, W., Ross, A.R. 1998. Tectonics, 17, 481-500.
Kind, R., Yuan, X., Saul, J., Nelson, D., Sobolev, S.V., Mechie, J., Zhao, W., Kosarev, G., Ni, J., Achauer, U., Jiang, M. 2002. Science, 298, 1219-1221.
Koulakov, I. 2009. Bulletin of the Seismological Society of America, 99, 194-214.
Koulakov, I. 2011. J. Geophys. Res., 116, B04301.
Koulakov, I., Maksotova, G., Mukhopadhyay, S., Raoof, J., Kayal, J. R., Jakovlev, A., Vasilevsky, A. 2015. Solid Earth, 6, 207-216.
Koulakov, I., Zaharia, B., Enescu, B., Radulian, M., Popa, M., Parolai, S., Zschau, J. 2010. Gcubed, 10, Q03002.
Kumar, P., Yuan, X., Kind, R., Kosarev, G. 2005. Geoph. Res. Lett., 32, L07305.
Li, C., van der Hilst, R.D, Meltzer, A.S., Engdahl, E.R. 2008. Earth Planet Sci. Lett., 274, 157-168.
Mitra, S., Priestley, K., Bhattacharyya, A.K., Gaur, V.K. 2005. Geophys. J. Internat., 160, 227- 248.
Molnar, P., Tapponnier, P. 1975. Science, 189, 419-426.
Mukhopadhyay, S., Sharma, J. 2010. Geoph. J. Int., 183, 850-860.
Nolet, G. 1987. Seismic Tomography. Edited by Nolet, G., Reidel, Dordrecht, 1-23.
Paige, C.C., Saunders, M.A. 1982. ACM Trans. Math. Soft, 8, 43-71.
Rai, S.S., Priestley, K., Gaur, V.K., Mitra, S., Singh, M.P., Searle, M. 2006. Geophys. Res. Lett., 33, L15308.
Ramesh, D.S., Kumar, M.R., Devi, E.U., Raju, P.S., Yuan, X. 2005. Geophys. Res. Lett.,32, 14301-14304.
Schulte-Pelkum, V., Sheehan, A., Wu, F., Billham, R. 2005. Nature, 435, 1222-1225.
Seeber, L., Armbruster, J.G., Quittmeyer, R. 1981. In: Zagros, Hindu Kush, Himalaya. Geodynamic Evolution. edited by: Gupta, H. K. and Delany, F. M.,Geodyn. Ser., 3, 215-242.
United States Geological Survey (USGS). 2015. Available at: http://earthquake.usgs.gov/ earthquakes/ eventpage/ us 20002926#scientific_finitefault
Zhao, D., Ochi, F., Hasegawa, A., Yamamoto, A. 2000. J. Geophys. Res., 105, 13,579-13,594.

Landslide susceptibility mapping of the Mussoorie Township and its environs using GIS and Frequency Ratio method

Meenakshi Devi, Vikram Gupta*
Wadia Institute of Himalayan Geology, 33 GMS Road, Dehradun 248 001, INDIA
**vgupta@wihg.res.in*

Landslides and related mass movement activities are common in the Himalayan region especially during or immediately after the rainy season. These not only cause immense damage to the infrastructure but result in the loss of life as well. In recent years, the frequency of these phenomena has increased, particularly in the Himalayan region. In order to assess the landslide hazards potential of an area, it is necessary to carry out the susceptibility mapping so that necessary precautions are made during further development of the area.

Mussoorie, a small township, located at an elevation of about 2000 m asl in the Garhwal Himalaya of Uttarakhand has been chosen for the present study. It is situated between latitudes 30º28'34.42"N and 30º24'4.00"N and longitudes 78º00'0.46"E and 78º05'56.27"E and covers an area of about 4881 m^2. Geologically, the Mussoorie township and its environs comprise rocks belonging to the Krol and Blaini formations having limestone as the dominant rock-type. The rockmass is highly jointed and shows the presence of numerous micro-cracks. The unconfined compressive strength (UCS) tests confirm these rocks as having low compressive strength. High hills and broad, narrow and elongated valleys are the characteristic features of the area.

High resolution satellite images of the area, viz., IRS-P5 PAN (Cartosat-1), Resourcesat-1 (Multispectral) and LISS IV, have been used for the present study. Digital elevation model (DEM) of the area has been generated using Leica photogrammetry suite. Eleven causative factors of landslides, viz., lithology, geomorphology, proximity to lineaments, land use, slope steepness, aspect, topographic wetness index, profile curvature, plan curvature and proximity to drainage, proximity to roads were taken into consideration and these thematic maps were prepared. An inventory of landslides has also been prepared using LISS IV image on scale of 1:10,000 and have been updated using field-survey.

In the entire area, 496605 pixels were present, of which 886 pixels covering an area of ~ 90 m^2 are present in the active landslides. Frequency ratio for different classes has been calculated and weights have been assigned to each class of all the thematic maps. Finally, landslide susceptibility index has been calculated by overlapping all the weighted thematic maps and landslide susceptibility map prepared classifying areas into high, moderate and low landslide susceptibility.

Prospective of an active back-thrust in the Kashmir Seismic Gap

Shraddha N. Jagtap, R. Jayangondaperumal
Wadia Institute of Himalayan Geology, 33 GMS Road, Dehradun 248001, INDIA

A >11 m slip deficit (Schiffman et al., 2013; Vassallo et al., 2012) vestiges in the Kashmir seismic gap between the 2005 Kashmir Mw 7.6 and 1905 Kangra Mw 7.8 earthquakes owing to the lack of historically documented surface rupture faulting due to earthquake. Paleoseismological investigation carried out in Kashmir shows evidence for the A.D.1555 Kashmir event and thus implies a five century long quiescence period until the last 2005 Kashmir event (Vassallo et al., 2012). However, the 2005 Kashmir earthquake may not have occurred on the Main Himalayan Thrust (MHT) (Gahalaut, 2006), thus the full potential of strain accumulated on the MHT awaits to be unleashed. These studies converge for the expectance of great damaging events of Mw >8 in the future (Schiffman et al., 2013; Vassallo et al., 2012; Gahalaut, 2006; Vassallo et al., 2015).

Geodetic measurements in the Kashmir region infer a 12 mm/yr, out of the total 16 mm/yr convergence between India and Tarim Basin, to be accommodated across the southernmost 250 km of the ranges (Schiffman et al., 2013). A recent study in the Riasi area characterizes the Late Quaternary deformation across three south verging frontal thrusts, namely, the Main Boundary Thrust (MBT), Medicott-Wadia Thrust (MWT) and the Himalayan Frontal Thrust (HFT) or the Main Frontal Thrust (MFT) (Vassallo et al. 2015). By using multiproxy dating techniques of fluvial markers, they estimate high fault slip rates of the order 1-2 cm/yr across the MWT and HFT and the inactivity of MBT since ~30 Ma and the lower bounds of their ages are consistent with the geodetic rates. Of these, a 9±3.2 mm/yr shortening rate is calculated across the HFT where a frontal anticline develops over the HFT in this region. The surface trace of HFT here is obscure unlike that of west of river Beas, where it is demarcated by a sharp escarpment between the Gangetic plains and overriding Siwaliks. This anticline mapped by ONGC workers is known as the Surin Mastgarh anticline (SMA) which extends for nearly 200 km between Chenab and Ravi rivers and hosts several en echelon faults running parallel in the crest. In addition to these faults, data from satellite imageries show a back facing scarp in the hinterland of the SMA which extends for nearly 60 km along strike with an offset of ~5 mts on lowermost terrace of Ujh river. Following a NNW-SSE strike, its western extent merges with the Mandili Kishanpur Thrust (MKT) which is an eastward extension of the Riasi Thrust/MWT. This fault, known as the Naun fault, thrusts the north-dipping Middle Siwalik rocks over the Quaternary deposits overlying the Upper Siwalik rocks. Field investigations revealed a 3-4 m vertical offset across this scarp in a younger terrace of the Bhini river. A (sand) bar in the Bhini river bed crossing the fault shows a scarp with a ~2 m displacement. A back-tilting surface was also identified. The sharp termination of the Middle Siwalik units and the occurrence of thick Upper Siwalik units further north of this fault indicate that this fault may have been active during the exhumation of the anticline.

Therefore, a possibility exists for a change in scenario for the previously documented deformation pattern in the region in which the MWT and HFT emerge in focus. The MWT forms the eastward extension of the Balakot-Bagh fault, causative fault for the 2005 Kashmir earthquake and the HFT which does not emerge on the surface. On the contrary, the existence of a back thrust is widely speculated in the previous studies carried out in the area (Schiffman et al., 2013; Vassallo et al., 2012; Vassallo et al., 2015).

What role the Naun fault plays in the kinematics of the growing SMA is unknown. Paleoseismological studies may shed light on the seismogenic potential of this fault in the seismic gap region of Kashmir and the distribution of strain release across the frontal structures can be evaluated to assess the seismic hazard in this less explored region.

Gahalaut, V.K. 2006. 2005. Current Science, 90(4), 507-508.
Schiffman, C., Bali, B.S., Szeliga, W., Bilham, R. 2013. Geophysical Research Letters, 40(21), 5642-5645.
Vassallo, R., Mugnier, J.L., Vignon, V., Malik, M.A., Jayangondaperumal, R., Srivastava, P., Carcaillet, J. 2015. Earth And Planetary Science Letters, 411, 241-252.
Vassallo, R., Vignon, V., Mugnier, J.-L., Jayangondaperumal, R., Srivastava, P., Malik, M.M., Mouchené, M., Jouanne, F. 2012. European Geosciences Union General Assembly 2012, Vienna, Austria 22-27 April 2012.

Is the Himalayan Frontal Fault System capable of an megathrust (M >9) Earthquake? A review of paleoseismic data

Tina M. Niemi
Dept. of Geosciences, University of Missouri-Kansas City, 5110 Rockhill Road, Kansas City, MO 64110, U.S.A.

Himalayan seismic hazards have been difficult to assess because of uncertainties in basic fault parameters, including (i) the location and rupture length of historical earthquakes, (ii)

segmentation models, (iii) earthquake recurrence intervals, (iv) coseismic slip, and (v) slip rates. These parameters are used to make predictive probabilistic models for magnitude and likelihood of future earthquakes. The Himalayan Frontal Thrust (HFT), sometimes also referred to as the Main Frontal Fault, is the 2500 km-long fault system that marks the active southward verging collision of the Eurasian plate with the Indian subcontinent. The HFT marks the contact of Tertiary Siwalik Sub-Himalayan sediment with Quaternary sediment and deformation. Large magnitude, twentieth century earthquakes, including the 1905 Kangra, 1934 Nepal-Bihar, and 1950 Assam earthquakes, and historically documented earthquake of 1255, 1344, 1505, 1555, 1803, 1833 have likely ruptured the HFT. Defining the rupture segments of these earthquakes has been a challenge. The central seismic gap was defined as the fault segment between the proposed 1905 and 1934 earthquake damage zone (e.g. Khattri, 1987). Some researchers have suggested that the 1505 earthquake may have filled this gap in the past.

A survey of the published literature shows less than twenty paleoseismic sites that have provided data to help resolve these issues. These data provide an emerging model for earthquake recurrence that I summarize in this paper. Deciphering the earthquake recurrence and fault segmentation of these historical earthquakes remains a primary research objective.

Chronology of Glaciation and middle to late Holocene climatic changes along Triloknath glacier valley, Lahul Himalaya

Rameshwar Bali[1], S. Nawaz Ali[2], Imran Khan[1], S.J. Sangode[3], A.K. Mishra[1]

[1]Centre of Advanced Study in Geology, University of Lucknow, Lucknow 226001, INDIA

[2]Birbal Sahni Institute of Palaeobotany, Lucknow 226001, INDIA

[3]Savitribai Phule Pune University, Pune, INDIA

Most of the southern and eastern parts of the Himalaya receive a summer precipitation from the Indian Summer Monsoon (ISM) that declines sharply northward across the Higher Himalaya. Mid-latitude Westerlies (MW) are responsible for the winter precipitation mainly over the extreme western Himalaya, Trans-Himalaya and Tibetan plateau. The Lahul Himalayan region is influenced by both these major weather systems with variable temporal and spatial influence. A number of studies suggested that the ISM strength and glacier response in the Himalaya have a direct connection, although the role of the Westerlies (MW) cannot be ruled out and the exact mechanism, timing and geographic extent of monsoonal influence is still debated.

The present study carried out on the Triloknath glacier, which receives precipitation dominantly from the ISM with contributions from the MW, is an attempt to examine the combined role of these two weather systems to govern the glacier dynamics in the Lahul valley of western Himalaya. Reconstruction of moraine morpho-stratigraphy based on the relative positions of lateral moraines, degree of lithification, vegetation cover, morphology, and soil formation revealed at least four stages of glaciation in the area. The farthest extent of glaciation being represented by a latero-frontal moraine preserved along an adjacent valley at Jhalma has been OSL dated and suggests that the maximum advancement of the glaciers in the Chandra Bhaga valley occurred at around 8.9 ka BP. The other three moraine stages are preserved in the Triloknath valley at a distance of around 5, 3 and 1 km, respectively, from the present day glacier snout. The interpretation of these glacial stages for regional and global climatic correlation relies on the absolute chronology which is under progress.

Besides the glacial chronology, two palaeolacustrine deposits have been located within the Kame terraces along the left and right valley walls. A 2.13 m pit along the right valley wall (32˚39′57′′Lat. and 76˚40′08′′ Long.) shows sub-angular matrix supported lithoclasts at the base followed by alternating layers of medium to fine sand/coarse sand/intercalations of silt and clay.

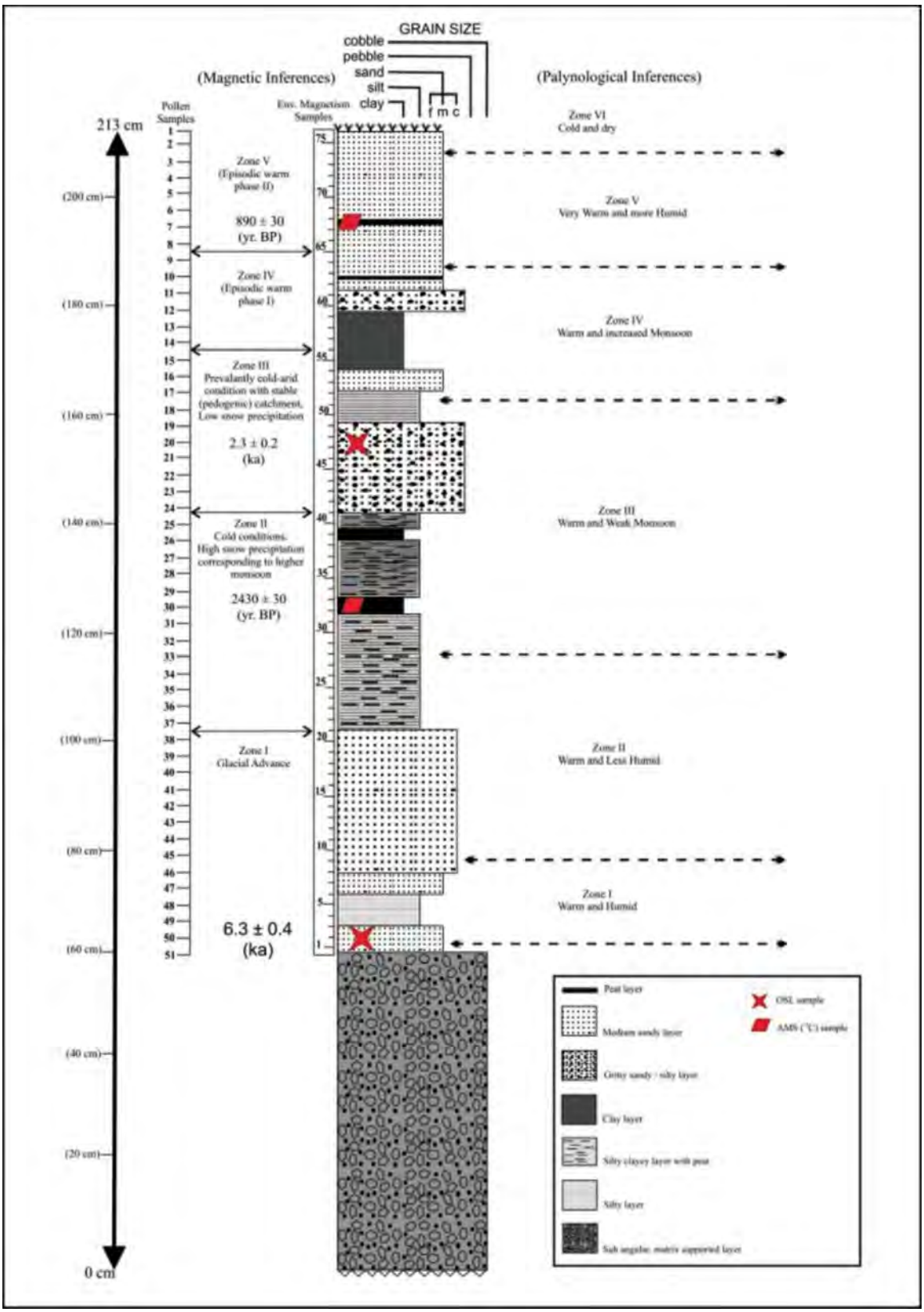
GRAIN SIZE
cobble
pebble
sand
silt
clay
f m c
(Magnetic Inferences)
(Palynological Inferences)
Pollen Samples
Env. Magnetism Samples
213 cm
(200 cm)
(180 cm)
(160 cm)
(140 cm)
(120 cm)
(100 cm)
(80 cm)
(60 cm)
(40 cm)
(20 cm)
0 cm
Zone V (Episodic warm phase II)
890 ± 30 (yr. BP)
Zone IV (Episodic warm phase I)
Zone III Prevalantly cold-arid condition with stable (pedogenic) catchment, Low snow precipitation
2.3 ± 0.2 (ka)
Zone II Cold conditions, High snow precipitation corresponding to higher monsoon
2430 ± 30 (yr. BP)
Zone I Glacial Advance
6.3 ± 0.4 (ka)
Zone VI Cold and dry
Zone V Very Warm and more Humid
Zone IV Warm and increased Monsoon
Zone III Warm and Weak Monsoon
Zone II Warm and Less Humid
Zone I Warm and Humid
Peat layer
Medium sandy layer
Grittsy sandy / silty layer
Clay layer
Silty clayey layer with peat
Silty layer
OSL sample
AMS (14C) sample

Prominent layers of charcoal have been found at various levels. Two OSL and two AMS dates complement each other and are useful to develop palaeoclimatic history of the region.

The 213 cm vertical pit profile is grouped into five distinct Zones (Fig. 1) based on mineral magnetic and lithological variations representing change in depositional conditions in response to the glacial conditions elaborated here.

Earthquake effect on Kathmandu basin-fill sediments

Mukunda Raj Paudel
Department of Geology, Tribhuvan University, Trichandra Campus, NEPAL
Mukunda67@gmail.com

Kathmandu basin is situated on the Kathmandu Nappe. The rocks of this nappe are ranging in age from Precambrian to Paleozoic of the Kathmandu complex (Stocklin and Bhattarai, 1981). Evolution of the Kathmandu basin and other contemporaneous basin along the 2400 km long Himalayan range have own Quaternary geological history. Kathmandu basin has been evolving as a tectonic basin in Lesser Himalaya of Central Nepal since the Quaternary period. The lesser Himalaya is the terrain with altitude less than 3000 m bounded in the north by the Main Central Thrust (MCT) and in the south by the Main Boundary Thrust (MBT). Based on surface geological mapping in the south and subsurface information from drilling data a Quaternary geological sedimentary history for unconsolidated sediment has been proposed (Sakai, 2001; Paudel and Sakai, 2008, 2009). The evolution of the basin started in Neogene-Quaternary time as a consequence of higher rate of uplift in the south in relation to north as a response to evolving Himalaya thrust tectonics. The initial sedimentation occurred in a fluvial basin and blankets the buried bedrock topography. The fluvial facies is characterized by granular sediments mainly consisting of gravel, and sands with some beds of silt and muddy sediments. After sedimentation of more than 100 m thickness the fluvial basin evolved into a lacustrine basin started from the south than expanded to the central part of the Kathmandu valley. The lacustrine sedimentary facies is characterized by unconsolidated sediments consisting mainly of clay and silty clay. The northern part of the present valley has been evolving all the time as a fluvial basin while proximal lacustrine facies consisting of sandy, silty and clayey sections are occuring in the southern part. The transition zone in the north near the boundary of lacustrine domain is characterized by lake-delta deposit. During the draining out of the lake a sandy section of about 40 m thickness has been deposited at the top of lake deposit known as Sunakothi formation in the south (Paudel and Sakai, 2009).

Different geological units are exposed on the surface of the Kathmandu basin. Ancient sediments within this basin show many types of deformation structure which also support the ancient seismic effect within these valley sediments. Present April earthquake within the Kathmandu basin also showed different effect within the different geological units of the Kathmandu basin-fill sediments.

Paudel, M.R., Sakai, H. 2008. Bulletin of the central Department of Geology, Tribhuvan University,Kathmandu, Nepal, 11, 61-70.
Paudel, M.R., Sakai, H. 2009. Jour. Nepal Geol. Soc., 39, 33-44.
Stocklin, J., Bhattari, K.D. 1981. HMG Nepal/UNDP report, 64.
Sakai, H., Fujii, R., Kuwahara, Y. 2001. Jour., Nepal Geol., Soc., 25 (Sp issue), 9-18.

Tectonic and exhumational variability between the Higher and Lesser Himalayan Crystallines, Kumaon-Garhwal region, NW-Himalaya, India

R.C. Patel[1,*], Mohit Kumar[2], Paramjeet Singh[3], Ashok Kumar[4]

[1]Department of Geophysics, Kurukshetra University Kurukshetra 136119, INDIA
**patelramesh_chandra@rediffmail.com*
[2]Department of Geology, Kumaon University, Nainital 263002, INDIA
[3]Wadia Institute of Himalayan Geology, 33, GMS road, Dehradun 248001, INDIA
[4]Department of Electronics, DAV College, Ambala City, Ambala 134002, INDIA

In the Himalaya of Kumaon-Garhwal, NW-India, the Higher Himalayan Crystalline (HHC) and the Lesser Himalayan Crystalline (LHC) are two important tectonic sheets which have suffered maximum deformation, uplift and exhumation during collisional evolution of the Himalaya. During continent-continent collision between India and Eurasia since ~55 Ma, the HHC has been intensively deformed, extruded and thrust over the Lesser Himalayan meta-sedimentary (LHMS) zone between the Main Central Thrust (MCT) at the base and the South Tibetan Detachment System (STDS) at the top. Various tectonic models such as wedge-extrusion (e.g., Burchfiel and Royden, 1985; Grujic et al., 1996; Kohn, 2008), channel flow (e.g., Beaumont et al., 2001; Hodges et al., 2001) and tectonic wedge (Yin, 2006; Webb et al., 2007) explain the tectonics of the HHC. On the other hand, our understanding of the tectonics of the LHC within the LHMS is very limited. Wedge-extrusion and channel flow models do not clearly address the issues of emplacement and exhumation of the LHC within the LHMS zone and their relationship with the emplacement of the HHC between the MCT and the STDS. The tectonic wedging model describes the emplacement of LHC as the basal Tethyan Himalayan Sequence (THS) rocks sliding along the MCT to the south of a branch line merging the MCT and STDS. But, it requires more detail studies in different parts of the Himalaya.

We conducted an integrated structural and thermochronological studies of the LHC (Chiplakot Crystalline belt (CCB) and Almora klippe within the LHMS in the Garhwal-Kumaon region of NW-Himalaya. Structural observation reveals that the emplacement of the CCB within the LHMS took place along a broad NE-dipping shear zone developed within the duplex structure that formed south of the MCT. The broad ductile shear zone is described as deep crustal deformation that resulted in crustal thickening during the Himalayan orogeny. Similarly, the structural studies across the Almora klippe indicate thrusting along both north and south dipping South Almora (SAT) in the south and North Almora (NAT) Thrust in the north of the Almora klippe, respectively.

The exhumation history inferred from the published Apatite Fission Track (AFT) data from the Almora klippe and Ramgarh thrust sheet, and the published Ar-Ar dating on white mica in the Dadeldhura klippe along with metamorphic and deformation temperature (400 to 600°C) constrains the emplacement of ~13 to 20 km thick crystalline thrust sheets between the MCT and the STDS over the LHMS between 23 and 17 Ma (Srivastava and Mitra, 1996; Célérier et al., 2009; Antolín et al., 2013; Patel et al., 2015). Lack of migmatites, leucogranite, high grade metamorphic rocks and inverted metamorphism (as present in the HHC) in the LHC thrust sheet does not agree that this thrust sheet was part of the HHC, but might be its origin, emplacement and exhumation histories are different than the HHC. Based on our published AFT data and new Zircon Fission Track (ZFT) data, we propose a new model for emplacement and exhumation history of the Almora klippe. Our Fission Track data not only help in understanding the superposed tectonic history but also reveal the pop-up emplacement of the Almora klippe which is responsible for its uplift and exhumation.

Antolín, B., Godin, L., Wemmer K., Nagy, C. 2013. Terra Nova, doi: 10.1111/ter.12034.
Beaumont, C., Jamieson, R.A., Nguyen, M.H., Lee, B. 2001. Nature 414, 738-742.
Burchfiel, B.C., Royden, L.H. 1985. Geology 13, 679-682.

Célérier, J., Harrison, M.T., Yin, A., Webb, A.A.G. 2009. Geological Society of America Bulletin 121(9/10), 1262-1280. doi: 10.1130/B26344.1.
Grujic, D., Casey, M., Davidson, C., Hollister, L.S., Kundig, R., Pavlis, T., Schmid, S. 1996. Tectonophysics, 260, 21-43.
Hodges, K.V., Hurtado, J.M., Whipple, K.X. 2001. Tectonics 20, 799-809.
Kohn, M.J. 2008. Geological Society of American Bulletin 120, 259-273.
Patel, R.C., Singh, P., Lal, N. 2015. Tectonophysics, v. 653, pp. 41-51, DOI: 10.1016/j.tecto.2015.03.025.
Srivastava, P., Mitra, G. 1996. Journal of Structural Geology 18, 27 - 39.
Webb, A.A.G., Yin, A., Harrison, M.T., Célérier, J., Burgess, W.P. 2007. Geology 35 (10), 955-958.
Yin, A. 2006. Earth-Science Review 76, 1-131.

Geometry of the Main Himalayan Thrust and Moho beneath the Satluj Valley, NW Himalaya using receiver function method

Monika Wadhawan*, Devajit Hazarika, Arpita Paul, Naresh Kumar
Wadia Institute of Himalayan Geology, 33 GMS Road, Dehradun 248001, INDIA
**monika.geophysics@gmail.com*

The crustal structure in the Satluj Valley region of the Northwest Himalaya has been studied using teleseismic waveform data recorded by a seismological network consisting of 18 broadband seismographs. The seismological stations cover the geotectonic units starting from the Himalayan Frontal Thrust (HFT) in the south to the Tethyan Himalaya to the north. Receiver Function method has been adopted to analyze about 250 teleseismic data of epicentral distance within the range of 30-90° and body wave magnitude >5.5. The receiver functions estimated at the stations located south of the HFT and corresponding inverted velocity models show extremely low shear wave velocity (~0.7-1.2 km/s) in the upper most 3-4 km of the crust indicating the thickness of the sedimentary column of the Indo-Gangetic plain which is filled with alluvium deposited by major rivers like the Ganga and Yamuna. The depth of Moho is observed at ~46 km at the stations near the HFT which increases to ~53 km in the Higher Himalaya and ~60 km beneath the Tethyan Himalaya. The detachment surface separating the under-thrusting Indian plate from the overriding Himalayan wedge is referred to as the Main Himalayan Thrust (MHT) which is clearly observable at the stations north of the HFT. The inverted velocity models show that the depth of the MHT varies from ~15 km beneath the Sub-Himalaya to ~25 km beneath the Higher Himalaya and further north under Tethyan Himalaya it is detected at ~35 km depth. The study infers gentle dipping nature of the MHT rather than flat-ramp-flat geometry as reported in Nepal Himalaya and Garhwal Himalaya (Pandey et al., 1995; Caldwell et al., 2013). This observation also supports along the strike variation of geometry of the MHT as observed in case of seismicity in an around the study region (Arora et al., 2012). In general, the seismicity in the northwest Himalaya is concentrated in the Himalayan Seismic Belt (HSB), a narrow belt, straddling the surface trace of the MCT. However, clustered seismicity beneath the HSB as observed in Garhwal Himalaya is not observed in the study section, instead a cluster of seismicity is observed close to the Kaurik-Chango fault zone which is transverse to the strike of the Himalaya.

Arora, B. R., Gahalaut, V.K., Kumar N. 2012, Journal of Asian Earth Sciences, 57, 15-24.
Caldwell, W.B., Klemperer S.L., Lawrence J.F., Rai S.S., Ashish, 2013. Earth Planetary Sci. Letters, 367, 15-27.
Pandey, M.R., Tandukar, R.P., Avouac, J.P., Lave, J., Massot, J.P. 1995. Geophysical Research Letters, 22, 741-754.

Detrital modes and provenance of the Middle Miocene Siwalik Foreland Basin, eastern Uttarakhand region

Tanuja Deopa*, Pradeep K. Goswami
Centre of Advanced Study, Dept. of Geology, Kumaun University, Nainital 263002, INDIA
**deopa.tanu@gmail.com*

The Siwalik peripheral Foreland Basin accumulated sediments derived from the eroding, uplifting and tectonically active Himalayan orogenic belt following the collision of Indian-Eurasian plates during the Neogene times. Detrital modes of these sandstones record the history of Himalayan uplift and tectonism. The present study focuses on the petrography and petrofacies analysis of two hitherto unstudied areas of the fluviatile Siwalik foreland basin of the Eastern Uttarakhand region. Detrital modes of both the regions reflect the recycled orogen provenance.

The Lower Siwalik sandstones of the region are characteristically grey to buff in colour, friable and salt and pepper textured and can be broadly classified as matrix-poor and matrix-rich sandstone. Based on the modal composition, the sandstone of the eastern part of the study area is: lithic arenite - $Q_{63}F_6L_{18}$:Mx_{13}, sublithic arenite - $Q_{73}F_4L_8$:Mx_{15} and lithic greywacke - $Q_{59}F_3L_{15}$:Mx_{23}. The gross modal composition of sandstone indicates its greater affinity towards the lithic greywacke types having $Q_{62}F_4L_{16}$:Mx_{18} components. Whereas, the average modal composition of the sandstone of the western part of the area is: lithic arenite - $Q_{62}F_4L_{23}$:Mx_{11}, sublithic arenite - $Q_{66}F_4L_{16}$:Mx_{14}, and lithic greywacke - $Q_{55}F_3L_{17}$:Mx_{25}. The gross modal composition is $Q_{62}F_4L_{18}$:Mx_{16}. The abundance of low-medium and few high grade metamorphic rock fragments and subordinate sedimentary rock fragments suggests derivation from metamorphic and sedimentary source rocks. However, the scarcity of detrital feldspar and volcanic fragments rules out the possibility of a magmatic arc source. The high proportions of carbonates indicate contribution by limestone formations. The presence of Glauconite in considerable proportions confirms the reworking from a marine source. Nevertheless, the high proportions of lithic fragments reflect the rapid and progressive uplift of the Himalaya and intense unroofing of the mid-crustal terranes.

Ascertaining neotectonic activities in the southern part of Shillong Plateau through geomorphic parameters and remote sensing data

Watinaro Imsong[1,*], Swapnamita Choudhury[1], Sarat Phukan[2]
[1]Wadia Institute of Himalayan Geology, 33 GMS Road, Dehradun 248001, INDIA
[2]Department of Geological Sciences, Gauhati University, Guwahati 781013, INDIA
**watinaro@wihg.res.in*

Shillong Plateau in the Northeast Sub-Himalaya is a detached block of a subducted wedge of the Indian Peninsula. The plateau is also considered as a tectonically active pop-up continental block (Kayal, 1998; Nandy, 2000; Bilham and England, 2001; Rajendran et al., 2004). The Dauki Fault which runs along the border between the Shillong Plateau and the Sylhet Basin of Bangladesh marks a spectacular topographic discordance in the region. The Precambrian basement in the Sylhet Basin of Bangladesh is found at a depth of about 18 km, which is exposed only at a few hundred meters below the surface along the southern fringe of the Shillong Plateau. The southern margin of the Shillong Plateau, thus, represents an active plateau margin. Tectonic behavior of the Shillong Plateau is believed to be diverse in different segments.

Considering the tectonic configuration, it is expected that the drainage basins would respond to the cumulative accumulation of compressive stress (neotectonics). Geographic Information

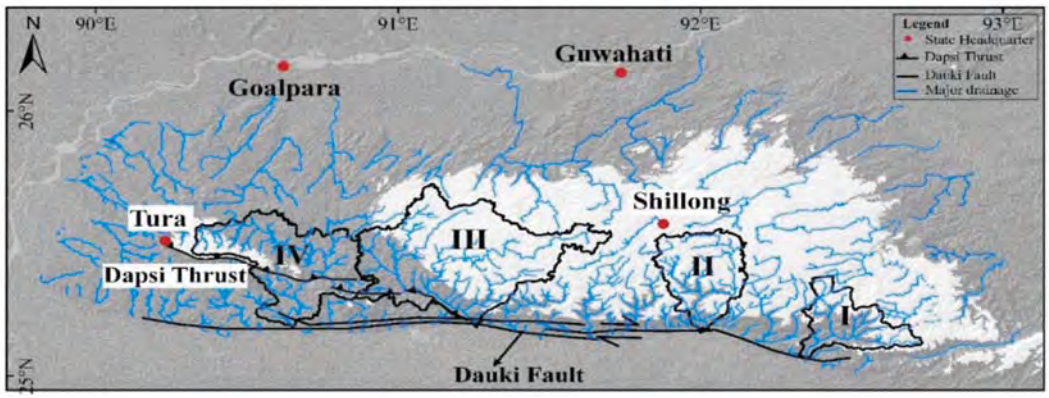

Fig. 1. Drainage map of the study area and location of the four river basins investigated in the present study. The basins are from east to west Lubha River Basin (I), Umngot River Basin (II), Jadukata River Basin (III), and Simsang River Basin (IV).

System (GIS) based morphometric studies were performed on four basins which drain towards the southern boundary of Shillong Plateau. These are from east to west (i) Lubha River Basin, (ii) Umngot River Basin, (iii) Jadukata River Basin, and (iv) Simsang River Basin (Fig. 1)

Morphometric indices calculated through the analysis suggest that the southern part of the plateau involving the study area is undergoing deformation, and incision and uplift seem to be in equilibrium. The hypsometric curves and indices of the river basins demonstrate similar observations indicating that the entire plateau is undergoing uplift. However, the longitudinal profiles of the Simsang River (western segment) and the Lubha River (eastern segment) are found to be more eroded than the Jadukata and Umngot Rivers (central part of the plateau). Major knick points in all the river channels show prominent topographic breaks. The Dapsi Thrust extends NW-SE in the southern part of the plateau. The Simsang River cuts across this thrust towards west and the Jadukata River cuts across the fault in the south-central region. The Dapsi Thrust merges with the Dauki Fault along the Jadukata River. Activity in Dapsi Thrust may be the cause of presence of steeper courses in the middle reaches of the Simsang River and the lower reaches of the Jadukata River implying the structural control on river morphology. The higher surface uplift of the central part of the plateau compared to the western and eastern parts are also reflected in the analysis of mountain front sinuosity (Smf). Duarah and Phukan (2011) have also identified relatively young landforms in the central part as compared to deeply eroded eastern and western parts. The Smf of the eastern part of the plateau is found to be the highest which is associated with less activity. Valley profiles and basin asymmetric factor of Simsang River shows slight tilt towards west whereas the Jadukata, Umngot and Lubha River Basins show obvious tilting towards the east. Correspondingly, numerous small channels (3rd and 4th order streams) around the central section on the southern periphery of the plateau show right lateral component (deflecting towards the east) in the channels. This supports the sense of movement suggested by Evans (1964) for the Dauki Fault. The study suggests that though the entire Shillong Plateau is undergoing tectonic instability, however, the central segment of the plateau is witnessing accelerated deformation/uplift. Further, the study indicates that the observed deformation in the river basins is associated with the episodic activity along the Dapsi Thrust and the Dauki Fault.

Bilham, R., England, P. 2001. Nature, 410, 806-809.
Duarah, B.P., Phukan, S. 2011. Geol. Soc. Ind., 77, 105-112.
Evans, P. 1964. Geol. Sco. Ind., 5, 80-96.
Kayal, J.R. 1998. J. Geophys., 19, 9-34.
Nandy, D.R.2000. Indian Jour. Geol., 2000, 72(3), 175-195.
Rajendran, C.P., Rajendran, K., Duarah, B.P., Baruah, S., Earnest, A. 2004. Tectonics, 23(4), 1-12.

Reconstruction of Indian monsoon variability between 3.1 to 5.7 ka BP using Speleothems $\delta^{18}O$ records from the Central Lesser Himalaya, India

Lalit M. Joshi[1], Bahadur S. Kotlia[1], S.M. Ahmad[2], C.C. Shen[3], Jaishree Sanwal[4], Waseem Raza[2], Anoop. K. Singh[1]

[1]Centre of Advanced Study in Geology, Kumaun University, Nainital, 263002, INDIA
[2]CSIR-National Geophysical Research Institute, Hyderabad 500007, INDIA
[3]Department of Geosciences, National Taiwan University, Taipei, TAIWAN, ROC, 10617
[4]Jawaharlal Nehru Centre for Advanced Scientific Research, Bangalore, INDIA

We present the first record of the monsoon precipitation variability between ~5.65 and ~3.17 ka BP from the Central Lesser Himalaya using $\delta^{18}O$ measurements of Tityana cave stalagmites (hereafter refer to as TCS). Presently, the cave receives the precipitation from both ISM (Indian Summer monsoon) and the Westerlies. A 13 cm long TCS is composed entirely of calcite and grew at a growth rate of 0.02 to 0.12 mm/yr. The $\delta^{18}O$ variation of -8.04 to -10.46‰ and five ^{14}C AMS radiocarbon dates (as the $^{230}Th/U$ ages uncertainties) allow us to identify the mid to late Holocene multi-decadal climatic oscillations. A significant $\delta^{18}O$ variation of >2.5‰ may have been resulted due to the amount effect. The low $\delta^{18}O$ (more negative) may represent the strengthening of the monsoon. The larger amplitude of $\delta^{18}O$ values with drop of >1.5‰ centred around 5.2, 3.5 and 3.2 ka BP seems the monsoon breaking events which are reported throughout the ISM/Asian Summer Monsoon (ASM) regimes. The climate was more unstable between 5.1 to 3.6 ka BP with the drop of $\delta^{18}O$ values between ~0.75 to 1‰, peaking around 4.7 ka BP and ~4.2 to 4 ka BP, indicating of the weakening of monsoon precipitation. However, the magnitude of 4.2 ka BP event was smaller over NW Himalaya due to two different source of moisture e.g., ISM winter western disturbance. During the transition of mid to late Holocene, the highest drop of $\delta^{18}O$ (>1.75‰) around 3.5 ka BP may represent the collapse of the civilization. The, close correlation of TCS data with records from the Asian monsoon regimes and westerlies suggest the possible relationship between North Atlantic oscillation and Asian monsoon system.

Surface wave group velocity assessment along different azimuths In the western part of Himalaya-Tibet region

Amit Kumar[1,*], Naresh Kumar[2], Sagarika Mukhopadhyay[1]

[1]Department of Earth Sciences, Indian Institute of Technology Roorkee, INDIA
**akiitkgp08@gmail.com*
[2]Wadia Institute of Himalayan Geology, 33 GMS Road, Dehradun 248001, INDIA

We performed surface wave group velocity analysis, and this data is inverted to obtain the sub-surface shear wave structure of the upper lithosphere for the western part of Himalaya-Tibet collision zone. We used broadband seismic data of 63 earthquakes of magnitude range 5.0 to 7.2 that occurred during 2006-2011 in the Western part of the Himalaya and Tibet regions. These earthquakes are located in the northern, western and eastern part of the NW Himalaya and further north in the Tibetan plateau (Fig. 1). The data is recorded at regional distances at two stations located in the southern part of the Himalaya. The epicenters are distributed in such a way that, the ray paths samples many different structures. The region is very complex containing different geological units and the lithosphere structure varies significantly from place to place. The data is divided into different clusters/groups such that the ray paths of each cluster sample different structural elements. These clusters are well separated from each other and the ray paths are located at different azimuths from recording stations in the western Himalayan syntaxis zone and surrounding parts of Himalaya and Tibet (Fig. 1). The paths between clusters and recording station cover different zones with different orientations with respect to the strikes of major structural elements of the the Himalaya and southern Tibet.

The major tectonic features of the region are Himalayan Frontal Thrust (HFT), Main Boundary Thrust (MBT), Main Central Thrust (MCT), South Tibetan Detachment (STD), Indian-Tsangpo Suture Zone (ITSZ), Karakoram Fault (KF), Main Karakoram Thrust (MKT) and Sargoda Ridge Thrust (SRT). The main geological units divided by these tectonic discontinuities are Siwalik (Outer) Himalaya, Lesser Himalaya, High Himalayan Crystalline, the Tibetan plateau and the Indo-Gangetic plains (IGP) are situated respectively to the north and south of the Himalaya. The ray paths traversed by the surface waves are perpendicular as well as parallel to the tectonic discontinuities and some paths also cover the western part of the Indo-Gangetic plains. Most of the ray paths sample the Himalayan region, and partly the south Tibetan detachment zone and the Indo-Tsangpo suture zone, as well as the Karakoram fault zone and Tibetan plateau regions. The IGP has thick sediments (5-8 km) in the upper most crust, however the crustal thickness is low compared to other above mentioned parts of the study region (Bhatachayra, 1992; Powers et al., 2001; Kumar et al., 2011). Similar to the variation of topographic elevation, the crustal thickness increases towards north starting from IGP, which has maximum value close to the collision zone (Mishra et al., 2004; Kumar et al., 2011).

For each cluster, the dispersion curves of both Rayleigh and Love waves are obtained from each earthquake event using Frequency and Time Analysis (FTAN) method of Levshin et al. (1972) and then average trend is calculated for one cluster of events. Based on a technique of Kumar et al. (2015), the weighted averaging of computed dispersion curve for a group of events of a single cluster is obtained based on the fitting of higher order polynomial and also the standard deviation is measured. For both Rayleigh and Love waves, the observations are performed for periods in the range 5-60 sec, and most of the data are within the period range 10 to 50 sec as per the selection criteria of high signal-to-noise ratio. The evaluated results of dispersions four clusters obtained at Shimla station are shown in figure 1. The dispersion curves of one particular cluster has nearly same trend of velocity variation with increasing period. Therefore, the variation of fundamental group velocity for the events of single cluster is small, however a higher variation is exhibited among different paths. A high variation at intermediate period ranges for different paths could be due to effect of thick crust for the parts having high topography. This variation is for both waves although

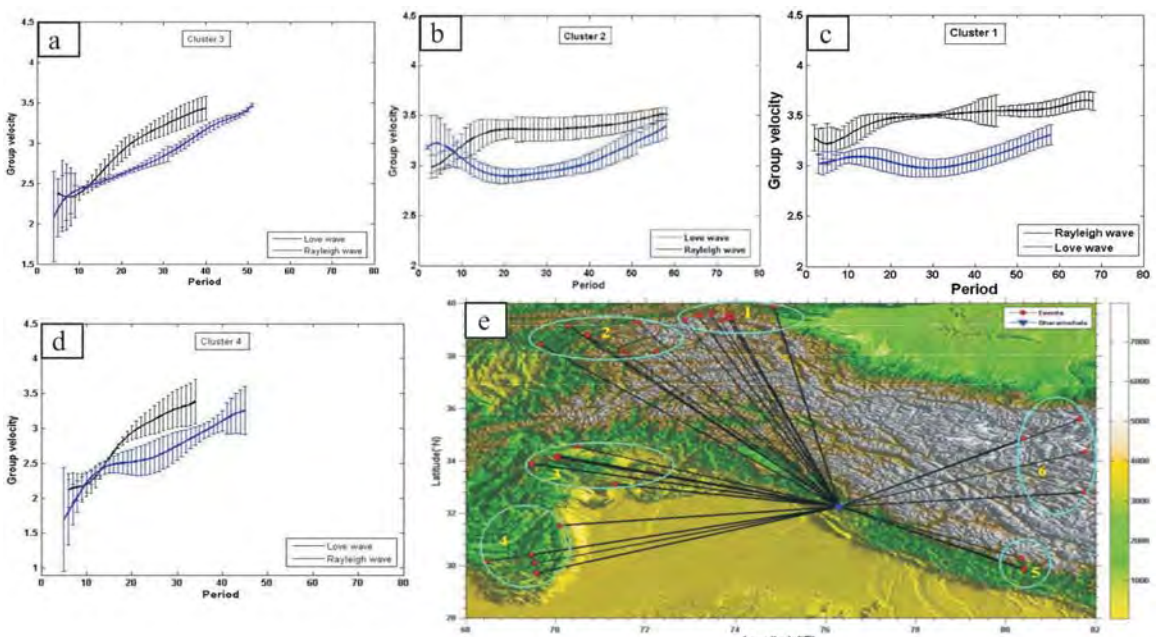

Fig. 1. The average dispersion curves of different clusters: (a) cluster 3, (b) cluster 2, (c) cluster 1, (d) cluster 4, along with (e) surface relief map of the study region that also contains ray paths from Shimla station.

higher variation is found in case of Rayleigh wave (Figs. 1b and 1c). The paths passing through the IGP indicates very low velocities for both Rayleigh and Love waves for periods less than 15 sec (Fig. 1e) which matches with earlier results (Bhatacharya, 1992; Kumar et al., 2011). This observation can be explained in terms of presence of low velocity sediments in the IGP. The waves passing perpendicular to the major structural elements have high variation in velocities in the period range 10 to 30 sec (Figs, 1b and 1c) which is specifically due to the low velocities of Rayleigh wave and it has been noticed earlier also (Shaprio et al., 2004; Kumar et al., 2011).

The extraction of low velocities may be related to the existence of fluid filled fractures in the middle and lower crust, however the contribution of anisotropy effect is not ruled out for which the inversion of both dispersion curves (Rayleigh and Love wave) is performed using the method of Herrmann and Ammon (2002) to obtain the shear wave structure. These differences of velocities are assessed to measure the anisotropic effects at different depths in the crust. In an overall attempt, the variation of group and inverted shear wave velocities are weighted to account for the effects of anisotropy, tectonics and partially fluid saturated zones in different depth sections.

Bhattacharya, S.N. 1992. Curr Sci 62:94-100.
Herrmann, R.B., Ammon, C.J. 2002. Dept. Earth Atm. Science, St Louis Unversity, St Louis, MO USA.
Kumar, N.K., Aoudia, A., Guidarelli, M. 2011. T43D-2303, AGU Fall meeting San Francisco, 5-8 Dec., 2011.
Kumar, A., Kumar, N., Mukhopadhyay, S. 2015Int. J. Earth Sci (Under Review).
Levshin, A., Pisarenko, V., Pogrebinsky, G. 1972. Ann Geophy 28, 211-218.
Mishra, D.C., Laxman, G., Arora, K. 2004. Curr Sci 84, 224-230.
Powers, P.M., Lillie, R.J., Yeats, R.S. 1998. Geol Soc Am Bull 110:1010-1027
Shaprio NM, Ritzwoller MH, Molnar P, Levin V (2004). Science 305:233-236.

Fractal analysis of aftershock sequence of the 2015 Nepal earthquake (Mw=7.8): A wavelet-based approach

Sushil Kumar[1,*], Chandra Shekhar[2], Mayank Poddar[2], Ravindra K. Arvind[2], Mahesh Prasad Parija[1], Sandeep K. Chabak[1]
[1]Wadia Institute of Himalayan Geology, 33 GMS Road, Dehradun 248001, INDIA
**sushil_rohella@yahoo.co.in*
[2]Birla Institute of Technology and Science, Pilani, INDIA

The Nepal Earthquake, worst natural disaster to strike Nepal since the 1934 Nepal-Bihar earthquake, hit the Gorkha district killing more than 8,000 people. It occurred at 12:35 IST on 25 April, with a magnitude of 7.8 (Mw). Its epicenter lies near the village of Barpak, Gorkha district (28.28° N, 84.79° E), and its hypocenter was at a depth of approximately 15 km (ISC). The main shock was followed by a number of aftershocks. The spatial distribution the aftershock sequence (N=388 with M $\geq$1.5, where N is the number of aftershocks and M stands for magnitude), indicates that the clustering (Fig. 1) is located in the south eastern segment of the mainshock and above the Main Boundary Thrust (MBT). The decay of Nepal aftershock sequence exhibits a power law relationship with time evident from Omori's curve implying that a scaling property exists in the time dimension.

In the present work, the observed non-stationary time series of the Nepal earthquake aftershock sequence has been analysed using wavelets. The wavelet variance analysis of the aftershock sequence yielded better estimates of fractal dimension, slip ratio and b-value of the region. The data was analysed at different resolutions using wavelets to segregate the large-scale features containing the broader information from the small-scale features containing detailed information present in the sequence.

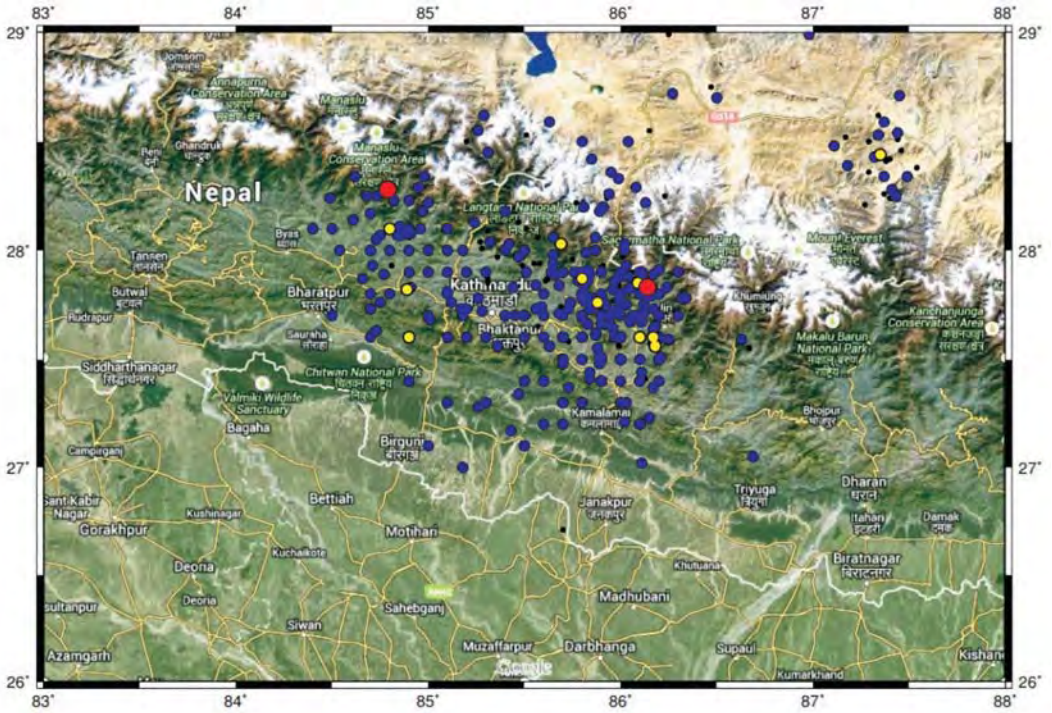

Fig. 1. The distribution of the aftershock sequences of Nepal earthquake. Clustering is located in the south eastern segment of the mainshock and above the Main Boundary Thrust (MBT).

Wavelet-based fractal analysis of the 388 aftershock data (M≥1.5) of the disastrous Nepal earthquake (25 April 2015) has been carried out to understand the behavior of the aftershocks. The Omori's curve suggests that the decay of aftershocks follows a power law relation with time. The p-value, known as 'decay constant' is found to be 0.62. The b-value of the region as obtained by wavelet variance analysis is close to 1, which is in agreement with the normal value for tectonically active regions. The results obtained from the multi-scale analysis of the aftershock sequence using the wavelets indicate that the fractal behavior of aftershock data sustains up to certain scales only. Using the wavelet variance, the fractal dimension of the source is obtained as 2.64, which indicates that it is a 2D plane that is being filled up by the source fractures. The slip ratio that determines the fraction of total slip occurring on the primary fault is computed to be 0.22, which reveals that 22% of the total slip has occurred on the primary fault.

Strain release by normal faulting in the hanging wall of the Himalayan mega thrust: reactivation along the Main Boundary Thrust at Logar in the northwestern Kumaon Sub Himalaya, India

G. Philip*, N. Suresh, R.J. Perumal
Wadia Institute of Himalayan Geology, 33 GMS Road, Dehradun 248001, INDIA
**drgphilip@gmail.com*

A prominent NW-SE trending linear fault, the Logar fault, which vertically displaced the Quaternary alluvial fan was delineated at Logar village in northwestern Kumaon Sub Himalaya (Valdiya, 1992). This fault cut across the Logar mega fan within the vicinity of the Main Boundary Thrust (MBT) and maintains a distinctive linear south side up scarp throughout its length. Paleoseismological

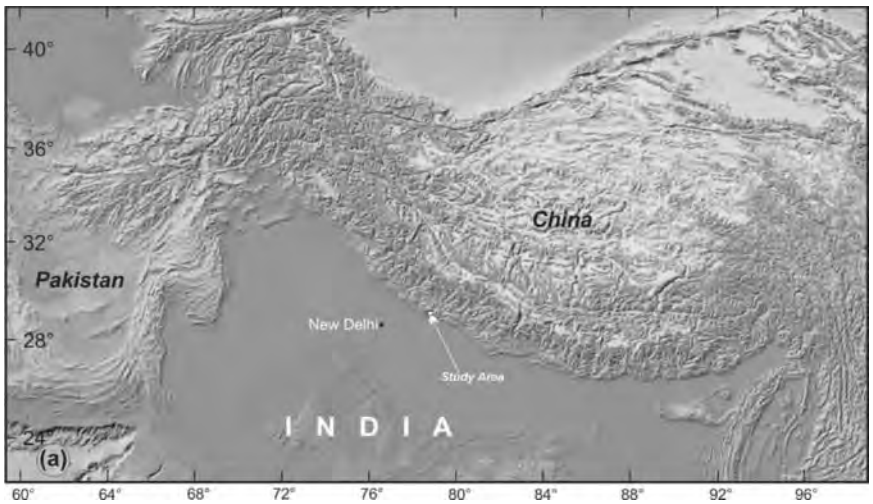

Fig.1. Satellite image (DEM) showing the regional location of the study area.

investigations carried out across this fault show evidences of large magnitude multiple paleoearthquakes that have produced surface rupture in the Late Quaternary with age constraints using luminescence chronology. The hanging wall of the MBT in the area is occupied by the Pre Tertiary rocks of the Lesser Himalaya (Bhowali-Bhimtal Formation) which has a definite tectonic contact with the Upper Tertiary (Siwalik) group of rocks (Varadarajan and Rawat, 1976; Karunakaran and Rao, 1979). The Tertiary rocks (~Dharamsala Formation of Oligocene-Lower Miocene overlain by the Siwalik group of rocks of post Miocene) form the footwall. The Quaternary alluvial fan developed at Logar comprises of clasts both derived from the Pre Tertiary (Bhowali-Bhimtal Formation, Amritpur granite) and the Tertiary group of rocks. Based on the surface expression of the discontinuous scarp, and its expression on the satellite data, the fault has been further extended on either side to a total length of ~7.5 km which in part follows the older mega thrust zone of weakness, the MBT.

The fault maintains a distinctive linear south side-up scarp throughout its length and has created a linear depression in front of the north facing scrap, which got subsequently filled-up by fluvial sediments. The generation of the fault scarp sharply deflected tributaries of Logar Gad also. The faulted and uplifted fan shows wind gaps and water gaps in the hanging wall besides depressions (sag ponds) developed in its front. A trench excavation survey across the Logar fault scarp for paleoseismic investigation was carried out at Bairasari village. The sedimentary units defined in the trench were divided into seven separate sub litho-units. The orientation of the clasts and the finer stratification within the units clearly suggest the fluvial depositional environment. The distribution and relative placing and their pattern of deformation of the units in the trench suggest normal faulting. A parallel trench excavated verified the distribution of the lithological units and their lateral extent.

Composed of loose and unconsolidated material, the height of the fault scarp (15 to 38 m) suggest multiple faulting events that occurred along the same fault plane/system with which the scarp obtained a cumulative vertical height upto 38 m. The OSL sample collected from the top surface of the south side-up scarp of the fan shows the age as <20 ka indicating the upper age of the fan before the faulting. The OSL age 20 ka in the bottom unit of the trench suggest commencement of post faulting deposition of the units.

The sequence of faulting of Logar mega fan suggests its genetic link with seismic activity in this region. The mappable length (7.5 km) of the Logar Fault indicate that it is not long enough to produce a great earthquake (Mw >8). However is capable of generating secondary faulting (Wells and Coppersmith, 1994). The geomorphic expression of the Logar Fault which also coincides to the Himalayan mega thrust, the MBT, suggests subsequent tectonic activity along the MBT. The Logar

Fig. 2. Corona satellite photograph showing the coalesced Logar mega fan (Fan boundary is outlined in white dashed line) displaced by a NW-SE linearly trending normal fault (F-F). The geomorphic southside-up fault scarp is indicated by white arrows. The expression of the discontinuous fault scarp is shown by white dashed line on the satellite photograph. The trench excavation site is also shown on the image.

active fault identified north of the HFT indicates that elastic strain release within the hanging wall is not limited to the front, but it is dispersed above the decollement over a broad area.

The Logar Fault may be one of several secondary hanging wall structures initiated to accommodate rupture during large magnitude Himalayan earthquakes. Repeated reactivation of the MBT substantiates high seismic potential of the Sub Himalaya and calls for more extensive study of paleoearthquakes of this vastly populous mountainous region. The losses in terms of life and property would be much higher than for the great earthquakes experienced in the past hundred years because of the explosive growth of population and industrial establishments in the northwestern Sub Himalayan and Frontal Himalayan region in the last half a century.

Karunakaran, C., Ranga Rao, A. 1979. Geological Survey of India, Miscellaneous Publication, 41, 1-66.
Valdiya, K.S. 1992. India.-Annals Tecton-icae 6,54-84.
Varadarajan, S., Rawat R.S. 1976. Himalayan Geology, 6, 467-484.
Wells D.L., Coppersmith, K.J. 1994. Bulletin Seismological Society of America, 84, 974 -1002.

Influence of aqueous fluids in strain localization and fault rock Behaviour in Frontal Thrust zones of the eastern Himalaya: Evidence from Main Boundary Thrust zone

Dilip Saha*, Abhijit Patra
Geological Studies Unit, Indian Statistical Institute, Kolkata 700108, INDIA
**sahad.geol@gmail.com*

Fault rocks varying from cataclasite to mylonite or phyllonite usually occur along the Main Boundary Thrust (MBT, cf. Ramgarh thrust) and the Main Frontal Thrust (MFT) in eastern Himalaya. In the foothills to low altitude Lesser Himalayan part of eastern Himalaya in Jalpaiguri and Darjeeling districts, deformed Gondwana sandstones including the Rangit pebble slates (Talchir Formation) constitute the fault rock protolihts in the footwall of the MBT. Here, micaceous quartz mylonites

(Daling Group) are thrusted over Gondwana sandstones along the MBT, henceforth referred to as the MBT1. Several tens of metres below the MBT1, intact Gondwana rocks preserve primary sedimentary structure and recognizable plant fossils. Within a metre of the contact (fault core) between Daling and Gondwana rocks, cataclasites or foliated cataclasites/phyllonite mark the footwall Gondwana sandstones, the latter (foliated cataclasites) often showing marked grain size reduction and increase in the relative proportion of phyllosilicate (illite/muscovite, chlorite). The occurrence of thin quartz-chlorite±calcite veins parallel or transverse to the foliation in the fault zone indicates local foliation parallel or transverse fracturing during progressive deformation and foliation development. Presence of folded veins with vein quartz grains showing undulosity and local bulging recrystallization and of deformation twins in calcite indicates syn- to late-tectonic nature of the veins.

In the Lish River traverse, the Gondwana rocks are thrusted over the Middle-Upper Siwalik coarse to pebbly sandstone. This north dipping thrust contact is referred to here as the MBT2 (cf. South Kalijhora thrust); the thrust zone is marked by development of cataclasite, common mm-cm thick deformation bands, metre scale faults and fractures affecting both the Gondwana and Siwalik sandstones. In the footwall of the MBT2, the Siwalik sandstones show multiple fracture sets at cm to m scale enclosing imbricate blocks of intact sandstone. Evidently the mesoscopic fracture density is much higher in a ~50 m wide zone of pebbly sandstone below the MBT2, compared to middle Siwalik sandstone further south.

Preliminary bulk and trace element chemistry of fault rocks collected from the vicinity of the MBT, show that there is marked decrease in SiO_2 content, and increase in FeO^T, Al_2O_3, (Na_2O+K_2O) and marginal increase in CaO in the thrust zone samples showing strong foliation compared to weakly deformed Gondwana sandstone samples. The relative change in bulk chemistry corresponds well with increase in modal phyllosilicate contact, foliation parallel chlorite grains and pronounced chlorite rich beard structure at pressure fringes of quartz or altered feldspar porphyroclasts. There is also relative increase (four to six fold) in ΣREE abundance in the strongly foliated samples. There is textural/microstructural evidence (like corroded quartz porphyroclast boundary or pressure solution seams with concentration of ferruginous matter) for silica dissolution in the MBT1 fault zone samples. Mineralogical changes together with increase in other major element (Fe, Al, alkali) and trace element abundances suggests the episodic, mass transfer assisted by multiple passes of advective circulation of hydrothermal fluids preferentially along the fault zone. Aqueous fluid channeling is possibly linked to episodic increase in porosity in the fault zone rocks usually mediated by transgranular to intragranular fracturing of quartz and feldspar clasts (e.g. Jeffries et al., 2006). Multiple passes of hydrothermal fluid enhance phyllosilicate generation reducing the permeability in the resulting phyllosilicate rich foliated fault rock. Appreciable thickness (a few metres to 10 m) of the foliated cataclasite/phyllonite renders weakening and strain localization near the fault core (e.g. Stewart et al., 2000). Transient porosity and permeability decrease lead to enhanced local fluid pressure, which results in cyclic brittle failure, as evidenced by foliation transverse, syntectonic quartz-chlorite and calcite veins.

Unlike the MBT1, foliated cataclasites are rare in the MBT2 fault core separating compact Gondwana sandstones from friable Middle to Upper Siwalik pebbly to coarse sandstones. In the MBT2 fault core, thin deformation bands of various orientations show grain size reduction by cataclasis, increased phyllosilicate proportion, common intragranular to transgranular fractures through feldspar and quartz clasts. Here also the development of fault zone rock is apparently controlled by hydrothermal pumping and secular variation in fluid pressure. Development of deformation bands in unconsolidated sands to weakly lithified sandstone around active fault segments, for example in the San Andreas Fault, has been interpreted in recent years as indicators of seismic creep (Cashman et al., 2007; Balsamo and Storti, 2011). The preponderance of deformation bands in the MBT2 fault core in the Lish River section opens up the possibility of tracking paleoseismicity in the eastern Himalayan foothills.

Balsamo, F., Storti. F. 2011. Geological Society of America Bulletin, 123, 601-619.
Cashman, S.M., Baldwin, J.N., Cashman, K.V., Lawrence, K.S., Crawford, R. 2007, Geology, 35, 611-614.
Jeffries, S.P., Holdsworth, R.E., Wibberley, C.A.J., Shimamoto, T., Spiers, C.J., Neimeijer, A.R., Lloyd, G.E. 2006. Journal of Structural Geology, 28, 220-235.
Stewart, M., Holdsworth, R.E., Strachan, R.A. 2000. Journal of Structural Geology, 22, 543-560.

A conceptual model of connectivity structure during Himalayan floods

Vimal Singh
Department of Geology, University of Delhi, Delhi 110007, INDIA
Vimalgeo@gmail.com

The biggest challenge posed by the rivers is floods, which impacts the communities and have socio-economic and environmental consequences. It has both positive and negative impacts depending upon the location and vulnerability. Several factors such as rainfall, sediment supply, anthropogenic activity, soil erosion etc. have been recognized to contribute to the floods. But how are these processes interconnected and how are floods in the mountains different from the floods in the plains? Do they have similar connectivity structure or is it different? This study addresses some of these questions and proposes a conceptual connectivity model for the Himalayan rivers based on wide range of studies carried out in the Himalaya and other active landscapes.

The floods in the Himalaya (or any mountainous terrain) can be divided in to two - normal flood (it can be further sub-classified on the basis of its intensity) and flash flood. Apart from the rainfall - the major driving factor of the floods - lake bursts also cause flooding in the Himalaya. Continuous and heavy rainfall may give rise to floods, whereas cloud burst and lake burst could give rise to a flash flood. The question is how different are these two events? A sudden increase in the volume of water in the rivers can cause severe damage and loss of lives as witnessed during recent Kedarnath 2013 event; but in normal flood the volume of water increases at relatively slower rate therefore, loss of lives could be reduced in this case.

On a regional scale the connectivity between the rainfall and the topography governs the normal floods. However, on investigating closely around several compartments (glacier, hillslope, valley bottom, active landslide, inactive landslide, tributary, trunk river, etc.) can be recognized in a Himalayan terrain. In addition, precipitation acts as another important compartment. While, link between the rainfall, surface runoff, streams and rivers are most important, the link between the rainfall, sediment storages and rivers is also equally important. As sediments are integral part of floods, the primary source of the sediments i.e. the hillslopes form a vital compartment that could be further divided in to smaller compartments based on its curvature. There are other compartments like active and inactive landslides, which provide significant sediment flux. Valley bottom is another important compartment as its width defines the degree of connectivity between the rivers and the hillslope compartments; in wide valley bottoms the connectivity between the river and the hillslope is poor whereas it is strong in narrow valleys.

There exists a difference in connectivity structure of a normal flood and a flash flood. In contrast to the flash floods, where longitudinal connectivity is strongest, in normal floods all the compartments, are connected i.e. there exists longitudinal, horizontal and vertical connectivity. For example, a recent study (Devrani et al., 2015) showed a strong longitudinal connectivity during 2013 Kedarnath event. Another important difference between these floods is the sediment size transported during these two events. In comparison to the normal floods, larger sediments are transported during the flash floods. When compared with the floods in the plains, the major difference exists in terms of lateral connectivity. Although both the terrains show lateral connectivity, in mountains lateral areas

act as sources for sediment flux whereas in plains adjacent areas act as sinks for the sediment flux. The longitudinal connectivity is similar for suspended loads in the channel but different for the bed load. The proposed connectivity structure in the Himalaya also provides insight into the functioning of long-term fluvial processes in an active landscape.

Devrani, R., Singh, V., Mudd, S.M., Sinclair, H.D. 2015.. Geophysical Research Letters, 42, 5888-5894.

The Siwalik Group in and around Itanagar, Western Arunachal Himalaya: Disposition of Formations and a Preliminary Study of the Associated Depositional Environments

Subhra Mullick
Geological Studies Unit, Indian Statistical Institute, Kolkata 700108, INDIA
Subhra.mullick@gmail.com

The Himalayan Foreland Basin (HFB), similar to other collision-related foreland basins, is developed in front of an active orogenic belt because of lithospheric subsidence induced by topographic load of the hanging wall; as well as sedimentary load in the basin (Burbank, 1996). The Siwalik group of the HFB in India is exposed in the southern frontal area of the Himalaya in a WSW to ENE trending belt. Our study incorporates the Miocene- lower Pleistocene Siwaliks of the Western Arunachal Himalaya (Chirouze, 2012), in the road-cut sections in and around Itanagar and some river sections of the area. The general dip of Siwalik in the study region is towards northernly to north-westernly.

Previously, Yin et al. (2010, Part 2) had named the thrust between the Siwalik Group and the sandstone-black shale-coal bearing Permian strata overlying it, as Main Boundary Thrust and the thrust separating Permian Gondwana and gneissic Lesser Himalayan succession was termed as Bome Thrust. According to that, in the study area, the Siwalik Group is bounded by the Main Boundary Thrust (MBT) to the north and Himalayan Frontal Thrust (HFT) demarcates its southern boundary.

In the footwall of the MBT, the overall coarsening upward sequence of Siwalik group has been divided into three formations based on their lithology. The Kimin Formation, correlated with the Upper Siwalik formation of Western and Central Himalaya (Kumar, 1997; Singh, 2007) is comprises of thick, poorly sorted conglomeratic beds with the alternation of sand and silt. Conglomerate beds are sheet-like, massive or stratified in some places, with limited or insignificant basal erosion. The fine sandstone units, interlayered with conglomerates, are parallel laminated and massive and ripple laminations are common in siltstone-mudstone unit. The whole succession is thought to represent an alluvial fan setting.

Kimin Formation is underlain by the Subansiri Formation, which is correlatable with the Middle Siwalik formation, and comprises of medium to very coarse grained, salt and pepper textured sandstone with occurrence of calcareous concretion of various shape and sizes. Sandstones are at places pebbly and pebble conglomerate beds with erosional base are encountered but less common in the succession. Large fragments of fossil wood and other vegetal matter occur throughout the Subansiri Formation. In upper part of formation, beds are up to 10 m. thick and show large scale cross-stratification and erosional surfaces that are lined with patches of pebbles. The amalgamated large sandstone bodies shows a systematic association of planar and trough cross stratification along with the presence of large scours. The large cross-strata are organized in downcurrent accreting compound bedforms where individual cross strata thickens as they grow on downcurrent inclined surfaces and eventually thins out further downstream. Paleocurrent direction is dominantly towards South-South East to South - South West. Presence of large erosively based sandstone bodies,

downcurrent accreting bedforms, paucity of mud throughout the formation and low dispersal of paleocurrent altogether indicates a deposition from a braided channel system.

The lowermost formation of the Siwalik group in the study area is Dafla formation and is correlatable with the Lower Siwalik Formation. The Dafla Formation occurs as a thrust sheet over the Upper Siwalik Kimin Formation over north dipping Tipi Thrust. Dafla Formation comprise fine - medium grained massive sandstone bodies, 2-10 m thick, harder as compared to Subansiri Formation, less micaceous and more quartzose, and are interlayered with thinner beds of shale and clay with a few nodular and silty beds. In a few well exposed sections the sandstones are dominated by low-angle to parallel strata. Outcrops of Lower Siwalik Dafla Formation occurs within the kilometer thick Tipi Thrust zone, and in most places is highly tectonised, hindering detailed sedimentological investigation.

In the study area, occurrence of Lower Siwalik demarcates the northern boundary of Siwalik Group and Lower Gondwana sandstone-black shale-coal beds overly it through the MBT. Here the Gondwana succession occurs as a thin thrust sliver over Siwalik and in north it is overlain by the Lesser Himalayan gneisses (e.g. Bomdila Gneiss in the particular area) through the Bomdila Thrust or Bome Thrust, this thrust zone is defined by the presence of mylonitic-ultramylonitic fault rocks in the study area.

Burbank, D.W., Beck, R.A., Moulder, T. 1966. The Himalayan foreland basin, The tectonic Evolution of Asia, Cambridge University Press, p. 666.

Chirouze, F., Doupont-Nivet, G., Huyghe, P., Beek, P.V., Chakraborty, T., Bernet, M., Erens, V. 2012. Journal of Asian Earth Sciences, 44, 117-135.

Kumar, Gopendra 1997. Geological Society of India, (1st edn.)

Singh, T. 2007. Journal of Geological Society of India, 70, 339-352.

Yin, A. 2006. Earth Science Reviews, 76, 1-131.

Yin, A., Dubey, C.S., Webb, A.A.G., Kelty, Harrison T.M., Chou, C.Y., Celerier, J. 2010.. Geological Society of America Bulletin, 122, 360-395.

Deformation pattern of Almora klippe south-eastern Kumaon Lesser Himalaya, Uttrakhand, India

Mohit Kumar[1,*], P.D. Pant[1], R.C. Patel[2]

[1]Department of Geology (CAS), Kumaun University, Nainital 263002, INDIA

**puniyamohit@gmail.com*

[2]Department of Geophysics, Kurukshetra University, Kurukshetra 136119, INDIA

The Almora klippe within the Lesser Himalayan Sequence (LHS) in the Kumaon region, NW- Himalaya is the largest klippe in the Himalaya. It is bound by the south-dipping North Almora Thrust (NAT) in the north and the north-dipping South Almora Thrust (SAT) in the south. The Ramgarh thrust sheet in the south of the SAT is bound by the Ramgarh Thrust (RT). It is made of quartzite, biotite augen gneiss, Champawat granitiods and Ramgarh porphyry. Structural field data, quartz c-axis and finite strain data are analysized to understand the kinematics and deformation of the Almora klippe. Study shows that Almora klippe has suffered by polyphase deformations i.e. D1, D2 and D3. Structural analysis of main foliation and lineation shows a major asymmetrical synformal structure between the NAT and the SAT. The synform is characterized by southern long and gently to moderately northward dipping limb and northern short and moderately to steeply southward dipping limb. The hinge zone of the regional synform is refolded into synform and antiform whose axes parallel to the axis of regional synform structure.

Strain analysis across the Almora klippe from the NAT to the RT has been carried out using Rf/Ø and Centre-to-centre Fry techniques. Strain pattern determined by both methods represents flattening strain ($k<1>0$). Finite strain is maximum along the NAT and the SAT but relatively low in

the middle part. Lattice preferred orientation data of quartz rich rocks shows triclinic symmetry along the NAT and the SAT and orthorhombic symmetry in the middle part of the Almora klippe. The RT zone is characterized by Monoclinic to orthorhombic symmetry. C-axes data of quartz shows top-to-NE movement along the NAT while top-to-SW along the SAT. Sense of movement along the RT is found to be top-to-SW. Based on the deformation pattern of quartz, feldspars and micas minerals, the NAT and the SAT zones have undergone high temperature deformation while the RT zone has undergone low temperature deformation.

Spatially variable subsidence and sediment characteristics across the Ganga Plain: implications for fluvial channel morphology

Elizabeth Dingle[1,*], H.D. Sinclair[1], M. Attal[1], D.T. Milodowski[1], V. Singh[2]
[1]*School of GeoSciences, University of Edinburgh, Drummond Street, Edinburgh, UNITED KINGDOM*
**elizabeth.dingle@ed.ac.uk*
[2]*Department of Geology, University of Delhi, Delhi 110007, INDIA*

Rivers draining the east Ganga Plain are described as shallow aggrading systems that frequently flood and avulse over the surface of well-defined alluvial mega fans, whilst those further west are more deeply incised systems that are less prone to flooding where channels are laterally constrained within broad valleys (Gibling et al., 2005; Sinha et al., 2005). Understanding the controls on these contrasting dynamics is fundamental to determining the sensitivity of these systems to projected increases in monsoonal storm events and continued anthropogenic development on the Ganga Plain. In addition, this has implications for predicting the long-term stratigraphic architecture of the subsurface stratigraphy.

A new basin scale approach to quantifying floodplain and channel relief has been developed that easily identifies areas where channels are super-elevated or perched above their adjacent floodplain. This is important as areas at a lower elevation than the nearest channels are most at risk of inundation should the channel flood or avulse. We quantify the geomorphic signal of super-elevation or incision of the principal rivers of the Ganga Basin through detailed analyses of the digital topography using a new generalised swath profile methodology (e.g. Hergarten et al., 2014; Fig. 1). This information has been combined with new depth to basement maps beneath the foreland basin and with grain size data down the principal rivers to determine probable controls on the observed geomorphic signal.

Basin subsidence plays a key role in the long-term pattern of sediment deposition across the Ganga Plain. However, there is little understanding of how long-term (millennial) subsidence patterns control the geomorphic character or longitudinal profiles of transverse rivers draining the Ganga Plain. By combining depth to basement beneath the foreland basin succession, with known shortening rates, it is possible to approximate subsidence rates (Sinclair and Naylor, 2012). Using new depth to basement maps derived from seismic data, we suggest that subsidence rates in the west Ganga Plain are approximately half those in the east. However, it is acknowledged that the most recent component of subsidence history is somewhat constrained by the paucity of depth to basement data close to the mountain front. Therefore, we combine these observations with additional constraints from the grain size distributions in the main river channels. Downstream grain size fining rates have been shown to reflect the spatial distribution of tectonic subsidence within sedimentary basins (Paola et al., 1992; Robinson and Slingerland, 1998; Fedele and Paola, 2007; Duller et al., 2010; Whittaker et al., 2011).Therefore, to further substantiate these first-order estimates of basin subsidence rate we present new grain size data from each of the major rivers between the mountain front and the gravel sand transition. The data demonstrate that downstream fining rates are slower and that the gravel sand transition is farther downstream in the west compared to the east, again supporting slower subsidence rates in the west.

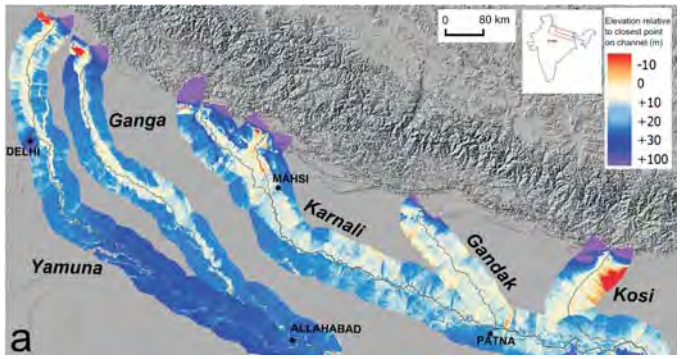

Fig. 1. Swath results when applied to a 90 m SRTM DEM of the Ganga Plain.

In summary, we interpret that higher subsidence rates at the mountain front in the east have encouraged lower proximal fan surface gradients due to trapping of coarse sediment close to the mountain front and rotation of fluvial profiles. In contrast, lower subsidence rates in the west promote progradation of the gravel front further into the basin producing steeper fan surfaces at the mountain front. Whether individual systems incise or aggrade in response to shorter term (e.g. Milankovitch timescale) top-down changes in sediment to water discharge ratios is dependent on the gradient of the revised equilibrium channel relative to that of the older fan or Plain surface. For a constant climatic forcing of channel lowering along the strike of the Ganga Plain, incision will only occur where this lowering rate outpaces subsidence.

Duller, R.A., Whittaker, A.C., Fedele, J.J., Whitchurch, A.L., Springett, J., Smithells, R., Fordyce, S., Allen, P.A. 2010 J. Geophys. Res. 115, F03022. doi:10.1029/2009JF001495

Fedele, J.J., Paola, C. 2007. J. Geophys. Res. 112, F02038. doi:10.1029/2005JF000409.

Gibling, M.R., Tandon, S.K., Sinha, R., Jain, M. 2005. Journal of Sedimentary Research 75, 369-385.

Hergarten, S., Robl, J., Stüwe, K. 2014. Earth Surface Dynamics 2, 97-104. doi:10.5194/esurf-2-97-2014.

Paola, C., Heller, P.L., Angevine, C.L. 1992. Basin Research 4, 73-90. doi:10.1111/j.1365-2117.1992. tb00145.x

Robinson, R.A.J., Slingerland, R.L. 1998. Journal of Sedimentary Research, 68.

Sinclair, H.D., Naylor, M. 2012. Geological Society of America Bulletin 124, 368-379. doi:10.1130/B30383.1,

Sinha, R., Jain, V., Babu, G.P., Ghosh, S. 2005. Geomorphology 70, 207-225. Doi:10.1016/j.geomorph. 2005.02.006

Whittaker, A.C., Duller, R.A., Springett, J., Smithells, R.A., Whitchurch, A.L., Allen, P.A. 2011. Geological Society of America Bulletin 123, 1363-1382. doi:10.1130/B30351.1

Comparison of fluvial facies and geochemistry in two differing River systems of the Neogene Siwalik Group, Nepal Himalaya

Swostik K. Adhikari[1,*], Tetsuya Sakai[1], Barry P. Roser[1], Ashok Sigdel[2]

[1]Department of Geoscience, Shimane University, Matsue 690-8504, JAPAN

**swostik_adhikari@hotmail.com*

[2]Soil, Rock and Concrete Laboratory, Nepal Electricity Authority, Kathmandu, NEPAL

This study characterizes the fluvial facies and geochemistry of the Lower and Middle Siwaliks in the Khutia Khola section of far-western Nepal. The results are compared to those from equivalent sediments in the adjacent Karnali River section, which are known to have been deposited by the large paleo-Karnali River system. The river deposits in these two sections are important records of tectonism and climatic change in the western part of the Nepal Himalaya, and the local variation of these key processes during middle to late Miocene times.

Depositional facies description from the Khutia Khola section shows the sequence of facies associations is the same as that recognized in other Siwalik Group sections, namely: fine-grained meandering river system (FA1), flood-flow dominated meandering river system (FA2), deep (FA3) and shallow (FA4) sandy braided river systems, from the oldest to youngest. FA1 and FA2 correspond to the Lower Siwalik, and FA3 and FA4 to the Middle Siwalik. Muddy facies are more common in the Khutia Khola section than in other Lower Siwalik sections in Nepal. Most of FA1 and FA2 are composed of red paleosols. A fluvial channel deposit represented by sandstone beds up to 3m thick is dominant in FA2. Lateral accretion pattern is typical, but the top of each laterally-accreted packet is marked by a rooted horizon with a mud drape. Calcite nodules tend to be more abundant in the upper part of each single channel sandstone succession, with increments in nodule size. This type of channel fill is uncommon in FA1. These characteristics suggest that the most of the channels are of ephemeral stream origin. A thicker fluvial channel deposit (ca. 5 m) is less frequent, and is characterized by parallel stratification, antidune stratification, and trough cross-stratification, indicating the predominance of upper flow regime sedimentary structures in FA1 and FA2. These are of perennial stream origin. The FA2 interval contains more frequent flood-related deposits. A couplet of sandstone (SST: up to 0.1 m) and mudstone (MST: up to 10 mm) in an SST-MST alternation records inundation and desiccation events, respectively. Most of this SST-MST alternation is interpreted as being of seasonal lake origin. Frequency of thick sandstone beds of braided stream origin is less in the FA3 and FA4 intervals than in the Karnali River section, and most of these associations consist of ephemeral stream deposits and the SST-MST alternations described above.

The facies characteristics suggest that small ephemeral river deposits are predominant within the Khutia Khola section. The timing of the appearance of FA2 is crucial for determining the timing of increase in precipitation due to monsoon intensification and sediment supply increment associated with tectonic uplift. FA2 appears at 12.5 Ma in the Khutia Khola section, compared to 13.5 Ma in the adjacent Karnali River section.

Changes in geochemical indices including provenance, sorting effect, and intensity of weathering are well synchronized with the changes in depositional facies. Comparable provenance indices suggest the same source for the Karnali River and Khutia Khola sediments. Stratigraphic ratio plots show more intense weathering, uniform source, and greater sorting fractionation in the meandering river systems. Systematic upward changes in elemental ratios reflect change in fluvial style in the Lower to Middle Siwaliks, from meandering to braided river systems.

Collectively, the above features imply that the Khutia Khola section was located at the western margin of the paleo-Karnali River system. The appearance of FA2 in the Khutia Khola section is later than in the Karnali River, as noted above. Appearance of FA2 is associated with increased frequency of ephemeral river deposits. This implies increased discharge and enhanced erosion from the frontal part of the Himalaya around 12.5 Ma (mostly in the Lesser Himalaya) in the Khutia Khola, significantly after that in the larger Karnali river system.

Magmatic fluid invaded at penultimate stage of Himalayan orogeny During Miocene period

Aditya Kharya*, H. K. Sachan
Wadia Institute of Himalayan Geology, 33 GMS Road, Dehradun 248001, INDIA
**aditya@wihg.res.in*

An accretionary prism represents the history of last tectonic event between two tectonic plates of an orogenic belt. In the Himalayan orogeny, Ladakh Accretionary Prism (LAP) was developed in the fore arc basin of the Ladakh magmatic arc along the Indus Tsangpo Suture Zone

(ITSZ). Numerous quartz and calcite veins are omnipresent in low grade Miocene metamorphic rocks of ITSZ/LAP, which helps to understand the penultimate stage history of Himalayan orogeny through the eye of fluid inclusion and elemental geochemistry.

The quartz and calcite veins are comprised of monophase CH_4, CO_2 and bi phase H_2O-NaCl fluid inclusions. The monophase CO_2 and CH_4 inclusions were homogenized between -2.2 to -10.5°C and -159.4 to -82.6°C, respectively. The final melting temperature of primary biphase H_2O-NaCl inclusions are in range -8.9 to -0.4°C, which homogenized between 331 and 223°C. Whereas the secondary H_2O-NaCl inclusions were homogenized between 199 and 103°C with final melting temperature range -10.0 to -0.1°C. The presence of CH4 inclusions confirmed by the Raman spectroscopy with the Raman shift at ~2910 cm^{-1} in both quartz and calcite minerals. Some typical re-equilibration textures were also observed during the petrography including implosion, 'C' shape and starched (few in one direction and other in both directions), suggest the rapid tectonic activity and isothermal decompression. The formation temperatures of these veins were estimated/calculated based on microstructures and oxygen isotope thermometry between 152 to 528°C. The thermometric data define a P-T region for entrapment of primary fluids initially at 528°C: 4.7 kbar and subsequently up to 315°C and 1.7 kbar. The secondary aqueous fluids were trapped at 4.1 kbar at 450°C to 1.3 kbar and 180°C. The P-T path for the entrapment defines an initial isothermal segment, and at the last by isochoric stage. The average $\delta^{13}C$ and $\delta^{18}O$ value of calcite vein is -7.7±6.9‰ VPDB and 13.9±9.6‰ VSMOW, respectively, suggesting the mantle/magmatic derivation of fluid source. The calculated $\delta^{18}O$ value of fluid in quartz and calcite between -3.5 to +8.6‰ VSMOW, indicating it's magmatic or ophicarbonate fluid source. Hence, the stable isotopic study of quartz and calcite vein along with $\delta^{18}O$ value of fluid suggest the possibility of mantle/magmatic fluid mixing with ophicarbonate or oceanic-crust derived fluids, which entrapped about 15 km depth at 528°C.

Thus it can be concluded that the vein forming fluid in Ladakh accretionary prism were derived from the deeper domain of the Earth along the downgoing slab of Indian plate during the Miocene period. Our results also suggest a surge of tectonic activity during a rapid exhumation phase at the penultimate stage of the Himalayan orogeny that has caused the high volume of fluid flow.

Geochemical characteristics of gypsum deposits from Sahastradhara-Chamsari section of Lesser Himalaya

Sakshi Maurya*, Santosh K. Rai
Wadia Institute of Himalayan Geology, 33 GMS Road, Dehradun 248001, INDIA
**sakshimaurya26@gmail.com*

Earth as a dynamic system, is operated by different forces like weathering (chemical physical and biological), erosion, volcanism and solar insolation etc. Among these, chemical weathering plays an important role in regulating the geochemical cycling of different element in varying reservoirs. Himalaya consists of Precambrian rocks to as young as Quaternary in age. It is a young mountain chain evolved out of continental collision between the Indian plate and the Eurasian Plate. It is attributed with three principal lithotectonic zones, based on internal stratigraphy and bounding faults which were activated during the Cenozoic of collision of India with Asia (Gansser, 1964; Lefort, 1975). It is divided into Outer Himalaya, Lesser Himalaya, Higher Himalaya Tethys Himalaya and Trans Himalaya on the basis of history and evolution of this mountain chain (Biyani et al., 2006). In Lesser Himalaya, carbonate rich rocks contain certain pockets of gypsum which are formed by the process of leaching.

In this work, a set of 11 gypsum samples were collected from the Sahastradhara-Chamsari section of Lesser Himalaya and an attempt has been made to understand the nature of weathering and

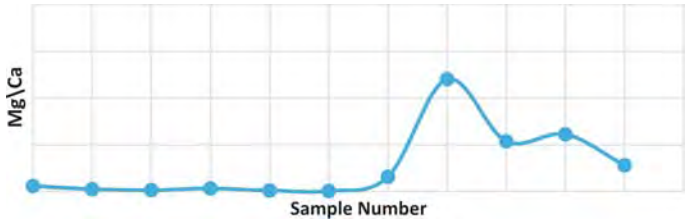

Fig 1. Variation of Mg/Ca in Gypsum, Carbonates and Shales.

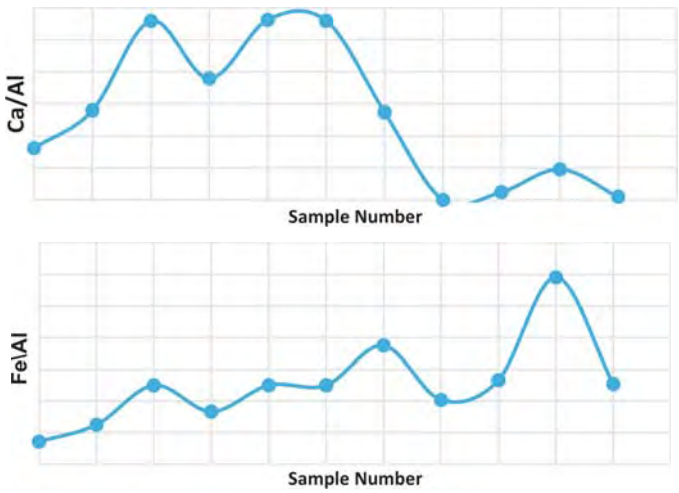

Fig. 2. Variation of Ca/Al and Fe/Al in Gypsum, Carbonates and Shales.

their relation with formation of gypsum. Towards this, geochemical proxies (major elements, trace element and isotopes) are used to trace these processes in space and time. Geochemical analysis were done for gypsum sample using modern analytical instrument like XRF and ICPMS. The accuracy and precision was also checked with the help of repeat analysis and running International Standard which were better than 5%. Results indicate that Mg/Ca ratios in gypsum are very low (0.06) which is highest (1.2) in shales. This shows that gypsum does not take Mg in its crystal. However, sulfur can get associated with the lattice of gypsum with fairly constant quantity (~23.4±1%; N=7) which are evident from figure1.

One of the important observations is that aluminium does not go well with gypsum under natural conditions which is evident from its lower concentration (~0.01-0.05%) and it is relatively more compatible in shales. These observations are consistent with Goldschmidt's rule of substitution of cations in a crystal lattice. Analytical results indicate that Ca-Mg is supported by sulphur in these gypsum samples. It was revealed that the possible mechanism for this gypsum mineralization could be the leaching of host rock including sulphide and black shale in the nearby study area. However, further analytical studies on sulphur isotope will be helpful to trace the origin of these gypsum deposits.

Biyani, A.K. 2006. Dimensions of Himalayan Geology, p. 4-5.
Gansser, A. 1964. Geology of the Himalayas London, Intersa. Publisher, 299.
Lefort, P. 1975. America Journal of Science, 275 A, 1-44

Morphotectonics of Manabhum anticline: A spectacular active Quaternary fold in the eastern Himalayan syntaxial zone

Chandreyee Goswami Chakrabarti[1], B.C. Poddar[2], Abhijit Chakraborty[3]
[1]Department of Geology, University of Calcutta, Kolkata, INDIA
[2]BE-367, Salt Lake City, Kolkata 700064, INDIA
[3]Department of Geology, Jogamaya Devi College, Kolkata 700026, INDIA

The Manabum area is situated in the south bank of the Brahmaputra, within the fore deep region of the Himalayas in the north, Mishmi Hills in the east and north east, partly in Belt of Naga Schuppen (thrust belt) to the south east, facing the Upper Assam foreland shelf in Arunachal Pradesh. It is characterised by the presence of a spectacular antiformal structure with a NNW-SSE direction of fold axis within the Quaternaries (Fig. 1).

The Manabum area lies in the eastern part of the Upper Assam basin, the junction of the east-west folding of Naga Hills and the northwest-southeast folding parallel to Mishmi hills. The area is flanked by the lesser Himalayan crystalline rocks present in Dapha Bum and Mishmi Hills in the eastern and north-eastern part, the Disangs and the Barails along the Patkoi Bum in the south western part and Namsang, Girujan and Siwalik/Dhekiajuli(Recent) formation in southern part (Mandal, 2013). The area is thickly covered by dense vegetation; one part is within the Namdapha Reserve Forest. The Noa Dihing River flows northerly from the Patkai Bum range in Vijaynagar and takes a sharp westerly bend from the Namdapha and flows towards west as Buri Dihing, but from Miao it again takes a northerly bend as Noa Dihing to meet the Brahmaputra. The Noa Dihing River is shifting easterly in its northerly flowing tract abandoning earlier river courses due to tilting of the surface towards east (Ramesh, 1988).

The rocks exposed in the Noa Dihing river section, small nallah sections and road cuttings are mainly grey to greenish grey colour medium to coarse grained arkosic sandstone with salt and pepper appearance with abundant coal fragments or fossilised woods associated with pebble and

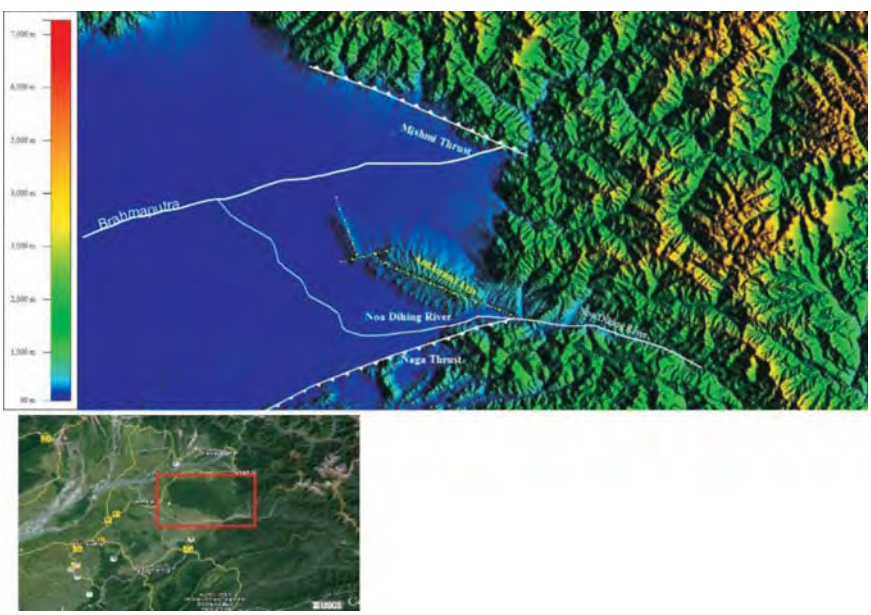

Fig. 1. The Quaternary Manabhum anticline and major structural trends within the Quaternaries. Inset: the location in the Google Earth.

boulder beds. These rocks are reported as Tipam sandstone in earlier literatures (Shrivastava and Sharma, 1986) but according to Mandal (2013) these may be of Girujan and Namsang formation. This older sandstones are folded into an antiform with the western limb dipping 40 to 450 towards west and the eastern limb dipping 30 to 350 towards east (Fig. 2). So the antiform is an asymmetric plunging antiform.

These older sandstones are overlain by deformed Quaternary Dhekiajuli sediments forming higher river terraces. The oldest Quaternary formation overlying the sandstones are boulders and pebbles embedded in silt and clay matrix. It is highly oxidised and colour is deep reddish brown. It is difficult to differentiate the upper Namsang/Girujan boulders from the oldest Quaternary boulders (Fig. 3). The matrix is reduced in the sediments overlying it forming thick pebble and boulder beds which are again overlain by sand and silt beds with almost no boulders and topped by clay beds. The Quaternary Dhekiajuli rocks are showing the similar folding but the dip of the beds is very gentle, 10 to 15°.

The higher river terraces are extensive in the northern bank of Noa Dihing River whereas the southern bank shows terraces with smaller extent. There are three major structural trends within this small area. The Noa Dihing river flows the trend parallel to the Naga thrust cross cutting the axis of the Manbhum anticline, the axis of the Manabhum anticline shows an offset perpendicular to it in its northern part which is nearly parallel to the HFT (Himalayan Frontal Thrust) but the major structural trend that is the trend of the fold axis of the Manabhum anticline and the present course of northerly flowing Noa-Dihing river is neither parallel to the Himalayan thrusts nor the Naga thrust but parallel to the NW-SE trending Mishmi thrust. The anticline is growing over an easterly dipping thrust fault (Barthakur et al. 2013). The western limb of the anticline shows a break in slope along an E-W line whereas the slope of the eastern limb is continuous (Fig. 4). This may be interpreted as a fault propagation fold over an easterly dipping thrust and the eastern limb is on the hanging wall side. This area is prospective for the hydrocarbon.

The tilting of the river terraces and changing course of the rivers suggest that the anticline is still growing. A detailed work on this anticline will definitely throw light on the genetics of the eastern Himalayan syntaxial zone.

Fig. 2. Eastern limb of the antiform along the Noa Dihing River section showing steep dip towards east.

Fig. 3. Quaternary Dhekiajuli boulder beds overlying Namsang boulder beds.

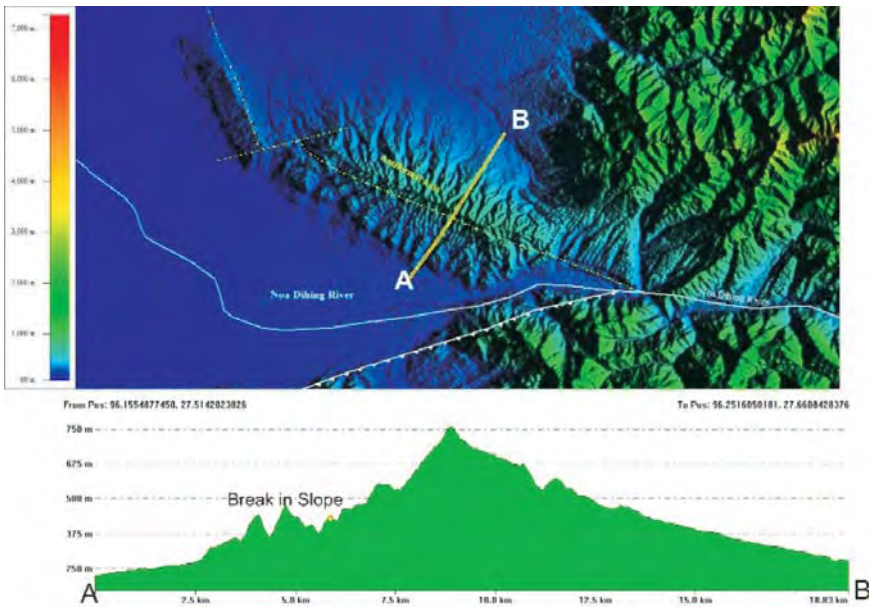

Fig. 4. The western limb of the Manabhum anticline shows a break in slope whereas the eastern limb is continuous.

Borthakur, A.N., Ahmed, J.P., Singh, S.P. 2013. 10th Biennial International Conference & Exposition, p370.
Mandal, K. 2013. South East Asian Journal of Sedimentary Basin Reasearch, 1 (1), 3-9.
Ramesh, N.R. 1988. Journal of Engineering Geology, XVII(3&4).
Shrivastava, R.N., Sharma, S.K. 1986. GSI Progress Report for the Field Season 1985-86. GSI portal.

Distribution and its sedimentary process of river terrace deposits Along the middle Kali Gandaki, central Nepal

Takahiro Yoshida[1,*], Yusuke Suganuma[1,2], Tetsuya Sakai[3]
[1]Dept. of Multiple Science SOKENDAI, Tokyo, 190-8518, JAPAN
**yoshida.takahiro@nipr.ac.jp*
[2]National Institute of Polar Research, Tokyo, 190-8518, JAPAN
[3]Shimane University, Shimane, 690-8504, JAPAN

"Kali Gandaki" is the river runs through the Himalayas from Tibetan plateau to Indian plain. A number of river terraces are distributed along the middle part of the Kali Gandaki. Recently, several studies have reported that catastrophic events such as glacial lake outburst flood (GLOF) and large-scale slope failure had strongly affected developments of river terraces in the Himalayas (Takada, 1992; Schwanghart et al., 2014). The river terraces along the Kali Gandaki have also thought to be composed of GLOF deposits (Upreti and Yoshida, 2014), although the detailed sedimentological feature of river terrace deposits to identify those deposits was not reported in this study. Because of the large population along the Kali Gandaki, it is very important to understand the geomorphological development of this region, including a possible scale of the GLOF event.

Sharma (1980) and Yamanaka (1982) originally classified the river terraces based on aerial photo interpretation. Although these pioneering studies have contributed greatly to our understanding of the geomorphological development of the terraces, the classification needed to be

examined by using modern highly-accurate altitude measurements, such as GPS. In addition, lithofacies of the river terrace deposits have not been described, which hampers understanding of the depositional processes of the terraces and its origin. Therefore, we carried out re-classification of the terraces by GPS and GIS, and sedimentological description of the terrace deposits along the middle Kali Gandaki (Beni-Kusma-Phalebas) to understand the geomorphological development, including their depositional process and its origin.

Here, we report five achievements as follows.

Based on detailed geomorphological analyses by using GIS software coupled with absolute altitude measurements (GPS), the river terraces along the middle Kali Gandaki are re-classified.

Lithofacies of the terrace deposits, which were originally described as a single gravel bed, are subdivided into six different types. They often include debris flow deposit, mudflow deposit, and delta deposit. The delta deposit indicates that the lake has developed at the south of the Kusma in the past.

At Kusma area, lower part of terrace deposits consist of a large-scale mudflow deposit. Unlike to the other deposits, the large-scale mudflow deposit contains 80% of Tethys-Himalayan gravels. Estimated source area of the mudflow is 50 km upper stream of Kali Gandaki, or Annapurna sanctuary area (40 km upper stream of Kusma along tributary). Because of the scale and composition of the mudflow deposits, the origin of the deposits is most likely a GLOF event.

The GLOF deposits are unconformity with overlaid later terrace deposits. It suggests the GLOF event was occurred prior to the terrace development.

At the confluence of rivers, lithofacies of the river terraces laterally change to be finer from the mainstream to tributaries. It indicates a rapid accumulation of the river terrace deposits along the mainstream of Kali Gandaki.

These achievements indicate that the river terraces that distributed along the middle part of the Kali Gandaki have been formed by the temporal development of the lake and following river incision. A cause of the development of the lake remains uncertain. The mudflow deposits at Kusma area suggest the GLOF event prior to the developments of the river terraces.

Schwanghart, W., Bernhardt, A., Stolle, A., Adhikari, B., Korup, O. 2014. Reassessing Catastrophic Infill of the Pokhara Valley, Nepal Himalaya, 16 (1982), 15787.
Sharma, T., Upreti, B.N., Vashi, N.M. 1980. Tectonophysics.
Takada, M. 1992. .Quaternary, 101(4), 283-297.
Upreti, B.N., Yoshida, M. 2014. Geology and natural hazards along the Kaligandaki Valley, Nepal, 2nd editon. Department of Geology, Tribhuvan University.
Yamanaka, H., Iwata, S. 1982. Journal of Nepal Geological Society, 2 , 95.

Petrographic and Sr-Nd isotopic geochemistry of the Lesser Himalayan Clastic Sediments: constrains on their provenance and model age

Manju Negi*, Santosh K. Rai, S.K. Ghosh
Wadia Institute of Himalayan Geology, 33 GMS Road, Dehradun 248001, INDIA
**manjunegi@wihg.res.in,*

The Indian Lesser Himalaya covering Garhwal-Kumaun regions is structurally separated by the Main Boundary Thrust (MBT) in the south and the Main Central Thrust (MCT) in the north with presence of Siwaliks and Higher Himalaya, respectively (Fig. 1). In between the MBT and the MCT, there lies intervening thrusts namely the Ramgarh, Almora, Tons and Munsiari with their corresponding surface manifestations. Based on the significant variations in lithological, stratigraphic and tectonic

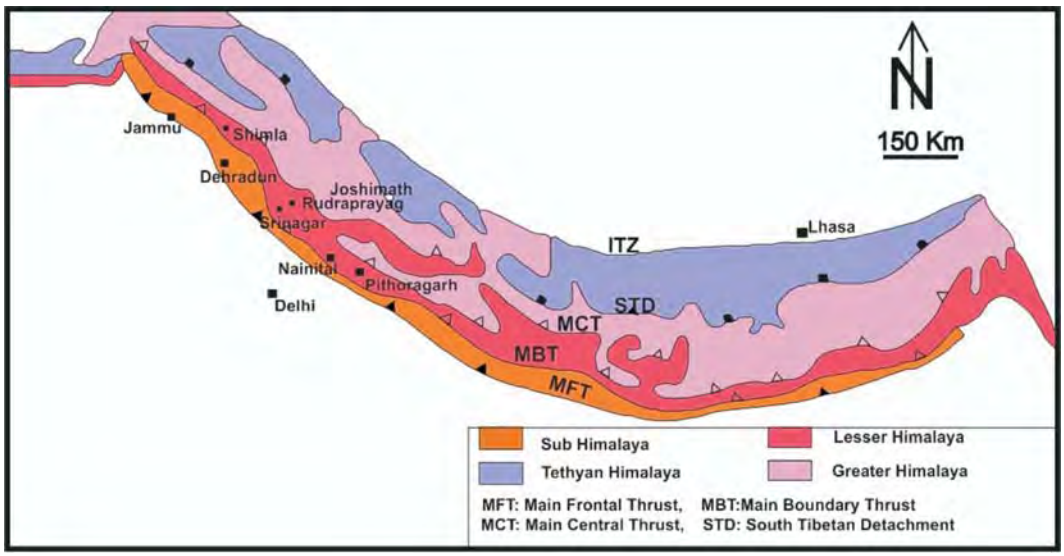

Fig. 1: Simplified geological map of Himalaya (modified after Valdiya, 1995).

settings between the northern and southern parts of the Lesser Himalaya, it can traditionally be divide it into two zones namely the Inner Lesser Himalaya (ILH) and the Outer Lesser Himalaya (OLH) (Valdiya 1980). These are separated by the North Almora Thrust/Tons Thrust).

Clastics form the major part of the sedimentary rocks in the Himalaya that had deposited in the Lesser Himalaya and exhibit varying chemical composition, protoliths, age (pre-Himalayan) and depositional settings. However, the information about the variability in their sources of sediments, chemical composition and nature of sedimentation remains unclear (Ahmad et al., 2000; Jain, 1972; Spencer et al. 2011). Petrography is a fundamental tool in understanding the textural and compositional properties of rocks. It is regarded as the most useful parameters for the reconstruction of the source lithology, digenetic and depositional attributes which are normally used as for the provenance identification. However, in many cases, such as metamorphism and intense weathering where the rocks lose their original texture, structures and the composition, the petrographic parameters do not work. Therefore, in these cases, geochemical and isotopic studies are helpful for the determination of the provenance, lithology of source area and depositional process which can be used in determining the age of rocks. These clastic sediments are unfossilliferous and thus most of the stratigraphic division are placed on the basis of the lithological and petrographic studies.

Further, the sediments of the Lesser Himalaya are characterized by the higher degree of digenesis and low grade metamorphism and therefore petrographic studies alone may not be sufficient for their provenance identification. Majority of the work regarding the lithology of the Lesser Himalaya shows that the variation in the southern and the northern Lesser Himalaya and hence it can be divided into two separate zones namely the Outer Lesser Himalaya (OLH) and the Inner Lesser Himalayan (ILH) sequence. However, the major problem regarding these two zones is about their relative age. Whether they are of the same age? If not then which one is the younger? In order to find out the age problems and the source region of the Lesser Himalaya sediments, the petrographic and isotopic studies are regarded as the helpful tool.

Present study shows that $^{87}Sr/^{86}Sr$ and $^{143}Nd/^{144}Nd$ values in clastic rocks ranges from 0.7414 to 1.4789 and 0.51150345± 0.000589 respectively. The corresponding ε_{Nd} values range from -6.6 to -37.6. This infers that these clastic sediments have diverse sources in terms of Vindhyans and Aravalies. Further attempts are being made to fix these end members by analysing representative rocks from the region.

Ahmad, T., Harris, N.B.W., Bickle, M.J., Chapman, H., Bunbury, J., Prince, C. 2000. Geol. Soc. Amer. Bull.,112, 467- 477.
Jain, A.K. 1972. Journal. Sed. Petrology. 42, 4, 941-960.
Spencer, et al. 2011. J. Asian Earth Sci. 41 (2011) 344-354.
Valdiya, K.S. 1980. Geology of Kumaun Lesser Himalaya. WIHG, Dehradun, 288p.
Valdiya, K.S. 1995. Precambrian Research 74, 35-55

Ionosphere modelling for earthquakes precursor study from GNSS data

Gopal Sharma[1], P.K. Champati Ray[1], S. Mohanty[2]
[1]Geosciences and Geohazard Department, Indian Institute of Remote Sensing, Dehradun 248001, INDIA
[2]Department of Applied Geology, Indian School of Mines, Dhanbad, INDIA

At low altitudes, electron content in the ionosphere shows substantial variation due to phenomena such as solar flares, magnetic storms and/or large magnitude earthquakes (Liu et al., 2006, Fatkulin et al., 1989). Most of the ionospheric studies have been carried out using ground based ionosonde and satellite radio beacon (Deshpande et al., 1976; Garg et al., 1977; Rastotgi et al., 1979) and considerable emphasis has also been given on GPS (Global Positioning System) based Total Electron Content (TEC) measurements (Calais and Minster, 1995). In present study, we compiled the different techniques adopted so far for examining pre-earthquake ionospheric anomalies by analysing the Total Electron Content (TEC) in the ionosphere. The various post processing techniques and its results are also discussed which could be of great important for adaptation of better methodology and processing techniques in future research. The study has been performed to understand a relationship between ionospheric electron content and earthquakes occurrences with special emphasize on Indian subcontinent and provides information on spatio-temporal variation of TEC from GNSS observation stations vis-à-vis prominent earthquakes of the region including 2015 Nepal earthquakes.

Calais, E., Minster, J.B. 1995. Geophys. Res. Lett., 22, 1045-1048.
Deshpande, M. R., Rastogi, R. G., Bhonsle, R. V., Sawant, H. S., Iyer, K. N., Dhar, B., Janve, A.V., Rai, R. K.,
Fatkullin, M.N., Zelenova, T.I., Legenka, A.D. 1989. Phys. Earth Planet. Inter., 57, 82-87.
Garg, S.C., Vijayakumar, P.N., Singh, L., Tyagi, T.R., Somayajulu, Y.V. 1977. J. Radio Space Phys., 6, 190-196.
Liu, J.Y., Chen, Y.I., Chuo, Y.J., Chen, C.S. 2006. Journal of Geophysical Research, 111, A05304
Rastogi, R.G., Sethia, G., Chandra, H., Deshpande, M.R., Davies, K., Murthy, B.S. 1979. J. Atmos. Solar Terr. Phys., 41, 561-564.

Influence of Himalayan Tectonics on uplift and exhumation of the Shillong Plateau and Mikir Massifs: New constraints from Apatite Fission Track Analysis

Akhil Kumar[1], Vikas Adlakha[2], Vinay[3], R.C. Patel[1,*]
[1]National Facility on low-temperature thermochronology, Department of Geophysics, Kurukshetra University, Kurukshetra, INDIA
**Patelramesh_chandra@rediffmail.com*
[2]Wadia Institute of Himalayan Geology, 33 GMS Road, Dehradun 248001, INDIA
[3]Geological Survey of India, Dehradun 248001, INDIA

A dramatic and unique feature of the eastern Himalaya system is the deformation of the Indian foreland basement beneath the Shillong Plateau. The Shillong Plateau occupies a region between the nearly orthogonal thrust belts of the south-vergent eastern Himalaya and the west-vergent Indo-Burman ranges, which accommodate convergence between India and Eurasia and

oblique convergence between India and the Burma micro-plate, respectively. The Plateau is bounded by two major thrusts i.e. Dauki Thrust in the south and Oldham Thrust in the north. The Shillong Plateau is separated from the Mikir Hills by NW-SE trending Kopili Fault. The Shillong Plateau and Mikir Massifs which were together have undergone deformation and uplift since continent-continent collision i.e. 55-60 Ma.

To test this interpretation, it is essential to constrain the timing and rate at which the plateau was uplifted and the amount of partitioning of the India-Asia convergence into the plateau. We used apatite fission track analyses to unravel the thermal histories of 16 basement samples collected along N-S transect across the central Shillong plateau and around Mikir Massifs. We find that the uplift and exhumation of the Shillong plateau and Mikir Massifs began together at the time of continental collision between Indian and Eurasian plates at about ~60 Ma. It appears that both Shillong Plateau and Mikir Massifs was single block before collision but during collision, the Mikir Massifs was detached from the Shillong Plateau along the Kopili tear Fault.

Architecture of Quaternary alluvial fills of Bhagirathi Valley, NW Himalaya

Yogesh Ray[1,*], Pradeep Srivastava[2]

[1]National Centre for Antarctic and Ocean Research, Headland Sada, Vasco da Gama, Goa, INDIA

**yogeshray@gmail.com*

[2]Wadia Institute of Himalayan Geology, 33 GMS Road, Dehradun 248001, INDIA

Quaternary sedimentation in the upper reaches of Ganga river system is influenced by tectonic and climatic conditions prevailing in the Himalayan thrust and fold belt. These physical forces are governing factors for the development of landforms, such as alluvial fans, fluvial and glacio-fluvial terraces, landslide dammed lakes etc. Majority of the terraces are cut and fill type formed due to aggradation of river valley.

The stratigraphy of fill terraces studied using the best available sections exposed along the bluffs of different terraces. These deposits are formed by the channel migration and deposition by accreting gravel bars, having considerable amount of sand lenses and sand bodies. The overall sedimentary architecture of the fill is found dominantly comprised of channel bound deposits grouped as Lithofacies Association-A (LF-A). The channel bound depositional sequence may often be interrupted by the deposition of debris flows generated locally as well as distally and grouped under Lithofacies Association-B (LF-B). They suggest valley filling via channel bar aggradation and sediments supplied from landslides and debris flows.

Optically Stimulated Luminescence (OSL) dating of quartz from the sandy bodies of these deposits shows that these phases are concentrated at around 49-25 ka and 18-11 ka, followed by incision. These were phases when sediment supply significantly increased, probably due to the two phases of deglaciation in the catchment area during the last ~63 ka. Several of these terraces represent a continuous valley fill it is suggested that in the Quaternary some zones of Himalaya (which is an active orogen) might be tectonically quiescent for several thousand years.

The seismicity pattern study using scale invariant property of recent 25th April 2015 Nepal Earthquake (7.8 Mw) sequence

Sonali Sahana*, P.N.S. Roy
Department of Applied Geophysics, ISM Dhanbad, Dhanbad 826004, INDIA
**sonalisahana401@gmail.com*

Recent 25th April 2015 Nepal earthquake (7.8 Mw) killed more than 9,000 people and injured more than 23,000. The epicenter was east of the district of Lamjung and its hypocenter was at a depth of approximately 8.2 km. It was the worst natural disaster to strike Nepal since 1934 Nepal-Bihar earthquake. Geophysicists and other experts had warned for decades that Nepal was vulnerable to a deadly earthquake, particularly because of its seismotectonics, urbanization, and architecture. Continued aftershocks occurred throughout Nepal within 15-20 minute intervals, with one shock reaching a magnitude of 6.7 on 26th April.

In this context b-value of earthquakes is very useful to forecast the occurrence of aftershocks in a given region. The b-value characterizes the release of energy due to stress accumulation in the rocks through an earthquake and is a direct indicator for the prediction of aftershocks in the region. Fractal analysis is also used in this study to determine the spatio-temporal pattern by calculating the fractal correlation dimension of the same earthquake sequence. This method guarantees high accuracy results through a limited dataset. Repeated earthquakes were analyzed between 1973 and 2015 in Nepal, and the b-value was found for these earthquakes.

The b-value analysis and determination is also done using ZMAP software (Fig 2). The b-value of recent 25th April 2015 Nepal earthquake (7.8 Mw) was 0.63. The b-value is related to the stability of the crust and when it is perturbed from its state of equilibrium it tends to go back to its original state by oscillating back and forth in terms of its b-value. These oscillations are manifested as earthquakes. The low b-values and low seismicity at depth range of 20-30 km may be associated with low degree of heterogeneity and high rheological strength in the crust. It is found that the observed b-values are controlled by the variations in the proportion between weak and strong earthquakes. The observed changes in the b-value with increasing depth could probably be due to the increase in the strength of crustal material caused by the growth in temperature and confining pressure. The correlation is established between the crustal areas with low b-values as well as fractal correlation dimension and the locations of the strongest earthquakes in the region. It is suggested that the three-dimensional mapping

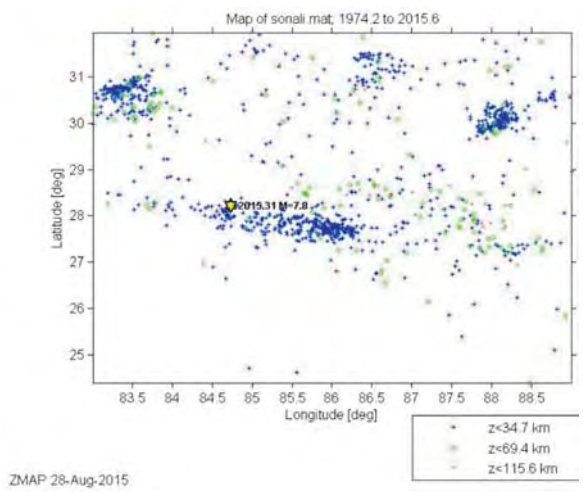

Fig 1: Seismicity map.

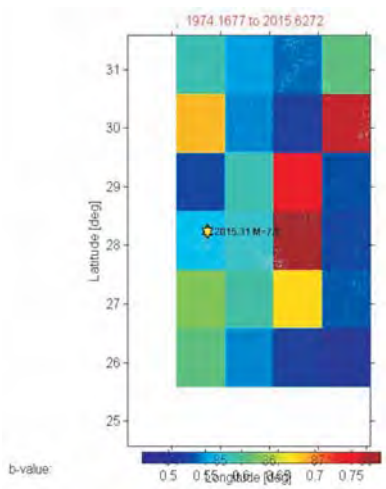

Fig. 2. Spatial variation of b value.

of the b-value can be helpful for estimating the location, depth, and maximal magnitude of the probable strong earthquakes in seismically active regions and can be used to assess seismic risks.

Oceanic and continental lithospheric subduction in the Trans-Himalaya and NW-Himalaya

A.K. Jain
CSIR-Central Building Research Institute, Roorkee 247667, INDIA
Himalfes@gmail.com

Since the postulate of the Himalayan orogen as a product of continent-continent collision between the Atlantic-type margins of the Indian and Asian Plates (Dewey and Bird 1970), many authors have opined that the Himalaya evolved through other alternative models (Powell and Conaghan 1973, 1975; Matte et al., 1997; Patriat and Achache, 1984; Hodges, 2000; Yin, 2006). Prior to advent of the Plate Tectonics, Argand (1924) explicitly demonstrated the configuration of the India-Asia "collision" zone as large-scale underthrusting of India below Asia till beneath Kun-Lun, and its "collision" with the Asian continent beneath this mountain, and "not" in the Himalaya. Further, he documented ductile deformation of the Indian continental crust and thrusting of Asia over India in the diagram along with doubling of continental crust beneath Himalaya and its rise to the south.

As vast Neo-Tethyan Ocean, separating the northern parts of Indian continental lithosphere from the southern Asian Plate (Patriat and Achache, 1984; Stampfli and Borel, 2002), closed along the Shyok and Indus-Tsangpo Suture Zones (SSZ and ITSZ) during late Mesozoic, continental lithospheres of these plates did not initially collide with each other. Instead, the Tethyan oceanic lithosphere subducted and partially melted to produce an intra-oceanic calc-alkaline Shyok-Dras Volcanic Arc, followed by its subsequent subduction and melting beneath the Asian Plate to produce Karakoram Batholith. Younger calc-alkaline Trans-Himalayan plutons such as the Ladakh Batholith, intruded this volcanic arc along with final closure of the Neo-Tethys along the ITSZ (Honegger et al., 1982; Searle et al., 1987; Jain and Singh, 2009).

The estimated timing of the Neo-Tethys closure, thereby impingement/'collision' between India and Asia, ranges between 65 and 35 Ma from geological and geophysical evidences (Garzanti, 2008; Bouilhol et al., 2013). However, comparison of bulk ages of the Ladakh Batholith with subducted ultra-high pressure (UHP) metamorphosed Indian continental lithosphere in Tso Morari

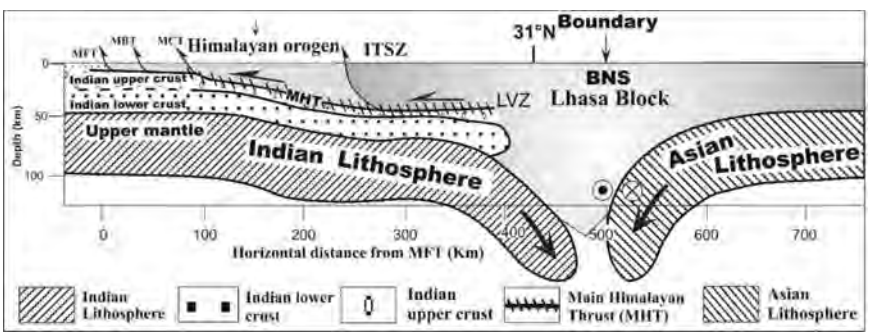

Fig. 1. Large-scale tectonics of the Himalayan orogen as a scrapped crustal wedge above the MHT. Simplified geophysical cross-section of the India-Asia convergence beneath the Himalaya and Tibet from Hi-CLIMB profile, depicting "collision" between two plates in the BNS. Redrawn after Tilmann et al. (2003), Nábělek et al. (2009) and Liang et al. (2012).

(Mukherjee and Sachan, 2001) indicate that the Indian continental lithosphere first impinged the Trans-Himalayan magmatic arc at ~58 Ma (Leech et al., 2005). The Himalaya first emerged from this deeply exhumed terrane between 53 and 50 Ma. Repeated sequential subduction and imbrication of the Indian continental lithosphere followed at ~48-35 and ~25-15 Ma to produce Eo- and Neo-Himalayan metamorphism and associated exhumation episodes during rise of the Himalayan Mountains from north to the south.

Geological and geophysical evidences from the Himalaya and nearby mountains bespeak about steep subduction and imbrication of the Indian continental lithosphere since ~58 Ma (Guillot et al., 2008). Present-day subhorizontal subduction of the Indian Plate (Gokarn et al., 2002; Arora et al., 2007; Miglani et al., 2014) and its episodic northward push along the Main Himalayan Thrust (MHT) (Zhao et al. 1993) has rotated these imbricates so that these follow the geometry of the Indian continental lithosphere. Overriding scrapped sequences thrust southwards and deform into the Himalayan crustal wedge. It is only in the Bangong-Nujiang Suture (BNS) in Central Tibet that true "collisional" signatures of large-scale opposing vergence of the India-Asia Plates are witnessed (Matte et al., 1997; Kind et al., 2002; Nábělek et al., 2009; Tilmann et al., 2003; Liang et al., 2012).

Argand, E. 1924. Proc. 13th International Geological Congress, 7, 170-372.
Arora, B.R., Unsworth, M.J., Rawat, G. 2007. Geophys. Research Letters, 34, L04307, doi:10.1029/2006 L029165.
Bouilho, L.P., Jagoutz, O., Hanchar, J.M., Dudas, F.O. 2013. Earth & Planetary Science Letters, 366, 163-175.
Dewey, J.F., Bird, J.M. 1970. Journal of Geophysical Research, 75, 26252647.
Garzanti, E. 2008, Aitchison J.C., Ali J. & Davis A.M. Journal of Geophysical Research, 113, Bo4411, doi: 10.1029/2007JB005276, 2008.
Gokarn, S.G., Gupta, G., Rao, C.K., Selvaraj C.B. 2002. Geophysical Research Letters, 29 (8), 1251, 10.1029/2001GL014325.
Guillot, S., Mahéo, G., De Sigoyer, J., Hattori, K.H., Pecher, A. 2008. Tectonophysics, 451, 225-241.
Hodges, K.V. 2000. Geological Society of America Bulletin, 112, 324-350.
Honegger, K., Dietrich, V., Frank, W., Gansser, A., Thoni, M., Trommsdorff, V. 1982. Earth & Planetary Science Letters, 60, 253-292.
Jain, A.K., Singh, S. 2009. Geological Society of India Bangalore, India, 1-179.
Kind, R., Yuan, X., Saul, J., Nelson, D., Sobolev, S.V., Mechie, J., Zhao, W., Kosarev, G., Ni J., Achauer, U., Jiang, M. 2002. Science, 298, 1219-1221.
Leech, M.L., Singh, S., Jain, A.K., Klemperer, S.L., Manickavasagam, R.M. 2005. Earth & Planetary Science Letters, 234, 83-97.
Liang, X., Sandvola, E., Chen, Y.J., Hearn, T., Ni, J., Klemperer, S., Shen, Y., Tilmann, F. 2012. Earth & Planetary Science Letters, 333-334, 101-111.
Matte, Ph., Mattauer, M., Olivet, J.M., Griot D.A. 1997. Terra Nova, 9, 264-270.
Miglani, R., Shahrukh, M., Israil, M., Gupta, P.K., Varsheney, S.K., Sokolova, Elena. 2014. Journal of Earth System Science, 123 (8), 907-918.
Mukherjee, B.K., Sachan, H.K. 2001. Current Science, 81, 1358-1361.
Nabelek, J., Hetenyi, G., Vergne, J., Sapkota, S., Kafle, B., Jiang, M., Su, H., Chen, J., Huang, B-S., The Hi-CLIMB Team 2009. Science, 325, 1371-1374.
Nelson, K.D., Zhao, W., Brown, L.D. INDEPTH Team. 1996. Science, 274, 1684-1688.
Patriat, P., Achache, J. 1984. Nature, 311, 615-621, doi:10.1038/311615a0.
Powell, C. McA., Conaghan, P.J. 1973. Earth Planet. Sci. Lett., 20(1), 1-12.
Powell, C. McA., Conaghan, P.J. 1975. Geology, 3(12), 728-731.
Searle, M.P., Windley, B.F., Coward, M.P., Cooper, D.J.W., Rex, A.J., Rex, D., Tingdong, L., Xuchang, X., Jan, M.Q., Thakur, V.C., Kumar, S. 1987. Geological Society of America Bulletin, 98, 678-701.
Stampfli, G.M., Borel, G.D. 2002. Earth & Planetary Science Letters, 196(1), 17-33,.
Tilmann, F., Ni, J., Science, 300, 1424-1427.
Yin, A. 2006. Earth Science Reviews, 76, 1-31.
Zhao, W., Nelson, K.D., Che, J., Quo, J., Lu, D., Wu, C., Liu, X. 1993. Nature, 366, 557-559.

25 April 2015 (M 7.8) Nepal earthquake: Role of transverse faults in constraining rupture lengths in Himalaya

N. Purnachandra Rao*, Ch. Nagabhushan Rao, M. Ravi Kumar, D. Srinagesh
CSIR-National Geophysical Research Institute, Uppal Road, Hyderabad 500007, INDIA
**pcrao.ngri@gmail.com*

Transverse faults have been commonly observed across Himalaya and are known to occur on deep seated, vertical sub-crustal faults unlike their thrust counterparts occurring on shallow-focus low-dip-angle faults. It is also known that they are responsible for partitioning the Indian plate convergence into various segments in the Himalayan belt. But recent seismological and geodetic data in the Himalayan region is pointing to newer possibilities. Based on analysis of the recent 25 April 2015 Nepal earthquake of M 7.8, we propose that the trans-Himalayan faults play a key role in confining the rupture length, and hence the magnitude of the earthquakes. Additionally, they also accommodate a large part of the convergent strain budget in Himalaya through transverse plate tectonics, similar to the eastward extrusion in Tibet further north, thereby greatly reducing the seismic hazard levels in Himalaya.

Deformation analysis of Nepal earthquake

Somalin Nath, Rohit Kumar, R.S. Chatterjee, P.K. Champati Ray
Geosciences and Disaster Management Studies, IIRS-ISRO, Dehradun 248001, INDIA

Nepal Himalaya is one of the hot spots of seismicity as it has been experienced many medium to large earthquakes in the past. The 7.8 Mw Nepal earthquake of April 25, 2015 is major event associated with the Main Central Thrust (MCT) at a depth of 15 km that had occurred on a relatively quiet block within tectonic framework of Nepal Himalaya. Understanding the nature of the MCT is important as it is a gliding plane for most thrust sheet. The earthquake also triggered a major avalanche on the southern slopes of Mt. Everest, located approximately 160 km east-northeast of the epicenter. The avalanche destroyed the base camp of climbers. Khumbu region considered as one of the top tourist destination in Nepal was affected severely due to this crustal movement.

The study area includes a part of Khumbu glacier where the Base Camps are located on the Nepal side of Mt Everest and other glacier valleys such as Ngajumba, Lunag, Panbuk and Mehlung glaciers, the Dudh Kosi and Tamakosi river valleys, Sagarmatha National Park and Gaurishankar Conservation area. Geologically the epicenter lies in the Lesser Himalayan region between the MBT and the MCT, more close to the MCT. This event was attributed to thrust faulting initiated at shallow depth defining a relation with décollement associated with the HFT and the subduction interface between India and Eurasian plate. Study reveals direction of the tectonic movement of Mt. Everest at a rate of 4.5 cm/yr with an azimuth of approximately 25° (Poretti et al., 2010). The study area consists of high-grade rocks, e.g. kyanite-sillimanite gneiss, schist and quartzite and is mostly characterized by ductile deformation defined along the MCT.

In the present study, L-band ALOS-2 PALSAR data (both pre- and post-event scene w.r.t. the main shock) was used for DInSAR based analysis of the western side of Mt Everest including a number of glacial, fluvio-glacial and river valleys. 1 arc second (30 m) SRTM DEM was used for topographic phase compensation in DInSAR processing. The data pair has a normal spatial baseline of 55.9 m which amounts to 826 m altitude ambiguity. Therefore, the topographic phase error appears to be bare minimum. In the differential interferogram, we observed three distinct fringe patterns: (i) deformation fringes aligned along the axis of Ngajumba glacier valley, (ii) deformation fringes aligned along the

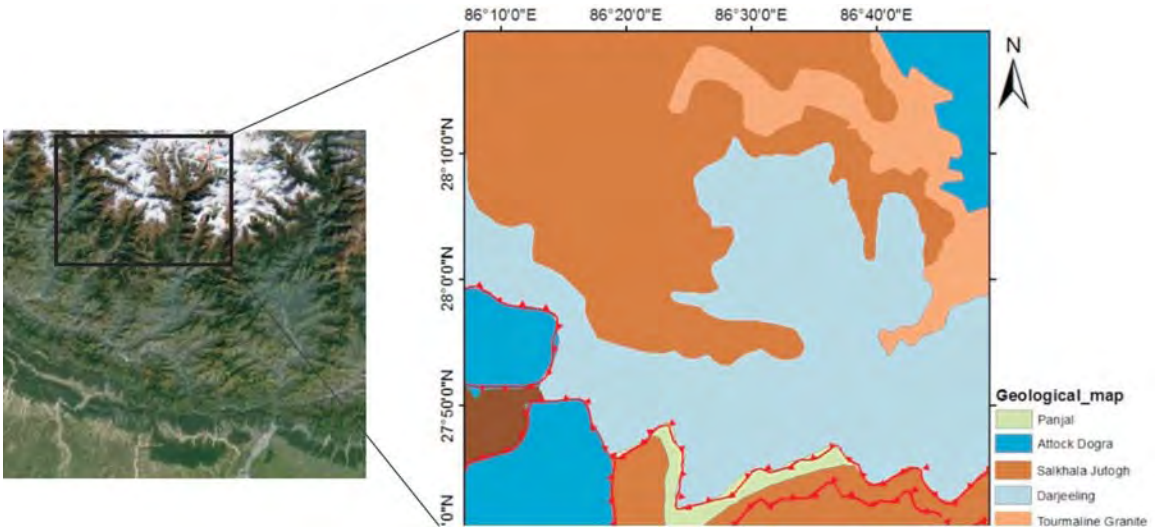

Fig. 1. Location of study area with geological map showing different formations (Map Source: Gansser, 1964).

river valleys of Tamakosi River, and (iii) high deformation areas other than glacier and river valleys are areas around Gaurishankar peak to the east of Lambagar. The differential fringe patterns suggest three types of deformation such as (a) snow cover deformation and glacier movement during the observation period, (b) soft sediment movement along the river valley, and (c) enhanced crustal deformation in and around the structurally weak planes. The differential interferogram was carefully filtered initially by InSAR coherence guided Goldstein approach to retain deformation fringes as far as possible followed by Boxcar algorithm. We unwraped the differential interferogram by MCF algorithm and produced LOS displacement map. It was observed that a maximum relative displacement of upto 82 cm in the study area. The maximum deformation was found along Tamakosi and Rolwaling valleys and along the structurally weak planes to the west of Gaurishankar peak.

Poretti, G. Calligaris, C., Tariq, S., Khan, H. 2010. Journal of Nepal Geological Society, Volume 41.

Changes in glacier facies and behavior of clean and debris covered Glaciers in Upper Indus Basin, Western Himalayas

Aparna Shukla[1], Iram Ali[2,*], Shakil Ahmad Romshoo[2]
[1]Wadia Institute of Himalayan Geology, 33 GMS Road, Dehradun 24800, INDIA
[2]Dept of Earth Sciences, University of Kashmir, Srinagar 190006, INDIA
**geoiram@gmail.com*

Over the years, the problem of understanding the response of Himalayan glaciers to climate change has received much attention (Bolch et al., 2012). Besides, the debris covered glaciers respond differently to a given set of climatic conditions than clean glaciers (Jansson and Fredin, 2002). Thus, the continuous assessment and monitoring of both debris covered glaciers and clean glaciers is crucial to understand the variability of their observed fluctuations for the management of water resources and future projections (Scherler et al., 2011). With the wide variety of satellite data becoming available, monitoring changes in the glacier facies in response to the climatic controls has gained much attention, particularly with respect to debris covered glaciers (Racoviteanu et al., 2015). The current research is an attempt to investigate the changes in the glacier facies, length and inter-conversion of clean glaciers to debris cover glaciers over a period of 12 years from 2003 to 2014 in

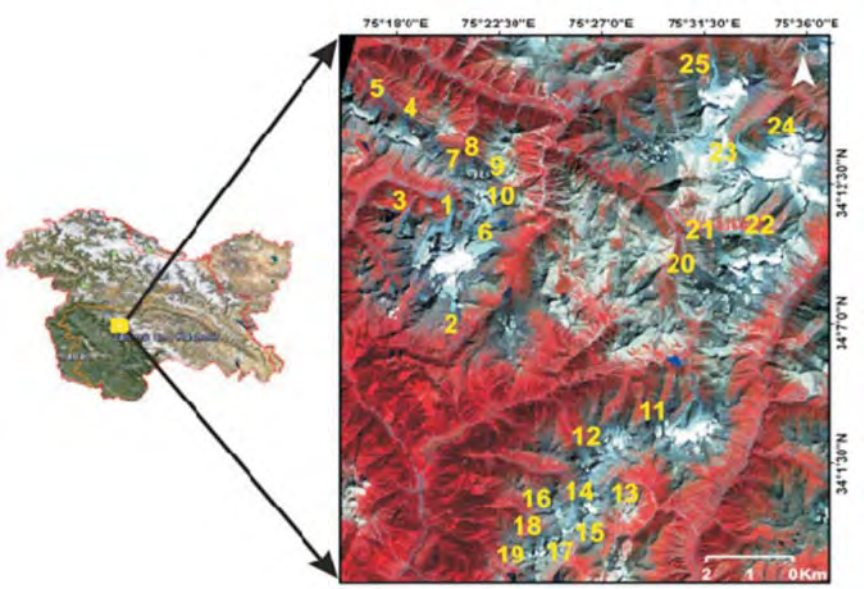

Fig. 1. Location map of the study area with the spatial distribution of 25 glaciers. The background image is an ASTER (20th September 2003) false colour composite (321).

Upper Indus Basin, Western Himalayas. The study includes 25 glaciers which are distributed in the Lidder Valley and Sindh regions between 34°18' to 33°56'N latitude and 75°15' to 75°36'E longitudes. Figure 1 denotes the geographical location of the glaciers along with their glacier Ids.

Primarily, the glacier facies were mapped by adopting hierarchical knowledge-based classification approach (Shukla and Ali, 2016) on two datasets viz. ASTER 2003 and Landsat8 OLI 2014 alongwith the input of slope from ASTER DEM. The methodology involves the mapping of glacier cover classes particularly snow-ice, ice mixed debris and supraglacial debris by using various ratios and indices viz NIR/SWIR, Normalized Difference Glacier Index (NDGI), Normalized Difference Debris Index (NDDI) and thermal glacier mask and non-glacier cover classes such as vegetation, water, periglacial debris and shadow by Normalized Difference Vegetation Index (NDVI), Normalized Difference Water Index (NDWI) and slope.

The glaciers with debris extent of <25% are considered as clean glaciers and the glaciers with debris covered area of above 50% are recognized here as debris covered glaciers (Banerjee and Shankar, 2013). Based on this criterion, 3 glaciers (with glacier Ids 3, 18, 20) were found to be debris covered and rest as clean glaciers on 2003 dataset. The total glacierised area from the same dataset yielded 53 km^2 of which 48.5 km^2 (91.4%) pertains to clean glaciers and 4.6 km^2 (8.6%) to debris covered glaciers. For a period of 12 years, the glacierised area in the basin reduced by 5.96 km^2 (11.23%) with maximum reduction of 4.76 km^2 (8.97%) in clean glaciers and 0.33 km^2 (0.63%) in debris covered glaciers. Considering the debris cover change on a glacier by glacier basis, there has been variable increase in the debris cover both on clean glaciers as well as debris covered glaciers. A closer examination of the clean glaciers revealed that the percentage increase of debris cover on certain glaciers ranged between 25-50% which can be thus categorized as partially debris covered glaciers in the study (Table 1). The increase in the debris cover on the glaciers depends on several factors controlling the generation and transport of supraglacial debris (Krikbride and Deline, 2013). The other reasons for increase in debris cover may be due to inter-conversion of debris cover classes such as ice mixed debris (IMD) to supraglacial debris (SGD) at IMD/SGD boundary which transports and exposes basal and intraglacial debris to the surface, rise in equilibrium line altitude (ELA) and low ice-flow velocity.

Table 1. *Glacier area count and area of clean glaciers, partially debris covered glaciers and debris covered glaciers as obtained from two datasets 2003 and 2014.*

Glacier Type	2003		2014	
	No. of glaciers	% Area	No. of glaciers	% Area
Clean glaciers	22	91.4	7	59.7
Debris covered glaciers	3	8.6	14	10.1
Partially debris covered glaciers	-	-	4	30.2

Table 2. *Comparative analysis of the facies variability over clean glaciers and debris covered glaciers over a period of 12 years (2003-2014). Here SI= snow-ice, SGD= supraglacial debris, IMD=ice-mixed debris, PGD= periglacial debris, VR= valley rock and Veg= vegetation.*

Year	Glacier cover classes (Area km^2)				Non-glacier cover classes (Area km^2)				
	Clean Glaciers		Debris covered Glaciers						
	SI/IMD	SGD	SI/IMD	SGD	PGD	Water	VR	Shadow	Veg
2003	41.51	7.001	1.96	2.62	128.83	48.59	359.08	2.07	597.22
2014	31.89	10.47	1.0	3.76	149.7	47.6	381.89	2.36	560.21

Analysing the change in the length of clean glaciers and debris covered glaciers, both the glacier types are retreating, though at variable rates. The highest frontal retreat rates were observed in clean glaciers which ranged between 18-93 m from 2003-2014. However, contrary to it, debris covered glaciers showed a retarded retreat rate ranging between 11-60 m during the same span of time. The reason for reduced rate of retreat by debris covered glaciers than clean glaciers may pertain to decreased albedo and increased insulating effect caused by the debris layer which thus prevents the direct contact of heat radiations to the snow surface resulting in reduced ablation.

In addition to the change in the glacier area and the rate of retreat, an attempt was made to understand and estimate the variation in glacier cover classes (snow-ice, IMD, SGD) and non-glacier cover classes (vegetation, water, valley rock, periglacial debris (PGD), shadow). An increase of 3.47 km^2 (49.57%) in the area under SGD was observed in clean glaciers and increment of 1.14 km^2 was evaluated in case of debris covered glaciers from 2003 to 2014 (Table 2). Increase in PGD is linked with conversion of SGD to PGD at the PGD/SGD boundary and hence related with glacier retreat, because when glacier ice at the snout melts, it dumps the SGD which then converts to PGD and cease to be a part of the glacier. Expansion in PGD cover is also greatly affected by increased denudational activity along the valley slope probably due to increase in evacuated slopes free from snow or vegetation cover. Further, decrease in vegetation and increase in valley rock areas are again linked because due to the rise in temperature the tree line has shifted up, exposing bare valley rock.

Banerjee, A., Shankar, R. 2013. Annals of Glaciology, Vol. 59, No. 215, 2013. doi:10.3189/2013JoG12J130.
Bolch, T., Kulkarni, A., Kääb, A., Huggel, C., Paul, F., Cogley, J.G., Frey, H., Kargel, J. S., Fujita, K., Scheel, M., Bajracharya, S., Stoffel, M. 2012., Science, 336, 310-314, doi:10.1126/science.1215828.
Jansson, P., Fredin, O. 2002 Quaternary International, 95-96, 35-42.
Kirkbride, M.P., Deline, P. 2013. Landforms, 38, 1779-1792.
Scherler, D., Bookhagen, B., Strecker, M.R. 2011. Letters Nature Geosci., 4, 156-159 (doi: 10.1038/ngeo1068).
Shukla, A., Ali, I. 2016. Annals of Glaciology 57(71) doi: 10.3189/2016AoG71A046.

3-D monitoring of glaciers in the parts of Chandra Basin, Himachal Pradesh, India

Purushottam Kumar Garg[1,*], Reet Kamal Tiwari[1], Aparna Shukla[2], D.P. Dobhal[1]

[1]*Centre for Glaciology, Wadia Institute of Himalayan Geology, 33 GMS Road, Dehradun 248001, INDIA*

**garg.glacio@gmail.com*

[2]*Wadia Institute of Himalayan Geology, 33 GMS Road, Dehradun 248001, INDIA*

Mountain glaciers are sensitive indicators of climate change and important component of global hydrological cycle (Scherler et al., 2011). Therefore, systematic and accurate assessment of their temporal changes is important for assessment of their response to climate change. Moreover, it has been reported, for many mountain chains of the world including the Alps and the Himalaya, that the heterogeneity in glacier response exists (Kulkarni et al., 2006; Paul and Haeberli, 2008; Fujita and Nuimura, 2011; Scherler et al., 2011). The glacier response includes changes in the glacier parameters like length, area, surface elevation, flow velocity and extent of debris cover. Due to inaccessible terrain and harsh weather conditions in mountainous regions, field based glacier monitoring is quite a challenge (Bhambri et al. 2011). In this regard, remote sensing acts as an effective technology for monitoring vital glacier parameters (Racoviteanu et al., 2008). Thus, in this study, an attempt has been made, using remote sensing techniques, to assess the impact of forcing factors on 3-dimensional glacier response by monitoring important glacier parameters (area, length, glacier thinning and surface ice velocity). For this, satellite images of ablation period (September-November) of Landsat TM/ETM/OLI (1991-2014) and ASTER (2003-2014) were used as a main data source. Landsat images were mainly used for mapping of length and area changes while ASTER data were used for estimating thickness change and velocity estimation.

The study was carried out on three proximal glaciers in Chandra basin of Lahul-Spiti district of Himachal Pradesh namely Bara Shigri (142.898 km^2), Chhota Shigri (14.7 km^2) and Sakchum glacier (14.1 km^2), all of which have, however, nearly similar orientations but varied extents of debris cover and different geometry. Study area is bound by latitude 32°04'30" N to 32°18'03" N and longitude 77°23'30" E to 77°49'30" E. Altitudinal range varies from 6632 to 3440 m.a.s.l. (Fig. 1).

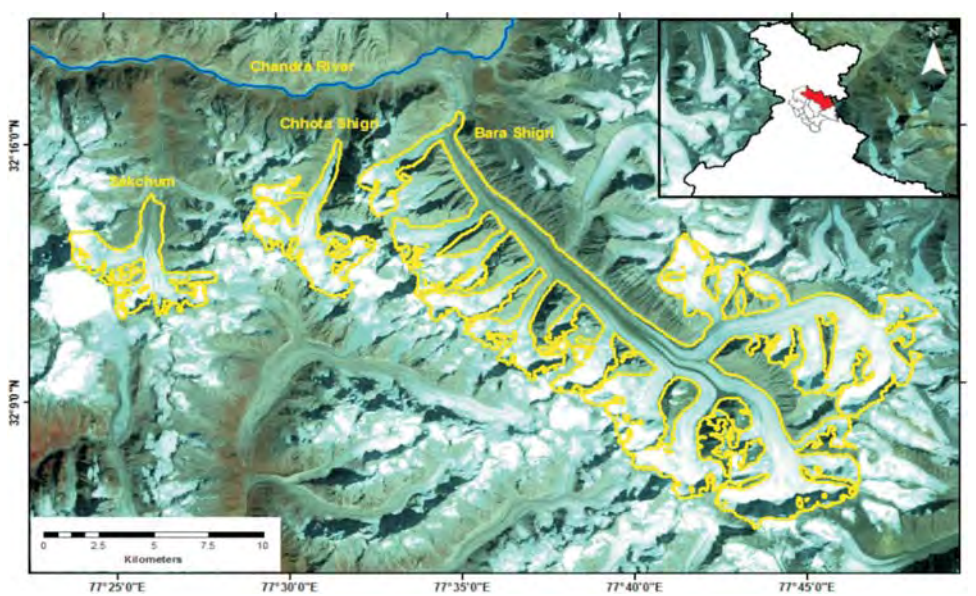

Fig. 1. Study area: Randolph Glacier Inventory (RGI) glacier boundaries overlaid on Landsat-7 ETM of October 15, 2000.

The remote sensing data sets were, firstly, subjected to geometric and radiometric corrections. Several combinations of Landsat bands (e.g. 321, 432, 543 etc.) along with band ratios (e.g. Red/SWIR for dark shadow zones) facilitated the length, area and debris-extent extractions. Digital Elevation Models (DEM), generated from ASTER stereo-pairs for the year 2003 and 2014, were used for estimation of glacier surface elevation change. Glacier surface ice velocity was calculated, on ASTER data (2003-2014), using Image correlation (COSI-Corr) (Leprince et al., 2008) technique.

An inter-comparative study of derived glacier parameters reveals the overall trend of glacier depletion during the last 23 years but the rate of change is found heterogeneous for all three studied glaciers. We interpret, as the recession has taken place, extent of supraglacial debris-cover also increased. Thus, shrinkage of glaciers seems to be intricately linked with debris-cover extents. The glacier surface thinning was calculated for year 2003-2014. It was observed that debris-cover plays a major role in controlling the surface lowering of the glaciers as the major loss of glacial ice has been observed in ablation zones of the studied glaciers. Variation in surface ice velocity was observed for different glacier zone in different years for all the three glaciers. Observed changes in surface velocity appear to be a function of variation in snow/ice overburden, differences in bed slopes and to extents of debris cover. Therefore, the results suggest that debris-cover extents, topography and size of glaciers have considerable control over the changes in three dimensional glacier parameters.

Bhambri, R., Bolch, T., Chaujar, R. K. 2011. Inter. Jour. Remote Sensing, 32(23), 8095-8119.
Fujita, K., Nuimura, T. 2011. Proc. of the National Academy of Sciences, 108(34), 14011-14014.
Kulkarni, A.V. 2006. Inter. Soc. Optics and Photonics, 2006.
Leprince, S., Berthier, E., Ayoub, F., Delacourt, C., Avouac, J. P. 2008. Eos, 89(1), 1-2.
Paul, F., Haeberli, W. 2008. Geophysical Research Letters, 35(21).
Racoviteanu, A.E., Williams, M.W., Barry, R.G. 2008. Sensors, 8(5), 3355-3383.
Scherler, D., Bookhagen, B., Strecker, M.R. 2011. Nature geoscience, 4(3), 156-159.

Nature of silicate weathering in the Indus River System, Ladakh, India

Santosh K Rai*, Sameer K.Tiwari, Anil K. Gupta, A.K.L. Asthana, S.K. Bartarya
Wadia Institute of Himalayan Geology, 33, GMS Road, Dehradun 248001, INDIA
** rksant@wihg.res.in*

Denudation of continents rocks influence the geochemical cycles of elements in different reservoirs including atmosphere, oceans and surface sediments. Chemical weathering of silicate rocks have significant control on the CO_2 budget of the atmosphere on longer time scales. Therefore, nature and intensity of silicate weathering may be regarded as a driver of climate. Towards this, the Himalayan uplift has produced fresh rocks to the surface and hence has contributed significantly to accelerate the silicate weathering on geological time scales. In this context, the Himalayan fluvial systems, specially the Indus-Ganga-Brahmaputra (I-G-B) system has been studied for chemical weathering in great detail (Ahmad et al., 1998; Pande et al., 1994; Karim and Veizer, 2000; Singh et al., 1998; France-Lanord and Derry, 1997; Krishnswami et al., 1999; Sarin et al., 1992). These rivers are characterized with high water discharge and act as the major pathway for the transport of weathered material from the Himalaya to the oceans. Present study addresses the nature of the weathering in the Indus River System covering the Ladakh region and is based on the major ions and stable isotopes ($\delta^{13}C_{DIC}$) in dissolved phase.

Ladakh forms a part of the Trans Himalaya which lies North West of the Indian subcontinent. Indus, originating from Kailash Mountain, is the main river of Ladakh region that flows in a NW direction along the Indus Suture Zone (ISZ) and debouches into Arabian Sea. From south to north, Ladakh region is divided into four geological units namely (i) Zanskar Suture Zone

(ZSZ) having Precambrian basement overlain by Phanerozoic rocks, (ii) ISZ comprising of remnant oceanic lithosphere with melange rocks, volcanogenic sediments and Ladakh plutonic complex, (iii) Shyok Suture Zone (SSZ) characterized with the relics of the back-arc basin dominated by mélange and volcanic rocks, and (iv) Karakoram Plutonic Complex (KPC). Therefore, it shows that the Indus catchment has the silicate lithology in considerable proportion. River water samples collected along the Indus River and its tributaries (Shyok, Zanskar and Nubra etc.) in the Ladakh Himalaya in September 2011 and major ions and stable isotopes were measured in these samples to infer about the nature of weathering (silicate vs carbonate) in this drainage.

Results (Fig. 1) of the stable isotopes ($\delta^{13}C$ VPDB range 0.4 to -5.7‰) and silica (73 to 280 µE) generally agree with the earlier studies (Ahmad et al., 1998; Pande et al., 1994; Karim and Veizer, 2000). Silicate weathering is a key process in Indus River catchment which has implication on the Global CO_2 budget.

This process operates as follows:

Silicate weathering (1): $CaSiO_3 + \downarrow 2CO_2 + 3H_2O \rightarrow Ca^{+2} + 2HCO_3^- + H_4SiO_4$

Carbonate weathering (2): $CaCO_3 + \downarrow CO_2 + H_2O \rightarrow Ca^{+2} + 2HCO_3^-$

Carbonate (in oceans) (3): $Ca^{+2} + 2HCO_3^- \rightarrow CaCO_3 + \uparrow CO_2 + H_2O$

Net (1 & 3) effect (~1 My time scale): $CaSiO_3 + \downarrow CO_2 \rightarrow CaCO_3 + SiO_2$

$\rightarrow CO_2$ mediated Silicate weathering is a sink of $Co_2 \rightarrow$ Cooling effect

Other possibility: Sulphuric acid mediated (Black Shales & Pyrites) Silicate weathering:

$4FeS_2 + 15O_2 + 8H_2O \rightarrow 2Fe_2O_3 + 8H_2SO_4$;

$H_2SO_4 + 9H_2O + 2NaAlSi_3O_8 \rightarrow Al_2Si_2O_5(OH)_4 + 2Na^+ + 2SO_4^{2-} + 4H_4SiO_4$

$\rightarrow$ No Co_2 is consumed $\rightarrow$ No net effect on climate on longer time scale.

Variation of $\delta^{13}C$ VPDB measured in Dissolved Inorganic Carbon (DIC) with concentration of SiO_2 in Indus River waters shows that the Alkalinity in these rivers is linked with silicate weathering. However, co-variation of $[HCO_3+SO_4]$ with [Ca+Mg] indicates that the alkalinity in these rivers may be linked with silicate weathering mediated by H_2SO_4 or dissolution of Halites. Therefore, the silicate weathering seems to serve as a dominant mechanism to produce the alkalinity in these rivers. This observation is also supported by the fact that the silicates (granites, gneisses, schists etc) in the Indus valley comprise mainly of minerals including quartz, plagioclase, alkali feldspar, biotite and muscovite and dissolution of these can produce silica and Alkalinity together in solution. The possibility of pronounced silicate weathering in the Indus River system also finds support from the

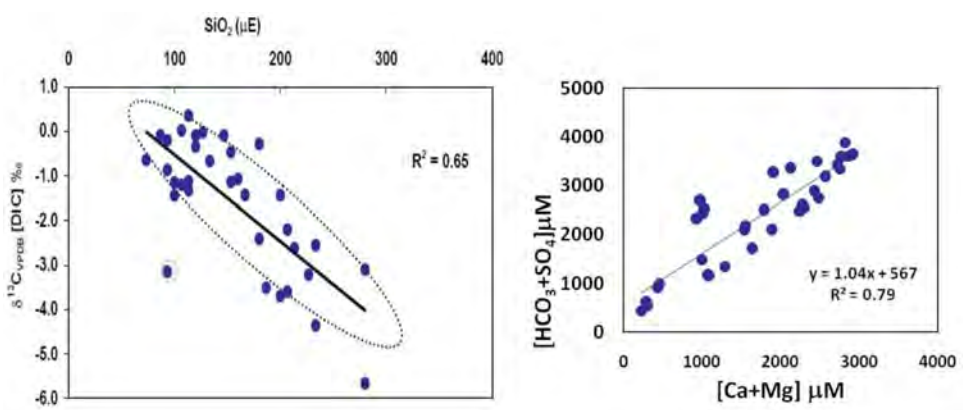

Fig 1. (a) $\delta^{13}C$ VPDB [DIC] with SiO_2 in Indus River system indicates that the Alkalinity in these rivers are linked with Silicate weathering.(b) $[HCO_3+SO_4]$ with [Ca+Mg] points that the alkalinity may be linked with Silicate weathering mediated by H_2SO_4 or dissolution of Halites

fact that it is flowing through the Indo-Tsangpo Suture zone with a high tectonic activity and highly fractured/sheared rocks which are prone to weathering. This work provides a testing tool for the nature of silicate weathering in the Indus catchment.

Ahmad, T., Khanna, P.P., Chakrapani, G.J., Balakrishnan, S. 1998. J Asian Earth Sci. 16 333-346
France-Lanord, C., Derry, L.A. 1997. Nature 390, 65-67.
Karim, A., Veizer, Jan 2000. Chemical Geology, 170, 153-177.
Krishnaswami, S., Singh S.K., Dalai, T. 1999. Indian National Science Academy and Akademia International, New Delhi, pp 23-51.
Pande, K., Sarin, M.M., Trivedi, S., Krishnaswami, K.K., Sharma, K.K. 1994. Chem. Geol. 116, 245-259.
Sarin, M.M., Krishnaswami, S., Dilli, K., Somayajulu, B.L.K., Moore, W.S. 1989. Cosmochim. Acta 53, 997-1009.
Singh, S.K., Trivedi, J.R., Pande, K., Ramesh, R., Krishnaswami, S. 1998. Cosmochim. Acta 62, 755-773.

Exhumation of the Lesser Himalaya of Northwest India: Zircon (U-Th)/He thermochronometric constraints and implications for Neogene seawater evolution

C.L. Colleps[1,*], N.R. McKenzie[1,2], D.F. Stockli[1], B.P. Singh[3], A.W. Webb[4], N.C. Hughes[5], P.M. Myrow[6], B.K. Horton[1]

[1]*Jackson School of Geosciences, University of Texas, 2305 Speedway, Stop C1160, Austin, TX 78712, USA*
**ccolleps@utexas.edu*
[2]*Geology and Geophysics, Yale University, 210 Whitney Ave, New Haven, CT 06511, USA*
[3]*Center for Advanced Study in Geology, Panjab University, Chandigarh 160014, INDIA*
[4]*School of Earth and Environment, University of Leeds, Leeds, LS2 9JT, UNITED KINGDOM*
[5]*Department of Earth Sciences, University of California, Riverside, 1242 Geology Building, Riverside, CA 92521, USA*
[6]*Department of Geology, Colorado College, 14 E. Cache La Poudre, Colorado Springs, CO 80903, USA*

The timing of Lesser Himalayan (LH) uplift in the Uttarakhand-Himachal region of Northwest India remains a topic of debate, the resolution of which may provide insight into the relationship between the weathering of chemically distinct Himalayan source rocks and the Neogene isotopic evolution of seawater osmium and strontium. Two contrasting models have been proposed to explain the origin of the southward dipping Tons Thrust, which separates the LH into the inner LH (iLH) of late Paleo-Mesoproterozoic rocks and the younger outer LH (oLH) of low grade Cryogenian to Cambrian metasedimentary rocks. One model suggests that the Tons Thrust shared an original decollement with the South Tibetan Fault System and that the oLH is a far-traveled klippe emplaced against the iLH during the Eocene-Oligocene prior to out-of-sequence activation of the Main Central Thrust (MCT). In contrast, a second model suggests that the oLH is a short travelled, in sequence thrust sheet emplaced in the Late Miocene, post-dating movement along the MCT. Given a time discrepancy for oLH emplacement of at least 14 Myr and broad constraints on the thermal history of the oLH, iLH, and MCT hanging wall, zircon (U-Th)/He (ZHe) thermochronology can effectively be used to test these hypotheses. New bedrock ZHe data yield average cooling ages of 10.5±3.6 Ma for the iLH, 16.2±1.5 Ma for the middle oLH, and 23.0±4.1 Ma for MCT hanging wall rocks in and around the Shimla and Mussoorie synclines of the frontal Himalayan system. These data suggest rapid passage of the oLH through the ZHe cooling window due to displacement along the Tons Thrust at ~16 Ma and provides support for the short-traveled kinematic model for oLH emplacement. ZHe ages from the oLH are also in agreement with predicted ages for the exhumation of black shale units enriched in ^{187}Os within the oLH, the weathering of which has been proposed to drive a global increase in seawater $^{187}Os/^{188}Os$ at ~16 Ma. Preliminary detrital ZHe ages from the Upper Dharamsala Formation (depositional age of 17-13 Ma) confine a depositional lag time of 0-3 Myr, suggesting surface exposure of the oLH and the black

shales within between 16-13 Ma. With better constrained detrital zircon U-Pb-He double dating of foreland basin deposits coupled with a higher spatial resolution of ZHe cooling ages from the hinterland, LH thrust kinematics can be further constrained and we can more confidently link the weathering of LH source rock to the observed shifts in seawater compositions.

Crustal deformation analysis using Finite Element Method (FEM) in Garhwal-Kumaon Himalaya, India

Anjali Brahma, Saksham Arora, Param Kirti Rao Gautam
Wadia Institute of Himalayan Geology, 33 GMS Road, Dehradun 248001, INDIA

The Kumaon region in eastern part of Uttaranchal India represents one of the most seismically active areas in its domain. In order to estimate the stress pattern of the region we performed 2-D finite element method (FEM) simulations for convergent displacement caused by northeastward movement of the Indian plate with respect to the Eurasian plate. Various rock properties (density, Poisson's ratio, Young's modulus, cohesion, and angle of internal friction) are used to evaluate failure and faulting patterns. Two plane strain models with appropriate boundary conditions were also calculated. The predicted maximum compressive stress ($\sigma 1$) shows a preferred orientation that helps explain the tectonic environment and the fault pattern. The best-fit model suggests that a compressive stress regime is dominant in the study area everywhere except for the uppermost part of the crust where extensional stress dominates. With increased progressive convergent displacement, the modeled $\sigma 1$ are predicted to rotate counterclockwise around the fault zones. The simulation results suggest that the north dipping Munsiari Thrust in the MCT region plays a significant role in the development of stress and deformation distribution in the area. We also infer that the tectonically induced deformation in the region is restricted to mainly within the crust (<30 km).

Response of fluvial architecture and vegetation with change in rainfall amount during the late Miocene time: Compound specific isotopic evidence from the NW Siwalik, India.

Sambit Ghosh[1,*], Prasanta Sanyal[1], Melinda Kumar Bera[2]
[1]Department of Earth Sciences, IISER, Kolkata 741246, INDIA
**sambitju@gmail.com*
[2]Department of Geology and Geophysics, IIT, Kharagpur 721302, INDIA

The collision between Indian and Eurasian continental landmass at ~55 Ma has resulted in the formation of the Himalayan mountain chain. At the late stage of Himalayan orogeny at ~20 Ma, flexural downwarping of overriding Indian plate has produced world largest terrestrial foreland basin in the foothill of Himalaya. During the late Miocene, rise of the Himalaya and Tibetan Plateau triggered the initiation of Indian Monsoon which enhanced the physical and chemical weathering of the Himalayan rocks. The eroded sediment deposited in the foreland basin gave rise to the Siwalik Group of rocks. Thus this foreland sediment is an excellent archive to unfold the late Miocene climatic condition existed over the northern part of India. However, previous reconstruction of timing of monsoon initiation and its effect on ecosystem and fluvial architecture using the Siwalik Group of rock is equivocal. The major goal of this study is to understand the effect of monsoon on vegetation using NW Indian Siwalik paleosol derived long chain n-alkane δD and $\delta^{13}C$ value along with fluvial architecture analysis. The paleosol serived leaf wax long chain n-alkane δD based rainfall reconstructions show variations in rainfall amount between 10.5 to 2 Ma with three episode

of high rainfall at ~9 Ma, ~5.5 Ma and ~3.6 Ma. The foreland sedimentary record depicts varying degree of creation of accommodation space during this interval: high accommodation space and immature soil development during the higher rainfall compared to the low rainfall regime. The change in the amount of rainfall is also reflected in the varying abundance of C4 plant reconstructed from the long chain n-alkane $\delta^{13}C$ value. However, rainfall amount and abundance of C4 plant is not well correlated. The appearance and expansion of C4 plant has earlier been documented from the different part of the globe and it shows timing of C4 advent is not synchronous in basin scale. This asynchronous nature of C4 plant appearance points towards the regional heterogeneity in climatic factors and soil morphology during the late Miocene time.

Present day crustal configuration and seismotectonics of northwest India-Asia collision zone

Devajit Hazarika*, Arpita Paul, Monika Wadhawan, Koushik Sen, Naresh Kumar
Wadia Institute of Himalayan Geology, 33 GMS Road, Dehradun 248001, INDIA
**devajit@wihg.res.in*

The crustal architecture of the northwest India-Asia collision zone extending from the Tethyan Himalaya to the Karakoram fault zone (Eastern Ladakh) is inferred on the basis of seismological data recorded by 13 broadband seismological stations under operation during 2009-2012. About 300 teleseismic waveform data recorded by these stations were analyzed using receiver function method. We observe strong azimuthal variation of P-to-S converted phase, which do not show a clear Moho discontinuity in the Indus Suture Zone (ISZ). The receiver functions computed from teleseismic P-waveforms and corresponding inverted shear wave velocity models obtained at each station reveal an Intra-Crustal Low Velocity Zone (IC-LVZ) at a depth of ~15-40 km. By integrating geological and geophysical parameters, the IC-LVZ is interpreted as a zone of fluid/partial melt. Our analysis suggests presence of 4-8% fluid/partial melt in the IC-LVZ. The crustal thickness obtained in this study varies from ~60 km beneath the Tethyan Himalaya to as high as ~80 km beneath the Karakoram fault zone. Shear wave velocity model also reveals a layer at a depth of ~47-50 km inferred as the eclogitized Indian continental crust. This eclogitized layer is ~25 km thick having S-wave velocity of 4.0-4.2 km/sec. The probable cause of sudden velocity jump at ~47-50 km depth is the presence of serpentinized ultramafic layer overlying the eclogitized Indian lower crust.

The seismotectonic scenario of this region is also explored by analyzing the local earthquakes data. Depth distribution of earthquakes and Fault Plane Solution (FPS) of local earthquakes ($M \geq 3.5$) obtained through waveform inversion reveals the kinematics of the major fault zones present in the Eastern Ladakh. Two clusters of micro seismicity is observed at a depth range of ~5-20 km at north western and southeastern fringe of the Tso Morari gneiss dome which can be correlated to the activities along the Zildat fault and Karzok fault respectively. The FPS estimated for representative earthquakes show thrust fault solutions for the Karzok fault and normal fault solution for the Zildat fault. It is inferred that the Zildat fault is acting as detachment, facilitating the exhumation of the Tso Morari dome. On the other hand, the Tso Morari dome is thrusting over the Karzok ophiolite on its southern margin along the Karzok fault, due to gravity collapse. The shallow level seismicity is also facilitated by presence of hydrothermal fluid/partial melts which may have generated decompression melting of the Tso Morari dome. The most pronounced cluster of seismicity is observed in the Karakoram Fault (KF) Zone upto a depth of ~60 km. The fault plane solution reveals transpressive environment with the strike of inferred fault plane roughly parallel to the KF. It is inferred that the KF penetrates up to the lower crust and is a manifestation of active under thrusting of Indian lower crust beneath Tibet.

Glacio-chemical study of Gangotri Glacier, Central Himalaya India: Implication for solute acquisition process

Shipika Sundriyal[1,*], Sameer K. Tiwari[1], D.P. Dobhal[1]
[1]Centre for Glaciology, Wadia Institute of Himalayan Geology, 33 GMS Road, Dehradun 248001, INDIA
**shipika@wihg.res.in*

The growing demand for availability of freshwater in downstream is important to study the chemical constituents of Himalayan glaciers. The glaciochemical studies at first order streams in Himalaya provide an ideal environment to understand the water-rock interactions and their natural/anthropogenic inputs at higher altitude. Solutes are the chemical constituents originate through water rock interaction and sub glacial weathering operating at zones of ice-water-rock contact. The present study is undertaken to understand ionic sources and flow pathway of major ionis in Gangotri Glacier of Uttarakhand Himalaya. The samples were collected from proglacial stream emerging from the snout of the Gangotri Glacier. They have been analyzed for its ionic composition through Ion Chromatograph and insitu measurement of its physical parameters by pH and conductivity meter.

The results showing the pH value of snow melt water from 5.8 to 7.7 with an average of 6.5 indicating slightly acidic nature of the melt-water. The concentration of major ions are showed here in increasing order of abundance in melt water stream (SO_4^{2-} >Ca^{2+} >NO_3^- >Na^+ >Mg^{2+} >HCO_3^- >Cl^- >K^+ >F^-). Elevated concentration of sulphate indicates the dominance of mineral dust, oxidation of sulphur emitted by the different sources like marine biota, volcanic emission and anthropogenic emissions via SO_2 whereas Ca^{2+} indicated the dominance of crustal source. However, the factor analysis calculation shows highest concentration of sulphate (47%) in factor 1 followed by nitrate (31%) in factor 2 and HCO_3^- (30%) in factor 3 respectively. This database provides a baseline against which to assess natural and anthropogenic influence on water chemistry in these environments.

The generated data of Gangotri glacier shows that carbonate derived calcium and magnesium are the major contributors of the total cations in all the samples. The higher (~0.85) (Ca+Mg/TZ+) and lower (~0.15) (Na+K/TZ+) equivalent ratios indicates that the carbonate weathering of granites could be the major source of dissolved ions in the melt-waters with small contribution from silicate weathering (Figs. 1 and 2) respectively. High equivalent ratio of (Ca+Mg)/(Na+K) ranging from 1 to 13 (mean=8) and high (Ca/Na) ratio ranging from (1 to 18.7) (mean=11) also confirmed that carbonate weathering of granite rocks is the major source of dissolved ions in the Gangotri glacier. The data of major ions chemistry of Gangotri glacier shows diurnal

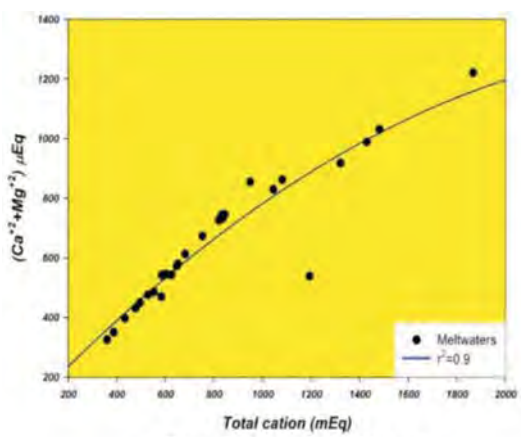

Fig: 1 (Ca+Mg/TZ+)

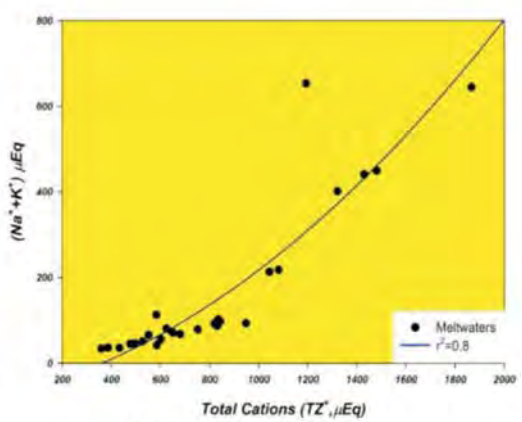

Fig: 2 (Na+K/TZ+)

variation in major ions and physical parameters. The diurnal variation in the magnitude and pattern of discharge, major ions and physical parameters are indicative of timing of the melt-waters transmission through subglacial discharge. Drainage pattern of glacier consists of a mix superglacial, englacial, and subglacial components and chemical weathering rates can vary among these components.

Proterozoic clastic sedimentary rocks and associated mafic magmatism of Lesser Himalaya: their relationship, geochemistry and tectonic significances

R. Islam*, Sumit K. Ghosh, S. Vyshnavi
Wadia Institute of Himalayan Geology, 33 GMS Road, Dehradun 248001, INDIA
**rislamwihg@gmail.com*

The Lesser Himalayan sequence ranging in age from Paleoproterozoic to Paleocene represents the oldest sedimentary basin in the Himalaya. It is bounded by the Main Boundary Thrust (MBT) in the south and the Main Central Thrust (MCT) in the north. The Lesser Himalayan package is disposed in two linear belts viz., the Outer Lesser Himalaya (OLH) in the south and the Inner Lesser Himalaya (ILH) in the north. Both the units consist of pelitic to arenitic sediments indicating a shallow marine condition. In addition, a thick pile of basic volcanic rocks in the form of sills and dykes are intruding these shallow marine siliciclastic rocks. Present study focused on geochemical aspects of the Lesser Himalayan siliciclastics packages from both OLH and ILH (Pre-Vendian) and associated basic volcanic rocks.

The bulk rock chemistry of the Lesser Himalayan sediments shows similarities with Post-Archean Average Australian shale (PAAS), North American Shale Composite (NASC) and Upper Continental Crust (UCC). Chemical variations in these rocks are produced by mineral specific grain size sorting during transport and deposition. The clastic sediments of Lesser Himalaya are enriched in LREE with pronounced negative Eu anomalies. HREE patterns are moderately depleted in nature. High Zr and Th contents and Th/Ni, La/Sc and $(La/Yb)_N$ ratios as well as Sc vs Th/Sc relationship suggest a dominant felsic source for these rocks.

The basic volcanic rocks of the Lesser Himalaya, mainly associated with Nagthat Formation of OLH and Rudraprayag/Rautgara Formation of ILH, range in composition from sub-alkaline basalt through andesite to andesitic basalt. Further, minor trace elements also suggest that these volcanics are identified as Fe- tholeiites of continental character. Chondrite normalized REE data of these basic rocks exhibit remarkable similarities and characterized by enriched LREE and relatively flat HREE pattern along with a weak negative Eu anomaly. Primitive mantle normalized multi-element spider diagram exhibit an enriched incompatible trace element pattern especially in LILE and distinct negative anomalies for Sr and HFSE for all the basic suites. The above trace and rare earth element character is similar to that in rocks of Aravalli and Bundelkhand regions of the Indian shield. Therefore, it is suggested that the Aravalli, Bundelkhand and Lesser Himalayan region may be forming a large igneous province in the northern part of Indian shield (?). The gradual change from pelite dominated to quartzite dominated succession with erupted volcanics and the occurrence of seismites and pebble bed at the upper part of succession is suggestive of deposition in unstable shallowing upward basins.

Evolutionary entities from the Krol-Tal Belt, Lesser Himalaya, India: A synoptic view

Rajita Shukla, Meera Tiwari, Harshita Joshi
Wadia Institute of Himalayan Geology, 33 GMS Road, Dehradun 248001, INDIA

The history of life on Earth during the Precambrian-Cambrian time is well documented in the Krol-Tal Belt of Lesser Himalaya, India. This belt occurs as a series of synclines from Solan (Himachal Pradesh) in the north-west to Nainital (Uttarakhand) in the south-east. Many palaeobiological entities namely cyanobacteria, algae, acritarchs, trace fossils and sponge spicules have been recorded from various lithostratigraphic divisions of this belt. Encompassing a time span from Ediacaran (base of the Blaini pink/cap carbonates) to Early Cambrian (Tal Group), the Krol-Tal Belt reveals records of evolution from primitive to increasingly complex life forms.

The early part of the Ediacaran Period is characterized by large acanthomorphic acritarchs. These acritarchs are morphologically complex, stratigraphically restricted, and largely facies independent, suggesting their utility in biostratigraphic correlation and subdivision of the Ediacaran time span. These l*arge acanthomorphic acritarchs have been reported from Infrakrol and Krol 'A' formations. Tianzhushania spinosa,* recently recorded from the Infrakrol Formation, is comparable with the Lower Biozone of Doushantuo Formation in China. The assemblage from the lower part of Krol 'A' Formation viz., *Appendisphaera grandis*, *Asterocapsoides sinensis*, *Cavaspina acuminata*, *C. basiconica*, *Eotylotopalla dactylos*, and *Knollisphaeridium* however, shows greater similarity with the Upper Doushantuo Biozone of China. Several taxa recognized from the Krol Group occur in successions from South China, Australia, the Siberian Platform, the East European Platform, and Svalbard.

The Chert Member of the lower Tal contains well preserved small acanthomorphic acritarchs, sphaeromorphic acritarchs, cyanobacterial filaments, sponge spicules and thallophytic remains. The assemblage, rich in small acanthomorphs, appears to be best developed in upper Nemakit-Daldynian beds. Based on acritarch biostratigraphy, a Nemakit-Daldynian to Early Tommotian age has been suggested for the Chert Member. The assemblage shows low diversity of species, characteristic of inshore biota. The assemblage is correlatable to the Precambrian-Cambrian boundary microbiotic assemblage from China, Central Asia and East European Platform.

The Tal Group also contains a variety of trace fossils, most of which are facies independent. The traces are mainly dwelling traces made by filter feeding organisms. A trace fossil assemblage comprising *Cruziana acacensisplana, Cruziana pectinata, Dimorphichnus* isp., *Diplichnites* isp., *Merostomichnites* isp., *Monomorphichnus lineatus, Neonereitesbiserialis, Phycodes curvipalmatum, P. palmatus, Palaeophycus* isp., *Planolites montanus, Rusophycus isp., Skolithos* isp., *Treptichnus pedum* amongst others, has been recorded from the lower part of Upper Tal in Mussoorie and Nigalidhar synclines, This assemblage matches with a majority of the Precambrian-Cambrian sections of the world and specifically with the Meischucun section of China and indicates an Early Cambrian age for the Tal Group. The above data from the Krol-Tal Belt adds to the biostratigraphic correlation of coeval sequences across the world.

Classical Structural analysis-a useful tool for identification of Fold-and-Thrust Structures

Deepak C. Srivastava*, Jyoti Shah
Department of Earth Sciences, IIT Roorkee, Roorkee 247 667, INDIA
*dpkesfes@gmail.com

This study shows the potential of classical structural analysis in distinguishing between the map scale flat-over-flat and flat-over-ramp structures. Two case studies are presented from the outer Lesser Himalaya India, where the original fault-related-folds have been overprinted by the buckle folds at various scales. The first example is from the Kumaun Himalaya where the Nagthat Formation, Ramgarh Group and Nathuakhan Group overlie successively from south to north. The contact between the Nagthat Formation and the Ramgarh Group is a regional thrust mappable as the Ramgarth Thrust. Similarly, the contact between Ragmgarh Group and the Nathukhan Formation is Chamaria/Lohali Thrust. The second case study is from the Garhwal Himalya, where the Krol Group consisting of Blaini-Krol-Tal formations is overlain by the Chakrata Formation along a well exposed regional Thrust.

All the three rock sequences, the Nagthat Formation, the Ramgarh Group and the Nathuakhan Formation are dominantly folded by buckling mechanism at scales ranging from outcrop to map. Systematic structural analysis and critical comparison of results reveals a striking parallelism between the fold axial planes and hinge lines across the three sequences. The intensity and tightness of folds, however, increases from south to north. The concordance of structures across various thrust implies these sequences initially defined a flat-over-flat structure of a large scale fault bend fold.

The second case study is from Garhwal Himalaya where the Krol Group consisting of Blaini-Krol-Tal formations is overlain by the Chakrata Formation along a prominent Thrust. Both the rock sequences are buckled by map scale upright and non-plunging to low plunging folds, although the mesoscopic folds are rare due to large thickness of the beds. The results of structural analysis reveal a sharp structural discordance between the Krol Group and the Chakrata Formation. In the Krol Group, folds hinge lines are predominantly NW-SE directed. By contrast, the Chakrata Formation is folded on NE-SW directed non-plunging hinge lines. The structural discordance between these two rocks sequences points to the presence of a large scale ramp-over-flat or flat over-ramp structure in the Outer Lesser Garhwal Himalaya.

Inception of the Indian monsoon and its abrupt behaviour since the latest Pleistocene

Anil K. Gupta[1,2], Prakasam M.[1], Yuvaraja, A.[1], Som Dutt[1], Moumita Das[2], Raj Kumar Singh[3], Velu A.[2]
[1]Wadia Institute of Himalayan Geology, 33 GMS Road, Dehradun 248001, INDIA
[2]Department of Geology & Geophysics, IIT Kharagpur, Kharagpur 721302, INDIA
[3]School of Earth, Ocean and Climate Sciences, Indian IIT Bhubaneswar, Bhubaneswar 751007, INDIA

The Indian or South Asian monsoon is one of the most spectacular climatic features in the tropics, catering to the water needs of a very large population. The monsoon provides moisture to the glaciers of the Himalayan-Tibetan region and feeds to large river systems of the Asian region. The evolution and timing of the onset of the Indian monsoon system has mystery to climate workers. The Himalaya-Tibetan plateau (HTP) complex has been implicated as the main factor in the evolution of Indian monsoon circulation and seasonal changes. However, there are genuine questions as to the role of the HTP complex in driving the Indian monsoon. The model simulation suggests a major intensification of the Indian

monsoon as early as ~30 Ma or before, whereas marine records from the Arabian Sea indicate a major strengthening of Indian summer or southwest monsoon winds between 10 and 8 Ma. The continental records from the Siwaliks, on the other hand, indicate a major transition in vegetation from C3 to C4 type during 8-7 Ma. Recent studies from Ocean Drilling Program holes located off the Oman margin and on the Owen Ridge, western Arabian Sea suggest that present day South Asian monsoon wind system began to develop during the late Middle Miocene (~13 Ma) and summer monsoon has been in its full strength since the late Miocene (~7 Ma).

Continental and marine records captured centennial to millennial scale weak phases in the Indian summer monsoon which are aligned with cold phases of the North Atlantic. Recent speleothem proxy records from northeastern (NE) India reflect seasonal changes in Indian summer monsoon strength as well as moisture source and transport paths. A 35,000 year old new speleothem record from Mawmluh Cave, Meghalaya, India suggests abrupt increase in strength of the Indian monsoon during the Bølling-Allerød and early Holocene periods and pronounced weakening during the Heinrich and Younger Dryas cold events. The marine records indicate weak summer monsoon winds during cold phases of the North Atlantic. We infer that these changes in monsoon strength were driven by changes in temperature gradients which drive changes in winds and moisture transport into Indian interior.

Preliminary palaeoseismic investigations along the Mishmi Thrust at Roing, Arunachal Pradesh, NE Himalaya, India

Arjun Pandey[1], I. Singh[1], R.L. Mishra[1], P.S. Rao[2], G.R. Bhatt[3], P. Srivastava[1], R. Jayangondaperumal[1], H. Baruah[4]

[1]Wadia Institute of Himalayan Geology, 33 GMS Road, Dehradun 248001, INDIA
[2]Present Address: Geological Survey of India
[3]University of Pondicherry, Pudducherry, INDIA
[4]Arya Vidyapeeth College, Guwhati, INDIA

The area of interest lies in Northeast Himalaya at the eastern flank of eastern syntaxis along the northern segment of Mishmi Thrust. The Mishmi Thrust (MT) shows regional NS to NW-SE strike that defines a boundary between Precambrian Mogok belt of Myanmar and Brahmaputra Quaternary flood plains (Fig. 1). The region has witnessed the past century great Assam earthquake Mw ~8.5 (1950), with estimated rupture length of >250 km (Bilham and Wallace, 2005). Our investigation lies in the meizoseismal region of the A.D. 1950 Assam earthquake with an aim to find out whether the Assam earthquake produced the surface rupture or it remains blind like that of the 2015 Gorkha-Nepal earthquake. The present study incorporates geomorphic, trench investigation, stratigraphic and structural analyses approach to understand the paleoearthquake history along MT and its control on development of geomorphic landforms. Field survey was carried out with the help of CARTOSAT imageries along with high resolution field survey instruments (Real Time Kinematic Global Positioning Satellite or RTK-GPS), Robotic Total station (RTS) and drone (UAV, unmanned aerial vehicle) were used to generate high resolution micro-topographic map and profile of the fault scarp.

At Roing park (28.15°N, 95.84°E), a beautiful scarp was identified with ~N-S strike, and it is perpendicular to the Deopani River course. The scarp extends ~0.5 km with height varies from 8 to 3 m. A micro-topographic survey was carried out using RTK-GPS and RTS across a 3 m high NS trending fault scarp (Fig. 1). Two trenches (50 m length, 8 m width and 5 m depth) were excavated across the fault scarp to investigate the paleoearthquake history. The excavated exposures were thoroughly cleaned and grids of 1x1 m were laid using strings with leveler. Photo and hand-drawn logs of the both trench walls (exposures) were prepared for detailed study of the fault displacement and displaced soil horizons. Detrital charcoals for radiocarbon (AMS) dating and OSL samples

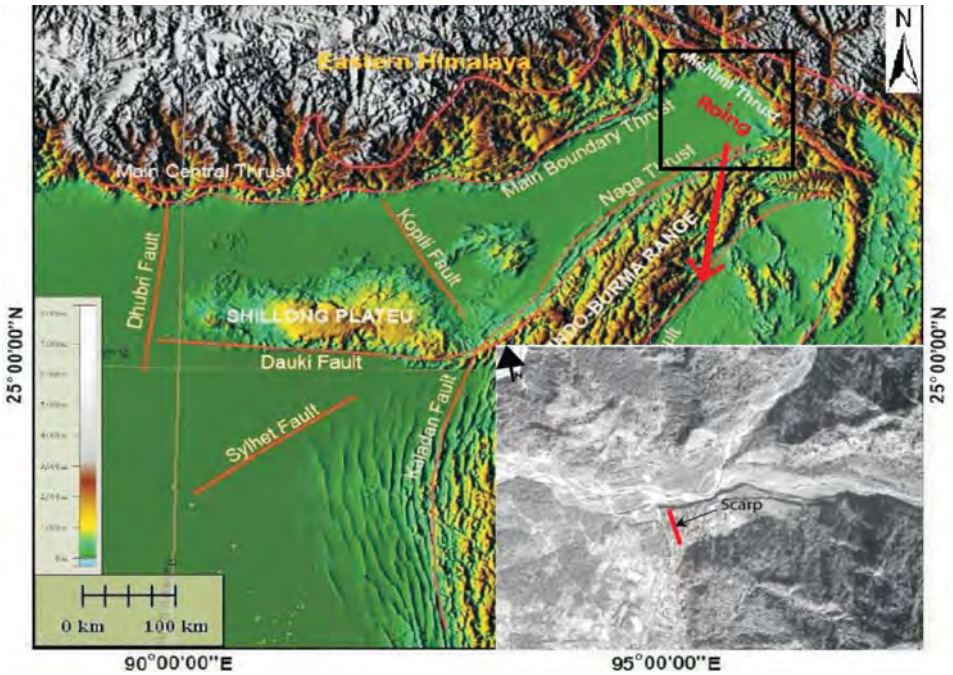

Fig. 1. Regional thrust faults and strike slip faults in NE Himalaya (after Nandy, 2001; Murthy et al., 1969) a small black color square defines our study region and inset in left down side is marked with NW-SE trending scarp where trench work carried out.

indicated by colored flags in the trench log, were taken from the displaced units of the trench walls to bracket the age of displacement and thereby, the earthquake event. For making photo mosaic and logs, photographs of each 1 m grid of the exposure was taken using the same resolution and camera adjustments. Though there was no evidence of faulting found in the trenches, we presume that it may be lying at a depth greater than the limit of the excavated trench. However, we found prominent fault exposure on the right bank river cut sections along the Devpani River (28°09'49.8" N; 95°50'16.5" E) and its tributary Iphipani River (28°10'55.2" N; 95°50'14.8" E). We collected several optical stimulated luminescence (OSL) and charcoal samples to constrain the ages of the paleo-events and to understand the long term uplift rates of the MT.

Tectonic and genetic implications of the mantle peridotites from the Tethyan ophiolites of the Eastern Himalaya, Northeast India

A. Krishnakanta Singh*, R.K. Bikramaditya Singh, S.S. Thakur, S. Khogenkumar
Wadia Institute of Himalayan Geology, 33 GMS Road, Dehradun 248001, INDIA
**aksingh_wihg@rediffmail.com*

The Tethyan ophiolite suite of rocks of the W-E trending Indus-Tsangpo Suture Zone (ITSZ) turn sharply southwestward at the Eastern Himalayan Syntaxis, are offset northward by the Sagaing Fault, and continue southward along the Indo-Myanmar Orogenic Belt of Northeast India. It further extends to the Andaman-Nicobar Islands Arc and continues to the Mentawai Islands representing the outer Indonesian Island Arc (Gansser, 1980). The Tidding-Mayodia ophiolite (TMO) of the Eastern Himalaya forms the southeast extension of the ITSZ which demarcates a collisional boundary

between the Indian subcontinent and the Eurasia (Mitchell, 1981). Mantle peridotites of the TMO exposed in the Tezu-Hayuliang section and Roing-Hunli section are variably serpentinized and metamorphosed. No other primary silicate minerals are survived except for spinel and less amount of olivine grains. Pseudomorphic textures after Opx and Cpx, olivine pseudomorphs after serpentinization are observed. Spinel grains are preserved primary igneous compositions in the core parts and their rim have been metamorphosed into ferritchromite.

Whole rock rare earth element (REE) characteristics along with the magmatic compositions of spinel and olivine were used to deduce the genesis and tectonic environments for the formation of the investigated TMO peridotites. Most of the investigated mantle rocks are enriched in REE and LREE (La_N/Yb_N = 3.0-8.6) resulting for the negative slopes of their REE patterns. Some of the peridotite samples also display mildly concave shaped chondritic-normalized REE patterns. Spinels in these peridotites show very high Cr# (0.63-0.93), Mg # (0.49-0.64) and very low TiO_2 content (<0.08 wt. %) which may reflect the crystallization of Chromian-spinel from a boninitic magma source (Zhou et al., 2005). Peridotites of the TMO have low to intermediate platinum group elements (PGE) contents and they exhibit more or less flat to slightly positive slopes with positive anomaly in all samples in spidergrams. Their PGE patterns are mostly similar to those of other ophiolitic harzburgites and dunites worldwide. Petrogenetic modeling suggests that these mantle rocks were produced by partial (12-25%) melting. Whole rock geochemistry, mineral chemistry in conjunction with PGE geochemistry of these investigated mantle peridotites indicate that the TMO of Eastern Himalaya, Northeast India was generated from an arc-related magma with boninitic affinity above a supra-subduction tectonic setting.

Gansser, A. 1980. In: Tater, J.M. (Ed.), The alpine Himalayan Region. Tectonophysics, 62, 37-52.
Mitchell, A.H.G. 1981. Jour. Geol. Soc. Lond., 138,109-122.
Zhou, M.-F., Robinson, P.T., Malpas, J., Edwards, S.J., Qi, L. 2005. Jour. Petrol., 46, 615-639.

Miocene mammals from Himalayan and Indian Shield regions, insights through their updated record

Ansuya Bhandari
Wadia Institute of Himalayan Geology, 33, GMS Road, Dehradun 248001, INDIA

In India the pre-Siwalik Miocene mammals are known through latest ongoing phase of paleontological investigations in Dharmsala and coevals (Murree and Dagshai/Kasauli) in the NW Outer Himalaya from Ladakh Molasse Group in Trans-Himalaya, and Kutch in western India. Dharmsala vertebrate fossil studies were initiated on the basis of clues by Verma and Verma (1979) in their abstract. Tiwari et al. (1991) published cyprinid fish teeth, crocodile teeth and ostracods from the Upper Dharmsala. Subsequently deinothere dental material too was put on record from the Upper Dharmsala (Tiwari et al., 2006). Still subsequently through persistent efforts an isolated rodent premolar recovered after maceration of >1000 kg of bulk sample from dark grey facies of Dharmsala Group and referred to Hodsahibia azrae. This find is a part of enormous microfossil assemblage comprising fish teeth, ostracods, charophytes, crocodile teeth, gastropods, etc. Though the molar shows insufficient crown details but has distinctive dimensions leading to its assignment to Hodsahibia, a baluchimyine taxon. Besides rodent records from Bugti localities in Pakistan, studies on fossil rodents from neighbouring localities of older Subathu, coeval Murree, and younger Siwalik beds and from other key horizons and localities provid an appropriate background to our present study. This rodent find from Dharmsala Group is said to mark small but significant paleontological beginning though has fallen short of expectations regarding biostratigraphy aspects because of lack of crown morphology (Bhandari and Tiwari, 2014).

Miocene Mammals from Indian Shield are dominantly the terrestrial fossils that have been recently added through extensive field works from two main fossil localities, namely, Pasuda and Tapar in central Kutch. Eight terrestrial mammal taxa comprising *Deinotherium sindiense,* Gomphotheriidae indet., *Brachypotherium* sp., *Parabrachyodus hyopotamoides, Sivameryx palaeindicus, Conohyus sindiensis* or *Tetraconodon malensis, Giraffokeryx punjabiensis,* and *Dorcatherium minus* were described from Khari Nadi Formation in Gujarat, India (Bhandari et al., 2010). This treasure of Miocene mammals with some early Miocene elements include exotics from Africa provide biogeographic insights, especially with regard to the opening of terrestrial routes between Africa and Eurasia via Arabian landmass. Larger vertebrate taxon with enormous migrating capacity in our collection is *Deinotherium*; this is significant in the context of palaeobiogeography, as its early Miocene record from Dharamsala as well as from Kutch assemblage, indicates the connection of African and Indian land masses. Remarkable records of *Hipparion* isolated teeth along with fossils of *Kachchhchoerus salinus* and *Tetraconodon indicus* in our collection from near Tapar in Kutch marks the presence of late-Miocene sediments in the region (Bhandari et al., 2015).

From indications that come to fore from Miocene mammal studies, it appears that a huge terrestrial bioprovince encompassing the entire Himalayan region and adjoining regions towards south in Indian Shield and north in the Chineses territory emerged at the beginning of Miocene to get fragmented subsequently as the orogen dynamics progressed; for precise view in this regard we have to have more Miocene mammals from different localities and for that work is in progress.

Bhandari, A., Mohabey D.M., Bajpai, S., Tiwari, B. N., Pickford, M. 2010. Neues Jahrbuch Fur Geologie Palaontogie Abhandlungeh, Stuttgart, 256(1), 69-97.
Bhandari, A., Pickford, M., Tiwari, B.N. 2015. Munchner Geowissenschfliche Abhandlungen 43(A) 1-40 (in press).
Bhandari, A., Tiwari, B.N. 2014. Jour. Geological Society of India, 83, 676-680.
Tiwari, B.N., Misra, P.S., Kumar, M., Kulshrestha, S.K. 1991. Jour. Palaeontological Soc. India, 36, 31-41.
Tiwari, B.N., Verma B.C., Bhandari, A. 2006. Jour. Palaeontological Soc. India, 51(1) 93-100.
Verma B.C., Verma. N.K.R. 1979. Neogene/Quaternary Boundary Conference, Chandigarh, Abstracts, p. 14.

Focal mechanisms of the aftershock sequence of the 25 April 2015 Gorkha Earthquake, and their relation to the Main Himalayan Thrust

Anna Foster[1*], S. Wei[1], B. Wang[2]
[1]*Earth Observatory of Singapore, Nanyang Technological University, 50 Nanyang Av., SINGAPORE 639798*
**aefoster@ntu.edu.sg*
[2]*Institute of Geophysics, China Earthquake Administration, Beijing, CHINA*

The destructive Mw 7.8 Gorkha earthquake on 25 April 2015 produced an aftershock sequence that is still ongoing. As of 20 August, this sequence includes over 270 earthquakes above Mb 4.0. Here, we use several examples to explore the levels of uncertainties in the results, particularly in the dip and depth. We use the Cut and Paste (CAP) method (Zhu and Helmberger, 1996), which uses waveform misfits to optimize the focal mechanism solution. The waveform is broken into two segments, one for body waves and one for surface waves, allowing equal or weighted contributions to the misfit from each. Amplitude information is retained, and is scaled by distance to give equal weight to all stations.

We get basic event information, including event location, from the NEIC catalogue. We use two separate data sets: (i) local body and surface wave data from 7 stations, most of which belong to the Chinese network and all but one of which are located to the north of the events, and (ii) teleseismic body wave data from the Global Seismic Network, available from the IRIS DMC, with distances ranging from 30-90˚. We compare the results from the two data sets with each other, and with other reported focal mechanisms, such as the Global CMT, where available. We examine the solutions

obtained to date in the context of geologic structure. The primary goal of the study is to produce a well-constrained, consistent survey of the depths and dips of earthquakes in this area, with the aim of helping to constrain the geologic model of the active faults in Central Nepal.

Dziewonski, A.M., Chou, T.-A., Woodhouse, J. H., 1981. J. Geophys. Res., 86, 2825-2852.
Ekström, G., Nettles, M., and Dziewonski, A.M., 2012. Phys. Earth Planet. Inter., 200-201, 1-9.
Zhu, L., Helmberger, D.V., 1996. Bulletin of the Seismological Society of America 86.5, 1634-1641.

Ooids-stromatolite associations as proxies for environmental conditions and depositional setting: A case study from Proterozoic Kunihar Formation, Simla Group, Himachal Himalayas, India

Alono Thorie*, Ananya Mukhopadhyay, Tithi Banerjee, Priyanka Mazumdar
Department of Earth Sciences, Indian Institute of Engineering Science and Technology, Shibpur, Howrah 711103, INDIA
**allan_thr@yahoo.com*

Numerous occurrences of ooid-stromatolite associations have been accounted in the Kunihar Formation, Proterozoic Simla Group at different locations in and around Arki Town, Solan district, Himachal Pradesh, India, which have been linked to various environmental and depositional setups, varying from beach to intertidal zones. Ooids in packstones and grainstones ranging in size from 0.01-0.7 mm are micritised and composed of nuclei of peloidal, sparry and/or micritic carbonate clasts. Ooids show internal fabrics with radial and radial-concentric cortex accompanied with few radial laminae, representing their deposition in an agitated beach environment above wave base with abundant microbial activity. Presence of ooids with fine radial laminae indicates their emergence from high energy shallow marine waters influenced by tide and storm activities. Microbial metabolic activities contributed to the calcification of the ooid cortex. Stromatolites occur on top of the oolites with sharp contact and at places laterally adjacent to the ooids. Exhibiting circular domes in plan view and having intact tops, the stromatolites indicate the absence of current influence under wave base. Lack of allochthonous coarse grain within the stromatolitic fabric depicts an overall low sediment rate, low energy environment and deposition during a transgressive phase. Syndepositional products like pyrites in the stromatolitic fabric indicate association of sulphur reducing bacteria, pointing to increased alkalinity. The plethora of ooids and microbial communities in Kunihar formation exhibits deposition in shallow marine environments with low salinity and significantly higher pH and alkalinity to induce carbonate precipitation.

Process studies and varve chronology using multiproxy palaeoclimate reconstructions from the sediments of Lake Bharatpur, Upper Lahaul Valley, NW Himalaya, India

Archna Bohra[1*], B.S. Kotlia[2], N. Basavaiah[3]
[1]Centre for Glaciology, Wadia Institute of Himalayan Geology, Dehradun 248001, INDIA
**archana@wihg.res.in*
[2]Centre for Advanced Studies in Geology, Kumaun University, Nainital, INDIA
[3]Indian Institute of Geomagnetism, New Panvel, Navi Mumbai, INDIA

The varved lake sediments are one of the important archives for high-resolution palaeoclimate and palaeo-environment reconstructions. Varved deposits in a lake formed by seasonal

variation in sediment release can be used to reconstruct the conditions that control sediment delivery. The main aim of this study is to reconstruct palaeoenviromental changes at Bharatpur in Upper Lahaul, NW Himalaya during Late Quaternary. At Bharatpur (77°27' E: 32°48' N, altitude 4,692 m), the exposed section has ca. 4.5 m thickness and consist of mainly the laminated sediments. The sedimentation may have taken place under the glacial/peri-glacial environment resulting in finely laminated, alternating dark and light layers of fine grained sequence, which at times also includes mm to cm scale thick layers of the highly angular gravel layers. The thin gravel horizons are composed of highly angular clasts of the country rocks, probably indicating comparatively more clastic input from the catchment during the warmer events. The proxies used were lithological details, chronology (AMS/radiocarbon dating), clay mineralogy, geochemical analysis, total organic carbon (TOC), loss on ignition (LOI), and mineral magnetism. Several parameters were also used, major being C/I, K/C, CIA, CIW, Al_2O_3/SiO_2, CaO/TiO_2, Al_2O_3/TiO_2, K/Al, Na_2O/TiO_2, K_2O/TiO_2 etc. Based on the available chronology, an average accumulation rate in the Bharatpur profile is estimated as ca. 28 cm/1000 yrs, and the basal most glacial outwash event (responsible for lake creation) can be estimated as ca. 24 ka BP. The laminated section indicates the continuity of sedimentation processes from Late Quaternary to Holocene.

Antigorite polysomatism during prograde metamorphism of Trans-Himalayan Tidding peridotite, eastern Arunachal Pradesh, India

Alik S. Majumdar*, D. Salvi, B. Borgohain, G. Mathew#
Department of Earth Sciences, IIT Bombay, Powai, Mumbai 400076, INDIA
** asmajumdar@iitb.ac.in, #gmathew@iitb.ac.in*

Peridotites are mainly composed of olivine and pyroxenes and exposed at shallower depth (<7 km) in various geological settings, including oceanic spreading centers, suture zones and continental margins. These peridotites, when interacts with an out-of-equilibrium fluid phase, texturally and chemically modifies the mineral assemblages, mainly via hydration and carbonation reactions. However, the interpretation of the replacement process during peridotite alteration is commonly complicated by multiple textural and chemical overprints related to different metamorphic events and/or evolution of reactive fluid chemistry on a micro-meter (μm) scale. Recent studies on equilibrium modelling suggested that the variation in activity of SiO_2 (aq), H_2O and O_2 (or H_2) (Frost & Beard, 2007) at the reaction interface and $Fe^{2+}Mg^{-1}$ chemical exchange potential (Evans, 2008) of the equilibrating system, i.e. $\Delta\mu$ ($Fe^{2+}Mg^{-1}$), dictate the secondary phase compositions during peridotite hydration. In addition, complexity may also arise due to a wide range of pressure (P)- temperature (T) stability of the serpentinite system (Evans, 2004) that commonly depends on the microstructure (Baronnet et al., 2006), and mineral chemistry (Majumdar et al., 2014 and references therein) of the serpentine phases. Additionally, the understanding of the mineral replacement mechanism is also important to decipher P-T evolution of serpentinization as the process of lizardite versus antigorite serpentinization operates between two end-member mechanisms i.e., solid-state diffusion-controlled or dissolution-precipitation-controlled processes (Evans, 2010).

The Cenozoic collisional zone between the Eurasian and Indian plate have imprints of oceanic and continental lithosphere simultaneously. The serpentinized peridotites present along the Indo-Tsangpo suture zone and its counterparts can thus provide insights towards collisional zone serpentinization processes. In this regard, the Trans-Himalayan Unit (THU) exposed at the eastern limb of the Siang Antiform (Singh, 1993; Acharyya, 1998) in eastern Arunachal Pradesh provide an unique setting to understand coupling between serpentinization and deformation process. The THU is composed of a lower ophiolite mélange sequence of the Tidding formation and the upper plutonic complex of the Lohit formation (Gururajan & Choudhuri, 2003).

Misra (2009) lithological documented that, along the Lohit and Dibang valley of the eastern Arunachal Pradesh, the Mishmi crystallines of the Higher Himalaya extends up to the Mayodia Pass. However, Ningthoujam et al. (2015) recently identified a klippe of Tidding formation within the Mishmi crystallines near Mayodia pass. Following this, the serpentinized peridotite samples for our study are collected from the serpentinite exposure within the klippe structure. The serpentinized peridotite appeared greenish in colour, friable, and has a soapy feel with a greasy lusture. Significant foliation is also developed in these rocks, however, the orientation of the foliation planes changes across locations.

Whole-rock powder XRD analyses have identified the presence of olivine, serpentine, magnetite, tremolite-actinolite and magnetite in all samples. We have performed detailed microtextural-chemical analyses across reaction interfaces using Raman spectroscopy, SEM and Electron Microprobe Analyses. The Raman spectroscopy analyses identified two different types of antigorites (Atg 1 and Atg 2) along microlithons (S1 foliation) and crenulation cleavages (S2 foliation) respectively within a crenulation structure that varies in FWHM and area in their SiO_4 antisymmetric peak position at ~1045 cm^{-1}. Atg 1 possesses lower value of FWHM and higher area under the curve of 1045 cm^{-1} peak whereas Atg 2 shows higher value of FWHM and lower area under the curve for the same peak. Compositionally, Atg 1 contains lower value of Al wt. % than that of Atg 2.

The P-T stability field of different serpentine phases indicates that stable antigorite can form in between 300-375°C whereas below 300°C stable lizardites are commonly produced (Andreani et al., 2007 and references therein). However, with increasing proportions of trivalent cations like Al^{3+}, Cr^{3+} in serpentine stoichiometry, the stability of serpentine also increase due to more equivalent dimensions of the tetrahedral and octahedral sheets within the crystal structure (Majumdar et al., 2014 and references therein). Hence, it appears that Atg 2 may have been produced at a higher temperature condition than that of Atg 1. The decrease in FWHM value of 1045 cm^{-1} peak from Atg 1 to Atg 2 can be attributed to the result of a decrease in the uniformity in a-axis length from Atg1 to Atg 2 as observed by Mellini et al. (1987) on different types of antigorites across contact aureoles. In addition, the formation of secondary tremolites (Tr) after replacing Atg 1 indicates that Atg 1 to Tr reaction temperature was within tremolite stability field (>476°C). Hence, given the higher temperature of formation of Atg 2 phase than that of Atg 1, we suggest that Atg 2 was produced at a temperature range in between 500-600°C as a result of progressive regional metamorphism in the Tidding peridotites.

Acharyya, S. 1998. Jour. Nepal Geol. Soc 18, 1-17.
Andreani, M., Mével, C., Boullier, A., Escartin, J. 2007. Geochemistry, Geophysics, Geosystems 8.
Baronnet, A., Grauby, O., Andreani, M., Devouard, B. 2006. Macla 6, 15-17.
Caruso, L.J., Chernosky, J. 1979. International Geology Review 46, 479-506.
Evans, B.W. 2008. Journal of Petrology 49, 1873-1887.
Evans, B.W. 2010. Geology 38, 879-882.
Frost, B.R., Beard, J.S. 2007. Journal of Petrology 48, 1351-1368.
Gururajan, N., Choudhuri, B. 2003. Journal of Asian Earth Sciences 21, 731-741.
Majumdar, A.S., King, H.E., John, T., Kusebauch, C., Putnis, A. 2014. Chemical Geology.380, 27-40.
Mellini, M. 1982. American Mineralogist 67, 587-59E.
Mellini, M., Trommsdorff, V., Compagnoni, R. 1987. Contributions to Mineralogy and Petrology 97, 147-155.
Mellini, M., Viti, C. 1994. American Mineralogist 79, 1194-1198.
Misra, D. 2009. Journal of the Geological Society of India 73, 213-219.
Ningthoujam, P., Dubey, C., Lolee, L., Shukla, D., Naorem, S., Singh, S. 2015. Journal of Asian Earth Sciences.
Singh, S. 1993. Jour. Himalayan Geol 4, 149-163.
Valdiya, K.S. 1998. Dynamic Himalaya. Universities press.
Wadia, D. 1931. Rec. Geol. Surv. India 65, 189-220.

Seismotectonics of the Garhwal Himalaya region of Central Seismic Gap in Northwest Himalaya, India

Arun Prasath R.[1,*], Ajay Paul[1], Sandeep Singh[2]
[1]*Wadia Institute of Himalayan Geology, 33 GMS Road, Dehradun 248001, INDIA*
**devanthran@hotmail.com*
[2]*Department of Earth Sciences, Indian Institute of Technology, Roorkee 247667, INDIA*

This work is a result of an analysis of 353 earthquakes of western Central Seismic Gap recorded by a seismic network in Garhwal region. The data magnitudes (ML) range from 1.8 to 4.9 in the span of six and half years from July 2007 to December 2013. The epicentral location map indicates that the seismicity in Garhwal Himalaya is concentrated in a narrow 25-35 km wide zone trending parallel to the Main Central Thrust (MCT). On the basis of the magnitude, epicentral location and hypocentral proximity, six clusters along the three profiles are selected for further analysis. From the Composite Focal Mechanism Solutions (CFMS) of these clusters and dip angles, we suggest that the MCT is active in eastern and western parts in contrast to the central part of Garhwal Himalaya. The location of events in the central part and their dip angle (20º) from the CFMS suggests that these earthquakes have their origin from the mid-crustal ramp that lies in the transition zone between the seismically active detachment under the Lesser Himalaya and aseismically slipping detachment under the Higher Himalaya at 16º. It is inferred from CFMS that compression in the NW-SE direction is the main stress in Garhwal Himalaya.

Influence of site conditions on ground response at stations in Bihar and Uttar Pradesh due to Nepal Earthquake

Babita Sharma, Sumer Chopra, Varun Sharma
National Centre for Seismology, New Delhi, INDIA

A large earthquake of magnitude 7.9 occurred in the central Nepal region on 25th April, 2015 at 11:41 hrs (IST). The epicentre of this earthquake was at 28.1°N and 84.6°E. The earthquake occurred at a depth of around 15 km. The earthquake was located 34 km ESE of Lamjung and around 80 km NW of Kathmandu city. The earthquake has occurred at the detachment where Indian plate is subducting below the Eurasian plate. The earthquake has ruptured a large, gently dipping thrust fault. The Indian plate is subducting below the Eurasian plate at a rate of 17-21 mm/yr and the resulting strain is periodically released during major/large/great earthquakes. In 1934, an earthquake named as Bihar-Nepal earthquake with magnitude 8.1 occurred in this region (Kayal, 2014). The April 25, 2015 earthquake has occurred about 200 km west of the 1934 earthquake. In the present study, the effect of ground geology on the acceleration response spectra is evaluated at 11 sites situated in Uttar Pradesh and Bihar States of the India. For this purpose, Nepal Earthquake (Mw 7.9) of 25th April, 2015 and its associated aftershocks (Mw 6.6 and 6.9) along with an earthquake occurred on 12th May, 2015 (Mw 7.2) have been used for the analysis. All the sites used it the present analysis are located on alluvium deposits. Peak Ground Acceleration (PGA) ranges from 3 to 80 cm/sec^2 for the network of UP and Bihar for the epicentral distance range of 120 km to 495 kms in case of Nepal earthquake. The Peak Ground Velocity (PGV) varies from 1 to 16 cm/sec while the Peak Ground Displacement (PGD) lies in between 1 to 37 cm for the same sites. Normalised responses spectra are determined from the strong ground motions recorded from these sites related to Nepal Earthquake are evaluated. It has been observed that stations located on alluvium deposits show peak at 0.24 seconds for horizontal components and at 0.19 seconds for vertical components. It has been observed that acceleration response spectra at sites are influenced by local site conditions. The results obtained are compared

with the BIS code which shows that the current Indian code applicable for the entire country is within the structural limits proposed for the seismic forces at all periods for alluvium sites. These response curves are useful for the engineering practices to implement new projects in the area of study or to strengthen the existing structures.

A sedimentological reappraisal of the Oligocene unconformity at the Bhainskati-Dumri transition in Nepal Himalaya

Bithika Das*, Arpita Sreemany, Melinda Kumar Bera
Department of Geology and Geophysics, IIT Kharagpur, Kharagpur 721302, INDIA
**dasbithika31@gmail.com*

A peripheral foreland basin, bordering the Himalayan mountain chain to the south, started forming after the collision between India and Asia at ~50 Ma (Najman et al., 2004; Green et al., 2008). It is long believed that the silicate weathering in the front of the rising Himalayan mountain chain is responsible for consumption of atmospheric carbon dioxide thus promoting late Cenozoic (Eocene-Oligocene Boundary) climate change from greenhouse to icehouse Earth (Raymo and Ruddiman, 1992; Zachos et al., 1999; DeConto and Pollard, 2003; Pearson et al., 2009). It has been considered that the sediments deposited in this peripheral foreland basin preserve the record of this climatic shift (DeCelles et al., 1998, 2004; Najman et al., 2004). Earlier works on these sediments proposed an initial phase of marine sedimentation and followed by continental fluvial sediment during Middle Eocene to Early Miocene. Presence of a long duration unconformity (~14 Ma), which is separating the marine and fluvial deposits, spanning Late Eocene-Oligocene has been proposed by the earlier workers using

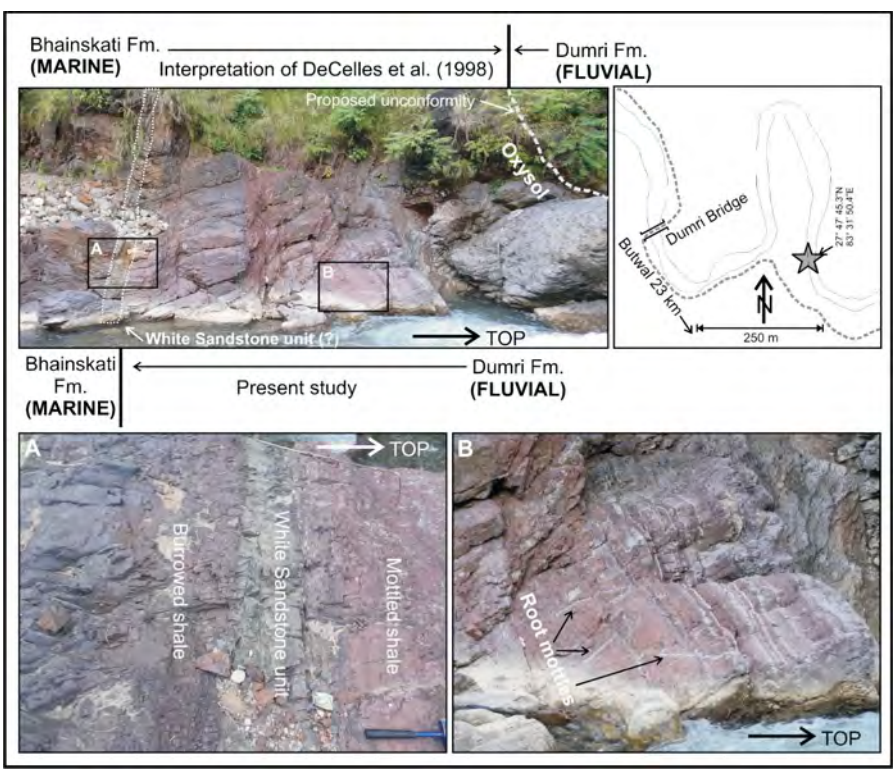

Fig. 1. Showing the location and field photograph of the Bhainskati-Dumri transition in t.....

detrital chronology (DeCelles et al., 1998, 2004; Najman et al., 2004). However, detailed field documentation and sedimentary processes based study of the unconformity, so critical to our understanding of the tectonically forced Late Cenozoic climate change, is still lacking. Controversy exists regarding the presence or absence of the unconformity and its duration (DeCelles et al., 1998, 2004; Najman et al., 2004, 2005; Bera et al., 2008, 2010; Bera and Mandal, 2013). Field observations in the type locality near Dumri Bridge, where the transition from marine Bhainskati to fluvial Dumri Formation rocks are exposed in the lesser Himalaya of Nepal, suggest soil development starts well before the proposed unconformity related oxysol (Fig. 1). This red shale unit lying below the oxysol horizon shows characteristic vertical to sub vertical mottles characteristic of root traces. Further down in the sequence, a characteristic greenish-white coloured, tabular sandstone unit of 35 cm thickness has been observed. Amalgamated lenticular bed sets, mud rip up clasts at base, and wave ripples at top indicates its deposition in a marginal marine environment: possibly shoreface. Interestingly, this unit separates the burrowed shale at below from the mottled red shale at top. Based on the above evidences we suggest that this unit to be equivalent of the White Sandstone unit exposed throughout the entire western Himalayan foreland in India (Bera et al., 2008, 2010; Bera and Mandal, 2013). No signature of very long ranging unconformity above the White Sandstone unit in Nepal has been documented in the present study and indicates a more gradual marine to continental transition in the Nepal Himalayan foreland without a long duration unconformity.

Quantitative geomorphic analysis indicating rejuvenation of the Main Central Thrust in Beas Basin within Larji-Kullu Window Domain, Higher Himalayas, India

Brijendra K. Mishra[1,*], G. Prusty[1], A. Chattopadhyay[2]
[1]Defence Terrain Research Laboratory DRDO, New Delhi 1100541, INDIA
[2]Department of Geology, University of Delhi, New Delhi 1100072, INDIA
**brijsmishra@gmail.com*

Himalaya is one of the most active and fragile mountain ranges in the world with numerous fault systems causing mass erosion. The north dipping Main Central Thrust (MCT) is assumed to be stable in terms of tectonic upliftment since the last tectonic activity in the early Miocene age (An Yin 2006, Webb et al, 2011). Geomorphic signatures are the key factors to identify or observe the ongoing tectonics in the Himalayan belt (Valdiya, 2002). Hypsometric Integral value (Strahler, 1952) and Elongation ratio factor of individual drainage basins are very sensitive to both tectonic uplift rates and variations in erosional resistance of different lithological and tectonic units. The present study is focused on the quantitative analysis of the geomorphic characteristics and the geometry of the Beas basin within the Larji-Kullu tectonic window to determine the ongoing tectonic signals if any. The study area is located in the Beas basin (Lat. 31°57'30" N; Long. 77°06'41" E) of Himachal Pradesh (India) in the Western Himalayas with an area of 4236.45 sq km. The MCT and the Kullu thrust are the two major tectonic attributes of the Largi-Kullu window domain cross-cutting the upper Beas basin. Here, the entire study area is categorized into three lithotectonic segments namely, (i) above the MCT, (ii) between MCT and Kullu Thrust, and (iii) below the Kullu Thrust (Fig. 1). Interestingly, it is observed that all the three segments have similar lithological units' viz. quartzite-schist-phyllite-gneisses and any dependence of morphologic parameters on lithology could not be inferred.

Our study characterizes the Larji-Kullu window domain with respect to the lithotectonic domain and identifies the second and third order drainage basins for the analysis. Twenty-one drainage basins have been identified using ASTER DEM (30 m) and LISS-III Imageries of IRS P6 satellite for the morpho-metric analysis irrespective of scale.

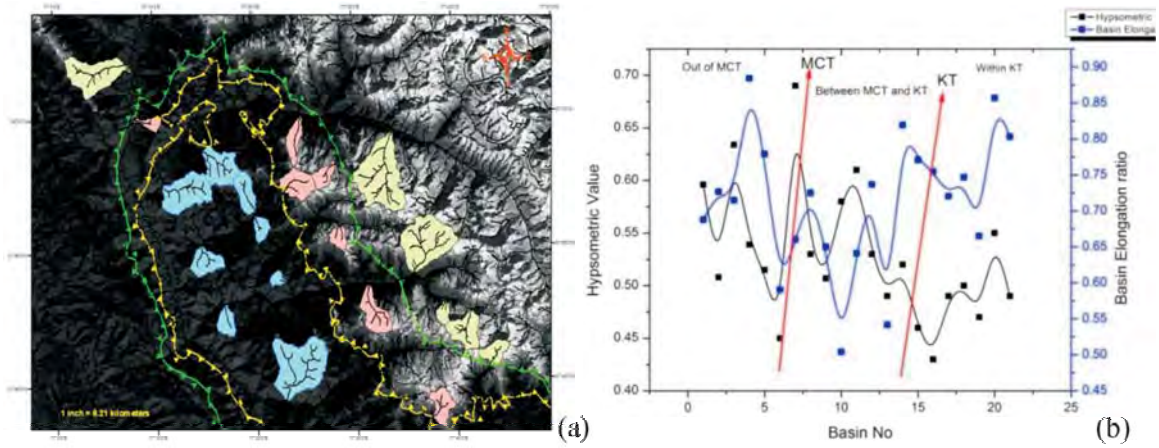

Fig. 1. Shows the basin selected for the study and, figure 2 graphs indicate the results of and correlation of the HI value and ER value and observe good correlation and picked the anomaly *HI- Hypsometric Integral , ER- Elongation Ratio.

The hypsometric integral, which expresses the morphological characteristics of a drainage basin by a single value, the curves with integrals larger than 0.60 were considered to be in an "inequilibrium stage" i.e, tectonically active and those with the values in the range of 0.60 to 0.40 in an "equilibrium stage" (Strahler, 1952; Ohmori, 1993). It was further stated that the basin elongation ratio (ER) between 0.60 and 0.80 indicates the basin is elongated with higher level of denudation occurring in the basin. Closer inspection of the observed results of the analysis demonstrates that the outer segment i.e., Above the MCT or the hanging wall block of the MCT is characterized by the HI values ranging between 0.49 and 0.65 and the ER values from 0.53 to 0.73. In contrast, the middle segment between MCT and Kullu Thrust has the HI values ranging from 0.59 to 0.79 and ER values are between 0.45 and 0.69. However, the inner loop below Kullu Thrust has HI and ER value ranging from 0.33 to 53 and 0.69 to 0.81, respectively (Fig. 2). The digital geomorphic attributes of the study area were analyzed for an in-depth interpretation of the tectonic setup.

The extracted Quantitative records of hypsometric integral curves and elongation ratio of the 21 sub-basins indicates that the window domain is undergoing tectonic disturbances in the recent time. The study also reveals that the Beas basin within the Larji-Kullu Window can further be categorized into relative active tectonic zone. The middle zone characterized by footwall block of MCT and hanging wall block of Kullu Thrust (Fig. 1) is tectonically most active whereas the inner loop zone below the Kullu Thrust is least active. The earlier researchers have concluded that MCT is inactive since Miocene age. Our findings based on morphotectonic indices have revealed the rejuvenation of MCT in this part of Himalayas within the Larji-Kullu window and it is leading to higher denudation processes.

Alexander, A., Webb, G., Yin, A., Harrison, T.M., Célérier, J., Gehrels, G.E., Manning, C.E., Grove, M. 2011. Geosphere 7 (4), 1013-1061.
Ohmori, H. 1993Geomorphology, 8, 263-277.
Strahler, A.N. 1952. Bulletin of the Geological Society of America 63, 1117-1142.
Valdiya, K.S. 2002. Progress in Physical Geography 26 (3), 360-399.
Yin, A. 2006. Earth-Science Reviews 76, 1-131.

Impact of 25th April 2015 Nepal Earthquake in Bangladesh

A.K.M. Khorshed Alam[1,*], Aktarul Ahsan[2]
[1]*Bangladesh Geological Society, BANGLADESH*
**akmkhorshed@gmail.com*
[2]*Geological Survey of Bangladesh, 153 Pioneer Road, Segunbagicha, Dhaka 1000, BANGLADESH*

The 25th April 2015 Nepal Earthquake of 7.8 magnitude shook almost entire Bangladesh and afterwards the necessity to assess and document the impact of the quake in the country was felt. The main objective of the work was to record the impacts with an intension that the document might be used as future reference. It is based on the information published in the national daily newspapers, interviews with local residents, information from government documents, data from different relevant national and foreign websites, and site visits only in Dhaka city. The document describes the feelings of the people, impact on natural objects and man-made structures. The main shock and aftershocks resulted in few casualties and little damage to structures, but those created panic among the large population of the country including the capital city. Most of the frightened people ran away from homes, offices and workplaces out of fear, and many of them became injured and some of them needed hospital treatment. However, result of the study brought the panicky situation created among the majority of the population at the fore front. This event has given us a lesson that our people needs to be aware and trained to cope with the earthquake occurrence. But long term preparedness for the safety of about 160 million populations from earthquake hazard must be taken from geologic and engineering points of view considering Bangladesh's location in a tectonically active region with mostly thick cover of unconsolidated Holocene alluvial and deltaic sediments.

Effect of changing snow grain size on its Albedo

Ankur Dixit, Vaibhav Garg, Shiv Prasad Aggarwal
Water Resources Department, Indian Institute of Remote Sensing, ISRO, Dehradun 248001, INDIA

Cryosphere plays a significant role to control radiation budget of the earth. The snow is a part of cryosphere which is present in the porous form of ice and mixed with air and other impurities like dust. The reflectance of snow is very high in visible region of electromagnetic spectrum but decrasing towards the near infra-red. The snow albedo also depends on its grain size (Wiscombe and Warren, 1980; Warren and Wiscombe, 1980; Aoki et al., 2003; Negi and Kokhanovsky, 2011), so this may be a factor which can be essential to study climate change studies. After the deposition of fresh snow it changes its properties like shape, size, density, etc cause of metamorphism. This snow cover is also very important for various other fields such as water resources, climate change, hydropower projects etc. So the monitoring of the snow cover can help in many ways to the human and other living species on the planet. In this study snow grain size has been calculated for the Beas river basin in Himachal Pradesh, part of North Western Himalaya. Since grain size affects its albedo so this study is focused to find out the trend of albedo due to changing snow grain size. To calculate the grain size we have used hyperspectral dataset Hyperion. The snow grain size has been calculated and compared with the albedo of the area. Since the albedo of freshly fallen snow is very high in the visible region of spectrum and decreases with the age of snow but in near-infrared this decrement is in considerable figure (O'Brien and Munis, 1975; Warren and Wiscombe, 1980; Wiscombe and Warren, 1980; Singh et al., 2010).

O'Brien, H.W., Munis, R.H. 1975. CRREL Res. Rep., 332.
Negi, H.S., Kokhanovsky, A. 2011. The Cryosphere.

Singh, S.K., Kulkarni, A.V., Chaudhry, B.S. 2010. Annals of Glaciology.
Wiscombe, W.J., Warren, S.G. 1980. J. Atmos. Sci., 37, 2712-2733. doi:10.1175/1520-0469(1980)037.
Warren, S.G., Wiscombe, W.J. 1980. J. Atmos. Sci., 37, 2734-2745. doi: 10.1175/1520-0469(1980)037.

$\delta^{18}O$, δD and $^{87}Sr/^{86}Sr$ isotope characteristics of the Indus River Water System

Anupam Sharma[1,*], Shailesh Agrawal[1], Amzad Laskar[2], Sunil Kumar Singh[2]
[1]Birbal Sahni Institute of Palaeobotany, 53 University Road, Lucknow 226007, INDIA
**anupam110367@gmail.com*
[2]Physical Research Laboratory, Navrangpura, Ahmedabad 380009, INDIA

The Indus River originating from the northern slope of mount Kailash near Mansarovar Lake in Tibet forms the largest fresh water system, which is comprised of several west flowing rivers of the Indian subcontinent, finally debouching in the Arabian Sea. The Indus and its major tributaries (Zanskar, Shyok, etc.) in the trans-Himalayan upper reaches are commonly fed by glaciers, however, in relatively lower reaches, the contribution from SW monsoon is equally important. Since, the Indus River System (IRS) constitutes one of the most fertile lands of Punjab in the Indian subcontinent, it is important for us to understand the moisture source to this system having wider implications including climate change for which the signature are preserved in different palaeoclimatic archives.

The isotopic (hydrogen, oxygen, and strontium) characteristics of Indus River, particularly in the Indian sector was studied earlier on very limited extent as compared to the Pakistan's counterpart (Pandey et al., 1994, 2000), the present work would complement the previous studies and bring new insights to our understanding. In the current investigation, $\delta^{18}O$ and δD values of water from IRS (Indus River System) have been integrated with the current work and data of Karim and Veizer (2000) to understand the spatial variations in the isotopes of water and d-excess as well as sources of moisture. The headwaters of the IRS largely receives water from the glacier melting and the moisture sources for these glaciers are derived both from the monsoonal air-mass from the Bay of Bengal, Arabian Sea and mid-latitude Central Asian air-mass sources. River water samples were collected from Loma to Batalik of the Indus main channel and its tributaries such as Zanskar, Shyok, Tangse etc. and several other relatively smaller streams (nallahs) (Fig. 1), the water of IRS is characterized by distinct isotopic trend. The $\delta^{18}O$ values of IRS ranges from -16.9 to -12.5‰, whereas δD values range from -122.8 to -88.5‰. Indus river and its tributaries like Zanskar, Nubra and Shyok rivers are characterized by relatively lower $\delta^{18}O$ values whereas Tangse and other small tributaries contributing to the Indus are relatively enriched in heavey isotopes (in $\delta^{18}O$). In the upstream part (between Loma and Choglamsar) of the Indus River, the $\delta^{18}O$ values vary between -14.8 to -14.3‰ only, however, the $\delta^{18}O$ values remarkably drop from Spituk site onwards. The lower $\delta^{18}O$ values may be explained if there is mixing of very low $\delta^{18}O$ containing water. Interestingly, the $\delta^{18}O$ value of Zanskar River before the confluence with Indus River is -16.9‰. The mass balance calculation suggests that if the Zanskar and Indus rivers contribute 55% and 45% of water with $\delta^{18}O$ values of -16.9‰ and -15.4‰, respectively then an average value of -16.1‰ can be achieved, however, individual streams (nallahs) do not affect the isotope chemistry of the Indus River due to their low water discharge rate compared to major tributaries or the main channel of the Indus itself. The cross plot between δD and $\delta^{18}O$ values for IRS shows linear correlation (correlation coefficient r = 0.97) and the best fit line set point derived is $\delta D = 7.876*\delta^{18}O + 11.41$ which is very close to Global Meteoric Water Line (GMWL). It indicates that little evaporation occurs in these high altitude streams because steep gradient reduces the residence time of water in the Ladakh region. The Deuterium excess (d-excess) in the IRS varying between 7‰ and 17‰, which is distinctly higher than the long-term average for the Indian monsoon (~8‰) indicating contributions from the Mediterranean (22‰) or other inland seas.

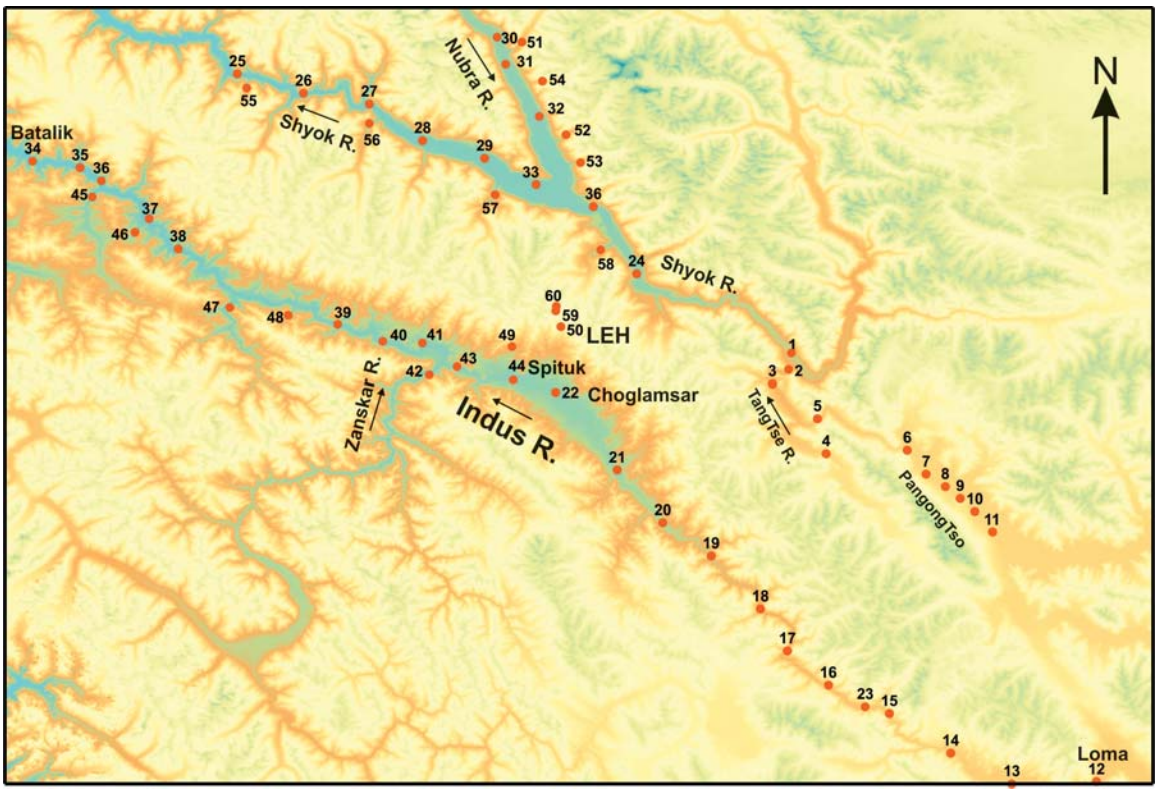

The Sr isotope of IRS varies between 0.70515 and 0.71291, wherein the Indus, Shyok and Nubra rivers are characterized by relatively high Sr isotope ratios (avg. 0.71086-0.71243) compared to the Zanskar and Tangtse rivers (Sr ~0.709). Similarly, small streams (nallahs), which joins the Indus and Shyok rivers, are also very unradiogenic ($^{87}Sr/^{86}Sr \leq 0.70878$). Overall, the relatively high Sr isotope ratio of the Indus, Shyok and Nubra rivers may be the result of higher abundance of granitoids (Ladakh and Karakoram granitoids) in their catchments.

Karim, A., Veizer, J. 2000. Chemical Geology, 170,153-177.
Pande, K., Sarin, M.M., Trivedi, S., Krishnaswami, K.K., Sharma, K.K. 1994. Chemical Geology 116, 245-259.
Pandey, K., Padia, J.T., Ramesh, R., Sharma, K.K. 2000. Proc. Indian Acad. Sci. (Earth Planet. Sci.) 109, 109-115.

Evidence of granulite grade metamorphism from Almora Nappe, Kumaun Lesser Himalaya

Mallickarjun Joshi[1,*], Ashutosh Kumar[1], S.B. Dwivedi[2]

[1]Centre of Advanced Study in Geology, Banaras Hindu University, Varanasi 221005, INDIA
**joshimallickarjun@gmail.com*
[2]Dept. of Civil Engineering, IIT (BHU) Varanasi 221005, INDIA

Crustal shortening during the Himalayan orogeny (Eocene-Oligocene) resulted in the southward tectonic transport of several metamorphic nappes and klippes from the Higher Himalaya that presently rest over the Lesser Himalayan sedimentaries with a tectonic discontinuity at their base. This tectonic discontinuity named variously in different areas is largely accepted to be a continuation of the Main Central Thrust (MCT) separating the Higher Himalayan metamorphics

from the tectonically underlying low grade metasedimentary sequences. One of the largest such nappe, viz. the Almora Nappe located in the Kumaun Lesser Himalaya is accepted by almost all workers to be conforming to this tectonic set up. The Almora Nappe comprises multiply folded interbanded sequence of metapelites and metapsammites comprising the Late Palaeoproterozoic Almora Group dated by Trivedi et al. (1984) at ~1860 Ma by Rb-Sr method. These metapelites have reached the granulite grade conditions of metamorphism. Based on field, petrographic and P-T pseudosection studies it is demonstrated that the metamorphics definitely crossed the second sillimanite isograd, viz. the reaction, quartz+muscovite = K-feldspar+sillimanite+ H_2O (1) Petrographic evidence further suggests that the next higher temperature reaction viz. quartz+plagioclase+muscovite = K-feldspar+sillimanite+H_2O (2) was also touched as there are clear reaction boundaries between quartz and plagioclase, quartz and muscovite and muscovite and plagioclase. The boundaries among quartz, plagioclase and muscovite are corroded evidencing the arrested reactions (1) and (2). Both the reactions led to the anatectically produced K-feldspar-sillimanite bearing Almora Gneisses. A P-T pseudosection in NCKFMASH system with phases involving garnet, biotite, muscovite, plagioclase, K-feldspar for the Almora Gneisses clearly documents the P-T field (2-8 kbar/400-1000°C) of the mineral phases, the biotite-garnet-sillimanite-K-feldspar-plagioclase-perthite-quartz at the specific bulk composition of the studied gneisses. The peak metamorphic conditions for the Almora Nappe calculated by Joshi and Tiwari (2009) are located within the P-T space computed for the pseudosection in the present work as the P-T range (6.9-7.9 kbar/694-709°C) falls largely within the field of the biotite-garnet-plagioclase-K-feldspar-sillimanite-quartz assemblage. It is evident from the pseudosection thermometry in conjunction with the textural relations that the temperatures of at least 760°C were exceeded in the area. Thus the area has reached the granulite grade metamorphism for certain.

Root zone of the Almora Nappe is largely accepted to be the Munsiari Formation comprising the lower most part of the inverted metamorphic sequence in the Higher Himalaya by earlier workers (Valdiya, 1980 and others). However, it is clear that the grade of metamorphism affecting the Munsiari Formation (450°C/4 kbar) is far lower than that of the granulite grade conditions reached by the Almora Gneisses of the Almora Group. Moreover, Joshi and Tiwari (2009) have documented that the metamorphic isograds in the Almora Nappe are folded and the Almora Nappe cannot be considered to be part of an inverted metamorphic sequence. Thus it is inferred that the largely accepted correlation of the Almora Group of rocks with the Munsiari Formation of the Higher Himalaya does not seem valid and the root zone of Almora Nappe lies elsewhere.

Organic matter preservation and mobilization of REE and trace element in paleolsol: a multiproxy study from the Siwalik paleosols Of Nurpur, Himachal Pradesh

Biswajit Roy*, S. Ghosh, P. Sanyal
Department of Earth Sciences, IISER Kolkata, Mohanpur 741246, INDIA
**br13ip038@iiserkol.ac.in*

The distribution and preservation of Soil Organic Matter (SOM) depends on productivity and grain size of soil (Wynn and Bird, 2006, 2007). The climatic parameters play key role in controlling productivity as well as sedimentation in overbank area of fluvial system. Although many studies have been carried out to understand the productivity (past vegetation) and climate using SOM but the factors which control preservation of SOM in overbank sediments have not been well studied. For example, $\delta^{13}C$ values of SOM from the late Miocene Siwalik paleosol have been used extensively (Sanyal et al., 2004, 2005, 2010) but factors controlling the preservation of SOM is unexplored. The

soil forming processes remobilizes the elemental concentration in different horizons of soil. The relation between pedogenesis and remobilization of elements in paleosol is also unknown. In this study, an attempt has been made to understand the preservation of SOM and mobilization of elements by using major oxide, REE along with long chain n-alkane δD and concentration from the Nurpur Siwalik of Himachal Pradesh.

In Nurpur area, the overbank sediments are characterized by siltstone, mudstone and considerable amount of paleosols. The paleosols are accretionary in nature and thus preserve the effect of deposition and removal at successive flooding events. The paleosol derived long chain n-alkane δD, a proxy to understand paleo-rainfall show good correlation with n-alkane (C25-C35) concentration suggesting climatic influence on SOM mobilization within overbank area. Chemical Index of Alteration (CIA) value of these paleosol unit indicate moderate to high pedogenesis (McLennan, 2001; Abdou and Shehata, 2007) and it is also confirmed by positive correlation with Ba and n-alkane concentration.

These fine grained overbank units show a major control on the accumulation of REE, mostly the HREE. It is evident from the positive correlation between n-alkane concentration and Al_2O_3 (wt.%) with HREE. Both played an important role in remobilization of trace elements from overlying layers (O/A horizon) to underlying horizons. As the LREE are less immobile than HREE, during weathering process the HREE is removed from top layer of soil and accumulated in the underlying layer. The positive correlation of δD value with HREE implies mobilization of HREE (Yb, Tb, Lu) is more effective than LREE. The δD value along with Al_2O_3 (wt.%) also shows good relationship with trace elements like Uranium indicating rainfall and substrate control on mobilization of element in fluvial system.

Abdou, A.A., Shehata, M.G. 2007. Australian Journal of Basic and Applied Sciences, 1(4), 553-560.
McLennan, S.M. 2001. Geochemistry, Geophysics, Geosystems, 2(4).
Sanyal, P., Bhattacharya, S.K., Kumar, R., Ghosh, S.K., Sangode, S.J. 2004. Palaeogeography, Palaeoclimatology, Palaeoecology, 205(1), 23-41.
Sanyal, P., Bhattacharya, S.K., Kumar, R., Ghosh, S.K., Sangode, S.J. 2005. Palaeogeography, Palaeoclimatology, Palaeoecology, 228(3), 245-259.
Sanyal, P., Sarkar, A., Bhattacharya, S.K., Kumar, R., Ghosh, S.K., Agrawal, S. 2010. Palaeogeography, Palaeoclimatology, Palaeoecology, 296 (1), 165-173.
Wynn, J.G., Bird, M.I., Vellen, L., Grand-Clement, E., Carter, J., Berry, S.L. 2006. Global biogeochemical cycles, 20(1).
Wynn, J.G., Bird, M.I. 2007. Global Change Biology, 13(10), 2206-2217.

Role of a blind duplex in controlling shortening partitioning in the Darjeeling Sikkim Himalayan Fold Thrust belt

Chirantan Parui*, Kathakali Bhattacharyya
Department of Earth Sciences, IISER-Kolkata, Mohanpur 741246, INDIA
**cp13ip039@iiserkol.ac.in*

Lateral variation in structural architecture is observed in major Fold Thrust Belts (FTB) at various scales. Variation in stratigraphic thicknesses of the initial sedimentary basin, presence of transverse zone, along-strike lithological variation along the basal detachment zone are some of the recognized causative factors for such variation in FTBs. Existing mechanisms do not completely explain the lateral variation in the structural architecture observed in the Sikkim Himalayan FTB. The Lesser Himalayan duplex (LHD) geometry significantly varies laterally in this region with the structurally lower system, the Rangit Duplex (Bhattacharyya and Mitra, 2009), not well exposed east of the Teesta River (Fig. 1). Additionally, the number of Lingtse imbricates in its hanging wall are greater in the eastern part (Fig. 1; Parui and Bhattacharyya, 2014, Bhattacharyya et al., 2015). At a first order, such a lateral variation in the structural architecture indicates strain partitioning at the

scale of the constituent thrust sheets. In this study, we document and quantify the observed strain partitioning at both orogenic transverse- and grain-scales. Such a study can also provide insights into the structural and kinematic evolution of a deforming wedge as a whole.

In order to constrain the lateral variation in the structural architecture, we have initiated mapping over an area of ~1056 km^2 at 1:25,000 along four N-S and two E-W transects in the eastern Sikkim Himalaya. In this region, the convergence-related shortening is accommodated by a series of south-vergent folded thrust sheets: the Main Central thrust (MCT), Pelling Thrust (PT), LHD, Ramgarh Thrust (RT), Main Boundary Thrust (MBT), Main Frontal Thrust (MFT) (Fig. 1). In the hinterland, the MCT sheet is folded into a regional synform along 23°, 047° and carries the

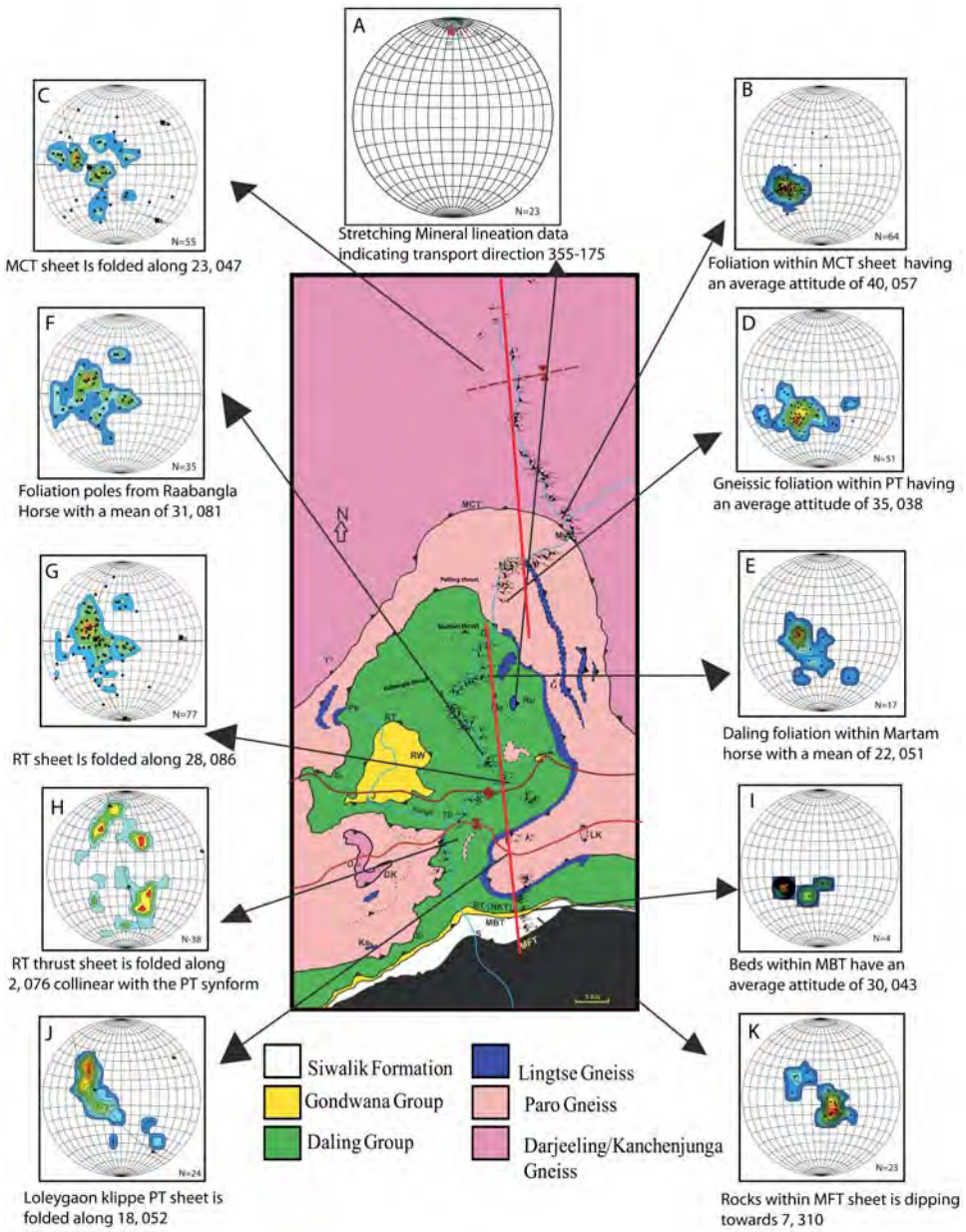

Fig. 1. Regional map of Darjeeling Sikkim Himalayan FTB modified after Bhattacharyya & Mitra (2009) with equal area projection of folded litho tectonic units. Red line marks the line of Cross Section.

Kanchenjunga gneiss of the Greater Himalayan sequence (GHS) in its hanging wall. The MCT fault zone is exposed near Mayangchu; the mylonitic foliation has an average attitude of 40°, 057° (Fig. 1B). In the footwall of MCT lies the PT that carries the Paro-Lingtse gneiss in its hanging wall (Bhattacharyya and Mitra, 2014). These form the lower Lesser Himalayan sequence (LHS). MCT and PT sheets are regionally folded into an antiform in the north along 28°, 086° (Fig. 1G) and a synform along 18°, 052° (Fig. 1J) in the south with a wavelength of ~29 km; the synformal core forms the Labha-Loleygaon klippe in the eastern Sikkim Himalaya (Fig. 1). In the immediate footwall of PT lies the structurally higher Daling duplex of the LHD with the northern Martam thrust, and the southern Rabangla thrust (Fig. 1). This imbricates repeat the quartzite and phyllite of the Daling Group of the lower LHS. The mean foliation in the Martam and Rabangla sheets are 22°, 051° (Fig. 1E) and 31°, 081° (Fig. 1F), respectively. The RT is the next major footwall imbricate that is folded along with the MCT-PT sheets, and is exposed south of the klippe. In the north of the klippe, the RT sheet is tightly folded into an antiform (10°, 107°) - synform pair (25°, 090°) with a wavelength of ~6.5 km. We interpret this structure as due to movement associated with underlying blind horses within the LHD. The next exposed imbricate is the MBT that carries Gondwana Group in its hanging wall. The MFT forms the major footwall imbricate of the MBT that separates the hanging wall Siwalik Group from the footwall Quaternary deposits.

We have used dip-spectral analysis, 'return to regional dip' principle, stratigraphic thickness data, template constraint and geophysical data to construct a preliminary, retrodeformable balanced cross section through the eastern Sikkim Himalaya (Fig 1). We have used stretching mineral lineation, hinge line data to constrain the regional transport direction at 355°-175°. We fixed the pin lines at the core of the northenrmost MCT sheet antiform in the N and at the undeformed footwall of the MFT in the S. Based on the "return to regional dip" argument, we estimated the dip of the basal detachment at 3.5° N. The basal detachment climbs from >25 km below the northern pin line, reaches a depth of ~10 km below the Daling horse and ramps at ~7 km north of the blind Rangit duplex. The Daling duplex comprises two hinterland-dipping, structurally upward facing horses (Mitra and Bhattacharyya, 2011). The PT is the roof thrust and the MHT is floor thrust of the duplex. The Rangit duplex is not exposed. Based on the balanced cross section, we interpret at least seven blind horses forming an antiformal stack to foreland dipping duplex. The roof thrust of the blind Rangit duplex is the RT, and the floor thrust is the MHT. Based on the preliminary cross section, we estimate a total, minimum shortening of ~483 km in the eastern Sikkim Himalaya; this does not include the shortening in the Tethyan Himalayan sequence (THS) that lies north of our study area. Using modified Fry method (Vollmer, 2011), we estimated penetrative strain from quartzite of the various thrust sheets. Preliminary strain analysis results suggest that there is no systematic decrease in the strain from the hinterland to the foreland. The PT records higher plastic strain than the MCT fault zone. The penetrative strain in quartzite from the Rabangla fault zone lying immediately north of the klippe is significantly high. Long axis of this strain ellipse is steeply plunging to the S. We interpret this orientation and magnitude of the strain ellipse as due to the effect of the underlying folded RT sheet, which in turn is folded by the growth of the blind duplex. We have initiated 3D strain elliposoid construction; they record flattening deformation.

A comparison of the existing shortening data from the western Sikkim transect (Mitra et al., 2010; Bhattacharyya et al., in revision; Bhattacharyya and Ahmed, in review) with these preliminary data from the eastern Sikkim Himalaya indicates that the total shortening accommodated within the LHS and the LHD are comparable from both these transects. Therefore, although the map pattern indicates a strong lateral variation in structural geometry of the LHS in this area, construction of a restorable balanced cross section reveals that the subsurface structural geometry remains somewhat similar in both the transects.

Bhattacharyya, K., Ahmed. F.(in review).
Bhattacharyya, K., Mitra, G. 2009. Gondwana Research, 16(3), 697-715.
Bhattacharyya, K., Mitra, G. 2014. Journal of Asian Earth Sciences, 96, 132-147.

Bhattacharyya, K., Mitra, G., Kwon, S., (in revision).
Bhattacharyya, K., Dwivedi, H. V., Das, J. P., Damania, S. 2015. Journal of Asian Earth Sciences.
Mitra, G., Bhattacharyya, K., Mukul, M. 2010. Special Issue J. Geol. Soc. India 75, 289-301.
Mitra, G., Bhattacharyya, K. 2011. Himalayan Geology, 32(1), 25-42.
Parui, C., Bhattacharyya, K., 2014. Rock Deformation and Structures (RDS-III) abstract, 13-14.
Vollmer, F.W. 2011. In: Geological Society of America Abstracts with Programs, 43 (1), 147.

Flash Floods in Gangotri and Kedarnath Region, Garhwal Himalaya, India

Dhruv Sen Singh
Centre of Advanced Study in Geology, University of Lucknow, Lucknow 226007, INDIA
Dhruvsensingh@rediffmail.com

The Gangotri and Chorabari glaciers are located at the head of the Bhagirathi valley and Mandakini valley, respectively, in the Garhwal Himalaya. They are characterized by thick supraglacial moraines, crevasses, kame terraces, lateral moraines, recessional moraines and out wash plains. Himalaya, birth place of perennial rivers of India which supports our agriculture system, has witnessed many disasters including the flash floods. The flash flood events are natural and had happened many times in the Himalayas in the past, however, the loss of life and properties have increased many times in recent years due to ignorance of natural laws and scientific facts and human intervention in the cycle of the natural system.

Flash floods are caused by bursting of glacial lakes or lakes which are formed by the blocking of rivers by landslides during heavy rain. The flash floods on 6th June, 2000 in Gangotri Glacier region was landslide lake outburst flooding (Singh and Mishra, 2001) and on 13th June, 2013 in Kedarnath Region was both glacial lake and landslide lake outburst flooding (Singh, 2013, 2014). The heavy rain and flash floods differentially erode the fine grained sediments from the pre-existing glacial landforms and deposit 1-3 m thick poorly sorted sediments on the outwash plain and river valley. Thus the facies of pre-existing landforms changes from matrix supported boulders to clast supported boulders and the new deposited sediments are matrix supported boulders.

The redistribution of enormous amount of sediments resulted in the modification of pre-existing glacial landforms/landscape. The modification of landforms and distribution of diamictons everywhere in these glaciated areas creates confusion and leads to misinterpretation. It leads to misconception of data in glaciated terrain presumably due to (i) directional and lithological similarity of lateral moraines of tributary glaciers to that of the recessional moraines of the main glacier, and (ii) modification of landforms by flash floods. Therefore, the flash floods are identified as event which, distributes the diamictons in the region and changes its facies from matrix supported boulder to clast supported boulder in the pre-existing landforms and matrix supported boulders in new deposits.

Variation of stress pattern in different sectors of north-west Himalaya and its implication on regional tectonics

Dilip Kumar Yadav*, Naresh Kumar, Devajit Hazarika
Wadia Institute of Himalayan Geology, 33 GMS Road, Dehradun 248001, INDIA
**yadavdk@wihg.res.in*

The Himalayan mountain chain is one of the most seismically active belts of the world that formed through collision and convergence of Indian and Eurasian plates over the last ~55 Ma. To understand the geodynamics and origin of clustered seismicity in NW Himalaya, it is essential to

investigate the existing stress beneath the region. The stress patterns of different seismic regimes of NW Himalaya are examined based on focal mechanism solutions (FPS) of moderate to higher magnitude earthquakes. The stress tensor inversions were carried out using FPS data. The selected FPS database includes about 150 earthquakes, recorded by present regional seismic network of the Wadia Institute of Himalayan Geology, Dehradun along with focal mechanism solutions of earlier published data (Yadav et al., 2009) as well as from published Centroid Moment Tensor solution of 50 selected earthquakes have been utilized for stress tensor analysis. The epicenters of these 50 events are mainly within higher Himalaya close to the Main Central Thrust (MCT) and few events are from the South Tibetan Detachment (STD) zone. Except few earthquakes of magnitude >6, rest of the mechanisms are oblique in nature with higher proportion of reverse/thrust components. Some events of Kinnaur region and the northern part of the India-Nepal border show normal faulting mechanism. The scrutiny of tectonic features suggests that these normal fault mechanisms are associated with South Tibetan Detachment (STD) where extension tectonic deformation exists.

The generated data set of fault plane solutions is utilized to extract the pressure and tension axes from each solution which are projected on the tectonic map to evaluate the linkage of stress pattern with tectonic elements. It is observed that most of the P-axes are oriented towards NE and nodal planes are aligned in NW-SE direction showing conformity with ongoing stress and orientation of existing major thrust faults/lineaments of NW Himalaya. The majority of nodal planes of these events are trending in N-S direction with T-axes trend in the E-W direction. This indicates the effect of E-W extension in these two regions and that is basically perpendicular to the strikes of major tectonics of the Himalaya. The stress tensor inversion study shows compressional stress regime for the Kangra-Chamba and the Garhwal-Kumaon regions and extensional regime for the Kinnaur region and in the northeastern part of study zone comprising the strata of south Tibet plateau. The occurrence of normal fault mechanism for deeper earthquakes (focal depth ~10-15 km) in the Kangra-Chamba region was also reported by previous study (Kumar et al., 2013). Based on earthquake data, the present study suggests diversity in the ongoing stress pattern in the NW Himalaya.

Kumar, N., Arora, B.R., Mukhopadhay, S., Yadav, D.K. 2013. J. Asian Earth Sci., 62, 638-646.
Yadav, D.K., Kumar, N., Paul, A. 2009. Himalayan Geology, 30 (2), 139-145.

Geochemical evolution of groundwater in the intermountain Una Basin, Himachal Pradesh, India

Divya Thakur, S.K. Bartarya*, Sameer K. Tiwari, H.C. Nainwal
Wadia Institute of Himalayan Geology, 33 GMS Road, Dehradun 248001, INDIA
H.N.B. Garhwal University, Srinagar, INDIA
**skbartarya@wihg.res.in*

Groundwater is the most prominent source of water for drinking and agriculture purposes. In India groundwater supports more than 60% irrigated agriculture and more than 85% drinking water supplies (World Bank reports, 2012). A noticeable decrease in groundwater level and its quality has been observed in many areas during the last few decades due to increased withdrawal to meet the water requirement for urban development, industrialization and irrigation. So there is an urgent need to understand the effects of natural and anthropogenic activities on groundwater level and its quality in the region. Because of the synclinal form, intermountain basins are natural hydrologic basins and have potential to hold good amount of water. The present study discusses geochemical evolution of groundwater in the Una Basin in the Outer Himalaya. Geologically, the basin consists of sandstone, clay, mudstone, shale and conglomerate of the middle and the upper

Siwalik Subgroups near the watershed boundary in the peripheral hilly region, and unconsolidated sand, gravels, cobbles and pebbles of quartzite, sandstone and shale set in a matrix of clay and sand in the valley fill deposits of central synclinal zone. Terraces, alluvial fans, hilly uplands and valley fills are the major geomorphic features in the area. The groundwater flows from hill towards valley through the geomorphological features.

The hydrochemical analysis of the water samples collected in the pre-monsoon season indicates Ca-Mg-HCO_3 type of water. Relatively higher concentration of Ca^{2+}, Mg^{2+}, K^+, Na^+, SO_4^{2-} and Cl^- are observed in hilly areas in comparison to valley area. Fence diagram and lithologs of the wells revealed that valley fills are dominated by gravel and sandy layers and medium fine sands. The scatter diagrams of SO_4+HCO_3 vs Ca+Mg, and Na vs Cl indicate predominance of ion exchange processes. The scatter plots of ions indicate that carbonate weathering is the main source of ions in the basin. As groundwater moves through sandstone, clay and mudstone rocks of the Siwalik succession, water-rock interaction increases Ca at the expense of Mg, Na, and K. Further down gradient, the concentration of ion decreases due to dilution from irrigation and low residence time of water to interact with aquifer material owing to high porosity and permeability of quaternary deposits. The higher concentration of ions in hill area than in valley fill suggests longer evolution period of groundwater in hill area than in valley fill. The correlation matrix of groundwater suggests that the variations in ionic relationships are due to the impact of lithology and groundwater level variation in the valley fill.

Similar Similar trend was observed in the isotopic ($\delta^{18}O$ and δD) ratio. A more depleted ratio of $\delta^{18}O/\delta D$ in the central synclinal region (valley fill) was observed indicating effect of local precipitation in recharging groundwater in this area. The source of water in the basin is primarily rain. Further d-excess (14 to 16 %) indicate that the source of water in the basin is primarily derived from SW monsoon.

Structural geometry of the Siang Window: Insights into far eastern Himalayan structural evolution

Farzan Ahmed*, Jonti Gogoi, Kathakali Bhattacharyya
Dept. of Earth Sciences, IISER Kolkata, INDIA
**fa13ip036@iiserkol.ac.in*

The Lesser Himalayan structures that lie in the footwall of the Main Central Thrust (MCT) accommodate ~50-75% of the convergence-related total shortening in the Himalayan Fold Thrust Belt (FTB) (Bhattacharyya and Ahmed, in review). These structures in the far-eastern Arunachal Himalaya are reasonably well exposed along the ~N-S trending Siang Valley, and therefore, provide a perfect platform to examine their role in the kinematic evolution of this segment of the Himalayan FTB (Ahmed et al., 2014). To decipher the kinematic sequence and to estimate the minimum shortening in this region, we have initiated construction of a regional, transport-parallel, balanced cross-section. We estimate grain-scale strain from the various thrust sheets to understand how strain is partitioned across these sheets in this region.

We have mapped 2800 km^2 area along transects oriented along N-S, E-W and SW-NE. We mapped the Ramgarh thrust (RT) at the western most part of our study area that separates the Daling Phyllite and schist in the hanging wall from the footwall carbonate and quartzite of the Buxa Formation of the lower Lesser Himalayan Sequence (LHS; Fig. 1). The RT is folded in an antifom along 8°, 031°. The Main Boundary thrust (MBT) is the next footwall imbricate carrying the Buxa carbonate in the hanging wall over the Abor volcanics in the footwall; the MBT develops transport-

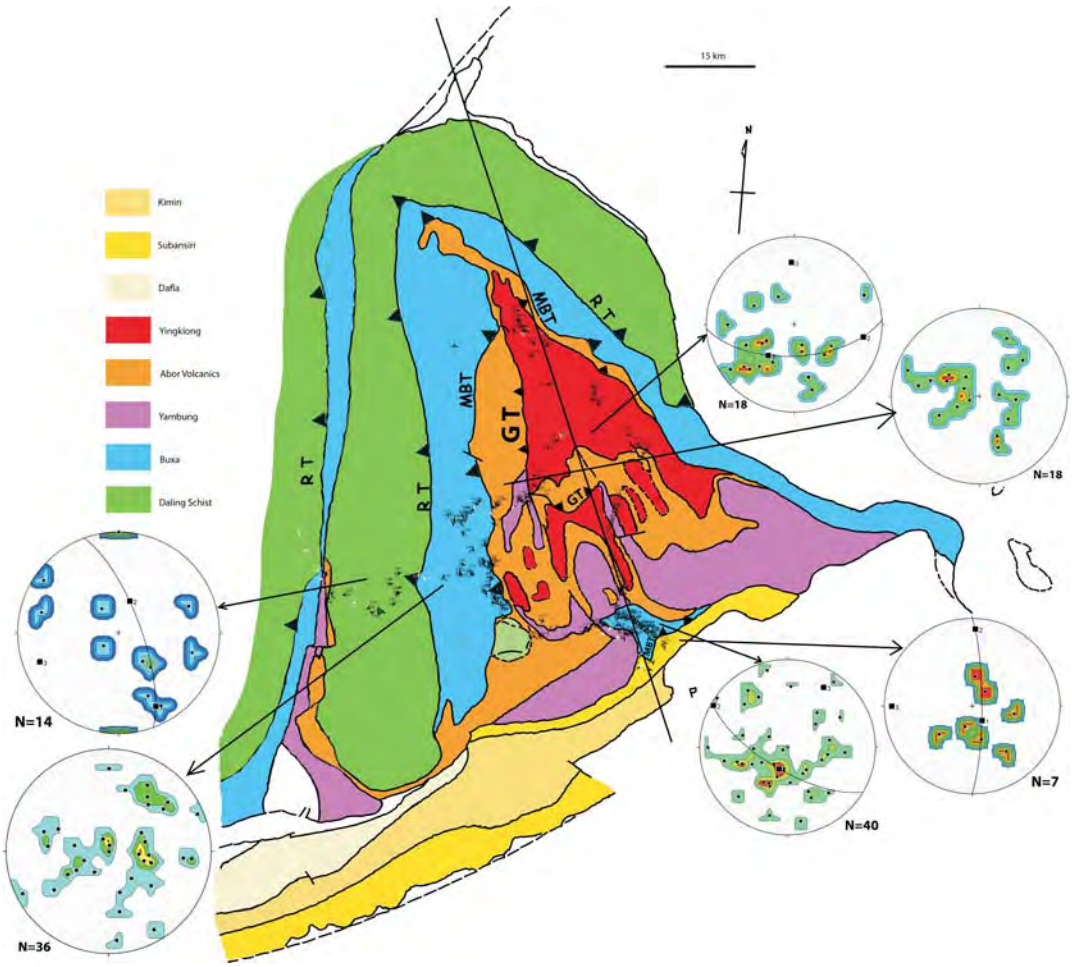

Fig. 1. Structural map of the Siang Valley (Modified after Acharyya, 1994), Arunachal Pradesh showing the different lithotectonic units, with structural data and poles of foliations of lihto-tectonic units plotted on stereoplots. MBT= Main Boundary Thrust, RT=Ramgarh Thrust, GT=Geku Thrust. R=strain ratio. Locations: P=Pashighat, A=Along.

perpendicular doubly plunging fold along 26°, 279° and 12°, 120°. The Abor volcanics lie in structural contact with the structurally underlying, younger, Yingkiong Formation along the Geku thrust (GT). The GT sheet also forms a doubly plunging fold along 29°, 280° and 17°, 040°. The MBT is repeated in the foreland and carries Buxa Formation over Subansiri Formation. The RT, GT and MBT are repeated at least twice and we identified at least six imbricates based on field work.

The doubly plunging folds are restricted to the middle of transect, and dies out in the southern imbricates. Such structures indicate structural culmination, possibly associated with structurally underlying duplex (Mitra and Bhattacharyya, 2011) (Fig. 1). To understand this structural geometry, we have initiated constructon of a preliminary balanced cross section in across this region.

Based on orientations of hinge lines in the foreland thrust sheets and stretching lineations, the transport direction is estimated at 342°-162°; the cross section is constructed along this transect. We estimated the thicknesses of the various thrust sheets with respect to outcrop widths, average foliation data, and slope of transects. The regional dip of the detachment is estimated at 2.2° from the hinge of the synform. Erosion through the RT and the MBT has exposed the footwall rocks in this region forming the Siang window. The undeformed footwall template is estimated at ~13 km. Based on our

preliminary data, we interpret the detachment to ramp from a depth of at least ~16 km in the northern end of the cross section where it breaks through the Yinkiong Formation. The footwall rocks Yingkiong and Abor volcanics are repeated at least in two and four imbricates, respectively. These imbricates define transport-perpendicular fault bend folds. In the foreland, the Buxa Formation is repeated in at least six imbricates. With progressive footwall imbrication, the detachment climbs up the stratigraphic section in the foreland part where it reaches a depth of ~7 km below the Siwalik Group. In the forelandmost MBT sheet the forelimb of the fault-bend fold is constrained by the southern dip of the Siwalik Group. The lower Siwalik unit is not exposed along our line of cross section.

In order to examine grain-scale strain partitioning among the various thrust sheets, we quantified 2D penetrative strain using modified Fry Method (Vollmer, 2011) from hinterland towards foreland starting from RT in the north followed by MBT and GT. We carried out the strain analysis in quartzite, sandstone and vesicular basalt. The penetrative strain progressively decreased in the thrust sheets from hinterland to foreland suggesting a forelandward progression of deformation. The strain also varied within the same thrust sheet as a function of its position within the sheet. For example, plastic strain decreased away from the MBT, the GT and the MFT fault zones. However, in the RT sheet that lies along the western end of our study area, the strain increases away from fault zone. This indicates the control of footwall structures that will be resolved through this study. Orientations of strain ellipses reveal ~55% transport-perpendicular and ~45% transport-parallel strain. These orientations suggest the control of the footwall imbricates of the RT on the hanging wall strain geometries. These rocks record overall flattening strain. Comparison of our data with the nearest available data from the Bhutan Himalaya (Long et al., 2011) suggests lateral variation in strain partitioning in the Himalayan FTB. Vorticity analysis using rigid grain method indicates overall general deformation of the studied thrust sheets in Arunachal Himalayan FTB.

Acharyya, S.K. 1994. Himalayan Geology.
Ahmed, F., Gogoi, J., Bhattacharyya, K. 2014. S III 2014.
Bhattacharyya, K., Ahmed, F. (under review).
Bhattacharyya, K., Mitra, G. 2011. Jour. Structural Geology, 33, 1105-1121. doi:10.1016/j.jsg.2011.03.008.
Bhattacharyya, K., Mitra, G., Kwon, S. (under review).
Long, S., McQuarrie, N., Tobgay, T., Hawthorne, J. 2011. Journal of Structural Geology, 33(4), 579-608.
Mitra, G., 1994. Journal of Structural Geology, 16 (4), 585-602.
Vollmer, F.W. 2011. Geological Society of America Abstracts with Programs, 43(1).

Tracking collision tectonics in Himalaya using Magnetotelluric investigations

Gautam Rawat
Wadia Institute of Himalayan Geology, 33 GMS Road, Dehradun 248001, INDIA
**rawatg@wihg.res.in*

Electrical resistivity, sensitive to rheological properties, is an important parameter to understand geodynamic evolution of Himalaya, particularly understanding of the seismogenesis of earthquakes. Magnetotelluric (MT) investigations in order to derive subsurface electrical resistivity variations are now routinely being employed in Himalaya. Although, few profiles across different sector of Himalaya has been covered but most of them are delimited with the inaccessibility factors in this mountain terrain. Therefore most of profiles do not reflect image of all the tectonic units accessible in Indian region. We have attempted a profile of Broadband MT from Bijnaur to Mallari covering right from the Indo-Gangetic plains to Southern Tibetan Detachment (STD). Electrical resistivity cross-section across this profile in Garhwal Himalaya is dominated by low-angle north-east dipping intra-crustal high conducting layer (IC-HCL) with a ramp at the transition from the

Lesser to Higher Himalaya. We interpret the low resistivity of IC-HCL layer in a depth range of 10-15 km is caused by the fluid reservoirs formed by stalling of upward propagating metamorphic fluids and/or tectonically induced neutral buoyancy. The effect of fluids counteracts the fault-normal stresses, facilitating brittle failure at lower threshold and therefore explained clustering of hypocentres of great earthquakes on a surface defining the seismically active detachment beneath the Sub and Lesser Himalaya. Ramp symbolizes block of low shear strength and high degree of strain, which under the deviatoric stresses releases accentuated stresses into the brittle crust to generate small but more frequent earthquakes in the narrow Himalayan Seismic Belt. In the compressional regime of the Himalaya, the upward propagation of fluid fluxes through the over pressured zones allows to see mega thrust and shear zone as locales of concentrated seismicity. Integrating the resistivity cross section of Darcha-Mallari profile, which complement the Bijnaur- Mallari profile from STD, with this section shows continuation of mid crustal conductor toward north side, indicating the role of channel flow model in Himalayan tectonics. In this paper brief details of completed few magnetotelluric profiles along different sector of Himalaya with emphasis on Bijnaur-Mallari profile will be discussed.

Development of empirical relationships between Ground-Motion parameters and modified Mercalli Intensity for Nepal Region

Harendra K. Dadhich*, Sanjay K. Prajapati, Babita Sharma, Sumer Chopra
National Center for Seismology, Ministry of Earth Sciences, New Delhi-3, INDIA
** dadhich.harendra@gmail.com*

The devastating Gorkha earthquake, Mw 7.8 struck Nepal on 25th April, 2015 (6:11:26 UTC) and resulted in more than 8000 deaths destroyed approximately million of houses. Infrastructure worth 25-30 billions of dollars are reduced to rumbles (Bilham, 2015). The earthquake was widely felt in the northern part of India and caused severe damage in Nepal. Maximum intensity IX, according to the USGS report was observed in the meizoseismal zone surrounding the Kathmandu region (Goda et al., 2015). In the present study, we compiled available information from the print, electronic media and reports of damages and other effects caused by the event, and interpreted them to obtain Modified Mercalli Intensities (MMI) at over 175 locations. We have collected strong motion data from UP, Bihar and Uttarakhand and derived the empirical relationship between MMI and ground motion parameters using the least square regression technique. We have compared our relationship with the empirical relationships available for other regions of the world (Linkimer, 2008). Further, seismic intensity information available for historical earthquakes (Mw 8.0: 1934; Mw 6.6: 1980; Mw 6.8: 1988; Mw 6.9: 2011) which have occurred in the Nepal Himalayas along with the present intensity data has been utilized for developing an attenuation relationship for the studied region using two step regression analysis (William and Boore, 1981). The derived attenuation relation will help in assessing damage from a large earthquake that may occur in near future (earthquake scenario-based planning purposes) for the Himalayan region and can be applied in seismic hazard assessment.

Bilham, R. 2015. Nature Geoscience, 8, 582-584.
Goda, K., Kiyota, T., Pokhrel, R.M., Chiaro, G., Katagiri, T., Sharma, K., Wilkinson, S. 2015. Front. Built Environ. 1:8. doi: 10.3389/fbuil.2015.00008.
Linkimer, L. 2008. Rev. Geol. Amer. Central, 38, 81-94.
William, B J., Boore, D.M. 1981. Bull. Seismol Soc. Amer, 71 (6), 2011-2038.

Engineering geological investigations for the assessment of rock fall hazards between Janki Chatti and Yamunotri Temple, Yamuna Valley, NW Himalaya

Imlirenla Jamir, Vikram Gupta*
Wadia Institute of Himalayan Geology, 33 GMS Road, Dehradun 248 001, INDIA
**vgupta@wihg.res.in*

Rock fall, the fastest type of mass movement, frequently occur in the mountainous terrain along a vertical or sub-vertical cliff, particularly during early spring where there is abundant moisture and repeated freezing and thawing conditions. It can be of any dimension ranging from few cm to tens and hundreds of meter and poses serious threat to lives and properties of the people living in the area. In order to assess the rockfall hazards of an area, it is of utmost importance to carry out the engineering geological investigations, involving engineering geological characterization of rocks, depicting the magnitude and directions of the stresses on the slope.

The present study encompasses the engineering geological study on six km long bridle path between Janki Chatti and the Yamunotri shrine. It is located in the upper Yamuna valley at an elevation ranging between 2550 and 3150 m and follows along the river Yamuna. Geologically, the study area is located to the north of MCT and consists of rocks of the Higher Himalayan Crystallines mainly comprising quartzite, marble, augen gneiss and garnet bearing mica schist. These generally trend NW-SE dipping northeastward at an angle ranging between 40-80º. However, due to complex structural set up and folding, variable attitudes of rocks have been observed. In general, three sets of joints with one random joint at places have been recorded. Geomorphologically, the area is characterized by high relief and moderately dissected topography carved into high ridges and deep valleys. The valley slopes are generally steep to very steep (60-80º).

In-situ rocks are exposed all along the six km long bridle path. DEM of the area has also been generated using high resolution Cartosat-1 data. Numerous cross sections across the bridle path have been drawn to assess the break in slope. Foliation and joints readings have been taken at an interval of about 250 m or where there is change in orientation of joints or lithology. Thus along the entire stretch, readings at 24 locations have been taken. The rock-mass has been classified as per the slope rock mass rating (SMR) and the geological strength index (GSI) methods. The kinematic analysis of these discontinuities have also been carried out which confirms that the entire rock-mass in the area falls under completely unstable to partially stable categories. There are six stretches in the area where the rock-mass is completely unstable. The rock-mass behind the Yamunotri shrine, where thousands of pilgrims visit particularly during summer, is also unstable. It is further to be noted that a ropeway is planned between Janki Chatti and the Yamunotri shrines, thus the area demands an immediate intervention in terms of any structural measures so as to minimize the rockfall hazards.

Metamorphism and CO_2 production in collisional orogens: petrographic characterization of different CO_2-producing lithologies (Central Himalaya)

Giulia Rapa[1,*], C. Groppo[1,2], F. Rolfo[1,2], P. Mosca[2], P.K. Neupane[3]
[1]Dept. of Earth Sciences, University of Torino, ITALY
**giulia.rapa@unito.it*
[2]CNR-IGG, Via Valperga Caluso 35, Torino 10125, ITALY
[3]Nepal Academy of Science and Technology, Khumaltar, Lalitpur, NEPAL

Decarbonation reactions during regional metamorphism in "large-hot" collisional orogens are an important source of atmospheric CO_2, able to influence global climate through geologic time

(Gaillardet and Galy, 2008). The petrologic study of the CO_2-source rocks is consequently the key to successfully investigate the metamorphic CO_2 flux in the past. This contribution focuses on the distribution and petrographic description of different types of CO_2-source rocks (i.e. calc-silicate rocks) in the archetype of "large-hot" collisional orogens, the Himalaya. Fieldwork performed in central and eastern Nepal highlighted that calc-silicate rocks are widespread in the Greater Himalayan Sequence (GHS) and occur as: dm- to m- thick layers or boudins within medium- to high-grade metapelites in the lower portion of the GHS, vs. tens to hundreds of meter thick layers within anatectic gneisses in the structurally upper GHS.

Three different groups of calc-silicate rocks have been recognized, corresponding to different protolith compositions, and they can be described in terms of relatively complex chemical systems: (i) CFMAS-HC (CaO-FeO-MgO-Al_2O_3-SiO_2-H_2O-CO_2) system, significantly more abundant in the lower GHS; (ii) NCFMAS-HC (Na_2O-CaO-FeO-MgO-Al_2O_3-SiO_2-H_2O-CO_2) and (iii) NKCFMAS-HC (Na_2O-K_2O-CaO-FeO-MgO-Al_2O_3-SiO_2-H_2O-CO_2) systems, widespread in both the lower and the upper GHS.

In all groups, mineral assemblages vary with increasing metamorphic grade from lower to upper structural levels. The CFMAS-HC assemblages are represented by: (a) Cal+Tr±Qtz±Pl in impure marbles and by (b) Grt+Amp+Qtz+Pl±Zo±Cal (Cpx-absent), (c) Grt+Cpx+Qtz+Pl±Zo±Cal and (d) Cpx+Qtz+Pl± Zo±Cal (Grt-absent) in calc-silicate rocks.

The NCFMAS-HC assemblages consist of: (a) Grt+Cpx+Qtz+Scp+Zo±Pl and (b) Cpx+Scp+Zo+Qtz+Pl+Cal (Grt-absent). In the NKCFMAS-HC group the following mineral assemblages can be observed: (a) Cal+Mu+Phl+Qtz±Pl±Tr impure marbles; (b) Mu±Bt+Cal+Qtz+Pl (Kfs, Cpx and Grt-absent) phylladic micashists; (c) Mu+Bt+Zo+Scp+Grt+Qtz+Pl (Kfs and Cpx-absent) micaschist; (d) Bt± Mu+Kfs+Scp+Qtz+Pl±Zo (Cpx and Grt-absent), (e) Bt±Kfs±Scp+Qtz+Pl+Czo±Amp±Cpx±Cal (Grt-absent) and (f) Kfs±Bt±Scp+Qtz+Cpx±Zo±Cal (Grt-absent) calc-silicate gneisses and granofelses.

Many of these assemblages, especially those equilibrated at lower temperatures and still containing abundant phyllosilicates, are not easy to be recognized in the field and have been probably considerably overlooked in the past. Most of them do not contain calcite anymore, because it was completely consumed during prograde metamorphism; nevertheless, their role in the orogenic-CO_2 cycle should be considered. Detailed fieldwork and petrographic analysis are therefore indispensable tools to estimate the volumes of potential CO_2-source rocks in collisional orogens.

Gaillardet J., Galy A. 2008. Science, 320, 1727-1728.

Ionosphere Modelling Techniques for earthquakes perturbation from GNSS data - A review

Gopal Sharma[1], P.K. Champati Ray[1], S. Mohanty[2]

[1]*Geosciences and Geohazard Department, Indian Institute of Remote Sensing, Dehradun 248001, INDIA*

[2]*Department of Applied Geology, Indian School of Mines, Dhanbad, INDIA*

At low altitudes, electron content in the ionosphere shows substantial variation due to phenomena such as solar flares, magnetic storms and/or large magnitude earthquakes (Fatkulin et al., 1989; Liu et al., 2006). Most of the ionospheric studies have been carried out using ground based ionosonde and satellite radio beacon (Deshpande et al., 1976; Garg et al., 1977; Rastotgi et al., 1979); considerable emphasis has also been given on GPS (Global Positioning System) based Total Electron Content (TEC) measurements (Calais and Minster, 1995). In present study, we compiled the different

techniques adopted so far for examining pre-earthquake ionospheric anomalies by analysing the Total Electron Content (TEC) in the ionosphere. The various post processing techniques and its results are also discussed which could be of great important for adaptation of better methodology and processing techniques in future research. The study has been performed to understand a relationship between ionospheric electron content and earthquakes occurrences with special emphasize on Indian subcontinent which enhances researchers of the region and manifest in better earthquake precursor.

Calais, E., Minster, J.B. 1995. Geophys. Res. Lett., 22, 1045-1048.

Deshpande, M.R., Rastogi, R.G., Bhonsle, R.V., Sawant, H.S., Iyer, K.N., Dhar, B., Janve, A.V., Rai, R. K., Singh, M., Gurm, H.S. 1976. Proc. Symp., Boston, Mass., (A77-30501 13-46) Boston, Boston Univ., 268-288.

Fatkullin, M.N., Zelenova, T.I., Legenka, A.D. 1989. Phys. Earth Planet. Inter., 57, 82-87.

Garg, S.C., Vijayakumar, P.N., Singh, L., Tyagi, T.R., Somayajulu, Y.V. 1977. J. Radio Space Phys., 6, 190-196.

Liu, J.Y., Chen, Y.I., Chuo, Y.J., Chen, C.S. 2006. Journal of Geophysical Research, 111, A05304

Rastogi, R.G., Sethia, G., Chandra, H., Deshpande, M.R., Davies, K., Murthy, B.S. 1979. J. Atmos. Solar Terr. Phys., 41, 561-564.

Kinematics of the Tengchong Terrane in SE Tibet from the late Eocene to Early Miocene: Insights from coeval mid-crustal detachments and Strike-slip shear zones

Zhiqin Xu[1,2*], Qin Wang[2, 1*], Zhihui Cai[1], Hanwen Dong[1], Huaqi Li[1], Xijie Chen[1], Xiangdong Duan[3], Hui Cao1,Jing Li[3], Jean-Pierre Burg[4]

[1]State Key Laboratory of Continental Tectonics and Dynamics, Institute of Geology, ChineseAcademy of Geological Sciences, Beijing 100037, CHINA

**Xuzhiqin@gmail.com*

[2]State Key Laboratory for Mineral Deposits Research, Department of Earth Sciences, Nanjing University, Nanjing 210046, CHINA

[3]Geological Survey of YunnanProvince, Kunming 650051, CHINA

[4]Geologisches Institut, ETH Zurich, 8092 Zurich, SWITZERLAND

It is generally believed that the extrusion of SE Tibet was bounded by the dextral Gaoligong and the sinistral Ailaoshan-Red River strike-slip shear zones from the Oligocene to early Miocene. This study integrates field mapping, structural analysis and geochronology in western Yunnan (China), where foliated Precambrian basement rocks and late Cretaceous to early Eocene plutons are exposed to the west of the Gaoligong shear zone. We found that late Eocene to early Miocene flat-lying ductile shear zones were kinematically related to steeply dipping strike-slip shear zones. Four elongated gneiss domes (Donghe, Guyong, Yingjiang and Sudian) are cored by high-grade metamorphic rocks and pre-kinematic granite plutons, and bounded by top-to-NE detachments and NE-trending dextral strike-slip shear zones. Zircon U-Pb ages from LA-ICP-MS analysis and $^{40}Ar/^{39}Ar$ ages of micas and hornblende demonstrate that the flat-lying DongheDetachment (>35-15 Ma) and the Nabang dextral strike-slip shear zone (41-19 Ma) were sites of prolonged, mostly coeval ductile deformation from amphibolite to greenschist facies metamorphism. The Gaoligong shear zone experienced dextral shearing under similar metamorphic conditions between 32 and 10 Ma. Consistent $^{40}Ar/^{39}Ar$ ages of hornblende from the three shear zones indicate their contemporaneity at mid-crustal depth, causing the rapid exhumation and SW-ward extrusion of the Tengchong Terrane.The strain geometry and shear zone kinematics in the Tengchong Terrane are interpreted with folding of the anisotropic lithosphere around a vertical axis, the northeast corner of the Indian plate since 41 Ma. The newly discovered NE-trending Sudian, Yingjiang, and Lianghe strike-slip shear zones are subordinate ductile faults accommodating the initially rapid clockwise rotation of the Tengchong Terrane.The detachments caused mid-crustal decoupling and faster SW-ward extrusion below the sedimentary cover,

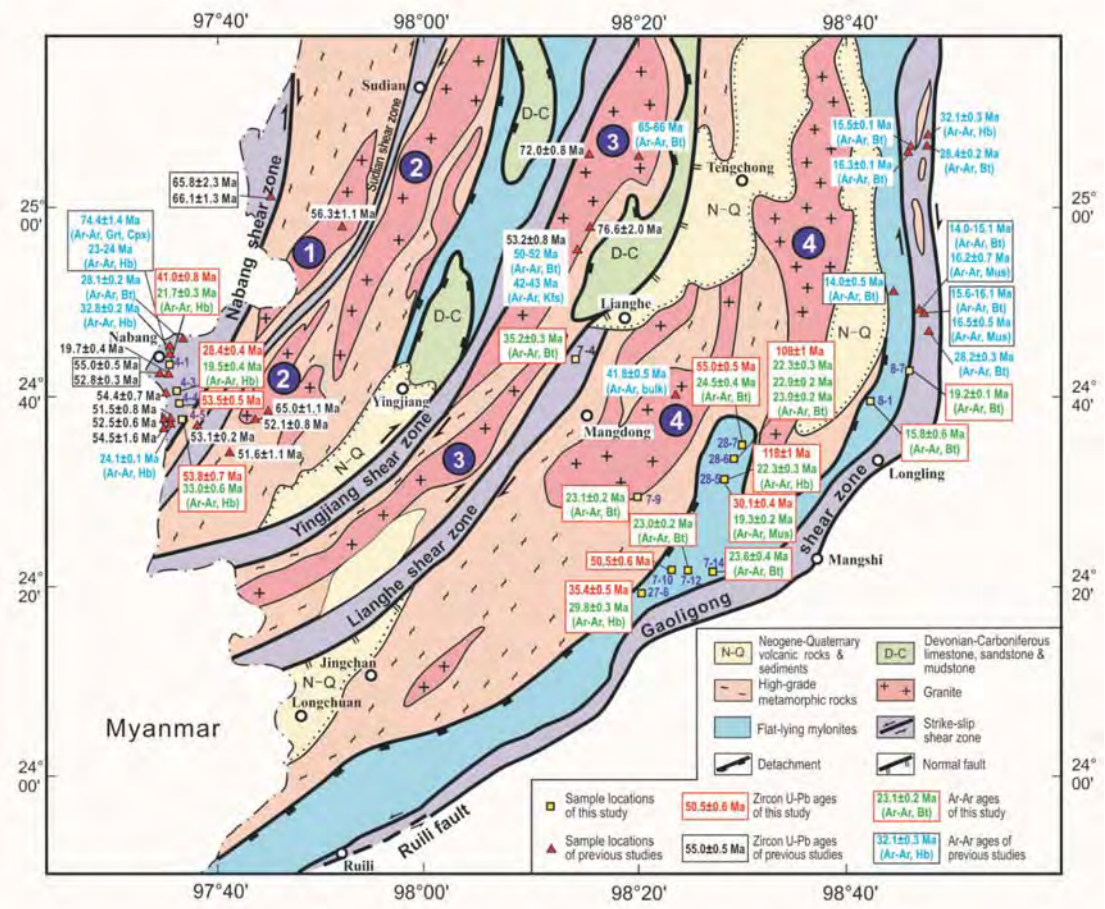

Fig. 1. Topography and schematic tectonic map of SE Tibet and adjacent regions. Bold yellow lines are major faults or ductile shear zone in the early Miocene, double lines show the Indus-Tsangpo Suture Zone (ITSZ), and dashed yellow thin lines indicate the dominant trend of stretching lineation in ductile shear zones. Red arrows in the inset map indicate motion of India, Indochina and eastern Tibet relative to Siberia from GPS observations (Shen et al., 2005; Zhang et al., 2004).The extrusion of SE Asia is bounded bythe sinistral strike-slip Ailaoshan-Red River shear zone (ARRSZ) in the northeast and the dextral strike-slip Sagaing fault in the west (Tapponnier et al., 2001). Abbreviations: GSZ, Gaoligong shear zone; LSZ, Lancangjiang shear zone; EHS, eastern Himalayan syntaxis; HM, Himalayan orogen; MBT, main boundary thrust; TC, Tengchong Terrane.

whereas the strike-slip shear zones accommodated extrusion and clockwise rotation of the Tengchong Terrane around the proto-Eastern Himalayan syntaxis since the late Eocene (Fig.1).

Modern pollen deposition in relation to vegetation distribution along the altitudinal gradient within Dokriani Glacial Valley, Garhwal Himalaya

Ipsita Roy, Parminder S. Ranhotra*, A. Bhattacharyya, Mayank Shekhar
Birbal Sahni Institute of Palaeobotany, 53 University Road, Lucknow 226007, INDIA
**ranhotra.p@gmail.com; pranhotra@yahoo.com*

The surface samples collected along the valley gradient from altitude ~2000 to 3800 m amsl within a stretch of ~27 kms in Dokriani Glacier valley, Garhwal Himalaya were analyzed for the

understanding of modern pollen deposition in relation to their nearest source taxa of this region. The valley widens at the top reaches of the valley, i.e., above ~3300 m amsl with the modern vegetation scenario of grassy meadows surrounded by the dense growth of broad leaved taxa, mainly *Quercus semicarpifolia, Rhododendron* and *Betula* and also conifers with the dominance of *Abies webbiana*. This broad leaved-conifer forest is followed by mixed conifer-broad leaved vegetation represented by *Juniperus,* few *Pinus, Picea* and *Cedrus*. *Abies webbiana*, grows densely on the morainic ridges at ~3-2 km downstream to the present glacier snout position along with few *Betula*, stunted *Rhododendron* and *Cassiope* are scattered till ~800 m downstream of the glacier snout. Regarding pollen deposition as a whole, arboreal taxa are dominant over the non-arboreal taxa. Between the ~3800 to 3300 m amsl *Quercus semicarpifolia* (20-50%) are more dominant followed by *Pinus, Abies* and *Juniper*. *Betula* is also represented in fair frequency with little more at altitudes between 3800 to 3600 m amsl. However the pollen of *Alnus*, a broadleaved taxa growing downstream, are more abundant than *Betula*, may be due to its high pollen productivity and easy wind transportation. Amongst non-arboreal taxa, the pollen of Apiaceae, Polygonaceae, Ranunculaceae, Asteraceae, Poaceae and Cyperaceae show good representation over others. Between 3300 to 3000 m amsl the pollen frequency of *Quercus semicarpifolia* (60-70%) increased with the lowering of *Pinus*, as the *Q. semicarpifolia* forms dense forest at this altitudinal range of the valley. At the elevations lower than ~3000 m amsl, the pollen representation of the arboreal taxa changed with the decline in pollen frequency of *Q. ssemicarpifolia*, *Abies*, and *Pinus*, whereas *Alnus* increased in good amount. Juniperus became much sparse, but the pollen of Urticaceae, which were absent in the high altitude samples, shows their presence in the lower altitude samples. Though pollen frequency of individual non-arboreal taxa remained less than 5% but the ferns (monolete and triletes) are conspicuous in their presence in samples of lower altitudes of the valley. Chenopodeaceae and Artemisia remained almost consistent throughout the valley gradient whereas the pollen of Liguliflorae (Asteraceae) is absent at the lower altitudes but present at the higher elevations ~3000 m amsl and above. Some temperate broad leaved taxa viz., *Juglans, Corylus, Carpinus* shows the presence of their pollen throughout the valley gradient without much change. Juglans pollen found slightly more in frequency at higher altitude, between 3800 and 3300 m amsl compared to its values at lower altitudes.

On the whole, modern pollen vegetation relationship of this area shows an altitudinal variation in the representation of taxa and this data base can be used as an analogue for the interpretation of sub fossil pollen spectra of dated sediment profile in terms of vegetation change vis-à-vis climate and glacial fluctuation.

Inferring the A.D. 1344 great earthquake surface ruptures using backthrusting and re-calibrated radiocarbon ages in the NW Himalayan Frontal Thrust System

R. Jayangondaperumal[1*], Y. Kumahara[2], V.C. Thakur[1], S. Dubey[3], Anil Kumar [1], Pradeep Srivastava [1], A.K. Dubey[1], V. Joevivek[1]

[1]Wadia Institute of Himalayan Geology, 33 GMS Road, Dehradun 248001, INDIA
**ramperu.jayan@gmail.com; ramperu@wihg.res.in*
[2]Graduate school of Education, Hiroshima University, Hiroshima, 739-8524 JAPAN
[3]Dept. of Geological Science, Indian Institute of Technology, Roorkee, India

Results of a paleoseismic trenching survey on a back thrust in the Janauri Hill, Sub-Himalayan range of the Himachal Himalaya are presented. The active back thrust revealed multiple events since 14 ka and the last event took place post 0.8±0.03 ka (i.e., post A.D. 1200 years). The age of the last earthquake event observed in the backthrust (~5.5 m fault dip slip) can be correlated with age of the forethrust displacement reported earlier at Bhatpur, NW Punjab Himalaya (Kumahara and

Jayangondaperumal, 2013). The long term uplift rate along the back thrust is 1.35±0.07 mm/yr. Further, the back thrust may be used as an indirect method of inferring the age of the last event that took place along the forethrust (i.e., HFT). Thus the study reveals the timing and net slip associated with the last event between 1210 A.D. and 1690 A.D., and long term uplift rate associated with the fault.

The Ox Cal Bayesian statistics method provides a strict age constraint of a great earthquake, which occurred in 1344 A.D. along the Himalayan Frontal Thrust (HFT) between the Ramnagar and Bhatpur sites, and corroborates with the last displacement recorded in the back facing fault scarp. Furthermore, Ox Cal modelled ages suggested two overlapping close interval earthquake events occurred between A.D. 1344 (Pant, 2002) and A.D. 1255 (Rajendran et al., 2015) at Ramnagar site, Kumaun Himalaya. These two events are in harmony with historical evidence obtained at monuments (Mugnier et al., 2013; Rajendran et al., 2013) located in Kashmir, Kumaun, Garhwal and Nepal Himalaya.

Kumahara, Y., Jayangondaperumal, R. 2013. Geomorphology, 180-181, 47-56.
Mugnier J.L., Gajure, A., Huyghe, P., Jayangndaperumal, R., Jouanne, F., Upreti, B.N. 2013. Earth Sci. Rev.,127,30-47.
Pant, M.R. 2002. Adarsa, 2, 29- 60.
Rajendran, C.P., Rajendran, K., Sanwal, J., Sandiford, M. 2013. Seism. Res. Lett., 84 (6), 1-13. Doi: 10.1785/0229130077.

Tree-Ring derived Satluj River Discharge Variability, Himachal Pradesh, India: A Review

Jayendra Singh[1*], Ram R. Yadav[2]
[1]Wadia Institute of Himalayan Geology, 33 GMS Road, Dehradun 248001, INDIA
[2]Birbal Sahni Institute of Palaeobotany, 53 University Road, Lucknow 226007, INDIA
**jayendrasingh@wihg.res.in*

Since Human History, Rivers, the main source of water, have played a significant role in development of the major human civilizations. In modern society, rivers not only fulfill the drinking water and agricultural needs but also serve the need of hydropower (electricity) requirements for domestic, industrial and other developmental activities of the society. In recent decades rapid population increase has enhanced the water requirement several times to meet the consistent socioeconomic needs.

Rivers originating from high Himalayas, continuously nourishing the local and downstream people's requirements are fed by the snow and glacier melt at upper elevations, whereas summer monsoon rainfall contributing in downstream region. Recent study of observational data (AD 1922-2004) of Satluj River, originating from Mansarovar and Raskal lakes in the Tibetan Plateau (~4572 m asl), flow showed decreasing trend in winter and monsoon season since 1990s, despite global warming are hypothesized to be because of glacier thinning (Bhutiyani et al., 2008). Such decreasing trends in river flow would be disastrous if it continues in future and warrants proper investigations in long-term perspective. Satluj river flow record (Singh & Yadav 2013) has been developed using tree-ring data from Kinnaur, Himachal Pradesh that provides valuable data base in understanding the Satluj River flow variability in context of past seven centuries. The reconstructed data is consistent with decreasing trend as noticed in the observational record. Reconstructed data also showed that such decrease in trend was also noticed earlier. Comparison of reconstructed 20-year low-pass filtered Satluj data with Indus flow (Cook et al., 2013) records showed good consistency. The other Satluj river discharge data (Misra et al., 2015) developed using seven site ring width chronologies from same region also showed similar high and low discharge period as noticed in Singh and Yadav (2013). Such similarity with other river discharge data reveal the potential of tree ring based river flow records in understanding hydrology of the region in long-term perspective and utility in future developmental planning.

Bhutiyani, M.R., Kale, V.S., Pawar, N.J. 2008. Current Science, 95 (5), 618-626.
Cook, E.R., Palmer, J.G., Ahmed, M., Woodhouse, C.A., Fenwick, P., Zafar, M.U., Wahab, M., Khan, N. 2013. Journal of Hydrology, 486, 365-375.
Misra, K.G., Yadav, R.R., Misra, S. 2015. Quaternary International, 371, 135-143, http://dx.doi.org/10.1016/j.quaint.2015.01.015.
Singh, J., Yadav, R.R. 2013. Quaternary International, 304, 156-162.

Indian monsoon and ITCZ dynamics recorded in stalagmites from Chakrata, NW Himalaya

Jooly Jaiswal
Wadia Institute of Himalayan Geology, 33 GMS Road, Dehradun 248001, INDIA
jooly1991@gmail.com

The Indian monsoon is a major weather system on the Earth and variations in its intensity have widespread socio-economic impacts on a very densely populated South Asian region. The monsoon winds blow from the southwest (SW monsoon) during summer (June-September) and from the northeast (NE monsoon) during colder months (October-March) of the year. Despite dedicated efforts by the scientists over the centuries, a comprehensive picture of variability in the Indian Summer Monsoon (ISM) and Westerlies for the Indian Himalayan sector has been elusive, especially on the time scales relevant to society. The absence of quantitative, long term high resolution (multi-annual to decadal) records and complexity and multiplicity of factors influencing the ISM have hindered the efforts to understand the behavior of ISM and Westerlies in the Himalaya. Absolutely dated speleothems (stalagmites), are found to be an excellent palaeoclimatic archives for the terrestrial environment, complementing the marine and ice-core records (Wang et al., 2001; Dykosk et al., 2005).

The stalagmite BH3 studied from Bhiar Dhar Cave (N 30°79'037" N: 77°77'65.6" E; elevation 2292 m.a.s.l.) Chakrata, NW Himalaya (Fig. 1) is located in Early-Neoproterozoic Deoban Limestone. The study area receives about 75-90 % of the rainfall during the SW monsoon season from June to September (Mooley et al., 1981) and remaining by western disturbances during winter. The temperature inside the cave is 14°C recorded in the month of July, 2014, which is close to the mean annual temperature of that area. The humidity is 92% inside the cave. The Intertropical Convergence Zone (ITCZ) was located over the study area during wetter/warmer season. Preliminary studies suggest that when it shifts southward, precipitation over the study area decreases significantly (Fleitmann et al., 2007).

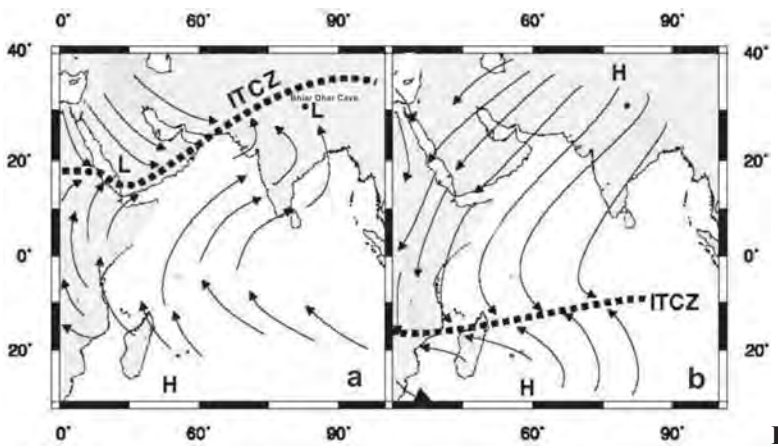

Fig. 1

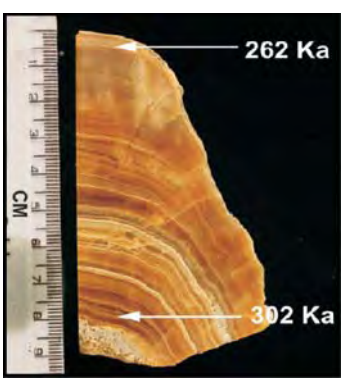

Fig. 2. Speleothem section cut along growth axis with age.

I present a continuous record of Indian monsoon variation during the 302 ka to 262 ka which comes under MIS 8 (Lisiecki et al., 2005). The chronology of Stalagmite (BH3) was constrained by two absolute U-Th series dates 302 ka (bottom) to 262 ka (top) determined by multiple collector-inductively coupled plasma-mass spectrometry using the technique as described by Cheng et al. (2013).

For stable isotopic study 160 powdered samples were microdrilled at 0.5 mm interval along the central growth axis of the stalagmite. The $\delta^{18}O$ and $\delta^{13}C$ values vary from -4.15 to -12.20‰ and 0.12 to -8.83‰ relative to the VPDB respectively. The $\delta^{18}O$ signatures reflect the variation in the intensity of ISM as well as the position of the ITCZ (Fleitmann et al., 2007). Wetter and drier phases can be interpreted by lesser and higher value of $\delta^{18}O$ respectively (Wang et al., 2001, 2005, 2008; Yuan et al., 2004; Zhang et al., 2008). Carbon isotope variations in the speleothems record changes in palaeovegetation pattern (Genty et al., 2001). C4 vegetations are rich in $\delta^{13}C$ show high $\delta^{13}C$ values. C3 vegetations are rich in $\delta^{12}C$ show low $\delta^{13}C$ values. High and low $\delta^{13}C$ values may indicate more C4 and C3 vegetation respectively. The results of this study augment the understanding of palaeoprecipitation of NW Himalayan region during MIS 8. However, further studies are required to reach a concrete conclusion.

Cheng, H. et al. 2013. Earth and Planetary Science Letters, 371, 82-91.
Dykoski, C.A. et al. 2005. Earth and Planetary Science Letters, 233(1), 71-86.
Fleitmann, D. et al. 2007. Quaternary Science Reviews, 26(1), 170-188.
Genty, D. et al. 2001. Geochimica etCosmochtimica Acta 65, 3443-57.
Lisiecki, L.E., Raymo, M.E. 2005. Paleoceanography, 20(1).
Mooley, D.A., Parthasarathy, B., Sontakke, N.A., Munot, A.A. 1981. Journal of Climatology, 1(2), 167-186.
Wang, Y. J. et al. 2001. Science, 294(5550), 2345-2348.
Wang, Y.J. et al. 2005. Science 308, 854-857.
Wang, Y.J. et al. 2008. Nature 451, 1090-1093.
Yuan, D.X. et al. 2004. Science 304, 575-578.
Zhang, P.Z. et al. 2008. Science 322, 940-942.

Meticulous investigation of near-surface wind flow pattern and its contribution to the surface melting of Chorabari Glacier, Central Himalaya, India

Kapil Kesarwani[1*], D.P. Dobhal[1], Manish Mehta[2], Alok Durgapal[3]
[1]Centre for Glaciology, Wadia Institute of Himalayan Geology, 33 GMS Road, Dehradun 248001, INDIA
**kapilcfg@gmail.com*
[2]Wadia Institute of Himalayan Geology, 33 GMS Road, Dehradun 248001, INDIA
[3]Dept. of Physics, D.S.B. Campus, Kumaun University, Nainital 263001, INDIA

Wind is one of the most significant factors affecting the transport of moisture, formation of clouds and occurrence of precipitation in the high altitude glacierized regions. In the complex relationship between glaciers and climate, one of the key processes is melting of snow and ice at the glacier surface. Surface melting of a glacier is strongly depends on the temperature gradient from atmosphere to surface and its spatial distribution created through the wind flow pattern. Thermodynamically, the surface melting of a glacier is highly influenced by the turbulent sensible and latent heat fluxes which are directly proportional to the change in wind speed. The surface mass loss of a glacier created through wind flow is observed highest in the poles and second highest after the radiative fluxes in the valley glaciers. To understand the phenomenon of glacier surface ablation through wind flow patterns in the valley glaciers, examination of the ways by which the glacier surface gains and losses heat under different wind conditions is necessary. Therefore, meticulous investigation of near-surface wind flow pattern of the Chorabari Glacier located in upper Mandakini basin (latitudes of N

30°45' to 30°48' and longitudes of E 79°2' to 79°4'), Central Himalaya, India and its contribution to the glacier surface melting is studied. The wind flow (speed and direction) data were collected through a network of two Automatic Weather Stations (AWS) setup at upper ablation zone (4270 m a.s.l. referred as K1) and at near the glacier's snout (3820 m a.s.l. referred as K2) during 2011-2012 and 2012-2013 mass balance years (1st November to 31st October of the following year). To scrutinize the glacier wind pattern in more detail the wind speed data were alienated in two different diurnal periods (day and night) and seasons (summer and winter) using frequency distribution analyses. The wind speed pattern was observed different for day (06:00-18:00) and night (19:00-05:00) time which varies with the change in season. Likewise, variations in day-time wind speed were observed over-and-above compared to the night-time. The frequency distribution analysis at diurnal scale suggested that the K2 site experienced high variations of wind speed in day time, whereas for K1 site, it was small as a consequence of low temperature differences between near-surface and atmosphere. Generally, mean diurnal maximum wind speed was observed in the summer around 13:00 to 14:00 h when the air is most subjected to terrestrial heating and vertical motion. Similarly, in the winter, it was around 06:00 to 07:00 h or before sunrise at the time of maximum diurnal cooling. Season wise analysis shows that wind speed increases in winter season (1.6 m s^{-1} for K1 and 2.9 m s^{-1} K2) as compare to summer (1.2 m s^{-1} for K1 and 2.3 m s^{-1} K2). Seasonal changes in wind speed pattern were classified into four sectors, (i) Light (0.0-2.0 m s^{-1}), (ii) Moderate (2.0-4.0 m s^{-1}), (iii) High (4.0-6.0 m s^{-1}), and (iv) Strong ($\geq$ 6.0 m s^{-1}). Based on the flow of the wind direction, the wind speed pattern was further categorized in Cold Katabatic and Warm Synoptic region. Results specified that the characteristics of wind speed and direction are highly influenced by the precipitation. During the summer higher frequency of light wind speed in all the stations were observed. However, the frequency of moderate wind speed was higher in the winter, which suggested that the glacier catchment area experienced highest wind speed under the cold katabatic region during the this season.

Change in the flow of katabatic and anabatic wind has the significant importance in the glacierized region as it directly controls the freezing or melting processes of snow/ice. The seasonal changes in the katabatic and anabatic wind flow were computed using frequency distribution analysis. The wind direction pattern at K1 site generally found in NNW-S or S-NNW direction, whereas for K2 it was N-S or S-N direction. Seasonal analysis of wind direction records showed that in summer the rate of recurrence of anabatic wind (valley wind) which results from the greater heating of the valley walls as compared with the valley floor has higher frequency leading to an increment of sensible heat flux that causes more melting on the glacier surface. However, in the winter there is a reverse process as the denser cold air at higher elevations drains into depressions and valleys resulting in katabatic wind. In this state, the adiabatic heating of air that travels down along the glacier is to a large extent compensated by cooling due to the exchange of sensible heat flux with glacier surface. At K1 site, the mean fraction of katabatic wind was estimated as 66%, which was more than the anabatic wind (34%), and of K2 site it was 63% (katabatic wind) and 37% (anabatic wind) resulting inadequacy in the glacier-wide surface melting produced by the sensible heat flux. Further, it is observed that the flow of katabatic and anabatic winds is greatly influenced by the winter precipitation than the summer in the catchment area.

Glacier Facies mapping using high resolution satellite Remote Sensing data

Kavita Mitkari*, Sahil Sharma, R.K. Tiwari, M.K. Arora, Kamal Kumar, H.S. Gusain
PEC University of Technology, Chandigarh 160012, INDIA
**mitkari.kavita@gmail.com*

Glaciers are large persistent bodies of ice which move due to stresses induced by its weight. Glaciers get formed where accumulation of snow exceeds its ablation (melting) over many years and

often centuries. When there is net accumulation at the end of a summer season, snow will densify into ice and will build up until it has become sufficiently thick to deform under its own weight and move downwards. Their importance is especially significant because they contain a considerable part of the world's fresh water and the accelerated melting and retreat of glaciers have severe impacts on the environment and human well-being, such as natural disasters, water supply, vegetation patterns, economic livelihoods, and specially they can contribute to sea level change (Singh et al., 2011). Information about the size and spatial extents of glacier is of utmost importance for many research applications such as mass balance studies, melt runoff modeling, glacier hazard prediction modelling and snow-line dynamics.

So, it is desirable to clearly distinguish the various components of glaciers such as snow, ice, ice-mixed debris, valley rocks, glacial lakes, moraines, crevasses and debris. Keeping in mind the difficult, vast, and inaccessible nature of mountain glaciers, remote sensing provides the most pragmatic tool for their extensive, cost-effective, and repetitive study. However, their mapping using satellite data is challenged by their spectral similarity. Although numerous techniques (Paul et al., 2000; Bolch et al., 2006; Keshri et al., 2008; Shukla et al., 2010) for mapping of glacier facies using remote sensing data (Landsat, ASTER, AWiFS, etc.) have been devised, mapping of glacier facies from Gangotri glacier using high spatial resolution remote sensing data still remains a bottleneck.

The high spatial and radiometric resolution optical data can grant an access to spectral regions where distinguishable differences exist between multiple classifications within the scene, which may be overlooked by more traditional MSI systems. Pixel based classification is considered to be appropriate and satisfactory for the classification of low to moderate resolution remote sensing data. But these datasets are fraught with mixed pixels, where per-pixel classification may not be appropriate. Salt and pepper effect is also one of the other disadvantages of pixel based classification.

In this study, we have made an attempt to demonstrate the performance of Object Based Image Analysis (OBIA) for mapping glacier facies of Gangotri glacier from high spatial MS remote sensing data of Worldview-2 satellite. Basic processing units in OBIA are thus image objects (group of pixels) and not single pixels. Therefore, the strength of OBIA is that the object characteristics such as shape, texture, spatial relationships (connectivity, distances and location etc.) can be used for classification along with spectral response. An overall accuracy of 90% is achieved and this signifies successful usage of OBIA in mapping glacier cover classes in Gangotri glacier region.

Bolch, T., Kamp, U. 2006. Proceedings of the 8th international symposium on high mountain remote sensing cartography, 20-27 March 2005, La Paz, Bolivia in print.
Keshri, A., Shukla, A., Gupta, R.P. 2009. International Journal of Remote Sensing, 30(2), 519−524.
Paul, F. 2000. EARSEL eProceedings No.1, 239−244.
Shukla, A., Arora, M.K., Gupta, R.P. 2010. Remote Sensing Letters, 1, 11-17.
Singh, V.P., Haritashya, U.K. 2011. Springer Science & Business Media, 2011.

Stable isotopic characterization of water samples from north-west Himalayan river basins and implications on glacio-fluvial coupling

L. Sardine Varay[1*], S.P. Rai[2], Vikrant Jain[3]
[1]*Department of Geology, Delhi University, Delhi 110007, INDIA*
**sardinevaray@gmail.com*
[2]*National Institute of Hydrology, Roorkee 247667, INDIA*
[3]*Discipline of Earth Sciences, IIT Gandhinagar, Gandhinagar 382355, INDIA*

Enhanced glacial melting in response to climate change may cause a major impact on river hydrological and morphological processes in downstream reaches (Goudie, 2006). Understanding

the process of glacial melt water component in river discharge is a major challenge in Himalayan river systems. The application of stable isotopes of oxygen and hydrogen in fingerprinting of melt water is one of the powerful tools for quantifying melt contribution to river discharge where direct monitoring of snow and ice melt is a challenge (Dincer et al., 1970; Unnikrishna et al., 2002). We report synoptic isotopic values of water samples (numbering 97) in two neighbouring river basins, to highlight the variability in glacial melt-water runoff. The study is carried out in the Spiti-Sutlej and Yamuna River basins in the northwest Himalaya, which are distinct in terms of glacial cover and geomorphic processes. The Sutlej River basin with an area of 54755 km^2 receives its precipitation from Western disturbance and Indian Summer Monsoon (ISM) (Bookhagen and Burbank, 2010). It has a glacier cover 2249 km^2 (SAC, 2011) i.e., about 4.1% of its basin area. Yamuna River basin on the other hand falls dominantly under the precipitation regime of Indian Summer Monsoon (Bookhagen and Burbank, 2010). With a total basin area of 7498 km^2, glacier cover an area of 166 km^2 (SAC, 2011) which works out to 2.2% of the total basin area. The analysis was carried out for two seasons, viz., 2013 post-monsoon and 2014 pre-monsoon (Fig. 1).

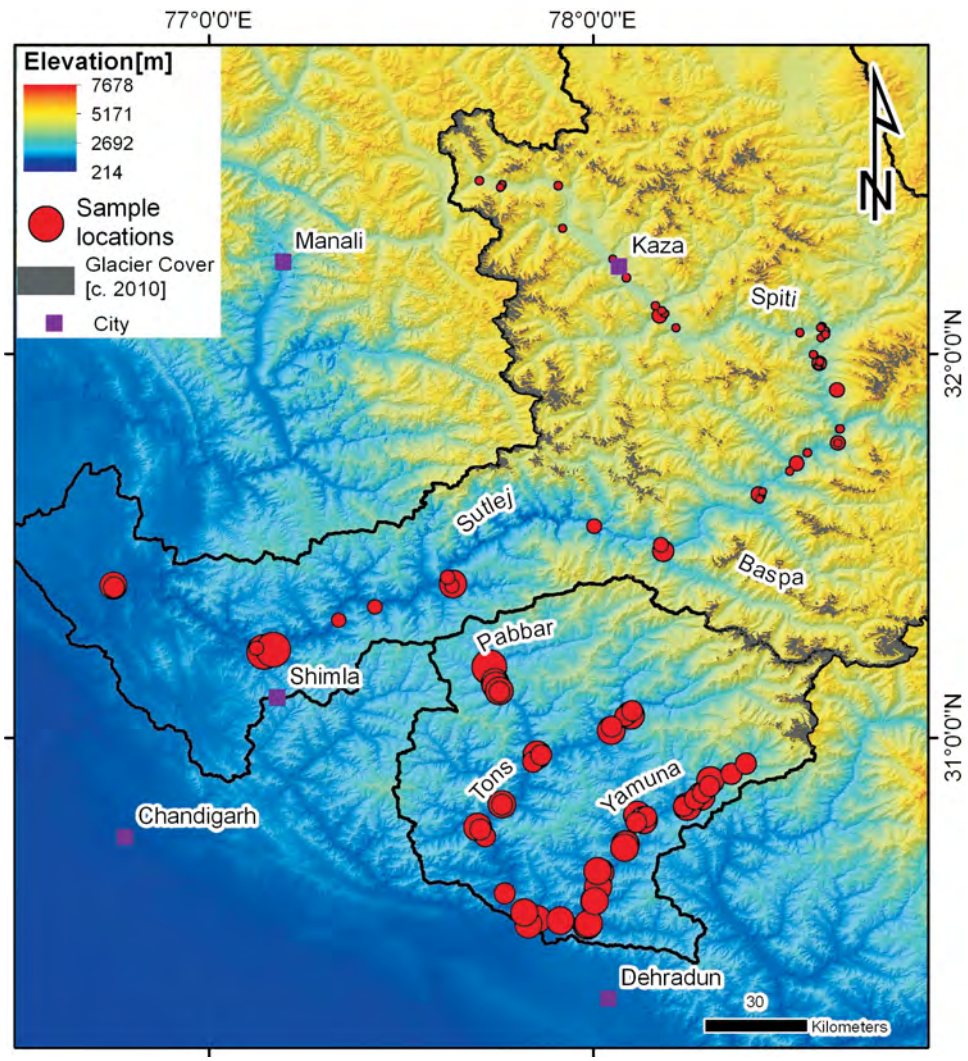

Fig 1. Map showing the sample location. The size of the circle is proportional to the value of averaged $\delta^{18}O$ of the two seasons; smaller circles being more depleted samples.

In the Spiti-Sutlej basins, the two seasons averaged $\delta^{18}O$ value ranges from -10.22‰ at Kandrour (537 m) to -14.28‰ at Taksa (4109 m) indicating an enrichment by about 4‰ from headwater region at Taksa to downstream at Kandrour. In the Yamuna basin, the value ranges from -9.16‰ at Dakpathar (483 m) to -10.17‰ at Hanumanchhatti (2036 m). For Tons, the value ranges from -9.27‰ at Dakpathar (510 m) to -10.54‰ at Netwar (1257 m). In general there is a gradual trend of enrichment from upstream to downstream. However this trend is more pronounced for Spiti-Sutlej mainstream samples than for Yamuna and its tributary Tons. In the Spiti-Sutlej basin, there is no straight forward seasonal variation. But in the case of Yamuna and its tributary Tons, the pre-monsoon samples are consistently more enriched compared to post-monsoon samples.

The relationship between $\delta^{18}O$ and $\delta^{2}H$ of river waters helps in understanding the effect of evaporation and other hydrological processes altering the isotopic composition. Meteoric Water Lines (MWL) of mainstream samples of Sutlej, Tons and Yamuna rivers were obtained from $\delta^{18}O$ versus $\delta^{2}H$ plots. The slope and y intercept of the water line for Sutlej river is higher than that of Global Meteoric Water Line (GMWL) [$\delta^{2}H = (8.20.1) \times \delta^{18}O + (11.30.7)$; Rozanski et. al., 1993] as well as LMWL developed by Kumar et al. (2010) indicating significant amount of snow and glacier melt contribution from the higher altitude regions in the Sutlej River. However, less slope and intercept values in Yamuna and Tons indicate evaporative enrichment of river water.

In the Spiti-Sutlej basin, the enrichment of $\delta^{18}O$ value in Sutlej River and its tributaries from upstream to downstream indicate the decreasing contribution of melt from upstream to downstream since snow/glacier melt water is the primary contributor to discharge in the headwater reaches. However, the tributaries originating from lesser altitude bear enriched isotopic composition due to altitude effect and absence of snow and glaciers in their catchments at low altitude. Contribution from stream catchments devoid of glacier cover to mainstream is expected to enrich mainstream samples. However this seems to be insignificant. Even with increasing river discharge from upstream to downstream, the trend of the tributaries shows significant deviation from mainstream sample trend, indicating that the contribution from these catchments are insignificant. In the case of Yamuna and its tributary Tons, the mainstream and tributary sample divergence of $\delta^{18}O$ values is less perceptible indicating that melt water contribution is very less in the Yamuna basin.

The separation of water samples from the two basins in the $\delta^{18}O$-$\delta^{2}H$ plot indicates that two basins belonged to different moisture regimes. The contribution of headwater sourced discharge inferred to be glacier and snow melt is more significant in the Sutlej basin as compared to Yamuna basin. This implies that the impact of changing melting dynamics in the Sutlej basin will be more significant as compared to Yamuna. Remote sensing based modelling has also suggested significant (60%) contribution of snow melt to the Sutlej river in comparison to only 11 % contribution of snow melt into the Yamuna River (Bookhagen and Burbank, 2010). These are the first isotope based data, which shows significant impact of glacial melt on the neighbouring river basins.

Bookhagen, B., Burbank, D.W. 2010. Journal of Geophysical Research, 115, F03019, doi:10.1029/2009JF001426.

Dincer, T., Martinec, J., Payne, B.R., Yen, C.K. 1974. Isotopes Techniques in Groundwater Hydrology, 1, 23-43.

Goudie, A. S. 2006. Geomorphology 79: 384-394.

Kumar, B., Rai, S.P., Kumar, U.S., Verma, S.K., Garg, P., Kumar, S.V.V., Jaiswal, R., Purendra, B.K., Kumar, S.R., Pande, N.G. 2010. Water Resource Research, 46, W12548, doi:10.1029/2009WR008532.

Rozanski, K., Araguas-Araguas, L., Gonfiantini, R. 1993. Geophys. Monogr. Ser., vol. 78, edited by P. K. Swart et al., pp. 1-36, AGU, Washington, D.C.

Space Applications Centre (SAC) 2011. Space Applications Centre, Ahmedabad - 380 015 May 2011.

Unnikrishna, P.V., McDonnell, J.J., Kendall, C. 2002. Journal of Hydrology, 260, 38-57.

Vacillating prolonged Tertiary sealevel record of the Tethys Sea in the Indo-Myanmar Range, Northeast India

Kapesa Lokho
Wadia Institute of Himalayan Geology, 33 GMS Road, Dehradun 248001, INDIA
kapesa@wihg.res.in

Extended continuation of the vacillating Tethys Sea in the Tertiary sequence of the Indo-Myanmar Range in northeast India is well reflected in its marine fauna, lithology and sedimentary geochemistry. Since fauna besides imparting temporal constraint to the stratigraphic sequence is foremost in providing a glimpse of the sea level changes, I intend to focus on faunal remains of the beds and their bathymetric inferences and will ultimately summarize these sealevel changes in the context of regional geological evolution transforming this region as an important oil and gas producing field.

Eocene record: Our earlier record of Eocene fossils include pteropods of the families Limacinidae, Creseidae, and Cliidae(?) and planktonic foraminifera consisting of *Hantkenina alabamensis, H. leibusie, Cribrohantkenina inflata, Turborotalia cerrozuolensis, T. pomeroli and Globigerinatheka seminvoluta and benthic Uvigerina facies consisting U. cocoaensis, U. continuosa, U. eocaena, U. glabrans, U. jacksonensis, U. longa, U. moravia, U. steyeri* and *U. vicksburgensis* from the Upper Disang Formation (UDF) of Nagaland. The present finding of foraminifera from the Naga Hills of Manipur consist of *Pseudohastegerina micra, Streptochilus martini, Chiloguembelina cubensis, Nonionella* sp., *Osangularia* sp., *Baggina* sp., *Cibicidoides* sp. The depositional setting inferred for the UDF range from outer neritic to upper bathyal paleobathymetry.

Eocene-Oligocene record: Earlier workers recorded 36 ichnospecies of 33 ichnogenera and grouped them into *Skolithos-Cruziana* mixed ichnofacies, *Cruziana* ichnofacies, *Skolithos* ichnofacies, *Zoophycos* ichnofacies, *Nereites* ichnofacies and *Teredolites* ichnofacies from Manipur. The present work reports megafossils leaf and ichnofossils from the Eocene-Oligocene boundary from the Naga Hills. The depositional setting of the Late Eocene-Early Oligocene of the Laisong Formation of Barail Group inferred is shallow marginal marine setting such as tidal flats, deltas and shoreface.

Early Miocene record: Besides earlier enumeration we recorded ichnofossils of Skolithos ichnofacies and Cruziana ichnofacies from the Middle Bhuban Formation (MBF) of Mizo Hills. Sedimentary structures associated with these traces are mainly cross bedding, flaser bedding and slump structures. Considering an integrated ichnological-sedimentological framework, the stratigraphic interval of the Middle Bhuban Formation was interpreted to have been deposited under a shallow, marginal-marine channel complex dominated by tidal channels developed in quiet, brackish-water portions of a delta plain.

Middle Miocene record: This author and other workers have documented Middle Miocene foraminiferal assemblage consisting of Ammonia umbonata, Baggina sp. Orbulina cf. bilobata, Praeorbulina glomerosa circularis, Praeorbulina cf. transitoria, Clavatorella cf. sturanii, Lagena sp. and Uvigerina sp. We also documented nannofossils indicating NN5 nannofossil Zone (Langhain age) consisting of *Helicosphaera, Coccolithus, Cyclicargolithus, Discoaster, Helicosphaera* and *Reticulofenestra* from the Mizo Hills. The assemblage of foraminiferal and nannofossil assemblage suggest a hemipelagic depositional setting with middle neritic shelf paleobathymetry for the Upper Bhuban Formation (UBF) of Mizoram.

Miocene-Early Pliocene record: Earlier workers recorded foraminiferal assemblage of *Streptochilus* cf. *globigerum, Globorotalia* (*T.*) *obesa, Globorotalia* (*T.*) *acoastaensis*,

Globigerinoides trilobus, *G. immaturus, Cassigerinella chipolensis, Globeigerina bulloides*, *Ammonia* sp., *Lenticulina* sp. and a record of palynoflora consisting of *Palmidites maximus, Podocarpidites* sp., *Verrutriletes* sp., *Meyerilollis* sp. from Cachar area of Assam and Tripura region. A good assemblage of calcareous nannofossil consisting of *Ceratolithus acutus, C. rugusus, Ceratolithus simplex, Catinaster coalithus, Catinaster* sp. *Coccolithus miopelagicus, C. pelagicus, Gephyrocapsa* sp., *Gephyrocapsa* sp., *Helicosphaera ampliaperta, H. californiana, H. carteri, H. intermedia, H. minuta, H. paleocarteri, H. walbersdorfensis, H. kamptneri, Helicosphaera* sp., *Pyrocyclus orangensis, Reticulofenestra haqii, Scyphosphaera globulata, Sphenolithus conicus, S. delphix, S. heteromorphus, S. moriformis, Tetralithoides symeonidesii, Triquetrorhabdulus rugosus, Thoracosphaera tuberosa, Umblicosphaera jafari, H. philippinensis, Holococcolith* sp., were recorded from the Mizo Hills by earlier workers and inferred a relatively shallow marine depositional environment for the Bokabil Group.

Pliocene record: Earlier workers recorded fossil woods namely *Swintonioxylon hailakandiense, Bombacacioxylon tertiarum, Dipterocarpoxylon jammuense* and *Bischofia palaeojavanica* from the Tipam Group of sediments from Mizoram. The recorded fossils indicate distribution of the modern equivalents

The continuance of deep to shallow marginal marine conditions sustained continuation of sedimentation of oil producing richly fossiliferous thick package for longer duration in the milieu of suitable geodynamics and availability of capping and reservoir horizons; these parameters together gave rise to a rich petroleum system in the Indo-Myanmar Range of northeast India.

Plant remains from the Paleogene sediments of Indo-Myanmar suture zone

Kapesa Lokho[1,*], Gaurav Srivastava[2]

[1]*Wadia Institute of Himalayan Geology, 33 GMS Road, Dehradun 248001, INDIA*

**kapesa@wihg.res.in*

[2]*Birbal Sahni Institute of Palaeobotany, 53 University Road, Lucknow 226007, INDIA*

The global climate during the Cenozoic shows an overall cooling trend, however, the Paleogene is considered as warm phase as compared to the Neogene. During the Paleogene, the most significant brief climate aberrations occurred at ~55, 34 and 23 Ma, all near or at epoch boundaries. The first aberration is popularly known as Paleocene-Eocene Thermal Maxima (PETM) which is characterized by a 5 to 6°C rise in deep sea water temperature, however, the other two climatic aberrations indicate cooler conditions which resulted in the formation of ice-sheets on South Pole. The last two events are popularly known as Oi-1 and Mi-1 events (Zachos et al., 2001). The aforesaid climatic aberrations are mainly recorded from the marine proxies. However, it is well known fact that the specific heat capacity of water is always greater than the atmospheric air. As a result the response time for any external environmental change will always be greater in the ocean as compared to atmospheric air temperature. So, to capture small fluctuations in the climate, land plants are considered as the best proxy because they are spatially fixed and directly respond to their external environmental conditions either in the form of their distribution or in their architectural features (Woodward et al., 2004; Yang et al., 2015).

In the present communication we report leaf megafossils from the Eocene-Oligocene boundary from the Indo-Myanmar suture zone. The fossils have been identified in the herbarium of Forest Research Institute, Dehradun. The identified fossils are *Artocarpus* of the family Moraceae, *Cynometra* of the Fabaceae, *Daphnogene* of the Lauraceae and palm leaves of the Arecaceae. The presence of typical pantropical aforesaid families indicates a warm and humid climate during the deposition of the sediments (Steenis, 1962). Moreover, the presence of legumes indicates seasonality

in the rainfall. The architectural features of the fossil leaves such as entire margin in all the leaf fossils again indicate a warm climate (Wolfe, 1993). The indication of warm and humid climate during the E/O boundary is not surprising because the fossil flora was growing near the Tethys Sea, as land connections in between Indian and Eurasian plates were not completed during the period (Chatterjee et al., 2013), where temperature and humidity remained same throughout the year.

Chatterjee, S., Goswami, A., Scotese, C.R. 2013. Gondwana Research 23, 238-267.
Van Steenis, C.G.G.J. 1962. Blumea 11(1), 235-372.
Wolfe, J.A. 1993. United States Geological Survey Bulletin, 2040, 1-73.
Woodward, F.I., Lomas, M.R., Kelly, C.K. 2004. Phil. Trans. R. Soc. Lond. B 359, 1465-1476.
Yang, J., Spicer, R.A., Spicer, T.E.V., Arens, N.C., Jacques, F.M.B., Su Tao, Kennedy, E.M., Herman, A.B., Steart, D.C., Srivastava G., Mehrotra, R.C., Valdes, P.J., Mehrotra, N.C., Zhou, Zhe-Kun, Lai, J-S. 2015. Global Ecology and Biogeography (In press; DOI:10.1111/geb.12334)
Zachos, J., Pagani, M., Sloan, L., Thomas, E., Billups, K. 2001. Science 292, 686-693.

Occurrences of Titan-augite within alkaline basaltic rocks of Zildat Ophiolitic Mélange, Indus Suture Zone, Himalaya: implications to the origin of subducted oceanic crust

Koushick Sen*, Barun Kumar Mukherjee
Wadia Institute of Himalayan Geology, 33 GMS Road, Dehradun 248001, INDIA
**koushick.geol@gmail.com*

Titanaugite is an aluminum and titanium rich pyroxene, commonly reported from lunar basalts, meteorites and a few terrestrial undersaturated alkaline basalts. The presence of titanaugite within alkaline lava does indicate an enriched magma source through which the rock was evolved. The present study reports the first data on the occurrence of Titanaugite within the meta-basic rocks of Zildat Ophiolitic Mélange, Indus Suture Zone, NW Himalaya, which opens a new prospect to understand the origin of the protolith and nature of the subducted oceanic crust. The studied rock is a medium-grained foliated meta-basic rock, mainly composed of Titanaugite, Titanite, Na-Amphibole, Albite, Epidote, chlorite and Iron-Oxides. Titanaugite occur as pink to brown in colour, euhedral to subhedral crystals up to 1 cm in size. Chemical zoning is common within these titanaugites with normal and oscillatory zoning. Mineralogical data suggests that the titanaugites are high in Ti and Al, the TiO_2 and Al_2O_3 concentrations are as high as 3.5% and 9%. Variation in elemental distribution pattern is observed within the individual titanaugite grains moving from core to the rim part of the grain. In cases, the rim part does show upto two fold changes of cation concentration, indicating a metamorphic overprint of titanaugite grains. Bulk rock geochemical analyses of the titanaugite hosed basic rock indicate their alkanine basaltic nature with low SiO_2 concentration. Following different discrimination diagrams for tectonic setting of these rocks suggests that the basalts are within plate alkali basalts. The normalized spider diagrams of rare earth elements of these basalts show enrichment of LREEs and depletion of HREEs suggesting their Ocean Island Basalt type characteristics. Putting all the evidences together and configuring them to the tectonic framework of Indus Suture Zone, this study reveals an enriched magma source of Tethyan oceanic crust prior to the subduction.

Palaeostress evolution of the MCT zone in the Joshimath area, Garhwal, India

Johann Genser[1,*], Waltraud Genser[2]
[1]*Dept. of Geography and Geology, University Salzburg, AUSTRIA*
**johann.genser@sbg.ac.at*
[2]*iC consulenten ZT GmbH, Zollhausweg 1, 5101 Bergheim-Salzburg, AUSTRIA*

Little is known about the palaeostress evolution of the MCT zone between ductile thrusting with consistent NNE-SSW trending stretching lineations and the present-day stress field with a NE-SW trending σ1 and subvertical σ3 (Mahesh et al., 2015). We investigated the brittle deformation in the triangular area south of the junction of Dhauliganga and Alaknanda rivers at Joshimath, where a number of faults crosscut ductile structures of the hanging-wall Joshimath Fm., part of the HHC, and the Helang Fm. in the foot-wall of the Vaikrita Thrust. The courses of the rivers in the area are also controlled by the trending of major faults, which range from sharp, discrete fault planes to brittle shear zone with several metres thick fault gouge. We measured orientations of slickenside surfaces and striations and determined shear senses of brittle faults, calculated palaeostresses from these data and correlate these with the main fault sets.

A total number of 225 slickensides were evaluated for palaeostress analysis. Pole points to slickenside surfaces and related striation measurements are shown in figure 1. Nine sets (clusters with poles of similar orientation) are distinguished from the data. The (N)NE-(S)SW-trending fault planes - assigned to the dominant palaeostress tensors I, II and IV (see below) - correlate well to the trends of prominent lineaments from aerial/satellite image analyses.

Palaeostresses were determined from slickenside data according to methods described by e.g. Célérier et al. (2012) with the programs Win-Tensor (Delvaux and Sperner, 2003) and Tectonics FP. Slickenside data were first separated into internally consistent data sets (homogenous subsets) by manual inspection and by a semi-automatic procedure implemented in the Win-Tensor program. Semiautomatic separation in Win-Tensor was done by the right dihedron method, which first extracts the dominant data set from all data. The procedure is then repeated with the remaining data. The dominant data set is the set with the largest number of measured slickensides, not necessarily the dominant faults. Palaeostresses for the separated sets were determined with the rotational optimization method implemented in Win-Tensor. The procedures search the reduced stress tensor that primarily minimizes the deviation between the observed striation and the calculated slip vector on any fault plane and in addition maximizes the resolved shear stress magnitude and minimizes the resolved normal stress magnitude on each plane. From slickenside data a reduced stress tensor with 4 (out of 6) stress components can be calculated, the orientation of the three principal stress axes and a shape factor $R = (\sigma2-\sigma3)/(\sigma1-\sigma3)$.

4 dominant and several minor stress tensors could be extracted from the data set. The major stress tensors are quite robust to the choice of fault planes, which belong to one stress regime, because they are represented by a high percentage of number of faults and clearly different orientations of the principal stress axes. Stress tensors that are calculated from slickensides, which do not belong to one of the dominant tensors, are very dependent on the choice of subsets and therefore less reliable. Numbering of the palaeostress tensors is according to their dominance (primarily number of measured slickensides) and not their chronology.

Palaeostress Tensor I: The dominant palaeostress tensor displays a major principal stress axis σ1 plunging 215/60, which is orthogonal to the main foliation, an intermediate principal stress axis σ2 plunging to the NNE and a horizontal minor principal stress axis σ3 trending WSW-ENE. The fault sets that were formed at this state of stress are steep, E-dipping and NW-dipping sets, a

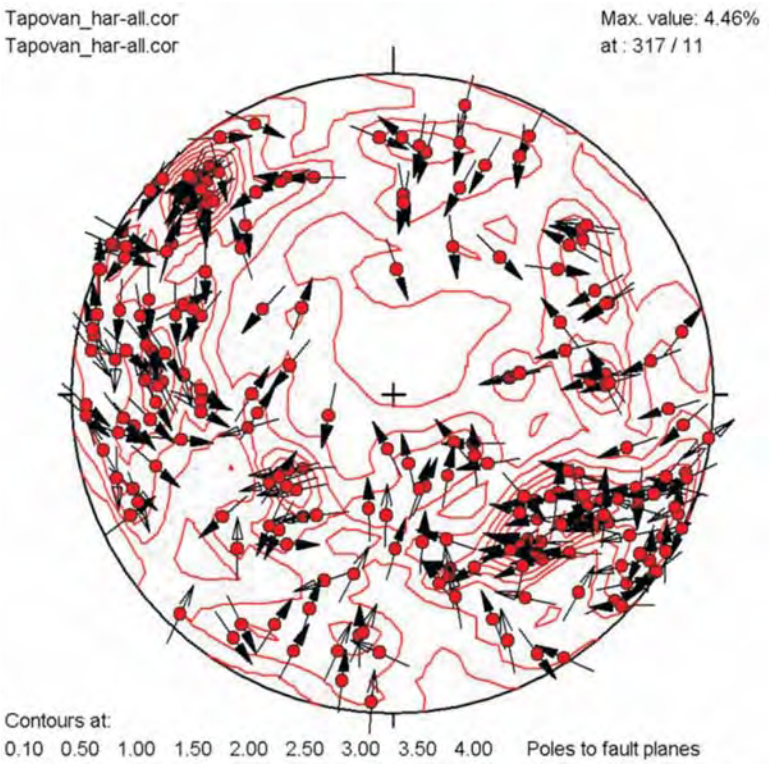

Fig. 1. Tangent-lineation diagram (equal-area projection) showing orientation of slickenside data. The arrows indicate the shearing directions of the hanging walls. Contours are densities of poles to fault planes.

conjugate fault system with oblique sinistral and dextral sense of shear, respectively, with a normal shear component.

Palaeostress Tensor II: The second palaeostress tensor shows a subvertical σ1, and a subhorizontal, NNE-SSW-trending σ3, thus displaying an extensional regime. It formed N-dipping normal faults, parallel to the main foliation and steep-dipping, and steep, SSW-dipping normal faults; in addition, it reactivated steep, SE-dipping faults as oblique normal dextral faults.

Palaeostress Tensor III: This palaeostress tensor displays again a subvertical σ1, thus an extensional stress regime, and a subhorizontal, but E-W-trending σ3. Only one fault set, normal faults with a minor sinistral component dipping to the W, was formed by this state of stress; no conjugate set was found in the working area.

Palaeostress Tensor IV: The fourth dominant stress tensor represents a compressional to strike-slip regime and shows a subhorizontal, WSW-ENE-trending σ1, with either σ2 or σ3 subvertical. This state of stress formed steep, SE-dipping, dextral, strike-slip faults. It could have formed a NE-dipping fault set as oblique sinistral reverse faults, if σ3 is subvertical.

Minor extracted stress tensors show NNW-SSE extension with a subvertical σ1 and a strike-slip regime with N-S compression and E-W extension, respectively. These stress regimes are not very robust and do not form one of the major fault sets seen in the working area, however, two of the palaeostress tensors and their related fault sets can be placed in a chronological order based on observed overprint relationships. The dextral, NE-SW-trending strike-slip faults of Tensor IV were formed in a compressional stress regime, before they were reactivated as oblique normal faults during the younger tensional stress regime of Tensor II.

In summary, after ductile, SSW-directed shearing in the MCT zone (mainly concentrated in the Helang Fm. beneath the Vaikrita Thrust), rocks of the HHC and LHC where deformed at semibrittle to brittle conditions. The presumably oldest deformation is related to stress Tensor IV, a compressional to strike-slip regime with WSW-ENE trending compression. The main structures that where formed during this phase are, steep, NE-trending, dextral strike-slip faults and reactivation of the main foliation as oblique-reverse faults. The course of the Alaknanda River west of Joshimath is parallel to the former fault set. The other three dominant stress regimes display either subvertical (Tenors II and III) or foliation-orthogonal orientations of σ1, hence extensional regimes. The main fault sets formed are steeply E-dipping, oblique dextral-normal (Tensor I) and steeply W-dipping, oblique sinistral-normal (Tensor III) faults. These N-S trending faults are prominently expressed in the topography, as e.g. in the course of the Alaknanda river north of junction with the Dhauliganga river and numerous fault traces. The conjugate fault set of Tensor I is dipping moderately to the NW and displays an oblique normal sinistral strike-slip displacement. It is trending parallel to the course of the Alaknanda River west of Joshimath too. The straight lower course of the Dhauliganga River follows a steeply SSW-dipping, normal fault set, which formed during stress regime II.

Célérier, B., Etchecopar, A., Bergerat, F., Vergely, P., Arthaud, F., Laurent, P. 2012. Tectonophysics 581, 206-219.
Delvaux, D., Sperner, B. 2003. Geological Society of London Special Publications, 212, 75-100.
Mahesh, P., Gupta, S., Saikia, U., Rai, S.S. 2015. Tectonophysics 655.

Deformation and Flow Character of the Higher Himalayan Crystallines (HHC) Belt in the Alaknanda-Dhauliganga Valleys, Garhwal Himalaya

Lawrence Kanyan[1,#], A.K. Jain[2]
[1]*Department of Earth Sciences, IIT Roorkee, Roorkee 247667, INDIA*
[#]*Present address: Geologist at Shell Technology Centre Bangalore, Bengaluru, INDIA*
[2]*CSIR-Central Building Research Institute, Roorkee 247667, INDIA*

The Channel Flow Model proposes that the Higher Himalayan Crystalline (HHC) rocks forming the anatectic core of the Himalayas have been extruded out from beneath the Tibetan plateau in form of a channel of weak mid-crustal rocks. Movement along the Main Central Thrust (MCT) in the south and the South Tibetan Detachment System (STDS) in the north, and exhumation along the Himalayan front played an important role in extrusion of this channel. However, this must be corroborated with real data and it is essential to quantify the flow in terms of Vorticity to characterize the kinematics of this crustal scale orogenic channel. Vorticity analysis of the samples collected from the Main Central Thrust Zone, Dhauliganga Valley section in Garhwal Himalaya, India, has been carried out through the use of rigid grains rotating in a ductile matrix. The analysis reveals that pure shear provides significant contribution (35% to 55%) to the deformation associated with southward thrusting along the MCT, with highest mean kinematic vorticity number (ω) values observed close to the shear zone boundaries. Vorticity numbers from within the anatectic core have not been reported as most of the vorticity gauges fail as deformation temperatures increase towards this region. The study also includes detailed field based structural analysis, petrographic analysis and study of quartz textures which reveal that the deformation temperatures increase as one moves to higher structural levels from the MCT. In the Vaikrita Group deformation temperatures >650°C are indicated by chessboard extinction and amoeboid boundaries of quartz grains.

Lithofacies analysis of the valley-fills in the middle part of Teesta River, Sikkim and Darjeeling Himalaya

Lukram Ingocha Meetei[1,*], Sampat Kumar Tandon[2,#]
[1]*M & CSD, Geological Survey of India, Visakhapatnam 530018, INDIA*
**ingocha2000@gmail.com*
[2]*Wadia Chair, IIT Kanpur, Kanpur 208016, INDIA*
[#]*sktand@rediffmail.com*

Lithofacies analysis of fluvial deposits was carried out along the Teesta river within the Main Central Thrust (MCT) and Main Boundary Thrust (MBT) in the lesser Himalayan region in Sikkim-Darjeeling Himalaya. The main fluvial landforms belong to river terraces (T1, T2, T3), fan lobes (F1 & F2), floodplain and channel bar deposits. Four major types of deposits, (i) Debris flow, (ii) Hyperconcentrated flow, (iii) Normal channel flow, and (iv) Sheet flow deposits, were identified. Debris flows are represented by mostly poorly sorted, weakly imbricated to disorganized matrix supported pebble to boulder gravels with silty sand. Hyperconcentrated flow deposits consist of clast-supported, poorly sorted polymodal gravel facies with poorly developed imbricated fabric, and generally occupy the lower parts of the terrace and fan sequences. The channel flow deposits constitute relatively well sorted, well imbricated and clast-supported gravels with coarse to medium sand matrix. Sheet flow deposits are characterized by clast supported well imbricated and horizontally bedded deposits, which were formed by high-velocity shallow flows as gravel bars without avalanche faces. Sub-facies units are classified into clast supported gravels, matrix supported gravels, granule facies, sandy facies, and palaeosol. Hyperconcentrated flow and debris flow deposits are mainly present in the terrace T2 and fanlobe F2. Normal channel flow deposits belong to braided channel facies and are mainly present in the terraces T3 and T1. Terrace T1 also shows the presence of Sheet flow and Hyperconcentrated flow units in its upper part. Granule facies deposited from the hyperconcentrated flow are present in the terrace T3 at Rangpo, Tumlang Khola and Kalijhora. In the middle part of fanlobe F1, both normal channel flow and hyperconcentrated flow deposits are present. The palaeosol are present in the upper units of the terrace T2 and fanlobe F2 in few places having a thickness of about 1 m. The colour of these palaeosol units vary from blackish to dark grayish and these are rich in humus as indicated by their high (2.3 to 6.1%) carbon content. The ^{14}C dates of the four palaeosol samples from the terrace T2 range from 1172 to 687 years B.P. It is evident that floodplains were widely formed at the end of the deposition of terrace T2 before the formation of terrace T1. The ^{14}C dates suggest that the floodplain was subjected to long-term exposure, during which humus soil was formed on it under humid climatic condition in the valley during 1,100 to 700 years B.P. Some of the lithofacies deposits also indicate that there were massive landslides along the valley walls indicated by the presence of Hyperconcetrated flood flow and debris flow deposits units during the formation of terrace T2 and Fanlobe F2. During these phases the basin might have been controlled by strong tectonic and high water discharge.

Do structural differences along strike of the Himalaya range represent changes in the pre-collision geometry of Greater India prior to collision?

Jess King
Dept. of Earth Sciences, University of Hong Kong, HONG KONG SAR
Jesking@hku.hk

Over the past few decades understanding of orogen development has evolved at a rapid pace, with classic geologic principles being combined with complex computer aided thermo-mechanical

simulations, to produce testable models of orogenic growth (Beaumont et al., 2004; Jamieson et al. 2004).

Typically, Greater India's pre-collisional northern edge, is usually modeled as a rifted passive margin. However, some workers (Ali and Aitchison, 2014) have argued for a quite different geometry resulting from its prior tectonic history. Whilst the western portion of the paleoboundary is seen as a Triassic rifted margin, the central and eastern portions developed more recently as India separated from Australia along a dextral 'scything' transform fault. This envisages the central-northern boundary to be a very narrow, weakly joined ocean-continent transition zone, with the North eastern corner attenuated into a series of half graben in response to shearing related to its motion along the original transform. Tentative models place the transition from passive rifted margin to 'scything transform' around longitude 77-80° East. Observable lines evidence presented for this transition are the restriction of ultra-high pressure metamorphic rocks to the north western Himalaya, and to ophiolite emplacement along the closing edge of the central portion of the India-Asia suture, and naturally, differences in the structural development of Himalayan front may also reflect this change.

Arguably, the most successful model to explain the development of the major structures of the central Himalaya is the so called, 'Channel Flow' model, where a key controversy is the mechanism by which flow initiates, and how long such a flow is sustained. In previous studies from Tibet (King et al. 2011), we identified low volume mid-late Oligocene Eohimalayan prograde (M1) granites consistent with those necessary to facilitate crustal flow and predicted that Oligocene melting should also be evident in the GHS of the southern Himalaya. However, despite recent studies having now began documenting similar prograde anatectic events both in the other North Himalayan gneiss dome, and also from very small late Eocene - early Oligocene prograde granitoid bodies (nanogranites) the GHS of central Nepal (Carosi et al., 2014; Iaccarino et al., 2015), and 33-28 Ma anatectic migmatites in the GHS of eastern Nepal (Groppo et al., 2010; Imayama et al., 2012), data for Himalayan prograde anatexis are still sparse. Furthermore, there still seems a paucity of any Himalayan age granitic bodies further west of Longitude ~82° East, compared to those found to the east. Do these observations throw light upon the state of the pre-collisional crust? And are these differences related to the paleoboundary of Greater India?

We speculate that the presence or absence of low volume prograde anatexis may relate to the geometry of the Indian crust, prior to plate collision, leading to either 'flow' or localised mid crustal ramping due to the availability, or lack, of more fusible lithologies. We present archive data, along with recent findings within this new context and suggest that the changes observed along strike of the orogen, allow us to gain a deeper understanding of not only the evolution of the Himalaya, but also of the pre-collisional geometry and nature of the plate boundaries of Greater India.

Ali, J.R., Aitchison, J.C. 2014. Basin Research, 26, 73-84

Beaumont, C., Jamieson, R.A., Nguyen, M., Medvedev, S. 2004. Journal of Geophysical Research, 109.

Carosi, R., Montomoli, C., Langone, A., Turina, A., Cesare, B., Iaccarino, S., Fascioli, L., Visonà, D., Ronchi, A., Rai, S.M. 2014. Geological Society of London Special Publications, 412, doi: 10.1144/SP412.1

Groppo, C., Rubatto, D., Rolfo, F., Lombardo, B. 2010. Lithos, 118, 287-301.

Iaccarino, S., Montomoli, C., Carosi, R., Massonne, H-J., Langone, A., Visonà, D. 2015. Lithos, 231. DOI:10.1016/j.lithos.2015.06.005

Imayama, T., Takeshita, T., Yi, K., Cho, D-L., Kitajima, K., Tsutsumi, Y., Kayama, M., Nishido, H., Okumura, T., Yagi, K., Itaya, T., Sano, Y. 2012. Lithos, 134-5, 1-22.

Jamieson, R.A., Beaumont, C., Medvedev, S., Nguyen, M. 2004. Journal of Geophysical Research, 109, doi:10.1029/2003JB002811.

King, J., Harris, N., Argles, T., Parrish, R., Zhang, H.F. 2011. Geological Society of America Bulletin, 123, 218-239.

Conglomerates in the Tibet-Himalayan region a decade and a half on: Some thoughts on sources, correlations, and interpretations

Jonathan C. Aitchison
School of Geography, Planning and Environmental Management,
University of Queensland, St Lucia, QLD 4072, AUSTRALIA
jona@uq.edu.au

At the onset of the 21st century Davis et al. (2002) published the first detailed account of a series of Paleogene-age arc-continent collision-related conglomerates from near Xigaze in southern Tibet that were then known to crop out along a strike length of around 120 km from near Lhatse eastwards to Baining. These distinctive conglomerates contain detritus that has unambiguously been sourced from the erosion of an intra-oceanic island arc (serpentinised ultramafic material, gabbros, basalts, chert, and other elements of the classic 'Penrose-style' ophiolite stratigraphy) combined together with sediments such as highly mature quartzose sedimentary lithologies of both fluvial and marine origin, limestones and other sedimentary rocks of passive margin affinity. Clearly these Luiqu Conglomerates had a mixed source and their existence represented something significant in terms of evolution of the Neotethyan realm. At rare locations depositional contacts could be observed. Elsewhere significant mismatches occur between the nature of proximal detritus and lithologies in adjacent units suggesting lateral offsets reminiscent of oblique-slip basins.

Our depositional model based on knowledge at that time suggested the Liuqu conglomerates accumulated in a series of narrow elongate strike-slip basins between a colliding oceanic arc and a passive continental margin. Two modern analogues for such settings being: The Longitudinal Valley in Taiwan between the colliding Luzon arc and the feather-edge of the Eurasian passive margin and; The Markham Valley in the Papua New Guinea collision zone of the western Solomon Sea where the intra-oceanic Bismarck arc is colliding with the leading edge of the Australian continent.

A younger, more extensively outcropping succession of conglomerates had been recognised at Mt Kailas by Gansser (1964) and these Oligo-Miocene units could be traced from east of Luobusa westwards across Tibet and to their lateral correlatives, the Hemis conglomerates, in the Indus valley in Ladakh. The stratigraphic nomenclature applied to these units reflected names applied in local mapping projects and as they traverse the breadth of Tibet and are best exposed on a revered mountain that is holy to several religion in far western Tibet we correlated them under the moniker 'Gangrinboche conglomerates', with Gangrinboche being one spelling of the Tibet name for Mt Kailas (Aitchison et al., 2002).

At that time of earlier investigations the transportation infrastructure in southern Tibet was extremely rudimentary. Much effort was required in order to travel to distant outcrops and many simply could not be visited for logistical or political reasons. Nonetheless, the preliminary picture that emerged from investigation of various conglomerate units was that they record key elements of the evolution of the India-Asia collisions system (Aitchison and Davis, 2004). In fact we regarded the presence/absence of conglomerate units and the nature of their source(s) to be a tectonic litmus test in the collision story (Aitchison et al., 2007).

In the decade and a half that has followed, we have been able to examine sections along the entire length of both the Yarlung Tsangpo and Indus sutures. Traversing west across Tibet we can recognise narrow zones of conglomerate that are essentially identical to Liuqu conglomerates in their type area. This includes outcrops north of Saga and immediately south of Mt Kailas in western Tibet. Further west the same units can be traced either side of the Karakoram Fault system with some spectacular outcrops cut along a new highway into the Zhada Basin. At each locality the conglomerates contain abundant material of ophiolite derivation together with copious red

radiolarian-bearing chert pebbles and accompanied by passive margin detritus likely derived from the northern margin of India.

In Ladakh study also reflects conditions of the time when conglomerates were first reported when most of a geologist's field time was spent trekking to outcrops rather than examining them. As with Tibet the transport infrastructure in Ladakh has continued to develop and access is much improved. Unraveling schemes of stratigraphic nomenclature in the Zanskar region, as well as elsewhere these conglomerates crop out in Ladakh, is not a task for the faint-hearted. This is in spite of (or perhaps because of) extraordinarily good outcrop. Various local schemes exist and units have been named, correlated and interpreted according to where they are seen to fit into the prevailing tectonic paradigm of the day. The success of this approach is at best mixed. Our investigations of the Ladakh region suggest that near-identical conglomerate units can be recognised and correlated with those in Tibet. Travelling NW along the Indus suture they can be recognised again at Lato thence in numerous outcrops along the northern flank of the Markha Valley crossing the Zanskar Valley at Chilling and continuing onwards towards Lamayuru. In some places massive proximal boulder conglomerates dominated by serpentinised harzburgite have been mistaken for ophiolite when in fact they are detrital units, albeit ophiolite-derived.

A key to working with these conglomerates is careful detailed field investigation. Of particular importance is the necessity to examine hand-specimens of conglomerate clasts in order to identify their lithology. Simple use of a hand lens to examine conglomerate clasts in the field provides unambiguous quantitative data with which to constrain source terranes. This first order methodology empowers sensible interpretation of the origins of sedimentary detritus. Reliance on detrital zircon analysis without recourse to knowing which clast lithologies are producing specific age populations commonly results in simplistic and inappropriate conclusions. Similar problems affect analysis of detrital sand grains where complex igneous lithologies are commonly milled down into less recognizable components.

Another important but seemingly lost art in the examination of sedimentary sections in the field is the necessity to map carefully and examine both structural and stratigraphic relationships using fossils as key data. Of particular note here are highly significant Paleogene sections south of the Yarlung Tsangpo suture zone. In these areas several recent studies have failed to recognize that sections reported as stratigraphically coherent are in fact zones of mélange. A lack of attention to this detail and fundamental inaccuracy in petrographic identifications has resulted in the publication of hugely erroneous statements. When combined with a lack of understanding of the subtle differences between accretionary (subduction) complexes and those of a collisional nature and the nature of serpentinite- vs. mud-matrix mélanges and their origins together with an astonishing unwillingness to even attempt to draw paleogeographically correct tectonic reconstructions it seems that in a supposedly data-rich age our understanding of this most majestic of collision systems is retrogressing.

Aitchison, J.C., Davis, A.M. 2004. Geological Society of London, Special Publication, 226, 217-233.
Aitchison, J.C., Davis, A.M., Badengzhu, Luo, H. 2002. Journal of Asian Earth Sciences, 21, 253-265.
Aitchison, J.C., Ali, J.R., Davis, A.M. 2007. Journal of Geophysical Research, Solid Earth, 112, B05423, doi:10.1029/2006JB004706.
Davis, A.M., Aitchison, J.C., Badengzhu, Luo, H., Zyabrev, S. 2002. Sedimentary Geology, 150: 247-273.
Gansser, A. 1964. The Geology of the Himalayas. Wiley-Interscience, New York. 289 pp.

A new approach of solving intricate structural problems: Use of angular balancing and shortening calculation across NW Sub-Himalaya

Joyjit Dey[1,*], Subham Sarkar[2], R. Jayangondaperumal[3], Anamitra Bhowmik[4], Shradha Jagtap[3], A. Lintoo[3], Pradeep Srivastava[3]

[1]*Indian Institute of Technology, Kharagpur 721302, INDIA*

**joy.ju.geology@iitkgp.ac.in*

[2]*Presidency University, College St. Kolkata 700073, INDIA*

[3]*Wadia Institute of Himalayan Geology, 33 GMS Road, Dehradun 248001, INDIA*

[4]*Jadavpur University, Raja S. C. Mallick Road, Kolkata 700032, INDIA*

In NW Sub-Himalayan frontal thrust belt the seismic interpretation of sub-surface geometry is ambiguous due to dissimilarity in the previously proposed models by various researchers. Though fault-bend and fault-propagation models have found to be convincing, but no simplified and direct method is yet to known to differentiate and testify various models for fault related folds. In this paper, a predicted angular function for quantitative geometric relationships between fault and fold shapes has been found to be a straight forward tool to test the structural complexity directly from the seismic profile. Use of distance-Displacement (dD) and excess area method in addition to measure the stretching/shortening amount and subsequent shortening rate on the seismic profile provides a measure to cross-check and predict the relative propagation rate of the fault and folds, and thus delivers a good mechanism to decipher the subsurface geometry of structures. Two seismic profiles Kangra-2 and Kangra-4 of Kangra re-entrant, Himachal Pradesh, were used in this regard, also shortening was calculated along the Jwalamukhi thrust and Jhor fault, found to be 6.06 km and 0.25 km respectively, that lie between Himalayan Frontal Thrust (HFT) and Main Boundary Thrust

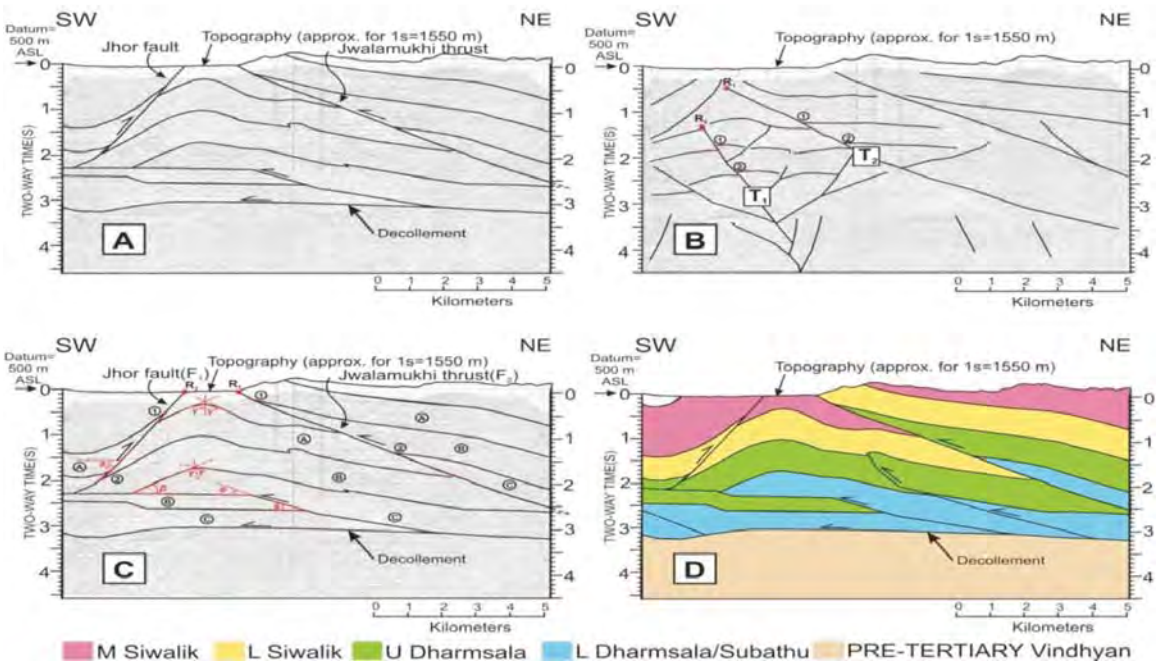

Fig.1. Seismic profile across Kangra-2 seismic section A) The seismic profile across Kangra-2 as interpreted by Powers et al. 1998. B) The same seismic profile as interpreted by Raiverman et al. Distance-displacement method has also been used on this profile considering R1 and R2 as reference points. C) The interpreted seismic profile of Kangra-2 by angular balancing method with cutoff angle Θ2/Θ and axial angle ϒ*/ϒ.

Table 1. *Comparison and calculation of shortening rate across various structures along the Sub-himalaya.*

Section	Method Applied	Thrust/ structures associate	Shortening Amount	Shortening Rate
Kangra 2 (Interpretated by Power et. al. 1994)	Distance-displacement method & Fault angle measurement	Jhor Fault Plane (F1)	10-30%	-
		Jwalamukhi Thrust Plane (F2)	70-80%	-
		Jhor Fault Plane (F1)	0.25 km	-
		Jwalamukhi Thrust Plane (F2)	6.06 km	-
Doon Seismic Profile	Fault angle measurement	HFT assuming straight ramp as marked by Power et. al. (Fig:)	0.44 km	0.93-1.8 mm/yr
		Assuming multi bend	4.06 km	16.67 mm/yr
Surinsar Seismic profile	Excess area method	Assuming the ancient folded topography of SMA anticline	—	12±1.6 mm/yr (considering wt. mean OSL age)
			—	14.29±1.95 mm/yr (considering least OSL age)

(MBT) in the frontal fold-thrust belts. For Paror anticline final cut off angle β 35° was obtained using transformation of seismic time profile to depth profile by time-depth conversion diagram, and it has been used to identify whether the interpreted structures are reasonable.

Also, this method has been applied to delineate subsurface feature and corresponding surfacial manifestation above the HFT of Dehradun re-entrant to find out the multi bending geometry of the buried thrust. Lastly, this method has been used to draw the intricate subsurface geometry of Surinsar Anticline, based on an OSL age of 18.7±2 ka at the strath contact along Chenab River and calculated shortening rate of 14.8±2.11 mm/yr. But here we had taken varying depth of decollement unlike the previous studies which fails to give account for the absurd shortening rate and dissimilarity between calculated and geodetic data, by taking this analogy we further provided evidences of lower and upper flat of MHT and also the presence of lithological heterogeneity beneath SMA anticline.

Our study signifies a great insight in the interpretation of subsurface seismic pattern and provides an important and simplified tool for the geologists to interpret and predict the existence of fault related fold and associate structures in the subsurface. Thus very useful to understand structures associated with active orogeny like Himalaya.

Barnes, J.B., Densmore, A.L., Mukul, M., Sinha, R., Jain, V., Tandon, S.K. 2011. Journal of geophysical research, 116, F03012, 1-19.
Boyer, S.E., Elliot, D. 1982. American Association of Petroleum Geology Bulletin v. 96, p. 1196-1230.
Chapman, T.J. 1983. Proc. Ussher Soc., 5, 460-464.
Chapman T.J., Williams G.D. 1984. Journal of the Geological Society, 141, 121-128.
Chen, J., Lu, H., Wang, S., Shang, Y. 2005. Journal of Asian Earth Sciences, 25, 473-480.
Coward, M.P., McClay, K. 1983. Journal of Geological Society of London, 140, 215-228.
Hossack, J.R. 1979. J. Geol. Soc. 136, 705-711.
Jamison, W.R. 1987. Journal of Structural Geology, 9 (2), 207-219.
Karunakaran, C., Rao, R.A. 1979. Misc. Pub. Geol. Ind. 41, 1-66.

Lu, H.F., Deng, X.Y. et al. 1989. Types Journal of Nanjing University (earth sciences), 4, 32-42.
Mishra, P., Mukhopadhyay, D.K. 2002. Journal Geological Society of India, 60, 649-661
Nakata, T. 1989. Geological Society of America Special Paper 232, 243-264.
Nakata, T., Otsuki, K., Khan, S.H. 1990. Tectonophysics, 181, 83-95.
Powers, M.P., Lillie, R.J., Yeats, R.S. 1998. Geological Society of America Bulletin 110, 1010-1027.
Raiverman, V., Srivastava, A.K., Prasad, D.N. 1993. Journal of Himalayan Geology, 4, 237-256.
Raiverman, V., Srivastava, A.K., Prasad, D.N. 1994b. Himalayan Geology, 15, 263-280.
Srinivasan, S., Khar, B.M. 1996. Geol. Surv. India Spec. Publ. 21, 295-405.
Suppe, J. 1983. American Journal of Science 283, 684-721.
Suppe, J., Medwedeff, D.A. 1984. Geological society of America Abstracts with programs, 16, 670.
Suppe, J., Medwedeff, D.A. 1990. Eclogae Geologicae Helveticae, 83, 409-454.
Wernicke, B., Burchefiel, B.C. 1982. Journal of Structural Geology, 4, 105-115.

Metamorphic study of deep structural level of the Songpan Garze belt along the Xuelongbao massif (Longmen Shan, Sichuan, China): evidence for two main phases of thickening in the eastern Tibetan plateau

Julia de Sigoyer*, Alexandra Robert, Manuel Pubellier, Audrey Billerot, Pierre Lanari, Damien Deldicque, Yong Li
ISTerre - University Joseph Fourrier, BP 53, 38041 Grenoble cedex 9, FRANCE
**Julia.de-sigoyer@ujf-grenoble.fr*

Different models are proposed for the formation of the Tibetan plateau. Most of them try to explain the thickening and uplift of the plateau since Cenozoic time, while it is well known that the formation of the plateau results from a polyphased history that began during Late Paleozoic. To take into account the inherited part of the plateau formation it is important to characterize the different stages of thickening of the plateau in its central part. In the Longmen Shan belt, located at the eastern border of Tibetan plateau, border of the Songpan Garze unit (Sichuan, China) the basement has been exhumed along the Beichuan and Wenchuan fault zone (Fig. 1). This basement supports the Songpan Garze sedimentary cover that has been deformed and metamorphosed during Mesozoic thickening. The contact between sedimentary cover and the basement crops out in the Xuelongbao massif in the internal part of the Longmen Shan belt that represents a tectonic window into a deep crustal level (Fig. 1).

A structural, microstructural, metamorphic observations, PT estimates (graphitization of carbonaceous material, quantified X-ray images, chlorite-phengite-quartz-water multi-equilibrium and thermodynamic modelling) and U-Pb geochronology are used to describe the tectono-metamorphic evolution of the Xuelongbao area. The Xuelongbao granite is dated at 765±7 Ma (in situ U/Pb dating on zircon), indicating that it forms part of the western Neoproterozoic South China block basement. The deformation in the western sedimentary cover above the Xuelongbao massif is intense, with step cleavage, twisted fold axes and CS structures with top to the SE thrusting vergence. In the cover above the Xuelongbao basement, four stages of deformation are described, three of them are related to the Mesozoic wedge thickening, and the last one is due to the Cenozoic deformation. An inverted metamorphic gradient from 470°C, 8 kbar to 620°C, 13 kbar is identified above a decollement zone, suggesting a stack of small sedimentary slices during the propagation of the Mesozoic accretionary wedge onto the South China block margin. This decollement zone has been exhumed during the Cenozoic reactivation of the Wenchuan thrust that also exhumed the Xuelongbao basement. This stage of deformation D4 is associated to greenschist metamorphic facies overprint.

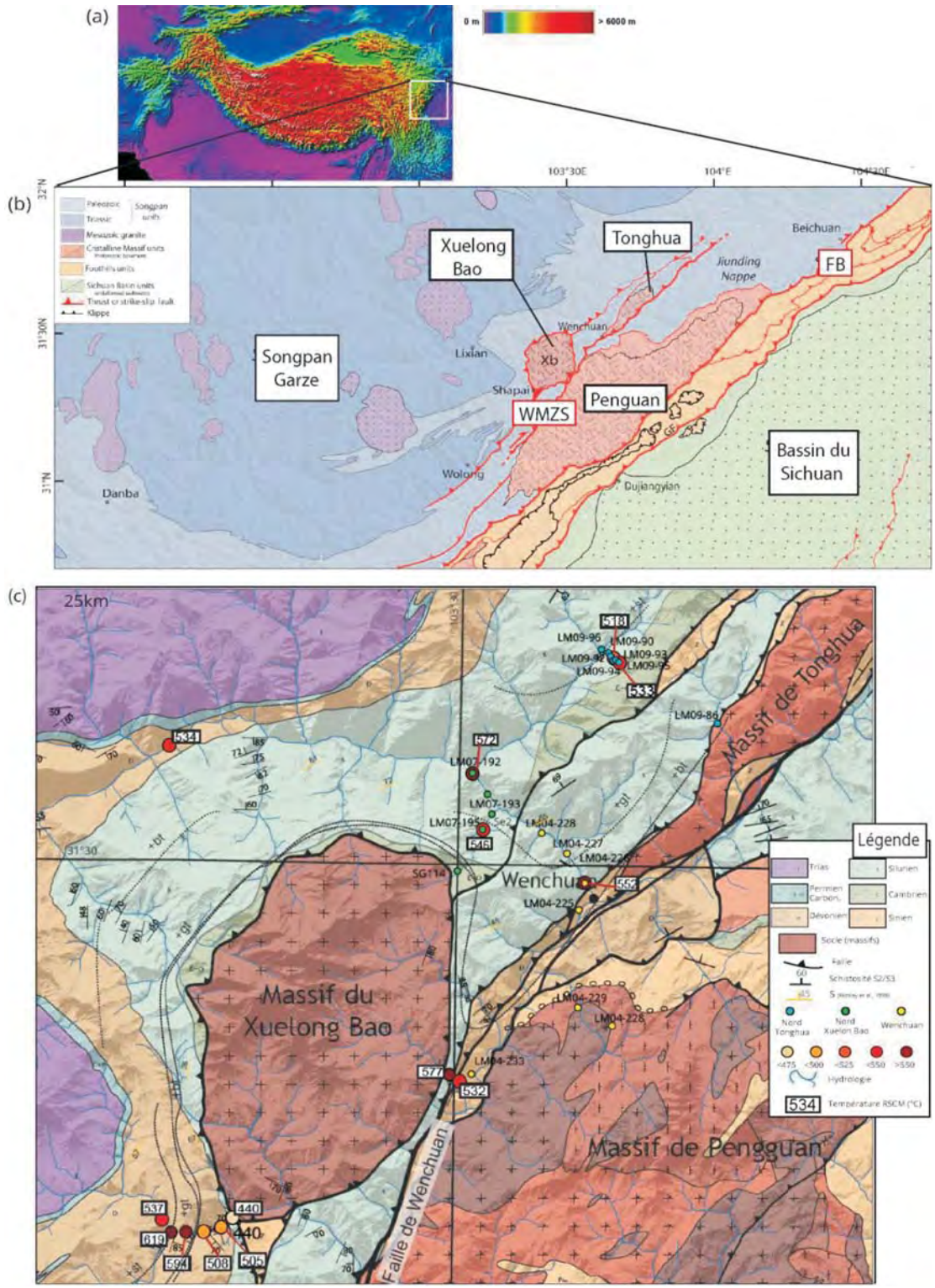

Fig. 1. (a) SRTM of the Tibetan plateau showing the location of the Longmen Shan. (b) Simple geological map of the Songpan Garze and Longmen Shan mountain belts at the eastern margin of Tibetan plateau. (c) Geological map of the Xuelongbao massif.

Extreme floods in the Tsangpo Gorge, observations from recent events And ancient evidence

Karl A. Lang[1*], Michael D. Turzewski[2], Katharine W. Huntington[2]
[1]*Department of Geosciences, University of Tübingen, Tübingen 72076, GERMANY*
**karl.lang@ifg.uni-tuebingen.de*
[2]*Department of Earth and Space Sciences and Quaternary Research Center, University of Washington, Seattle 98195, Washington, USA*

Extreme outburst floods resulting from landslide and glacial dam failure are a powerful agent of geomorphic change and a potential hazard along steep Himalayan Rivers. The potency of such events is magnified in the steep and narrow Tsangpo Gorge, a ~2 km deep knickzone crossing the young Namche Barwa metamorphic massif in the eastern Himalayan syntaxis. Evidence for extreme flood events in the gorge persists downstream where a series of slackwater flood deposits line the Siang River up to 211 m above the river channel (Lang et al., 2013). These meter-thick deposits drape preexisting topography and are often buried by landslide deposits. In contrast to alluvial deposits in the active river channel and terraces, flood deposits are very-fine to coarse sands, finely laminated and exhibit small scour features within fining upward and massive sequences. To interpret the record of extreme flood events, we investigate the provenance of these deposits, complimenting detrital zircon U-Pb and petrographic modal analyses with numerical simulations of recorded flood events.

Relatively unweathered and well exposed deposits at elevations within ~40 m of the channel are interpreted to be derived from an historical outburst flood in 2000 when a ~2 km^3 lake breached a landslide dam along the Yigong River, a Tsangpo Gorge tributary, resulting in peak discharges exceeding 105 m^3s^{-1} (Delaney and Evans, 2015). U-Pb dating of detrital zircons from these deposits is consistent with sources in Transhimalayan plutonic rocks exposed in the Yigong River valley with an additional contribution from metamorphic bedrock exposed in the Tsangpo Gorge. We simulated the 2000 flood using GeoClaw open source software for modeling geophysical flows (Berger et al., 2011). Simulations produced estimates of river discharge and flood wave arrival-time similar to observations recorded 450 km downstream and simulated inundation matches the distribution of high water marks mapped in the field and with remote sensing data. Hydrodynamic conditions favorable for localized deposition were reproduced in the regions where slackwater deposits are observed and conditions favorable for sustained erosion were reproduced within constricted reaches of the Tsangpo Gorge where shallow landsliding was observed in satellite imagery following the 2000 flood event (Larsen and Montgomery, 2012). Flood-triggering of landslides is an intriguing phenomenon that suggests a possible mechanism for extreme floods to preferentially remove material within the Tsangpo Gorge, focusing erosion within the knickzone (Lang et al., 2013).

Detrital zircon U-Pb ages from ten weathered slackwater flood deposits (including four deposits published in Lang et al., 2013) found over 40 m above the river channel indicate a sedimentary provenance in source rocks upstream of the Tsangpo Gorge, with a greater contribution of material from metamorphic bedrock exposed within the Tsangpo Gorge than both active channel deposits or deposits from the 2000 flood. Single-grain infrared stimulated luminescence (IRSL) dating of feldspars from eleven deposits yields ages of 14-35 ka, comparable to the timing of extensive lake deposition in the immediate headwaters of the Tsangpo Gorge (Guangxiang and Qingli, 2012). These deposits provide strong evidence that outburst flooding was an active geomorphic process in the Tsangpo Gorge during the Late Pleistocene, potentially evacuating lakes as large as 800 km^3 in volume (Montgomery et al., 2004). Evacuation of such large lakes through the Tsangpo Gorge would have confined flood discharges exceeding 106 m^3s^{-1} through a river channel,

less than 200 m wide, resulting in channel shear stresses capable of transporting virtually any size of preexisting bed material or contemporaneous landslide debris (Lang et al., 2013).

From a broader perspective, this story illustrates the potential for infrequent, but large magnitude geomorphic events to shape landscapes. While the specific contribution of these events is difficult to quantify without additional constraints on their reoccurrence, it is important to consider the influence of such extreme flood events in models explaining the intermontane deposition above the Tsangpo Gorge and incision within it.

Berger, M.J., George, D.L., LeVeque, R.J., Mandli, K.M. 2011. Advances in Water Resources, 34, 1195-1206.
Delaney, K.B., Evans, S.G. 2015. Geomorphology, 246, 377-393.
Guangxiang, Y., Qingli, Z. 2012. Journal Geological Society of India, 79, 295-301.
Lang, K.A., Huntington, K.W., Montgomery, D.R. 2013. Eastern Himalaya, Geology, 41, 1003-1006.
Larsen, I.J., Montgomery, D.R. 2012. Nature Geosciences, 5, 468-473.
Montgomery, D.R., Hallet, B., Yuping, L., Finnegan, N., Anders, A., Gillespie, A., Greenberg, H.M. 2004. Quaternary Research, 62, 201-207.

Iron Ooid beds of the Palaeogene Subathu Formation, foothills of NW Himalaya, India: Source of iron, origin and palaeoclimatic significance of Ooidal Ironstone

N. Siva Siddaiah
School of Environmental Sciences, Jawaharlal Nehru University, New Delhi 110 067, INDIA
nssiddaiah@gmail.com

Ooidal ironstone beds of the Palaeogene Subathu Formation, foothills of Northwest Himalaya were investigated using field, optical, geochemical and electron probe methods to shed light upon source of iron, origin of ooids as well as their palaeoclimatic and tectonic significance. The ironstone beds are associated with carbonaceous shales, and consist predominantly of berthierine/chamosite, as both ooids and matrix. Ooids are spherical displaying regular and continuous concentric cortical laminae surrounding nuclei. The ooidal ironstone consists of 40-60 wt. % Fe_2O_3 and 13-30 wt. % SiO_2. It has high abundance of Zr (180-716 ppm), Nb (10-42 ppm) and ΣREE (250-612 ppm). Their chondrite-normalised REE patterns are LREE enriched, negative Eu anomalies and relatively flat to positively sloped HREE. These patterns are similar to those reported for volcanic ash (tonsteins) fall deposit in the basin. The chemical composition, and Al/Si and Mg/Fe ratios of berthierine from the Subathu ironstone are consistent with that of berthierine formed in marine environment. The lithological association, distinct mineralogy, their textures and chemistry, suggest that the mineralogy of the ooidal ironstone is in-situ, formed in shallow-marine environment (prodeltaic to estuarine) under conditions of low net sediment accumulation during marine transgression. Similarity of the REE patterns and the incompatible trace element contents of the ironstone with those of volcanic ash beds as well as the occurrence of coeval basalts in the basin strongly suggest that they share a similar source. Volcanic ash by direct fallout and/or fluvial reworking was an important source of Fe, Al and Si required for berthierine formation. These sources promoted the authigenic or early diagenetic formation of berthierine in the Subathu Formation indicating a link between volcanic activity and ooidal ironstone formation. The stratigraphic position of ooidal ironstone coincides with the early Eocene volcanism, associated greenhouse conditions, and the transgressive flooding of shallow shelves.

Zircon U-Pb ages of the Mansehra Granite in the Lesser Himalaya, Pakistan

Masatsugu Ogasawara[1,*], Mayuko Fukuyama[2], Rehanul Haq Siddiqui[3], Ye Zhao[4]
[1]*Geological Survey of Japan, AIST, Tsukuba, JAPAN*
**masa.ogasawara@aist.go.jp*
[2]*Akita University, Akita, JAPAN*
[3]*Balochistan Univ. of Information Technology, Engineering and Management Sciences, Quetta, PAKISTAN*
[4]*Nu Instruments Ltd, Wrexham, UK*

Mansehra Granite occurs in the Lesser Himalaya zone of Pakistan, covering more than 2,000 km^2 area (Calkins et al., 1981; Kazmi and Jan, 1997; Arif et al., 1999). It is coarse-grained biotite granite with large porphyritic crystals of K-feldspar. The coarse-grained orthogneisses with augen texture are present north of the Mansehra Granite, and are included as member of the Mansehra Granite. The Mansehra Granite is considered as the typical plutonic unit within the Lesser Himalaya zone of Pakistan. Petrological and chemical data of the Mansehra Granite (Le Fort et al., 1980) suggest that it has S-type characteristics. It has been dated by Rb-Sr isochron method at 516±16Ma (Le Fort et al., 1980). Present study provides new zircon U-Pb ages to understand precise timing of the magmatic intrusion and discusses its significance.

A sample (MS02A) was collected in the Mansehra city along the road side cutting (34°20'17.4" N: 73°11'31.8" E). The sample shows typical characteristics of the Mansehra Granite. A tourmaline-bearing leucocratic muscovite granite body is present northwest of the Mansehra town (34°20'47.1" N: 73°11'10.6" E), and a sample was also collected for analysis (MS01A). The tourmaline-bearing leucocratic muscovite granite is considered that it intruded the main type of the Mansehra Granite. Zircons were separated from the samples with standard magnetic and heavy liquid methods. The zircon grains from the two samples have been mounted in an epoxy resin with standard zircons. LA-MC-ICP-MS U-Pb analysis was performed with NWR213 laser system and Nu Plasma II multi-collector ICP-MS at application laboratory of Nu Instruments Ltd. MS02A contains large zircon crystals, typically 200 μ long. The most of zircon grains show igneous oscillatory zoning. Though, considerable amounts of zircons from the MS02A contain inherited cores, and shape of the cores suggests detrital origin. The presence of the zircon core with detrital origin supports the model that the Mansehra granite was formed by partial melting of the sedimentary rocks. The zircon grains in the tourmaline-bearing leucocratic muscovite granite (MS01A) also show similar characteristic to MS02A. The 42 spot analyses were obtained on MS02A sample, and 38 analyses were made on MS01A. It is a prime objective to obtain igneous crystallization ages, however, it is also focused to obtain ages of the inherited core to examine characteristics of magma source.

Analytical results of 16 magmatic zircons from the Mansehra Granite, MS02A, yield a weighted mean $^{206}Pb/^{238}U$ age of 457.8±3.9 Ma with 4.4 of MSWD. Although the age obtained is about 60 Ma younger than the Rb-Sr isochron age of Le Fort et al. (1980), this age is now provide timing of intrusion of the Mansehra Granite. $^{206}Pb/^{238}U$ ages of inherited core in zircons from MS02A range from 716 to 2293 Ma. The ages of 20 inherited cores out of 26 of those are in the range from 716 to 852 Ma, giving narrow time span. The results indicate that the source sedimentary rocks which formed the Mansehra granite melts were derived from a region containing considerable exposures of 716-852 Ma magmatic rocks. The inherited zircon age suggests Paleoproterozoic history similar to the other part of Lesser Himalaya zone (Kohn et al., 2010). The minimum age of the inherited core, should indicate maximum age of the sedimentary rocks which were source of the Mansehra granite melt. Thus sedimentary rocks deposited between 458 and 716 Ma became the source of the Mansehra granite melt.

A weighted mean $^{206}Pb/^{238}U$ age of 20 magmatic zircons from the tourmaline-bearing leucocratic muscovite granite, MS01A, is 454.7±3.5 Ma with 4.3 of MSWD. The age is identical to

that of the main Mansehra Granite within the analytical uncertainty. Slightly younger mean age of the MS01A might explain the geological evidence. $^{206}Pb/^{238}U$ ages of inherited core in zircons from MS01A range from 719 to 1336 Ma. Most of the ages fall in interval between 719 and 846 Ma. This time range of the inherited core is similar to that of the main type of the Mansehra Granite, suggesting that the tourmaline-bearing leucocratic muscovite granite was derived from same source materials.

Several granitic gneisses are known in the Himalaya zone of northern Pakistan. The Choga granite gneiss in the Swat district has been dated by conventional U-Pb method (Anckiewicz et al., 2001). The well-defied discordia line yields an upper concordia intercept at 870±7 Ma and a lower intercept age of 468±5 Ma. Anckiewicz et al. (2001) interpreted lower intercept age to approximate the timing of magmatic emplacement, and upper intercept age to plutonic or volcanic protolith residing at exposed levels of the Indian continental crust. New $^{206}Pb/^{238}U$ age of 457.8±3.9 Ma of the Mansehra Granite is identical to the lower intercept age. Furthermore, upper Concordia intercept age of the Choga granite is almost similar to the age of the inherited zircon ages of the Mansehra Granite. Similar ages are obtained for the Chingali orthogniess in the Peshawar Plain, northern Pakistan (Ahmad et al., 2013).

Present study provided the precise $^{206}Pb/^{238}U$ age of 457.8±3.9 Ma for the Mansehra Granite, the age is about 60 million years younger than the frequently referred the Rb-Sr isochron age, indicating that the granite is of Ordovician, and not Cambrian age. The protolith of the Mansehra Granite should be sedimentary rocks containing zircons derived from plutonic or volcanic rocks of 700-800 Ma at exposed levels of the Indian continental crust. Igneous rocks with age of about 700-800 Ma are exposed in the northwest of India (e.g., Gregory et al., 2009), the rocks can be correlated with rocks supplied zircons to the plotolith of the Mansehra Granite. New data will help to construct pre-Himalayan history in the Lesser Himalaya zone in the northern Pakistan.

Ahmad, I., Khan, S., Lapen, T., Burke, K., Jehan, N. 2013. Journal of Asian Earth Sciences, 62, 414-424.
Anczkiewicz, R., Oberli, F., Burg, J.P., Villa, I.M., Gunther, D., Meier, M. 2001. Earth Planetary Science Letters, 191, 101-114.
Arif,M., Mulk, A., Mehmood, M.T., Shah, S.M.H. 1999. Geol. Bull. Univ. Peshawar, 32, 41-49.
Calkins, J.A., Offield, T.W., Abdullaah, S.K.M., and Ali, T. 1975. USGS Professional Paper, 716-C, 29p.
Gregory, L.C., Meert, J.G., Bingen, B., Pandit, M., Torsvik, T.H. 2009. Precambrian Research, 170, 13-26.
Kazmi, A.H., Jan, M.Q. 1997. Graphic Publishers. Karachi, 554p.
Kohn, M.J., Paul, S.K., Corrie, S.L., 2010. GSA Bulletin, 122, 323-335.
Le Fort, P., Debon, F., Sonet, J. 1980. Geol. Bull. Univ. Peshawar, 13, 51-61.

Sub-surface structure investigation and characterization of Moho geometry under the Himalaya-Karakoram-Tibet collision using surface wave Seismic tomography

Naresh Kumar[1,*], Abdelkrim Aoudia[2], Devajit Hazarika[1], D.K. Yadav[1], Dherandra Yadav[1]
[1]*Wadia Institue of Himalayan Geology, 33 GMS Road, Dehradun 248001, INDIA*
**nkd@wihg.res.in*
[2]*The Abdus Salam Intl. Centre for Theoretical Physics, ESP, Strada Costiera 11, 34151 Trieste, ITALY*

We used surface wave data of more than 300 earthquakes to investigate the sub-surface structure of the western part of Himalaya-Tibet collision zone. The data is first used to obtain the group velocities for each path between earthquake source and the station location. We extracted group velocities for the period range of 5 to 60 sec of fundamental mode of Rayleigh wave using Frequency Time Analysis (FTAN) technique of Levshin et al. (1972). The dispersion curves have variable trends in different direction of the study region. The variation are observed for all the time

period range, for the lower period the velocity was low for the paths passing through the sedimentary strata such as the Indo-Gangetic plains. However, in the intermediate period (25-40 sec) the paths passing through the India-Tibet collision zone and under the Tibetan plateau, the velocity is low compared to other parts.

The combined data of dispersion curves of whole study region is inverted to obtain the 2D tomography maps at different period. The inversion is performed using the technique of Yanovskaya and Ditmar (1990) to obtain average weighted dispersion curves at different grid point. The method of Yanovskaya (1997) is formulated to use the density of ray paths to obtain the resolution of tomography maps for different periods and the present data set has average spatial resolution of 200 km for whole region but in some parts also have even fine resolution. This technique also measures the elongation parameter, ε, of the averaging area which is the ratio of the difference between the maximum and the minimum sizes of the area to its mean size. Both these evaluated parameters are used to describe the quality of source receiver path coverage and we created the tomography maps after passing the data of these tests.

The constructed 2D tomography maps suggest changes of shear wave velocities for the study region indicating a high variation at intermediate period ranges for different paths. For period less than 15 sec, the low velocities are detected for the Indo-Gangetic plains which thick deposits of sediments however the velocities are higher in the India-Tibet collision zone including Karakoram fault region. Around 20 sec, the difference in velocities for different periods are very less suggesting homogeneity of acoustic impedance for whole study region. Further increase of period shows reversible results, the velocities in the collision zone start appearing as low velocities while in the southern part in Indo-Gangetic plains the velocities are comparatively higher. Around 30 sec period, prominent low velocity is appeared in the collision and whole part of the Tibet and this trend is prevalent upto 45 sec. It clearly indicates partial melting and partly fluid filled zones in the middle and lower crust. It also highlights the thicker crust which is the resultant of high topography and plate collision tectonics. Therefore the crustal strata in this part may be deeper depth compared to the respective part under the Indian plate and there is low velocity anomaly.

From the constructed 2D tomographic maps of group velocities at different period, the dispersion curves are extracted at different grids spacing of 1x1°. We then invert the dispersion curves based on the method of Herrmann (2013) to construct 1D shear wave velocity at each node. The inversion is a non-linear technique which also depends upon the initial model. To overcome this dependency, more than 250 inverted models are obtained from single dispersion curve after introducing changes in each initial model at different depths and then weighted average structure is extracted (Rapine et al., 2003) The shear wave velocities have similar manifestation as per obtain in the tomography maps of dispersion curves. The Karakoram fault zone is also not have uniform crustal shear wave structure where the lower crust in the southern part is coupled with high velocity. The obtained crustal thickness is less in this part and the mantle part of Indian plate is clearly visible at shallow depth compared to the northern part. The crustal thickness increases as moving towards north along the Karakoram fault and further north is the Hindukush region where it was not possible to clearly extract the Moho discontinuity.

Different profiles aligned to N-S direction, NW-SE perpendicular to the major tectonic features and along the strike of the Karakoram fault are taken to formulate the shear wave velocity structure. The inverted shear wave velocity for the upper part of the lithosphere indicates variable depth of the Moho discontinuity. As reported by Rai et al. (2006) the Moho depth of the Indian plate is ~40 km in the Indo-Gangetic plains towards south that increases to 75-80 km on the boundary of India-Eurasia plates. The similar observations are for the part of Tibetan plate (Wittlinger et al., 2004). The results shed new light on the long-lasting debates regarding processes governing continental deformation of mountain ranges and the formation of the Tibetan plateau.

Herrmann, R.B. 2013. Seism. Res. Lettr. 84, 1081-1088.
Levshin, A. L., Pisarenko, V. F., Pogrebinsky, G. A. 1972. Ann. Geophys., 28, 211-218.
Rai, S. S., Priestley, K., Gaur, V.K. et al. 2006. Geophy. Res. Lett., 10.1029/2006GL026076.
Rapine, R., Tilmann, F., West, M., Ni. J., Rodgers, A. 2003. J. Geophys. Res., 108(B2), 2120, doi: 10.1029/2001JB000445.
Wittlinger, G., Vergne, J., Tapponnier P. et al. 2004. Earth Planet Sci. Lett., 221, 117-130.
Yanovskaya, T.B. 1997. Izvestia Phys. Solid Earth, 33(9), 762-765.
Yanovskaya, T.B., Ditmar, P.G. 1990. Geophys. J. Int., 102, 63-72.

Precursory signatures observed at MPGO Ghuttu associated with Mw 7.8 Nepal earthquake of 2015

Naresh Kumar*, Vishal Chauhan, P.K.R. Gautam, S. Dhamodharan, Gautam Rawat, Devajit Hazarika
Wadia Institute of Himalayan Geology, 33 GMS Road, Dehradun 248001, INDIA
**nkd@wihg.res.in*

On 25 April 2015 the Mw 7.8 Gorkha earthquake shattered whole part of the Nepal and strongly hit the surrounding region of India and Tibet. As usual, still the aftershock activity is taking place, however, a strongest event of Mw 7.3 occurred on 12 August, 2015 after 17 days is the unusual aftershock in account of its larger size than expected. To the west of epicentre at 636 km, India is operating its first Multi-Parametric Geophysical Observatory (MPGO) established by the Wadia Institute of Himalayan Geology, Dehradun at Ghuttu, Garhwal Himalaya. Since over 7 years, the MPGO is accumulating continuous time series of different geophysical parameters to carry out earthquake precursory research in an integrated manner. The occurrence of this earthquake in the seismic gap is the first major event to examine the strength of multi-parameter observation for precursory research in this part of central Himalaya. The MPGO records the temporal variation in radon emanation (both within soil and underground water), electro-magnetic field changes, gravity changes, geodetic data, seismic activity (weak and strong motion) observation and supporting geo-hydrological and atmospheric parameters (Arora et al., 2012; Kumar et al., 2013).

The MPGO is located close and to the south of Main Central Thrust (MCT), situated within the seismic gap between Kangra earthquake of 1905 to its west and the Nepal-Bihar earthquake of 1935 to its east. The well documented high Himalayan seismic belt is around the surface trace of MCT in the Garhwal Himalaya (Mahesh et al., 2013) and also other part of the Himalaya. The past records of different parameters of MPGO, since its installation in 2007 have documented some anomalous behaviour prior to the occurrence of few nearby moderate size earthquakes (Choubey et al., 2009; Arora et al., 2012). On these observations, the data processing techniques of MPGO observations have been formulated, however, the amplitudes of anomalous changes are not much stronger which vary with the earthquake size and epicentre distance. Sometimes the data is influenced by the environmental and hydrological effects and the behaviour of anomalous changes may be different depending upon the earthquake source parameters.

The radon, one of most reported earthquake precursors is collected continuously at 15 minute interval within soil and underground water at 10 m and 50 m depths respectively within a 68 m borehole. The radon monitoring site is located to the south of the MCT, which is the part of the fault zone where high seismic activity is taking place and every major and higher magnitude earthquake of the Himalayan region is causing geotectonic sub-surface changes along this fault. The rupture zone area due to the occurrence of major and higher magnitude earthquake is created along the Main Himalayan Thrust (MHT). It is the discontinuity upon which the under-thrusting Indian plate is detached with the over-ridding Himalayan wedge and Eurasian plate. Basically the rupture starts on a

ramp structure vertically down from the surface trace of the MCT at a depth ~15 km and propagated southward updip, the similar observations are reported during recent Gorkha Nepal earthquake (Avouac et al., 2015). It indicates that high deformation (pre-, co- and post) are expected close to the MCT where the MPGO is located although the observatory is 636 km away towards west. A careful scrutiny of radon data during April 2015 and of previous period revealed prominent anomalous changes associated with Mw 7.8 Nepal earthquake.

The amount of radon emanation is reported to vary in the region surrounding to earthquake focus on the basis of well-accepted dilatancy diffusion model of Schoz et al. (1973). This concept is related to the changes of stresses during earthquake preparation and occurrence period which was reported for the first time at the time great Tashkent earthquake of 1966. In the Himalayan region the anomalous changes were observed few days before the occurrence of Chamoli earthquake of 1999 (Virk et al., 2001). In the present study also prominent changes are observed before the occurrence of Mw 7.8 Gorkha Nepal earthquake. Both in soil and underground water a similar behaviour of deviation from the average emanation trend is observed in two occasions. This is unique feature for the whole data set of over 7 year period and treated as precursory signatures to this earthquake. However, the characteristic of these anomalous changes in continuous time series does not fully match with earlier previous studies which may be related with geological and tectonic complexities of the crust.

The scrutiny of 2015 radon data of MPGO Ghuttu highlight that first time ~45 days before the Nepal earthquake origin time, the radon concentration within soil suddenly deceases. The similar behaviour is observed in the underground radon concentration ~8 days later on. These changes in both time series account a huge reduction in radon emanation and may be related with the enhancement of stress during the preparation zone of earthquake occurrence. It was followed with a constant but little bit change in radon emanation for over 35 days. Then suddenly radon concentration started increasing again first in the soil and then in the underground water (Fig. 1). Brief information of this precursory signature is reported by Kumar et al. (2015) however now a detail work is being performed with addition of previous and some post seismic data. The anomalous changes are also noticed in other parameters of MPGO Ghuttu but the amount and duration are variable. These observations suggest strong pre-seismic changes in radon while pre-, co- and post-seismic changes

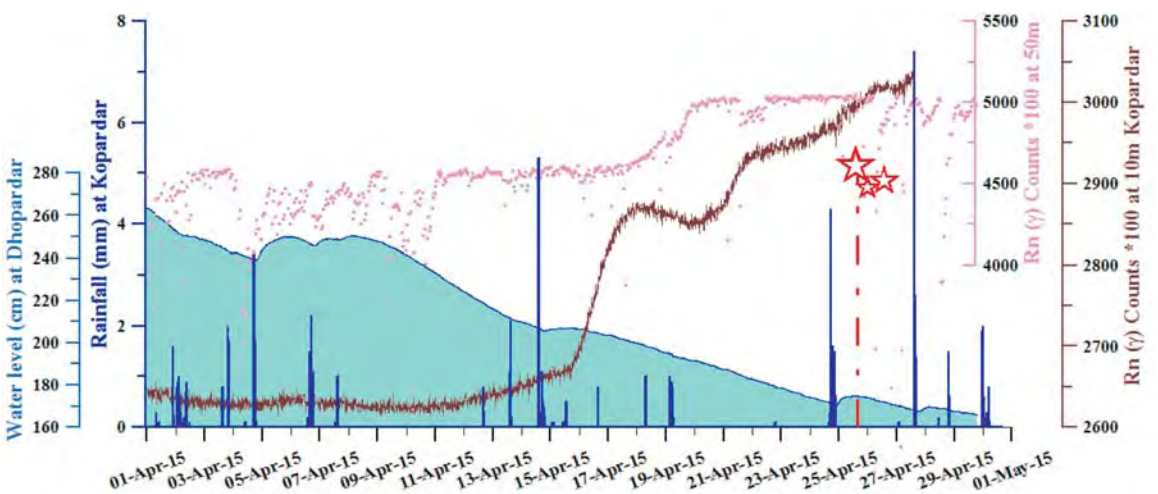

Fig. 1. Temporal variation of different parameters of MPGO Ghuttu (modified after Kumar et al., 2015). Variation in soil radon, underground water radon, Water table fluctuation within borehole and rainfall precipitations are shown with brown, pink, sky blue and blue colours respectively. Star denotes the occurrence time of Mw 7.8 and two strong aftershocks.

are observed in the gravity, sub-surface temperature and geodetic deformation. The different characteristics of anomalies in different parameters indicate non-linear relations among geophysical fields to the sub-surface deformation during earthquake generation and occurrence process. The deviation of nonlinear relations from one earthquake to another may indicates complexities in the sub-surface structure of the earth crust.

Arora, B.R., Rawat, G., Kumar, N., Choubey, V.M. 2012. Curr. Sci., 103 (11), 1286-1299.
Avouac J.-P., Meng L., Wei S., Wang W., Ampuero J.-P. 2015. Nat. Geosci. 10.1038/ngeo2518.
Choubey V.M., Kumar, N., Arora, B.R. 2009. Sci. Tot. Environ., 407, 5877-5883.
Kumar N., Rawat, G., Choubey, V.M., Hazarika, D. 2013. Acta Geophy., 61(4), 977-999.
Kumar, N., Chauhan, V., Dhamodharan, S., Rawat, G., Hazarika, D., Gautam, P.K.R. 2015. Curr. Sci. (Under Review).
Mahesh, P., Rai, S.S., Sivaram, K., Paul, A., Gupta, S., Sarma, R., Gaur, V.K. 2013. Bull. Seismol. Soc. Am., 103, 328-339.
Scholz, C.H., Sykes, L.R., Agarwal, Y.P. 1973. Science, 181, 803-810.
Virk, H.S., Walia, V., Kumar, N. 2001. Jour. Geodyn., 31, 201-210.

Understand the role of active structure on drainage evolution

Nilesh Kumar Jaiswara*, Prabha Pandey, Anand K. Pandey
CSIR-National Geophysical Research Institute, Uppal Road, Hyderabad 500007, INDIA
**nilesh_js@outlook.com*

In an active orogeny, like Himalaya, the geometry and evolution of drainage networks are sensitive to surface uplift, which is a function of tectonic history of the region (Seeber and Gornitz, 1983; Clark et al., 2004). The drainage basin morphology reflects the steady state condition of the substrate during active deformation (Hallet & Molnar, 2001) and therefore helps in understanding the control of geological structure on drainage basin evolution (Strahler, 1964; Esper Angillieri, 2008). Drainage patterns and deviation anomalies can provide information on evolving regional relief and tectonic deformation experienced by the catchment region (Howard, 1967).

NE Himalaya is a locus of active tectonics with the rapid exhumation of Namche Barwa syntaxis causing large scale deflection along Tsangpo-Siang and Lohit rivers during Quaternary in Himalayan terrain (Lang et al., 2014). The Dibang River, lying between Siang and Lohit, remained unaffected and hold clue to understand the regional drainage migration in response to active tectonics of the region. We carried out geomorphic indices analysis, which represent a quantitative approach to differential geomorphic analysis related to gradational processes of river channel including long profile, valley morphology and tectonically sensitive parameters (Homdouni, 2008).

The Dibang river drains through Lohit Granitoid complex, Higher Himalayan sequence, Lesser Himalaya, Sub Himalaya and Quaternary alluvium before merging with the Brahmaputra river system cutting across Lohit Thrust, MCT and MBT in Himalayan terrain (Fig. 1) The morphometric indices of the Dibang drainage are being extracted from merged SRTM and ASTER GDEM V2 data to improve data quality. The topographic metrics, swath profiles, geomorphic indices, longitudinal profiles, hypsometric integral (HI), basin asymmetry factor (AF) and stream-length gradient (SL) are calculated at basin and sub-basin levels. In order to differentiate lithological influence from structural control, different levels of average rock strength were defined and correlated with the derived parameters. The Dibang River show a dendritic pattern over the Lohit batholith and trellis pattern in the Higher and Lesser Himalayan terrain with the trunk channel run parallel to the structural elements. The basin asymmetric factor remains 51% suggesting no lateral tilting. The hypsometric curves of the Dibang basin and its sub-basins in the Himalayan terrain shows convex upward with high value HI ranging from 0.51 to 0.63 youthful channel draining through a tectonically active region.

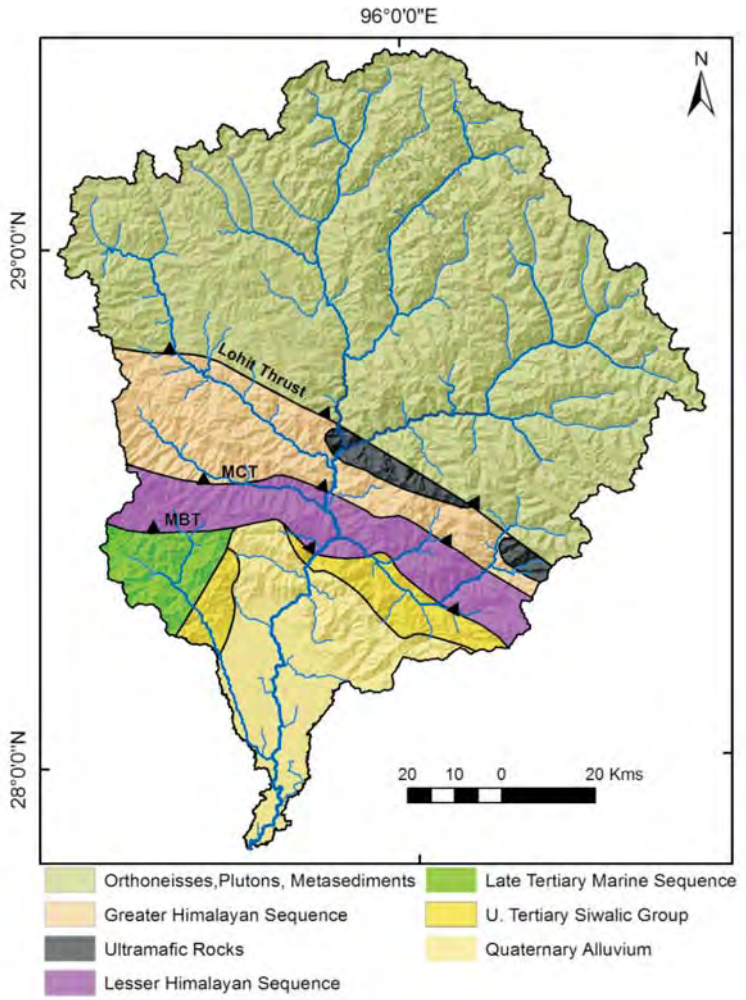

Fig. 1. Geology of Dibang basin (after Yin & Harrison, 2000).

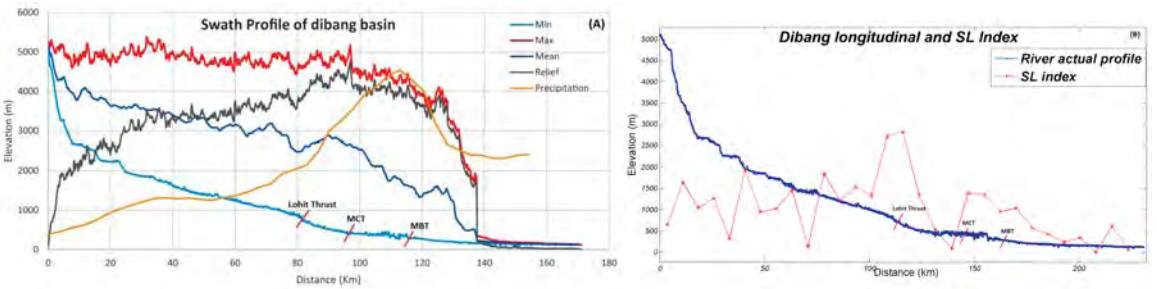

Fig. 2. (a) Longitudinal swath profile of Dibang river basin and (b) SL Index.

The longitudinal profile of the Dibang River shows three prominent knick point separating varying channel gradients, indicating the tectonically active zone. They correspond to the Lohit Thrust, MCT and MBT (Fig. 2a). The stream length gradient index discriminating the active segment of the river profile suggests two dominant zone across Lohit Thrust and MBT zone (Fig. 2b) suggesting them to be active structure. The same may be observed in the form of high topographic relief downstream of MCT and high precipitation (TRMM data) along the zone marking the

localization of tectonically induced uplift and precipitation induced incision leading to high exhumation in the zone.

Clark, M.K. et al. 2004. Tectonics, Vol.23, TC1006.
Esper Angillieri, M.Y. 2008. Environmental Geology, 55, 107-111.
Hallet, B., Molnar, P. 2001. J. Geophys. Res., 106, 13, 697-13,709.
Hamdouni et al. 2008. Geomorphology 96, 150-173.
Howard, A.D. 1967. AAPG Bull., 51, 2246- 2259.
Karl, A., Lang et al. 2014. EPSL 397 145-158
Seeber, L., Gornitz, V. 1983. Tectonophysics, 92, 335 - 367.
Strahler, A.N. 1964. Handbook of Applied Hydrology. Mc Graw Hill Book Company, New York, 4:39-76.
Yin, A., Harrison, T.M. 2000. Annu. Rev. Earth Planet. Sci. 28:211-80

Variation in uplift rate along Alaknanda valley, Garhwal Himalaya, India: a chronological and geomorphic approach

Naresh Rana[1*], Y.P. Sundriyal[1], G.S. Rawat[1], Navin Juyal[2]
[1]*Department of Geology, HNB Garhwal University, Srinagar 246174, INDIA*
**naresh_geo@yahoo.co.in*
[2]*Physical Research Laboratory, Ahmedabad, INDIA*

Alaknanda valley, a part of the Central Himalaya lies in Central Seismic Gap and therefore, has been considered as a potential area for future earthquakes. In Alaknanda valley the seismicity is concentrated near MCT and immediate south of it which has been ascribed as the manifestation of the geometry of the active detachment (Main Himalayan Thrust). Our study based on the optical chronology of fluvial terraces, river long profile and geomorphometry delineate the zones of differential uplift in Alaknanda valley.

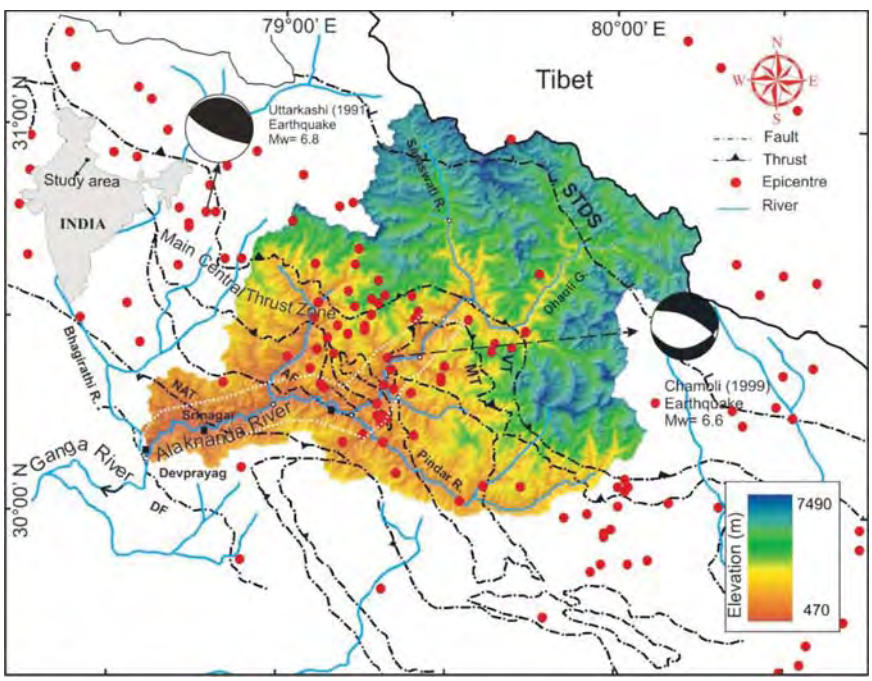

Fig. 1. Tectonic boundaries and distribution of seismicity in Alaknanda valley. VT=Vaikrita Thrust, MT=Munsiari Thrust, AF=Alaknanda Fault, NAT=North Almora Thrust, DF=Devprayag Fault.

It has been observed that in the Lesser Himalaya, morphology of the strath and the sedimentary architecture of the fill sequences indicate that the valley-fill sediments are incised into eleven surfaces of varying dimensions. The incision of the valley-fill sequence is ascribed to the reduction in the hydrological discharge (climate). In terms of bedrock incision, we observed significant spatial variability. For example, highest bedrock incision rate of 4.5 mm/yr is obtained from the southern mountain front (MCT), followed by significant reduction of 0.66 mm/yr in the vicinity of Alaknanda Fault (AF) and renewed increase of 3.15 mm/yr in the outer lesser Himalaya.

We ascribe the highest incision rate in the south of the MCT to the accelerated erosion caused by a combination of focused high intensity rainfall and active deformation (Wobus et al., 2005; Thiede, et al., 2009) which is in agreement with the GPS results of plate convergence along Garhwal Himalaya (Banerjee and Burgman, 2002). In this presentation, we will be discussing the results obtained using basin morphometry, chronologically constrained fluvial landform/valley-fill sediments and estimation of the bedrock incision history during the late Quaternary.

Benerjee, P., Bürgmann, R. 2002. Geophysical Research Letter 29 (13), 10.1029/2002GL015184, 2002
Thiede, R.C., Ehlers, T.A., Bookhagen, B., Strecker, M.R. 2009. Jour. Geophy. Res. 114, F01015, doi:10.1029/2008JF001010.
Wobus, C., Heimsath, A., Whipple, K., Hodges, K. 2005. Nature 434, 1008-1011.

Kinematics and strain partioning of Baijnath Klippe along Dewal-Narainbagarh section Inner Lesser Himalaya, Uttarakhand, India

Neha Joshi*, Sonam Singh#, Mohit Kumar, P.D. Pant
Department of Geology, Kumaun University, Nainital 263001, INDIA
**joshineha108@gmail.com, #sonamgeology@gmail.com*

The Baijnath Klippe lies in the Inner Lesser Himalaya, is derived from the Almora nappe of the Kumaun Himalaya. It forms a synformal structure bounded by NW-SE dipping Baijnath thrust. The kinematics and strain partitioning along Dewal-Narainbagarh transect of NW Kumaun Himalaya (Uttarakhand) provide us with the view of intensity of deformation in Baijnath Klippe. Due to movement in the Baijnath thrust, area had experienced polyphase deformation (D1, D2 and D3).The rocks from Baijnath crystalline (mylonites) form the hanging wall while the rocks from Berinag formation (quartzite) form the footwall. The macroscopic structures are evident for three phases of deformation and microscopic structures are evident for two phases of deformation. Ultimately the kinematics of Baijnath thrust in the northern part is and in the southern part it strikes towards NE-SW.

Rf/ϕ and Fry analysis are used to delineate the finite strain pattern in twelve samples. The data revealed oblate strain symmetry (flattening i.e. $0<k<1$) and the strain magnitudes showed considerable increase towards the tectonic contacts. Finite strain values are heterogeneous in nature and shows triaxial oblate geometry across the Baijnath thrust. It is suggested that the accumulation of finite strain was associated with significant volume change.

The ductile shearing in the area has led to the development of mylonites with mylonitic foliation. Kinematics indicators include S-C foliation, mantled porphyroclasts, myrmekite, micro-shears with bookshelf gliding, and mineral fishes exhibit strong dextral and sinistral sense of ductile shearing across the Baijnath thrust. The textural features of the minerals especially that of quartz and feldspar, indicate temperature of mylonitisation ranging between 300 and 500°C in the upper greenschist facies.

Interseismic deformation in the Darjiling-Sikkim-Tibet Himalayan Wedge, India

Malay Mukul[1*], S. Jade[2], K. Ansari[1], A. Matin[3], V. Joshi[4]

[1]*Dept of Earth Sciences, Indian Institute of Technology Bombay, Mumbai, INDIA*

**malaymukul@iitb.ac.in*

[2]*CSIR-Fourth Paradigm Institute (Formerly CSIR-CMMACS), Wind Tunnel Road, Bangalore, INDIA*

[3]*Dept of Geology, University of Calcutta, Kolkata, INDIA*

[4]*G. B. Pant Institute of Himalayan Environment and Development, Gangtok, INDIA*

The Darjiling-Sikkim Himalayan (DSH) region (Fig. 1a) is located in a fold-thrust, salient-recess setting together with transverse and oblique strike-slip faults (Mukul, 2010). The DSH region has not experienced a historical great earthquake and is dominated by moderate strike-slip rather than thrust earthquakes typically observed in the Himalaya (e.g. Ni and Barazangi, 1984). Coeval strike-slip and thrust seismotectonics occurs here with hypocenters located at depths both above and below the Main Himalayan Thrust (MHT) or the basal decollément of the Himalayan wedge (Mukul et al., 2014; Fig. 1) suggesting a seismogenic upper crust in the Darjiling-Sikkim Himalaya (Paul et al., 2015). However, only strike-slip, and not thin-skinned style thrust earthquakes, can account for the hypocenters that are deeper than the maximum decollément depth of ~20-30 km in the region (de la Torre et al., 2007; Mukul et al., 2014; Paul et al., 2015). In such a seismotectonic setting, does the strike-slip seismicity decrease the decollément related seismic hazard? We explored this question using long time series high-precision Global Positioning System data in the Darjiling-Sikkim Tibet (DaSiT) Himalayan wedge at ~88.5ºE longitude. The ITRF 2005 velocity in the DSH decreased northwards from ~53 mm/yr in the rigid Indian Plate to ~45 mm/yr near the Indus-Zangbo suture; it was ~48 mm/yr near the South Tibet Detachment at the Indo-Tibetan border. This implied an N-S convergence of ~9 mm/yr that was almost equally distributed within the LHD (~4-5 mm/yr) and the Higher Himalaya (~4 mm/yr). The north-component of the measured India-fixed convergence velocities, relative to the pole of rotation at Latitude 52.97±0.22º, Longitude -0.30±3.76º, and Angular Velocity 0.500 ± 0.008º/Myr (Banerjee et al., 2008), in the DaSiT wedge varied systematically from ~0-1 mm/yr in the frontal DSH to ~12.5-15.5 mm/yr in the Tibet Plateau indicating that thrust-seismotectonics was active in the DaSiT wedge. These results are similar to those observed in Central Nepal (Grandin et al., 2012). The east-component of the measured India-fixed convergence velocities, were statistically insignificant indicating that the strike-slip seismotectonics had not affected surface GPS velocities in the wedge probably because of their high depth.

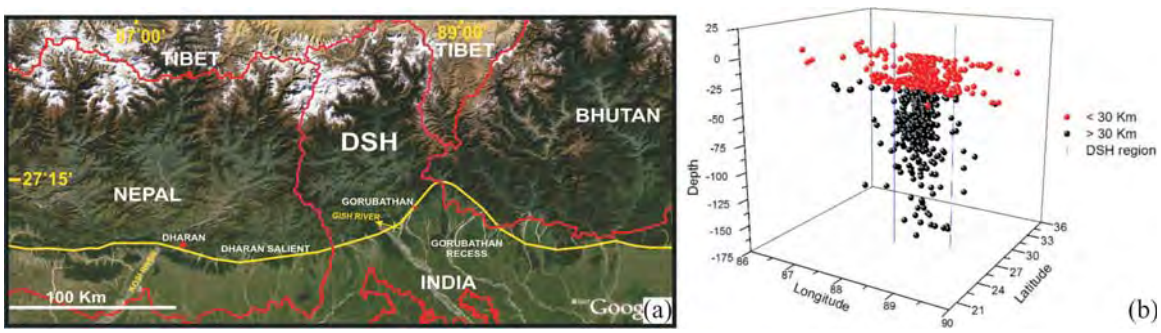

Fig. 1. (a) Location of the Darjiling-Sikkim Himalaya (DSH) (b) Seismicity in the Darjiling-Sikkim Himalaya (DSH) during 2008-2009 from local seismic network stations (Mishra et al., 2010). The seismicity ranges in magnitude (Mc) from 1.5 to 6.7 and exhibits a large hypocentral cluster indicating seismicity both above (red) and below (black) the MHT. Vertical blue lines define the DSH region. The Lesser Himalayan Duplex (LHD) (Bhattacharyya and Mitra, 2009; Mitra et al., 2010) has been mapped in the region between Lat. N 27.07 to 27.50 and Long. E 88.23 to 88.62 suggesting that it may be seismically active in the DSH.

Dislocation modelling of the measured India-fixed north convergence velocities in the DaSiT wedge indicated that the MHT is locked at a depth of ~16 km at ~27.7ºN to the north of the LHD (N 27.07 to 27.50); the frontal ~100 km transport- parallel width of the MHT is locked. The dip of the MHT is modelled to be 6ºN with a top-to-the-south reverse slip of ~18 mm/yr indicating again that strike-slip seismotectonics had not affected the slip and strain accumulation on the MHT in the DaSiT wedge. It has also been postulated that almost 10-18 m of slip potential on the MHT exists in the DaSiT wedge resulting in a Mmax of 8.7 earthquake (Bilham et al., 2001). The GPS measurements seem to be consistent with the decollément (MHT) slipping aseismically in the hinterland at ~18 mm/yr and locked just north of a seismically active LHD suggesting that the DSH could be the location of the next large decollément earthquake in the Himalaya.

Banerjee, P., Burgmann, R., Nagarajan, B., Apel, E. 2008. Geophysical Research Letters, 35, L18301, doi: 10.1029/2008GL03 5468.

Bhattacharyya, K., Mitra, G. 2009. Gondwana Res.,16, 697-715.

Bilham, R., Gaur, V.K., Molnar, P. 2001. Science, 293, 1442-1444.

de la Torre, T.L., Monsalve, G., Sheehan, A.F., Sapkota, S., Wu, F. 2007. Geophys. J. Int., 171, 718-738.

Grandin, R., Doin, M-P., Bollinger, L., Pinel-Puysségur, B., Ducret, G., Jolivet, R., Sapkota, S.N. 2012. Geology, 40 (12), 1059-1062.

Mishra, O.P., Chakrabortty, G.K., Singh, O.P., Ghosh, D.C., Mukherjee, K.K., Das, P.C. 2010. GSI Report (FSP: SEI/CHQ/CGD/2007/070), p. 57.

Mitra, G., Bhattacharyya, K., Mukul, M. 2010. J. Geol. Soc. India, 75, 276-288.

Mukul, M. 2010. Journal of Asian Earth Sciences, 39, 645-657.

Mukul, M., Jade, S., Ansari, K., Matin, A. 2014. Current Science, 106 (2), 126-131.

Ni, J., Barazangi, M. 1984. J. Geophys. Res., 89(B2), 1147-1163.

Paul, H., Mitra, S., Bhattacharya, S.N., Suresh, G. 2015. Geophysical Journal International, 201(2), 1070-1081, May 2015. doi:10.1093/gji/ggv058

Spatial and temporal variability of climate change in high-altitude regions of NW Himalaya: Implications on recent mass movements in the Nubra Valley in Karakoram Himalayas

M.R. Bhutiyani

Director, Defence Terrain Research Laboratory, Delhi 110 054, INDIA

mahendra_bhutiyani@yahoo.co.in

The high mountain areas such as the Alps, the Rockies, and the Himalayas etc. are considered as the 'hotspots' over the surface of the earth where impacts of climate change are being positively felt. The analyses of the temperature data collected manually at different observatories in NW Himalayas during the period from 1866 to 2012 show significant rate of warming during the winter season (1.4ºC/100 years) than the monsoon temperature (0.6ºC/100 years), due to rapid increase in both, the maximum as well as minimum temperatures, with the maximum increasing much more rapidly. Studies have confirmed significant spatial and temporal variations in magnitude of winter as well as summer warming at different ranges. While windward side of the Pirpanjal and parts of Greater Himalayan and Karakoram ranges have shown statistically significant winter and summer warming, leeward sides of these ranges have not shown much change. Significant decreasing trend in winter warming experienced at almost all stations above equilibrium line (>5300 m in altitude) points towards an anomaly which needs to be further explored. Spatial and temporal variations in winter and summer warming and consequent precipitation changes in different ranges/regions of the NW Himalayas are attributed to varying scales of anthropogenic activities and growing urbanization of the areas.

Climate change in high altitudes of the Karakoram Himalayas appears to have impacted geomorphological characteristics of the mass movements. Two recent mass movement events of reasonably large magnitude in the Nubra Valley, one classified as a 'rock avalanche' over the North Terong Glacier and other one as a debris-earth flow over main Siachen Glacier, are studied using multi-date remote sensing data (LANDSAT imageries), snow-meteorological data of a nearby station of last 30 years, TRMM (Tropical Rainfall Measurement Mission) data, seismic data recorded by seismic stations located in the area and data collected during field investigations. Abnormally high temperatures causing rapid thaw cycles and persistent light to moderate rainfall, resulted in instability in the scree-filled slope and subsequent massive failure. Occurrence of debris-earth flow, a rarity in high attitudes of the Karakoram Himalayas, indicate a warming climate and change in nature of natural hazards in this part of Himalayas.

First event on the North Terong Glacier appears to have increased glacier surface velocity leading to almost two-fold increase in post-event period and triggering a surge, an earthflow over the Siachen Glacier has led to a formation of large supra-glacial lake on the debris. Consequent glacier lake outburst flood (GLOF) or a Jökulhlaup poses a potential threat to the lives of civilian population inhabiting downstream areas. The study will help the soldiers of the Indian Army and mountaineers in identifying similar areas vulnerable to rock avalanches and debris-earth flows and saving their precious lives.

High resolution 1600 year climatic records inferred from Tso-Moriri lake Ladakh, north western Himalaya, India

Narendra K. Meena*, Prakasam M, Sudipta Sarkar, Pranaya Diwate
Wadia Institute of Himalayan Geology, 33 GMS Road, Dehradun 248001, INDIA
**naren@wihg.res.in*

The paleoclimate records from the cold dessert of Ladakh, northwestern India are important for understanding the relationship between the Westerlies (winter rainfall) and Indian Summer Monsoon (ISM) rainfall in Ladakh Himalaya. The lakes of Ladakh region are ideal for such studies as they record the signal of the past climatic changes in sediment column. Therefore, we acquired one sediment core sample measuring 5 m from the Tso-Moriri lake of Ladakh. A 1600 year BP (Before Present) multipoxy (carbon isotope, environmental magnetism and geochemistry, etc.) climatic records were reconstructed from AMS ^{14}C dated core sample. The $\delta^{13}C$ isotope values of core fractionate between -25 to -13‰ indicates the presence of both C3 and C4 vegetation in the region. The time between 400 and 1600 AD shows abundance of the C3 plants with a $\delta^{13}C$ value of -25‰ that indicate a wet phase of the climate in which the Tso-Moriri area received higher rainfall. The time between 1600 and 1800 AD we observed a sharp decreased in $\delta^{13}C$ value from -24 to -13‰ with fluctuations. The sudden fall in $\delta^{13}C$ indicates dominance of the C4 plants in the Tso-Moriri area that infer dry climate with low rainfall. After 1800 AD the $\delta^{13}C$ shows mixed values raging from -22 to -18‰ with fluctuation that advocates moderate rainfall in region. The heavy metal Ti (%) and magnetic susceptibility (χlf) also shows higher values in wet and warm phase of the climate and supports to the $\delta^{13}C$ interpretation.

Origin of the Manipur Ophiolite Complex, NE India: Constraints from geochemical and Sr-Nd isotopic studies

Oinam Kingson Singh*, Sibin Sebastian, Rajneesh Bhutani, S. Balakrishnan
Dept. of Earth Sciences, Pondicherry University, Puducherry 605014, INDIA
**kingsonoinam39@gmail.com*

The Manipur Ophiolite Complex (MOC) is the southern continuation of the Nagaland Manipur Ophiolite belt (NMOB) which is a part of the Indo-Myanmar Orogenic Belt (IMOB). It is believed that the IMOB is formed due to the subduction and obduction processes caused by collision of the Indian plate and Burmese plate (Acharyya et al., 1989; Bhattacharjee, 1991; Mitchell, 1993; Singh, 2008). It occurs as a narrow belt, of approximately 200 km in length, 2-20 km in width and covers an area of approximately 2000 km^2. The MOC is composed of dismembered ophiolite sequence containing serpentinised peridotites, pelagic sediments, podiform chromitites with minor mafic and felsic intrusive. Origin of the ophioilite, in MOC, remains an outstanding issue. Based on the chromite chemistry Tapan Pal et al. (2014) have suggested a subduction zone setting while Singh et al. (2008, 2009, 2012a,b); Nightojoum et al. 2012 and Singh 2013 based on the whole-rock and mineral elemental chemistry favoured MORB origin of these rocks.

We present here new elemental and isotope data from the MOC and attempt to understand the petrogenesis of the serpentinized peridotites. We show that the existing whole-rock elemental data are not able to discriminate the tectonic setting of the origin unequivocally, a fact that not only reflects on the limitations of the tectonic discrimination diagrams (Li, 2015), but also the complex origin of the MOC.

The new whole-rock REE data along with the existing data in the literature are compared with that of from different tectonic settings (Fig. 2a). Based on geochemistry, the samples are classified into three groups: peridotite samples show LREE depletion when normalized to the N-MORB, while the mafic intrusives are LREE enriched and also plot in the range of Izu-Bonin arc as well as in the range of Lau back arc samples and serpentinites show variable mobility of some elements, probably related to the serpentinisation process. The depletion of LREE in the peridotites and enrichment in the mafic intrusives of the MOC, appear complementary to each other. This is confirmed with a melting model that indicates that peridotites are residual solids after 10-15% melt is extracted from a spinel-lherzolite source. The mafic intrusives show similar pattern as the extracted melt. The ambiguity related to the tectonic setting is also reflected in the standard tectonic discrimination diagrams using other trace elements. For example, Nb/Yb vs Th/Yb discrimination diagram (Fig. 2b) is successfully used to discriminate between the subduction-related and subduction-unrelated ophiolites (after Pearce, 2008), however, the results from the MOC samples plot in both the fields. The peridotites indicate subduction-related while mafic intrusives plot in the subduction-unrelated fields. This ambiguity could be because the back-arc spreading centers such as presently active Valu Fa Ridge, Lau basin produce basalts that are difficult to distinguish from the MORBs. It is, therefore, possible that while peridotite are the residual mantle wedge or depleted slab of the subduction zone while the mafic intrusives are the back-arc basalts.

Radiogenic isotope ratios do not get fractionated during melting or magmatic processes and thus provide unambiguous information about the source. We are in process of generating Sr-Nd isotope ratios of the peridotites and the results would be discussed during the presentation. The preliminary results of Nd isotope ratios indicate that the source was depleted to the same range as the normal MORB mantle.

We conclude, taking into consideration all the available geochemical data that rocks in the MOC represent residual mantle as well as extracted melt. We propose that a new model of origin that

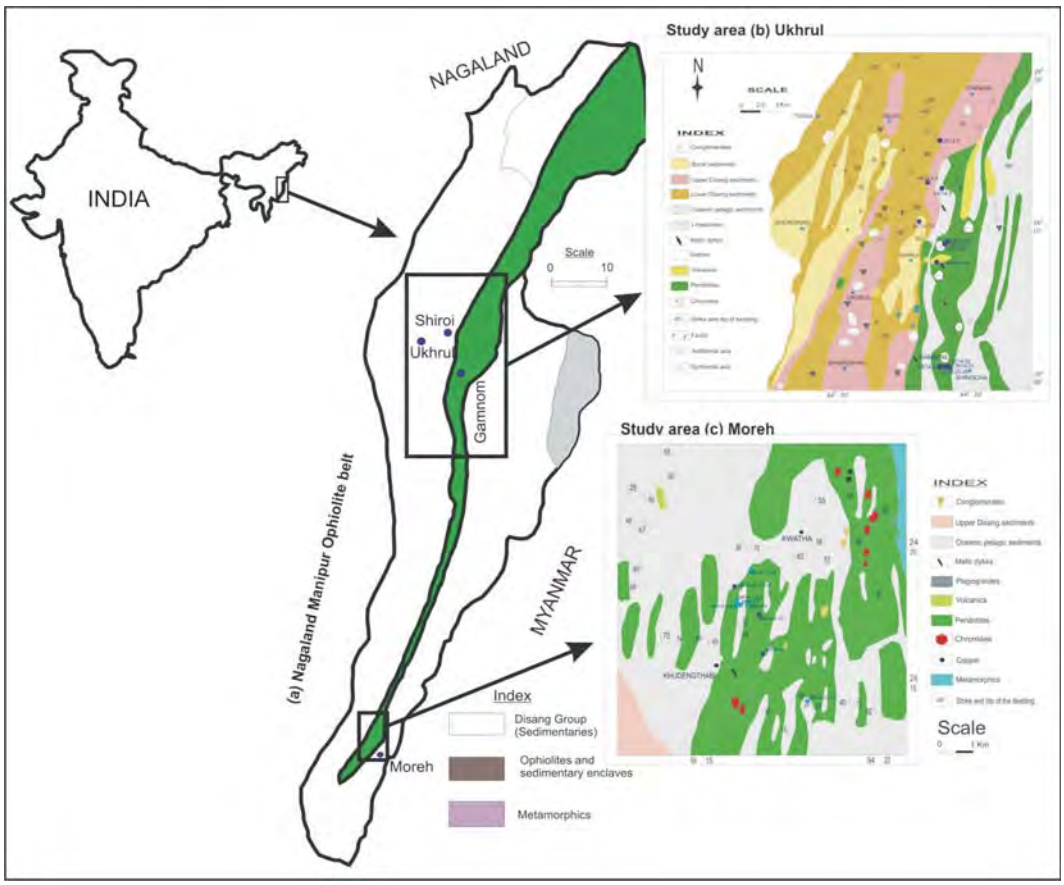

Fig.1. (a) Geological map of the MOC (after Singh et al., 2013); (b) Geological map of Ukhrul (after Singh, 2013) and (c) Geological map of Moreh (after Singh, 2013). Study areas are shown along with the sample locations.

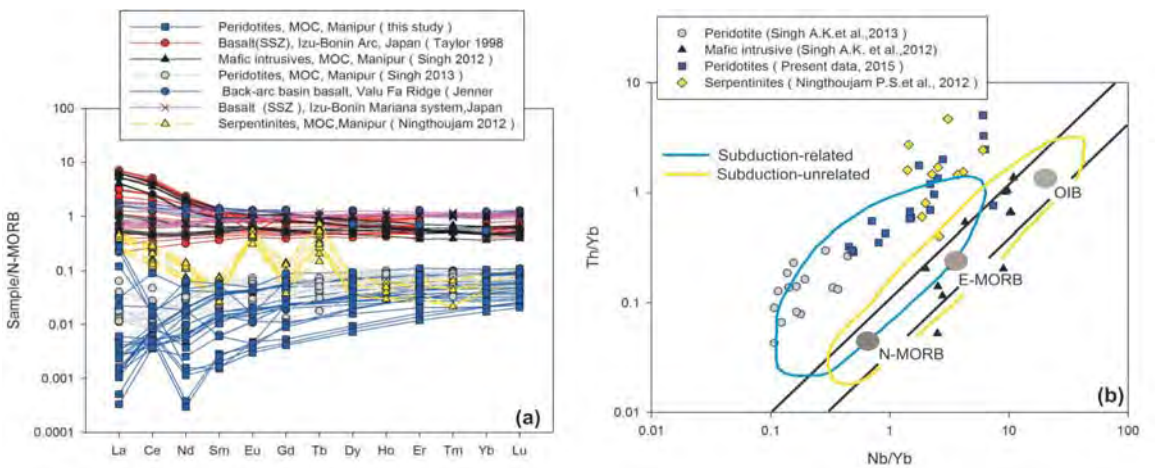

Fig.2. (a) N-MORB normalized rare earth elements for serpentinites (Ningthoujam *et al.* 2012) , peridotites (Present study; Singh 2013) , mafic intrusives (Singh *et al.* 2012) of the MOC ; back-arc basin volcanics for Valu Fa ridge, Lau basin (Jenner *et al.* 1987); basalts of Izu Bonin Arc, Japan (Taylor *et al.* 1998); basalts from Isu-Bonin-Mariana system,Japan (Reagan *et al.* 2010). Normalised value are from Sun and McDonough (1989) (b) Nb/Yb-Th/Yb discrimination diagram (after Pearce, 2008).

involves subduction zone and back-arc juxtaposition in the present MOC should be explored fully before finalizing on the tectonic setting of the MOC.

Acharyya, S.K., Ray, K.K., Roy, D.K. 1989. Jour. Geol. Soc. India, 33, 4-18.
Bhattacharjee, C.C. 1991. Tectonophysics, 191, 213-222.
Jenner, G.A., Cawood, P.A., Rautenschlein, M., White, W.M. 1987. Jou. Volcanol. Geothermal Res., 32, 209-222.
Li, C., Arndt, N.T., Tang, Q., Ripley, E.M. 2015. Trace elements indiscrimination diagrams. Lithos, 232, 76-83.
Mitchell, A.H.G. 1993. Journal of the Geological Society of London, 150, 1089-1102.
Ningthoujam, P.S., Dubey, C.S., Guillot, S., Fagio, A.S., Shukla, D.P. 2012. J. Asian Earth Sci, 50, 128-140.
Pal, T., Bhattacharya, A., Nagendran, G., Yanthan, N.M., Singh, R., Raghumani, N. 2014. Miner Petrol, 108, 713-726.
Pearce, J.A. 2008. Lithos, 100, 14-48.
Singh, A.K. 2008. Jour. Geol. Soc. India, 72, 649-660.
Singh, A.K. 2009. Curr. Sci., 96, 973-978.
Singh, A.K. 2013. J. Asian Earth Sci., 66, 258-276.
Singh, A.K., Devi, L.D., Singh, N.I., Singh, R.K.B., 2012b. Frontier of Earth Science Research. Proceedings of the Seminar. Gulbarga, India, 103-105.
Singh, A.K., Devi, L.D., Singh, N.I., Subramanyam, K.S.V., Singh, B.R.K., Satyanarayanan, M. 2013. Chemie der Erde, 73,147-161.
Singh, A.K., Ibotombi, N.I., Devi, L.D., Singh, R.K.B. 2012a. J. Geol. Soc. India, 80, 231-240.
Singh, A.K., Singh, N.I., Devi, L.D., Singh, R.K.B. 2008. Jour. Geol. Soc. India, 72, 168-174.
Singh, N. I, Devi, L.D., Chanu, Th. Y. 2013. Journal Geological Society of India, Vol.82, pp.121-132.
Taylor, R.N., Nesbitt, R.W., 1998. Earth and Planetary Science Letters, 164, 79-98.

Petrological and geochemical characteristics of the ultramafic rocks of the Indo-Myanmar Ophiolite Belt, Northeastern India

B. Maibam[1], Kh. Nirupama[1], S.F. Foley[2]
[1]Department of Earth Sciences, Manipur University, Imphal 795003, INDIA
**nirukh@gmail.com*
[2]CCFS and Dept. Earth and Planetary Sciences, Macquarie University, North Ryde, Sydney, NSW 2109, AUSTRALIA

Ophiolites are remnants of oceanic lithosphere (oceanic crust and upper mantle) that are preserved in the continental margins during the closure of the oceanic basins (e.g., Coleman, 1977; Dilek and Furnes, 2011). Upper mantle peridotites exposed in ophiolites represent residues after various degrees of melt extraction from the primitive mantle, and hence the fragments of previously depleted, ancient peridotites. Fragments of the ancient upper mantle peridotites provide critical information on the mode and nature of magmatic, tectonic, and geochemical processes controlling the evolution of the oceanic lithosphere (Dilek and Furnes, 2011). Geochemical and petrological data from ophiolitic and abyssal peridotites have presented new insights into our understanding of the compositional heterogeneity of the upper mantle that has been mainly induced by varying degrees of partial melting in earth history (Niu et al., 1997; Takazawa et al., 2000; Choi et al., 2008; Dilek and Morishita, 2009).

The ophiolite belt of Indo-Myanmar Range which evolved as a result of obduction of the Indian and Burmese plates forms a belt extending about 200 km from Phokhpur (Nagaland state) in the north to Moreh (Manipur state) in the south (Fig. 1). The rootless allocthonous ophiolitic belt consists of different igneous, metamorphic and sedimentary sequences. Ultramafic rocks forming the main component of the belt consists of mantle sequence of tectonised peridotites with mafic intrusives, volcanic rocks, pelagic sediments. In general, localized along the suture zones, ophiolites and associated ophiolitic mélanges witness the closure of an oceanic domain during continent-continent

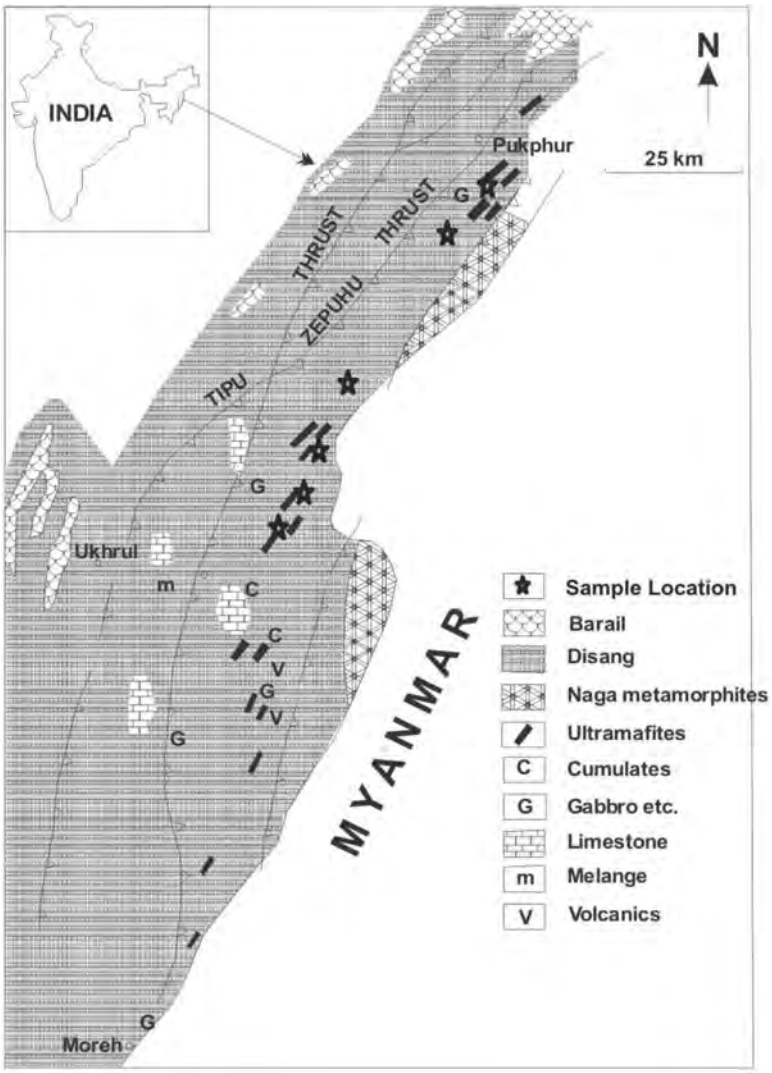

Fig. 1. Geological map of the area around Indo-Myanmar Ophiolite belt.

convergence. The southern part of the belt falling in the Manipur state is dominated by mantle peridotites with minor basic rocks and extrusive volcanics. In contrast the northern part which falls in the Nagaland is represented by peridotite, cumulate mafic-ultramafic, mafic volcanics, eclogite, glaucophane schist, amphibolite and late felsic intrusives. The abundant mantle fragments and variable size provide an opportunity to study the mantle processes of the belt. Considering the difference in the nature of distribution and associated lithounits in the entire ophiolite belt, an understanding of the origin and nature of the ultramafite sequence is necessary. It is possible that variable degrees of melting may have preserved some compositional characteristics of the mantle prior to the subduction process. In general, as the ultramafic rocks are prone to serpentization, characterization of the relict mineral phases in these rocks would give a clear picture of the mantle processes.

In this study we use whole rock geochemical and phase chemistry data of the mantle sequence ultramafic rocks of the Indo-Myanmar Ophiolite Belt (IMOB) to determine the petrogenesis and tectonic setting of the ophiolite. The aim of the proposed study is to carry out compositional characterization of the mineral phases and rocks, establish crystallisation environment and probable mantle processes of the rock and tectonic implication of the ultramafites.

Representative samples of ultramafic rocks were collected from the central (Ukhrul District, Manipur) and northern (Phek District, Nagaland) parts of the ophiolite belt. Thin sections were studied by petrological microscope. Major element composition of the mineral phases was determined by electron microprobe Jeol JXA 8900 RL with wavelength dispersive mode. Olivine, orthopyroxene, clinopyroxene, and spinel were analyzed using an accelerating potential of 20 kV, a beam current of 12 nA, and a spot size of 2 micrometres. Counting times varied between 20 and 80 s on the peak and 10 and 40 s on the background. We used natural minerals and oxides (Si, Ti, Al, Fe, Mg, Mn, Cr and Zn) and pure element standards (V, Co) as standards. The oxide minerals were measured with five WDS spectrometers at 20 kV acceleration voltage, a probe current of 12 or 20 nA and either a focussed beam or a beam diameter of 2 μm. The spinel stoichiometry was calculated assuming that all Ti is in the ulvöspinel component and that all V is present as $Fe_7V_2O_{10}$. Ferrous and ferric irons were then calculated assuming stoichiometry. Whole rock geochemical data is also generated for selected rocks.

Mineralogical study of peridotite samples reveal olivine, orthopyroxene, clinopyroxene and spinel as the primary mineral phases and serpentine as the most common secondary mineral, altered mainly from olivine and orthopyroxene. Composition of olivine from EPMA analysis gives a consistent (Fo≈90) for Manipur samples and (Fo_{84-94}) for samples of Nagaland. Clinopyroxene composition for the two set of samples are ($En_{47-52}Fs_{4-5}Wo_{44-49}$) and ($En_{32-49}Fs_{7-23}Wo_{41-50}$) respectively. Orthopyroxene values ranges from ($En_{88-90}Fs_{9-11}Wo_{0.8-2}$) in samples from Manipur to ($E_{88-90}Fs_{8.5-10}Wo_{0.8-5}$) in Nagaland samples. Equilibrium temperatures for the first set of samples were calculated between 1038-1206°C using two-pyroxene thermometry (Nickel et al., 1985). For the samples from Nagaland, temperature was calculated between 1000-1383°C using spinel-olivine geothermometry (Fabries, 1979). Oxygen fugacity (following Ballhaus et al., 1991) was calculated between 0.39 to 0.69 ΔQFM. The studied ultramafic rocks were formed due to various degree of melting ranging between 0.5 to 11%. Various tectonic discrimination diagrams show that majority of the samples were found to be plotted within and in the margin of abyssal peridotite field. From our present study, we can conclude that peridotites from both sections of the IMOB were crystallized in upper mantle environment and had experienced multi stage melting history representing the heterogeneous character of the preserved oceanic lithosphere.

Ballhaus, C., Berry, R.F., Green, D.H. 1991. Contrib. Mineral. Petrol., 107, 27-40.
Choi, S.H., Shervais, J.W., Mukasa, S.B. 2008. Contribution to Mineralogy and Petrology. 156, 551-576.
Coleman, R.G. 1977. Ophiolites. Springer Verlag, New York, 220 pp.
Dilek, Y., Furnes, H. 2011. Geological Society of America Bulletin, 123, 387-411.
Dilek, Y., Morishita, T. 2009. Island Arc, 18, 551-554.
Fabries, J. 1979. Contribution to Mineralogy and Petrology 69, 329-336.
Nickel, K.G., Brey, G.P., Kogarko, L. 1985. Contrib. Mineral. Petrol., 91, 44-53.
Niu, Y., Langmuir, C.H., Kinzler, R.J. 1997. Earth and Planetary Science Letters, 152, 251-265.
Takazawa, E., Frey, F.A., Shimuzu, N., Obata, M. 2000. Goechemica et Cosmochemica Acta, 64, 695-716.

Tectonic framework and geochemical characteristics of granitoids of Nubra-Shyok Valley, Ladakh Trans-Himalaya and Karakoram

Nazia Kowser, Rakesh Chandra
Department of Earth Sciences, University of Kashmir, Hazratbal, Srinagar 190006, INDIA

The rocks of Shyok Suture Zone (SSZ) are delineated by the Pangong Tso Lake-Indus River in the east and continue to the valley of Lower Shyok, Indus and Shigar, all the way to Nanga Parbat. The rocks of this tectonic zone comprise thrust slices of Khalsar Formation, Shyok Volcanics, Saltoro Flysch, Saltoro Molasse, Ophiolitic Melange sandwitched between Ladakh Batholiths to the south and Karakoram Batholith to the north. Besides the marginal granitoids of Ladakh and Karakoram Batholiths,

there are several WNW-ESE aligned isolated granitic bodies intruding the rocks of Shyok Suture Zone (SSZ) collectively named as Tirit Granitoids. Detail geochemical of Tirit Granitoids reveals that these granitoids are sub-leucocratic-mesocratic and ranges in composition from granodiorite-tonalite to gabbro diorite. Tirit Granitoids have a wide range of chemical compositions with SiO_2=52.1-72.11 wt.%, Al_2O_3=11.42-13.52 wt.% and CaO=3.24-9.31 wt.%, relatively high in total alkalis, with K_2O=2.96-5.55 wt.% and Na_2O=2.84-4.73 wt.%. However, Karakoram Batholiths are leucocratic-sub-leucocratic and are classified as granite, granodiorites and tonalites along the northern margin. Whereas, the southern margin of Karakoram Batholiths is two-mica Granitoids. At places Karakoram Batholith is defined by mylonites along the Karakoram Fault. The SiO_2 content of Karakoram Batholiths from 60.36 to 72.38 wt.% is more than that of Tirit Granitoids. Al_2O_3=12.95 to 15.25, CaO=1.72 to 6.76, K_2O=2.93 to 5.55 and Na_2O=2.84 to 4.51wt.%. Normalized Rare Earth Elements (REE) and multi elements patterns show enriched characteristics in terms of Light Rare Earth Elements (LREE) and depletion of Heavy Rare Earth Elements (HFSE) in both these granitoids. The Tirit and Karakoram Granitoids substantiate met-aluminous character with high A/NK ratios (1.0-1.8, 1.0-1.7) relative to A/CNK (0.0-0.7, 0.7-0.8) respectively. These granitoids are of calc-alkaline affinity and represents the I-type, Volcanic Arc Granitoids (VAG). The integrated field, Petrographic and geochemical study reveal that Karakoram Granitoids are the result of the subduction along the Shyok Suture Zone of the Neo-Tethyan oceanic plate under the Karakoram Block. Whereas, Tirit Granitoid resulted either from the melting of lower crust due to thermal relaxation following continental collision along Indus-Tsangpo Suture Zone (ITSZ) or from melting of the upper mantle that accompanies post-collision uplift and erosion.

Lateral variation in climate and weathering in the Himalaya since Miocene

Natalie Vögeli[1,*], P. Van Der Beek[1], Y. Najman[2], P. Huyghe[1], P. Wynn[2]
[1]Institut des Sciences de la Terre, Université Grenoble Alpes, 38401 Grenoble, FRANCE
**natalie.voegeli@ujf-grenoble.fr*
[2]Lancaster Environment Centre, Lancaster University, Lancaster LA1 4YQ, UK

The link between tectonics, erosion and climate has recently become an important subject of ongoing research (Clift et al., 2008, amongst others). The Himalayan orogen represents a key natural laboratory for its study. The major force driving the evolution of this mountain belt is the India-Asia convergence. Whilst the Himalaya has a major influence on global and regional climate, it is suggested that the monsoonal climate also plays a major role in controlling the erosion and relief pattern (Bookhagen and Burbank, 2006; Clift et al., 2008; Iaffaldano et al., 2011). Understanding the past variations in monsoonal strength and weathering regime along strike is crucial to understand the role of climate in the evolution of the mountain belt.

The Neogene sedimentary foreland basin of the Himalaya contains a record of tectonics and paleoclimate since Miocene times, within the molassic sediments of the Siwalik Group. Several sedimentary sections within the foreland basin of the Himalayan range have previously been dated and studied with the aim of determining hinterland exhumation rates, provenance and paleoclimatology (e.g. Quade and Cerling, 1995; Ghosh et al., 2004; Sanyal et al., 2004; van der Beek et al., 2006). Lateral variations in hinterland exhumation rates have been observed. However, the record of climate change in the past, especially the strengthening of the Asian summer monsoon along strike of the range, remains debated.

In this study we use a multiproxy geochemical approach to better understand variations in weathering intensity, monsoonal evolution and associated vegetation from the Western to the Eastern part of the Himalaya. To this aim, previously dated Siwalik Group sedimentary sections in the West, namely the Joginder Nagar, Jawalamukhi and Haripur Kolar sections (Najman et al., 2009; Meigs et

al., 1995; Sangode et al., 1996; White et al., 2001) and the Kameng river section in the East (Chirouze et al., 2012) were newly sampled and analyzed. Sedimentary records span from 20-1 Ma in the West and 13-1 Ma in the East.

Major elements were analyzed in order to calculate the Chemical Index of Alteration (CIA), to identify a trend in the weathering intensity over the time span. Ratios of mobile to immobile elements were used to show different trends of weathering intensity. In order to track vegetation as a marker of monsoonal intensity and seasonality, we analyzed $\delta^{13}C$ on soil carbonate and associated $\delta^{13}C$ on bulk organic carbon.

The presence of soil carbonate in the West, but its absence in the East is a first indication of lateral climatic variation. $\delta^{13}C$ in soil carbonate shows a shift from around -10 to -2‰ at 6 Ma in the West. This is confirmed by $\delta^{13}C$ analyses on bulk organic carbon, which show a shift from around -24 to -19‰ at the same time. Such a shift in isotopic value is likely associated with a change in vegetation type from C3 to C4 plants. In contrast, $\delta^{13}C$ on bulk organic carbon remains relatively stable at around -24‰ in the East. Whether the lateral difference in change of vegetation is caused by relief building or climate remains to be discussed.

Bookhagen, B., Burbank, D.W. 2006. Geophysical Research Letters, 33(8), L08405.
Chirouze, F., Dupont-Nivet, G., Huyghe, P., van der Beek, P., Chakraborti, T., Bernet, M., Erens, V. 2012. Journal of Asian Earth Sciences, 44, 117-135.
Chirouze, F., Huyghe, P., van der Beek, P., Chauvel, C., Chakraborty, T., Dupont-Nivet, G., Bernet, M. 2013. Geological Society of America Bulletin, 125(3-4), 523-538.
Clift, P.D., Hodges, K.V., Heslop, D., Hannigan, R., Van Long, H., Calves, G. 2008. Nature Geosci, 1(12), 875-880.
Garzanti, E., Vezzoli, G., Andò, S., France-Lanord, C., Singh, S.K., Foster, G. 2004. Earth and Planetary Science Letters, 220(1-2), 157-174.
Ghosh, P., Padia, J.T., Mohindra, R. 2004. Palaeogeography, Palaeoclimatology, Palaeoecology, 206 (1-2), 103-114.
Huyghe, P., Mugnier, J.-L., Gajurel, A.P., Delcaillau, B. 2005. The Island Arc, 14, 311-327.
Iaffaldano, G., Husson, L., Bunge, H.-P. 2011. Earth and Planetary Science Letters, 304(3-4), 503-510.
Meigs, A.J., Burbank, D.W., Beck, R.A. 1995. Geology, 23(5), 423-426.
Najman, Y., Garzanti, E., Pringle, M., Bickle, M., Stix, J., Khan, I. 2003. Geological Society of America Bulletin, 115 (10), 1265-1277.
Najman, Y., Bickle, M., Garzanti, E., Pringle, M., Barfod, D., Brozovic, N., Burbank, D., Ando, S. 2009. Tectonics, 28, TC5018, doi:10.1029/2009TC002506.
Quade, J., Cerling, T.E. 1995. Palaeogeography, Palaeoclimatology, Palaeoecology, 115(1-4), 91-116.
Sangode, S.J., Kumar, R., Ghosh, S.K. 1996. Journal Geological Society India, 47, 683-704.
Sanyal, P., Bhattacharya, S.K., Kumar, R., Ghosh, S.K., Sangode, S.J. 2004. Palaeogeography, Palaeoclimatology, Palaeoecology, 205 (1-2), 23-41.
van der Beek, P., Robert, X., Mugnier, J.-L., Bernet, M., Huyghe, P., Labrin, E. 2006. Basin Research, 18(4) 413-434.
White, N.M., Parrish R.R., Bickle, M.J., Najman, Y.M.R., Burbank, D., Maithani, A. 2001. Journal of the Geological Society, 158 (4) 625-635.

A satellite-based assessment of river aggradations and degradation due landslides triggered by the Uttarakhand extreme rainfall event in 2013

Priyom Roy*, Tapas R. Martha#, K. Vinod Kumar
Geosciences Group, National Remote Sensing Centre, IRSO, Hyderabad 500037, INDIA
**roy.priyom@gmail.com*
#*tapas_martha, vinodkumar_k@nrsc.gov.in*

Satellite images have inherent advantage of extracting landslide information in highly inaccessible mountainous areas. Availability of high resolution data from Indian Remote Sensing

(IRS) satellites such as Resourcesat-2 LISS-IV Mx, Cartosat-1&2 in conjunction with ISRO's geoportal i.e. Bhuvan, has culminated to a mechanism from timely data acquisition to dissemination, which is vital for assessment as well as management of landslide disaster (Martha and Vinod Kumar, 2013). A comprehensive assessment of the landslides triggered during the recent 2013 Uttarakhand disaster was carried out by NRSC. An exhaustive landslide inventory was created for the entire Bhagirathi and Alaknanda valley. Landslides were detected from post-landslide Resourcesat-2 LISS IV Mx images using a semi-automatic Object-based image analysis (OBIA) technique developed by NRSC (Martha et al., 2011; Martha et al., 2012). Consequent to this, an assessment of river aggradation/degradation was carried out by assessing the impact of these landslides and estimating the sediment influx due to these landslides, into the Mandakini catchment.

A total of 6585 landslides with an area of 52 km^2 were mapped in the Bhagirathi and Alaknanda valleys using high resolution satellite data. The assessment showed that 3,472 landslides

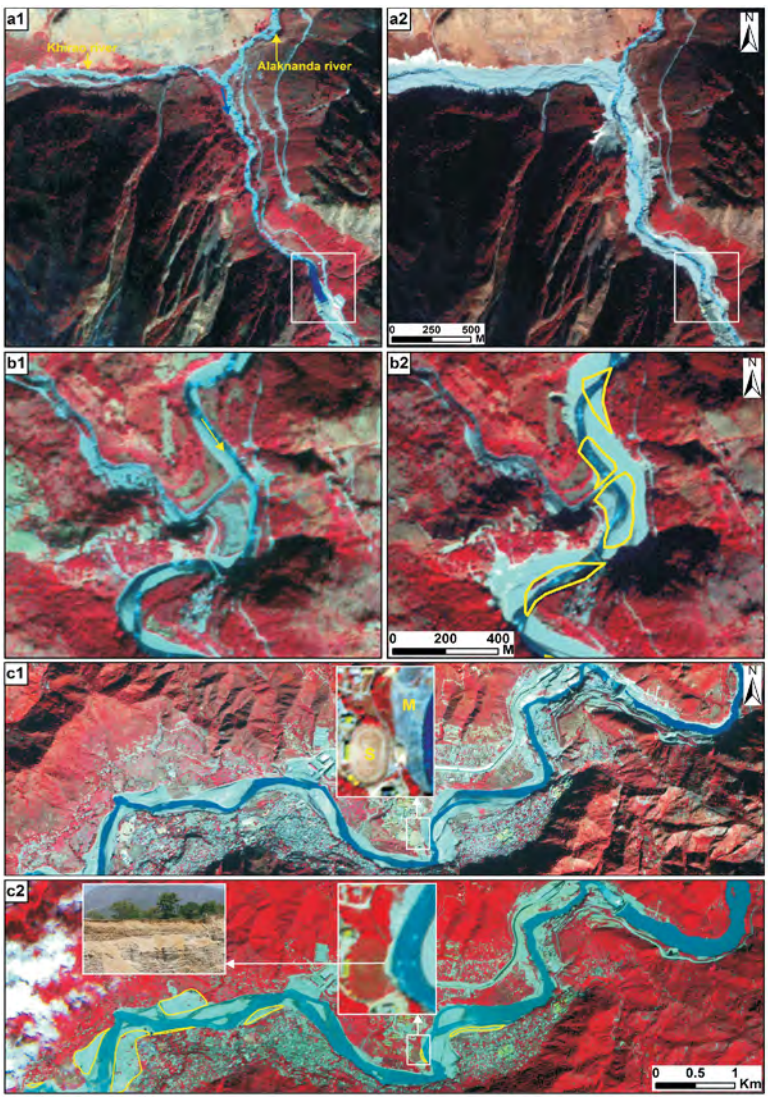

Fig. 1. (a) Severe damage to river terraces on either side of Khirao River in Alaknanda valley as seen from pre (a1) and post (a2) images. (b) River bed erosion around pre (b1) and post (b2) images. (c) Damage to river terrace around Srinagar seen from pre (c1) and post (c2) image S=sports stadium and M=Muck deposit.

with 30.4 km^2 area are new ones, 1,137 landslides with 9.1 km^2 area can be classified as old ones and 1,401 landslides with 11.7 km^2 area can be classified as reactivated ones (Martha et al., 2014). Furthermore, a total area of 2 km^2 of river terrace at 89 locations along the two river valleys was damaged (Fig. 1). Maximum loss of fluvial terrace was seen in the Alaknanda river valley in comparison to the Bhagirathi river valley.

An estimate of the sediment influx in the Mandakini catchment using landslide volumes calculated from landslide area-volume empirical relationship ($V=0{\cdot}1549A^{1{\cdot}0905}$) proposed by Gurthrie and Evans (2004). Proximity analysis showed that, out of 860 new landslides in the Mandakini catchment, 511 landslides have contributed sediments to the Mandakini River and therefore were considered for volume estimation and sediment influx into the rivers. The total volume of landslides estimated as ~3.59*106 m^3 can be assumed as total sediment influx to the Mandakini catchment by the extreme rainfall event, since other sources of sediment influx are insignificant (Roy et al. 2014). The sub-catchment-wise statistic shows that Madhyamaheswar river has contributed maximum volume of sediments (~7.67*105 m^3). Deposition of sediments in the Mandakini catchment was verified at several places (e.g., Sonprayag, Rudraprayag, etc.) using high resolution satellite images and also during a fieldwork carried out after the disaster.

Guthrie, R.H., Evans, S.G. 2004a. Earth Surface Processes and Landforms, 29, pp. 1321-1339.

Martha, T.R., Kerle, N., van Westen, C.J., Jetten, V., Vinod Kumar, K. 2011. IEEE Transactions on Geoscience and Remote Sensing, 49, pp. 4928-4943.

Martha, T.R., Kerle, N., van Westen, C.J., Jetten, V., Vinod Kumar, K. 2012. ISPRS Journal of Photogrammetry & Remote Sensing, 67, 105-119.

Martha, T.R., Vinod Kumar, K., 2013. Landslides, 10, 469-479.

Martha, T.R., Roy, P., Govindaraj, B., Vinod Kumar, K., Diwakar, P., Dadhwal, V.K. 2015. Landslides DOI 10.1007/s10346-014-0540-7.

Roy, P., Martha, T.R., Vinod Kumar, K. 2014. ISRS proceedings. ISPRS Technical Commission VIII Symposium, Special Interactive Session, 09-12 December 2014, Hyderabad, India.

Formation of the Main Boundary Thrust (MBT) and its role in exhumation Of the Amritpur granite in Kumaon Himalaya, NW-India

Paramjeet Singh[1*], R.C. Patel[2]

[1]Wadia Institute of Himalayan Geology, 33 GMS Road, Dehradun 248001, INDIA

**paramjeetsingh@wihg.res.in*

[2]Department of Geophysics, Kurukshetra University Kurukshetra 136119, INDIA

Since the onset of collision between India and Eurasia, at ~50-55 Ma, maximum contraction and formation of the Himalayas was accommodated by shortening within the Indian continental crust mainly along SW directed thrust faults that divide the Himalaya into several sub-parallel tectonic units. Along each of these thrusts, tens to hundreds of kilometres of the displacement between India and Eurasia have been accommodated. From north to south and in order of decreasing age and structural position, they are (1) the Indus-Tsangpo suture, (2) the South-Tibetan Detachment System (STDS)-the Main Central thrust (MCT); (3) the Main Boundary thrust (MBT) and (4) Main Frontal Thrust (MFT). Whereas the age of initiation and duration of thrusting on MCT and detachment along the STDS have received considerable study, the history of the MBT is less studied owing to poorer exposure and fewer radiometric dates associated with it.

The MBT is defined as the thrust that places meta-sedimentary rocks of the lesser Himalaya over un-metamorphosed sedimentary rocks of the sub-Himalaya. A unique feature in the Kumaon Himalaya is that a Precambrian Granite body (Amritpur Granite) of lensoid shape has been emplaced

over the sedimentary rocks sub-Himalaya along the MBT. The Amritpur Granite in the north is bound by NE-dipping Amiya Thrust along which meta-sedimentary rocks of the Lesser Himalayan Sequence (LHS) have been thrust over the Amritpur Granite. New 17 Fission Track (09 Apatite Fission Track (AFT) ages and 08 Zircon Fission Track (ZFT) ages) ages from the Amritpur Granite and 3 AFT ages from the meta-sedimentary rocks in the hanging wall of the Amiya Thrust have been obtained to constrain the activity of the MBT and Amiya Thrust and their role in uplift and exhumation of the Amritpur granite. The AFT ages in the Amritpur Granite range between 11.3±1.6 and 14.7±1.0 Ma while ZFT ages between 12.4±1.2 and 15.4±1.7 Ma while AFT ages in the hanging wall of the Amiya Thrust range between 4.2 and 3.6 Ma. It appears that the Amritpur granite which was buried below ~8 to 9 km depth, uplifted and exhumed to depth of ~3-4 km rapidly between 15 and 11 Ma. It was probably time during which the MBT was formed along which the Amritpur granite thrust directly over the sedimentary rocks of the sub-Himalaya. It was then followed by northward shifting of activity along the Amiya Thrust as out-of-sequence thrusting during 4 Ma.

Last five decadal heavy metal pollution records in the Rewalsar Lake, Himachal Pradesh, India

Prakasam M[1*], Narendra Kumar Meena[1], Sudipta Sarkar[1], Ravi Bhushan[2]
[1]Wadia Institute of Himalayan Geology, Dehradun 248001, INDIA
**prakasam@wihg.res.in*
[2]Physical Research Laboratory, Navrangpura, Ahmedabad 380009, INDIA

The pollution and increasing environmental degradation of the aquatic systems have become a global concern. The lakes of the Himalaya are also degrading due to human interference. Sediment cores were recovered to study the pollution loading in the Rewalsar Lake, Himachal Pradesh, India. The ^{137}Cs and ^{210}Pb isotope based sedimentation rate study suggests rapid sedimentation in the lake during the last ~50 years. The concentrations of Mn, Cu, Zn, Cd, Pb, Co, Ni, Cr metals in the Rewalsar Lake sediments owe its contributions both to the natural and anthropogenic sources. Prior to ca 1990 AD metal loading was mainly dominated by the lithogenic input, whereas the post ca 1990 AD the metal loading seems to be controlled by the anthropogenic factor. The Pb concentration in the lake gradually increased during 1990-2004 and then decreased significantly till present. The higher concentration of Pb seems to be derived from the fossil fuel burning, while the Cr concentration in the

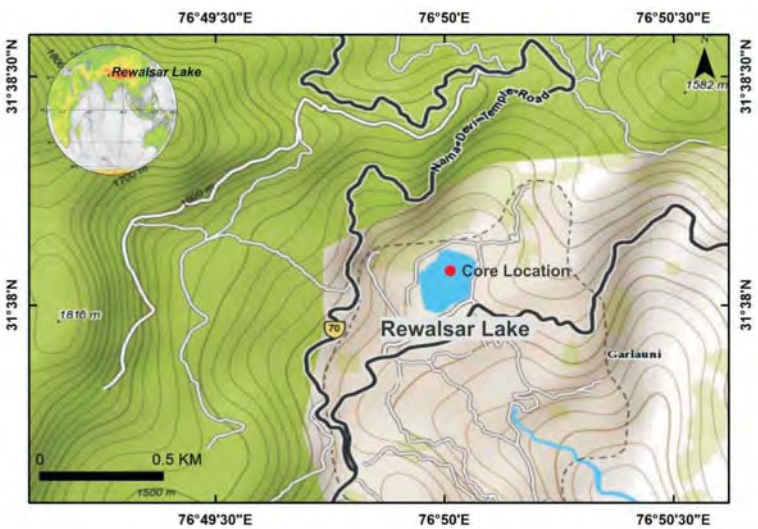

Fig. 1. Topographic map of the study area (red colour dot shows core location on the Rewalsar Lake).

lake indicates the use of fertilizer in the catchment area. The lowest concentrations of elements around ca 1990 AD seem to have occurred due to channelization of the lake feeding system.

Development of braided fluvial deposits in response to base-level changes - A case study from the Sanjauli Formation, Proterozoic Simla Group, Lesser Himalaya, India

Priyanka Mazumdar*, Ananya Mukhopadhyay, Alono Thorie, Tithi Banerjee
Department of Earth Sciences, IIEST, Shibpur, Howrah 711103, INDIA
**priyancam8@gmail.com*

Fluvial pattern recorded in the Sanjauli Formation of Proterozoic Simla Group indicates fluctuations in the rate of accommodation space generation. The dominant facies assemblages recognised in the Sanjauli Formation are braided-channel deposits, sheet-flood deposits and floodplain deposits. Three systems tract have been delineated from the fluvial facies associations: lowstand systems tract (LST), transgressive systems tracts (TST) and highstand systems tract (HST). The prograding braided-channel deposits of the Sanjauli Formation which has been found incised on an ancient fan-delta deposit represent a lowstand systems tract (LST) which has developed in response to high-clastic supply during falling base level. The subaerial erosional surface (subaerial unconformity-Type-1 unconformity) has formed coevally with the deposition of braided-channel deposits. The lower unit (braided-channel deposit) of the Sanjauli fluvial clastics initially records little available accommodation space. Slow rates of base-level rise resulted in amalgamated fluvial channel complexes. The development of sheet-flood deposits on top of the LST reflects high degree of reworking resulting in sheet-like, high-energy, bed-load-dominated, braided river deposits lacking recurrent facies patterns. As accommodation space increased during base level rise, reduction in reworking has been characterised by the development of fining- and thickening-upward muddy-silty fluvial cycles. More rapid rates of base-level rise produced vertically isolated sandstones, thick extensive shale beds, laminated silt with occasional presence of mud drapes and bi-directional foresets, which mainly characterise the TST. The culmination of transgression is marked by development of thin dark shale bed on top of the sheet-flood deposits and has been interpreted as a condensed section representing the maximum flooding surface. The highstand systems tract (HST) has been deposited during gradual slowing down of rise in base level giving rise to decreasing accommodation space (continued subsidence still creates some accommodation). The HST is mainly characterised by lateral accretionary deposits with minor accumulations of fine-grained vertically accreted sediment.

Structure of the Triyuga Valley piggy-back basin from active source seismology

Rafael Almeida[1*], Anna Foster[1], Lee Liberty[2], Judith Hubbard[1], Som Sapkota[3]
[1]*Earth Observatory of Singapore, Nanyang Technological University, SINGAPORE*
**ralmeida@ntu.edu.sg*
[2]*Department of Geoscience, Boise State University, Boise, ID, USA*
[3]*Department of Mines and Geology, Kathmandu, NEPAL*

In this study we acquired four seismic lines in the Triyuga Valley of eastern Nepal. The data were acquired using a 6000 kg vibroseis truck in the spring of 2015. Thirty km of data was acquired using 264 channels with 5 m spacing. The data were processed using the following flow: 1) Vibroseis correlation; 2) Geometry assignment; 3) Amplitude recovery; 4) Spectral whitening; 5) Top mute

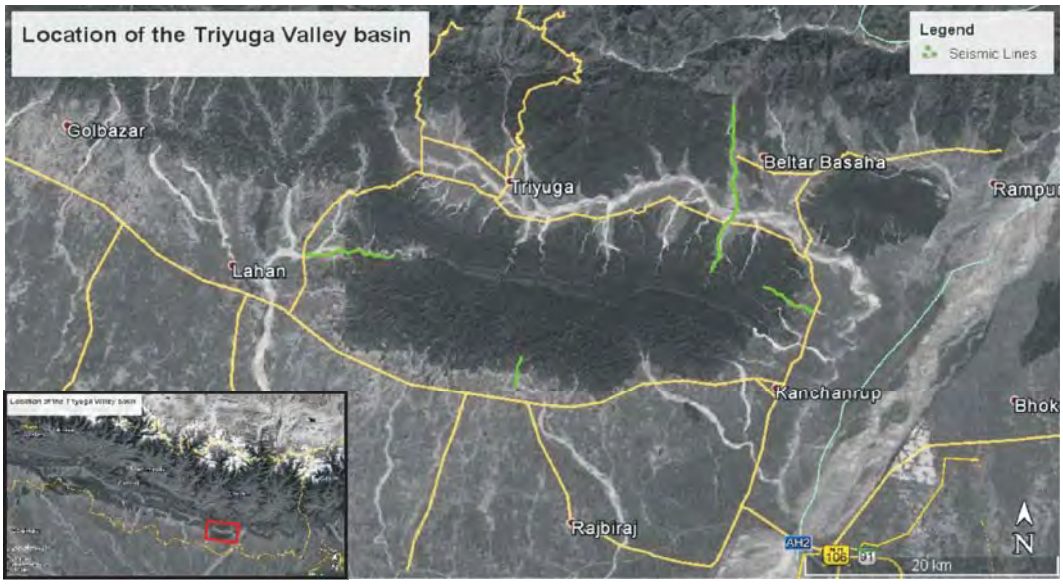

(remove refractions) and bottom mute (remove noise cone); 6) Velocity analysis of supergathers; 7) Normal move-out (NMO) correction; 8) Dip Move Out correction; 9) Inverse NMO; 10) Velocity Analysis (steps 6-10 are iterative); 11) CDP stacks with automatic gain control and a band-pass filter.

The lines can image the subsurface down to 1.5-2 km. They follow several of the dry riverbeds in the area and are generally orthogonal to the foothills that bound the Triyuga Valley within the Siwalik Group. These Miocene-Pliocene age foreland sediments are strongly folded in this region. Measurements of bedding attitudes were done throughout the area to complement the seismic data. Folding near the outcropping faults is asymmetric, typically with steep, narrow forelimbs and shallow, wide back-limbs.

The seismic lines show that the east and west boundaries of the basin are not formed by strike-slip faults as previously interpreted but rather by thrust faults. This implies that the basin-bounding faults are overthrusting the foreland basin in 3 directions. This requires that internal deformation of the thrust sheet be accommodated on secondary structures. A fault, inferred to be strike-slip, was identified within the basin, and may be a product of this internal deformation. More studies need to be done to further constrain this.

On the eastern side of the basin there are a series of aggradational terraces ~5 m above the present local base level. Our data show that these are not uplifted structurally and may reflect local changes in base level. This has implications for the determination of tectonically induced terrace uplift and paleoseismological analysis.

Implication of methane trapped in Himalayan lithotectonic domains

Rajesh Sharma, Rakhi Aswal*, A.K. Singh
Wadia Institute of Himalayan Geology, Dehradun, India
E-mail: rajesh_fluid@rediffmail.com
***Present address:** Oil and Natural Gas Corporation, Dehradun*

The C-O-H fluids with CO_2- H_2O composition are unequivocally participated in much of the Himalayan tectonometamorphic events, and the enrichment of CO_2 have been interpreted either a

result of higher metamorphic grades or the deep fluid migrated along the thrusts. However, methane enrichment in these fluids is unusual and attracts our understanding on the processes operated at the preferred domains. The knowledge on the origin of methane in geofluids suggests that it can be present significantly in the fluids originating from mantle or can generate through near surface processes (Symonds et al., 2003). Recent studies and available work from Himalaya show that significant CH_4 is found in inclusions from (i) selected areas of Lesser Himalayan crystallines, (ii) ophiolite sequence and of Ladhakh and (iii) chromites from the ophiolites. The fluid inclusion and micro Raman spectroscopy has been vital to trace the records of methane in Himalayan rocks.

Substantial methane with Raman band at 2917 ±2 cm^{-1} has been noticed in fluid inclusions in graphitic schists of Almora Crystallines, and the granite gneisses with intruding deformed mineralized quartz veins in Precambrian Askot Crystallines, both these representing lesser Himalayan crystallines thrusted over the metasedimentary sequence. Presence of substantial CH_4 is unusual in the Himalayan metamorphics. Present study on fluid compositions confirms that the H_2O-CO_2-CH_4-N_2 fluid was present during graphite crystallization. The reported $\delta^{13}C$ values of Almora graphite from -23.2 to -31.9 ‰, with mean value of -29.08‰, corroborate that the graphite was formed through the thermal conversion of organic carbonaceous material (Rawat and Sharma, 2011). Restricted occurrence of the CH_4 with H_2O-CO_2 fluids in graphite bearing assemblage favour the contention that methane was released from biogenic material during its conversion to graphite and is result of fluid equilibration during graphite crystallization. The occurrence of CH_4 during thermal maturation and cycling of organic carbon in subduction zones are also demonstrated in Myanmar region (Shi et al., 2005). The fluids trapped in the mineralized gneisses and veins of Askot Crystallines are C-O-H with low salt contents. Significant CH_4 is present together with CO_2 and the evidences of aqueous fluid boiling are also discernible. The chemical and sulphur isotope signatures of Askot sulphides infer that they were formed in submarine volcano sedimentary environment with exhalative fluxes (Sharma, 2008), and based on geochemical studies the granitoid rocks in the Askot klippen are considered to have derived from the mafic/intermediate magmatic products in a volcanic arc setting during Proterozoic time (Rao and Sharma, 2009). In view, it is attributed that CH_4 in Askot rocks was evolved from high temperature magmatic fluids in subvolcanic hydrothermal environment.

Although CH_4 was also noticed in the fluid inclusions in olivine from partially serpentinized harzburgite and dunite from the Nidar ophiolite complex (Sachan et al., 2007), but this was concluded to be result of the serpentinization of ultramafic rocks. Further occurrence of methane is observed in the fluid inclusions in chromite from the Indus Suture zone. Monophase and biphase inclusions filled with CH_4+CO_2 fluid are seen in the chromite mineral grains. Since the primary fluid in chromite may likely represent the fluid released from mantle, this can be significant evidence of the fluid exsolved from magmatic system of the than forming oceanic crust.

Rao, D.R., Sharma, R. 2011. Island Arc, 20, 500-519.
Rawat, Rakhi, Sharma, Rajesh 2011. Journal of Asian Earth Sciences, 42, 51-64.
Sachan, H.K., Mukherjee, B.K., Bodnar, R.J. 2007. Earth and Planetary Science Letters, 257, 47-59.
Sharma, Rajesh, Rao, D.R. 2008. ,Current Sci., 95, 527-531.
Shi, U.G., Tropper, P., Cui, W., Tan, J.,Wang, C. 2005. Geochemical Jour., 39, 503-516.
Symonds, R.B., Poreda R.J., Evans, W.C., Janik, C.J., Ritchie, B.E. 2003. USGS Open-File Report, 03-436.

Identification of vulnerable zones of Climatically and Geomorphologically sensitive Mandakini Valley by Weights of Evidence Method using Pre-disaster Satellite Data and verification of the results with Post-disaster Satellite Data

***Poonam[1], P.K. Champati Ray[2], Naresh Rana[1], Pradeep Srivastava[3], Y.P. Sundriyal[1]**
[1]Department of Geology, H.N.B. Garhwal University, Srinagar (Garhwal), Uttrakhand
**poonam.hnbgu02@gmail.com*
[2]Geoscience and Geohazard Department, Indian Institute of Remote Sensing, Dehradun, Uttrakhand
[3]Wadia Institute of Himalayan Geology, Dehradun, Uttrakhand

Geomorphologically Mandakini valley is highly sensitive and the main landforms on which the infrastructure sites are located include moraines, reworked moraines, alluvial fans, debris flow deposits, modified palaeo-landslides, colluvial and fluvial terraces. All these all landforms are highly sensitive to river erosion. Mandakini valley receives average rainfall of 2500 mm annually, so high rainfall is considered as one of the triggering climatic factors of erosion and associated mass wasting phenomena. Tectonically the valley is also active as four major thrusts are running from south to north in the study area: Ramgarh Thrust, Munsiari Thrust, Vaikrita and Pindari Thrust beside various transverse faults. Cloudburst (high intensity precipitation) and prolonged precipitation is considered as the main triggering factors of slope failures causing enormous losses to lives and infrastructures. This phenomenon has become recurring during the rainy seasons in the valley but June, 2013 event was highly disastrous in terms of damage as it was one of the extreme high precipitation event accompanied by moraine dammed lake outburst flooding. High rainfall and weak geological setup are not solely responsible for the large scale slope failures, the anthropogenic factors also contribute to the slope failure phenomena in the recent time. Weight of Evidence is a data- driven method which is basically a Bayesian statistical approach using the pre- and post-(predicted) probability of phenomena and is applied where sufficient data is available to estimate the relative importance of evidential themes by statistical mean. In this method, landslide inventory maps are compared with each causative factor map to obtain the weight of the parameter and then all the causative factor maps are integrated according to the weights derived by this method. In the present study we tried to identify vulnerable zones of Mandakini valley using LISS IV orthorectified pre-disaster data by applying the weight of evidence method and then the results were compared with the post disaster LISS IV orthorectified data which indicated that 77.67% of the landslides have occurred where the maximum slope failures were expected (very high and high susceptibility class). Validation of the model was carried out by Prediction Rate Curve (PRC), which provides an estimate of occurrences of actual landslide events in predicted classes of highest susceptibility and area under this curve is 83.15% which is an estimate of accuracy of the model. Applying this method it is possible to identify the vulnerable zones in all other river valleys of the Himalaya and the nearby habitat can be informed well in advance to take remedial measures.

Exhumation path of the Chiplakot Crystalline Belt, Kumaun Himalaya, India, deduced from fluid inclusion study

Dinesh S. Chauhan[1*], Rajesh Sharma[#]
Wadia Institute of Himalayan Geology, Dehradun, India
**dinesh_geo@rediffmail.com, [#]rajesh_fluid@rediffmail.com*
[1]Present address: 102/ Janta Colony, Behind Rameshwer Nagar, Jodhpur, (Raj.) India.

The Himalaya represents classic example of continent-continent collision resulted in the development of broad ductile shear zones throughout its strike length. These shear zones unroofed

the basement rocks to the present level of their exhumation that was often rapid. The Tertiary tectonics of Himalaya has produced numerous remnant nappe and klippen offering debatable emplacement perceptions viz. remnants of the southward travelled thrust sheets or pop-up structure. The rocks of these klippen provide ample evidences for their exhumation history that can be investigated from the mineral assemblages and/or interacting fluids. Chiplakot Crystalline Belt (CCB) is one such klippen representing detached thrust sheet of the Paleo-Proterozoic crystalline rocks exposed in the northeast Kumaun, India, and in the adjoining northwest Nepal. The CCB comprises augen gneiss, mylonitic granite gneiss, granite gneiss, quartz-sericite schist and amphibolites. The detached CCB is believed to be equivalent of Higher Himalayan Crystallines thrusted upon the metasedimentary sequence of Lesser Himalaya. The CCB represents a duplex slab within the Lesser Himalayan zone. It has both southern and northern boundaries as north dipping thrust named as Chiplakot Thrust. The signatures of poly-phase deformation are preserved in the CCB. The present work focuses on the fluid inclusion study of various stages of structural evolution to investigate exhumation path of CCB. Samples from well-developed D1-D3 quartz veins and late injections have been studied.

The earliest record of fluid inclusion is noticed in the relict quartz grains in the granite gneisses with typical occurrence of high saline aqueous inclusion with low density CO_2 (0.53 to 0.67 gm/cc) representing fluid of the granite crystallization. The isochors of these inclusions suggest >7 kb pressure of granite crystallization at the mid-crustal level. In addition, aqueous-carbonic fluid is also found in Type 2 inclusions in gneisses showing total homogenization about >400°C. The fluids linked to the Tertiary metamorphism are wide spread in the studied samples. In the quartz vein representing D1 deformation H_2O-CO_2, CO_2-H_2O and aqueous biphase inclusions are present, wherein density of the histogram peak of predominant H_2O-CO_2 inclusions is 0.71 gm/cc. The quartz veins representing D2 deformation has carbonic density of 0.83 gm/cc. Most of these inclusions were not homogenized. The secondary H_2O-CO_2 inclusions in D2 deformation provide lower CO_2 density of 0.56 gm/cc. The isochors characterizing synchronous D2 deformation mineralizing fluid in CCB indicate PT: about 4 kb and 450-500°C. The CO_2 density in D3 deformation veins is 0.54 gm/cc and total homogenization is between 240-360°C. Their obtained isochor is at lower PT level. The H_2O-CO_2 inclusions in oblique late quartz veins show lower total homogenization viz. 260-320°C. A pervasive saline aqueous fluid is unequivocal in all the samples representing circulation of late low temperature water circulation. Furthermore, the study of the existing geothermal springs in the CCB suggests reservoir temperatures upto 129°C.

The integration of all these data can deduce an uplift path for the CCB. The present work proposes one such uplift path advocating isothermal decompression applicable to Himalayan collision tectonics. The slope of this uplift path suggests exhumation from >5 kb pressure within temperature drop of 200°C. This study also assesses the thermal regime and fluid conditions during evolutionary stages of CCB.

The Raman Spectroscopy evidence for the granulite metamorphism of Almora Crystallines, Kumaun Himalaya, India

Rakhi Aswal[1,*], Rajesh Sharma[#]
Wadia Institute of Himalayan Geology, Dehra Dun, India
**rakhi84@rediffmail.com, [#]sharmarajesh@wihg.res.in*
**Present address: Oil and Natural Gas Corporation, Kaulagarh, Dehradun*

The carbonaceous material (CMs) is widely distributed in the meta-sedimentary rocks of the Lesser Himalaya. The studies performed on these CMs reveal that these are metamorphogenic

impure graphite (Rawat and Sharma, 2011). They would represent metamorphic conditions attained by the host rocks because the crystallinity of graphite increases with metamorphic grade and graphitization is an irreversible process, and hence graphite temperatures are considered as a reliable geo-thermometer (Beyssac et al., 2002; 2004; Rahl et al., 2005). The studies are performed on the graphite present in the meta-sedimentary rocks of the Gumalikhet Formation, Almora Group in Kumaun Lesser Himalaya. Of the three subdivisions of the Almora Group viz. Saryu Formation, Champawat Granodiorite and the Gumalikhet Formation, graphite is by and large confined to the youngest Gumalikhet Formation comprising of garnetiferous mica schist, quartzites, carbonaceous phyllites and the graphitic mica schist. The graphite of Almora Group has been focused here as a typical representative of the Lesser Himalayan graphite. The studied graphite occurs in the form of lenses, pods, nodules, layers and pockets. Thin bands to the sizable deposits of graphite are noticed, which are economically as well as geological significant. In the present work, this graphite has been investigated for the graphite crystallization temperatures and interns imply the metamorphism attained during its crystallization. Extensive Laser Micro Raman Spectroscopy has been carried out for this purpose, and carbon isotope of graphite is used to endorse its genesis.

The graphite from the Almora Cystallines show ordered to well-ordered graphitic material. The micro Raman spectroscopic data of this graphite has characteristic first and second order spectra, which is useful for distinguishing between various crystallite (La) stages. Typical Raman bands of graphite are obtained, and intensification of the G-band, absence of D2-band and low intensity of the D1-band is noticed in the first order spectra. The second order spectra show splitting of the S1-band and disappearance of S2-band. The designated G-band in the first order spectra of Almora graphite occurs at 1578.19 to 1583.56 cm^{-1}, with an average ~1580±2 cm^{-1}. Whereas, the position of defect bands (D1-band) varies from 1351.08 to 1359.52 cm^{-1} and which at times disappear in the highly crystalline form. The average position of D1-band and D2-band are ~1355 cm^{-1} and ~1620 cm^{-1} respectively, wherein the D2-band appears rarely (cf. Cuesta et al., 1994; Beyssac et al., 2002, 2004). In the studied graphite, the S1-band peak at ~2700 cm^{-1} is asymmetrical and split into two peaks at ~2688 cm^{-1} and ~2721 cm^{-1}. The S1-band also occurs as wide band at ~2700 cm^{-1} in the samples with disordered graphite. The S2 Raman band position at ~2955 cm^{-1} is visible with the symmetrical S1 Raman band at ~2700 cm^{-1}, but it is absent if S1-band splits into two peaks (close to 2688 $cm^{-1}$and 2721 cm^{-1} respectively). The G-band is intensified in most of the samples with the absence of D2-band and low intensity of the D1-band, in the first order spectra. On the other hand, in the second order spectrum, splitting of the S1-band and disappearance of S2-band is observed, which suggests that the material is well organized.

These results based on the evaluation of the different quantitative parameters such as position, width, intensity ratio (R1) and area ratio (R2) of the Raman spectra for the estimation of the temperature of graphite formation and crystallite size indicated that the graphitic in Almora Crystallines reached crystallite size and temperatures of 509<La>5600 Å, 418 to 714°C respectively. It is also observed the folded/nodular graphite reveal higher temperatures and crystallite size. In view, it is attributed that the crystallinity of Almora graphite was enhanced during Himalayan orogeny. The metamorphic temperature and high carbon contents was vital in improving its crystallinity. The synthesis of data and various plots of well-ordered to ordered graphite overall points that Almora Crystallines achieved metamorphism upto granulite grade.

Beyssac, O., Goffe, B., Chopin, C. and Rouzaud, J-N., 2002a. Journal of Metamorphic Geology, 20, 859-871.
Beyssac, O., Bollinger, L., Avouac, J.P. and Goffe', B., 2004. Earth and Planetary Science Letters, 225, 233-241.
Cuesta, A., Dhamelincourt, P., Laureyns, J., Martinez-Alonso, A., Tascon, J.M.D., 1994. Carbon, 32 (8), 1523-1532.
Rahl, J.M., Anderson, K.M., Brandon, M. and Fassoulas, C., 2005. Earth and Planetary Science Letters, 240, 339-354.
Rawat, R. and Sharma, R., 2011. Journal of Asian Earth Sciences, 42, 51-64.

Mapping of reach scale stream power variability using SWAT model in Kosi River Basin, India

Rahul K. Kaushal[1*], Punit K. Das[2], Vikrant Jain[1]
[1]*Earth Sciences Discipline, IIT Gandhinagar, Palaj, Gandhinagar 382355, INDIA*
**rahul.kaushal@iitgn.ac.in*
[2]*Civil Engineering Discipline, IIT Gandhinagar, Palaj, Gandhinagar 382355, INDIA*

Sediment delivery from upstream to downstream is spatially variable and is governed by stream power of river. Stream power represents the driving force in a fluvial system (Bagnold, 1966). Total stream power (Ω), is defined by the rate of liberation of kinetic energy from potential energy (Bagnold, 1966) and is a function of water discharge (Q) and energy slope (s). Unit or specific stream power ($\omega = \gamma.Q.s/w$) defined as stream power per unit bed area, characterizes effective utilization of available energy for geomorphic work. Stream power provides an expression of the rate of energy expenditure at a given point in a river system and is inherently linked to sediment- transport competence. This aspect may be applied to use the spatial distribution pattern of stream power in mapping of erosion pattern. A basin scale work in the Andes mountain has shown that specific stream power (SSP) distribution pattern in a river basin can be used as a proxy for spatial variation in erosion (Bookhagen and Strecker, 2012). A recent work on the Yamuna River basin in the Garhwal Himalaya also suggests a strong but nonlinear control of SSP distribution on erosion processes (Scherler et al., 2014). The stream power per unit length or cross-sectional stream power (Ω) is defined as (Bagnold, 1966)

$$\Omega = \gamma.Q.s \qquad (1)$$

where γ is the unit weight of water (=9800 N/m^3), Q is discharge (m^3/s), and s is energy slope (m/m), which is considered equivalent to bed slope. Equation (1) indicates that there are two variable components of stream power, namely discharge (Q) and slope (s). Mapping of stream power distribution pattern needs spatial distribution of slope and discharge data in the basin. Hence, the Soil and Water Assessment Tool (SWAT) is used in this study to simulate the reach scale stream power variability.

SWAT model is a continuous-time, semi-distributed, processes-based river basin scale model. This model was developed to forecast the influence of land management practices on water, sediment and chemical yields from agricultural basins with varying soil, LULC and management settings over long period of time (Arnold et al., 1998; Neitsch et al., 2005). SWAT model can delineate sub-basins from large basin and each sub-basin is linked through a stream channel. The sub-basins can be divided into Hydrologic Response Unit (HRU), a unique combination of land use, soil and slope (Arnold et al., 2011).

We used SWAT model to extract stream power variability at reach scale in Kosi River basin (Fig. 1). The dynamics nature of Kosi River causes frequent flooding in this region. The importance of this study is to identify potential contributing zones of sediment to the downstream region. We estimated Subbasins scale discharge using SWAT model. The basic inputs such as precipitation, temperature, elevation, land use land cover and soil data were used to drive SWAT model. Spatial variation in channel slope has been carried out based on topography data such as DEM. The reach scale discharge and slope obtained from SWAT model was used to evaluate spatial distribution of stream power.

We observed that the estimated stream power is higher in channel reaches of Sun and Arun Kosi (Fig. 2). It shows a close proximity with the spatial variability in slope data. Since channel slope is higher in western and main channel so stream power is also higher in these channels. Further, rainfall distribution is also plotted to see its impact on the stream power distribution pattern. We

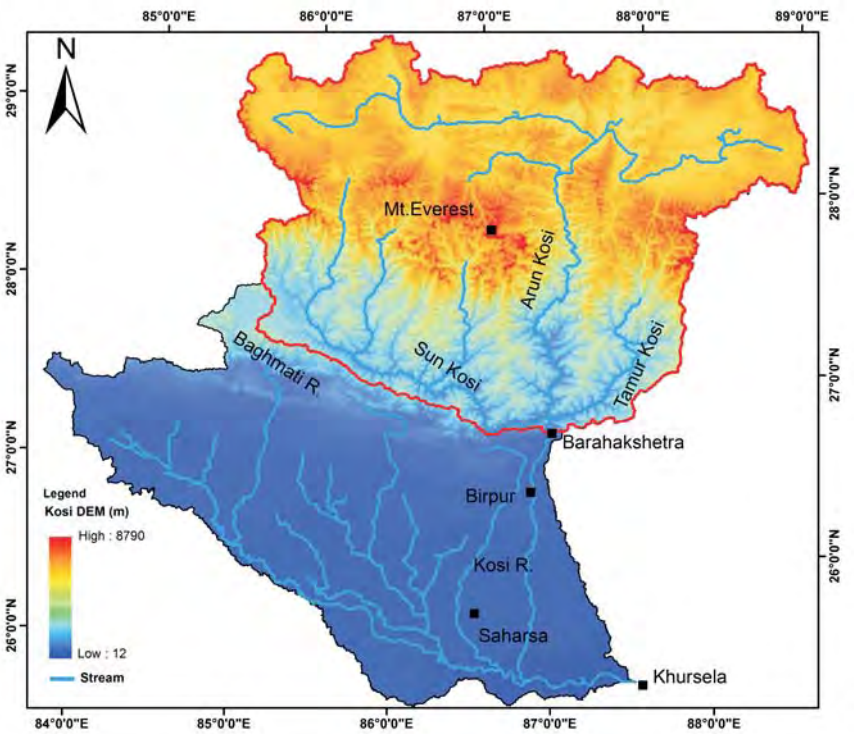

Fig 1. Map showing a study area and major tributaries.

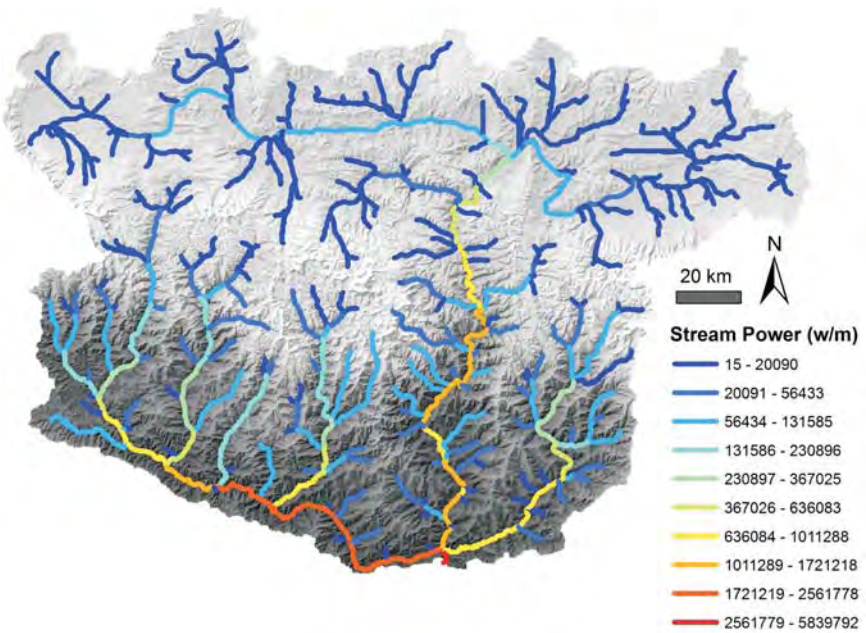

Fig. 2. Spatial distribution of stream power over the Kosi River basin (at upstream part of Barahkshetra).Stream power is estimated for period of 1985-1995.

found that western and eastern part of the lower reaches receives higher rainfall. Stream power has been mapped at reach and basin scale to see spatial variation. We observed that the spatial variability in stream power is directly related with slope variability and rainfall distribution.

Arnold, J.G., Kiniry, J.R., Srinivasan, R., Williams, J.R., Haney, E.B., Neitsch, S.L. 2011. Grassland Soil and Water Research.

Arnold, J.G., Srinivasan, R., Muttiah, R.S., Williams, J.R. 1998. Journal of American Water Recourses Association, 34(1),73-89.

Bagnold, R.A. 1966. Geological Survey Professional Paper, 422- I, I1- I37.

Bookhagen, B., Manfred R.S. 2012. Earth and Planetary Science Letters, 327-328, 97-110.

Neitsch, S.L., Arnold, J.G., Kiniry, J.R., Williams, J.R. 2005. Grassland Soil and Water Research Laboratory, Agricultural Research Service: Temple, TX, USA.

Scherler, D., Bodo B., Manfred, R.S. 2014 Journal of Geophysical Research: Earth Surface 119 (2): 2013JF002955.

Temporal variation of shear wave splitting parameters: a case study for earthquake precursory research in Garhwal region of Himalaya

Rakesh Singh*, Ajay Paul

Wadia Institute of Himalayan Geology, 33 GMS Road, Dehradun 248001, INDIA

**rakeshgosain@wihg.res.in*

The current micoseismicity trend in the Garhwal region of Himalaya is coinciding with the high conductivity zone (Rawat et al., 2014) and the metamorphic fluid facilitates the micro-fracturing by mechanical weakening. Shear Wave Splitting (SWS) can be described in terms of two parameters: the fast polarization direction (ø) and the time lag between fast and slow shear waves (δ_t). The time delays observed between the slow and fast shear waves give information about the density of cracks in the medium. SWS measurements can be used to monitor stress levels in the earth and to map the network of the subsurface fractures. To delineate the network of these subsurface fractures, measurement of SWS parameters is being carried out by using MFAST technique. This is for the first time that this technique has been attempted in the Garhwal region to monitor the temporal variation in the polarization and delay time. The preliminary observations of variation in SWS measurements show increase in delay time before the occurrence of 4.9 M Chamoli earthquake of 1st April 2015 and it decreases after the main shock. The analysis of more earthquake events, with reference to SWS, need to be carried out before any conclusive result towards precursory signature can be ascertained.

Rawat, G., Arora, B.R., Gupta, P.K. 2014. Tectonophysics 637, 68-79.

Significance of fossils from Kasauli and Nyoma in understanding the timings of Indo-China collision, evolution and upliftment of Himalaya

Ritesh Arya

168 Arath Bazaar, Kasauli Himachal Pradesh, INDIA

Aryadrillers@gmail.com

Mega floral fossis assemblage found in Kasauli during late 1990's belonging to *Garcinia, Gluta, Syzygium, Clinogene, Combretum* and palms from the Kasauli Formation had shown beyond doubt the similarity with the extant taxa from coastal regions of Indo-Malayan Archipelago including Borneo and Sumatra and Andaman Nicobar Islands which indicate hot and humid equatorial climatic conditions with major representation of evergreen elements typical of tropical or near equatorial conditions and near shore coastal marine influence on otherwise terrestrial environment that prevailed during thatt time (Arya and Awasthi, 1994). Fossils of mega plants from the Indian Himalaya showing similarity with Indo- Malayan and Indonesian islands establish land connections

for their migration during those times. This fact on environmental regime (near coastal/marine transgression) at the time of deposition is further supported by fossil and sedimentological findings in Kasauli, Dharamsala, Udhampur, Jammu, Kalakot, Kargil, Alchi, Nimmu, Stok, Kangri range and Nyoma in the northwestern Indian Himalaya and further in the Chitarwata Formation, west central Pakistan; and the equivalent formation in Darjeeling, West Bengal, North Eastern India and Bhutan in North eastern sector all shallow marine coastal regimes. All these localities marked on the map show an interesting structural pattern revealing a lot about the history of their genesis in geological time. Interestingly, on ground all the fossil plant assemblage localities show great similarity in lithologies, fossils and type of preservations with each other. The most important being the taphonomic relationship between the fossil wood and the sandstone facies which is quiet homogenous with other homotaxial localities or basins described above and show unmatched similarity in the environments of the deposition specially in the basins of Kasauli-Dagsahi, Dharamsala, Murree and along Indus in Ladakh.

Based on the fossil findings of *Mitrgyana* from the Kasauli sediments by the author elevation was also found to be less then 1300 m in contrast to the present height of about 2000 m. This really meant that the Himalaya attained sufficient height to block the rain laden winds and thus the concept of monsoons was born. Presence of diverse assemblage of fossil flowers shows that seasonal changes had initiated during those times.

Recent findings of *Turritella, Venericardia, Glyptoactys, Cordiopsis* and hundreds of yet to be identified fossil specimen in author's collection from Nyoma in Ladakh along with oysters show close resemblance with the fossils from the Subathu Formation which confirms beyond doubt that Subathu basin extended uptil Nyoma and enjoyed tropical/equatorial latitudinal position during the Lower Eocene. Since fossils from Kasauli show similar affinities with extant taxa of Indo-Malayan region it can be very well be interpreted that the Kasauli Formation and its equivalent also enjoyed near coastal equatorial to subequatorial climatic conditions and latitudes may be around 10 degrees +5 north of equator at the time of deposition in contrast to 32 degrees which the place is presently located. This implies that the major tectonic forces which were to give rise to the future Himalayas were not very active during those times. Northward dragging of the uplifted Tethyan basin (during Dagsahi times) along with the Indian subcontinent took place much later than 18.2 Ma ago (age of the Kasauli Formation based on the findings of *Stephenochara ungri* by the author). If this is to be believed then the rate of northward drifting can be calculated and actual timing of collision and upliftment of Himalayas being known. Accordingly age of Himalayas should be much less than 10 million years. Paper also highlights the role of mighty Ladakh Batholith in giving birth to the baby Himalaya.

Need for preservation of Aryas C structures discovered from Ladakh batholith in understanding cyclicity of climate change

Ritesh Arya
168 Arath Bazar, Kasauli Himachal Pradesh, INDIA
Aryadrillers@gmail.com

Present paper highlights the need to preserve the paleoclimatic signatures made by the Indus River on the granites of Ladakh batholith. Author discovered these signatures in 2010 while exploring, drilling and developing groundwater on Indo-China (Changthang) and Indo-Pakistan (Siachen, Kargil) boders in the NW Indian Himalaya. These signatures resemble alphabet C, hence named Aryas C cycles. Cyclicity of cooling, warming and again cooling can be well understood by writing alphabet C. The starting point of alphabet C represents the cooling phase (ICE age) and as we continue to draw the curve there is gradual curvilinear transformation from cooling maxima to

warming phase. Half of the C curve represents the warming maxima (an event marked by flooding, cyclones, sea level rise, desertification, biodiversity explosion, increase in GHGs) and completion of alphabet C represents the culmination of the gradual curvilinear transformation from warming to cooling coinciding with ICE age (marked by squeezing and freezing of water resources, glaciations, desertification, competition, mass extinctions, decrease in GHGs). Transferring this sentence geologically means that since there is less water in the system during ICE age so there is less erosion hence we get starting and end of C cycle but as the temperature increases the rate of erosion increases hence the curvilinear depressions are created making the upper half of the warming cycling, center of alphabet C is marked by warming maxima. Then there is again gradual transformation from warming to cooling and as the water in the system decreases there is less erosion therefore we get a geomorphological feature which resembles the lower half of alphabet C finally ending into the ICE age. So uniformity in the paleoclimatic signatures dicovererd in Ladakh Himalaya which resembles alphabet C, for the first time geologically and scientifically explains cooling, warming and again cooling phase in nature to be a natural climate cyclic process.

Granites played important role in the preservation of these climatic signatures because they are very hard and compact as compared to other rocks found in the Himalaya which are fragile and susceptible to faster rate of weathering and erosion making preservation of the signatures a tedious task. Taphonomical analysis of these C curves in massive granites show great role of lithology and geomorphology in preservation and understanding the cyclicity of these climate signatures which have been beautifully preserved in the Ladakh Batholith in NW Himalaya. Author observed 10 such cycles, 8 complete and 2 half cycles. Geomathematical modeling of these paleoclimatic signatures show that after every 4 cycles there is a half cycle. According to this model each complete C cycle is of 1338.6 years and half C cycle is 669.3 years.

Based on this model author has tried to correlate the paleoclimatic and geological events in the past and found that lot of events can be explained by Aryas C cycles. Important question now is which part of the C cycle are we in now. Seeing the paleoclimatic signature in the Batholiths of Ladakh we are presently in the warming maxima times and are curvilinearly moving into the cooling phase finally culminating into ICE age in 2344 years, represented by the lower part of alphabet C. So enjoy global warming by building sustainable habitats in geologically favorable locations because the next warming maxima will be in 3014. Today these are the only structures which give complete documentation of the climate change history outside the 2 poles. These structures are being naturally destroyed by the actopn of extreme climatic conditions in Ladakh on one hand and on the other the expansion of the roads is posing a great threat to these geomorphological features. Need of the hour is to preserve them and make a geo heritage site so that the future generations can understand the cyclicity of climate change and live happily with warming process.

Cenozoic mammalian dispersal patterns indicate significant uplift of the Himalaya between 10-8 Ma

Ramesh Kumar Sehgal
Wadia Institute of Himalayan Geology, 33 GMS Road, Dehradun 248001, INDIA
Rksehgal@wihg.res.in

The uplift of the Himalaya, as a result of collision between Indo-Eurasian plates, played a vital role in the dispersal of the mammalian faunas across its width. The initial timing of the continental collision and evolution of primitive Himalaya is largely debated. The general consensus places it around 50-60 Ma (Yin and Harrison, 2000; Spicer et al., 2003), while other estimations range from 34 to 70 Ma (Sahni et al., 1981; Jaeger et al., 1989; Aitchison et al., 2007; Najman et al., 2010).

The biological dispersal during the Cenozoic era was largely controlled by the uplift of the Himalaya. The correlation of the faunas, occurring north and south of the Himalaya, reveal that during early Cenozoic Himalaya was not a formidable barrier for to and fro migration of the faunas. A large number of terrestrial genera were common on both northern and southern sides of the Himalaya. The pre-Siwalik faunas belonging to the Subathu Group (Paleocene-Eocene) show wide ranging faunal exchanges between India and central Asia (West, 1980). Similarly, the faunas from Kargil Molasse of Trans Himalaya (Oligo-Miocene) and Bugti Fauna of Chitrawata Formation of Pakistan (Oligo-Miocene) show good linkages with the faunas occurring north of the Himalayan arc (Raza and Meyer, 1984). The Lower Siwalik faunas (18-10 Ma) also show considerable links with contemporaneous faunas from Europe, Africa and central Asia. However, it was during the Nagri Formation of the Siwalik Group (10-8 Ma), the faunas across the width of the Himalaya show very poor links (Nanda, 2015). It is inferred that around 10 Ma, the Himalaya attained a significant height to act as a barrier for faunal migration. For the first time, dispersal patterns of the Cenozoic mammalian assemblages (especially the Neogene mammalian assemblages), occurring north and south of the Himalaya, have been linked with the uplift of the Himalaya, which is widely considered responsible for the onset of monsoon conditions in the Indian subcontinent, in the geologic past. The linkage between the Cenozoic mammalian assemblages of the Outer Himalaya and their equivalent correlatives in Europe, Africa and central Asia has been derived by comparing a large number of fossil mammalian genera reported from these regions. The linkage has been worked out at generic level.

Aitchison, J.C., Ali, J.R., Davis, A.M. 2007. Journal of Geophysical Research, 112, 43-51.

Jaeger, J.J., Courtillot, V., Tapponnier, P. 1989. Geology, 17, 316-319.

Najman, Y., Appel, E., Boudagher-Fadel, M., Bown, P., Carter, A., Garzanti, E., Godin, L., Han, J.,Liebke, U., Oliver, G., Parrish, R., Vezzoli, G. 2010 Journal of Geophysical Research, 115, B12416.

Nanda, A.C. 2015. Siwalik mammalian faunas of the Himalayan foothills-with reference to biochronology, linkage and migration. In press.

Raza, S.M., Meyer, G.E. 1984. Mem. Geol. Surv. Pakistan, 11, 43-63.

Sahni, A., Bhatia. S.B., Hartenberger, J.L., Jaeger, J.J., Kumar, K., Sudre, J., Vianey-Liaud, M. 1981. Bull. Geol. Soc. France, 23(6), 689-695.

Spicer, R.A., Harris, N.B.W., Widdowson, M., Herman, A.B., Shuangxing, G., Valdes, P.J., Wolfe, J.A., Kelley, S.P. 2003. Nature, 421, 622-624.

West, R.M. 1980. Journal of Paleontology, 54(3), 508-533.

Yin, A., Harrison, T.M. 2000. Annual Review of Earth and Planetary Sciences, 28, 211-280.

Out-of-sequence structures in the eastern Himalaya: constrains from LA-ICP-MS monazite U-Pb age of Greater Himalayan Sequence in Arunachal Pradesh, NE India

R.K. Bikramaditya-Singh[1,2,*], Clare J. Warren[3], A. Krishnakanta Singh[1], N.M.W. Roberts[4]

[1]Wadia Institute of Himalayan Geology, 33 GMS Road, Dehradun 248001, INDIA

[2]Geosciences Department, National Taiwan University, Taipei106, TAIWAN

**rkbikramadityasingh@gmail.com*

[3]Department of Environment, Earth & Ecosystems, The Open University, Milton Keynes MK7 6AA, UK

[4]NERC Isotope Geosciences Laboratory, British Geological Survey, Nottingham NG12 5GG, UK

The high structural levels of the Greater Himalayan Sequence (GHS) in western Arunachal Pradesh, NE India are mainly comprised of high-grade sillimanite-bearing migmatitic gneisses. Toward Tawang, the migmatitic gneisses are overlain by kyanite schists, which grade upwards into staurolite-garnet schists and garnetiferous schists. The Lumla Formation (LF) that affinity to Lesser Himalaya Sequence is exposed as a window through the GHS at Lumla. It comprises quartzites and

phyllites, that grade upwards into garnet bearing lithologies near the tectonically contacts with the overlying the higher grade metasedimentary rocks. The Lumla Thrust cuts parallel to the foliation and may be a northerly exposure through the MCT, similar to the structure separating the Paro window from the GHS in southwestern Bhutan (Tobgayet al., 2010). To the north of Lumla, high-grade garnet-bearing mica schists and gneisses are over-thrust by garnet-free sillimanite-bearing augen gneisses along the Zimithang Thrust, a possible out-of-sequence structure correlated with the Kakhtang thrust in Bhutan (Yin et al., 2010).

Monazite U-Pb, muscovite $^{40}Ar/^{39}Ar$ and thermobarometric data from rocks in the hanging and footwall of the Zimithang Thrust constrain the timing and conditions of their juxtaposition across the structure, and their subsequent cooling. LA-ICP-MS U-Pb analyses of monazite from sillimanite bearing gneiss in the hanging wall yield an ages of 16±0.2 to 12.7±0.4 Ma and the garnet-staurolite mica schists in the footwall yield an older monazite ages of 27.3±0.6 to 17.1±0.2 Ma. Single grain fusion $^{40}Ar/^{39}Ar$ muscovite data from samples either side of the thrust yield ages of ~7 Ma. Temperature estimates from titanium-in-biotite and garnet-biotite thermometry suggest similar peak temperatures were achieved in the hanging and footwalls (~525-650°C). Monazite from a sample collected in the high stain zone itself grew in association with fabric-forming biotite between 14.9±0.3 and 11.5±0.3 Ma at temperatures of ~680°C. Together the $^{40}Ar/^{39}Ar$ and U-Pb data suggest that the ZT had juxtaposed the hanging and footwalls between ~11.5 and 7 Ma, at the closure temperature of Ar diffusion in muscovite had been reached. The new data lend strength to the suggestion that the Zimithang Thrust is the eastwards continuation of the out-of-sequence Laya and Kakthang Thrust mapped in Bhutan. This structure consistently appears to juxtapose younger metamorphic rocks on top of older metamorphic rocks, although the pressure-temperature variation across the structure is not as pronounced as in Bhutan. These data confirm previous suggestions that major orogenparallelout-of-sequence structures disrupt the Greater Himalayan Sequence at different times during Himalayanevolution, and highlight an eastwards-younging trend in $^{40}Ar/^{39}Ar$ muscovite cooling ages at equivalentstructural levels along Himalayan strike.

Tobgay, T., Long, S., McQuarrie, N., Ducea, M.N., Gehrels, G. 2010. Tectonics, 29, TC6023.
Yin, A., Dubey, C.S., Kelty, T.K., Webb, A.A.G., Harrison, T.M., Chou, C.Y., Célérier, J. 2010. Geological Society of America Bulletin, 122, 360-395.

Differential behaviour of a Lesser Himalayan watershed in extreme rainfall regimes

Pankaj Chauhan[1,*], Nilendu Singh[1], Devi Datt Chauniyal[2], Rajeev Saran Ahluwalia[1], Mohit Singhal[1]
[1]Centre for Glaciology, Wadia Institute of Himalayan Geology, 33 GMS Road, Dehradun 248001, INDIA
[2]School of Earth Science, HNB Garhwal University, Srinagar 246174, INDIA
**pchauhan1008@gmail.com*

Climatic extremes including precipitation are bound to intensify in the global warming environment (Good et al., 2015; Lehmann et al., 2015). Understanding the effects of extreme precipitation events on the watershed processes will be helpful in managing natural resources while sustaining hydropower projects. Present study intends to understand the response of a lesser Himalayan watershed (Fig. 1) in three entirely different hydrological years (July 2008-June 2011) in terms of discharge, erosion, sediment flux and denudation rates (headwater of the Ganga River system). In this study computations are based on the systematic sampling collected two to four times per day. Within uncertainty limit of ±20%, mean interannual water discharge (5.74±1.44 m^3s^{-1}) (±SE), was found highly variable (0.8-38 m^3s^{-1}) (Coefficient of variation (CV): 151%). In a normal

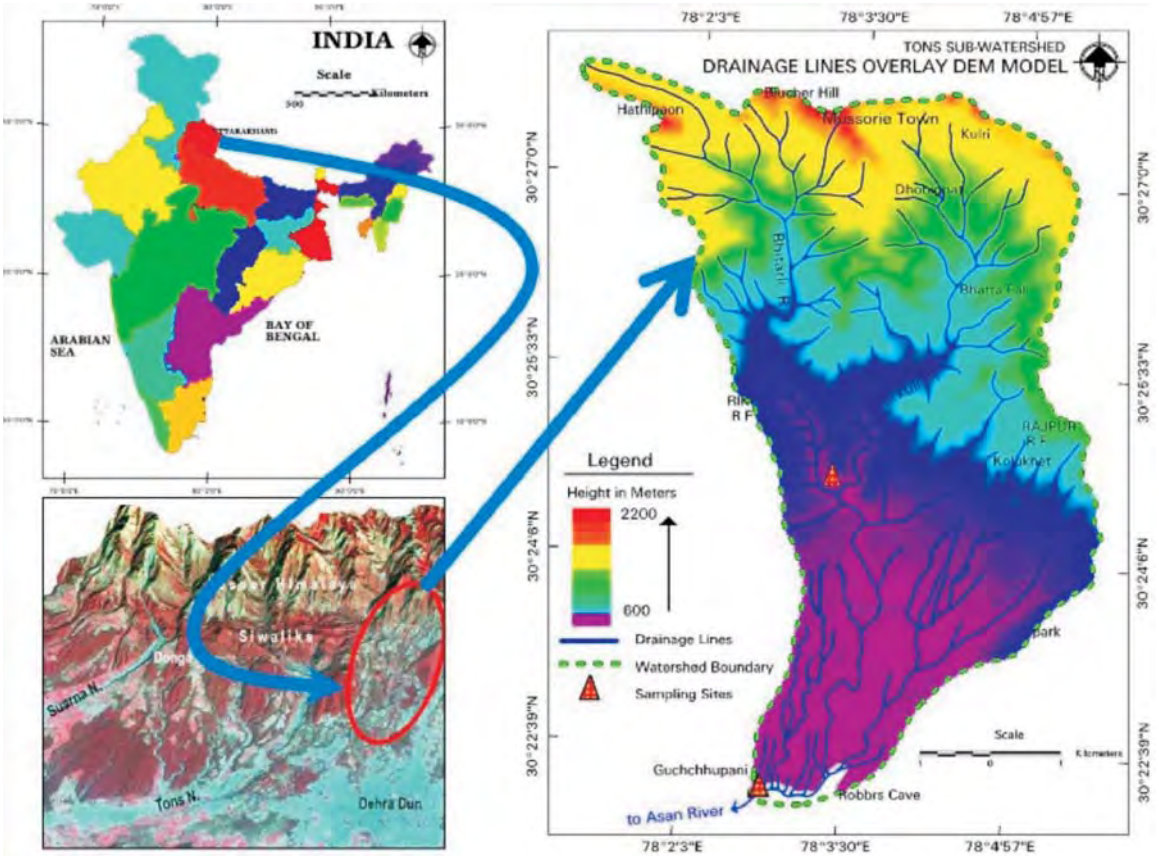

Fig. 1. Location map of the Tons River basin (sub-watershed), satellite data in lower left panel shows topography and the river systems around the study area, DEM model in right panel shows drainage and sampling sites within the catchment.

rainfall (P) year (2008-09; ~1550 mm) mean discharge was 5.12±1.75 m^3s^{-1}(CV: 120%), whereas in a drought year (2009-10; ~1200 mm), discharge was 3.6±0.9 m^3s^{-1} (CV: 85%). In an excessive rainfall year (2010-11; ~3050 mm), mean discharge was 8.45±3.9 m^3s^{-1} (CV: 159%). The rainfall event in 2010 was once-in-a-century event, during which discharge was ~200% higher relative to the long-term regional average (Fig. 2). Mean monthly discharge was least in summer month (April) and highest in peak monsoon (July-Aug). Rainfall explained more than 85% of the discharge variation in this typical lesser Himalayan watershed with ~45% vegetation cover. Interannual mean total suspended solids (TSS) and total dissolved solids (TDS) was 4027±1566 and 2134±762 metric tons, respectively. Monsoon months (July-Sep) accounted for 97% and 93% of the annual load transport respectively. More than 200% upsurge in total solid load was observed in the excessive rainfall year (2010). Remarkably, TDS variation was similar in normal and drought year, whereas suspended solid (TSS) varied significantly in both the years (Fig. 3). Consistently, dissolved load was found higher than suspended load in the drier months (winter, summer) (except monsoon). Irrespective of the rainfall behaviour in the three year, TDS/TSS (C/P) ratio was consistently low (<1) during monsoon months and higher (1-7) during rest of the dry period. C/P ratio was inversely (R^2 = 0.49) but significantly (P<0.001) related to the rainfall. This shows that erosion rate is closely linked with rainfall and runoff and its relation with the tectonics remains invariant in the region.

Average mechanical erosion rate in the three different rainfall year was 0.24, 0.19 and 1.03 mm yr^{-1} respectively, whereas, chemical erosion was estimated at 0.12, 0.11 and 0.46 mm yr^{-1},

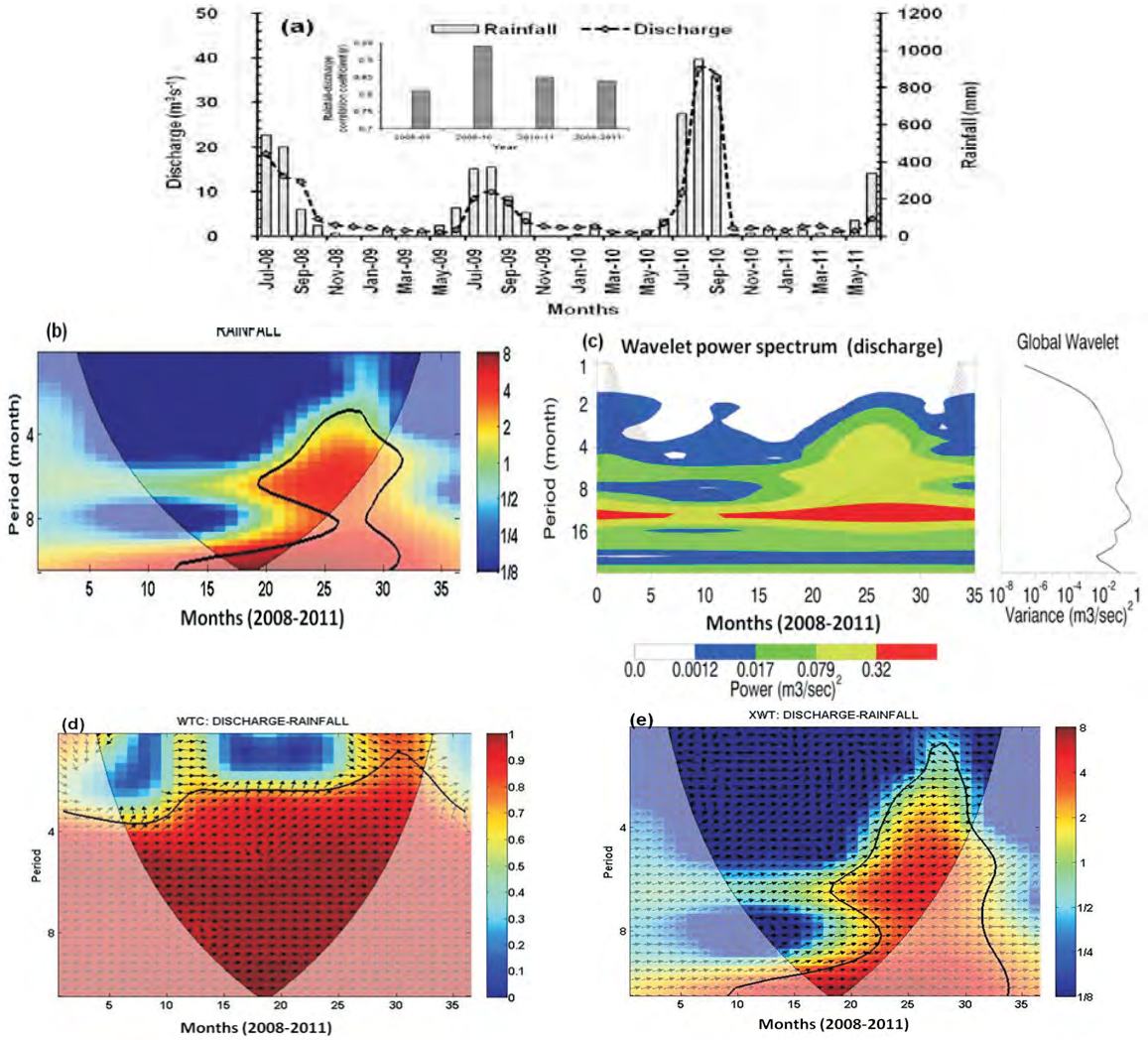

Fig. 2. (a) The rainfall-discharge behaviour of the catchment in the study period (inset figure shows correlation coefficient "r" in the different hydrological years). The continuous wavelet power spectrum of (b) rainfall during study period (thick black contour designates the 5% significance level against red noise and the cone of influence) (c) the wavelet power spectrum of discharge and its global wavelet power spectrum (the cross-hatched region is the cone of influence where zero padding has reduced the variance). There is more concentration of power between the 1113 month band, which shows that this time series has a strong annual signal (d) squared wavelet coherence (e) cross wavelet transform between the standardized discharge and rainfall time series (The 5% significance level against red noise is shown as a thick contour. All significant sections show in-phase behaviour. Arrows show the phase shift between the respective time series. Colors indicate the measure of coherence: red color implies high degree of coherence. Arrows pointing right indicate that the two time series are in phase. Arrows pointing down indicate that precipitation leads discharge).

respectively, for three years. Thus, the average denudation rate of the Tons sub-watershed has been estimated at 0.33 mm yr^{-1} (excluding extreme rainfall year: 1.5 mm yr^{-1}). Our results have implications for the proposed and upcoming several small hydropower plants in the region in the context of regional ecology and natural resource management.

Good, Stephen P., David Noone, Gabriel Bowen. Science, 2015 doi: 10.1126/science.aaa5931.
Lehmann, J., Coumou, D., Frieler, K. Climatic Change, 2015; doi: 10.1007/s10584-015-1434-y.

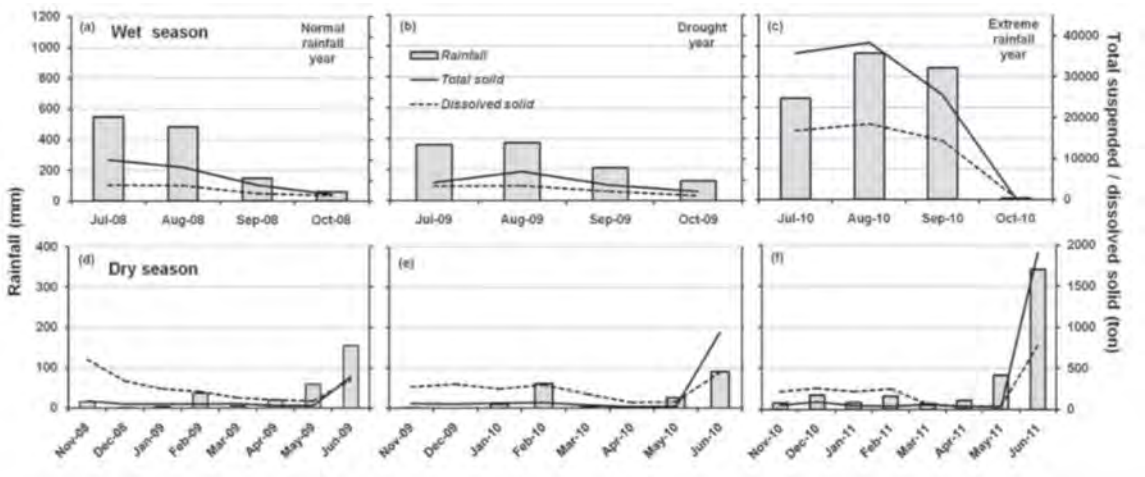

Fig. 3 (a-f). Temporal relation between rainfall and load (total suspended and dissolved) transport behaviour indifferent precipitation regime and in dry season.

Evidence of A.D. 1255 earthquake at Panijhori tea garden, Sikkim Himalaya along the north eastern Himalayan Front, India

Rajeeb L. Mishra[1*], I. Singh[1], A. Pandey[1], P.S. Rao[2], R. Jayangondaperumal[1]
[1]*Wadia Institute of Himalayan Geology, 33 GMS Road, Dehradun 248001, INDIA*
[2]*Geological Survey of India, Hyderabad, INDIA*
**rajeebmishra88@gmail.com*

Himalayan arc has experienced many medium, large and great earthquakes since its evolution. Those earthquakes which have proved to be fatal for the human civilizations bear patchy historical documentation by various people in historic times and thus prevent us from quantifying the seismic hazard precisely. In order to understand the timing, size, rupture extent, recurrence interval and the mechanics involved in the process of faulting associated with the devastating earthquakes of the past, a number of trench excavations have been conducted so far. Till date ~27 trenches have been dug out by various workers all along the Himalayan Frontal Thrust (or Main Frontal Thrust) in India as well as Nepal.

As an addition to the paleoseismic investigations done so far, we present here the results of a trench survey conducted at Panijhori village near Chalsa town, located ~500 m west of a trench excavated previously (Kumar et al., 2010). Though the site is located within the meizoseismal zone of A.D. 1934 earthquake, trenching was carried out with an intention of finding any signature of surface faulting associated with it. Six detrital charcoal samples collected from Units 1 and 2 observed in the Panijhori trench were analyzed by Accelerator mass spectrometer radiocarbon (^{14}C), which provided ages widely ranging from cal year B.C. 1690 to cal year A.D. 1150. Since the samples are not in proper stratigraphic sequence, the detrital charcoal samples are interpreted to have been reworked due to transportation and re-deposition by surface processes. Variability in ages of the samples provide no scope for constraining the age and timing of faulting event observed in the trench, except the sample P2 which gives an age range of cal A.D. 990-1150. Since the sample is located at the fault tip, it is more likely to pre-date the earthquake event. Relevantly, damage due to the A.D. 1255 event has earlier been reported in Nepal. Based on reported age ranges of A.D. 700-1300, evidence of A.D. 1255 event has been reported in a trench at Sir Khola, located towards east of

Kathmandu in Nepal (Sapkota et al., 2013). More recently, on the basis of the radiocarbon age ranges of A.D. 1050-1259, evidence of the same earthquake was inferred from a trench investigation at Belparao village near Ramnagar, India in NW Himalaya (Rajendran et al., 2015). Hence, in validation of the consensus that the A.D. 1255 event was a giant event (Pant, 2002; Mugnier et al., 2013) and as our site is at a distance of ~300 km from Sir Khola trench in Central Nepal, we assert that, a fault slip of ~5 m observed in the present trench at Panijhori is an outcome of the historically documented 7th June, A.D. 1255. If this is reasonably true, then the A.D. 1255 earthquake would have a rupture extent of ~990 km.

Kumar, S., Wesnousky, S., Jayangondaperumal, R., Nakata, T., Kumahara, Y., Singh, V. 2010. J. Geophys. Res.,115, B12422, doi: 10.1029/2009JB006789.

Mugnier, J.-L., Gajurel, A., Huyghe, P., Jayagondaperumal, R., Jouanne, F., Upreti, B. 2013. Earth Sci. Rev., 127, 30-47.

Pant, M.R. 2002. Journal of the Samsodhanamandala, pp. 29-54.

Rajendran, C.P., John, B., Rajendran, K. 2015. J. Geophys. Res. Solid Earth, 120, doi:10.1002/2014JB011015.

Sapkota, S.N., Bollinger, L., Klinger, Y., Tapponnier, P., Gaudemer, Y., Tiwari, D. 2013. Nat. Geosci., 6, 71-76, doi:10.1038/ngeo1669.

Primary surface faulting of the A.D. 1697 and A.D. 1950 great earthquakes along the Main Frontal Thrust, Arunachal Pradesh, NE Himalaya

Priyanka Singh Rao[1,2], Arjun Pandey[1], Ishwar Singh[1], R.L Mishra[1], G. Bhat[2], Hrishikesh Baruah[3], Pradeep Srivastava[1], R. Jayangondaperumal[1*]

[1]Wadia Institute of Himalayan Geology, 33 GMS Road, Dehradun 248001, INDIA

**ramperu@wihg.res.in*

[2]Present Address: Geological Survey of India

[3]Dept. of Geology, Pondicherry University, Port-Blair, INDIA

[4]Arya Vidyapeeth College, Guwahati, INDIA

The 1950 A.D. Assam earthquake (M ~8.7) is the most intense (Tandon, 1950; Tillotson, 1951; Chen and Molnar, 1977) amongst many historical earthquakes (e.g., A.D. 1803 Garhwal, A.D 1883 Nepal, A.D. 1905 Kangra, A.D. 1934 Bihar-Nepal earthquakes) along the Himalayan arc. However, no surface ruptures associated with the 1950 earthquake have been documented so far. To hunt for surface ruptures associated with the A.D. 1950 Assam earthquake, a field work was carried out for two months in and around the meisoseismal zone (Poddar, 1950; Kingdon-ward, 1953) at Pasighat town, Roing and Niglok villages, Arunachal Pradesh with aid from high resolution Pleiades and Cartosat imageries.

The field survey provides evidence of tectonic surface uplift and recent active faulting in discontinuous young fault scarps along the Himalayan Frontal Thrust (HFT, also referred as Main Frontal Thrust, MFT). To quantify the vertical offsets of uplifted and disjointed Quaternary alluvial or fluvial terraces and fault scarp along the HFT, we carried out mircro-topographic mapping of disjointed geomorphic markers and prepared topographic profiles across the identified fault scarp using RTK-GPS (Real Time Kinematic Global Position Satellite) and Robotic Total Station. Aerial photography was performed using Drone for trenched sites to generate a high resolution digital elevation model (DEM). We report the first evidence of surface faulting associated with the A.D. 1697 and A.D. 1950 earthquakes in Pasighat, and Niglok villages.

At Pasighat town, a prominent fault scarp was identified with ~N-S strike, which parallels the regional Himalayan structural grain in the area. The 20±01 m high scarp extends for ~7 km at southern end that displaces higher surface. The scarp becomes 3±01 m high at the northern end,

where it cuts the lower terrace at west bank of the Siang River. A trench (25x5x5 m length, width and depth respectively) was excavated across the fault scarp to identify the co-seismic fault slip and to infer the timing of the deformation event. We collected several charcoals and caesium samples for constraining the chronology of the faulting event. In the Pasighat trench both trench walls were mapped using total station and 15 charcoal samples were dated for AMS radiocarbon dating that suggests A.D. 1697 and A.D. 1950 earthquake associated surface ruptures.

At Niglok village, multiple fault scarps were identified in the field. The scarps extend nearly 2 km with a NW-SE strike. At the south-western segment, the fault scarp displaces T2 terrace with 15±01 m high scarp, whereas in the north-eastern trace, the fault scarp displaces the T1 terrace that shows 2.5-3 m high scarp. Two trenches were excavated across T2 and T1 fault scarps, respectively. Both these trenches reveal splay faults that were mapped using Robotic total station. Several charcoal samples including OSL samples were collected. In addition, two caesium profiles at 20 cm intervals were collected one, near the fault tip and the other away from the fault tip. In the T1 trench, 11 charcoal and in the T2 trench, 17 charcoal samples were dated using the AMS radiocarbon dating suggesting A.D. 1697 earthquake associated surface ruptures. Our inferred surface rupture events correspond to the historically documented A.D. 1697 and A.D. 1950 earthquakes (Iyengar et al., 1999).

Chen, W.P., Molnar, P. 1977. Journal of Geophysical Research, 82(20), 2945-2969
Iyengar, R.N., Sharma, D., Siddiqui, J.M. 1999. Indian J. Hist. Sci., 34, 181-237.
Kingdon-Ward, F. 1953. The Geographical Journal, 119/2, 169-182.
Poddar, M.C. 1950. Indian Minerals, 4/4, 167-176.
Tandon, A.N. 1950. Science and Culture, 16/4, 147-155.
Tillotson, E. 1951. Nature, 167, 128-130.

Late Holocene vegetation and climate reconstruction from the Central Tibet

Parminder S. Ranhotra[1,2*], Cheng Sen Li[1#], Jin Feng Li[1,]**
[1]State Key Laboratory of Systematic and Evolutionary Botany, Institute of Botany, Chinese Academy of Sciences, Xiangshan, Beijing, CHINA
**pranhotra@yahoo.com; ranhotra.p@gmail.com*
***lijinfeng@ibcas.ac.cn*
[2]Birbal Sahni Institute of Palaeobotany, 53 University Road, Lucknow 226007, INDIA
#lics@ibcas.ac.cn

The vegetation and climate change since ca. 2000 yrs BP have been reconstructed on centennial to decadal scale by palynological analysis of the subsurface sediments from Cuona wetland (~4600 m amsl), Central Tibet. Study shows an abrupt change in vegetation since ca. 760 yrs BP (1240 AD) marked by the increase in pollen frequency of few local non-arboreals (Cyperaceae, Asteraceae (Liguliflorae), Ephedra and Chenopodiaceae) and extra-local arboreal taxa (Pinus, Abies and Tsuga) at the expense of Artemisia, Ranunculaceae (including Thalictrum), Polygonaceae and other local herbs. The pollen assemblages combined with the various semi-quantitative methods put forth the existence of meadow type vegetation under the warm conditions (high Artemisia/Cyperaceae ratio) with good soil moisture (high Artemisia /Chenopodiaceae and Artemisia/Ephedra values and low Dryness Indicator (DI) values between ca. 2000 to 760 yrs BP. The warm-moist conditions of relatively higher magnitude than present were peaked between 1612 to 760 yrs BP that may correspond to Medieval Warm Period (MWP). After 760 yrs BP the change in pollen assemblage with decrease of pollen ratios (Artemisia/Cyperaceae, Artemisia/Chenopodiaceae and Artemisia/Ephedra) and increase of DI values indicate shift to steppe type vegetation under colder conditions with less soil moisture. This cold-dry phase, related to Little

Ice Age (LIA), peaked around 1500 to 1800 AD. During MWP the Asian summer monsoon (ASM) might have been stronger over the Central Tibet with its boundary towards west as compared to present ASM boundary, whereas weaker ASM with subsequent shift of its limit towards east of present limit during LIA phase. The abrupt increase of extra local arboreal pollen since ca. 1240 AD might be due to change of arboreal vegetation from the warm temperate broad-leaved to cool temperate conifers in the temperate montane forest belts near the eastern margins of the QTP during the last millennia, subjected to the climate change as well as increased human activities.

Constraints on the stratigraphic architecture of the Uttarakhand-Himachal Lesser Himalaya: implications for the evolution of the North Indian margin

N.R. Mckenzie[1,2*], N.C. Hughes[3], P.M. Myrow[4], B.P. Singh[5], Q. Jiang[6], N.J. Planavsky[2], A.A.G. Webb[7], C.L. Colleps[2], D.M. Banerjee[8], M. Deb[8], D.F. Stockli[2]

[1]Geology and Geophysics, Yale University, 210 Whitney Ave, New Haven, CT 06511, USA
[2]Jackson School of Geosciences, Univ. of Texas, 2305 Speedway, Stop C1160, Austin, TX 78712, USA
**ryan.mckenzie@yale.edu*
[3]Dept. of Earth Sciences, University of California, 1242 Geology Building, Riverside, CA 92521, USA
[4]Department of Geology, Colorado College, 14 E. Cache La Poudre, Colorado Springs, CO 80903, USA
[5]Center for Advanced Study in Geology, Panjab University, Chandigarh 160014, INDIA
[6]Department of Geoscience, University of Nevada, Las Vegas, Nevada 89154-4010, USA
[7]School of Earth and Environment, University of Leeds, Leeds, LS2 9JT, UK
[8]Department of Geology, University of Delhi, Delhi 110007, INDIA

Thick Proterozoic sedimentary successions distributed across the Indian subcontinent record important information on regional tectonics and evolution of the Earth system. However, these strata have been underappreciated due to a general lack of age constraints, which has led to disparate and controversial age designations for these units. Integrative detrital zircon U-Pb geochronologic, lithological, biostratigraphic, and sedimentary geochemical (e.g., ε_{Nd} and $\delta^{13}C$) data derived from Himalayan and cratonic sedimentary successions provide age constraints for these deposits and allow for broad regional correlations. A regional ~500 Ma unconformity exists between late Paleoproterozoic and late Mesoproterozoic strata across northern India. Prominent late Paleo-, late Meso- and Neoproterozoic siliciclastic successions were deposited during intervals of convergent margin tectonism, and are all capped by coeval carbonate successions, with phosphatic stromatolites present in distinct late Paleoproterozoic deposits-some of the oldest sedimentary phosphorites known in the rock record. Contemporaneous strata in all sectors yield similar age populations of detrital zircon grains, with similar stratigraphic variation in age distributions, implying shared provenance. These data combined with facies analysis suggests all strata were part of broad contiguous sedimentary systems with the Vindhyan deposited in a proximal epicontinental setting and the Aravalli-Himalaya along the distal continental margin. This interpretation contrasts classic widely held views that strata in all regions were deposited in a series of discrete isolated basins.

Stable isotope ($\delta^{13}C_{DIC}$, $\delta^{18}O_{H2O}$ & δD_{H2O}) studies of geothermal springs from Himachal & Ladakh Himalaya, India: sources and the nature of geothermal fluids

Sameer Kumar Tiwari[1]*, Santosh K. Rai[1], S.K. Bartarya[1], Anil K. Gupta[1]
[1]Wadia Institute of Himalayan Geology, Dehradun 248001, INDIA
**sameer@wihg.res.in*

Carbon Dioxide (CO_2) is one of the major greenhouse gases in the Earth's atmosphere where its concentration influences the climate on longer time scales. Several processes contribute to the atmospheric CO_2 levels either as a source or as a sink. These include photosynthetic fixation of CO_2 by plants, chemical weathering of silicate rocks, and oxidative weathering of organic matter (OM) during riverine transport, burial of organic carbon (in flood plains and coastal oceans), volcanic emissions and metamorphic degassing of CO_2 in the active mountain belts etc. These processes eventually regulate the Global Carbon Cycle and hence the long-term (million year or more) evolution of climate. Prevailing uncertainties in this geological carbon cycle still remain to be addresses in terms of the amount of carbon entering the atmosphere now and in the past. Towards this the degassing flux of Carbon were estimated based on volcanic emissions in different geodynamic contexts including the mantle (magmatic) as well as from rocks in subduction zones (metamorphic). Such estimates do not address the CO_2 derived from the regions of mountain building. As a result of continental collision these regions may have organic rich sediment and limestone buried at depths at which CO_2 is formed by metamorphic reactions.

Active mountain range of the Himalaya has been witnessing the process of subduction and has the potential to generate metamorphic CO_2 along its structural boundaries. Therefore its roles in regulating the atmospheric CO_2 budget may be significant and needed to be quantified. Towards this, the natural hot springs situated along the Main Central Thrust (MCT) zone of the NW Himalaya provide an opportunity to address their origin in terms of metamorphic degassing of CO_2 (Becker et al., 2008; Galy *et al.*, 2007; Evans *et al*., 2008) have recently attempted to estimate the flux of metamorphic CO_2 based on the chemistry of Himalayan hot springs in Central Nepal. They used the isotopic proxies exploiting the fact that carbon isotopes are fractionated when dissolved carbon species are transformed into gaseous Co_2. A fluid containing dissolved carbon will preferentially lose the light isotope of carbon (^{12}C). The isotopic composition of the remaining carbon in the fluid can then be used to estimate the intensity of degassing. As the mountain ranges have varying impacts on the global carbon cycle, their contribution as sources or sinks can only be resolved by considering the importance of different processes at their relevant time scales and special distributions.

Geothermal activity in northwest Himalaya (Himachal Pradesh and Jammu & Kashmir) is probably related to northward migration of hydrothermal activity due to under plating. Some of the present-day hot spots and associated activities with relatively higher heat flow induce the geothermal activities. A Systematic observation of geothermal sites was initiated in India by Geological society of India, which identified 112 hot spring localities of northwest Himalaya region (Ravishankar, 1988). Among these, 20 geothermal springs covering different River Valleys have been selected for the present study. These are Changlung, Pulthang and Panamic from Nubra valley; Gaik, Chumathang from Indus valley; and Puga from Puga valley; Ladakh region along the Indo-Eurasian plate boundary and Sumdo, Thopan, Tapri, Naptha, Jeori, Jhakri, Tattapani from Satluj and Spiti valley; Bashist, Khiral-Bahal,Kalath from Beas valley; (Kullu Ramshila, Manikaran, Kasol) Parvati valley; along the Main central thrust of Himachal Pradesh. This study focuses on the stable isotopic composition ($\delta^{13}C_{DIC}$, $\delta^{18}O$ and δD) of geothermal springs which were measured against PDB with a

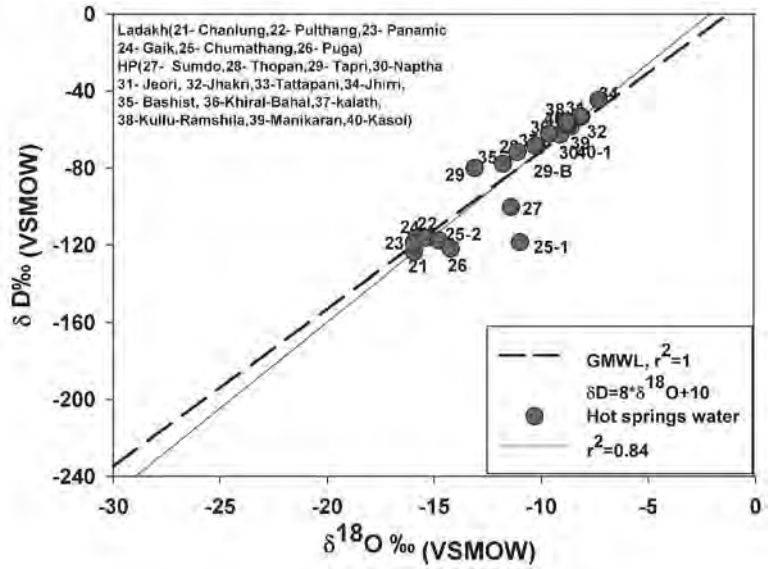

Fig 1. This X-Y plot of δD and $\delta^{18}O$ of is showing hot springs fluid correlation with global meteoric water line. Some of the hot springs does not very significantly from meteoric water line defined by (δD= 8.17* $\delta^{18}O$+10.35).

Delta V Plus stable isotope Ratio Mass Spectrometer at the Wadia Institute of Himalayan Geology Dehradun India. The precision of measurements of $\delta^{18}O_{SMOW}$ and $\delta^{13}C_{PDV}$ were (±0.1‰) and that for δD_{SMOW} was (±1‰).

Surface temperature of the geothermal springs is varying from 20.6-94.5°C which is well above the river waters and pH ranges from slightly acidic to highly alkaline (6.23-8.9). Geothermal springs of Ladakh and Himachal region have very high concentration of Dissolved Inorganic Carbon (DIC) with concentrations of HCO_3 (1300 to 13400 µEq/L) indicating these fluids carry large fluxes of CO_2 derived from metamorphic reaction. The $\delta^{13}C_{DIC}$ of these springs show a strong variation from -8.4 to +1.7‰ $_{(PDB)}$ pointing towards the varied sources of their origin. These values are similar to those in the active volcanic region and comparable to the values (-13 to +13‰) reported in the Marsyandi valley, central Nepal (Evans et al., 2008). Higher $\delta^{13}C_{DIC}$ indicate a deeper origin for these springs. Water isotopes were also measured (against SMOW) in thermal springs where $\delta^{18}O$ range between -16 to -7.3 ‰ and δD vary from -123.5 to -44.8‰. This shows that the thermal waters are mixing with a meteoric dominated reservoir because most of the samples fall near the GMWL line (Fig. 1).

Two of the samples from Puga and Chumathang fall below on the GMWL indicating a non surface origin. This characteristic of the fluids shows a relatively short residence time with limited water-rock interaction. Major ion composition shows a high concentration of Na^+ ion (1231 to 20703 µEq) and low concentration of Ca^{+2} (12-4312 µEq) indicating their interaction with silicate rocks that are dominant in the study area. The atomic ratio of the dominant Cations and Anions present in the thermal fluid point to partial magmatic source of heat supply. The reservoir temperature have also been estimated applying standard Si and Ca corrected alkali chemical geothermometer to springs chemistry produces estimates for euilibrium reservoir temperature range 44-189°C.

Becker, J.A. et. al. 2008. Earth & Planetary Science Letters 265, 616-629.
Evans, M.J., Derry, L.A., France-Lanord, C. 2008. Geochem. Geophys. Geosyst. 9, Q04021, doi:10.1029/2007GC001796.
*Galy, V., France-Lanord, C., Beyssac, O., Faure, P., Kudrass, H., Palhol, F. 2007. Nature, **450**, 407-410.*
Ravishankar 1988. Indian Minerals, 42, 89-110.

Incorporation of slope variability in channel network extraction from DEM

Vikrant Jain[1*], Rahul K. Kaushal[1#], Vaibhav Kumar[1,2]**

[1]*Earth Sciences Discipline, IIT Gandhinagar, Palaj, Gandhinagar 382455, INDIA*

**vjain@iitgn.ac.in; #rahul.kaushal@iitgn.ac.in*

[2]*Center for Urban Science and Engineering, IIT Bombay, Powai, Mumbai 400076, INDIA*

***vaibhav.kumar.cs10@gmail.com;*

Identification and extraction of actual drainage networks is a key component in many geomorphic and hydrological analyses. Drainage network pattern is governed by its magnitude, which is defined by the number of its first order tributaries. The initiation of first order tributaries is a function of slope and rainfall (Montgomery and Dietrich, 1988). Hence, the drainage network evolution and its patterns are governed by tectonics (slope) and climate (rainfall) variability. The standard algorithms for drainage network generation are based on the threshold of constant basin area. The exclusion of slope parameter in the algorithms results insensitivity of drainage pattern to tectonic processes. Here we proposed a new algorithm based tool for extracting the channel network from DEM by incorporating the slope characteristics. This proposed algorithm can be served as an extension of previously developed basic methods (Jenson and Domingue, 1988) used by ArcGIS and other GIS environment. The initial study was carried out in the Nahan area covering Siwalik rocks and alluvial plain area.

The automatic extraction methods of geomorphic features from Digital Elevation Models (DEM) have been there over the past several decades (O'Callaghan and Mark, 1984). However, available methods are based only on catchment area as threshold for generation of first order tributaries and overall pattern of drainage network (Gardner et al., 1991). It defines the uniform drainage pattern for a river basin, even if the basin is characterized by different topographic classes. The slope dependent contributing area thresholds assume channel heads are developed due to erosional threshold approach (Montgomery and Dietrich, 1988), and hence it will be a process based criteria. However, this criterion has not been included in the standard algorithms for drainage network generation. Empirical studies shows that channel initiation process and channel head location can be explained by incorporating the 2nd order value of slope variability (AS2) (Montgomery and Dietrich, 1994). The similar relationship as product of area and slope (AS2) was used as threshold in our algorithm to generate drainage network from DEM data.

The drainage network generated from proposed algorithm provides channel head locations, which are sensitive to topographic characteristics. Drainage network generated by the proposed algorithm has disconnectivity due to certain error in input data sets. To further create a connected drainage network a new connectivity algorithm is proposed in this study. This connectivity algorithm is applied on the previously generated disconnected network. Connectivity algorithm is applied in 2 different steps: a) single pixel connectivity b) multipixel connectivity, using flow direction dataset as one of the inputs. The above whole process is developed as an open source front end application for the ease of user, developed in Python environment. Simulation and generation of drainage network are carried out on DEM of Nahan salient area, NW Himalaya. We observed a quite distinct variation in drainage networks generated by the proposed algorithm and ArcGIS 10.0 (Fig. 1a, b). The current algorithm with inclusion of slope dependent threshold provides a closer match with existing river networks in different topographic setting.

Inclusion of slope variability in drainage network algorithm will help in analysing the tectonic signature in the pattern of drainage network across different thrust sheets. In general, an uplifted block is characterised by higher drainage density due to enhanced channel incision in response to headward erosion and base level change (Singh and Jain, 2009). However, DEM derived drainage network only on the basis of area threshold will not be able to represent the topographic input on the drainage network. In that case, morphometric parameters related with drainage networks

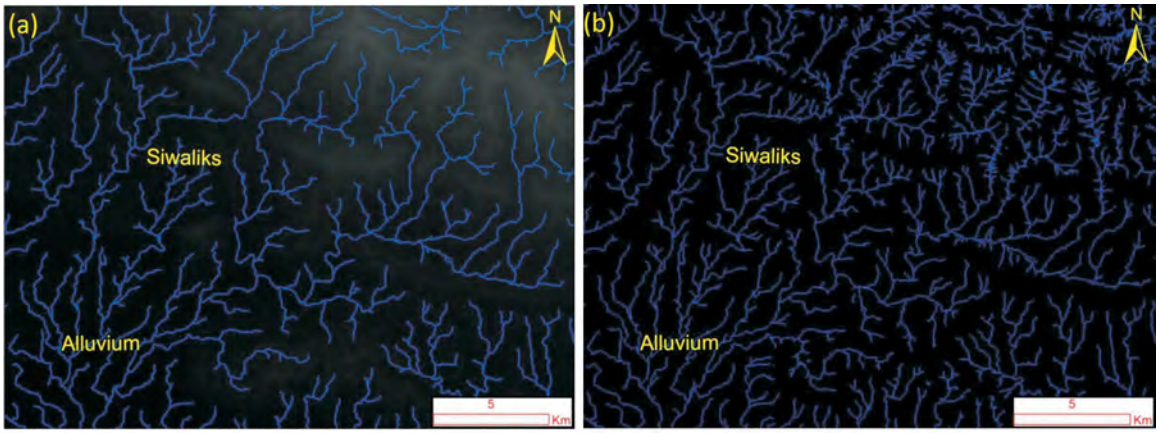

Fig.1. Drainage networks generated using (a) Existing ArcGIS methods Jenson and Domingue (1988) and our proposed algorithm (b) using slope dependent threshold (AS2 relationship).

may not provide any tectonic signal (Hurtrez et al., 1999). The new algorithm with inclusion of slope variability in threshold condition will provide a drainage network pattern, which will be more sensitive tectonic processes.

Gardner, T.W., Sasowsky, K.C., Day, R.L. 1991. Z. Geomorphol. Suppl., 80, 57-68.
Hurtrez, J.-E., Lucazeau, F., Lavé, J., Avouac, J.-P. 1999. J. Geophys. Res. Solid Earth, 104, 12779-12796.
Jenson, S.K., Domingue, J.O. 1988. Photogrammetric Engineering and Remote Sensing 54(11), 1593-1600.
Montgomery, D.R., Dietrich, W.E. 1988. Nature, 336, 232-234.
Montgomery, D.R., Dietrich, W.E. 1994. Geomorphology, John Wiley & Sons, Chichester, 221-246.
O'Callaghan, J. F., Mark, D.M. 1984. Computer Vision, Graphics and Image Processing, 28, 323-344.
Singh, T., Jain, V. 2009. Geomorphology, 106, 231-241.

Geological evaluation of high resolution EIGEN-6C4 gravity model over the Karakoram Shear Zone, Leh, India

A. Sai Krishnaveni*, Priyom Roy, K. Vinod Kumar
National Remote Sensing Center, Indian Space Research Organisation, Hyderabad 700037, INDIA
**saigeophysics@gmail.com*

The Earth's gravity field reflects the mass distribution in the Earth's interior and on its surface. In recent times, Earth's gravity field models are being derived from satellite measurements, combined with field derived gravity anomalies or GPS leveling derived/altimetry derived gravity data, thus yielding higher spatial resolution and accuracy.

In the present study, we use gravity field and derivatives generated from high resolution EIGEN-6C4 gravity model (Förste et al., 2014) of degree/order 2190 for a geological appraisal/evaluation, in and around Karakoram Shear Zone, Leh, India. The model with aforesaid degree/order corresponds to a approximate spatial resolution of 9 km. Bouguer anomaly, regional residual maps, derivative maps (x, y and z), analytical signal (AS, Nabighian, 1972) and tilt derivative (TDR, Miller and Singh, 1994) maps of EIGEN-6C4, over the study area, has been generated, to derive the litho-boundaries from respective gravity signatures. These maps have been superimposed on the lithological boundaries derived from existing geological map (Roy et al., 2010). Further, three across strike profiles have been derived to substantiate lithological boundaries/structural features vis-à-vis change/breaks in gravity signatures. It is seen that the major and distinct gravitational signatures, from

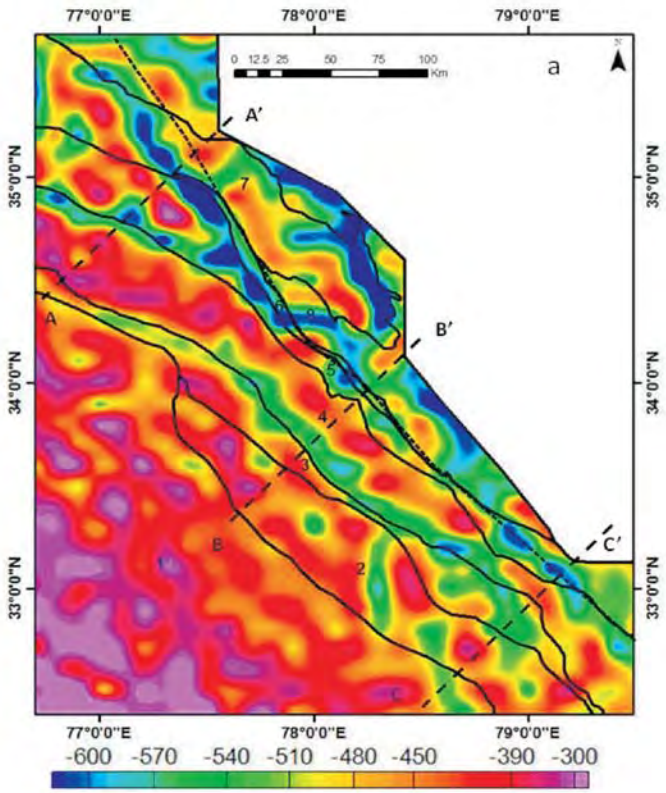

Fig. 1. a: EIGEN-6C4 derived bouguer gravity map of the study area. Litho-boundary map (Modified from Roy et al., 2010) has been underlain. Litho units as shown in (a) are marked as follows: 1.Tethyan Sedimentary zone; 2. Tso Morari Crystallines; 3. Indus Suture Zone. 4. Darbuk Granites; 5. Shyok Suture Zone; 6. Karakoram Shear zone; 7. Karakoram Batholith; 8. Karakoram Metamorphic complex.

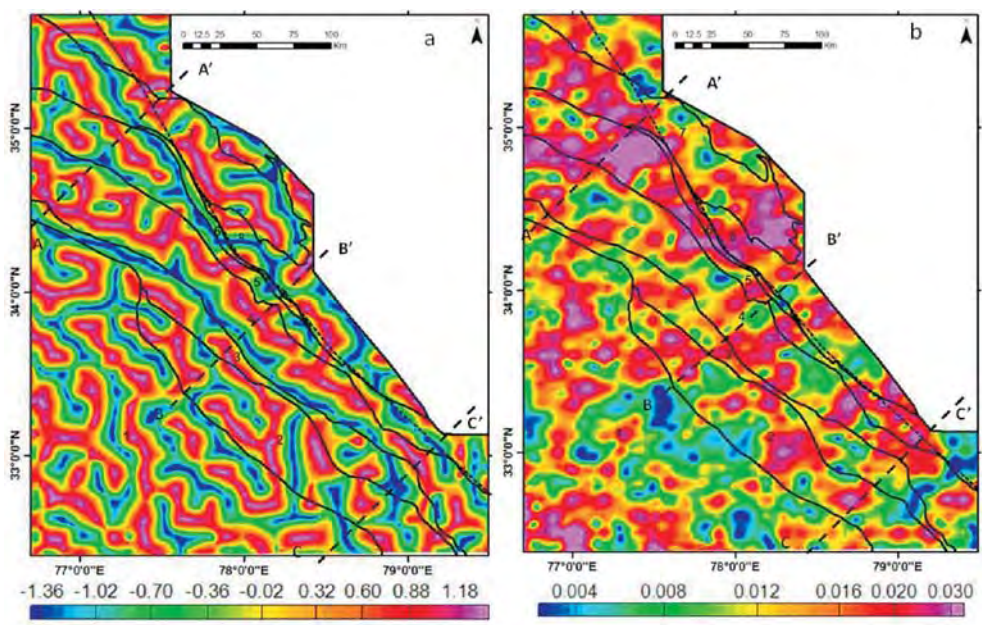

Fig. 2. a: Analytical signal map and b: Tilt derivative (TDR) map generated from EIGEN-6C4 Bouger gravity data of the study area. Lithological boundary map has been superimposed.

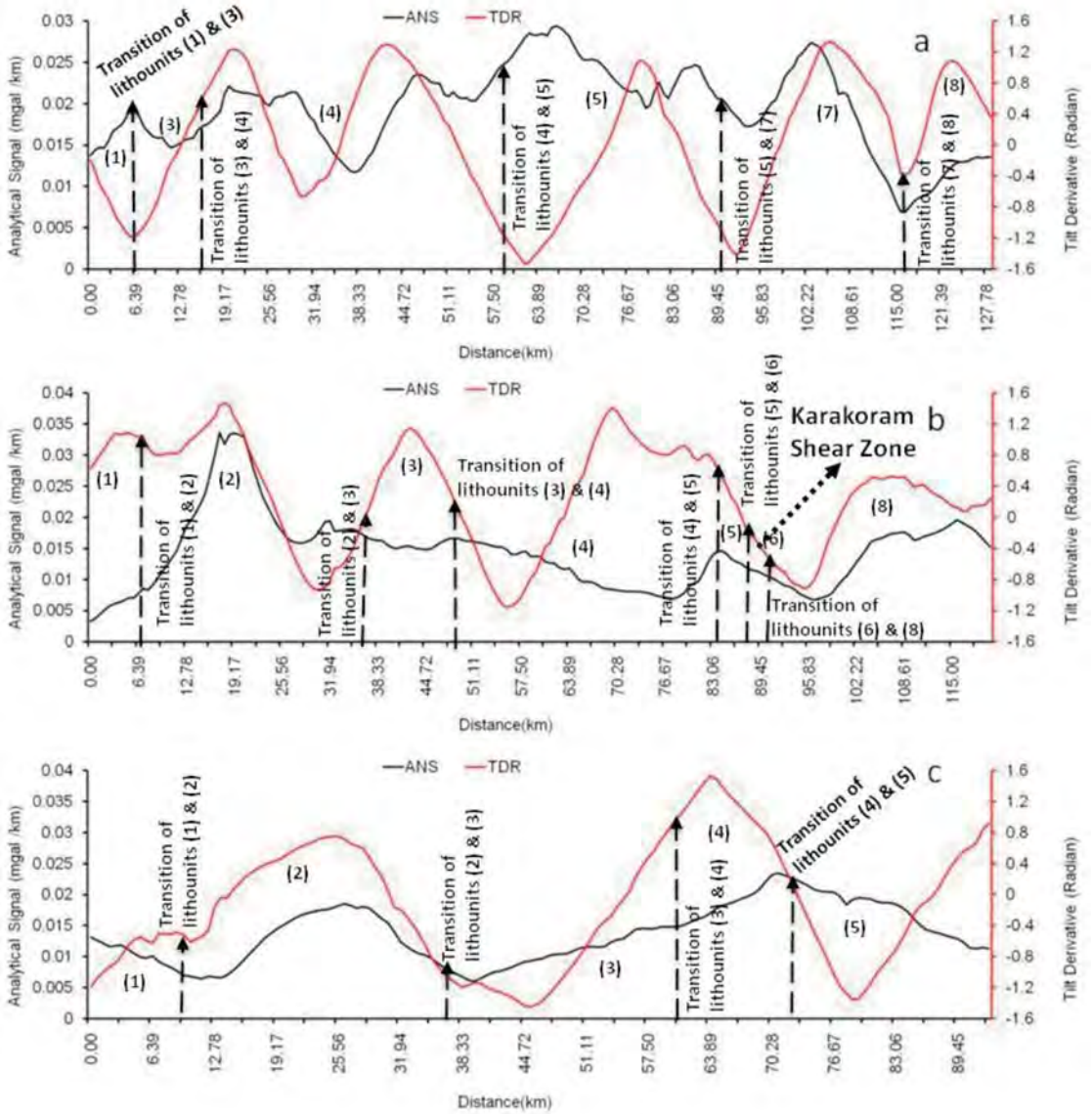

Fig. 3. Plots of Analytical Signal and Tilt Derivative generated from EIGEN_6C4 Bouguer anomaly along profile AA', BB' and CC'. Different lithological units/boundary and structural units have been delineated as observed with distinct or change slope in the profile (lithounits have been marked as serial nos. 1-8 as described in fig.1).

different derivative maps, AS and TDR maps, are correlated well with the existing litho-units (Fig. 1). The AS and TDR indicate the litho-boundaries with reasonable accuracy (Fig 2). The derivative profiles also correlate well with the litho-boundary transitions (Fig 3). The observations illustrate that, the gravity data generated from EIGEN-6C4 model correlates well with the lithology in and around the KSZ. Further the gravity model provides sufficient resolution for understanding of the geological settings in and around the Karakoram Shear zone.

Förste et al. 2014. In: 5th GOCE User Workshop, Paris. 25-28 November 2014. http://icgem. gfz potsdam.de/ ICGEM/documents/Foerste-et-al-EIGEN-6C4.pdf.

Nabighian, M.N. 1972. Geophysics 37 (3), 507-517.
Miller, H.G., Singh, V. 1994. J. Appl. Geophys. 32, 213-217.
Roy, P., Jain, A.K., Singh, S. 2010. Journal of the Geological Society of India, 75(5), 679-694. Http://doi.org/10.1007/s12594-010-0065

Examining microstructural and kinematic evolution of dominant thrust faults from hinterland of the Sikkim Himalayan FTB: Insights into orogenic wedge deformation

Pritam Ghosh*, Kathakali Bhattacharyya
Department of Earth Sciences, Indian Institute of Science Education and Research Kolkata (IISER), Mohanpur 741246, INDIA
**pg14rs039@iiserkol.ac.in*

We evaluate the structural evolution of two dominant thrust faults, with mineralogically similar protoliths, from similar structural positions in the hinterland in a deforming orogenic wedge. We focus our study on the hinterland-most exposures of Main Central thrust (MCT) at Mayangchu and the Pelling thrust (PT) at Mangan in the Sikkim Himalayan fold thrust belt (FTB) (Fig. 1). Both the exposures lie on the northern limb of the folded MCT-PT antiform in the hinterland-most part of the wedge (Fig. 1). Both the MCT and the PT are folded in an E-W trending antiform-synform pair, by the growth of the underlying Lesser Himalayan duplex (Bhattacharyya and Mitra, 2009). We quantify the various operative deformation mechanisms and strain recorded in these two fault zones and evaluate a comparative study on their structural evolution. The coarse-grained, quartzo-feldspathic gneissic protoliths transform into quartz-mica mylonite zone defining both the fault zones.

The thicknesses of the amphibolite facies MCT mylonite zone and greenschist facies PT zone are somewhat similar in the hinterland at~1170 m and at ~938 m, respectively. However, in the foreland most part, the same fault zones become narrower with the PT 158 m thick (Bhattacharyya and Ghosh, 2014) suggesting that the deformation conditions spatially varied along the fault zones (Bhattacharyya and Mitra, 2014). The mylonitic foliation is dominantly defined by preferential orientations of recrystallized quartz along with muscovite, biotite and chlorite. The mean MCT mylonitic foliation at Mayangchu is 41°, 057° with a mean stretching lineation defined by stretched biotite and sillimanite at 15°, 030°; the latter also defines the regional transport direction. The easterly plunging pucker axis lineation (18°, 078°) indicates east-west trending fault bend fold and N-S plunging pucker axis lineations (28°, 203°) are associated with doubly plunging structure of the underlying Lesser Himalayan duplex. The average PT mylonitic foliation in Mangan is 32°,020°, pucker axis lineation is 22°, 013°, and a mean stretching mineral lineation defined by stretched biotite and chlorite is 25°, 016° (Fig. 1).

The pyroxene-amphibole bearing biotite rich quartz-feldspathic gneissic protolith has undergone ~ 70% grain size reduction in quartz and ~55% reduction in feldspar within the MCT zone. Similarly biotite rich coarse grained quartzo feldspathic protolith records ~85% grain size reduction in quartz and ~70% in feldspar within the PT mylonite zone. Quartz has undergone grain size reduction dominantly by dislocation creep and feldspar by microfracturing. Interestingly, microfracturing is more dominant in MCT zone than in PT for both quartz and feldspar grains. Additionally, pressure solution is significantly higher in PT ~(17%-20%) than in MCT ~(1%-3%). Therefore, there is a spatial variation in deformation mechanisms in the MCT and PT zones in the study areas. Shear-sense analysis on asymmetric feldspar porphyroclasts (~70%-85% porphyroclasts) record top-to-the south shearing from both the zones which agrees with the regional transport direction. Based on recrystallized quartz grain sizes (Stipp et. al., 2002), the temperatures at MCT and PT are estimated at 435-510°C and 405-425°C, respectively.

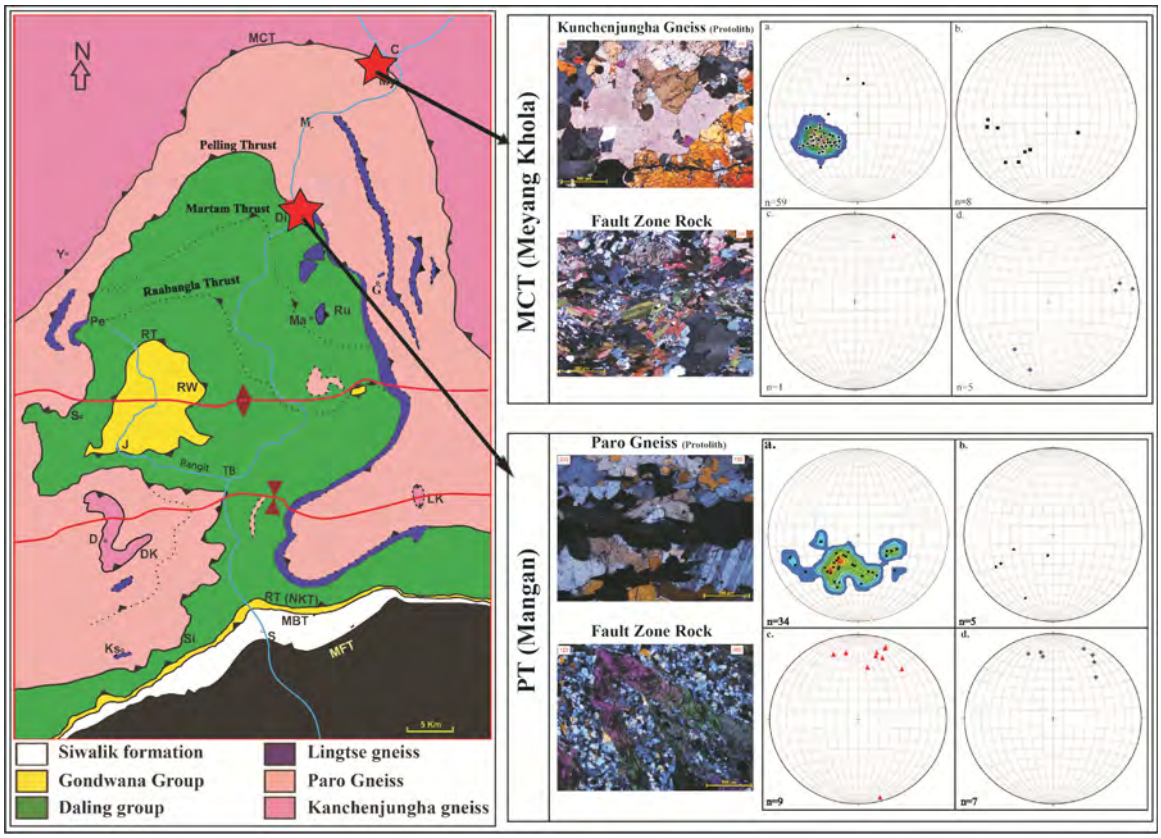

Fig. 1. Regional map of Darjeeling Sikkim Himalaya (Bhattacharrya and Mitra, 2009). The study locations are marked in red asterices. The stereographic projection of a. foliation plane, b. cleavage plane, c. stretched mineral lineation, d. pucker axis lineation data from both the zones. Pictorial representation of thin section images, to compare between fault rock and its hanging wall protolith from both the zones.

To quantify the strain partitioning between deformed quartz and feldspar grains, we estimated plastic strain from relict quartz and feldspar grains (Bhattacharyya et. al., 2015). Based on strain analysis, the MCT and PT zones both record strong flattening strain. Penetrative strain from deformed quartz grains and relict feldspar grains record stronger flattening in MCT zone than in PT fault zone. We propose that pressure solution and microfracturing have accommodated a significant proportion of strain in the fault rocks, thereby under-representation of the finite plastic strain from the strain markers. We have initiated vorticity analyses on the fault rocks using both porphyroclasts (Wallis et al, 1993) and subgrain (Das et al., 2014) methods. Based on porphyroclast analysis (Wk), the MCT and PT record ~28-42% simple shear and ~33-57% simple shear, respectively. Subgrain method (Wm) indicates ~42-65% simple shear in MCT and ~46-73% simple shear in PT. Therefore, at a first order, both the fault zones record non-steady deformation.

Bhattacharyya, K., Dwivedi, H.V., Das, J.P., Damania, S. 2015. Journal of Asian Earth Sciences, 107, 212-231.
Bhattacharyya, K., Ghosh, P. 2014. Rock Deformation and Structures (RDS-III) abstract, 13-14.
Bhattacharyya, K., Mitra, G. 2009. Gondwana Research, 16, 697-715.
Bhattacharyya, K., Mitra, G. 2014. Journal of Asian Earth Sciences, 96, 132-147.
Das, J.P., Dwivedi, H.V., Bhattacharyya, K. 2014. Rock Deformation and Structures, (RDS-III) Abstract, 27-28.
Wallis, S.R., Platt, J.P., Knott, S.D. 1993. American Journal of Science, 293, 463-495.

Weathering and phosphorus dynamics in the Late Holocene High Himalayan Triloknath palaeolake of Himachal Pradesh

Saurabh K. Singh[1], Amit K. Mishra[2], Rameshwar Bali[2], S. Nawaz Ali[3], Imran Khan[2], Jayant K. Tripathi[1*]

[1]Jawaharlal Nehru University, New Delhi 110067, INDIA
**jktrip@yahoo.com*
[2]Department of Geology, Lucknow University, Lucknow 226007, INDIA
[3]Birbal Sahni Institute of Palaeobotany, Lucknow 226007, INDIA

A 1.53 m thick sediment profile of a palaeolacustrine (lake) deposit (32°39'57.84" N: 76°40'1.26" E) located in the Kame terrace region (between the moraine and the right valley wall) of Triloknath glacier has been studied for weathering history and phosphorus biogeochemistry in the lake catchment. The lake deposit is situated in the Triloknath valley, where the Triloknath glacier and its meltwater stream flow northeasterly to join the river Chandrabhaga. The valley is situated in the north of the Main Central Thrust (MCT) and is mainly underlain by schist and gneissic rocks of the Central Crystalline Zone (CCZ). The OSL dating provides an age of 6.3 ka at 153 cm for the excavated profile. At around 18 cm depth of the profile the AMS age was found around 890 years B.P.

The lake at the height of 3457 m occupies a place in the rain shadow zone of the Lahul Himalaya. The water supply to the lake was mainly maintained from the snowmelt around the area. This lake must have been an oligotrophic lake (National Wetland Inventory and Assessment, 2011), which is an important requirement to use phosphorus fractions geochemistry for palaeolimnological study. The provenance lithology of the lake sediments is low to medium grade metamorphic rocks of the CCZ, and absence of any mixing from a dissimilar lithology becomes very useful in deciphering weathering history in the catchment of the lake. In this study we use three different geochemical proxies, i.e., chemical index of alteration (CIA: using geochemical analysis of Al_2O_3, CaO, Na_2O, K_2O by WD-XRF), organic phosphorus (OP: extracted using SMT protocol; Ruban et al., 2002) and apatite phosphorus (AP: extracted using SMT protocol). Since three different aliquots of sediment samples were used in the analytical procedures, independent analyses do not interfere or affect each other for any bias. Figure 1 shows patterns of changes in CIA, AP and OP through the Late Holocene lake deposit.

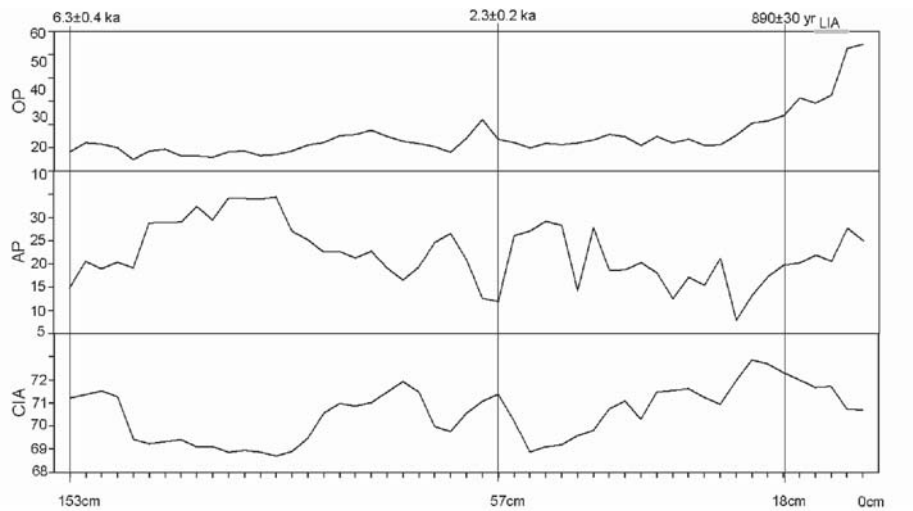

Fig. 1. Chemical Index of Alteration (CIA in %), Apatite phosphorus (AP in μg/g) and organic phosphorus (OP in μg/g) patterns through 153 cm thick Triloknath palaeolake sediment profile.

The chemical index of alteration of the lake sediments ranges between 69 and 73, suggesting limited extent of weathering in the catchment. Initially around 6 ka weathering started with the CIA value of 71 but soon dropped to 69 by around 5 ka. It again increased from around 3 ka and dropped after around 2.5 ka. Since 2 ka the weathering trend shows a gradual increase till around 1 ka but with a kink around Little Ice Age (LIA: 1400 to 1800 AD). Apatite phosphorus shows an opposite pattern to that of the CIA, complimenting weathering information. Increasing weathering in the catchment destroys apatite thereby supplying lesser amount of AP with sediments during higher weathering. The trends of CIA and AP together suggest a clear trend of gradual increase in weathering and decreasing supply of apatite bound fresh phosphorus to the lake after around 2 ka. The kink around LIA could be related to the colder event when extent of weathering decreased and supply of AP increased. Interestingly, trends of AP and CIA seem to be controlled by the global temperature pattern of the last 5000 years (Lewis and Maslin, 2015 and references there in).

The trend of OP also shows an interesting pattern, especially in the later stage. The OP shows a gradual increase in the supply of organically bound phosphorus to the lake since around 2 ka. It followed the CIA pattern as more weathering has supplied more available phosphorus to be associated with soil organic matter in the lake catchment. However, the OP did not revert to a lesser supply to the lake during the LIA period, except for a minor kink/flattening. Instead, in the latest phase the OP increased further up. The decoupling of OP from the CIA pattern after LIA indicates that there are two separate forcing for their patterns. The OP pattern since 2 ka seems to be related to increasing global CO_2 and CH_4 patterns (Lewis and Maslin, 2015 and references there in) in the atmosphere. The fertilization effect on biomass production could be a guiding factor for the OP pattern (Idso et al., 2014). However, CIA and AP patterns seem to be getting controlled by the climatic factor.

Idso, C.D., Idso, S.B., Carter, R.M., Singer, S.F. 2014. The Heartland Institute, Chicago, 1078p.
Lewis, S.L., Maslin, M.A. 2015. Nature, 519, 171-179.
National Wetland Inventory and Assessment. 2011. Space Applications Centre Indian Space Research Organisation, Ahmedabad, 21p.
Ruban, V., Lopez Sanchez, J. F., Rauret, G., Quevauviller, P. 2002. Buletin des laboratories des Ponts Et Chaussees, 240, 43-52.

Tista river response to uplift in the Himalayan Terrain: a morpho-tectonic approach

Sravan Kumar*, Prabha Pandey, Anand K. Pandey
CSIR-National Geophysical Research Institute, Uppal Road, Hyderabad 500007, INDIA
**kotlurisravankumar@gmail.com*

The topography of the Himalayan mountain belt is attained by foreland propagating thrust system which also influenced the growth of monsoon system in south Asia (Molnar and England, 1990), and related gradational process leading to the development of regional drainage patterns. In actively deforming mountain regions, the geometry and evolution of drainage systems are sensitive to surface uplift and in a steady state system erosion keeps pace with uplift (Seeber and Gornitz, 1983). The transverse drainages flowing perpendicular to the geologic structures of Himalayan belt are more efficient in negotiating the active structures and their geomorphic parameters better reflect the active tectonics of the region.

The Tista river originating from Cholamo glacier lake, at an altitude of ~5,300 above MSL in Tethys Himalaya flowing as transverse drainage through Higher-, Lesser-, Sub- Himalaya to debauch to Ganga-Brahmaputra plains. These litho-tectonic units are separated from each other by

South Tibetan Detachment System, Main Central Thrust (MCT), Main Boundary Thrust and Main Frontal Thrust, respectively from north to south, (Fig. 1). The Tista River drains through Tista & Rangit tectonic windows, which show unique domal upwarp and thereby affecting gradation and incision process as well. We analysis and interpretation of morphometric parameters, topographic metrics, geomorphic indices, swath profile and transverse river longitudinal profiles in different litho-tectonic domains as well as sub-catchments to understand the drainage geometry, gradation process and intensity deformation in different segments drained by the Tista river. The Tista

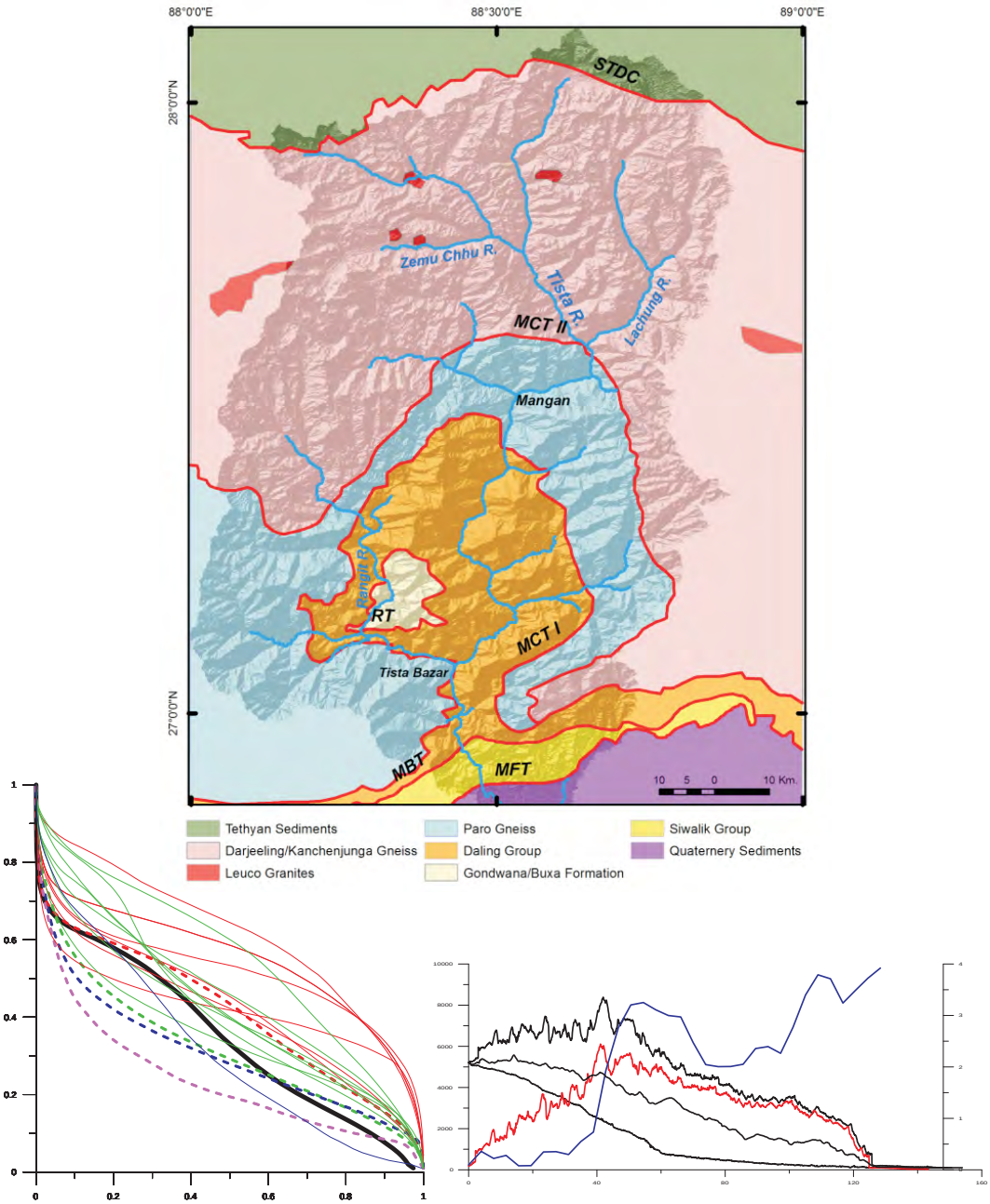

Fig.1. (a) A geological map of the Tista river catchment in Sikkim Himalaya. (b) Hypsometric integrals of the rivers in Tista catchment. The sub-catchments in different tectonic zones have similar colour codes. (c) Cross section of the Tista River. Balck line-Elevation, Red line- Relief, Blue line-Rain fall precipitation.

catchment has an asymmetry factor of 60 with eastward tilted suggesting lateral structural variation. The hypsometry equilibrium curve for the Tista river is 0.5, suggesting active channel with substantial erosion potential in response to the active uplift. The sub-catchments in Tethyan and Sub Himalayan terrain show below average and the Higher Himalaya is more active in comparison to the Lesser Himalaya. The valley width -height ratios across Tista River show narrow valley with high incision in the Higher and Lesser Himalaya, as well. The longitudinal profile along the Tista river show distinctive change in stream gradient from <15 m/km across the Sub Himalaya and Lesser Himalaya to >75 m/km across Higher Himalaya with knick point corresponding to the MCT zone. The high relief across the Tista River is observed in frontal foothills belt and the Higher Himalayan tectonic block, which also receive enhanced precipitation forming a distinct zone of focused denudation.

All the morphometric parameters suggests the Higher Himalayan terrain show convergence of high channel gradient, high uplift and steep slope and precipitation (≥4 m/yr) and the terrain also experienced high stream power suggesting that the topography growth in the hanging wall of the MCT is supporting focused gradation processes.

The MCT has been considered inactive for the past 10 Ma, but its footwall constituting the northernmost part of Lesser Himalaya is undergoing active deformation (Wobus et al., 2003; Burbank, 2005) over an out-of-sequence blind thrust, originating from the ramp on Himalayan Décollement thrust in the Himalayan crustal wedge. The observed terrain pattern in the Tista river section points towards similar tectonic setting causing the growth of Tista-Rangit window as a fault propagating fold, thereby actively exhuming the hanging wall of the blind thrust by focused erosion caused by localization of precipitation, which may also be an effect of the topographic growth.

Burbank, D.W. 2005. Cracking the Himalaya. Nature, 434, 963-964.
Molanar, P., England, P. 1990. Nature, 346, 29-34.
Seeber, L., Gornitz, V. 1983. Tectonophysics, 92, 335 -367.
Wobus, C.W. et al. 2003. Geology, 31, 861-864.

A complex tectonic model of Shillong Mikir Plateau-Northeast India: Inferred through waveform and stress tensor inversion with Successive seismic anisotropy and receiver function analysis

Saurabh Baruah
Geoscience Division, CSIR North East Institute of Science & Technology, Jorhat 785006, INDIA
saurabhb_23@yahoo.com

An evaluation of complex tectonic model of the Shillong Mikir Plateau, one of the most deformed and largest active basement fold structures in the world, lying between the eastern Himalayan thrust belt to the north, Bengal delta to the south and the Indo-Burma subduction zone to the east, is examined through multiple inversion method, stress tensor inversion, seismic anisotropy and receiver function analysis. The multiple inverse method separates stresses from a set of heterogeneous focal mechanism solutions obtained from waveform inversion for Shillong-Mikir Plateau which is affected by NNW-SSE directed maximum compression. Stress orientations corresponding to thrust and strike-slip faulting are most common within the assembled palaeostress results, followed by normal configurations with less frequency. So far kinematics of the region is concerned; the dominant N-S compression and E-W extension are the important parameters which measure the criticality of the region. Although an overall NNW-SSE compressional stress is observed in the area, the stress regime varies from western part to eastern part of the plateau. The

eastern part of the plateau is dominated by NNE-SSW compressional stress and the western part by NNW-SSE compression. The NNW-SSE compression in the western part is mainly due to the back thrust from the Himalayas, and the NNE-SSW compression in the eastern part may be attributed to the influence of oblique convergence of the Indian plate movement beneath the Indo-Burma ranges. The result inferred from anisotropy studies on the Plateau validates the current stress regime with the orientation of thrust axis along NNW. Simultaneously, the receiver function and the inverted velocity models reveal azimuthally varying crustal structure in the region where the Moho is thinner beneath the Shillong Plateau about 33-35 km and is the deepest beneath the Brahmaputra valley to the north about 39-41 km, deeper by 5-6 km below the Shillong plateau with the thinnest crust (~33 km) in the western part of the Shillong Plateau in the Garo Hills region.

Space-Time seismicity migratory behavior analysis of North West Himalaya

Sundeep Chabak*, Sushil Kumar
Wadia Institute of Himalayan Geology, 33 GMS Road, Dehradun 248001, INDIA
*chabaksk@gmail.com

On-going convergence of the Indian and pacific plates against the Asian landmass has produced devastating earthquakes. It is important to understand behavior of seismogenic faults and their nature and kinematics. Active faults and understanding their kinematics behavior vis-a-vis seismicity has direct societal relevance in earthquake hazard reduction. We analyse the seismic catalogue of western Himalaya, India for the period of 1990-2014. Compiled regional earthquakes ($M \geq 3.5$) show a migratory behavior of seismicity in western Himalaya. The three and five years' time window was examined covering 28-34°N latitude and 74-82°E longitude in Western Himalaya, India. The epicenters shows two major clusters centered over the Kangra (Himachal Pradesh) region at about 76.5°E longitude and the Garhwal-Kumaon Himalaya at about 79.5°E longitude with a well-defined seismic quiescence zone over Shimla sector at about 76.0°E longitude. In recent years, a few small clusters of earthquake epicenters are also seen southern region at about 29.0°N latitude. Investigated regional earthquakes $M \geq 3.5$ shows thrust faulting in Chamba Kangra and Garhwal-Kumaun regions and normal faulting in Kinnaur and Kumaun regions. It is observed that the regional seismicity pattern shows increase and shift in the seismicity with time and space perpendicular to the regional tectonics of the Himalayan region. It is also noticed that migration of earthquakes towards the Gangetic plane at about 30.0°N latitude takes place, which is associated with southern tectonic boundary of Himalaya i.e. Himalayan Frontal Thrust (HFT).

Rapid sedimentation history of Rewalsar Lake, Lesser Himalaya, India during the last fifty years - Estimated using ^{137}CS and ^{210}Pb dating techniques

Sudipta Sarkar[1*], Narendra K. Meena[1], Prakasam M.[1], Upasana S. Banerji[2], Ravi Bhushan[2], Pawan Kumar[3]
[1]Wadia Institute of Himalayan Geology, 33 GMS Road, Dehradun 248001, INDIA
**sudipta.iitkgp@gmail.com*
[2]Physical Research Laboratory, Navrangpura, Ahmedabad 380009, INDIA
[3]Dept of Environmental Sciences, Central University of Himachal Pradesh, Dharamshala 176215, INDIA

The pristine Himalayan lakes are under threat due to higher sedimentation, ecological degradation and pollution, especially due to human interference. The higher sedimentation reduces the depth and size of these lakes. This study is aimed at understanding the last ~50 year's record of

sedimentation and its shift in rates in the Rewalsar Lake, Himachal Pradesh, India. An effort has also been made to identify the natural, such as geological, esp. lithology and catchment slope and rainfall etc. and anthropogenic factors that could have governed the fluctuation in the sedimentation rates. The sedimentation rate of the Rewalsar Lake was measured on top 2 m core samples using isotopes of ^{137}Cs and ^{210}Pb dating techniques. Our study reveals that the Rewalsar Lake experienced an average sedimentation rate of 3.35 cm/yr during the last ~50 years which is the highest in comparison to the other lakes in the north-western Himalayan region. The 3.92 cm/yr of rapid sedimentation rate was observed during ca. 1995 to 1963 AD and 2.78 cm/yr after 1995 AD. At the Rewalsar Lake, the natural parameters, such as lithology, catchment area and slope, rainfall etc. do not appear to be the limiting factors controlling the rate of sedimentation. Rather, human interference, in terms of civil constructions and growth of township in the lake catchment area appears to be the most plausible factor controlling the sedimentation rate during the past fifty years. The study suggests an early action plan required to be followed up by the concerned authority to arrest the extremely higher sedimentation rate of the Rewalsar Lake and to protect the water body from faster degradation.

U-Pb geochronology and Lu-Hf isotopes of zircons from granitoids exposed along Kameng-Sela-Tawang corridor of western Arunachal Himalaya, Northeast India

Santosh Kumar[1*], M. Pathak[1,2], Fu-Yuan Wu[3], Wei-Qiang Ji[3],
[1]Department of Geology, Kumaun University, Nainital 263002, INDIA
**skyadavan@yahoo.com*
[2]Present Address: Geological Survey of India, Ahmadabad, INDIA
[3]Institute of Geology and Geophysics, Chinese Academy of Sciences, Beijing 100029, CHINA

Palaeoproterozoic to Tertiary felsic magmatic lithounits are extensively exposed all along the Kameng-Sela-Tawang corridor in the western Arunachal Himalaya. These lithounits are represented mainly by Ms-Bt granite gneiss (GGn) of batholithic dimension exposed in and around Bomdila, small stock-like Hbl-Bt (±Cpx) granite (HBG) body outcropping near Salari-But regions, an exposure of Hbl-Bt granite gneiss (HBGGn) near Sapper close to Main Central Thrust (MCT), Ms-Bt (±Tur±Gt) bearing leucogranite (TLG) after crossing the MCT on the way to Sela Pass, and Ms-Bt (±Gt±Sil) migmatite-like granite gneiss (TGN) bodies exposed in and around Tawang. Zircons separated from representative samples of granitoids and gneisses were subjected to in situ U-Pb and Lu-Hf isotopic investigations in order to infer timing of magmatism, protolith assessment and geodynamics of western Arunachal Himalaya.

Zircons from peraluminous GGn provide weighted mean $^{207}Pb/^{206}Pb$ age of 1752±23 Ma (MSWD=0.22). Some older zircons (2100-2400 Ma) found in GGn were inherited from source regions. Interestingly zircons from calc-alkaline metaluminous HBG, elsewhere called as Salari pluton, provide weighted mean $^{207}Pb/^{206}Pb$ age of 1749±22 Ma (MSWD=0.32) without any zircon inheritance. Zircons from metaluminous to peraluminous HBGGn yield weighted mean $^{206}Pb/^{238}U$ age of 520.7±6.4 Ma (MSWD=0.32), and some of them provide older ages in the range of 655-858 Ma. An younger zircon of 347±10 Ma has also been recorded in HBGGn. Zircons from migmatite-like TGN yield two distinct concordant ages, one clustering at 512.3±5.1 Ma (N=13; MSWD=0.24) and another at 462.2±6.3 Ma (N=6; MSWD=0.15), which most likely represent the timing of zircon crystallization in magmatic protolith, which was subjected to partial melting, and leucocratic melt respectively. Some older zircons (638-648 Ma) in TGN are also recorded, which could have been derived from source region. Zircons from TLG provide weighted mean $^{206}Pb/^{238}U$ age of 23.3±0.5 Ma, with an inherited zircon of 511±24 Ma.

Zircons from GGn display $\varepsilon_{Hf}(t)$ values between +5.06 and -7.99 and a wide range of older Hf model ages (3000, 2600-2200, 1800, 1000 Ma), which suggest contribution of Neoarchean to Neoproterozoic ancient crusts with a small juvenile input in the generation of GGn. Zircons from HBG provide $\varepsilon_{Hf}(t)$ values between -1.13 and -3.72 and older Hf model ages of 2320-2220 Ma, which pin -pointed sole involvement of ancient continental crust in the genesis of HBG melt. This feature is indeed contrary to the calc-alkaline metaluminous nature of HBG melt representing arc-type magmatism, and hence this requires further explanation. Zircons from HBGGn give $\varepsilon_{Hf}(t)$ values between +0.98 and -5.70 and older Hf model ages ranging from 950 to 1450 Ma, which affirm a major role of Proterozoic crust in the formation of HBGGn magma. Zircons from TGN yield $\varepsilon_{Hf}(t)$ values between +5.24 and -5.70 and older Hf model ages of 800-1300 that suggest involvement of largely the juvenile and minor amount of ancient crustal sources in the genesis of TGN. TLG is sole product of Proterozoic crust as indicated by negative $\varepsilon_{Hf}(t)$ (-3.54 to -16.30) and Hf model ages in the range of 1240-1380 Ma.

Geochronology, Lu-Hf isotopes and spatial organization of GGn and HBG suggest synchronous bimodal Proterozoic magmatism having Columbian Supercontinental affinity, whereas Cambro-ordovician TGN and HBGGn are the result of Pan-African thermal events. These felsic magmatisms were prevalent in the northern parts of Indian lithosphere and are now form integral parts of continental arc system in the Himalayan belt of India. Himalayan-type felsic magmatism in Sela region can be correlated well with the other Tertiary granitoids, which were formed by partial melting of ancient continental crust.

Optical dating of terraces in spring fed Ramganga River

Shipika Sundriyal
Centre for Earth Sciences, Indian Institute of Science, Bangalore 560012, INDIA
archie.hnb@gmail.com

Formation of river terraces depends on sediment supply, transport capacity, hydrology and base level change, and preservation potential. Thus a study of fluvial terraces has the potential to reveal information on catchment dynamics, climate and tectonics. Terraces along the major Himalayan rivers have been used to infer response of these rivers to climate change. Sediment source for these rivers are glacial deposits and higher Himalayan rocks, that are eroded by monsoon (Vance et al., 2003; Ray and Srivastava, 2010; Chaudhary et al., 2015). It is noteworthy that Himalayan rivers with non-glaciated catchment has not gained much attention. This is because of absence or poor preservation of river terraces in narrow valleys. Landslides in these valleys prevent preservation of terraces and often terrace deposits are mainly debris flow (landslide) sediments of local origin. Sediment accommodation in such valleys is mostly along weak fault zones where valley is wider due to higher erosion rate.

In the present work we examined terraces of a non-glaciated spring fed river Ramganga (a major tributary of Ganga river originating from Dudhatoli ranges of Lesser Himalaya) to understand its internal dynamics and response to climate. Two to three levels of terraces are preserved in this valley. Most extensive fluvial terraces were also the youngest (200-300 years) and occur 0.5 to 1 m above the present day river flood plain. This terrace is preserved over a 500-700 m wide region at Chaukhutiya (29°53.121′ N: 7921.081′ E) and Bhikiyasain (29°41.977′ N: 79°15.729′ E). Sedimentary facies suggest that its deposition occurred as braided river. At tributary junction (Buda Kedar) this terrace formation event is preserved as flood deposit and shows 5-7 flood couplets in the time span of ~100 years. Other levels of terraces are mainly fluvially modified debris flow deposits.

Around 1000-2500 years old debris flow terrace deposits are well preserved in the valley. These terraces are fluvially modified and correspond to major slope failure activity along present day

river. The thickest terrace deposit along main river course in the Ramganga basin is ~25 m and comprises multiple events of fluvially modified debris flow (landslide) deposits. The terraces far above the present river bed and along tributaries shows much older ages. The oldest terrace (debris flow terrace) is ~150,000 years old and lies close to the head of the river at Gairsain. OSL ages obtained from wide distribution of debris flow deposits are random and do not show any trend thus restricting their formation age with known climatic events.

Chaudhary, S., Shukla, U.K., Sundriyal, Y.P., Srivastava, P., Jalal, P. 2015. Quaternary International, 371, 254-267.
Ray, Y., Srivastava, P. 2010.. Quaternary Science Reviews, 29, 2238-2260.
Vance, D., Bickle, M., Ivy-Ochs, S., Kubik, P.W. 2003 Earth and Planetary Science Letters, 206, 273288.

Fossilized microbial growth structures from the mantle section of a Neo Tethyan ophiolite, Indus Suture Zone (ISZ)

Souvik Das[1], 2, Koushick Sen[2], Barun K. Mukherjee[2*]
[1]Physical Research Laboratory, Navrangpura, Ahmedabad 380009, INDIA
[2]Wadia Institute of Himalayan Geology, 33 GMS Road, Dehradun 248 001, INDIA
**barun@wihg.res.in*

Whether or not the life on the ancient ocean floor was triggered by the interaction between mantle rocks and the seawater is a long standing controversy. Since the discovery of deep marine serpentinite hosted ecosystem from the "Lost city" hydrothermal vents in mid-Atlantic ridges (Kelley et al., 2005) scientists started to think that life could have originated in a hostile condition even without sunlight. But these evidences are yet to be found form ancient sea floors and ophiolites. The present study reports the occurrences of stratified and laminated microbial structures from the ophicarbonates of a Neo Tethyan ophiolite (Nidar ophiolite, ISZ) in the Ladakh Himalaya. The ophicarbonates occur as veins (10-15 cm thick) within serpentinized (~30%) dunite at the lower part of the ophiolite. Whole rock XRD analyses suggest that the ophicarbonate is composed of mainly calcite and dolomite with minor serpentines. The $\delta^{13}C$ (-0.76 to -2.26‰ VPDB) and $\delta^{18}O$ (14.8 to 17.3‰ VSMOW) isotope values strongly suggest hydrothermal origin (Clerc et al., 2014) of these carbonate veins at a palaeo ocean floor. So the ophicarbonates in the basal part of Nidar ophiolite represent an ancient hydrothermal system beneath the surface as they are located below the petrological moho of the ophiolite suite. The carbonates bear euhedral crystals of calcite with dolomitic matrix. Within the dolomitic matrix 800 µm-1 mm long and 100-150 µm wide micro organic film like structures are observed. At higher magnification, ~2 µm thick numerous oriented dark threads are noticed in each layer. The individual layers are separated by ~5 µm wide median walls. Morphological characters are supported by Raman Spectroscopic study to claim these as fossilized organic microbial remnants. Laser Raman spectroscopy on these dark threads and walls confirms presence of disordered carbonaceous matter. This finding strongly indicates a micro organic activity in hostile environment beneath the ancient Neo Tethyan sea floor.

Clerc, C., Boulvais, P., Lagabrielle, Y., de Saint Blanquat, M. 2013. Int J Earth Sci., doi: 10.1007/s00531-013-0927-z.
Kelley, D.S., Karson, J.A., Fru¨h-Green, G.L. et al. 2005. Science, 307, 1428-1434.

India-Asia collision near the western syntaxis: paleomagnetic constraints from Late Cretaceous volcanic rocks at the western most Lhasa Terrane

Zhiyu Yi[1,*], Baochun Huang[2], Liekun Yang[3], Zhonghai Li[1], Zhiqin Xu[1]

[1]Institute of Geology, Chinese Academy of Geological Sciences, Beijing 100037, CHINA

**yizhiyu09@gmail.com*

[2]School of Earth and Space Sciences, Peking University, Beijing 100871, CHINA

[3]Institute of Geology and Geophysics of the Chinese Academy of Sciences, Beijing 100029, CHINA

The large-scale lithospheric deformation resulting from the India-Asia collision has created the Himalayan Orogen and Tibetan Plateau (Tapponnier et al., 1982; Chang et al., 1986; Yin and Harrison, 2000) with profound geodynamic and environmental consequences (Raymo and Ruddiman, 1992; Molnar et al., 1993; Royden et al., 1997). Restoration of the pre-collisional shape of continental India and Asia is closely related to a series of important scientific questions. These include the timing and position of the India-Asia collision and the amount and pattern of post-collisional crustal shortening (e.g. Dupont-Nivet et al., 2010a; van Hinsbergen et al., 2011; Yi et al., 2011). The Lhasa Terrane is critically positioned at the southern margin of Asia and its paleoposition is important for reconstructing the southern margin of Asia prior to the collision (Achache et al., 1984; Dupont-Nivet et al., 2010a; Liebke et al., 2010; Chen et al., 2010, 2012, 2014; Sun et al., 2010, 2012; Lippert et al., 2014).

We report the first combined geochronologic and paleomagnetic study of volcanic rocks from the Shiquanhe and Yare basins at the westernmost Lhasa Terrane, which aims to provide further constraint on the shape and paleoposition of the southern margin of Asia prior to the India-Asia collision. Three new $^{40}Ar/^{39}Ar$ ages of 92.5±2.9 Ma, 92.4±0.9 Ma and 79.6±0.7 Ma determined by fresh matrix or feldspar from lava flows suggest a Late Cretaceous age for the investigated units. Characteristic remanent magnetizations (ChRMs) have been successfully isolated from 38 sites which pass positive fold and/or reversal, conglomerate tests and are hence interpreted as primary in origin. The two paleopoles obtained from Yare and Shiquanhe yield consistent paleolatitudes at ~14°N (for a reference site of 31.5°N, 80°E) indicating that the southern margin of Asia near the western syntaxis was located far south during the Late Cretaceous time. A reconstruction of the Lhasa Terrane in the frame of Eurasia with paleomagnetic data obtained from its western and eastern parts indicates that the southern margin of Eurasia probably had a quasi-linear orientation prior to the collision formerly trending approximately 310°E. This is compatible with the shape of the Neo-Tethys slab observed from seismic tomographic studies (Van der Voo et al., 1999; Raplumaz et al., 2003, 2010, 2013). In addition, on the basis of compilation of the available paleomagnetic data (including 6 primary and 35 secondary components in Cretaceous-Paleogene ages) obtained from the area near the western syntaxis, the paleopositions of the terranes (including the western Lhasa-Karakorum, Kohistan-Ladakh and Himalaya terranes) has been achieved. The paleopostions of the subducted oceanic slabs and paleo-suture zone are evaluated which are in accordance with the global seismic tomography studies and numerical modeling. On the basis of the above information, the positions of continent-arc and continent-continent collisions are defined. Together with the motion images of continent India since ~100 Ma, the timing of initial contacts between India and Kohistan-Ladakh arc and Asia are evaluated on the assumption of different sizes of Greater India. Our findings provide a solid basis for evaluating Cenozoic crustal shortening in the Asian interior and the size of Greater India near the western syntaxis.

Achache, J., Courtillot, V., Zhou, Y.X 1984. J. Geophys. Res., 89 (b12), 10311-10339.
Chang, C.F. et al. 1986. Nature, 323(6088), 501-507.
Chen, J., Huang, B., Sun, L. 2010. Tectonophysics, 489(1-4), 189-209.
Chen, J., Huang, B., Yi, Z., Yang, L., Chen, L. 2014. J. Asian Earth Sci., 96, 162-177. DOI:

10.1016/j.jseaes.2014.09.007.
Chen, W., Yang, T., Zhang, S., Yang, Z., Li, H., Wu, H., Zhang, J., Ma, Y., Cai, F. 2012. Gondwana Res., 22(2), 461-469.
Dupont-Nivet, G., Lippert, P.C., van Hinsbergen, D.J.J., Meijers, M.J.M., Kapp, P. 2010a. Geophys. J. Int., 182(3), 1189-1198.
Lippert, P.C., van Hinsbergen, D.J.J., Dupont-Nivet, G. 2014., Geological Society of America, p. 1-21, doi: 10.1130.2014.2507(01).
Molnar, P., England, P., Martinod, J. 1993. Rev. Geophys., 31(4), 357-396.
Raymo, M.E., Ruddiman, W.F. 1992. Nature, 359(6391), 117-122.
Replumaz, A., Guillot, S., Villaseñor, A. et al. Gondwana Research, 2013, 24(3), 936-945.
Replumaz, A., Negredo, A.M., Villasenor, A. et al. 2010. Terra Nova, 22(4), 290-296.
Replumaz, A., Tapponnier, P. 2003. Journal of Geophysical Research: Solid Earth (1978-2012), 108(B6).
Royden, L.H., Burchfiel, B.C., King, R.W., Wang, E., Chen, Z.L., Shen, F., Liu, Y.P. 1997. Science, 276(5313), 788-790.
Sun, Z., Pei, J., Li, H., Xu, W., Jiang, W., Zhu, Z., Wang, X., Yang, Z. 2012. Gondwana Res., 21(1), 53-63.
Sun, Z., Jiang, W., Li, H., Pei, J., Zhu, Z. 2010. Tectonophysics, 490(3-4), 257-266.
Tapponnier, P., Peltzer, G., Ledain, A.Y., Armijo, R., Cobbold, P. 1982. Geology, 10(12), 611-616.
Van der Voo, R., Spakman, W., Bijwaard, H. 1999. Nature, 397(6716), 246-249.
van Hinsbergen, D. J. J., Lippert, P.C., Dupont-Nivet, G., McQuarrie, N., Doubrovine, P.V., Spakman, W., Torsvik, T.H. 2012. Proc. Natl. Acad. Sci., 109(20), 7659-7664.
Yi, Z., Huang, B., Yang, L., Tang, X., Yan, Y., Qiao, Q., Chen, L. 2015.Tectonics.
Yi, Z.Y., Huang, B.C., Chen, J.S., Chen, L.W., Wang, H.L. 2011. Sci. Lett., 309(1-2), 153-165.
Yin, A., Harrison, T.M. 2000. Annu. Rev. Earth Planet. Sci., 28, 211-280.

Recent seismological studies that advance our understanding of the Himalaya-Karakoram-Tibet orogen

Simon Klemperer[1*], XiaoBo Tian[2], XiaoFeng Liang[2], DaNian Shi[3], Rui Gao[4], ZhanWu Lu[4]
[1]Department of Geophysics, Stanford University, Stanford, CA 94305-2215, USA
**sklemp@stanford.edu*
[2]Institute of Geology and Geophysics, Chinese Academy of Sciences, Beijing 100029, CHINA
[3]Institute of Mineral Resources, Chinese Academy of Geological Sciences, Beijing 100037, CHINA
[4]Institute of Geology, Chinese Academy of Geological Sciences, Beijing 100037, CHINA

In previous decades, most interpretations of lithospheric structure of Himalaya and southern Tibet (between the two syntaxes) have tacitly assumed large-scale west-east uniformity of the orogen co-axial with the surface trace of the Yarlung-Zangbo Suture (YZS), and have assumed that the main structural elements can be captured with a single south-north cross-section. Iconic near-vertical reflection and receiver-function images from INDEPTH campaigns in the 1990s (Alsdorf et al., 1998; Kosarev et al., 1999; Kind et al.,, 2002) and receiver-function images from the HiCLIMB recordings in the 2000s (Nábělek et al. 2009) dominated discussions and led to a widespread consensus that Indian crust and subjacent Indian lithospheric mantle underplate southern Tibet nearly to the Banggong-Nujiang suture (BNS). Since the international INDEPTH and HiCLIMB transects, at least four additional "north-south" broadband seismic profiles have been completed by Indian and Chinese groups (Fig. 1) including NGRI-TW80 (National Geophysical Research Institute - Tibet West 80°) (Caldwell et al., 2013; Zhang et al., 2014); Westline (Zhao J. et al.,, 2010); Central line (Zhao J. et al., 2010); G92 (Gangdese92) (Shi et al., 2015a & b), so that transects now exist across the entire west-east extent of Tibet.

Broadband transects with >40 stations, medium-weight grey lines, ~north-south: NGRI-TW80 (Tibet West 80°) (Caldwell et al., 2013; Zhang et al. 2014); Westline (Zhao J. et al., 2010); HiCLIMB (Nábělek et al., 2009; Xu et al. 2011); Central line (Zhao et al., 2010); INDEPTH 2 and 3 (Zhao et al., 2011); G92 (Gangdese 92) (Shi et al., 2015a & b); and west-east line: 31N (Tibet 31°N) (Zhang et al., 2014; Chen et al., 2015; Tian et al., 2015).

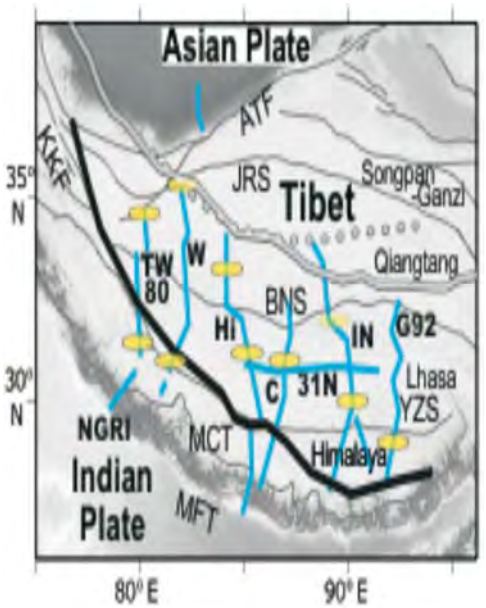

Fig. 1. Seismic interpretations of location of the mantle suture, superimposed on a shaded topographic relief map, with Tibetan terranes (Himalaya, Lhasa, Qiangtang, Songpan-Ganzi), terrane-bounding thrusts and sutures (from south, MFT Main Frontal Thrust, MCT Main Central Thrust, YZS Yarlung Zangbo suture, BNS Banggong Nujiang suture, JRS Jinsha River suture) and major dextral faults (ATF Altyn Tagh, KKF Karakoram).

Comparison of these profiles, as well as regional tomography, led some to a revised view (Li et al., 2008; Zhao J. et al., 2010) that there is a gradation from western Tibet where Indian mantle and/or crust is horizontally underthrusting Tibetan crust and forming the lower part of the lithosphere of the Tibetan Plateau (Fig. 2, top), to central/eastern Tibet where Indian mantle is delaminating from Indian crust and being subducted into the mantle beneath a warmer Tibetan mantle (Fig. 2, bottom). But seismic tomographic inversions that try to find a contrast between fast-wavespeed cratonic Indian lithosphere and slow-wavespeed, warmer, Tibetan or Asian mantle, have led different authors to very different conclusions. Some body-wave tomographies (Li et al., 2008) place the "mantle suture" (northern limit of the Indian plate at the Moho) along the Karakoram fault (KKF) and Yarlung Zangbo suture (YZS) in western Tibet (77-87°E) and south of the YZS in eastern Tibet (Fig. 1, thick black line) though others place the mantle suture close to the BNS in eastern Tibet (Tilmann et al., 2003). Some surface-wave tomographies (Priestley and McKenzie, 2006) and earthquake geothermometry (Craig et al. 2012) place the mantle suture north of the BNS (thick grey dashed & solid lines), whereas other surface-wave analyses show the mantle suture cross-cutting the YZS (Agius and Lebedev 2013). Other geophysical locations of the mantle suture, from Pn and Sn tomography (Beghoul et al. 1993; McNamara et al., 1997), shear-wave splitting of SXS phases (Chen and Özalaybey, 1998; Chen et al., 2010), and gravity modeling (Jin et al., 1996), fall between these southern (black) and northern (grey) lines. Although these different interpretations place the mantle suture all over the map (literally: Fig. 1), most recent papers have still presumed a continuous mantle suture, albeit no longer necessarily co-axial with the YZS.

In principle direct images of boundaries in the mantle can be made using P- and S-receiver-function (PRF, SRF) common-conversion point (CCP) images. CCP picks of the mantle suture rely on identifying weak dipping RF converters (or sometimes Moho offsets), so there is a lot of uncertainty about what to pick, and different analyses of similar datasets are often quite different (ovals on Fig. 1). For INDEPTH some proposed Indian mantle delaminates from Indian crust <100 km north of the YZS

and subducts into the deeper mantle (Kosarev et al., 1999; Zhao W. et al., 2011); others showed Indian mantle attached to its crust and underthrusting to the Banggong suture (Kind et al., 2002). HiCLIMB receiver-functions have been used to place the mantle suture at 31°N (Nábělek et al., 2009) or at >33°N (Xu et al., 2011). Similarly for the more recent Chinese profiles, interpretations of the mantle suture differ by hundreds of kilometers: on NGRI-TW80 Zhao Z. et al. (2014) vs Rai et al. (2006); on Westline Klemperer et al. (2013) vs Zhao J. et al. (2010) (light-grey ovals, Fig. 1).

The large discrepancies in inferred location of the mantle suture suggests the possibility that the concept of a single mantle suture as a key marker in geodynamic interpretations may be holding us back from a more realistic appraisal of the Indian slab as being laterally highly variable (Liang et al., 2012). A new Chinese west-east broadband transect 31N (Fig. 1) is particularly valuable in highlighting some of this variability. New finite-frequency P- and S-body-wave tomography incorporating the 31°N stations (Liang et al.,, 2015) shows fast-wavespeed anomalies interpreted as the northward-dipping Indian continental lithosphere. However, this is not a homogeneous body- rather, it is broken by three north-south low-wavespeed regions, extending from depths of 150-400 km up to the base of the crust. These low-wavespeed bodies are possibly but not clearly spatially associated with the Tangra Yum Co, Yadong-Golmud and Cona graben systems. Shear-wave splitting variations along the 31°N profile have been taken to indicate slab tearing in the down-dip direction (Chen et al., 2015), perhaps allowing linear upwellings of asthenospheric material from beneath the subducting Indian lithosphere. Virtual deep-seismic sounding (VDSS) along the same profile has identified likely Moho offsets controlling crustal thinning, one between the Tangra Yum Co and Pumqu Xianza rift and one just west of the Yadong-Gulu rift (Tian et al., 2015). At least the most prominent north-south graben, the Yadong-Gulu rift, is likely related to asthenospheric upwelling, but in general lithospheric extension may be decoupled from surficial extension by a

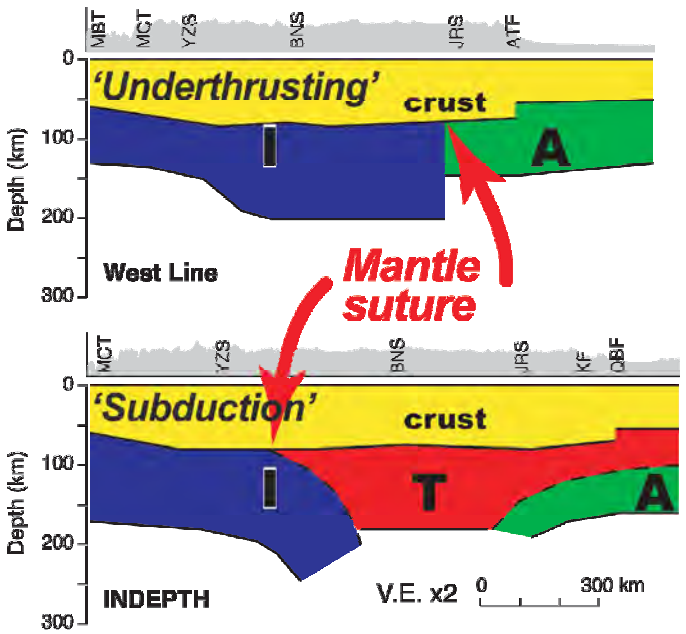

Fig. 2. Cartoon cross-sections of Tibet, interpretation of Zhao J. et al. (2010). Pale grey: crust (undifferentiated); light grey, "A": Asian lithospheric mantle; mid-grey, "T": Tibetan lithospheric mantle (high T, low V, likely incipiently melting); dark grey, "I": Indian lithospheric mantle (cratonic); Moho from P-receiver functions (P-RF) and S-receiver functions (S-RF) and CCP images; LAB only from S-RF. Sections drawn along Westline and INDEPTH passive broadband seismic transects (see Fig. 1). Westline: inferred underthrusting to Jinsha River suture (JRS), cf. HiCLIMB. INDEPTH: inferred delamination and subduction north of Yarlung Zangbo suture (YZS).

weak lower crust. The geometry of the Indian slab and its lateral discontinuities, and their temporal evolution, must surely be intimately related to the generation of Miocene post-collisional magmas across southern Tibet. Though geochronologists and geochemists have appealed to slab tears to explain the Neogene magmas (e.g. Zhang L. et al., 2014), a simple self-consistent model of the seismic and geochronological datasets has not yet been achieved.

Despite the west-east variability between subducting Indian continental lithosphere and asthenospheric upwelling that makes the interpretation of any individual north-south transect potentially problematic, there does seem to be a larger-scale west-east trend from large degrees of underthrusting beneath western Tibet, and more southerly delamination and roll-back of the Indian plate beneath eastern Tibet (Li et al.,, 2008; Zhao J. et al., 2010; Shi et al.,, 2015a & b) (Fig. 2). This large-scale pattern may be due in part to forces associated with subduction of India beneath Myanmar and the abrupt change in the orientation of subduction direction at the eastern syntaxis.

Our re-appraisal of the mantle suture leads us to ask whether we must similarly re-appraise the "crustal front", or northern limit of Indian crust above the Moho of the modern Tibetan Plateau. The location of the crustal front and the depth of the MHT beneath the Tethyan Himalaya and Lhasa Block are controlled by the proportion of the Indian crust that is underthrust beneath Tibet as opposed to transferred to the upper plate, so can help constrain whether the orogenic wedge between the MHT and the YZS is evolving by thrust-faulting in a critical-taper wedge or by southward extrusion of a ductile channel-flow. Although there is no geodynamic requirement that the mantle suture and crustal front be coincident or even parallel, in the absence of contrary evidence this has been the simplest assumption. However, recent broadband transects in the region of the INDEPTH reflection profiles are interpreted to show that the crustal front is decoupled from the mantle suture (Shi et al., 2015a & b). Indian crust seems to penetrate a fairly uniform distance beneath Tibet over a large sector of the orogen at least from 85° (HiCLIMB) to 92°E (Gangdese92), to the crustal front >150 km north of the YZS. This might suggest that underplating of Indian crust beneath the Lhasa Terrane in eastern Tibet is controlled by the geometry of collision as recorded by the YZS at the surface, in contrast to the location of detachment (delamination) of Indian mantle lithosphere from Indian crust that may be controlled by plate-scale subduction geometries. In eastern Tibet both INDEPTH and HiCLIMB receiver-function CCP images show the Main Himalayan Thrust (MHT) as sub-parallel to the Moho beneath the YZS (Kind et al., 2002; Nábělek et al., 2009). In contrast, a recent controlled-source reflection profile recorded by Sinoprobe in western Tibet at 81.5°E (Lu et al., 2012; Gao et al., 2015) traces the MHT as a steep ramp nearly down to the Moho directly beneath the YZS. This profile, which has considerably higher resolution than CCP images, implies that at 81.5°E, very little Indian crust underplates the Lhasa block. Although it is dangerous to generalize this result too far west and east, clearly there is much lateral variability in the proportion of Indian crust within the Lhasa block.

In summary, a plethora of new seismic transects within Tibet, both passive-source and active source, are demonstrating complex west-east variability in the geometry of both Indian crust and Indian mantle lithosphere in the convergence zone. The complexity is on a sufficiently small scale that even the six north-south seismic transects thus far accomplished in Tibet (Fig. 1) are insufficient to capture the 3D variability.

Agius, M. R., Lebedev, S., 2013. Geochemistry, Geophysics, Geosystems, 14, 4260-4281.

Alsdorf, D., Makovsky, Y., Zhao, W., Brown, L.D., Nelson, K.D., Klemperer, S., Hauck, M., Cogan, M.,Ross, A., Clark, M., Che, J., Kuo, J. (1998). Journal of Geophysical Research, 103, 26,993-26,999.

Beghoul, N., Barazangi, M., Isacks, B., 1993. J. Geophys. Res. 98, 1997-2016.

Caldwell, W.B., Klemperer, S.L., Lawrence, J.F. Rai, S.S., 2013. Earth Planet. Sci. Letts., 367, 15-27, 10.1016/j.epsl.2013.02.009

Chen, W.P., Özalaybey, S., 1998. Geophys. J. Int. 135, 93-101.

Chen, W.P., Martin, M., Tseng, T.L., Nowack, R.L., Hung, S.H., Huang, B.S., 2010. Sci. Letts., 295,297-304, doi:10.1016/j.epsl.2010.04.017.

Chen, Y., Li, W., Yuan, X., Badal, J., Teng, J., 2015, Sci. Letts., 413, 13-24.
Craig, T. J., Copley, A., Jackson, J., 2012. Sci. Letts., 353, 231-239.
Gao R., Lu, Z., Klemperer, S.L., Wang, H., Dong S., Li, W., 2015, in prep.
Jin, Y., McNutt, M.K., Zhu, Y., 1996. J. Geophys. Res. 101, 11275-11290.
Kind, R., Yuan, X., Saul, J., Nelson, D., Sobolev, S.V., Mechie, J., Zhao, W., Kosarev, G., Ni, J., Achauer, U., Jiang, M., 2002. Science 298, 1219-1221. doi: 10.1126/science.1078115.
Klemperer, S.L., Kennedy, B.M., Sastry, S.R., Makovsky, Y., Harinarayana, T., Leech, M.L., 2013. Sci. Letts., 366,59-70, 10.1016/j.epsl.2013.01.013.
Kosarev, G., Kind, R., Sobolev, S.V., Yuan, X., Hanka, W., Oreshin, S., 1999. Science 283, 1306-1309. Doi:10.1126/science.283.5406.1306
Li, C., van der Hilst, R.D., Meltzer, A.S., Engdahl, E.R., 2008 Sci. Letts. 274, 157-168. Doi:10.1016/j.epsl. 2008.07.016.
Liang, X., Sandvol, E., Chen, Y.J., Hearn, T., Ni, J., Klemperer, S., Shen, Y., Tilmann, F., 2012. Sci. Letts. 333-334,101-111, http://dx.doi.org/10.1016/j.epsl.2012.03.036.
Liang, X., Chen, Y., Tian, X.B., Wang, M.L., Xu, T., Chen, Y.J., Ni, J., Gallegos, A., Klemperer, S.L., Sun, C.Q., Si, S.K., Lan, H.Q., Teng, J.W., 2015, in prep.
Lu, Z., Gao, R., Klemperer, S.L., 2012. Am. Geophys. Un., Fall Meeting 2012, Abstract T22B-06 oral presentation.
McNamara, D.E., Walter, W.R., Owens, T.J., Ammon, C.J., 1997. J. Geophys. Res. 102, 493-505.
Sapkota, S., Kafle, B., Jiang, M., Su, H., Chen, J., Huang, B., Hi-CLIMB Team, 2009. Science 325, 1371-1374. doi: 10.1126/science.1167719.
Priestley, K., McKenzie, D., 2006. Sci. Letts., 244, 285-301.
Rai, S.S., Priestley, K., Gaur, V.K., Mitra, S., Singh, M.P., Searle, M., 2006. Geophys. Res. Letts. 33, L15308. doi:10.1029/2006GL026076.
Shi, D., Wu, Z., Klemperer, S.L., Zhao, W.J., Xue, G., Su, H., 2015a. Sci. Letts., 414, 6-15, http://dx.doi.org/10.1016/j.epsl.2014.12.055.
Shi, D., Zhao, W.J., Klemperer, S.L., Wu, Z.H., Mechie, J., Xue, G.J., Su, H.P., Shi, J.Y., 2015b in prep.
Tian, X.B., Chen, Y., Tseng, T.L., Klemperer, S.L., Thybo, H., Liu, Z., Xu, T., Liang, X.F., Bai, Z.M., Zhang, X., Si, Saokun, Sun, C.Q., Lan, H.Q., Wang, E.C., Teng, J.W., 2015. Sci. Letts. 430, 171-177.
Tilmann, F., Ni, J., INDEPTH III Science Team, 2003. Science, 300, 1424-1427.
Xu, Q., Zhao, J., Pei, S., Liu, H., 2011. Geophysical Journal International, 187, 414-420.
Zhang, L.Y., Ducea, M.N., Ding, L., Pullen, A., Kapp, P., Hoffman, D., 2014. Lithos, 210, 209-223.
Zhang, Z.J., Chen, Y., Yuan, X., Tian, X., Klemperer, S.L., Xu, T., Bai, Z.M., Zhang, H.H., Wu, J., Teng, J., 2013. Tectonophysics, 606, 178-186.
Zhang, Z., Wang, Y., Houseman, G.A., Xu, T., Wu, Z., Yuan, X., Chen, Y., Tian, X., Bai, Z., Teng, J., 2014. Sci. Letts, 408, 370-377.
Zhao, J., Yuan, X., Liu, H., Kumar, P., Pei, S., Kind, R., Zhang, Z., Teng, J., Ding, L., Gao, X., Xu, Q., Wang, W.,2010. Proc. Natl. Acad. Sci. 107, 11229-11233. doi: 10.1073/pnas.1001921107.
Zhao, J., Zhao, D., Zhang, H., Liu, H., Huang, Y., Cheng, H., & Wang, W., 2014. Gondwana Research, 25, 1690-1699.
Zhao, W., Kumar, P., Mechie, J., Kind, R. Meissner, R., Wu, Z., Shi, D., Su, H., Xue, G., Karplus, M., Tilmann, F. 2011. Nature Geoscience 4, 1-4. doi: 10.1038/NGEO1309.

Biostratigraphy, depositional environment and correlation of microfaunal assemblage from the Ordovician succession of Pin Valley, Spiti Basin

Shivani Pandey*, Suraj K. Parcha#
Wadia Institute of Himalayan Geology, GMS Road Dehradun 248001, INDIA
**shivani@wihg.res.in; #parchask@wihg.res.in*

The Spiti Basin is well-known for its splendid outcrops, richness of fossil contents and for its continuous stratigraphic record of rocks from Neoproterozoic to Cretaceous. The present study is focused in the Ordovician succession of Pin Valley. In the Spiti basin, the Ordovician succession separated from the underlying Cambrian successions by a break in the deposition, which is denoted by angular unconformity. The Ordovician sedimentary succession is typical of carbonate platform facies. The microscopic studies reveal abundant accumulation of calcareous algae along with,

bryozoans and other unidentified microfauna. Among these the widely spread forms are the green calcareous algae and bryozoans. The algal assemblages were consisting mainly of the order Dasycladales that were most numerous in the Ordovician-Silurian successions. Calcareous algae are relatively common biotic constituent in marine carbonate units and played the important role in rock-building and are important constituents in reef complexes in Ordovician period. These benthic marine chlorophyte groups, indicates shallower part of the infralittoral stage and are useful parameters to define the depositional environment of the sequence. Their relative abundance was probably controlled by substrate and rates of deposition. Calcareous algal remains are widespread in various facies in Ordovician carbonate complexes and it provides useful information about the paleoenvironments, which can complement interpretations based on other biota and depositional textures. The most frequent dasycladacean algal recognized in the carbonate facies is Vermiporella and Dasyporella; these forms are usually accompanied by Moniliporella. The various genera of bryozoans identified are as Calloporella, Cyphotrypa, Dekayai, Eridotrypa, Insignia, Trematopora, etc. The earlier bryozoans fauna reported from Tethys Himalaya indicates the age Late Ordovician but the recent studies show that they go even up to Late Silurian.

The presently described calcified algae show the resemblance from Tarim Basin, Kazakhstan, Baltica and North America, indicating cosmopolitan nature. Whereas, the studied bryozoans communities, indicates resemblance with the forms of southern China, Russia, Siberia, Kazakhstan and from Mongolia. The presence of calcareous algae and bryozoans from the Ordovician succession of the Spiti Basin reveals that these successions has shallow seas, mild climates and extensive areas of carbonate deposits, which were helpful to supplied the proper environmental background for extensive development of algae. Based on the faunal elements from these formational units, Middle to Late Ordovician age can be assigned to Thango Formation. The above described genera have relatively wide stratigraphic distribution in the Ordovician period and thus are used as indicator, particularly for shallow-marine, warm, well-oxygenated and relatively high-energy environments. In the light of these studies, an attempt been made to correlate it on the generic level with the analogous successions of the Spiti Basin and with the other well-known sections of the world.

Mineral magnetic record of Late Pleistocene-Holocene environmental changes in lake and peat deposits of Lahaul, NW Himalaya

Suman Rawat
Wadia Institute of Himalayan Geology, 33 GMS Road, Dehradun 248 001, INDIA
rsuman26@gmail.com

The Indian summer monsoon (ISM) is one of the important climate systems in the world providing moisture source for agriculture and socio-economic development of the South Asian countries which constitute two-third of world population (Benn and Owen, 1998). The weakening of the summer monsoon led to changes in and adaptability of various civilizations such as that of Harappa or Indus (Staubwasser et al., 2003; Leipe et al., 2014a; Dixit et al., 2014), whereas extreme events in the ISM precipitation cause floods (Wasson et al., 2013) and landslides in the Himalaya (Dortch et al., 2009). Such extreme events in the monsoon appears to have repeatedly occurred during the Holocene, allowing measures of adaptation and mitigation strategies by human civilizations as reported from the Indian subcontinent (Gupta et al., 2003, 2006). However, the intensity of ISM precipitation in different Indian basins was not uniform owing to variations in latitude, altitude and distance from the sea (Kale et al., 2003; Prasad et al., 2007). Thus, there is an increasing demand to generate high resolution record of ISM variability from different geographic

domains for better understanding of the human-climate interactions (Prasad and Enzel, 2006; Leipe et al., 2014a and references therein).

In the present study, we used the environmental magnetic technique to understand the iron oxide characteristics of the catchment and peat-lake sediment sequence from a small lake, developed over a glacially carved depression (~4,300 m altitude) in the Lahaul, Northwest Himalaya for reconstructing the Holocene palaeoclimate and pedogenic developments. The chronology of studied profile is based on 9 AMS ^{14}C calibrated dates (cal yr BP). The piece-wise linear regression analysis of age-depth model indicates non-linear sedimentation with higher sedimentation rate from ~4142 cal yr BP to the Present and lower accumulation during ~12,880 to 4142 cal yr BP. The mineral magnetic data showed three dominant assemblages of magnetic minerals with varying concentrations in peat-lake sediment sequence i.e. (1) mixed ferri- and antiferro-magnetic minerals between ~12,880 and 11,019 cal yr BP; (2) essentially dominant antiferromagnetic minerals from ~11,019 to 3172 cal yr BP, and (3) significantly increased mixed ferri- and antiferromagnetic minerals from ~3172 cal yr BP to the Present with characteristically increased ferrimagnetic concentrations after ~2032 cal yr BP. The increasing concentration of detrital antiferromagnetic minerals between ~10,398 and 5770 cal yr BP corresponds to increased ISM intensity during early to mid-Holocene in the NW Himalaya and distinctly increased concentration from ~6732 to 5770 cal yr BP indicates mid-Holocene climate optimum in the Lahaul Himalaya. The increased bulk ferri- and antiferromagnetic flux after ~3172 cal yr BP followed by higher ferrimagnetic concentration from ~2032 cal yr BP suggest relative pedogenic maturity of the catchment. The strengthening and weakening of ISM recorded in environmental magnetic signals during ~1260 to 852 cal yr BP and between ~852 and 239 cal yr BP corresponds to Medieval Warm Period (MWP) and Little Ice Age (LIA) events, respectively.

Benn, D.I., Owen, L.A. 1998. Journal of the Geological Society, 155 (2), 353-363.

Dixit, Y., Hodell, D.A., Petrie, C.A. 2014. Geology, 42 (4), 339-342.

Dortch, J.M., Owen, L.A., Haneberg, W.C., Caffee, M.W., Dietsch, C., Kamp, U. 2009. Quaternary Science Reviews, 28, 1037-1054.

Gupta, A.K., Anderson, D.M., Overpeck, J.T. 2003. Nature, 421, 354-357.

Gupta, A.K., Anderson, D.M., Pandey, D.N., Singhvi, A.K. 2006. Current Science, 90 (8), 1082-1090.

Kale, V.S., Gupta, A., Singhvi, A.K. 2003. Late Pliestocene-Holocene paleohydrology of Monsoon Asia, In Gregory, K.J. and Benito, G., editors,. John Wiley and Sons 213-232.

Leipe, C., Demske, D., Tarasov, P. 2014a. Quaternary International, 348, 93-112.

Prasad, V., Phartiyal, B., Sharma, A. 2007. Holocene. 17 (7), 889-896.

Prasad, S., Enzel, Y., 2006. Quaternary Research, 66 (3), 442-453.

Singhvi, A.K., Rupakumar, K., Thamban, M., Gupta, A.K., Kale, V.S., Yadav, R.R., Bhattacharyya, A., Phadtare, N.R., Roy, P.D., Chauhan, M.S., Chauhan, O.S., Chakravorty, S., Sheikh, M.M., Manzoor, N., Adnan, M., Ashraf, J., Khan, A.M., Quadir, D.A., Devkota, L.P., Shrestha, A.B. 2010. Instrumental, Terrestrial and Marine Records of the Climate of South Asia during the Holocene, Springer Netherlands, 54-124.

Staubwasser, M., Sirocko, F., Grootes, P.M., Segl, M. 2003. Geophysical Research Letters, 30(8).

Wasson, R.J., Sundriyal, Y.P., Chaudhary, S., Jaiswal, M.K., Morthekai, P., Sati, S.P., Juyal, N. 2013. Quaternary Science Reviews, 77, 156-166.

Siliciclastic-carbonate sedimentation and sequence stratigraphy of lower part of Prorerozoic Simla Group, western Lesser Himalaya, India: A journey from coastal to shallow marine environment

Tithi Banerjee*, Ananya Mukhopadhyay, Priyanka Mazumdar, Alono Thorie
Department of Earth Sciences, IIEST, Shibpur, Howrah - 711 103, INDIA
**tithi.geol@gmail.com*

Rifted continental margins are often characterised by accumulation of thick sedimentary sequences that are attributed to prolonged phases of subsidence due to gravity loading. The Proterozoic Simla Group of the western lesser Himalaya, India is a typical example of a rifted basin which comprises a 1500 m thick coarsening-upwards clastic succession characterised by the development of a mixed siliciclastic-carbonate platform topped by a regressive succession of a fan-delta deposit. The development of this fan-delta system was due to tectonic activity along the southern basin margin. Sedimentation took place due to vigorous uplift of the adjacent source terrene, which caused a high rate of supply of coarse detritus, and rapid basin subsidence. The Simla Group is divisible into the lower Basantpur, middle Chaaosa and upper Sanjauli Formations.

This study documents (1) outcrop based facies analysis, (2) temporal and spatial relationships of sedimentary facies associations, (3) delineation of different system tracts within well-preserved areas in the lower part of the Simla basin using physical tracing, field mapping and detailed sequence stratigraphic study. Facies and architectural analysis was performed on the lower part of the Simla basin, resulting in the identification of twelve distinct facies attributes: (i) minor tabular and lenticular sandstone (F1), (ii) finely laminated, calcareous siltstone (F2), (iii) flaser-wavy- lenticular bedded heterolithic facies (F3), (iv) interbedded fine sandstones and mudstones (F4), (v) ripple-laminated sandstones (F5), (vi) parallel-laminated sandstones (F6), (vii) carbonaceous mudstone (F7), (viii)shale dominated facies (F8), (ix) rare channel-hosted storm beds (F9), (x) stromatolitic dolostone facies (F10), (xi) siliciclastic-carbonate facies (F11), (xii) flaser-lenticular bedded quartzose dolosiltite & doloarenite (F12). The twelve facies attributes were categorised into three major facies associations (FA1, FA2, FA3) which reflect different transport/deposition mechanisms. FA1 and FA2 (F1-F9) delineated from the Lower Chhaosa Formation, in and around Sanjauli town have combined to develop tidally influenced muddy pro-delta part of the fan-delta system. Flaser- wavy- lenticular bedding, bipolarity of ripple cross-stratification, evenly laminated sand/silt-streaked shales, reactivation surfaces within cross-bedded sandstone sets, mud-drapes on foreset laminae and herringbone cross-stratification as well as small-scale vertical graded units (several fining-upward units) are diagnostic for tidal influence. FA3 (F10-F12) manifested in and around Baldeyan in the Upper Basantpur Formation reveals the signature of tide dominated inner carbonate ramp deposit. Facies distribution of the Lower Simla Group indicates development of two different systems tracts, highstand systems tract (HST) and regressive systems tract (RST) at two different stages of sea-level fluctuations. The development of HST (characterized by mixed siliciclastic inner ramp deposit) took place during sea level high stand where as the RST comprising muddy prodelta deposit developed during periods of high-clastic input and stable-to-rising relative sea level related to normal regression.

U-Pb ages and petrography of the detritus in Siwalik Group along Karnali river section-far western Nepal

Upendra Baral[1,2*], Ding Lin[1], Deepak Chamlagain[3]
[1]Chinese Academy of Sciences, Beijing 100101, CHINA
[2]University of Chinese Academy of Sciences
**ubaral@itpcas.ac.cn*
[3]Department of Geology, Tri Chandra Multiple College, Tribhuvan University, NEPAL

The Himalayan sediments were deposited in the northern margin of the Indian plate and crosscut by several magmatic units in various locations, which ultimately recycled, reworked and deposited in the foreland basin. These fluvial sediments hold the history of the Himalayan exhumation and geo-tectonic events (DeCelles et al., 1998a; DeCelles et al., 2004). This paper deals with the possible provenance of the middle Miocene to early Pleistocene fluvial sediments of the Siwalik Group along the Karnali River section (Far Western Nepal); the oldest Siwalik unit recorded in Nepal Himalaya (Gautam and Fujiwara, 2000) and adds some new insights on the Himalayan orogeny by means of optical petrography and detrital zircon U-Pb dating under LA-ICP-MS. Following the Gazzi-Dickinsion point counting method (Dickinson et al., 1983) the optical petrography has shown that the detrital sediments fall on 'recycled orogeny' field in a QFL plot indicating the sediments were significantly reworked and recycled during the mountain building process. The detrital zircons from the Lower Siwalik clusters around ~490-600 Ma and ~750-1300 Ma having major peaks at 560, 927 and 983 Ma with subordinate peaks at 494 Ma, 1127 Ma, 1604 Ma, 1877 Ma, and 2480 Ma. In the Middle Siwalik the detrital zircon U-Pb ages are clustered around ~299-727 Ma, ~750-1200 Ma, ~1650-1900 Ma having major peaks at 469 Ma and 905 Ma with minor peaks at 711 Ma, 808 Ma, 1148 Ma, 1844 Ma, 2038 Ma, and 2458 Ma. Correlating the ages obtained from the present study and correlating it with the ages of the Himalayan units; Tethys, Higher and Lesser Himalaya (Gehrels et al., 2011 and reference therein) we draw the conclusion that the fluvial foreland basin sediments were mostly derived from the Tethys, Higher, and upper Lesser Himalaya. However, since ~10 Ma ago after the input of the lower Lesser Himalayan sediments was relatively higher in the Siwalik Group, possibly due to the activation of Main Boundary Thrust (Huyghe et al., 2001).

DeCelles, P., Gehrels, G., Quade, J., Ojha, T., Kapp, P., Upreti, B. 1998a. Geological Society of America Bulletin, 110 (1), 2-21.
DeCelles, P.G., Gehrels, G.E., Najman, Y., Martin, A.J., Carter, A., Garzanti, E. 2004. Earth and Planetary Science Letters, 227 (3-4) 313-330.
Dickinson, W.R., Beard, L.S., Brakenridge, G.R., Erjavec, J.L., Ferguson, R.C., Inman, K.F., Knepp, R. A., Lindberg, F.A., Ryberg, P.T. 1983. Geological Society of America Bulletin, 94 (2) 222-235.
Gautam, P., Fujiwara, Y. 2000. Geophysical journal international, 142 (3), 812-824.
Gehrels, G., Kapp, P., DeCelles, P., Pullen, A., Blakey, R., Weislogel, A., Ding, L., Guynn, J., Martin, A., McQuarrie, N., Yin, A. 2011. Tectonics, 30 (5), TC5016.
Huyghe, P., Galy, A., Mugnier, J.-L., France-Lanord, C. 2001. Geology, 29 (11), 1007-1010.

Curious case of the Main Central Thrust in the Sikkim Himalaya

Sayantan Chakraborty*, Atirath Sengupta, Malay Mukul
Continental Deformation Laboratory, Dept. of Earth Sciences, IIT Bombay, Mumbai 400076, INDIA
**sayantanc@iitb.ac.in*

The Main Central Thrust (MCT) in the Himalaya was originally defined as the thrust that transports the Greater Himalayan crystalline Sequence (GHS) over Lesser Himalayan

metasedimentary sequence (LHS) (Heim and Gansser, 1939). The MCT along with the GHS has been extensively studied (e.g. Searle et al., 2008) but consensus is lacking on its geometry and its location in the Sikkim Himalaya. Different ideas exist on the position and definition of the MCT here (Fig. 1):

- MCT as a high-strain zone: (a) MCT is defined as a ~10-12 km thick ductile shear zone with distributed strain extending from garnet-grade Lesser Himalayan schists to muscovite-out isograd (zone between A'-A' and A-A; D-D and E-E in Fig. 1) in Higher Himalayan Gneiss (e.g. Harris et al., 2004; Dasgupta et al., 2004) (c) MCT is a ~5 km thick zone of "tectonic imbrication" that transports GHS in its hanging wall (characterized by U-Pb detrital zircon ages of c. 800-2500 Ma and $\varepsilon_{Nd}(o)$ values ranging from 18.3 to -12.1) over LHS in its footwall (with U-Pb detrital zircon ages c. 1800-3600 Ma and $\varepsilon_{Nd}(o)$ values ranging from -27.7 to -23.4) (Mottram et al., 2014a). (d) MCT is a ~10 km thick zone extending from biotite to muscovite-out isograd based on peak metamorphic ages (Catlos et al., 2004; Mottram et al., 2014b) (zone within D-D and D'-D' in Fig.1).
- Single MCT: (a) MCT is a discontinuity in the chlorite zone (B-B in Fig. 1) (Sinha Roy, 1982) (b) MCT is the base of the GHS and coincides with the muscovite-out isograd (D-D in Fig. 1) with the IMS (Inverted Metamorphic Sequence) entirely in the footwall within the LHS (e.g. Dasgupta et al., 2009) (c) MCT is plane of discordance between migmatitic gneisses and underlying mica schists (C-C in Fig. 1) characterized by a north-east dipping penetrative foliation associated with S-C fabric indicating top-to-the-south-west sense of shear (Gupta et al., 2010) (d) MCT coincides with garnet+ biotite zone (Searle and Szulc, 2005) and is the base of an extruding channel bound by MCT and STDS in the south and north respectively (Searle and Szulc 2005).
- Two MCTs: There are two MCTs; a structurally higher MCT 1 and structurally lower MCT 2 transporting crystalline rocks in their hanging walls (Fig.1) (Mitra et al., 2010; Bhattacharyya and Mitra 2011).

The MCT is a quasi-plastic shear zone (e.g. Grujic et al., 1996) and, therefore, should be characterized by mylonites and systematic fault-zone geometry (Newman and Mitra, 1993; Passchier and Trouw, 2005). We mapped the MCT fault zone in the light of modern concepts along the extensively studied, ~ 25 km N-S, Dikchu to Chungthang transect (e.g. Dasgupta et al., 2009; Mottram et al., 2014a, b) (Fig. 1) to work out its detailed geometry and deformation characteristics. Our results reveal that two distinct mylonite zones are present in the Sikkim Himalaya (Fig. 1) supporting the two-MCT hypothesis (Bhattacharyya, 2010; Bhattacharyya and Mitra, 2011). The MCT 1 and MCT 2 fault zones are ~760 m and ~3.8 km thick respectively. The MCT1 mapped by us coincides with the location of MCT 1 of Bhattacharyya (2010) and lies ~8 km south of MCT previously mapped in Sikkim (e.g. Dasgupta et al., 2009) in the Mangan-Chungthang transect. The MCT 1 fault zone shows a systematic grain size reduction and abundant strain softening features such as grain size sensitive dislocation creep, dynamic recrystallization and geometric softening. Deformation temperature based on quartz and feldspar microstructures (Passchier and Trouw, 2005 and references therein) indicate a normal temperature profile, i.e. the temperatures decreases upwards from the base of the mylonite zone. The deformation temperature in the upper part of the MCT 1 fault zone is ~425°C and increases to ~650°C at the base of the MCT 1 fault zone with no evidence of fluid assisted deformation as the feldspars and biotites are unaltered in this transect. The MCT 2 transports older Paro and Lingste Gneiss over younger Daling Group of rocks of chlorite grade. Both the lithounits are of Lesser Himalayan affinity and the MCT 2 lies ~10 km south of MCT 1. Thus, the MCT 2 is confined within the Lesser Himalayan Sequence and equivalent to the Munsiari thrust in the NW Himalaya (Ahmad et al., 2000). The MCT 2 fault zone boundary is characterized by protomylonites with bimodal distribution of quartz grains and decrease in proportion of relict grains towards the fault core. In the MCT 2 fault zone, the quartz grains deform primarily by grain size-sensitive dislocation creep and fracturing along with limited reaction softening. MCT 2 has been previously mapped as a distinct fault zone in Pelling (Bhattacharyya and Mitra 2011), Soreng and Sivitar (Bhattacharyya and Mitra, 2014).

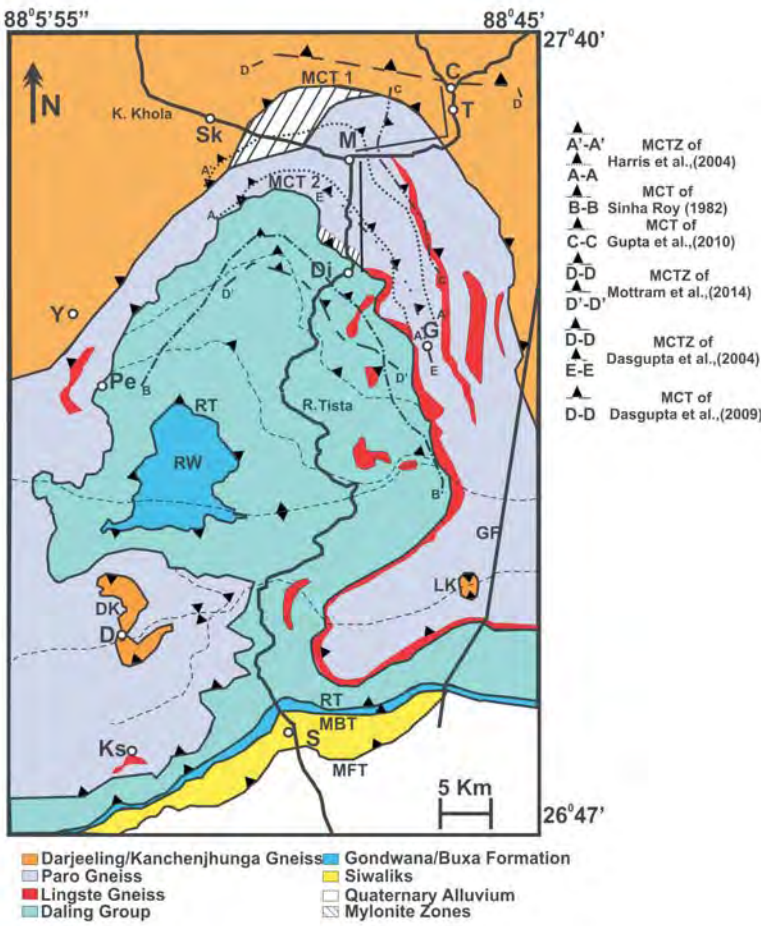

Fig.1. Geological map of Sikkim modified from Bhattacharyya and Mitra (2011); Sinha Roy (1982); Dasgupta et al. (2004); Harris et al. (2004); Gupta et al. (2010); Mottram et al. (2014 a,b) showing the transects marked in black. M = Mangan, T=Tung, My= Myang, C- Chungthang, Sk= Sakkyong, Di= Dikchu, G= Gangtok, S=Sevok, Ks= Kurseong, Y= Yuksom LK= Lava Klippe, DK=Darjeeling Klippe, RW= Rangit Window, GF= Gish Fault. The thick mylonite zones are marked by hatched white enclosures and the MCT mapped by previous workers are also shown.

Our results, therefore, indicate that the MCT 1 is marked by mylonite with a top-to-the-south thrust motion with the GHS in its hangingwall and LHS in its footwall. The MCT 2 is a distinct fault zone within the LHS ~10 km south of MCT 1 and should be renamed the Munsiari Thrust for regional correlation (like the Ramgarh Thrust) in the Himalaya. The MCT 1, in which case, is the MCT.

Ahmad, T., Harris, N., Bickle, M., Chapman, H., Bunbury, J., Prince, C. 2000. Geol. Soc. Am. Bull., 112, 467-477.
Bhattacharyya, K. 2010.. Univ. Rochester.
Bhattacharyya, K., Mitra, G. 2011. J. Struct. Geol., 33, 1105-1121.
Bhattacharyya, K., Mitra, G. 2014. Journal of Asian Earth Sciences, doi:10.1016/j.jseaes.2014.08.035
Catlos, E.J., Dubey, C.S., Harrison, T.M., Edwards, M. 2004. J. Metamorph. Geol., 22, 207-226.
Dasgupta, S., Chakraborty, S., Neogi, S. 2009. Am. J. Sci., 309, 43-84.
Dasgupta, S., Ganguly, J., Neogi, S. 2004. J. Metamorph. Geol., 22, 395-412.
Grujic, D., Casey, M., Davidson, C., Hollister, L.S., Kündig, R., Pavlis, T., Schmid, S. 1996.. Tectonophysics, 260, 21-43.
Gupta, S., Das, A., 11.Goswami, S., Modak, A., Mondal, S. 2010. J. Geol. Soc. India, 75, 313-322.
Harris, N.B.W., Caddick, M., Kosler, J., Goswami, S., Vance, D., Tindle, A. G. 2004. J. Metamorph. Geol., 22, 249-264.

Heim, A., Gansser, A. 1939. Mem. Soc. Helv. Sci. Nat., 73 (1), 1-245
Mitra, G., Bhattacharyya, K., Mukul, M. 2010. Journal of the Geological Society of India, 75(1), 289-301.
Mottram, C.M., Argles, T.W., Harris, N.B.W., Parrish, R.R., Horstwood, M.S. a., Warren, C.J., Gupta, S. 2014a. J. Geol. Soc. London, 171, 255-268.
Mottram, C.M., Warren, C.J., Regis, D., Roberts, N.M.W., Harris, N.B.W., Argles, T.W., Parrish, R.R. 2014b. Sci. Lett., 403, 418-431.
Newman, J., Mitra, G. 1993. J. Struct. Geol., 15, 849-863.
Passchier, C.W., Trouw, R.A.J. 2005. Microtectonics. Springer-Verlag, Berlin/Heidelberg.
Searle, M.P., Szulc, A.G. 2005. J. Asian Earth Sci., 25, 173-185.
Searle, M.P., Law, R.D., Godin, L., Larson, K.P., Streule, M.J., Cottle, J.M., Jessup, M.J. 2008. J. Geol. Soc. London, 165, 523-534.
Sinha-Roy, S. 1982. Tectonophysics, 84, 197-224.

Variability in Indian monsoon over past 5000 years: Impacts on Indian society

Som Dutt[1,*], Anil K. Gupta[1], Hai Cheng[2], Santosh K. Rai[1], Raj K. Singh[3]
[1]Wadia Institute of Himalayan Geology, 33 GMS Road, Dehradun 248001, INDIA
**somdutt@wihg.res.in*
[2]Department of Earth Sciences, University of Minnesota, USA
[3]School of Earth, Ocean and Climate sciences, Indian Institute of Technology Bhubaneswar, INDIA

The strength and timing of Indian monsoon play crucial role in flourishing of one thirds of world's population in Indian subcontinent. Seasonal rainfall from June to September controls the hydrological budget and inturn the agricultural economy of these developing countries. Extreme changes in the rainfall cause huge humanitarian, ecological, agricultural and property losses by the devastating floods and famines. But the relationship of Indian monsoon variability with the ancient cultural development/collapse in south Asia is still unknown due to paucity of high resolution paleoclimatic records from Indian continental part. Speleothems and lake sediments are the best archives to understand the paleoclimatic conditions in continental areas. Present study incorporates the multiproxy investigations using lake sediments from Western Himalayan and speleothem deposits from Eastern Himalaya. It documents significant changes in the ISM behavior over last 5000 years including the global events of 4.2 ka cooling, medieval warm period (MWP) and little ice age (LIA). These climatic oscillations were primarily induced by the changes in solar energy output. This study also reveals that the substantial abrupt and long term fluctuations in ISM strength caused major historical and cultural shits in Indian societies including the demise of Harappan civilization.

Isotopic and biotic footprints of the Paleocene-Eocene Thermal Maximum (PETM) in the Subathu Group, NW Sub-Himalaya, India

Smita Gupta*, Kishor Kumar[#]
Wadia Institute of Himalayan Geology, 33 GMS Road, Dehradun 248001, INDIA
**sggsmita@gmail.com; [#]kumark@wihg.res.in*

A pronounced global warming event referred to as the Paleocene-Eocene Thermal Maximum (PETM) occurred during the Paleocene-Eocene transition (~55 Ma) and lasted for ~170-200 Kyrs causing extraordinary changes on the earth's surface. The most noticeable manifestation of this event is a negative excursion of $\delta^{13}C$ known as Carbon Isotope Excursion (CIE) with as much as 2.5-6‰ drop recorded from marine as well as terrestrial sedimentary archives across the globe. The warming event resulted in widespread deep-ocean acidification, carbonate dissolution, changes in ocean geochemistry and major biotic turnovers as reflected in fossil records of many organisms throughout the world. The

CIE is globally used as a primary element of correlation to mark the PETM footprints. The secondary elements of correlation include turnover of larger benthic foraminiferids, diversification of planktic foraminiferids, *Apectodinium* (dinoflagellate cyst) acme, fluctuations in nannofossil assemblages and changes in ocean geochemistry, etc.

In the Himalayan region, the oldest unit of the Paleogene succession, i.e., the Subathu Group comprises a package of largely shallow marine sediments ranging in age between late Paleocene and middle Eocene and hence embodies the Paleocene/Eocene (P/E) boundary as well as the PETM span. We investigated a section of the basal part of the Subathu Group of the stratotype area in Himachal Pradesh (NW sub-Himalaya) using geochemical and biotic proxies to identify the signatures of the PETM event. In the studied section, carbonate dissolution of larger benthic foraminiferids, *Apectodinium* acme (including the species *Apectodinium parvum, A. homomorphum* and A. *quinquilatum*) and the carbon isotope excursion of 3.4‰ have been observed. The larger benthic foraminiferids are well preserved in the late Paleocene part of the studied section while dissolution features in them develop close to the P/E boundary and then the foraminiferids totally disappear owing to dissolution. The dissolution of calcareous tests of larger benthic foraminiferids is attributed to the warming event. The larger benthic foraminiferids appear later when the basin conditions become stable. The dinoflagellate zones D4 and D5 of Costa and Manum (1988) have been identified in the studied section which correspond to the P/E boundary and correlate closely with the PETM event. The *Apectodinium* acme coincides with the base of the CIE and is usually interpreted as an indicator of rise in temperature, sea level, and nutrient influx (e.g., Crouch and Brinkhuis, 2005; Sluijs et al., 2005).

The depositional scenario of the lower part of the Subathu Group encompassing the PETM event is reconstructed on the basis of the paleontological and isotopic studies. The fluctuations in the sea level are reflected by the presence of varying faunal assemblages in the basal beds. The onset of the PETM coincides with base of the CIE and is marked by carbonate dissolution of the calcareous fossils, *Apectodinium* acme and rise in the sea level is also registered during the same time. The peak PETM is marked by the peak negative values of $\delta^{13}C$ (-26.0‰), absence of calcareous larger and smaller benthic foraminiferids and fall in the sea level. The early recovery phase of the PETM is marked by the decrease in $\delta^{13}C$ values to about -24.6‰ and re-appearance of smaller benthic foraminiferids followed by small rise in the sea level.

Costa, L.I., Manum, S.B. 1988. Results of the International Geological Correlation Programme, Project No. 124, Geol. Jahrbuch A, 100, 321-330.
Crouch, E.M., Brinkhuis, H. 2005. Marine Micropaleontology, 56, 138-160.
Sluijs, A., Pross, J., Brinkhuis, H. 2005. Earth Sci. Rev., 68, 281-315.

Is the magnitude of extreme flood events in the Himalaya increasing? Insight from Ladakh 2010 and Uttarakhand 2013

H.D. Sinclair[1], S. Mudd[1], M. Naylor[1], K. Dallas[1], T. Le Divellec[1], V. Singh[2], R. Devrani[2]
[1]School of GeoSciences, The University of Edinburgh, Drummond Street, Edinburgh, EH8 9XP, UK
[2]Department of Geological Sciences, University of Delhi, INDIA

It has been demonstrated that the frequency and intensity of extreme precipitation events over the western Himalaya are increasing (Roy and Balling, 2004; Alexander et al., 2006); testament to this are the devastating floods in Pakistan in 2010 and Uttarakhand in 2013. However, understanding just how 'extreme' a particular event is, it requires knowledge of the longer term record of comparable events. The sedimentary and geomorphic record of extreme storms enables recent records to be placed in an historic context spanning thousands of years. In August 2010 a mesoscale convective storm hit the arid region of Ladakh devastating village communities in the tributaries

north of the Indus River (Kumar et al., 2012; Thayyen et al., 2013). Satellite derived TRMM data forms the basis for meteorological modelling of the storm (Rasmussen and Houze 2012; Kumar et al., 2014), however these satellites, and hence the models, missed the most intense convective storm that caused the damage. A geomorphic reconstruction of the storm limited its impact to a narrow (4-6 km) wide band along the range of the Ladakh Batholith (Hobley et al., 2012). In this study we extend this reconstruction using the geomorphic record of flood discharge in the main channels. For the first time, we also quantify the volume of sediment mobilised in debris flows during the event from individual catchments (Basgo and Sabu; Fig. 1). This mobilized volume is then compared to the background, long-term erosion rate derived from detrital cosmogenic ^{10}Be in quartz-rich sands. The analysis indicates that the 2010 storm event had the equivalent impact of approximately 1200 years of the background erosion rate.

In 2013, an intense monsoon storm caused heavy flooding and destruction along the Ganga River in Uttarakhand. Analysis of the geomorphic impact of the event demonstrated that in its upper reaches in the Mandakini tributary, the peak discharge obliterated 13,000 yr old glacial moraines, and

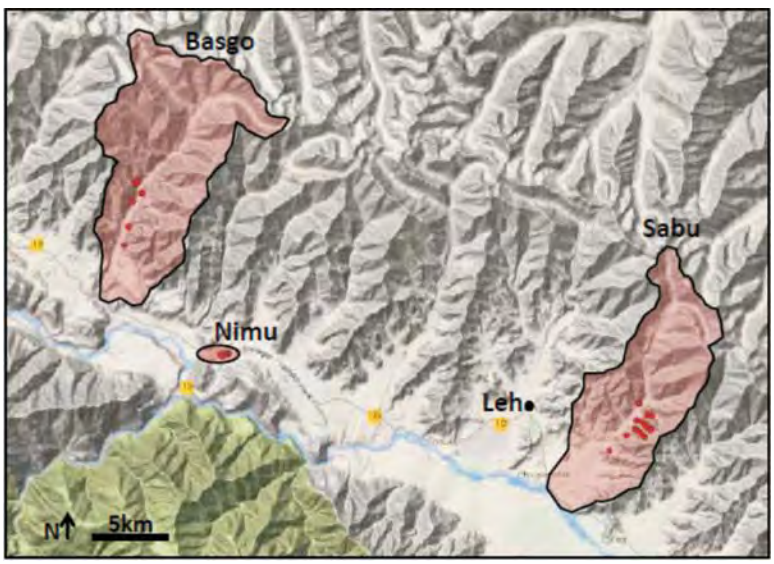

Fig. 1. Catchments analysed over the Ladakh Batholith for the intensity of debris flows associated with the Ladakh 2010 event.

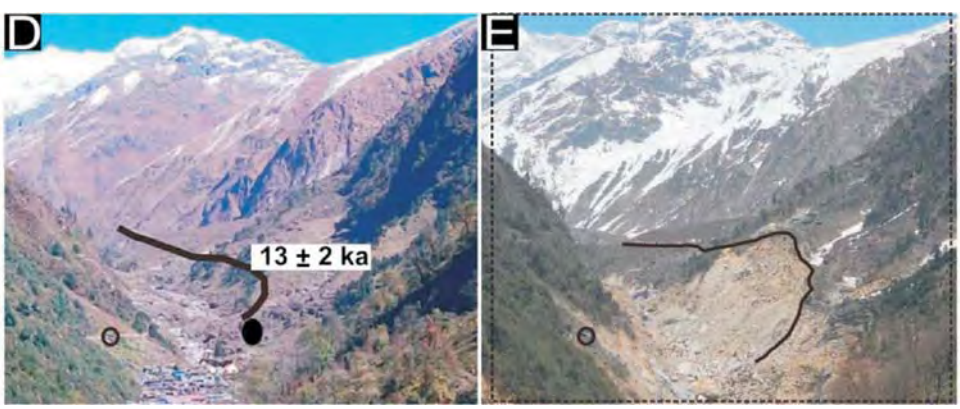

Fig. 2. Images of the upper Mandakini River near Kedarnath before and after the 2013 storm showing the erosional removal of 13 Ka moraines by the peak discharge (Devrani et al., 2015).

in its lower reaches, it developed high fill terraces that accumulated on top of older, perched terraces that are ~1000 yrs old (Wasson et al., 2013; Devrani et al., 2015). We conclude that as with the Ladakh event, the 2013 floods in Uttarakhand were the largest recorded in that catchment for >1000 yrs. The results suggest that not only the frequency of extreme storm events is increasing in the western Himalaya, but the magnitude of these events may also be increasing.

Alexander, L.V. et al. 2006. Journal of Geophysical Research: Atmospheres (1984-2012) 111.D5.
Devrani, R., Singh, V., Mudd, S.M., Sinclair, H.D. 2015. Geophysical Research Letters, 42(14), 5888-5894.
Hobley, D.E., Sinclair, H.D., Mudd, S.M. 2012. Geology, 40(6), 483-486.
Kumar, A., Houze Jr, R.A., Rasmussen, K.L., Peters-Lidard, C. 2014. Journal of Hydrometeorology, 15(1), 212-228.
Rasmussen, K.L., Houze Jr, R.A. 2012. Bulletin of the American Meteorological Society, 93(11), 1713-1724.
Roy, S., Balling, R.C. 2004. International Journal of climatology 24.4, 457-466.
Thayyen, Renoj J. et al. 2013, Natural hazards 65.3, 2175-2204.
Wasson, R.J. et al. 2013. Quaternary Science Reviews 77, 156-166.

Geological controls on the long profile shape of the major rivers of the Himalaya and its implications in geomorphic studies

Sonam*, Vikrant Jain#
Discipline of Earth Science, Indian Institute of Technology Gandhinagar, Palaj 382355, INDIA
**sonam@iitgn.ac.in; #vjain@iitgn.ac.in*

River long profile is one of the fundamental geomorphic parameter to analyze river response to tectonic disturbances (Hack, 1957; Knighton, 1984; Shepherd, 1985). The long profile of a river is shaped by geological processes and hence it is used to derive evolutionary trajectory of a landscape at 104-106 years' time scale. The long profile shape further governs the modern day (100-101 year time scale) fluvial processes by controlling the spatial variability of channel slope. Hence, long profile of a river provides a platform to analyze the interaction of geological and geomorphic processes at different time scales. This work highlights the variability in long profile shape of the Ganga River and its major tributaries and examines the geological control on long profile shapes. The impact of long profile shape on slope variability has also been analyzed to develop a relationship between river processes and geological setting.

The elevation versus channel length data to obtain long profile plots have been obtained in Arc GIS version 10 using the Cost Path Tool. Regression analysis was done in order to find the best suited mathematical function. The values of the exponents and constant in the equation were optimized up to the limit where the minimum value of the Sum of Square Error (SSE) was attained. A mathematical function has been proposed as the most representative curve of the river long profile. Second order exponential function provides the best representation of most of the long profiles, which is similar to other rivers in the passive tectonic setting (Jain et al., 2006; Singh, 2009). Hence, long profile in different tectonic setting may be represented by similar mathematical function. The coefficients of exponential curve were used to define the geological control on the long profile shape. The second order exponential curve also explains the dominance of two different set of processes in the evolution of long profile. The distribution of fast and slow decay components of the river long profile is not uniform for all river channels, and this variability has been defined by the extent of different thrust sheets in the basin area. The rivers with a major portion of their long profile segment in the Higher and Lesser Himalayas have a very rapid slope decay rate expressed by the high exponent value of the exponential profile.

The exponential curve was also used to derive the concavity of profile by integrating the long profile equation. The mathematical expression of profile concavity provides better representation of

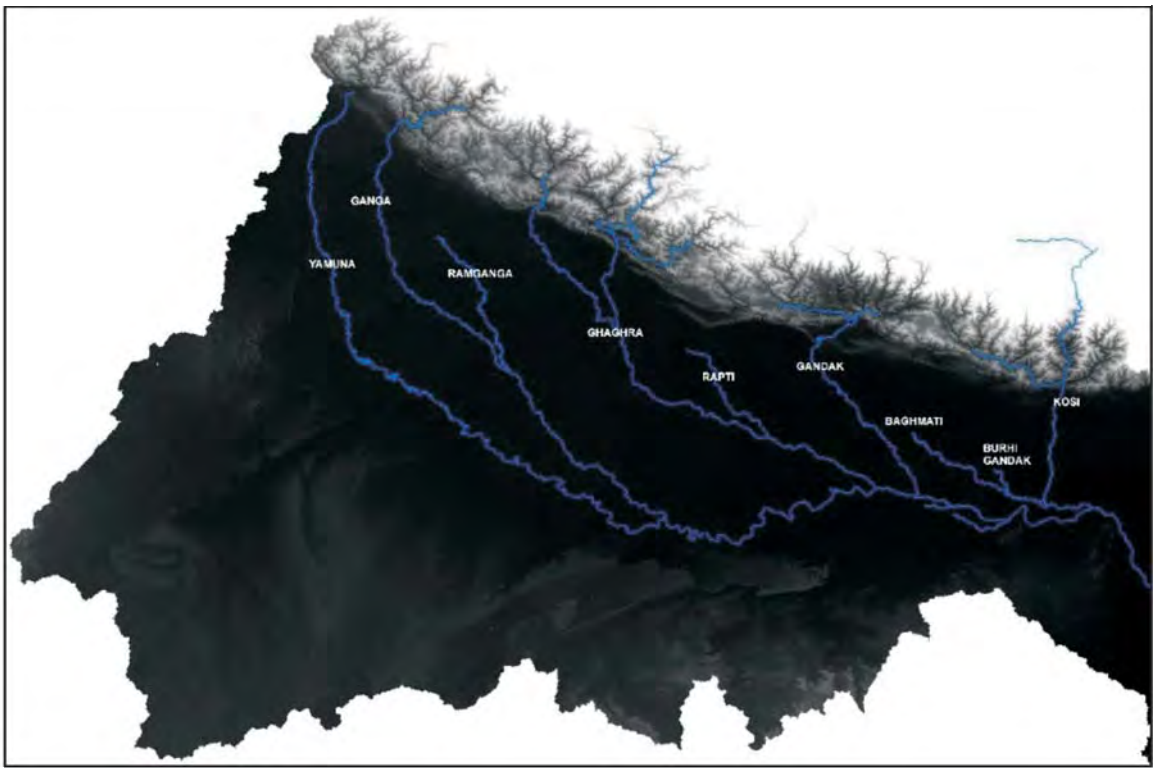

Fig. 1. Tributaries of Ganga River overlaid on Digital Elevation Model.

long profile concavity (after Langbein et al., 1964). The different profile concavity was further related with the geological differences in the basin area and the total elevation difference between channel head and mouth for a given basin. Also, concavity of a river channel is believed to be an indicator of the spatial distribution of channel denudation rate which is basically a function of channel slope, an important determinant of shear stress which drives erosion. Spatial variability in channel slope was derived through first derivative the exponential equation. Channel slope distribution pattern has also a significant relationship with the Geology of the study area. The bimodal distribution of channel slope as portrayed by the second order exponential function also indicates the variability in stream power distribution pattern and thus the locations of geomorphic process zones along the different channel of the Ganga River Basin. The distribution of the distinct process zones is governed by geological setting in the basin area.

Hack, J.T. 1857. USGS Professional Paper, 294-B.
Jain, V. et al. 2006. Geomorphology, 74.1-4, 297-317.
Knighton, D. 1984. Fluvial Forms and Processes. London: E. Arnold.
Langbein, W.B. 1964. Geological Survey Professional Paper, 501B, 119-122.
Morris, Peter, H., David, J.W. 1997. Earth Surf. Process. Landforms, 22.2, 143-163.
Shepherd, R.G. 1985. The Journal of Geology, 93.3, 377-384.
Singh, T., Jain, V. 2009. Geomorphology 106.3-4, 231-241.

Deciphering tectono-climatic variability from morpho-sedimentary records in the middle Damodar valley, Lower Gangetic Plain during Quaternary period

Sujay Bandyopadhyay[1*], Subhajit Sinha[2], Pradeep Srivastava[3]
[1]*Department of Geography, The University of Burdwan, Burdwan 713104, INDIA*
**sujaybandyopadhyayest@gmail.com*
[2]*Post-Graduate Dept. of Geology, Durgapur Govt. College, Durgapur 713214, INDIA*
[3]*Wadia Institute of Himalyan Geology, 33 GMS Road, Dehradun 248001, INDIA*

Over the last few decades, study of morpho-sedimentary architecture has become more and more important for the understanding of climate-tectonic interplay (Srivastava et al., 2009) during the Quaternary period. These are the excellent laboratory informing about the role of climate and tectonics which sculpt the landscapes through the production, transport and deposition of sediments. The development of fluvial landscape can be influenced by active and passive tectonic processes, climate-related variations in flood regime and sediment supply, and base level fluctuations that manifest in many ways, including drainage network positioning/configuration, accelerated river incision, differences in channel steepness, and asymmetries of catchments.

In the Indian context, detailed regional studies on the Quaternary fluvial deposits of lower Ganga plains and deltaic plains (Ganga fluvio-deltaic plains, GFDP) have been reported that climate and sea-level change have influenced the fluvial processes in this region (Mallick and Niyogi, 1972; Sinha et al., 2005; Tandon et al., 2008; Sinha and Sarkar, 2010). Some evidences of the link between climate and sedimentation have been documented based upon (i) playnological, micropaleontological and sedimentological investigations in onshore Kolaghat, West Bengal (Hait et al., 1996), (ii) correlation of sediment dispersal with intensity of South Indian Monsoon in Ganga-Brahmaputra delta (Goodbred and Kuehl, 2000; Goodbred, 2003), (iii) sedimentology, chronology, isotope (^{13}C) and sequence stratigraphic analysis of subsurface sediments of western delta plain of Ganges-Brahmaputra delta (Sarkar et al., 2009), and (iv) analysis of sediment microstructure from eastern margin of the lateritic area of Medinipur district between the Silabati River in the north and the Kansabati River in the south (Dey et al., 2009). In addition, the late Quaternary period witnessed intense tectonic movements (neotectonics) in the GFDP, due to several reasons such as reactivation of basement faults and tectonic subsidence which controls depositional pattern (Stanley and Hait, 2000; Goodbred and Kuehl, 2000) and produces active transgression during early Pleistocene and around 7-6 ka (Banerjee and Sen, 1987; Singh et al., 1998), fault lineament controlled drainage system (Roy and Chattopadhyay, 1997) and shifting (avulsion) of river courses (Chakrabarti et al., 2001; Gupta et al., 2014; Rudra, 2014). Therefore, understanding of fluvial systems in different climate and tectonic regime is cardinal to the understanding of geomorphic evolution of GFDP vis-à-vis climate and tectonic changes.

Here we present a study from the alluvial plain of middle Damodar River in GFDP, eastern India based on morpho-sedimentary records, highlighting the role of Quaternary tectonic and climatic variability in shaping the landscape of the region. These record form important continental archives for understanding landscape dynamics against the backdrop of Quaternary environmental changes driven by neotectonics (Sen, 1988) and palaeo-monsoonal dynamics. To understand the changes in stratigraphic architecture induced by perturbations in the tectono-climatic system, sedimentology, stratigraphy and luminescence chronology are used. This has been supplemented by detailed topographical analysis, geomorphometry, shallow sub-surface stratigraphic data and field documentary in order to examine the spatial and temporal relationship between changes in the landscape development. The Quaternary deposits of the middle Damodar valley is divided into very poorly indurated Older alluvium overlain by friable Newer alluvium. The Older alluvium unconformably overlies the Gondwana deposits, consisting mostly sandy facies with ca. 11° tilt towards SE.

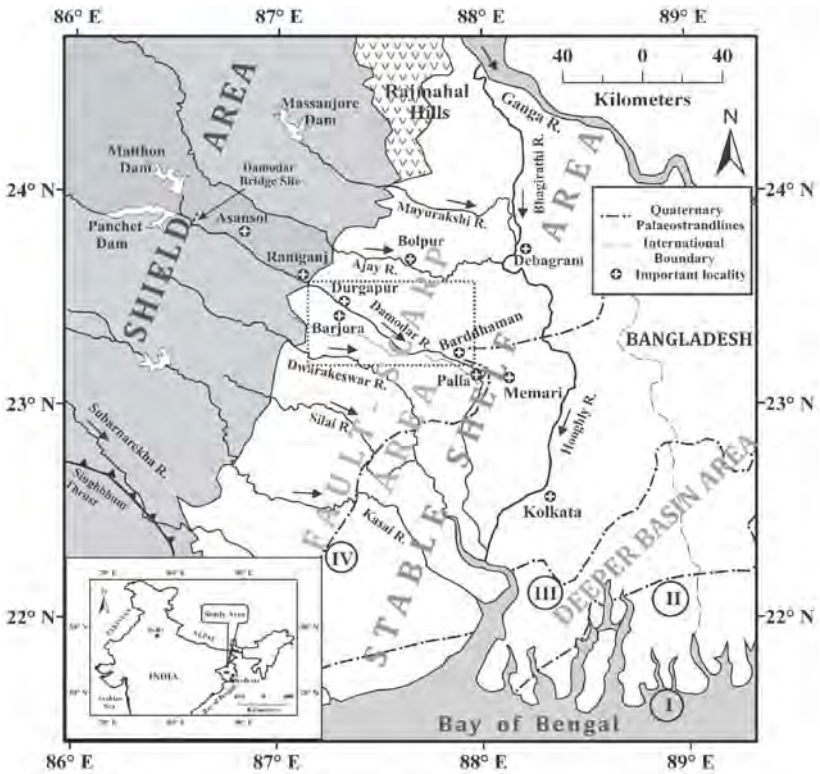

Fig. 1. Location map of the lower Gangetic plain (LGP) with structural units and palaeostrandlines (Modified after Sengupta, 1966; Agarwal and Mitra, 1991). The dotted line box represents the middle reach of the Damodar River. (Inset) Map showing the location of study area in India.

The analyses of the results revealed that during 90-82 ka (end of MIS-5), the region experienced aggradational fluvial activities due to higher sea level and frequent climatic fluctuations and continued till 74-64 ka. In addition, the area experienced dry climate indicated by the presence of pedocal soil and caliches nodules in the strata between 31-27 ka. This complex interaction between environmental change and earth surface processes provides an important framework for examining the present day landscape evolution. The climate and tectonic implications of this work in this less studied region will be presented.

Agarwal, R.P., Mitra, D.S. 1991.. Mem Geol Soc India, 22, 13-24.
Banerjee, M., Sen, P.K. 1987. Indian Journal of Earth Sciences, 14, 307-320.
Chakrabarti, P., Nag, S., Mitra, A.K. 2001. Indian Journal of Geology, 73 (1), 35-41.
Dey, S., Ghosh, S., Debbarma, C., Sarkar, P. 2009. Russian Geology and Geophysics, 50, 884-894.
Gibling, M.R., Bhattacharjee, P.S., Dasgupta, A.S. 2005. Himalayan Geology, 26 (1), 223-240.
Goodbred Jr, S.L., Kuehl, S.A. 2000. Geology, 28, 1083-1086.
Goodbred Jr., S.L. 2003. Sedimentary Geology, 162. 83-104.
Goodbred Jr., S.L., Kuehl, S.A. 2000. Sedimentary Geology, 133, 227-248.
Gupta, N., Kleinhans, M.G., Addink, E.A., Atkinson, P.M., Carling, P.A. 2014. Geomorphology 213, 15, 24-37
Rudra, K. 2014. C. Geomorphology, 227, 87-100.
Sarkar, A., Sengupta, S., McArthur, J.M., Ravenscroft, P., Bera, M.K., Bhushan, R., Samanta, A., Agrawal, S. 2009. Quaternary Science Reviews, 28, 2564-2581.
Sen, P.K. 1988. The Allahabad Geographical Society, Allahabad, 106-117.
Sengupta, S. 1966. Bulletin of American Association Petroleum Geology, 50 (5), 1001-1017.
Singh, L.P., Parkash, B., Singhvi, A.K. 1998. Catena. 33, 75-104.
Srivastava, P., Bhakuni, S.S., Luirei, K., Misra, D.K. 2009. Journal of Quaternary Science, 24 (2), 175-188.
Tandon, S.K., Sinha, R., Gibling, M.R., Dasgupta, A.S., Ghazanfari, P. 2008. Memoir Jour. Geol. Soc. India, 66, 259-299.

Geomorphically deduced uplift rate estimates from the Chittagong-Tripura Fold Thrust Belt (FTB)

Tejpal Singh[1*], Shakul Mittal[2], A.K. Awasthi[3]
[1]*CSIR-Fourth Paradigm Institute, Bangalore 560037, INDIA*
** geotejpal@yahoo.co.in*
[2]*Indian Institute of Technology Roorkee, Roorkee 247667, INDIA*
[3]*Graphic Era University, Dehradun 248001, INDIA*

Oblique convergence takes place along the eastern margin of the Indian plate. The southern part of this margin is largely submerged and had ruptured during the 2004 earthquake (Mw ~9). Northward, it continues over land and is manifested in the Chittagong-Tripura Fold Thrust Belt (FTB). The FTB is characterized by typical landscape gently sloping towards west. The westernmost hill ranges mark the general tectonic boundary and often overstep/overlap the adjacent ranges. In the normal direction, a series of parallel to sub-parallel hill ranges are separated by broad valleys.

Geologically, these hill ranges are made of Upper Tertiary sandy-argillaceous sediments have been folded into a series of long anticlines and synclines striking NNW-SSE. The seismic data suggest that some of these anticlines are cored by thrust fault ramps that extend to a large-scale décollement dipping gently to the east. The décollement likely deepens to the east.

Morphometric studies over the hill ranges provide information on the relative degree of tectonic activity that conforms to tectonic activity class 3 of Silva et al. (2003). These values provide semi-quantitative estimates of discrete uplift rates ~0.03 mm/yr. These estimates are consistent with geodetic and geological convergence rates that show an increase in convergence rates from west to east (0-2 mm/yr) across the FTB.

Seismic hazards in the Himalayas: Evaluation of seismicity and seismic characteristics

Uma Ghosh[1], Pankaj Mala Bhattacharya[2]
[1]*Lalbaba College (Calcutta University), Howrah 711202, INDIA*
[2]*Geological Survey of India, Kolkata, INDIA*

Spatial distribution of seismicity and seismic characteristics (fractal dimension, b-value, energy release, reoccurrence period) are assessed for the Himalayan Region (260-350 N and 720-980 E). The Engdahl, van der Hilst, and Buland (EHB) relocated earthquakes M ≥4.0 are selected for the period 1964-2009 from the International Seismological Centre (ISC) catalogues.

The Gutenberg-Richter frequency-magnitude relation (b-value) is calculated by the Maximum Likelihood Method (MLM) as well as by the new alternative Kaltek method. The fractal dimension is estimated using the correlation integral method. The total set of events was also used for estimating radiated energy in the region. The probability of the occurrence of strong earthquakes (M ≥6.0) during a specified interval of time has been estimated on the basis of three probabilistic models namely, Weibul, Gamma and Lognormal. The model parameters (probability distribution functions) have been estimated by the MLM.

The large data set in the Himalayas made it possible to examine the b-value, fractal dimension (D), energy release and probability of strong earthquakes/seismic hazards in the region. The results are corroborative, and the zones of impending strong/large earthquakes are identified. Low b-value contours are obtained in the Kangra (~0.58), Nepal (~0.48) and Sikkim (~0.68) areas, and the contours are parallel to the seismicity trends that also follow the Himalayan trend. These

zones are identified with prominent low fractal dimension, D ~1.3 contours. This indicates clustering to earthquake epicenters in this block. Energy release in Kangra, Nepal and Sikkim is Low (~0.04×10^{20} ergs, 4.71×10^{20} ergs and ~5.84×10^{20} ergs., respectively) and the contours trend along the MBT. Low energy released in the Nepal, Kangra and Sikkim region may be indicative of higher stress concentration for future release of the energy and is indicative for a probable earthquake in near future as energy is being accumulated here.

A comparatively higher b-value parallel to the seismicity trend is obtained in Uttarkashi (~0.8), Arunachal Pradesh (~0.76) and North East India (~0.77), and the trend is transverse to the Himalayan trend. Higher D (~1.97) values are obtained in Uttarkashi, Arunachal Pradesh and North East India. Pockets of high energy release contours in between these areas is visible in UttarKashi (~19.57×10^{20} ergs.), Northeast India (~9.77×10^{20} ergs), Arunchal Pradesh (~8.7×10^{20} ergs). Comparatively high b value, high fractal dimension and high energy released in these regions indicate remote probably of earthquake of magnitude more than 5.0 in near future.

The cumulative distribution of the observed time intervals using the Weibull, Lognormal and Exponential models was estimated. The cumulative probability is estimated for blocks containing Kangra, Nepal and Sikkm as these zones are indicative of probable earthquake in near future.

Thus the b-value maps have identified the variable stressed zones, and the fractal dimension maps the fractal characteristics of the active fault zones. The energy release map, on the other hand, identified the zones of higher and lower energy release, thus indicating the areas of future probable earthquakes. The vulnerable zones (Kangra, Nepal region and Sikkim) have been identified by these maps are further corroborated with the probabilistic models to assess the seismic hazards in the Himalaya region.

Overview of the NAMASTE seismic array recording aftershocks of the M7.8 Gorkha earthquake

Marianne S. Karplus[1*], Soma Nath Sapkota[2], John Nabelek[3], Mohan Pant[1], Aaron A. Velasco[1], Simon L. Klemperer[4], Jochen Braunmiller[5], Ezer Patlan[1], Abhijit Ghosh[6], Vaclav Kuna[3], Birat Sapkota[3], Keith Galvin[7], Jenny Nakai[8]

[1]Dept. of Geological Sciences, Univ. of Texas at El Paso, El Paso, TX USA 79968
**mkarplus@utep.edu*
[2]Geoscience Subdivision, Department of Mines and Geology, Lainchaur, Kathmandu
[3]College of Earth, Ocean, and Atmospheric Sciences, Corvallis, OR USA 97331
[4]Dept. of Geophysics, Stanford University, Stanford, CA USA 94305
[5]School of Geosciences, University of South Florida, Tampa, FL USA 33620
[6]Dept. of Earth Sciences, Univ. of California-Riverside, Riverside, CA USA 92521
[7]U.S. Geological Survey, Menlo Park, CA USA 94025
[8]Geological Sciences, Univ. of Colorado, Boulder, CO USA 80309

The collision of the Indian and Eurasian plates presents a significant earthquake hazard, as demonstrated by the recent, large, and devastating earthquakes in Nepal (April 25, 2015 M=7.8 and May 12, 2015 M=7.3). These recent earthquakes and their aftershocks provide a unique opportunity to learn more about this collision zone. Specifically, many important science questions remain about crustal architecture of the Himalaya, including distinguishing between different possible geometries of the Main Himalayan Thrust (MHT) and better defining structural causes and locations of rupture segmentation both along-strike and down-dip. The U.S. National Science Foundation funded the deployment of seismometers and strong motion sensors at forty-five sites across the rupture area of the April 25, 2015 M7.8 Nepal earthquake, an effort known as project NAMASTE (Nepal Array Measuring Aftershock Seismicity Trailing Earthquake). The sites consist of 10 short-period plus

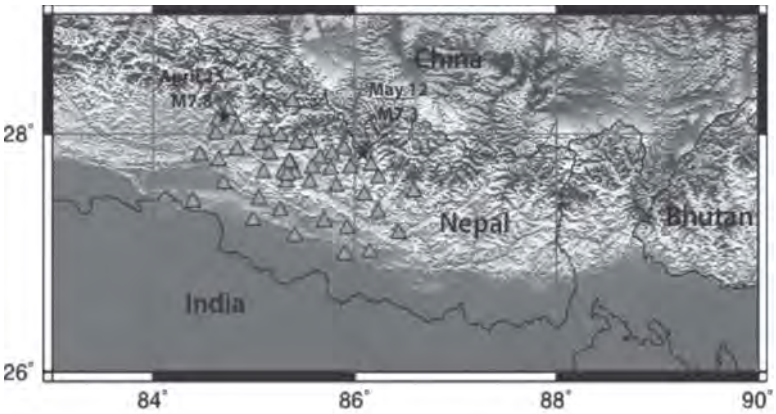

Fig. 1. Topographic map showing the locations of the 45 seismic stations (triangles) deployed across the rupture area of the April 25, 2015 M7.8 Nepal earthquake. Black stars: M7.8 April 25 (west) and M7.3 May 12 (east) earthquake epicenters.

strong motion stations, 25 broadband stations, 6 short period stations, and 4 strong motion stations (Fig. 1). With a dense array of seismometers deployed within and around the rupture area from June 2015 through winter or spring 2016, we will be able to determine accurate aftershock locations as well as use local earthquake tomography to test fault geometry models and better constrain the lithospheric structure. Distinguishing between different possible geometries of the Main Himalayan Thrust and better understanding structural causes and locations of rupture segmentation both along-strike and down-dip are essential for assessing future Himalayan seismic hazards.

Post glacial landform evolution in the middle Satluj River valley, India: Implications towards understanding the climate tectonic coupling

Shubhra Sharma, B[1,*], S.K. Bartarya[1], B.S. Marh[2]
[1]Wadia Institute of Himalayan Geology, 33 GMS Road, Dehradun 248001, INDIA
**shubshubhra@gmail.com*
[2]Department of Geography, Himachal Pradesh University, Shimla, INDIA

The Indian Summer Monsoon (ISM) is considered to have profound effect on earth surface processes and landscape evolution in the monsoon dominated Southern Mountain Front (SMF), located to the south of Main Central Thrust (MCT) in the Himalaya. The terrain experiences accelerated erosion due to a combination of focused high intensity rainfall and seismicity (Clift et al., 2012; Bookhagen et al., 2005; Wobus et al., 2005; Thiede, et al., 2004; Hancock and Anderson, 2002). It has been suggested that Himalayan fluvial system has a coupling between the ISM and fluvial dynamics as ~80% of the annual flow is discharged during ISM along with most of the sediment production and transportation (Wulf et al., 2012; Goodbred Jr., 2003).

Middle Satluj valley which lies in the trajectory of the Indian Summer Monsoon (ISM) has a rich repository of the late Quaternary landforms which involves the fluvial terraces (fill and strath), alluvial fans, debris flow and palaeoflood deposits.

The present study is an attempt to (i) reconstruct the evolutionary history of the landform (event stratigraphy), and (ii) to ascertain the role of ISM variability and the regional and local tectonics in the evolution of these landforms. Using the detailed field geomorphology, sedimentology supported by the optical chronology it has been observed that fluvial landforms dominate the study area followed by the

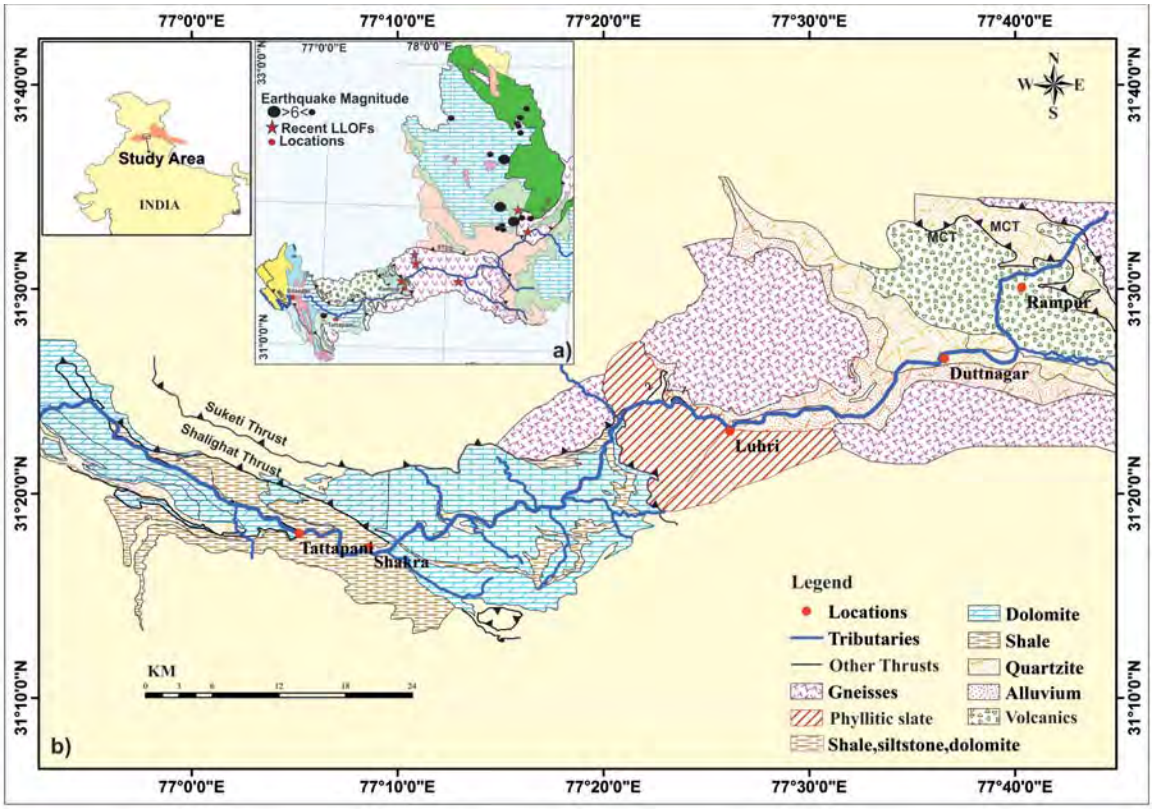

Fig. 1. Regional geological map of the Middle Satluj valley (modified after GSI memoirs, 1976 and Thakur and Rawat, 1992). a) Inset showing major earthquakes in the valley (modified after Wulf et al., 2012) and recent events of Landslide Lake Outburst (LLOFs) (Source: DDMA, Kinnaur; Gupta & Shah, 2008; and Wulf et al., 2012).

alluvial fans and debris flow. The palaeoflood deposits although constitute the minor constituent provide an important insight to the climatically governed extreme hydrological events. The study area has preserved three major events of valley-fill aggradation. Optical chronology suggests that the oldest aggradation event pre date the Last Glacial Maximum (LGM). The second valley wide aggradation event occurred during the post glacial strengthening of ISM and persisted intermittently till the middle Holocene (~17 ka and ~6 ka).Whereas, the younger aggradation phase with considerable contribution from local slopes is dated between ~5 ka to 1.4 ka and is attributed to the declining phase of ISM. The palaeoflood deposits are dated between early to mid-Holocene indicating episodes of high intensity rainfall induced landslide lake outburst in the Higher Himalaya. Landslides in higher Himalaya are known to occur due to the abnormal monsoon events during the early to middle Holocene period Bookhagen et al. (2005).

Debris flows and alluvial fans constitute the second major landform. Field stratigraphic relationship with that of the fluvial landforms and the chronology suggests that these landforms evolved during the LGM (weak ISM) and early to mid-Holocene transitional climate. Based on the terrace morphology, three events of relatively enhanced surface uplift are inferred. The oldest event of enhance uplift pre-dated the LGM and created accommodation space for post LGM fluvial aggradation by lateral planation and vertical incision. The second event after the early-Holocene, assisted the valley-fill incision and development of terrace T2, whereas, the third event after late Holocene was responsible for valley-wide strath terraces formation.

The study emphasizes the role of ISM and the ongoing regional and local tectonics in the post glacial landform evolution.

Bookhagen, B., Thiede, R.C., Strecker, M.R. 2005. Geology, 33 (2), 149-152, doi: 10.1130/G20982.1
Clift, P.D., Giosan, L., Blusztajn, J., Campbell, I.H., Allen, C., Tabrez, A.R., Rabbani, M.M., Alizai, A.,Lückge, A. 2012. Geology, 36, 79-82, doi: 10.1130/G24315A.1.
District Disaster Management Authority (DDMA), Kinnaur. http://hp.gov.in/ddma-kinnaur/page /History. aspx. Last accessed on 29 June 2015.
Goodbred Jr., S.L. 2003. Sedimentary Geology, 162, 83-104.
GSI. 1976. Memoirs of the Geological Survey of India 106 (I, II), Government of India.
Gupta, V., Shah, M.P. 2008. Natural Hazards, 45(3), 379-390.
Hancock, G.S., Anderson, R.S. 2002. Geological Society of America Bulletin,114 (9), 1131-1142.
Thakur, V.C., Rawat, B.S. 1992. Geological map of the Western Himalaya. WIHG, Dehradun.
Thiede, R.C., Bookhagen, B., Arrowsmith, J.R., Sobela, E.R., Streckera, M.R. 2004. Earth and Planetary Science Letters, 222, 791-806.
Wobus, C., Heimsath, A., Whipple, K., Hodges, K. 2005. Nature, 434, 1008-1011.
Wulf, H., Bookhagen, B., Scherler, D. 2012.. Hydrology and Earth System Sciences, 16, 2193-2217, doi: 10.5194/hess-16-2193-2012.

Climate-driven terrace formation in the Kangra Basin, NW Sub-Himalaya, India

S. Dey*, R.C. Thiede, T.F. Schildgen[#], H. Wittmann*, B. Bookhagen, M.R. Strecker
Institut für Erd & Umweltwissenschaften, Universität Potsdam, GERMANY
[#]GFZ, Potsdam, GERMANY
**geosaptarshi@gmail.com*

Fluvial terraces in intermontane basins record variations in sediment routing that causes aggradation during transport-limited episodes and incision during supply-limited conditions. These alternations occur commonly during the evolution of intermontane basins in the Himalaya, but the temporal constraints and the underlying mechanisms for changes in sediment routing are only known to a first order.

The Kangra re-entrant of the NW Sub-Himalaya hosts intermontane sedimentary basins that contain Quaternary valley fills that appear to be associated with severed drainage conditions caused by reactivated thrust faults in the Himalayan orogenic wedge. The valley fills in the Kangra Basin constitute alluvial-fan deposits that have been re-incised, creating a landscape with multiple terrace levels that afford an analysis of the forcing of erosional and depositional processes in the Sub-Himalaya. Four, 1-2 km2 gravel surfaces at 1100-1150 m elevation comprise previously undiscovered remains of a ~200 m thick fan-related sedimentary fill along the southern margin of Kangra Basin (E of the town of Kangra). We determined a cosmogenic radionuclide (CRN) ^{10}Be exposure age of 41±5 ka for that surface (terrace level T1), indicating that the filling (AF1) occurred earlier. Combining previous geochronological results with our new data, we distinguish at least three major aggradation phases in the Kangra Basin. Sediment removal from the first basin fill was superseded by a renewed aggradation phase, which formed a second fill generation (AF2) ~110 m below the T1 alluvial fan remnants. We determined a ^{10}Be exposure age of 15.2±2 ka for the T2 alluvial-fill surface, which is compatible with prior OSL dating by Srivastava et al. (2009) and Thakur et al. (2014). Interestingly, this fill event is thus broadly coeval with the termination of the last glacial maximum. Geomorphic and stratigraphic evidences record a subsequent phase of erosion of AF2, which was followed by a third episode of aggradation (AF3), which formed the best-preserved alluvial fans during the early Holocene. This aggradation phase appears to have been coeval with an early Holocene strengthened Indian Summer Monsoon. Similar to other Himalayan valleys, this fill was episodically incised, leaving a sequence of fluvial terraces with exposure ages of 8.4±0.8 ka, 6.6±0.7 ka, 4.9±0.4 ka, and 3.2±0.3 ka at successively lower levels.

The terrace exposure ages correlate with trends of oxygen-isotope data (Fleitmann et al., 2003; Wang et al., 2005) that record relatively weak Indian Summer Monsoon (ISM) phases, and they are coeval with dry episodes recorded in Tibetan lakes, similar to observations in the Lesser Himalaya of NW India (e.g., Bookhagen et al., 2006). Together, the data suggest that the pronounced early Holocene fill event and subsequent incision episodes in the Kangra Basin as well as from other sectors of the Himalaya were controlled by regional changes in climate.

Bookhagen, B., Fleitmann, D., Nishiizumi, K., Strecker, M.R., Thiede, R.C. 2006. Geology, 34 (7), 601-604.
Fleitmann, D., Burns, S.J., Mudelsee, M., Neff, U., Kramers, J., Mangini, A., Matter, A. 2003, Science, 300, 1737-1739.
Gasse, F., Arnold, M., Fontes, J.C., Fort, M., Gibert, E., Huc, A., Li, B.Y., Li, Y.F., Lju, Q., Melieres, F., Vancampo, E., Wang, F.B., Zhang, Q.S. 1991. Nature, 353, 742-745.
Gasse, F., Fontes, J.C., Van Campo, E., Wei, K. 1996.Palaeogeography, Palaeoclimatology, Palaeoecology, 120, 79-92.
Srivastava, P., Rajak, M.K., Singh, L.P. 2009. . Catena, 76 (2), 135-154.
Thakur, VC, Joshi, M., Sahoo, D., Suresh, N., Jayangondapermal, R., Singh, A. 2014. . International Journal of Earth Sciences, 103 (4), 1037-1056.
Van Campo, E., Cour, P., Sixuan, H. 1996, Palaeogeography, Palaeoclimatology, Palaeoecology, 120, 49-63.
Wang, Y.J., Cheng, H., Edwards, R.L., He, Y.Q., Kong, X.G., An, Z.S., Wu, J.Y., Kelly, M.J., Dykoski, C.A., Li, X.D. 2005 Science, 308, 854-857.

Probing the Himalayan Seismogenic Zone (HSZ)

Larry D. Brown[1*], Simon L. Klemperer[2]
[1]Department of Earth and Atmospheric Sciences, Cornell University, Ithaca, NY 14845-1504, USA
[2]Department of Geophysics, Stanford University, Stanford CA 94305-2215, USA
**ldb7@cornell.edu*

The Mw 7.8 Gorkha, Nepal, earthquake that occurred on April 25 of this year was a dramatic reminder that great earthquakes are not restricted to the large seismogenic zones associated with subduction of oceanic lithosphere. The latter have been the foci of a number of major geoscience initiatives over the past several decades, most notably the MARGINS SEIZE program, as well as the host of several recent great earthquakes, including the Mw 9.0 Tohoku earthquake of 2011 and the Mw 8.8 earthquake of Maule, Chile in 2010. The Himalayas seismogenic zone is in many respects the continental counterpart to these largely marine systems. As such it not only represents important scientific and societal issues in its own right, it constitutes a reference for evaluating general models of the earthquake cycle derived from the studies of the oceanic subduction systems.

The Himalayan seismogenic zone shares with its oceanic counterparts a number of fundamental questions, with respect to the accumulation of strain and its release by major earthquakes. These include:

a) What controls the updip and downdip limits of rupture?
b) What controls the lateral segmentation of rupture zones (and hence magnitude)?
c) What is the role of fluids in facilitating slip and or rupture?
d) What nucleates rupture (e.g. asperities?)?
e) What physical properties can be monitored as precursors to future events?
f) How effectively can the radiation pattern of future events be modeled?
g) How can a better understanding of Himalayan rupture be translated into more cost effective preparations for the next major event in this region?

However the underthrusting of continental, as opposed to oceanic, lithosphere in the Himalayas frames these questions in a very different context:

h) How does the greater thickness and weaker rheology of continental crust/lithosphere affect locking of the seismogenic zone?
i) How does the different thermal structure of continental vs oceanic crust affect earthquake geodynamics?
j) Are fluids a significant factor in intercontinental thrusting?
k) How does the basement morphology of underthrust continental crust affect locking/creep, and how does it differ from the oceanic case?
l) What is the significance of blind splay faulting in accommodating slip?
m) Do lithologic contrasts juxtaposed across the continental seismogenic zone play a role in the rheological behavior of the SZ in the same manner as proposed for the ocean SZ?

Major differences in the study of the continental vs oceanic seismogenic zone also relate to the opportunities for new geological observations. In contrast to the study of submarine seismogenic zones which lie beneath many kilometers of water, Himalaya structures are open to:

a) direct geological observation via field mapping
b) dense and wide aperture monitoring of surface strain via GPS and INSAR
c) extensive sampling of geofluids via surface flows and shallow drill holes
d) cost effective deployment of long term geophysical arrays (e.g. seismic and MT) designed to detect subtle variations if physical properties within the seismogenic zone, and ultimately,
e) a fixed platform for deep drilling of past and future rupture zones

The only logistical advantage of the marine environment for the study of the seismogenic zone is the relatively lower cost of multichannel seismic reflection profiling that forms the backbone of such initiatives. However, that advantage may be offset in part by new recording technologies for land acquisition, especially for 3D surveys. Moreover, in some respects the "fixed" land environment is more amenable for the design of cost-effective time lapse geophysical monitoring.

It remains to be established whether the Himalayan seismogenic zone has the potential for earthquakes of the greatest magnitudes (e.g. 9.0+). However, there is no question that future ruptures in this system represent a serious threat to major population centers (megacities) in the India subcontinent. For this reason alone the HSZ is deserving of a major effort exploiting the new generation of geophysical and geological tools.

Any Himalayan Seismogenic Zone effort will be international by the very nature of the target. Certainly one on the scale envisioned here will require the substantial resources that only a

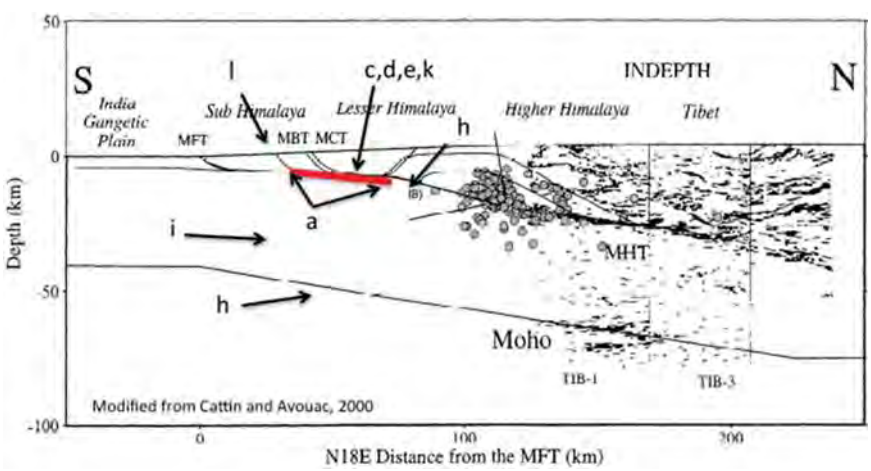

Fig. 1. The Himalayan Seismogenic Zone (Modified from Cattin and Avouac, 2001). Letters refer to issues enumerated above. MHT- Main Himalayan Detachment.

Fig. 2. A network of seismic reflection/refraction surveys would provide the necessary backbone for detailed mapping and monitoring of the Himalaya Seismogenic zone.

multinational consortium can rally. It must also respect the interests of the scientists and authorities of the countries most affected, especially Nepal, and should take advantage of special scientific assets in the regional, for example the geophysical capabilities of the National Geophysical Research Institute in Hyderabad. The workshop being proposed is a first step toward identifying and organizing these diverse interests and resourcs.

Experience with the MARGINS SEIZE initiative as well as numerous individual investigator efforts have clearly demonstrated the desirability of integrating results from multiple approaches. The most obvious components include: multichannel seismic reflection detailing of structure (e.g. Fig. 2), wide-angle seismic measurements of physical properties (e.g. bulk P and S wave velocity, reflector AVO, attenuation, anisotropy), passive seismic measurement of gross structure and physical properties (e.g. anisotropy), MT measurements of conductivity, laboratory measurements of relevant physical properties of local samples, field geological mapping of relevant surface structure and lithology, monitoring of ground water geochemistry, mapping and monitoring of heat flow, GPS and INSAR monitoring of surface strain accumulation and geodynamic modeling of realistic crustal structure. A particularly exciting prospect is time lapse seismic/MT imaging of subtle changes in physical properties within previous and potential future rupture zones.

Latest Ediacaran occurrence of the *Archaeonassa* in the Nigali Dhar Syncline, Lesser Himalaya, India

S.K. Prasad[1], Birendra P. Singh[1], O.N. Bhargava[2], C.A. Sharma[1], Naval Kishore[1], R.S. Negi[1]
[1]Center of Advanced Study in Geology, Panjab University, Chandigarh 160014, INDIA
[2]103, Sector-7, Panchkula, INDIA

We report the Ichnotaxon *Archaeonassa* Fenton and Fenton, 1937 is recorded from the basal part of the Earthy Siltstone Member (Shaliyan Formation, Tal Group) Nigali Dhar syncline (Sirmur

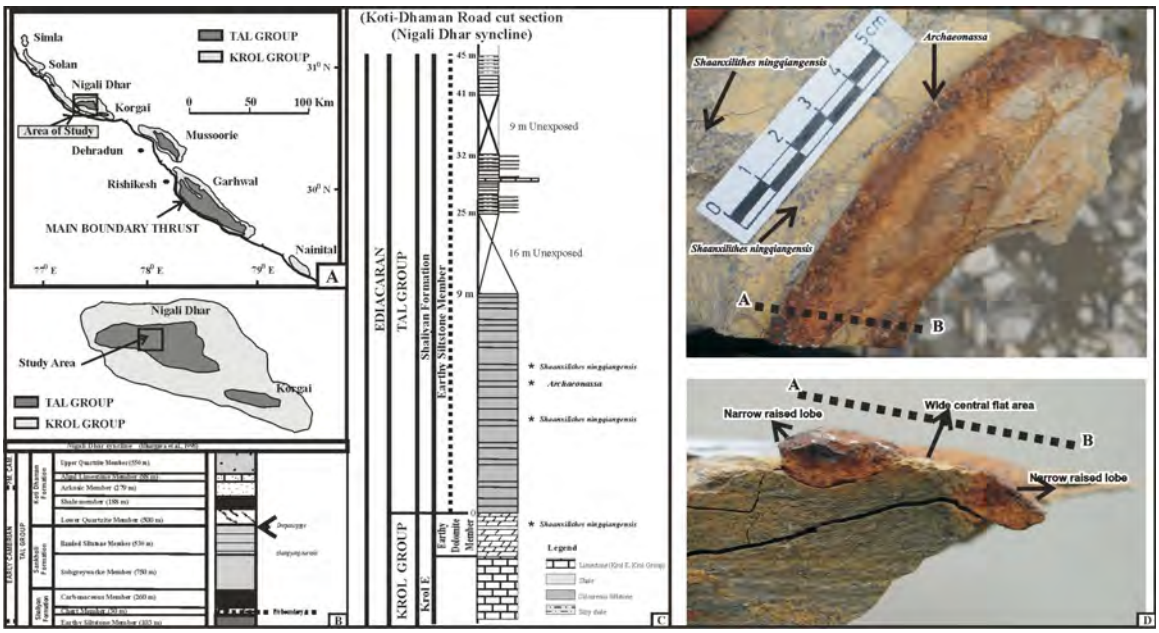

district), Himachal Pradesh (Fig. 1A-C). The trace is preserved on bedding plane of a fine grained calcareous earthy siltstone slab in association with the enigmatic Shaanxilithes ningqiangensis (Xing et al., 1984; Cai and Hua, 2011; Meyer et al., 2012). The section is exposed on the Koti-Dhaman road cut which is the probable section for the demarcation of Precambrian-Cambrian boundary (Tarhan et al., 2014). Chert Member occurs 80 m above than this Archaeonassa bearing level. Till so far Chert Member of Nigali Dhar syncline has not yielded Small Shelly Fossils (SSF) which generally used for demarcation of Precambrian-Cambrian boundary in the Lesser Himalaya (Azmi et al., 1981, Braiser and Singh, 1987; Bhat et al., 1983; Bhat, 1991. The trace is epichnial, horizontal trail (Fig. 1D), gently curved with a wide flat central area flanked by relatively narrow raised levees (Fig. 1D). The total length of the trail is 11 cm, and the lateral levees are 0.9 cm apart. The levees are 0.3-0.4 cm raised and the central flat region show variation in width. The ichnogenus *Archaeonassa* is a bilobed simple, unbranched, straight, curved to meandering, horizontal trail represented by a regular furrow flanked by two narrow lateral ridges; furrow usually v-shaped in cross-section.

Furrow rarely smooth, mostly crossed by rounded wrinkles (Häntzschel, 1975; Yochelson and Fedonkin 1997; Mángano et al., 2005). Wide accepted view for the origin of *Archaeonassa* is from the mollusk-like animals (Valentine, 1995; Jensen, 2003; Baucon and Carvalho, 2008; Mángano et al., 2005; Buatois and Mángano, 2002).

Azmi, R.J., Joshi, M.N., Juyal, K.P. 1981. Contemporary Geosciences Research in Himalaya,1, 245-250.
Bhat, D.K. 1991. Journal Palaeontological Society of India, 36, 109-120.
Bhat, D.K. Mamgain, V.D., Mishra, R.S., Srivastava, J.P. 1983. Geophytology, 13, 116-123.
Braiser, M.D., Singh, P. 1987. Geological Magazine, 124, 323-345.
Buatois, L.A., Mangano, G.M. 2002. Palaeogeography, Palaeoclimatology, Palaeoecology, 183, 71-86.
Cai, Y., Hua, H. 2011. Geological Magazine, 148, 329-333.
Fenton, C.L., Fenton, M.A. 1937. American Mid Naturalist, 18, 1079-1084.
Hantzschel, W. 1975. Supplement I. Geological Society of America., University of Kansas Press, New York, Lawrence, 1-269.
Jensen, S. 2003. Integrative Comparative Biology, 43, 219-228.
Mangano, M.G., Buatois, LA., Muniz G.F. 2005. Amegh, 42 (4), 641-668.
Meyer, M., Schiffbauer, J.D., Xi, A.S., Cai, Y., Hua, H. 2012. Palaios, 27, 354-372.
Tarhan, L.G., Hughes, N.C., Myrow, P., Bhargava, O.N., Ahluwalia, A.D., Kudryavtsev, A.B. 2014.

Palaeontology,57, 283-298.
Valentine, J.W. 1995. Genetics and paleontology 50 years after Simpson, 87-107.
Xing, Y., Ding, Q., Luo, H., He, T., Wang, Y. 1984. Geological Magazine, 121, 155-170.
Yochelson, E.L., Fedonkin, M.A. 1997. Canadian Journal of Earth Science, 34, 1210-1219.

Towards establishing rainfall thresholds for triggering landslides for the Uttarakhand Himalaya

Vikram Gupta
Wadia Institute of Himalayan Geology, 33 GMS Road, Dehradun 248001, INDIA
vgupta@wihg.res.in

Landslide, in general, is mainly affected by the internal geological conditions like lithology, structure, tectonics, terrain morphology, hydrological conditions and external triggering factors like earthquake and rainfall. Rainfall induced landslides and related mass movement phenomena occur almost every year, particularly during the monsoon, which usually lasts from June/July to September, and accounts for the loss of hundreds of lives and damage to private and public property. According to an estimate an average loss of ~400-500 crores Indian rupees incurs every year in India due to landslides and associated phenomena.

Uttarakhand Himalaya, having about 90% of its landmass under mountainous terrain, is plagued by landslides during or immediately after the monsoon, owing to its propensity towards unstable geological and structural setting, and steep slopes combined with severe weather conditions. It has been reported that two landslides occur in every square km of area per year in the Uttarakhand Himalaya. 1998 Surabhi Resort (near Mussoorie) landslides, 2003 Varunavat Parvat (near Uttarkashi) landslides, 2013 numerous landslides in the Yamuna, Alaknanda and Bhagirathi valleys, 2014 Balia Nala (Nainital township) landslide are some of the recently struck rainfall induced landslides that have caused great loss of life and property in the region.

With increasing number of rainfall induced landslides in recent years, particularly in the Uttarakhand Himalaya, an understanding of the relationship between rainfall and the incidence of landslides is of utmost importance. Though many studies related to the assessment of empirical rainfall thresholds for landslides initiation in order to predict landslide occurrence have been carried out all over the world, none of the established threshold value hold true for the Himalayan region, particularly for the Uttarakhand Himalaya.

The present study focuses on the studying typical rain triggered landslides vis-à-vis long duration daily rainfall data of the area. The study is based on the assumptions that there is a direct correlation between the occurrence of landslides and the quantity of rainfall, intensity and duration of the rainstorm events. The studied landslides are 1998 Surabhi Resort landslide (located on the Mussoorie-Kempty road), 2003 Varunavat Parvat landside (located in the Uttarkashi township), Wariya landslide in the Yamuna valley (located upstream of Barkot township), 2013 landslides in the Bhagirathi valley and 2014 Balia Nala landslide (located in the Nainital township). It has been observed that despite having different rainfall intensity in these different areas/valleys, there is greater probability of occurrence of landslides when the intensity of rainfall, in the monsoon season (total rainfall during rainy season/number of rainy days), in a particular area exceeds about 100% of the normal intensity of that area. However more landslide case-studies need to be investigated so as to establish the generalized rainfall threshold of the area.

Geometry and kinematics of the frontal Darjiling-Sikkim Himalaya

Vinee Srivastava*, Malay Mukul
Continental Deformation Laboratory, Dept of Earth Sciences, IIT Bombay, Mumbai 400076, INDIA
**vineesri@iitb.ac.in*

The Himalayan boundary is wedge-shaped in transport-parallel cross-sections (Mukul, 2010 and references therein) and sinuous in map view. The sinuosity is characterized by salient and recesses (Macedo and Marshak, 1999; Marshak, 2004; Mukul, 2010) that are separated by lateral/oblique ramps and steeply-dipping tear faults (Marshak, 2004). A salient-recess pair, viz., Dharan salient-Gorubathan recess, separated by a transverse, sinistral, tear fault, viz., the Gish Transverse Fault (GTF), has been recognized in the Darjiling-Sikkim, N-E Himalaya (Mukul et al., 2010).

The mountain front in the Dharan salient was defined by a set of 11 imbricate faults that repeated the Middle Siwalik section (Kundu, 2014) (Fig. 1a). North to south, the Ramgarh Thrust (RT) carried Daling over Gondwana, Main Boundary Thrust (MBT) carried Gondawana over Lower Siwalik, South Kalijhora Thrust (SKT) carried Lower Siwalik over Middle Siwalik rocks and Main Frontal Thrust (MFT) carried Middle Siwalik over Quaternary sediments respectively in the Darjiling-Sikkim-Tibet Himalayan wedge (Mukul, 2000; Kundu, 2014).

Several small fan surfaces composed of Quaternary sediments of climatic origin (Kar et al., 2014) have been deeply incised by tributaries of the Tista near the mountain front in the Gorubathan recess (Nakata, 1989). Several thrust-related fault scarps were recognized on these surfaces. The Gorubathan-Jiti fault was recognized at the mountain front and interpreted as MBT as it carried Lesser Himalayan rocks over Quaternary sediments (Nakata, 1989). This was reinterpreted to be the RT (Matin and Mukul, 2010) as hanging wall Daling phyllites were transported over footwall Gondwana sandstones. South of the Gorubathan-Jiti fault, the Matiali fault was recognized as a splay of the MBT carrying Lesser Himalayan rocks in its hanging wall. The Matiali fault displaced the Matiali, Rangamati and Samsing surfaces and formed the Matiali escarpment (Nakata, 1989). The Chalsa fault south of Matiali fault was interpreted as the MFT (Nakata, 1989) (Fig.1b).

The Chel River had incised through a flight of four terraces (T1 to T4) in the Gorubathan recess, the topmost of which was the Gorubathan surface (Nakata, 1989). The RT was seen exposed at the base of the Gorubathan surface (T4) near the Mountain front and was seen to override organic-rich clay horizon dated at 33,875±550 years (Guha et al., 2007) indicating that it was active after ~33 ka. In the Chel section, T1 and T2 terraces were symmetric and fill-terraces. The T3 and T4 terraces had Daling rocks exposed at their bases and were probably strath terraces. The terraces T1, T2 and T3 were paired and T4 was unpaired. Real Time Global Navigation Satellite System (RTK-GNSS) measurements indicated that the mean ellipsoidal elevation of the present-day channel of the Chel River was 297.5±4.2 m. The T1 and T2 terraces were close to the present-day water level at mean elevations of 306.6±5.5 m and 309±10.9 m respectively. Also, T3 in the east and west banks of the Chel River were located at mean elevations of 491.5±14 m and 349±7.5 m respectively. T1, T2 and T3 sloped south towards the foreland. The T4 or the Gorubathan fan surface exhibited a mean elevation of 631±3 m and was warped by neotectonic activity along the RT.

South of the RT, the Matiali escarpment was associated with the Matiali fault. The Matiali fault branched from the RT and rejoined it again near Thalijhora carrying Daling rocks in its hanging wall (Nakata, 1989) forming a rejoining splay of RT. RT and the Matiali fault warped the south-sloping Samsing surface whose mean elevation between the Neora and Murti rivers from RTK-GNSS measurements was 401±17.5 m. The age of the Matiali scarp and the activity along the Matiali fault was bracketed between 24 and 11 ka (Kar et al., 2014). The RT (and its splay, the Matiali fault) was, therefore, the mountain front defining fault in the Gorubathan recess of the Darjiling-Sikkim Himalaya (Fig.1b).

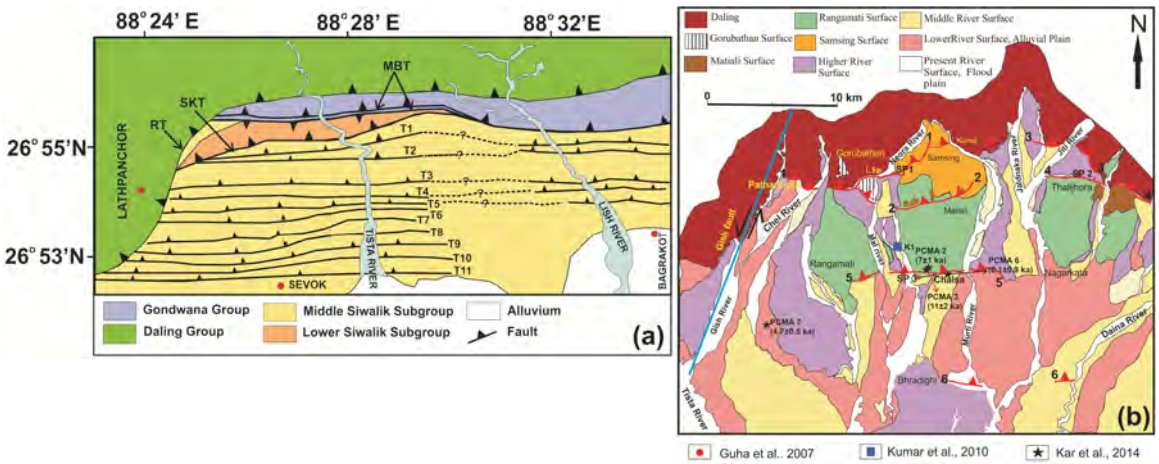

Fig 1. (a) Elevation imbricate thrusts in the footwall of the South Kalijhora Thrust in the Dharan Salient of the frontal Darjiling-Sikkim Himalaya (Kundu, 2014). (b) Active faults and deformed alluvial fans in the Gorubathan Recess in the frontal Darjiling-Sikkim Himalaya. The major active faults in the area are shown in red line: 1.

Gondwana sandstones were exposed in the footwall of the RT (Matin and Mukul, 2010) and formed the hanging wall of the Chalsa fault which was the next imbricate south of RT. Correlation with the Dharan salient indicated that the Chalsa fault was, in fact, the MBT and not the MFT. The MBT warped the Matiali surface forming the Chalsa scarp. The Matiali surface sloped south with a mean ellipsoidal height of 248±9.2 m. The Chalsa scarp was formed before ~22 k (Guha et al., 2007) and between 11-6 ka (Kar et al., 2014). The last activity on the Chalsa scarp was dated to be as recent as ~1100 A.D. (Kumar et al., 2010). South-dipping bedding in Quaternary terraces was also recorded near the Chalsa scarp (Kar et al., 2014) along with folded clay layers (Chakrabarti-Goswami et al., 2013).

Correlation between the fault of Dharan salient (Fig.1a) and Gorubathan recess (Fig.1b) completely breaks down south of the MBT because of lack of exposure of Siwalik rocks in the recess. The Bharadighi fault, reported by Nakata (1989), when correlated with Dharan salient could be any of the 12 faults south of the MBT and may be, tentatively, named the MFT. The Bharadighi fault was active later than the ~5 ka age (Kar et al., 2014) of the surfaces south of the Chalsa scarp.

The frontal Darjiling-Sikkim Himalaya, therefore, is composed of imbricate faults in both the Dharan salient and the Gorubathan recess. The Dharan salient is characterized by a greater number and more closely-spaced (12) imbricate faults defining a frontal schuppen zone in contrast with the single imbricate south of the MBT in the Gorubathan recess. Fault propagation folding (FPF) and/or ramp anticlines have been tentatively invoked to explain the warping of the fans and terraces (Goswami et al., 2012, Chakrabarti-Goswami et al. 2013) by blind thrust faults in the recess. However, better-constrained geometric and kinematic models are needed to explain the observed neotectonics in the Gorubathan recess.

Chakrabarti Goswami, C., Mukhopadhyay, D., Poddar, B.C. 2013. Quat. Int. 298, 80-92.
Goswami, C., Mukhopadhyay, D., Poddar, B.C. 2012. Frontier of Earth Science 6 (1), 29e38.
Kar R., Chkraborty T., Chkraborty, C., Ghosh, P., Tyagi, A.K., Singhvi, A.K., 2014. Geomorphology, 227,137-152. Http://dx.doi.org/10.1016/j.geomorph.2014.05.014
Kundu, A. 2014, Ph.d Thesis, Calcutta University. 187p
Macedo, J., Marshak, S. 1999. GSA Bulletin 111 (12), 1808-1822
Marshak, S. 2004. American Association of Petroleum Geologists Memoir 82, 131-156.
Matin, A., Mukul, M. 2010. Current Science 99, 1369e1377.
Mukul, M. 2010. Journal of Asian Earth Sciences, 39, 645-657

Mukul, M. 2000. Journal of Structural Geology 22, 1261e1283.
Nakata, T. 1989. Active Faults of the Himalaya of India and Nepal, vol. 232. Geological Society of America.

Structural geological model: An essential information for civil engineering works Tapovan HEPP, Himalaya, India

W. Genser[1,*], J. Kleberger[1], I. Poeschl[1], J. Genser[2]
[1]*iC consulenten ZT GmbH, Zollhausweg 1, 5101 Bergheim-Salzburg, AUSTRIA*
**w.genser@ic-group.org*
[2]*Dept. of Geography and Geology, University Salzburg, AUSTRIA*

The investigation area is situated south of the junction of Dhauliganga and Alaknanda River at the mountain range between Shelang, Joshimath, Auli and Tapovan. The alignment of an approximately 12 km long head race tunnel passes through metamorphic rocks of the Joshimath and the Tapovan Formation of the Crystalline Thrust Sheet in the Higher Himalayan (Fig. 1). Severe geotechnical problems during tunnel excavation resulted in a review of the predicted geological model (tender model). The findings of the review show that the actual geological conditions deviate substantially from the predicted geological model. Tectonic and structural geological issues were neglected in the predicted model (Fig. 2), although complex faulting controls geotechnical and geological conditions and behaviour of the rock mass during tunnel excavation. The encounter of these unpredicted and therefor unexpected ground conditions caused several collapse incidents that resulted in the trapping of the TBM (tunnel boring machine) and in extremely slow advance rates of drill & blast excavation. An improved structural model was required within short notice as excavation works were ongoing (Fig. 2).

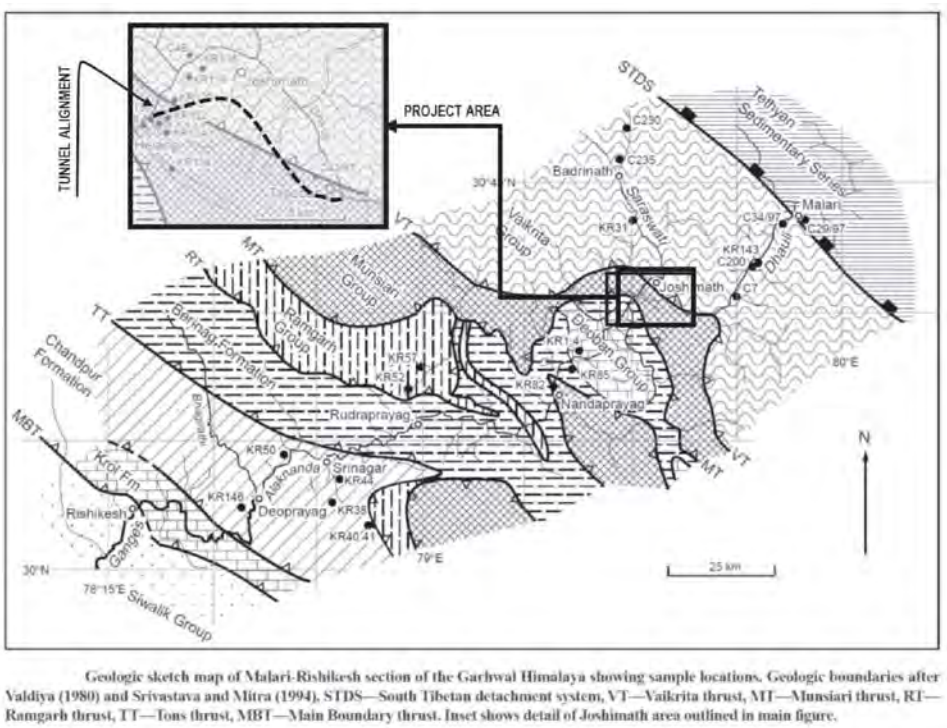

Geologic sketch map of Malari-Rishikesh section of the Garhwal Himalaya showing sample locations. Geologic boundaries after Valdiya (1980) and Srivastava and Mitra (1994). STDS—South Tibetan detachment system, VT—Vaikrita thrust, MT—Munsiari thrust, RT—Ramgarh thrust, TT—Tons thrust, MBT—Main Boundary thrust. Inset shows detail of Joshimath area outlined in main figure.

Fig. 1. Project area located south of the Dhauliganga/Alaknanda river junction and detail of the geological map at the studied area, Joshimath, Himalaya, India (from Ahmad et al., 2000).

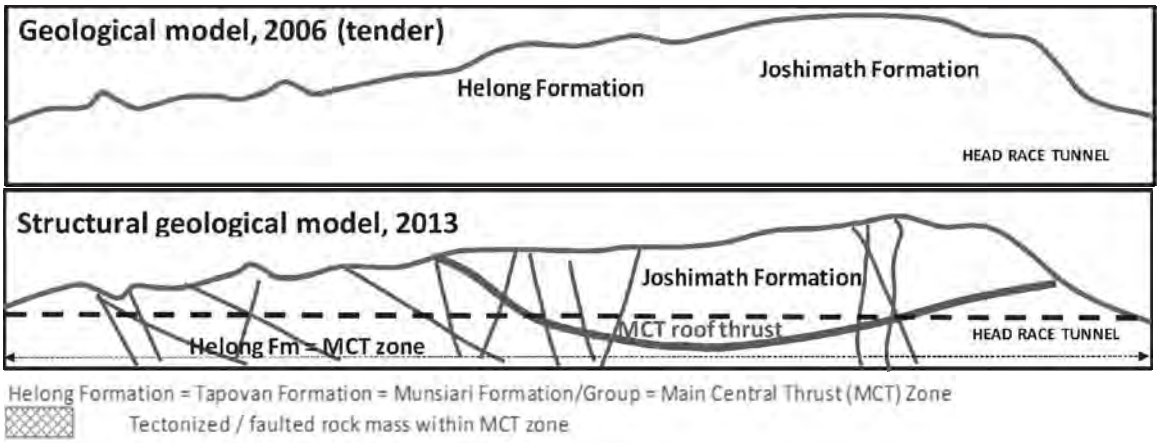

Fig. 2. Development of the revised geological/structural geological model along the head race tunnel alignment (Tapovan HEPP).

The present study was carried out to develop a revised structural (tectonic) model along the tunnel alignment (Fig. 1) on basis of data made available within a stipulated time period. Prior to structural geological mapping and sampling lineament analyses from satellite images, literature studies and evaluation of documentation data from the ongoing tunnel excavation were performed. The geotechnical behavior of rock mass is dominated by brittle structures and their characteristics. Two basic types of brittle tectonic features were identified. Low-angle features, including the foliation and low-angle shear planes, which were originally formed by ductile shearing along the MCT. Low-angle shear zones were at least partly reactivated by brittle faulting during later deformation phases. Medium- to high-angle features with varying orientations were created by younger deformation phases at brittle conditions (Fig. 2). These faults were investigated in more detail and classified based on orientation, dimension, filling and persistence.

One of the major issues with significant implications for the tectonic model along the tunnel alignment is the allocation of the roof thrust of the Main Central Thrust zone (MCT), which was stated to pass south of the project area. In contrast to the prediction, excavation data as well as various scientific papers (e.g. Sati 1988, Ahmad et al 2000) show that more than 65% of the tunnel passes through the tectonized MCT below the Vaikrita Thrust (=Roof Thrust of the MCT zone). To confirm the field evidence concerning the position of the Vaikrita Thrust, metamorphic-petrological studies on samples collected along the head race tunnel (HRT) were performed. Results of the petrological study mesh well with the conclusions published by Sati (1988) and Spencer et al. (2012), which report and prove a discordance and inversion in grade of metamorphism between the Helong and the Joshimath Formations, implying the presence of a thrust zone at the base of the Joshimath Formation.

The geothermobarometric data indicate peak Pressure (P)-Temperature (T) conditions of ~730°C/12 kbar in the Joshimath Formation, and a strong inverse metamorphic gradient in the

Table 1. *Conclusion of the metamorphic petrological studies from samples along the head race tunnel.*

Formation	Petrography/Microtexture	Pressure [kbar]	Temperature [°C]
Joshimath	static metamorphism	~12	730
			MCT
Helong	dynamic synmetamorphic deformation	~9 close to MCT (Vaikrita Thrust)	680
		~7 distantly from MCT (Vaikrita Thrust)	550

underlying Helong Formation, decreasing from ~680°/9 kbar close to the Vaikrita thrust to ~550°C/7 kbar in larger distance. Microtextures show almost static metamorphism in the Joshimath Formation and strong ductile, synmetamorphic deformation in the Helong Formation (Table 1). All data confirm that the Joshimath and the Helong Formations are tectonically separated by the Vaikrita thrust. The Helong Formation below the MCT (Vaikrita thrust) acted as a km-thick shear zone (MCT zone), which absorbed the southward displacement of the HHC over the LHS.

Ahmad, T. et al. 2000. GSA Bulletin, v. 112, no. 3, p. 467-477.
Sati, D.C. 1988. (unpublished Ph.D. Thesis).
Spencer, C.J., Harris, R.A., Dorais, M.J. 2012. Tectonics, Vol. 31, TC1007.
Valdiya, K.S., 1980. Geology of Kumaun Lesser Himalaya, WIHG, Dehradun, 291 p.
NTPC Limited, 2004 to 2006. Tender reports concerning Tapovan-Vishnugad Hydro-Electric Project (unpublished documents).

Rock-melt interaction beneath orogenic belt: experimental investigations On rheological and seismic consequences

Santanu Misra[1*], David Mainprice[2]
[1]*Department of Earth Sciences, IIT Kanpur, Kanpur 208016, INDIA*
**smisra@iitk.ac.in*
[2]*Geosciences Montpellier, Universite de Montpellier, FRANCE*

The mechanical behavior of binary systems, consisting of solid and fluid phases, is one of the key research areas in Earth Sciences as it has implications of understanding deep orogenic processes, particularly melt dynamics - generation, segregation, localization and movement of magma (fluid) within partially molten crystalline (solid) rocks.

This study investigates the large strain rheological behaviour of pelitic rocks undergoing syn-tectonic melting and subsequent crystallization. Constant strain rate ($\gamma=3x10^{-4}$ s^{-1}) torsion experiments were performed to achieve large strains ($\gamma_{max} = 15$) on synthetic aggregates of quartz and muscovite at 300 MPa confining pressure and 750°C temperatures. A set of hydrostatic experiments for equivalent times of torsion experiments were also conducted at 300 MPa and 750°C to appreciate the reaction kinetics and microstructures with and/or without deformation. Microstructures of the deformed samples reveal four distinct but transitional stages (Fig. 1) of crystal-melt interactions - (i) solid state deformation, (ii) initiation and domination of partial melting, (iii) simultaneous partial melting and crystallization, and (iv) domination of crystallization. These four microstructural stages are linked to the bulk mechanical response and rheology of the deforming samples. Partial melting starts at relatively low finite shear strains (γ=1-3) and is associated with strong (ca. 60%) strain softening. With further shearing (γ=4-10) the melt assisted bulk material shows a constant (steady state) flow at low stress with nucleation of new crystals. Growth of new crystals at the expense of partial melt at higher stains (γ=10-15) is characterized by weak strain hardening and finally the material fails by developing brittle fractures. The stress exponent (n) values, calculated at three different shear strains (γ=1, 5 and 10), show a continuous increase from ca 3 to 43 with incremental deformation indicating a transition from power to power law break-down or exponential flow of the bulk system. These new experimental data establish the fact that the partially molten rock does not always flow following a constant strain rate dependent power law (steady state) rheology. The rheological transition from strain rate sensitive to strain rate insensitive flow is interpreted to be a function of melt and solid proportions and their mutual interactions coupled with evolution of microstructures in the partially molten rock.

Fault propagation and damage in layered rocks: the effect of transverse anisotropy

Santanu Misra[1*], Susan Ellis[2], Nibir Mandal[3]
[1]Department of Earth Sciences, IIT Kanpur, Kanpur 208016, INDIA
**smisra@iitk.ac.in*
[2]GNS Science, 1 Fairway Drive, Avalon, Lower Hutt 5011, NEW ZEALAND
[3]Department of Geological Sciences, Jadavpur University, Kolkata 700032, INDIA

This study aims to probe the role of inherent mechanical anisotropy in controlling damage zone localization in both the tip and wall regions of a fault or fracture. Rocks are often mechanically anisotropic due to the presence of bedding planes, penetrative crystallographic or shape fabrics and compositional foliations. Inherent cracks, fractures and faults often act as mechanical flaws to intensify local stresses, leading to mechanical failure at their tips. Earth scientists have used flaw-controlled mechanics to understand a wide variety of geological and geophysical phenomena including flanking structures, wing fractures, secondary fracture-controlled hydraulic conductivity and growth of crustal-scale tectonic faults. In this study, analogue and numerical models were deformed under compressive stresses either parallel, perpendicular or at an angle to the plane of anisotropy under a constant strain rate. We show from our experiments that the damage localization can dramatically change depending on the orientation of the planar anisotropy (θ). Under layer-normal (θ=0°) and layer-parallel compression (θ=90°), pre-existing faults are reactivated. Fault slip leads to mechanical instabilities within the anisotropic layering, causing damage zones in the tip regions. For θ=0° the planar anisotropy arrests the propagation of tensile fractures across the plane of anisotropy and promotes localised plastic shear instabilities at the crack tips, whereas a combination of layer opening and distributed shear banding occurs when the plane of anisotropy is parallel to the compressive direction. For θ=45°, the faults experience little or no reactivation and instead, bulk (distributed) inter-layer slip occurs. Our results have implications for the deformation style of strongly anisotropic rocks such as schist. They show how the deformation mechanism and degree of localization will be strongly influenced by the orientation of principal stresses and inherited cracks to the plane of the foliation.

Leh Floods 2010 - Lessons unlearnt

Ritesh Arya[*],
168 Arath Bazar Kasauli, Himachal Pradesh, INDIA
**aryadrillers@gmail.com*

More than 5 years have passed but the flooding event at 23:45 hours on 5th August 2010 in Leh, Ladakh, India in which the author was also trapped and narrowly escaped his life. Later to study the event and describe it as an extreme geological event of this century in history of Himalayas for simple reason that sediment deposition of 3 to 8 m took place in <1 to 3 minutes in low lying areas and equal amount eroded from upstream parts widening and deepening the valleys. The event was sufficient to destroy and submerge habitations which fell in its natural course; Indus valley civilization in the past was no exception to this event. In Leh and Choglamsar, it was a single depositional event but in Tyagshi, Nubra Valley it was episodic and deposited in 2 short phases of <1 minute each in 2 days. In all 52 villages were effected, more than 191 lives lost (mainly in recent habitations constructed in traditionally unsafe areas), millions of trees and agricultural land destroyed in villages as the streams widened manifold, people (mainly non locals) still missing probably buried in thick pile of sediments or washed along the streams into Indus. People in the

effected villages rose the next morning to see all together a different geomorphological set up. Old men and women were crying as all their plantations and agricultural land was lost and instead the valley was just flowing very near to the houses.

Main aim of the report is to understand geo-mechanism of extreme geological event (land slide, mud slides and flooding) triggered by heavy rains falling for short time span of 5-10 minutes. No evidence of cloud burst are found in studied catchments as the plantation above flooding areas (4-8 m high and 8-15 m wide) is still intact. Had cloud burst theory been the phenomenon then the plants and small structures on the upstream side of the effected valleys been destroyed.

Paper proposed Reservoir Wall Rupture Theory to explain the geo-mechanism of flooding in Himalayas and selective destruction caused in adjacent catchments in spite of receiving similar rains. Dry glacio fluvial valleys brought in sediments along with water and the thickness of the slush was more than 12 m. Anticipated speed of these flood/mud slush is estimated to be around >120 miles/hour. Concrete buildings of upto 3 levels were just leveled to ground near Leh Bus stop within seconds on that night.

However traditional mud houses stood test of time, since time immemorial in this highest seismic areas of Ladakh with complex geology, extreme climate and fragile environment, because they were located in traditionally geological safe places. It is interesting to note negligible damage was done to old mud habitation in Ladakh below Mani Walls and on hills whereas recent (25-30 years) concrete structures constructed on paleo channels were completely destroyed. Clearly suggesting that flooding event was natural and followed its natural course but destruction was manmade as infrastructure/houses were built on paleo channels in traditionally unsafe areas.

Lastly paper had suggested sustainable habitat solutions to be built on hills (Gompas and palaces), using traditional (geological) wisdom practiced by ancestors. Flooding areas in the past were also demarcated by building huge boundary walls (Mani Walls, 600 m long and 11 m wide and up to 3 m, high and Stupas) 400-500 years ago to protect habitations.

But today all the habitations have sprung up in the same locations in the valley region very near to the killer streams of 2010. People and administration wants to worship Mani walls and Stupas but do not want to understand the ancestral wisdom of their construction pattern in particular geological locations to prevent the habitants from flash floods and avalanches in the past. If situation like 2010 is repeated in Leh more loss to life and property will happen. The bridge constructed by Himank in Choglamsar will turn out to be the worst geo-engineering blunder and would cause great damage to the habitants of Choglamsar by blocking the passage of the stream. No lessons seem to be learnt!!! Traditional Wisdom Lost.

Regional metamorphism along Pinder valley of the Central Crystalline rocks, Kumaun Himalaya, India

Manisha Sanguri*, A K Sharma
Department of Geology, Kamaun University, Nainital, INDIA
**Manisha.sanguri@gmail.com*

A number of geological processes including deformation and metamorphism occur deep inside the earth, and involve entrapment of fluids in minerals in the form of fluid inclusions during the processes which when clubbed with microscopic and P-T data are important in deciphering the unique and precise information of P-T-X evolution of the rocks. Metapelites of the Central Crystallines (between 30°4'and 30°15' N : 79°54'and 79°60' E) of Kumaun Himalaya exposed along the Pinder valley section show an

increase in grade of metamorphism towards north, and are constituted by mineral assemblage ky-grt-staur-bt-qtz-chl-ms±pl, with mag, ilm, tour and fsp occurring as minor constituents.

The textural features of the rocks suggest for three major phases of deformation viz. D_1, D_2 and D_3 to which these rocks were subjected. Metapelites are found associated with quartzites and gneisses while leucocratic rock with tourmaline needles (tourmaline pegmatite) are observed in the higher regions beyond the Vaikrita Thrust. The region also shows conspicuous presence of folded quartz in these rocks. Garnet, staurolite and kyanite are present in the form of porphyroblast which are also aligned parallel, and are elongated to S_1 schistosity formed during D_1 deformation. The S_1 schistosity is later folded during D_2 deformation as shown by folding of micaceous layers, followed by final development of S_3 schistosity during D_3 deformation, thereby displaying the evidences of multiple deformations in the region. Fluid inclusions were observed in mineral quartz present in the matrix, while few were also noticed in quartz occurring as inclusion within garnet and staurolite. The P-T estimations were made using different models of geothermobarometry so as to obtain a clearer picture on the evolution of these metapelites. The estimated P-T results suggest temperature in the range of 425 to 850^{o}C, while pressure values range between 4 and 13 kbar, and their increase towards north suggest inversion of isograds.

Author Index

LTSS No.....

WADIA INSTITUTE OF HIMALAYAN GEOLOGY

Publication & Documentation Section
33, General Mahadeo Singh Road, Dehradun – 248 001, India

REGISTRATION FORM

LIFE TIME SUBSCRIBER SCHEME
for
"HIMALAYAN GEOLOGY"
(for individuals only)

1. I would like to become a Life Time Subscriber for "Himalayan Geology".

2. The Life Time Subscriber fee for Rs.1000.00 (India) US $ 100.00 (Foreign) is enclosed herewith by Draft in favour of Director, Wadia Institute of Himalayan Geology. Kindly send the publications on the following address :

   Name ……..…

   Address ……..…

   ……...…

   ……...…

   E-mail/Fax ……..…

I certify that the subscription is for my personal use only and that print subscriptions will not be released to libraries or reading rooms for at least 2 years after publication.

SIGNATURE

Note: A free set of old volumes (1971 to 2005, subject to availability) of Himalayan Geology will be provided to the newly registered Life Time Subscriber Scheme Members for a limited time (Postage to be borne by the Subscriber).

Phone : 91-135-2525430 **Fax:** (91)0135-2625212 **Web:** http://www.himgeology.com
E-mail: himgeol@wihg.res.in, kaushikrb@wihg.res.in, publications@wihg.res.in

WADIA INSTITUTE OF HIMALAYAN GEOLOGY, DEHRA DUN
PUBLICATIONS AVAILABLE FOR SALE

HIMALAYAN GEOLOGY

(These volumes are the Proceedings of the Annual Seminars on Himalayan Geology organizsed by the Institute)

		(in Rs)	(in US $)
Volume 1	(1971)	130.00	26.00
Volume 2*	(1972)	50.00	-
Volume 3*	(1973)	70.00	-
Volume 4*	(1974)	115.00	50.00
Volume 5	(1975)	90.00	50.00
Volume 6	(1976)	110.00	50.00
Volume 7	(1977)	110.00	50.00
Volume 8(1)	(1978)	180.00	50.00
Volume 8(2)	(1978)	150.00	45.00
Volume 9(1)	(1979)	125.00	35.00
Volume 9(2)	(1979)	140.00	45.00
Volume 10	(1980)	160.00	35.00
Volume 11	(1981)	300.00	60.00
Volume 12	(1982)	235.00	47.00
Volume 13*	(1989)	1000.00	100.00
Volume 14* (in Hindi)	(1993)	600.00	-
Volume 15*	(1994)	750.00	

(Available from M/s Oxford & IBH Publishing Co. Pvt. Ltd., New Delhi, Bombay, Kolkata)

Volume 16*	(1999)	1000.00	100.00

Journal of Himalayan Geology

(A bi-annual Journal : published from 1990 to 1995)

Annual Subscription		(in Rs)	(in US $)
	Institutional	500.00	50.00
	Individual	100.00	25.00
Volume 1*	(1990)		
Volume 2	(1991)		
Volume 3	(1992)		
Volume 4*	(1993)		
Volume 5	(1994)		
Volume 6*	(1995)		

HIMALAYAN GEOLOGY

(A bi-annual Journal incorporating Journal of Himalayan Geology)

Volume 17 (1996)	Annual Subscription:	(in Rs)	(in US $)
	Institutional	500.00	50.00
	Individual	100.00	25.00
	Revised Annual Subscription:		
	Institutional	750.00	50.00
	Individual	100.00	25.00
Volume 18 (1997) to Volume 27 (2006)*			
Volume 28 (2007) to Volume 29 (2008)			
Volume 30 (2009) to Volume 32 (2011)*			
Volume 33 (2012)			
Volume 34 (2013) to Volume 35 (2014)*			
Volume 36 (2015)	Institutional	750.00	50.00
	Individual	100.00	25.00

OTHER PUBLICATIONS

Geology of Kumaun Lesser Himalaya, 1980 (by K.S. Valdiya)	Rs. 180.00 US $ 50.00
Geology of Indus Suture Zone of Ladakh, 1983 (by V.C.Thakur & K.K. Sharma)	Rs. 205.00 US $ 40.00
Bibliography on Himalayan Geology, 1975-85	Rs. 100.00 US $ 30.00
Geological Map of Western Himalaya, 1992 (by V.C. Thakur & B.S. Rawat)	Rs. 200.00 US $ 15.00
Excursion Guide :The Siwalik Foreland Basin (Dehra Dun-Nahan Sector), (WIHG Spl. Publ. 1,1991) (by Rohtash Kumar and Others)	Rs. 45.00 US $ 8.00
Excursion Guide : The Himalayan Foreland Basin (Jammu-Kalakot-Udhampur Sector) (WIHG Spl Publ.2,1999) (by A.C. Nanda & Kishor Kumar)	Rs. 180.00 US $ 15.00
Glacier Lake Inventory of Uttarakhand (by Rakesh Bhambri et al. 2015	Rs. 500.00 US $ 50.00
Siwalik Mammalian Faunas of the Himalayan Foothills With reference to biochronology, linkages and migration (by Avinash C. Nanda)	Rs. 1200.00 US $ 100.00
Atlas of early Palaeogene invertebrate fossils of the Himalayan foothills belt (WIHG) Monograph Series No. 1, 2000) by N.S. Mathur & K.P. Juyal (Available from M/s Bishen Singh Mahendra Pal Singh, 23-A New Connaught Place, Dehradun- 248001, Email: bsmps@vsnl.com	Rs. 1450.00 US $ 50.00

Note: 'Journal of Himalayan Geology' & 'Himalayan Geology' have been merged and are being published as Himalayan ' Geology' after 1996.

*** Out of Stock**

Life Time Subscribers for Himalayan Geology

India: Rs. 1000/- Abroad: US $ 100/=

Note: A free set of old volumes (1971-2005, subject to availability) of Himalayan Geology will be provided to the newly registered Life Time Subscriber Scheme Members for a limited time (Postage to be borne by the Subscriber).

Trade Discount (In India only)

1-10 copies: 10%, 11-25 copies: 15%
More than 25 copies: 25%

Publications: *may be purchased from Publication & Documentation Section and Draft/Cheque may be drawn in the name of The Director, Wadia Institute of Himalayan Geology, 33- General Mahadeo Singh Road, Dehra Dun – 248 001*

Phone: 0135-2525430 Fax: (91) 0135-625212 Website: http://www.himgeology.com E-mail: himgeol@wihg.res.in


वाडिया हिमालय भूविज्ञान संस्थान
WADIA INSTITUTE OF HIMALAYAN GEOLOGY
वाडिया हिमालय भूविज्ञान संस्थान
WADIA INSTITUTE OF HIMALAYAN GEOLOGY